VOL.
19
1961

Journal of Inorganic & Nuclear Chemistry

VOLUME 19 1961

EDITORS

JOSEPH J. KATZ, Argonne · A. G. MADDOCK, Cambridge · L. E. J. ROBERTS, Harwell · E. J. W. VERWEY, Eindhoven

EDITORIAL ADVISORY BOARD

U.K. and Commonwealth: J. S. ANDERSON, F.R.S., Melbourne · C. C. ADDISON, Nottingham · C. B. AMPHLETT, Harwell · F. M. BREWER, Oxford · G. E. COATES, Durham · J. S. DUNCAN, Melbourne · H. J. EMELÉUS, F.R.S., Cambridge · F. FAIRBROTHER, Manchester · J. H. GREEN, Kensington, N.S.W. · H. M. N. H. IRVING, Oxford · L. E. ORGEL, Cambridge · A. R. POWELL, F.R.S., Wembley · P. L. ROBINSON, Newcastle-upon-Tyne · R. SPENCE, Harwell · H. G. THODE, F.R.S., Hamilton · L. YAFFE, Montreal

U.S.A.: L. F. AUDRIETH and JOHN C. BAILAR JR., Univ. of Illinois · F. BASOLO, Northwestern Univ. · E. O. BRIMM, Linde Air Products · HERBERT C. BROWN, Purdue · ANTON B. BURG, Univ. South Calif. · CHARLES D. CORYELL, M.I.T. · R. W. DODSON, Brookhaven · W. CONARD FERNELIUS, Koppers Company, Penn. · WARREN C. JOHNSON, Chicago · H. B. JONASSEN, Tulane Univ. · JACOB KLEINBERG, Univ. of Kansas · K. A. KRAUS, Oak Ridge · W. F. LIBBY, Los Angeles · W. M. MANNING, Argonne · THERALD MOELLER, Univ. of Illinois · EARL L. MUETTERTIES, Wilmington, Delaware · EUGENE G. ROCHOW, Harvard · GLENN T. SEABORG, Univ. of California · P. W. SELWOOD, Evanston · F. H. SPEDDING, Ames · R. W. STOUGHTON, Oak Ridge · J. R. VAN WAZER, Missouri · DON M. YOST, Pasadena, Calif. · W. H. ZACHARIASEN, Chicago · R. A. PENNEMAN and B. B. CUNNINGHAM, Univ. of California · H. TAUBE, Chicago

Austria: E. BRODA, Vienna · BERTHA KARLIK, Vienna · V. GUTMANN, Vienna
Denmark: J. BJERRUM, Copenhagen
France: J. BÉNARD, Paris · J. CHÉDIN, Paris · J. GUÉRON, Paris · M. MAGAT, Paris
Germany: W. HIEBER, Munich · G. JANDER, Berlin · A. MUENSTER, Frankfurt
Netherlands: A. E. VAN ARKEL, Leiden · A. H. W. ATEN JR., Amsterdam · J. H. DE BOER, Geleen · J. H. VAN SANTEN, Eindhoven
Israel: M. BOBTELSKY, Jerusalem · *Italy:* V. CAGLIOTI, Rome
Norway: H. HARALDSEN, Oslo · ODD HASSEL, Oslo
Persia: H. A. C. McKAY, Tehran
Sweden: G. HÄGG, Uppsala · L. G. SILLÉN, Stockholm
Switzerland: G. SCHWARZENBACH, Zürich

Copyright © 1961 Pergamon Press Ltd.

PERGAMON PRESS OXFORD · LONDON · NEW YORK · PARIS

JOURNAL OF INORGANIC AND NUCLEAR CHEMISTRY

Editors:

JOSEPH J. KATZ: *Argonne National Laboratory, 9700 South Cass Avenue, Argonne, Illinois, U.S.A.*
A. G. MADDOCK: *University Chemical Laboratory, Lensfield Road, Cambridge, England*
L. E. J. ROBERTS: *Atomic Energy Research Establishment, Harwell, Didcot, Berks, England*
E. J. W. VERWEY: *Philips Research Laboratories, Eindhoven, The Netherlands*

NOTES FOR CONTRIBUTORS

I. General

1. Papers should, in general, be concerned with original work in the field of inorganic and nuclear chemistry. They should be submitted to the Editors, Dr. A. G. MADDOCK, Dr. L. E. J. ROBERTS, or Dr. J. J. KATZ, or, in the case of papers not in the English language, to Dr. E. J. W. VERWEY. The addresses are given above.

2. Fifty free reprints of each paper are supplied. Additional copies can be supplied at a reasonable cost if ordered at the time when the first proofs are returned. A reprint order form will accompany proofs.

II. Script Requirements

1. Scripts should be submitted in duplicate. They must be typewritten, and double-spaced. Authors are requested to make clear any Greek characters which may be confused with ordinary letters or with other characters. Authors will receive proofs for correction when their contribution is first set, but there is rarely time for page proofs also to be sent for checking. This will be done, however, where the amount of alteration makes it advisable.

2. Illustrations should be placed at the end of the manuscript, and legends should be typed on a separate sheet. It is requested that photographs should be kept to the minimum necessary. Line drawings or good photo-prints may be provided. Line drawings must include all relevant details: if they are already well drawn it may be possible to reproduce them direct from the original. It is not possible to reproduce from "dye-line" prints, or from prints with weak lines. Illustrations for reproduction should normally be about twice the final size required. Any lettering on diagrams—other than Greek letters, symbols, etc.—should be stencilled and should be sufficiently large and bold to permit reproduction when the diagram has been reduced to a size suitable for inclusion in the journal.

3. References should be clearly indicated in the text by superior numbers. Full references should be given in numbered footnotes containing author's name, initials, title of paper (where desired), abbreviated title of journal, year, volume number, and page number.

4. The text of articles submitted must be concise and in a readily understandable style. The technical description of the methods used should only be given in detail when such methods are new. The essential contents of each paper should be briefly recapitulated in an abstract. French and German papers should be submitted with English abstracts. **Four copies of the English abstracts are required with all papers, including those in the English language.**

5. To conserve space, authors are requested to mark less important portions of the paper (such as description of methods, record of experimental results, etc.) for printing in smaller type.

PERGAMON PRESS LTD.

HEADINGTON HILL HALL, OXFORD 122 EAST 55TH STREET, NEW YORK 22, N.Y.

VOL
19
196

LIST OF CONTENTS

NUMBERS 1/2

I. B. HÄLLER and G. RUDSTAM: Relative yields of the isomeric pairs ^{69g}Zn–^{69m}Zn and ^{52g}Mn–^{52m}Mm in some spallation reactions induced by 20–153 MeV protons . . . 1

R. D. MACFARLANE: Dysprosium-154, a long-lived α-emitter . . . 9

K. F. CHACKETT and G. A. CHACKETT: Light isotopes of rubidium formed in ^{3}He bombardments of bromine . . . 13

D. HALL and G. N. WALTON: Chemical effects in fission product recoil—V. The valency state of fission product iodines formed in uranyl iodate . . . 16

T. COSTEA: Associated processes to the Szilard-Chalmers effect in crystals—I. Hexammino-cobaltic nitrate, section 2. Thermal annealing of the crystalline defects after irradiation . . . 27

B. JEZOWSKA-TRZEBIATOWSKA and K. BUKIETYŃSKA: The electronic structure of uranium (IV) in complex compounds—I. Comparison of the absorption spectra of uranium (IV) and praseodymium (III) compounds . . . 38

H. A. BENT: Hybridization and bond properties. Effects of second-order hybridization on the σ-bonds in thionyl, sulphuryl, phosphorus, phosphoryl and thiophosphoryl halides . . . 43

C. FURLANI and A. FURLANI: Absorption spectra of some tetrahalogenomanganates (II) . . . 51

E. J. FELTEN: Preparation and properties of some rare earth borates . . . 61

A. D. KIRSHENBAUM and J. A. CAHILL: The density of molten thorium and uranium tetrafluorides 65

A. G. GALINOS: A group of complex metal halogen compounds . . . 69

L. SACCONI, M. CIAMPOLINI, F. MAGGIO and F. P. CAVASINO: Studies on co-ordination chemistry—VIII. Magnetic, spectrophotometric and dielectric measurements on a series of *bis*-(*n*-alkylsalicylaldimino)-copper (II) complexes . . . 74

L. MALATESTA and F. CANZIANI: Iridiumcarbonyl compounds—V. Bromo- and chlorocarbonyliridates . . . 81

F. G. SHERIF and Miss A. M. AWAD: The structure of uranyl azide—its instability constant in aqueous solutions . . . 94

J. SOBKOWSKI and S. MINC: Oxidation-reduction potential of UO_2^{2+}–U^{4+} system in perchloric acid 101

C. N. POLYDOROPOULOS and TH. YANNAKOPOULOS: Silver hyponitrite: solubility product and complexes in aqueous ammonia . . . 107

E. BLASIUS, W. PREETZ und R. SCHMITT: Untersuchung des Verhaltens der Chlorokomplexe der Platinelemente in Lösung und an Anionenaustauschern . . . 115

D. B. JAMES, J. E. POWELL and F. H. SPEDDING: Cation-exchange elution sequences—I. Divalent and rare-earth cations with EDTA, HEDTA and citrate . . . 133

J. KENNEDY and A. M. DEANE: The infra-red spectra of uranium species in carbon tetrachloride solutions of uranium (VI), dibutyl phosphoric acid and tri-*n*-octyl phosphine oxide . . . 142

P. A. D. DE MAINE and E. J. WALSH: Inorganic salts dissolved in non-aqueous or in mixed solvents—X. Conductance studies at 20 and 45°C for hydrated tin chlorides in methanol and in methanol-carbon tetrachloride . . . 156

H. SMALL: Gel-liquid extraction—II. The separation of metallic species using ion exchange resins in conjunction with water-immiscible organic extractants . . . 160

Notes:

I. MCLURE and T. D. SMITH: Aluminium hydride etherate formed from etherpentane solution . 170

K. J. H. MACKAY: Non-dispersive X-ray fluorescence analysis of uranium-containing solutions . 171

L. L. WILLIAMS, N. SUTIN and J. M. MILLER: The thermal annealing of ^{60}Co in irradiated tris-(ethylenediamine)-cobalt (III) nitrate . . . 175

B. D. JAIN and S. P. SINGHAL: Determination of zirconium in presence of common metals using 2:5 dihydroxy *p*-benzoquinine and the nature of metal complexes with this reagent . . . 176

D. V. S. JAIN and A. K. BANERJEE: On the structure of antimonates . . . 177

Y. K. GUPTA: Reduction of permanganate by iodide in a neutral medium . . . 179

F. KLANBERG and H. SPANDAU: Der Reaktionsdruck des Indium(I)sulfids . . . 180

M. C. PALCOS, R. RADICELLA and J. RODRIGUEZ: Search for an antimony isotope with a 30 days half-life . . . 182

D. ROBBINS: Formation of antimony orthophosphate, $SbPO_4$ . . . 183

G. TÓTH: Production of carrier-free I-131 from telluric acid by an adsorption method . . . 185

R. CHRISTELL, S. FORBERG and T. WESTERMARK: Some experiments on the use of the chelating ion exchanger Dowex A-1 in nuclear chemistry . . . 187

G. GORDON and H. TAUBE: The exchange reaction between uranyl ion and water in perchloric acid solution . . . 189

S. G. KOKALIS, K. JOHN, T. MOELLER and L. F. AUDRIETH: Hexa-*n*-alkylamino triphosphonitriles, $[NP(NHR)_2]_3$ . . . 191

Book Review:

"Théorie Fondamentale du Système Périodique des Eléments" (reviewed by C. A. COULSON) 194

Announcement:

Conference on Fission and Spallation Phenomena and their Application to Cosmic Rays . . . 195

NUMBERS 3/4

A. V. BELLIDO: New isotopes of emanation and francium: ^{223}Em, ^{224}Em and ^{224}Fr . . . 197

J. T. ALLAN, N. GETOFF, H. P. LEHMANN, K. E. NIXON, G. SCHOLES and M. SIMIC: Influence of carbon dioxide on the yields of hydrogen on irradiation of aqueous solutions of organic compounds with ^{60}Co γ-rays . . . 204

N. F. CURTIS: An infra-red spectroscopic investigation of the nature of the hydrogen halide in *trans*-dichloro *bis* ethylenediamine cobalt (III) chloride, hydrochloride dihydrate; and the bromide analogue . . . 208

VOL. 19 1961

W. B. Wilson: High-pressure high-temperature investigation of the uranium–oxygen system . . 212
P. H. L. Walter, J. Kleinberg and E. Griswold: The indium (I) bromide-indium (II) bromide system 223
W. D. Johnston and D. E. Sestrich: The MnTe–GeTe phase diagram 229
K. R. Hyde, P. L. Robinson, M. J. Waterman and J. M. Waters: Structural evidence on the beryl–sodium fluorosilicate reaction 237
W. W. Wendlandt and T. D. George: A differential thermal analysis study of the dehydration of the rare-earth (III) sulphate hydrates. The heats of dehydration 245
L. W. Holm, G. R. Choppin and D. Moy: Negative chelate complexes of lanthanide and actinide elements 251
B. J. Pullman and B. O. West: The reaction of trichloroiodomethane with some organometallic compounds of group VB elements 262
W. W. Wendlandt and G. R. Horton: The uranium(IV) complexes with 8-quinolinol and 5,7-dihalo-8-quinolinols 272
J. O. Wear, C. V. McNully and E. S. Amis: A study of transference and solvation phenomena—IV. Potassium chloride in water and water–ethanol solvents 278
R. W. Stoughton, A. J. Fry and J. E. Barney, II.: A study of thorium–iodate complexing in aqueous solutions 286
J. Krtil: Exchange properties of ammonium salts of 12-heteropolyacids—II. Separation of rubidium and caesium on ammonium phosphotungstate 298
J. C. Warf: The decomposition kinetics of copper hydride in the presence of electrolytes . . 304
T. V. Healy: Synergism in the solvent extractions of di-, tri- and tetra-valent metal ions—I. Synergic effects of different phosphate esters 314
T. V. Healy: Synergism in the solvent extractions of di-, tri- and tetra-valent metal ions—II. Synergic effects in so-called inert diluents 328
A. I. Popov and J. C. Marshall: Study of pure formic acid as solvent for acid-base equilibria 340
R. Stuart Tobias: The limitations of salt cryoscopy for the study of complex species in aqueous solution 348
Notes:
A. S. Kertes and M. Halpern: Hydrolytic and photolytic reactions in the system: water–hydrochloric acid–uranyl chloride–butyl phosphoric esters 359
Robert R. Holmes: Pressure measurements in the arsenic trichloride–chlorine system and the arsenic and antimony tribromide–bromine systems 363
Carl W. F. T. Pistorius: Polymorphism and melting in silver cyanide to 75,000 bars . . 367
R. A. Edge: The preparation and some properties of the intermediate product leading to the formation of red zinc oxide 370
C. M. Harris and E. D. McKenzie: Bivalent nickel complexes of 1,10-phenanthroline and 2,2′-bipyridyl 372
K. R. Applegate, E. M. Morimoto, M. Kahn and J. D. Knight: Redetermination of the half-life of bismuth (ThC) 375
John P. Buettner and Albert W. Jache: The ice region of the system $AgF.HF.H_2O$ at −15° 376
Letters to the Editors:
Henry Selig, Cedric L. Chernick and John G. Malm: The preparation and properties of TcF_6 377
John P. Oliver and L. G. Stevens: The preparation of trivinylgallium 378
B. A. Partridge: The thermodynamics properties of dilute solutions of UCl_3 in LiCl–KCl eutectic 379
B. J. Bowles: The half-life of Br^{83} 380
Book Reviews:
Emilio Segre "Annual Review of Nuclear Sciences" (reviewed by G. Wilkinson) . . . 382
D. P. Graddon "An Introduction to Co-ordination Chemistry" (reviewed by G. E. Coates) . 382

AUTHOR INDEX

(B denotes Book Review)

Allan, J. T. p. 204
Amis, E. S. p. 278
Applegate, K. R. p. 375
Audrieth, L. F. p. 191
Awad, A. M. p. 94
Banerjee, A. K. p. 177
Barney, II, J. E. p. 286
Bellido, A. V. p. 197
Bent, H. A. p. 43
Blasius, E. p. 115
Bowles, B. J. p. 380
Buettner, John P. p. 376
Bukietynska, K. p. 38
Cahill, J. A. p. 65
Canziani, F. p. 81
Cavasino, F. P. p. 74
Chackett, G. A. p. 13
Chackett, K. F. p. 13
Chernick, Cedric L. p. 377
Choppin, G. R. p. 251
Christell, R. p. 187
Ciampolini, M. p. 74
Coates, G. E. p. 382 (B)
Costea, T. p. 27
Coulson, C. A. p. 194 (B)
Curtis, N. F. p. 208
Deane, A. M. p. 142
Edge, R. A. p. 370
Felten, E. J. p. 61
Forberg, S. p. 187
Fry, A. J. p. 286
Furlani, A. p. 51
Furlani, C. p. 51
Galinos, A. G. p. 69
George, T. D. p. 245
Getoff, N. p. 204
Gordon, G. p. 189
Griswold, E. p. 223
Gupta, Y. K. p. 179
Hall, D. p. 16
Häller, I. B. p. 1
Halpern, M. p. 359
Harris, C. M. p. 372
Healy, T. V. pp. 314, 328
Holm, L. W. p. 251
Holmes, R. R. p. 363
Horton, G. R. p. 272
Hyde, K. R. p. 237
Jache, Albert W. p. 376
Jain, B. D. p. 176
Jain, D. V. S. p. 177
James, D. B. p. 133
Jezowska-Trzebiatowska, B. p. 38
John, K. p. 191
Johnston, W. D. p. 229
Kahn, M. p. 375
Kennedy, J. p. 142
Kertes, A. S. p. 359
Kirshenbaum, A. D. p. 65
Klanberg, F. p. 180
Kleinberg, J. p. 223
Knight, J. D. p. 375
Kokalis, S. G. p. 191
Krtil, J. p. 298
Lehmann, H. P. p. 204
Mackay, K. J. H. p. 171
Maggio, F. p. 74
de Maine, P. A. D. p. 156
Malatesta, P. p. 81
Malm, John G. p. 377
Marshall, J. C. p. 340
Macfarlane, R. D. p. 9
McKenzie, E. D. p. 372
McLure, I. p. 170
McNully, C. V. p. 278
Miller, J. M. p. 175
Minc, S. p. 101
Moeller, T. p. 191
Morimoto, E. M. p. 375
Moy, D. p. 251
Nixon, K. E. p. 204
Oliver, John P. p. 378
Palcos, M. C. p. 182
Partridge, B. A. p. 379
Pistorius, Carl W. F. T. p. 367
Polydoropoulos, C. N. p. 107
Popov, A. I. p. 340
Powell, J. E. p. 133
Preetz, W. p. 115
Pullman, B. J. p. 262
Radicella, R. p. 182
Robbins, D. p. 183
Robinson, P. L. p. 237
Rodriguez, J. p. 182
Rudstam, G. p. 1
Sacconi, L. p. 74
Schmitt, R. p. 115
Scholes, G. p. 204
Selig, Henry. p. 377
Sestrich, D. E. p. 229
Sherif, F. G. p. 94
Simic, M. p. 203
Singhal, S. P. p. 176
Small, H. p. 160
Smith, T. D. p. 170
Sobkowski, J. p. 101
Spandau, H. p. 180
Spedding, F. H. p. 133
Stevens, L. G. p. 378
Stoughton, R. W. p. 286
Sutin, N. p. 175
Taube, H. p. 189
Tobias, R. Stuart. p. 348
Tóth, G. p. 185
Walsh, E. J. p. 156
Walter, P. H. L. p. 223
Walton, G. N. p. 16
Warf, J. C. p. 304
Waterman, M. J. p. 237
Waters, J. M. p. 237
Wear, J. O. p. 278
Wendlandt, W. W. pp. 245, 272
West, B. O. p. 262
Westermark, T. p. 187
Wilkinson, G. p. 382 (B)
Williams, L. L. p. 175
Wilson, W. B. p. 212
Yannakopoulos, Th. p. 107

VOL
19
196

J. Inorg. Nucl. Chem., 1961, Vol. 19, pp. 1 to 8. Pergamon Press Ltd. Printed in Northern Ireland

RELATIVE YIELDS OF THE ISOMERIC PAIRS ^{69g}Zn–^{69m}Zn AND ^{52g}Mn–^{52m}Mn IN SOME SPALLATION REACTIONS INDUCED BY 20–153 MeV PROTONS

I. B. HÄLLER and G. RUDSTAM
The Gustaf Werner Institute for Nuclear Chemistry, University of Uppsala, Sweden

(*Received* 15 *July* 1960)

Abstract—The ratio between the spallation yield of the high-spin isomer and that of the low-spin isomer has been measured for the isomeric pairs ^{69g}Zn–^{69m}Zn and ^{52g}Mn–^{52m}Mn as a function of the irradiation energy and of the target used. For a given irradiation energy the yield ratio increases with increasing mass difference between target and isomer pair. A qualitative explanation of this effect is given.

VOL. 19 1961

1. INTRODUCTION

IN an earlier investigation one of the authors[1] measured the cross sections of the isomers ^{69g}Zn and ^{69m}Zn formed by spallation of arsenic with 49, 103 and 170 MeV protons. It was then found that the ratio between the yields of the high-spin isomeric state and the low-spin ground state decreases with increasing proton energy. This behaviour can be understood in terms of a simple model. At 49 MeV compound nucleus formation seems to be necessary in order to ensure sufficiently high excitation energy for the evaporation of seven nucleons. The average angular momentum of the compound nucleus would then be above $6\hbar$ according to calculations by MEADOWS *et al.*[2] Assuming that this momentum stays practically unchanged by the subsequent particle evaporation, the final, excited spallation product should also have a high angular momentum. The energy degradation of this nucleus by a γ-cascade is believed not to change the spin appreciably.[3] Therefore, the high-spin isomer should be favoured as found experimentally.

If the impinging proton is more energetic, on the other hand, only a small part of its energy need be deposited in the nucleus in order to make possible the production of ^{69}Zn. Most of the energy would then be carried away by the prompt cascade particles resulting from the nucleon cascade developed in the nucleus.[4] A Monte Carlo calculation of such cascades indicates that the residual nucleus in this case obtains a fairly low angular momentum.[1] At 170 MeV an average angular momentum of $3\hbar$ was found to be imparted to the residual nucleus by the cascade process. This could explain the experimental result that the low-spin isomer is formed in relatively larger yield when the irradiation energy is increased.

Another interesting result of the Monte Carlo calculation is that a correlation between angular momentum and excitation energy seems to exist. For a given irradiation energy, the angular momentum picked up by the residual nucleus increases with increasing excitation energy.

The considerations given above can be generalized as follows:

(1) The favoured spin state of an isomeric pair is that having its spin closest to the

[1] G. RUDSTAM, Inaugural dissertation, Uppsala (1956).
[2] J. W. MEADOWS, R. M. DIAMOND and R. A. SHARP, *Phys. Rev.* **102**, 190 (1956).
[3] L. KATZ, L. PEASE and H. MOODY, *Canad. J. Phys.* **30**, 476 (1952).
[4] R. SERBER, *Phys. Rev.* **74**, 1269 (1947).

angular momentum of the residual nucleus after the nucleon cascade (the compound nucleus in case of compound formation).

(2) The angular momentum of the residual nucleus is determined by a combination of the intrinsic spin of the target nucleus and the angular momentum picked up in the reaction itself. The latter part is largest when a compound nucleus is formed. When a cascade is developed the angular momentum is correlated with the excitation energy of the residual nucleus: higher excitation energy corresponds to higher average angular momentum.

The momentum distribution of the residual nuclei is certainly very wide and will be further broadened by the evaporation of nucleons.

Certain conclusions can now be drawn regarding the yield ratio high-spin isomer/low-spin isomer (irradiation energy of the order of 40–50 MeV or higher):

(a) For a given irradiation energy the yield ratio should increase with increasing complexity of the reactions leading to the formation of the isomers because more complex reactions require higher excitation energy, which is connected with higher angular momentum, of the residual nucleus. Thus, as a rule, the ratio should increase with increasing mass difference between target and isomer pair. This would hold best when all the targets have the same spin.

(b) The behaviour of the yield ratio as a function of the irradiation energy for a given target is more difficult to predict. For reasonably complicated reactions the yield ratio should decrease with increasing irradiation energy just as for the zinc isomers formed from arsenic. For very simple reactions, where only low excitation energies are required, the cascade process contributes little to the angular momentum of the residual nucleus. The effect of raising the irradiation energy might be very small.

Since these rules are based on the momentum picked up by the residual nuclei in the cascade reaction they will hold best when the target spin is low. A high spin of the target would tend to obscure the effects.

In order to test the ideas expressed above the earlier work on the zinc isomers was extended. The elements zinc, gallium, arsenic, bromine and rubidium were irradiated with protons of average energy from 20 to 153 MeV. A second isomeric pair, ^{52g}Mn–^{52m}Mn, was also studied. In this case manganese, cobalt, copper and gallium targets were used, and the proton energy was varied as before.

The zinc isomers have been studied by ZHEREBTSOVA *et al.*[5] using low energy neutrons and deuterons for the bombardments. The manganese isomers have not been systematically investigated, but a few scattered yield ratios can be found from different spallation studies.

The spin assignments of the nuclides of interest here (as given by STROMINGER *et al.*[6]) are tabulated in Table 1.

2. EXPERIMENTAL TECHNIQUE

2.1. *Irradiations*

All bombardments were carried out in the circulating beam of the synchro-cyclotron at the Gustaf Werner Institute for Nuclear Chemistry. The targets were irradiated with protons of mean energy 20, 49, 75, 103, 133, and 153 MeV. Data for the different bombardments are given in Table 2.

[5] K. J. ZHEREBTSOVA, T. P. MAKAROVA, IU. A. NEMILOV and B. L. FUNSHTEIN, *Soviet Phys.* JETP **8**, 947 (1959).
[6] D. STROMINGER, J. M. HOLLANDER and G. T. SEABORG, *Revs. Mod. Phys.* **30**, 585 (1958).

Several target elements were used, namely manganese, cobalt, copper, zinc, gallium, arsenic, bromine and rubidium. The target materials were of high purity and contained no impurity likely to interfere with the results.

TABLE 1.—SPIN ASSIGNMENTS

Nuclide	Abundance in natural element (%)	Spin
^{52g}Mn		6
^{52m}Mn		2
^{69g}Zn		$\frac{1}{2}$
^{69m}Zn		$\frac{9}{2}$
^{55}Mn	100	$\frac{5}{2}$
^{59}Co	100	$\frac{7}{2}$
^{63}Cu	69·0	$\frac{3}{2}$
^{65}Cu	31·0	$\frac{3}{2}$
^{69}Ga	60·1	$\frac{3}{2}$
^{71}Ga	39·9	$\frac{3}{2}$
^{70}Zn	0·63	0
^{79}Br	50·6	$\frac{3}{2}$
^{81}Br	49·4	$\frac{3}{2}$
^{85}Rb	72·2	$\frac{5}{2}$
^{87}Rb	27·8	$\frac{3}{2}$
^{89}Y	100	$\frac{1}{2}$

TABLE 2.—IRRADIATION DATA

Target element	Target material	Mean irradiation energy (MeV)	Monitor	Elements studied
Mn	Metal pieces	20, 49, 75, 103, 133, 153		Mn
Co	Metal powder	49, 103, 133	Aluminium and magnesium powder	Na, Mn, Fe
Cu	Metal foil	153	Aluminium foil	Na, Mn, Fe
Zn	Metal foil	20, 49, 75, 103, 133, 153		Zn
Ga	Powdered gallium oxide	153	Aluminium powder	Na, Mn, Fe
Ga	Powdered gallium oxide	20, 49, 75, 103, 153		Zn
As	Metal powder	75, 133		Zn
Br	Powdered potassium bromide	153		Zn
Rb	Powdered rubidium chloride	153		Zn

The main problem in this work was to determine relative yields. Absolute yields were also obtained in some cases, however, by comparing the yields with the yield of ^{24}Na formed from aluminium or magnesium. Depending on the form of the target a stack of foils or a mixture of powders was used.[1]

2.2. *Preparation of samples*

a. *Zinc samples*. The isomers of interest, ^{69m}Zn and ^{69g}Zn, have the half-lives 13·9 hr and 58·5

min, respectively. Two other zinc isotopes with similar half-lives, namely ^{62}Zn (9·3 hr) and ^{63}Zn (38 min) are also formed, in certain cases in much higher yields than the ^{69}Zn isomeric pair. To avoid difficulties in resolving the decay curves the zinc samples were prepared by electromagnetic isotope separation[7] except when arsenic was used as target. In the latter case the contamination was not serious.

When natural zinc was used as target it was brought into the isotope separator immediately after the irradiation, and the isotope ^{69}Zn was collected on a strip of 0·01 mm aluminium. The strip was then mounted for activity measurement. With gallium, bromine and rubidium as target materials, some zinc carrier was added to the target solution. The zinc was separated and purified by a procedure involving extraction of gallium chloride into ether, precipitation of the sulphides of copper, germanium, arsenic and selenium from acid solutions, and precipitation of zinc as zinc mercuric thiocyanate. The precipitate was dissolved, the mercury removed, and zinc was precipitated as the sulphide from ammoniacal solution. Finally, the zinc sulphide was converted to zinc chloride and inserted into the isotope separator. The isotope ^{69}Zn was collected on a strip of aluminium as before.

With arsenic as target the chemical procedure described by Rudstam[1] was used. The chemical yield of zinc was determined by a micro-titration method with EDTA.[8]

b. *Manganese samples.* The main difficulty in the manganese experiment is the short half-life (20·1 min) of the isomeric state ^{52m}Mn. Besides, the isotope ^{51}Mn has a half-life of 45·0 min.[1] A good determination of the yield of ^{52m}Mn can only be carried out if a fast chemical separation is performed. A separation method for manganese was worked out based on extraction with diethyl dithiocarbamate into carbon tetrachloride from solutions at pH 8·5 containing tartrate and cyanide to form complex with cobalt and nickel. After back-extraction into 1N hydrochloric acid, iron and vanadium were removed with cupferron and chloroform. The water phase was evaporated to dryness, and the residue was dissolved into a small volume of dilute nitric acid. From this solution 50 λ samples were pipetted onto a 0·01 mm aluminium foil, evaporated to dryness, and mounted for activity measurement. The chemical yield was determined spectrophotometrically.[9]

c. *Iron and sodium samples.* The yield of ^{52m}Mn has to be corrected for the growing-in from the mother nuclide ^{52}Fe. The cross-section of this nuclide was therefore determined in some bombardments. The separation methods for iron and sodium as well as the methods of analysis were those given by RUDSTAM.[1]

2.3. *Determination of spallation yields*

The activity measurements were carried out with G.M.-counters and flow-proportional counters. The counting rates were converted to disintegration rates using the correction factors given by RUDSTAM[1] and PAPPAS[10]. Corrections were also carried out for fluctuations in the beam intensity during the irradiation.

The decay schemes accepted for the calculations were taken from DUFFIELD and LANGE[11] and from SMITH[12] for the zinc isomers, from JULIANO *et al.*,[13] KONIJN *et al.*[14] and from ARBMAN and SVARTHOLM[15] for the iron and manganese isotopes, and, finally, from DANIEL[16] for ^{24}Na.

The decay curves of the managnese samples were resolved using a "Biller plot"[17] after previous subtraction of the contribution from the isotopes ^{52g}Mn, ^{54}Mn, and ^{56}Mn. The half-life of ^{51}Mn was taken to be 45·0 min. The method of least squares was used to evaluate the decay rate of ^{52m}Mn.

[7] G. ANDERSSON, *Phil. Mag.* **45**, 621 (1954).
[8] G. SCHWARZENBACH, *Die komplexometrische Titration.* Stuttgart (1956).
[9] H. SPECKER, *Z. Anal. Chem.* **143**, 425 (1954).
[10] A. C. PAPPAS, Technical Report No. 63, Laboratory for Nuclear Science, Massachusetts Institute of Technology (1953).
[11] R. B. DUFFIELD and L. M. LANGE, *Phys. Rev.* **89**, 854 (1953).
[12] A. B. SMITH, *Diss. Abstr.* **13**, 849 (1953).
[13] J. O. JULIANO, C. W. KOCHER, T. D. NAINAN and A. MITCHELL, *Phys. Rev.* **113**, 602 (1959).
[14] J. KONIJN, B. VAN NOOIJEN, H. C. HAGEDOORN, *Physica* **24**, 377 (1958).
[15] E. ARBMAN and N. SVARTHOLM, *Arkiv Fysik* **10**, No. 1 (1956).
[16] H. DANIEL, *Nucl. Phys.* **8**, 191 (1958).
[17] W. F. BILLER, Report UCRL–2067 (1953).

TABLE 3.—YIELD RATIOS OF THE ZINC ISOMERS

Target	Irradiation Energy (MeV)	$\sigma(^{69m}\text{Zn})/\sigma(^{69g}\text{Zn})$
Zn	20 ± 6	0·77 ± 0·05
Zn	49 ± 7	0·77 ± 0·05
Zn	75 ± 8	0·67 ± 0·03
Zn	103 ± 8	0·74 ± 0·08
Zn	133 ± 8	1·06 ± 0·07
Zn	153 ± 8	0·70 ± 0·04
Ga	20 ± 6	1·11 ± 0·10
Ga	49 ± 7	1·49 ± 0·13
Ga	75 ± 8	1·71 ± 0·17
Ga	103 ± 8	1·42 ± 0·24
Ga	153 ± 8	1·31 ± 0·21
As	75 ± 8	1·90 ± 0·10
As	133 ± 8	0·91 ± 0·09
Br	153 ± 8	2·67 ± 0·22
Rb	153 ± 8	5·9 ± 1·1

VOL. 19 1961

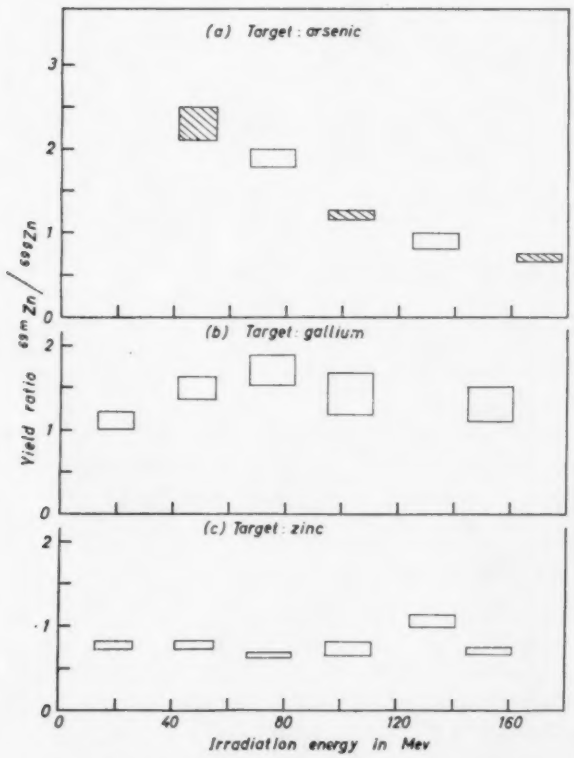

FIG. 1.—Yield ratio ^{69m}Zn/^{69g}Zn vs. irradiation energy.
Unfilled rectangles: this work.
Hatched rectangles: from reference (1).

The presence of a long-lived isomeric state decaying to the ground state will affect the counting rate of the state. This is important for the zinc isomers, and a correction was applied. The isomeric state ^{52m}Mn does not decay to the ground state but directly to ^{52}Cr.

3. EXPERIMENTAL RESULTS

3.1. *The isomeric pair* ^{69g}Zn–^{69m}Zn

The yield ratios ^{69m}Zn/^{69g}Zn are given in Table 3.

Figs. 1 and 2 illustrate graphically the variation of the yield ratio of the zinc isomers with irradiation energy (Fig. 1) and with the mass difference between the

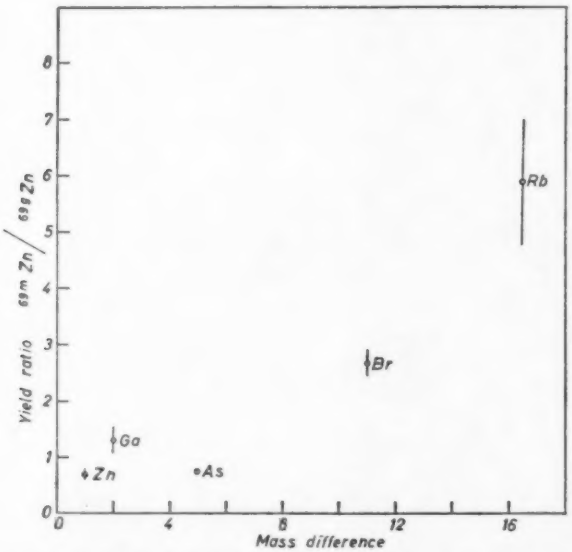

FIG. 2.—Yield ratio ^{69m}Zn/^{69g}Zn vs. the mass difference between target and isomer pair for mean irradiation energy 153 MeV. The target used is indicated in the figure. The yield ratio corresponding to arsenic was obtained by interpolation in Fig. 1.

target and the isomer pair (Fig. 2). Some results from reference (1) are also included.

A correction for growing-in from the mother nuclide cannot be performed because this nuclide is unknown. Yield estimates show, however, that such a correction would be very small (1).

3.2. *The isomeric pair* ^{52g}Mn–^{52m}Mn

The experimental data are collected in Table 4.

The absolute cross-sections were obtained using the formation cross section of ^{24}Na from aluminium determined by HICKS *et al.*[18] and the corresponding cross-section with magnesium as target calculated from the results by MEADOWS and HOLT[19] and CRANDALL *et al.*[20]

[18] H. G. HICKS, P. C. STEVENSON and W. E. NERVIK, *Phys. Rev.* **102**, 1390 (1956).
[19] J. W. MEADOWS and R. B. HOLT, *Phys. Rev.* **83**, 47 (1951).
[20] W. E. CRANDALL, G. P. MILLBURN, R. V. PYLE and W. BIRNBAUM, *Phys. Rev.* **101**, 329 (1956).

The yield ratio ^{52g}Mn/^{52m}Mn is plotted vs. irradiation energy in Fig. 3.

As an average of several determinations the half-life of ^{52m}Mn was found to be 19·5 ± 0·3 min.

TABLE 4.—MANGANESE CROSS-SECTIONS

Target	Irradiation energy in MeV	$\sigma(^{52g}\text{Mn})$ / $\sigma(^{52m}\text{Mn})$	$\sigma(^{52g}\text{Mn})$ (mbarns)	$\sigma(^{52m}\text{Mn})$ (mbarns)	$\sigma(^{52}\text{Fe})$ (mbarns)
Mn	49 ± 7	1·69 ± 0·11			
Mn	75 ± 8	1·39 ± 0·17			
Mn	103 ± 8	1·58 ± 0·14			
Mn	133 ± 8	1·40 ± 0·12			
Mn	153 ± 8	1·84 ± 0·22			
Co	49 ± 7	2·6 ± 0·6	2·0 ± 0·3	0·8 ± 0·2	0·015 ± 0·002
Co	103 ± 8	2·6 ± 0·4			
Co	133 ± 8	2·4 ± 0·2	10 ± 2	4·2 ± 0·7	0·50 ± 0·10
Cu	153 ± 8	3·0 ± 1·0	2·6 ± 0·5	0·9 ± 0·3	0·092 ± 0·013
Ga	153 ± 8	9 ± 5	0·27 ± 0·04	0·031 ± 0·016	0·039 ± 0·005

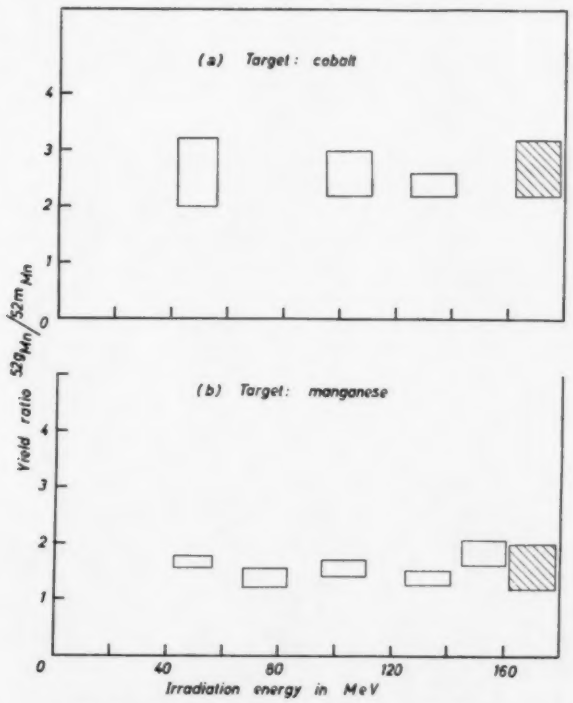

FIG. 3.—Yield ratio ^{52g}Mn/^{52m}Mn vs. irradiation energy.
Unfilled rectangles: this work.
Hatched rectangles: from reference (1).

4. DISCUSSION

The yield ratios of the zinc isomers agree rather well with the simple picture given in the Introduction. The low-spin isomer is favoured in the simple reaction ^{70}Zn

(p,pn)^{69}Zn, and the energy-dependence is small. In the slightly more complicated reaction ^{71}Ga(p,$2pn$)^{69}Zn the high-spin state is the more favoured one, the energy dependence still being small. In the reaction ^{75}As(p,$4p3n$)^{69}Zn there is a marked energy dependence of the results with decreasing yield ratio for increasing irradiation energy. Finally, Fig. 2 shows a fairly strong dependence on the complexity of the reactions.

The ratio between the yields of the manganese isomers is almost independent of irradiation energy. In the cobalt irradiations a decrease of the ratio between the yield of the high-spin isomer and that of the low-spin isomer with increasing irradiation energy might have been expected. As already pointed out in the Introduction, however, the high intrinsic spin of the target nucleus ($\frac{7}{2}$) would tend to wash out the dependence on irradiation energy.

The results given in Table 4 indicate that, for a given irradiation energy (153 MeV), the yield ratio high-spin isomer/low-spin isomer increases with increasing complexity of the reactions. In this respect the tendency is the same as for the zinc isomers.

It may be pointed out that the results by HÄLLER and ANDERSSON[21] on the isomer pair ^{80g}Br–^{80m}Br are in agreement with the results of the present investigation. With bromine as target (reaction ^{81}Br(p,pn)^{80}Br) the isomeric state is slightly favoured, and the energy dependence of the yield ratio is very small. With yttrium as target (reaction: ^{89}Y(p,$5p5n$)^{80}Br) the high-spin state is strongly favoured, and the yield ratio decreases with increasing irradiation energy.

Acknowledgements—We are grateful to Professor T. SVEDBERG for stimulating working conditions and to Dr. G. ANDERSSON for valuable discussions.

Furthermore, we want to thank Mr. R. RINGH for performing the mass separations and Mr. Å. SVANHEDEN and the cyclotron staff for carrying out the bombardments.

[21] I. B. HÄLLER and G. ANDERSSON, *J. Inorg. Nucl. Chem.* To be published.

J. Inorg. Nucl. Chem., 1961, Vol. 19, pp. 9 to 12. Pergamon Press Ltd. Printed in Northern Ireland

DYSPROSIUM-154, A LONG-LIVED α-EMITTER

R. D. MACFARLANE
Lawrence Radiation Laboratory University of California, Berkeley, California

(*Received* 16 *September* 1960; *in revised form* 27 *October* 1960)

Abstract—Gadolinium oxide, enriched in ^{154}Gd, was bombarded with 48 MeV α-particles to form dysprosium isotopes. α-Pulse-analysis of the chemically separated dysprosium resulted in the observation of a new weak α-activity of 2·85 ± 0·05 MeV energy. This activity was assigned to ^{154}Dy on the basis of a rough excitation function and consideration of α-decay systematics of the neighbouring dysprosium isotopes.

The α-half-life was calculated as approximately 1×10^6 years by estimating the amount of ^{154}Dy produced and comparing it with the α-count rate.

A lower limit of 10 years for the β-decay half life was established on the basis of the absence of the prominent γ-radiation of ^{154}Tb in the photon spectrum.

VOL.
19
1961

THE observation of α-activity in the rare earth elements is the result of an enhancement of α-decay energy due to the decrease in neutron binding energy of nuclides containing between eighty-four and eighty-eight neutrons.

In 1953, RASMUSSEN *et al.* reported results on α-emitters of europium, gadolinium, terbium, and dysprosium.[1] The dysprosium alpha emitters were later studied in greater detail by TOTH and RASMUSSEN, who identified the α-activities of ^{150}Dy, ^{151}Dy, ^{152}Dy, ^{153}Dy and ^{154}Dy.[2,3] The α-activity attributed to ^{154}Dy decayed with a half-life of 13 hr and possessed an α-energy of 3·35 MeV. From the observed α-counting rate, it appeared that the α:β branching ratio was indeed very small. However, no evidence for a β-decay branch was observed: neither a 13 hr decay component in the γ-spectrum nor the appearance of the daughter, ^{154}Tb, in the γ-spectrum. Toth postulated that this α-activity was due to an isomer of ^{154}Dy and that the ground state actually was long-lived.[4]

The purpose of this investigation was to test, in part, this hypothesis by searching for a long-lived α-emitting ^{154}Dy.

EXPERIMENTAL DETAILS

Two samples of 3 mg each of gadolinium oxide, enriched in ^{154}Gd to 33 per cent, were irradiated in a stacked-foil arrangement with 30μAhr of α-particles in the Berkeley 60 in. cyclotron. The first sample was bombarded at 48 MeV, and the second sample at 37 MeV.

Separation of dysprosium from the target material was accomplished by a cation-exchange method described elsewhere.[5] The eluting agent was 0·4 M α-hydroxy isobutyric acid buffered to a pH of 3·95.

After the rare earth separation, the dysprosium fraction was evaporated to dryness and the residue dissolved in concentrated hydrochloric acid. The solution was then passed through a Dowex-1 × 10 anion-exchange column in order to remove some of the inert material which had passed through the cation exchange column (mostly iron). The eluate was then taken to dryness and treated with aqua regia to remove most of the organic material present.

[1] J. O. RASMUSSEN, S. G. THOMPSON and A. GHIORSO, *Phys. Rev.* **89**, 33 (1953).
[2] K. S. TOTH and J. O. RASMUSSEN, *Phys. Rev.* **109**, 121 (1958).
[3] K. S. TOTH and J. O. RASMUSSEN, *J. Inorg. Nucl. Chem.* **10**, 198 (1959).
[4] K. S. TOTH, Report, UCRL-8192 (1958).
[5] S. G. THOMPSON, B. G. HARVEY, G. R. CHOPPIN and G. T. SEABORG, *J. Amer. Chem. Soc.* **76**, 6229 (1954).

Finally, the residue was taken up in a couple of drops of concentrated nitric acid and transferred to a 1 in. diameter platinum disk. The disk was heated to dryness and ignited to red heat. This procedure resulted in the formation of an essentially weightless deposit suitable for α-pulse-analysis. α-spectra were obtained by using a Frisch-grid argon–methane flow-type ion chamber. The spectrum was displayed on a 100-channel pulse-height analyser.*

Energy calibration was provided by ^{147}Sm (2·23 MeV)[6] and ^{148}Gd (3·16 MeV).[1]

TABLE 1.—ISOTOPIC ABUNDANCE OF TARGET GADOLINIUM

	152	154	155	156	157	158	160
Enriched ^{154}Gd	0·32	33·19	38·57	15·92	5·49	4·50	2·05
Natural Gd	0·20	2·15	14·73	20·47	15·68	24·87	21·90

RESULTS

1. α-*Decay properties*

Fig. 1 shows the α-spectrum of the dysprosium fraction from the 48 MeV bombardment taken three days after the end of the bombardment. A weak α-group of 2·85 MeV energy with an intensity of ~0·07 counts/min was observed. This activity was not observed in the sample from the 37 MeV bombardment.

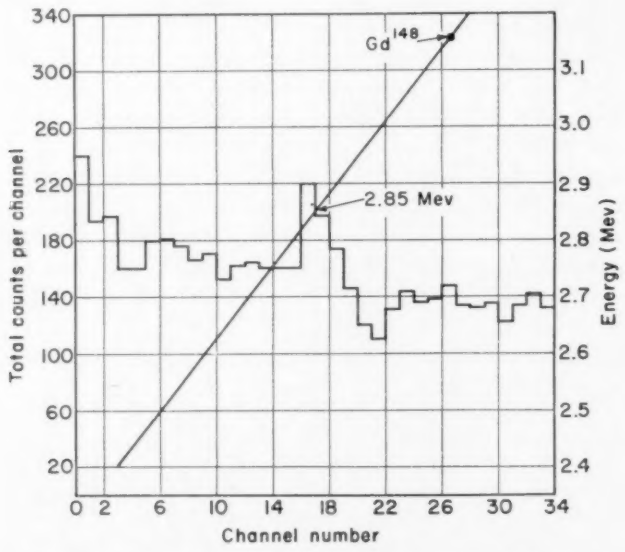

FIG. 1.—α-particle spectrum of ^{154}Dy counting time: 4269 min.

Assuming that the α-activity was due to ^{154}Dy, produced by an $(\alpha,4n)$ reaction on ^{154}Gd, the total number of atoms of ^{154}Dy produced was calculated by using an estimate of 1 barn for the cross section.[7]

From these data, the alpha half-life of ^{154}Dy was determined to be 1×10^6 years, uncertain by a factor of three.

* Manufactured by Pacific Electro-Nuclear Co., Culver City, California.

[6] R. D. MACFARLANE and T. P. KOHMAN, *Phys. Rev.* In press.

[7] E. L. KELLY and E. SEGRÈ, *Phys. Rev.* **75**, 999 (1949).

2. *Search for β-decay branch*

The α-spectrum was recorded at different intervals over a period of 10 months. As shown in Fig. 2, no decrease in the alpha-particle counting rate was observed.

Next, the γ-spectrum was studied 10 months after bombardment in order to see whether the β-decay daughter, 19 hr ^{154}Tb, was present. It is characterized by a strong 123 KeV γ-radiation.[8] The only peaks present, however, were those due to ^{153}Gd, arising initially from ^{153}Dy. The absence of the 123 keV γ-radiation of ^{154}Tb, was used to establish a lower limit for the β-half-life of 10 years. (It was estimated

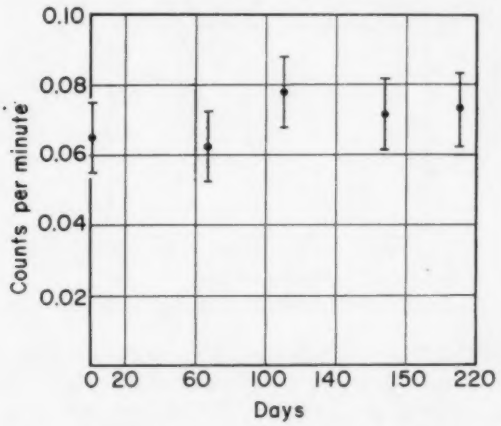

FIG. 2.—Decay rate of ^{154}Dy α-activity over a period of 10 months.

that the 123 keV gamma was present in at least 20 per cent abundance in the electron-capture decay of ^{154}Tb.)

3. *Mass assignment*

The assignment of the 2·85 MeV α-activity to ^{154}Dy was based on the following argument. That the activity was observed at a bombarding energy of 48 MeV and not at 37 MeV indicates that the activity was produced by an $(\alpha,4n)$ but not an $(\alpha,3n)$ reaction (very little $(\alpha,4n)$ product is formed at 37 MeV in the rare earth region). Of all the gadolinium isotopes present in the target material (see Table 1) only ^{152}Dy, ^{154}Dy and ^{160}Dy could be formed by an $(\alpha,4n)$ and not an $(\alpha,3n)$ reaction. ^{160}Dy was eliminated because it is a naturally occurring isotope with a very long α-half life. ^{152}Dy was also eliminated because its α-decay properties have already been characterized and are different from those observed in this work.[2] This left ^{154}Dy as the only other possibility.

From the trend of the α-decay energies of the other dysprosium isotopes, it appeared reasonable the ^{154}Dy should have the observed α-particle energy (see Fig. 3).

DISCUSSION

The discovery of long-lived ^{154}Dy provides an answer to the puzzling result of TOTH, who was unable to observe the growth of ^{154}Tb in samples known to contain ^{154}Dy.[4] It also relieves somewhat what appears to be an abnormally large difference

[8] J. W. MIHELICH, B. HARMATZ and T. H. HANDLEY, *Phys. Rev.* **108**, 989 (1957).

in alpha-decay energy between ^{154}Dy and ^{156}Dy compared with what has been observed from mass data for ^{152}Gd–^{154}Gd and ^{150}Sm–^{152}Sm.[9] (An upper limit of 2·0 MeV for the α-decay energy of ^{156}Dy has been established on the basis of the negative results obtained by Riezler and Kauw for natural dysprosium.[10])

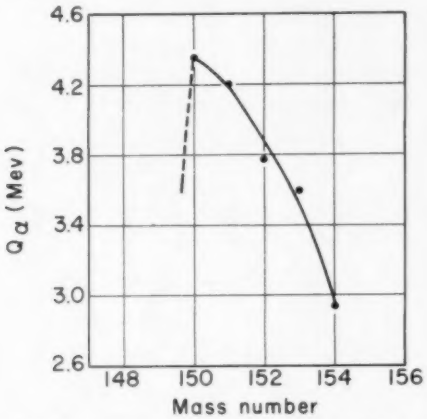

FIG. 3.—Variation of α-decay energy with mass number for the dysprosium isotopes.

The origin of the 13 hr α-emitter reported by TOTH and RASMUSSEN is still a puzzle. Preliminary results confirm the apparent existence of this alpha activity, but there is some indication that it is not due to ^{154}Dy.[11] Further work is in progress on this problem.

Acknowledgements—The assistance of the crew of the 60 in. cyclotron and the health chemistry group is gratefully acknowledged.

This work was performed under the auspices of the United States Atomic Energy Commission.

[9] W. H. JOHNSON, JR. and V. B. BHANOT, *Phys. Rev.* **107**, 1669 (1957).
[10] W. RIEZLER and G. KAUW, *Z. Naturforsch.* **13** A, 904 (1958).
[11] R. D. MACFARLANE, (Lawrence Radiation Laboratory) Unpublished data (1960).

J. Inorg. Nucl. Chem., 1961, Vol. 19, pp. 13 to 15. Pergamon Press Ltd. Printed in Northern Ireland

LIGHT ISOTOPES OF RUBIDIUM FORMED IN ^{3}He BOMBARDMENTS OF BROMINE

K. F. CHACKETT and G. A. CHACKETT
Physics Department, University of Birmingham

(*Received* 9 *September* 1960)

Abstract—A light isotope of rubidium ^{79}Rb, first noted by CHAMINADE *et al.*[1] in products obtained from copper bombarded by oxygen ions, has been prepared along with ^{81}Rb and ^{82}Rb by bombarding bromine with ^{3}He ions at 27 MeV. The mass assignment made by the earlier workers has been fully confirmed by a genetic experiment and characterization of the ^{79}Kr daughter. The half-life is 20·9 ± 0·8 min.

VOL. 19 1961

BECAUSE of its low binding energy the ^{3}He nucleus provides an interesting projectile with which to form neutron deficient isotopes. Thus if one considers the equivalent reactions

$$X + {}^3He \rightarrow Y + 3n + Q_1$$

$$X + {}^4He \rightarrow Y + 4n + Q_2$$

it is clear that

$$Q_1 - Q_2 = M_{^3He} + M_n - M_{^4He}$$
$$= 21{\cdot}4 \text{ MeV}.$$

This means that with the ^{3}He-ion energy available at the Nuffield 60 in. cyclotron (27·5 MeV) reactions such as (^{3}He, 3n) and (^{3}He, 4n) may be energetically possible, the the products being isotopes which are hardly obtainable with ^{4}He ions even at the 37 MeV available. As an example we have bombarded bromine in the form of lithium bromide and identified ^{79}Rb as one of the principal products.

EXPERIMENTAL

Lithium bromide was synthesized from pure lithium carbonate and hydrobromic acid, and then bombarded for periods ranging from a few minutes to half an hour in a 0·001 in. copper envelope in the external ^{3}He beam. Currents of up to 5 μA were used. After bombardment the lithium bromide crystals were dissolved in water containing potassium carrier as chloride, insoluble material being centrifuged out and rejected. Sources for counting experiments, carrying the rubidium activity, were then prepared by repeated recrystallization of potassium perchlorate from 50 per cent alcoholic solution. Activities in bromine were also investigated after isolation of silver bromide from the solution after removal of the potassium. Active samples were examined by end-window G-M counting and by scintillation spectrometry using a $1\frac{1}{2} \times 1$ in. sodium iodide (Tl) crystal.

Milking experiments were performed by dissolving an active sample containing Rb and bubbling hydrogen gas through it. Krypton was then stripped from the hydrogen stream on to charcoal in U-tubes cooled to −190°C, and subsequently desorbed *in vacuo*. Separated krypton samples, sealed off in thin-walled glass bulbs, were examined for half-life by G-M counting and for γ-ray spectrometry with the crystal. In one experiment krypton samples milked at exactly 20 min intervals were collected in six separate U-tubes; each sample was purified over metallic calcium at 700°C and then transferred quantitatively with an argon–alcohol mixture to a gas counter. The apparatus used in this experiment is shown diagrammatically in Fig. 1. The last krypton sample to be obtained was counted first, giving 10,280 counts/min at the time of counting when all corrections were applied. Samples collected earlier than this one were expected to be more active by a factor of about two and were therefore

[1] R. CHAMINADE, M. CROS, I. GRATOT and M. LE PAPE, *Nucl. Phys.* **2**, 634 (1957).

counted after a suitable delay and by transferring only a small known fraction of each to the G-M tube. Division of the active gas was achieved by using the gas space defined by the taps T_1 T_2 T_3 and T_4, and the bulb of the Toepler pump G as a gas pipette. The counting efficiency of the G-M chamber was also changed by counting with the mercury in G either at the top of the bulb or at a fixed level in the stem below it. In this way effective pipetting ratios of 3·17 and 13·9 were available, their exact values being determined by a subsidiary experiment using two active samples (Nos. 4 and 5) which were each counted by two pipetting techniques. By this means all the counting rates which were obtained lay between 2,430 and 10,280 count/min so that errors due to uncertainty of background and

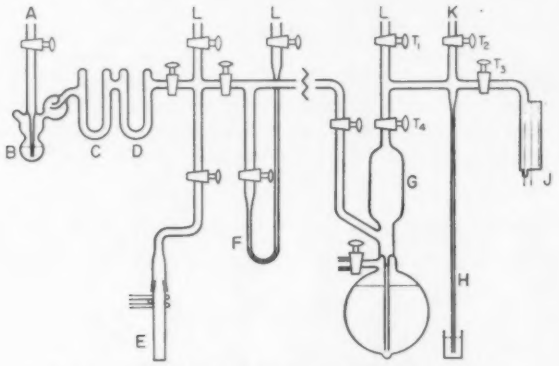

FIG. 1.—Apparatus for milking ^{79}Kr from parent ^{79}Rb.
A. Hydrogen inlet.
B. Active rubidium solution in 2 ml of water.
C. U-tube containing 10 g of KOH pellets.
D. U-tube containing 10 g of silica gel.
E. Stainless steel tube, with water-cooled standard-taper joint, containing 20 g calcium.
F. U-tube containing 0·1 g charcoal. In the actual apparatus there were six such U-tubes arranged closely enough to permit simultaneous cooling in liquid nitrogen.
G. Toepler pump, capacity 250 ml.
H. Manometer.
J. G-M tube (Twentieth Century Electronics).
K. Inlet for argon-alcohol mixture.
L. Vacuum connections.

counter dead time are inappreciable. With such high counting rates statistical errors were all less than 0·5 per cent (standard deviation).

In another milking-type experiment air was bubbled rapidly for a few minutes through a solution containing an active rubidium fraction. The γ-rays emitted from the solution were examined after stopping the gas flow to demonstrate the re-growth of fresh krypton activity.

RESULTS

Decay curves of the rubidium samples under an end-window G-M tube showed components of 20 min, about 1 hr, about 5·5 hr and of 35 hr. Of these the 1 hr component was very weak and could have been due to ^{81m}Rb although our half-life value would be nearly twice the period found by DOGGETT[2]. γ-ray spectrometry showed γ-rays of about 0·1 and 0·15 MeV which disappeared in the course of a few hours; in particular the 0·15 MeV line appeared to be associated with the 20 min period. Also present were several γ-rays of higher energy which clearly belonged to the well-known ^{81}Rb and ^{82}Rb (4·7 and 6·5 hr respectively. The presence of the 81 mass chain was confirmed also by the short-period milking experiment outlined

[3] W. O. DOGGETT, UCRL—3438 (1956) Unpublished.

above, in which the re-growth of the 0·19 MeV γ-ray of ^{81}Kr was observed with a growth period of 13 $\pm$ 1 sec.

The activity of the long-lived krypton isotope, separated after a 15 min growth from initially pure rubidium, showed a period of 34 hr, measured with an end-window G-M tube, and gave a γ-spectrum wholly consistent with ^{79}Kr. Complete confirmation that this isotope is the daughter of 20 min ^{79}Rb follows from the milking experiment in which six active gas fractions were obtained at 20 min intervals. The numerical results obtained are collected in Table 1.

TABLE 1.—MILKING OF ^{79}Kr FROM SEPARATED ^{79}Rb†

Sample	Counting rate (cpm)	Time and date	Time elapsed since milking (hr)	Pipetting factor	Counting rate at end of 20 min milking period.	Ratio
1	8,600	11.30 30/7	69·17	13·9	489,300	2·14
2	6,050	15.00 29/7	49·00	13·9	228,300	1·98
3	3,290	12.00 29/7	46·33	13·9	114,900	1·92
4	2,430	17.45 28/7	28·33	13·9	59,900	1·84
5	5,864	16.30 28/7	27·5	3·17	32,560	2·01
6	10,280	11.00 28/7	22·33	1·0	16,200	
					Mean ratio	1·98

† Bombardment time 11.30–12.00 on 27/7/1960. Milking of ^{79}Kr from separated ^{79}Rb commenced 12.20.

The mean ratio of the successive corrected activities is a little under two, indicating a half-life a little longer than the 20 min milking interval. A least-squares fit gave a best value of 20·7 min with a standard deviation of 0·5 min. If we take into account the likely errors in the pipetting ratio measurement (which however affect only samples 5 and 6) and the fact that our determination of the ^{79}Kr half-life (34 hr) is a little less than the accepted value (34·5 hr) we arrive at a final estimate of 20·9 $\pm$ 0·8.

A rough calculation of the thick-target yield of the Rb isotope gives about 400 μc/μA hr, or 4 μc/μA hr of the Kr daughter. The true figure may be considerably more than this because it is likely that only a small fraction of the measured beam current was incident on the actual target.

CONCLUSIONS

^{79}Rb formed by the (^{3}He, 3n) reaction on ^{79}Br decaying with emission of a γ-ray of 0·15 MeV, has a half-life of 20·9 $\pm$ 0·8 minutes and is the parent of 34 hr ^{79}Kr.

Acknowledgements—We should like to thank the cyclotron crew for the bombardments and Mr. B. SINGH and Miss R. EVESON for technical assistance.

VOL. 19 1961

J. Inorg. Nucl. Chem., 1961, Vol. 19, pp. 16 to 26. Pergamon Press Ltd. Printed in Northern Ireland

CHEMICAL EFFECTS IN FISSION PRODUCT RECOIL—V

THE VALENCY STATE OF FISSION PRODUCT IODINES FORMED IN URANYL IODATE

D. HALL* and G. N. WALTON
A.E.R.E., Harwell, Didcot, Berks

(*Received* 14 *July* 1960)

Abstract—When uranyl iodate is irradiated in a reactor the iodate ions are partly decomposed to form reduced forms of iodine. Several isotopes of iodine are formed as fission products, and are distributed in different proportions between the oxidised and reduced forms of iodine. The percentage in the reduced form for ^{131}I is 14 per cent and for ^{133}I 18 per cent; these values are independent of the amount of fission over a wide range. For ^{132}I the reduced form amounts to about 36 per cent, and for ^{135}I 54–68 per cent, dependent upon the amount of fission.

These results are discussed in terms of the independent yields of the various isobars involved in the fission process, and it is shown that the valency state adopted is modified by the environment in which they are formed.

FISSION products are initially formed as isolated atoms, and their chemical condition is expected to be very dependent on the material in which they are stopped and on the method by which they are subsequently extracted from it. By stopping the fission fragments in material containing carriers of the same element in different valency states it might be expected that uncertainties associated with the extraction process would be eliminated, and that measurements of the distribution of a fission product between the valency states would then give some indication of the factors affecting the chemical condition of the fission product at the time of its formation.

In previous studies of the decomposition of potassium iodate and of uranyl iodate in a reactor[1,2] it was observed that the distribution of fission product ^{131}I between the reduced iodine species and the undecomposed iodate was independent of the total amount of fission and also of the relative proportions of the amount of the reduced and oxidized states, provided that the overall decomposition of the iodate was small relative to the total iodate present. As the distribution was independent of the time of irradiation it was concluded that neither radiation-induced exchange nor radiation-induced recombination, such as that observed in bromates[3] and iodates,[4] is an important factor in controlling the distribution. The distribution was also measured at times short compared with the delay in the formation of ^{131}I from the decay of its 30-hr precursor ^{131m}Te, and it was found that the observed distribution was not due to a change in chemical state occurring in the isomeric transition $^{131m}\text{Te} \rightarrow {}^{131}\text{Te}$ analogous to that observed for instance in $^{80m}\text{Br} \rightarrow {}^{80}\text{Br}$[5,6] and in tellurates in aqueous solution.[7]

* Present address: Chemistry Department, University of Auckland, New Zealand.

[1] G. N. WALTON and I. F. CROALL, *J. Inorg. Nucl. Chem.* **1**, 149 (1955).
[2] D. HALL, *J. Inorg. Nucl. Chem.* **6**, 3 (1958).
[3] J. W. COBBLE and G. E. BOYD, *J. Amer. Chem. Soc.* **74**, 1282 (1952).
[4] R. E. CLEARY, W. H. HAMILL and R. R. WILLIAMS JR., *J. Amer. Chem. Soc.* **74**, 4675 (1952).
[5] R. S. H. CHIANG and J. E. WILLARD, *J. Amer. Chem. Soc.* **74**, 6213 (1952).
[6] A. W. ADAMSON and J. M. GRUNLAND, *J. Amer. Chem. Soc.* **73**, 5508 (1951).
[7] R. R. WILLIAMS, JR., *Radiochemical Studies: The Fission Products*, (Edited by C. D. CORYELL and N. SUGARMAN) NNES Plutonium Project Record Div. IV Vol. 9. Paper 20, McGraw-Hill, New York (1951).

The distribution of fission-product iodine between the reduced and oxidized states appears to be determined at an early stage in the process. A large proportion (86 per cent) of the ^{131}I activity was found in the iodate fraction, and it would seem likely that the majority of the primary fission fragments (which are mainly tin and antimony atoms) react to form oxy-ions which persist through the various stages of nuclear decay leading either to iodate ions or to species which hydrolyse to form iodate (or periodate) on dissolution. The remainder appeared as reduced iodine either due to rupture of an oxy-ion during one of the disintegrations before tellurium is formed, or because the initial reaction product was not an oxidized species.

The chemical changes which accompany nuclear transformations are by no means clearly understood. Disruption of molecules, oxidation and reduction have been shown in various studies to accompany beta-disintegration and the internal conversion of gamma rays,[7–10] although in other instances the parent species has appeared to survive the transformation.[6,10,11,12]

VOL. 19 1961

In order to obtain further information on whether the oxidation state of fission product iodine was determined mainly at the initial act of fission, or by the subsequent nuclear transformations following fission, it was decided to study the other iodine fission products, viz those of mass 132, 133 and 135, each of which arises from its precursors by a radically different route.

The relevant fission product chains are shown in Table 1.

EXPERIMENTAL

The techniques used in the irradiation, subsequent dissolution, and extraction of the reduced iodine, were essentially as previously described.[2] Uranyl iodate is sparingly soluble, and as discussed before, a solution of the complexing reagent sodium hexametaphosphate was used to dissolve it after irradiation. Short irradiations were accomplished using a pneumatic tube leading into BEPO.

Aliquots of the iodine and iodate fractions were radiochemically purified as before, precipitated as silver iodide, and counted using a double-crystal γ-ray scintillation spectrometer.[13] In this instrument the spectrum obtained with an anthracene crystal is subtracted from that with a thallium-activated sodium iodide crystal, after adjusting the distances of the crystals from the source in such a way that the response to the Compton continuum is the same from both crystals. By this means only the response due to the photoelectric effect is recorded. However, it was still found desirable to choose irradiation and cooling times such that the peak to be studied dominated the spectrum. The activities of the various isotopes were obtained from peaks corresponding to the following energies:—

^{131}I —0·36 MeV; ^{132}I —0·67 MeV; ^{133}I —0·53 MeV.

The γ-rays associated with the various iodine isotopes and their daughters are shown in Table 2.

The iodine-131 was readily obtained by allowing all the other iodines to decay. The 0·67 MeV peak of ^{132}I suffers interference from ^{131}I (0·637 MeV) but only 9 per cent of the ^{131}I disintegrations lead to γ-rays of this energy and there is a factor of 80 in favour of ^{132}I in the rate of decay; the ^{131}I contribution could therefore be neglected. The 0·53 MeV peak of ^{133}I suffers interference from the 0·528 MeV γ of ^{132}I and the 0·52 MeV γ of ^{135m}Xe. However, if the ^{133}I is separated from tellurium soon after the irradiation, ^{132}I (2·4 hr) can be allowed to decay so that only ^{133}I (20·8 hr) remained. At the same time, by waiting some 20 hr ^{135m}Xe from the ^{135}I (6·7 hr) also decays to an insignificant proportion. Rather than count ^{135}I directly, 12–20 hr decay was permitted and the 0·25 MeV peak of the daughter ^{135}Xe was then used, so avoiding the complexity of the short half-life spectrum. ^{133m}Xe (0·233 MeV)

(8) D. De Vault and W. F. Libby, *J. Amer. Chem. Soc.* **63**, 3216 (1941).
(9) T. H. Davies, *J. Phys. Chem.* **52**, 595 (1948).
(10) W. H. Burgus and J. W. Kennedy, *J. Chem. Phys.* **18**, 97 (1950).
(11) R. R. Edwards, J. M. Day and R. F. Overman, *J. Chem. Phys.* **21**, 1555 (1953).
(12) R. L. Wolfgang, R. C. Anderson and R. W. Dodson, *J. Chem. Phys.* **24**, 16 (1956).
(13) D. H. Pierson, *Nature, Lond.* **173**, 990 (1954).

interferes, but forms only a small percentage of the chain (2·4 per cent). After short irradiations no other activity was then detectable, and as the ^{135}Xe peak itself was only small, the Compton compensation (which necessarily reduces the observed count-rate) was not used. It has been shown that xenon formed by decay of iodine does not escape appreciably from a silver iodide precipitate.[14,15]

TABLE 1.—FISSION PRODUCT CHAINS FOR IODINE ISOTOPES

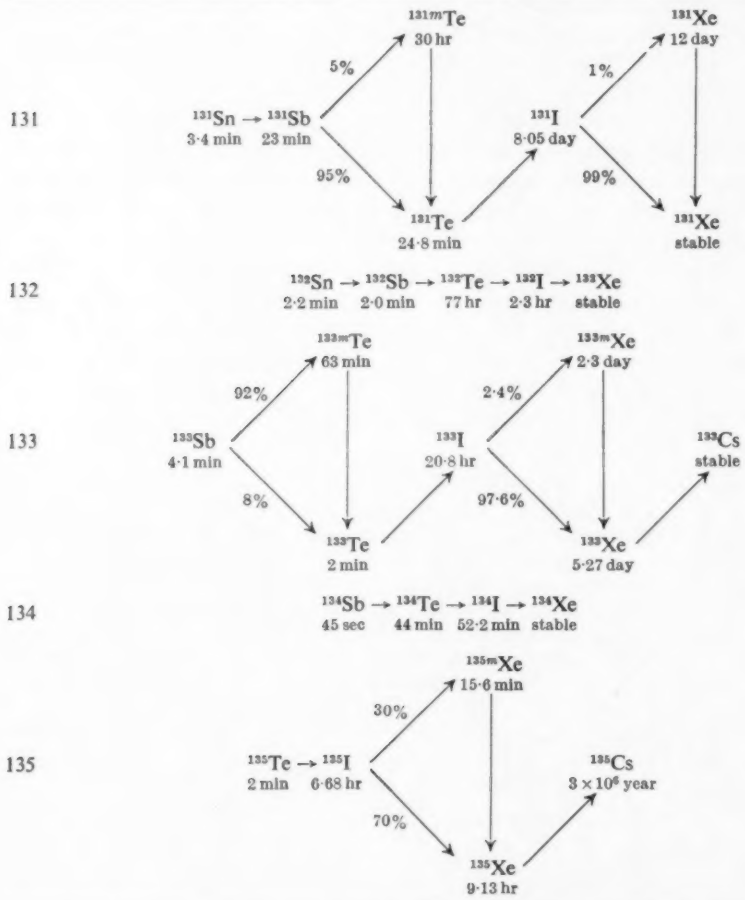

The radiochemical purifications of the iodate and the reduced iodine fractions were always performed rapidly and simultaneously, and the silver iodide samples were counted immediately one after the other. No allowance for decay was then necessary; only correction for chemical yield was required to give the extraction coefficient ϕ, i.e. the fraction of the total activity of the particular isotope extracted as a reduced species. Decay curves were plotted on each sample to ensure that the measured activity was identified by its correct half-life. Details of sample experiments are shown in Table 3.

[14] W. H. SULLIVAN, O. JOHNSON and R. NOTTORF, *Radiochemical Studies: The Fission Products* (Edited by C. D. CORYELL and N. SUGARMAN) NNES, Plutonium Project Record Div. IV, Vol. 9. Paper 139, McGraw-Hill, New York (1951).

[15] S. KATCOFF, C. R. DILLARD, H. FINSTON, B. FINKLE, J. A. SEILER and N. SUGARMAN, *Radiochemical Studies: The Fission Products* (Edited by C. D. CORYELL and N. SUGARMAN) NNES, Plutonium Project Record, Div. IV, Vol. 9, Paper 141. McGraw-Hill, New York (1951).

TABLE 2.—γ-RAYS ASSOCIATED WITH IODINE ISOTOPES

^{131}I	E_γ(MeV)	0·722	0·637	0·364	0·284					
	%	3	9	80	5·3					
^{132}I	E_γ(MeV)	2·2	1·96	1·40	1·16	0·96	0·777	0·673	0·624	0·528
	%	2	5	11	8	20	75	100	6	25
^{133}I	E_γ(MeV)	1·4	0·85	0·53						
	%	1	5	94						
^{133m}Xe	E_γ(MeV)	0·233								
	%	100								
^{133}Xe	E_γ(MeV)	0·081								
	%	100								
^{135}I	E_γ(MeV)	1·8	1·27							
	%	50	50							
^{135m}Xe	E_γ(MeV)	0·52								
	%	100								
^{135}Xe	E_γ(MeV)	0·60	0·37	0·25						
	%	4	1	96						

TABLE 3.—DETAILS OF SAMPLE EXPERIMENTS

Sample A

Irradiation—90 min at flux 6×10^{11} neutrons cm^{-2} sec^{-1}.
Decay—5 days before dissolving
Counted immediately

	Activity observed	Activity corrected for chemical yield
^{131}I—reduced fraction	635 cpm	1005 cpm
iodate fraction	810	5995
^{133}I—reduced fraction	635	1005
iodate fraction	610	4515
Fraction of activity in reduced form—^{131}I	0·143	
—^{133}I	0·182	

Sample B

Irradiation—7 min at flux 14×10^{11} neutrons cm^{-2} sec^{-1}.
Decay—4 hr before dissolving sample
^{135}Xe counted 18 hr later
^{133}I counted 3 days later

	Activity observed	Activity corrected for chemical yield
^{133}I—reduced fraction	520 cpm	655
iodate fraction	310	2985
^{135}Xe—reduced fraction	5900	7405
iodate fraction	650	6260
Fraction of activity in reduced form—^{133}I	0·179	
—^{135}Xe	0·541	

In most experiments sufficient decomposition of the iodate occurred to make the addition of carrier iodine unnecessary in determining chemical yields. For the distribution of ^{131}I after very short irradiations during which very little decomposition of the uranyl iodate occurred, a measured amount of carrier iodine (as the element) was added before dissolution of the sample. The activity from these short irradiations was too low for γ-counting, and the β-activity was therefore measured using a 2π

VOL. 19 1961

geometry internal-source β-proportional counter. Counting was started 10 days after irradiation, and decay was followed for several half-lives. Self-absorption corrections were applied[16] where the precipitates differed in mass.

RESULTS

The extraction coefficients observed for ^{131}I previously,[2] and for ^{131}I, ^{132}I, ^{133}I and ^{135}I in this study, are plotted against neutron dose in Fig. 1. The neutron dose was estimated from the overall amount of ^{131}I found in the sample, assuming a 3 per cent fission yield, and is a measure of the amount of fission that had occurred. The ϕ

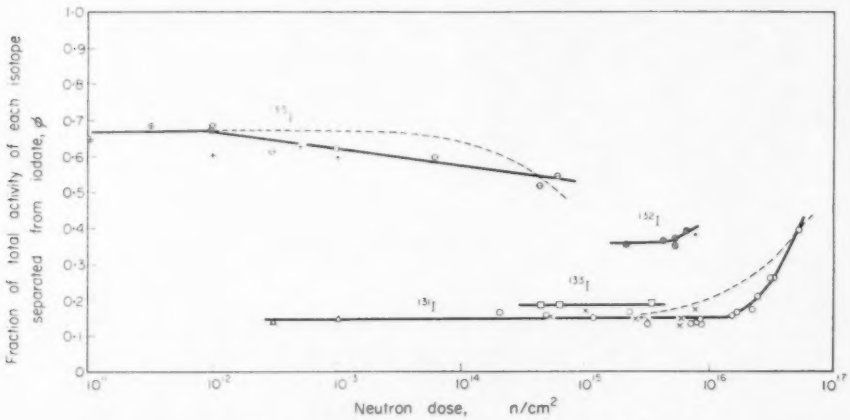

FIG. 1.—Valency states of iodine isotopes found in the irradiation of uranyl iodate. ○ ^{131}I—previous work, × ^{131}I—γ-counting, △ ^{131}I—$2\pi\beta$-counting, ⊗ ^{132}I, □ ^{133}I, ⊖ ^{135}I, + ^{135}I—thick glass capsule, ⊕ ^{135} I— pile operating at 100 kw. – – – – calculated values of ϕ.

value for ^{131}I, ϕ 131, was constant over a wide dose-range varying only when substantial decomposition had occurred, and ϕ 133 was also constant over the range considered. On the other hand, ϕ 135 decreased from 0·68 when irradiated for one second (flux $1{\cdot}4 \times 10^{12}$ neutrons cm^{-2} sec^{-1}) to 0·54 for 10 min. The ϕ values for the isotopes of mass 131, 133 and 135 are respectively 0·14, 0·18 and 0·5–0·7 i.e. there is an increase with the mass of the isotope.

To reduce the dose-rate the silica containing capsule was replaced by one of thick glass, which would absorb a large fraction of the thermal neutrons. This modification would however increase the relative flux of γ-rays to neutrons and, as discussed below, this is possibly the explanation for the slightly lower values of ϕ that were then obtained for ^{135}I. Operation of the very short irradiations was difficult, as the sample receives radiation not only during the time it is in the irradiation hole but also during the instant of transit through the reactor core. To over-come this difficulty the original silica capsules were used, but the reactor was run at only one-sixtieth of its normal power level. The irradiation hole used was not adjacent to the control rods, and the quality of the radiation should not have been greatly affected. Higher extraction coefficients for ^{135}I were again obtained, the limiting value being 0·68.

The extraction coefficient for ^{132}I was only very indirectly obtained. Uranyl iodate is only slightly soluble, and dissolves slowly even in complexing solvents. It is difficult

[16] J. G. CUNINGHAME, M. L. SIZELAND and H. H. WILLIS, AERE C/R 2054.

to dissolve the sample and complete the iodine extraction in less than thirty minutes. This is not important for the odd mass isotopes, the tellurium parents of which had in all cases decayed completely before dissolution, but the slow dissolution may affect the ^{132}I distribution. This isotope, with a half-life of 2·2 hr, will be formed from its 77-hr parent until separated from it, and a significant fraction of the iodine activity would grow from the parent during the 30 min dissolution period. Some estimate of the limiting value for the extraction coefficient before dissolution can be obtained by the following argument. It has been shown that when the $(^{132}Te\ O_3)^{2-}$ ion decays in acid solution seventy-five per cent of the resulting ^{132}I appears in the reduced form;[4] it is

TABLE 4.—OBSERVED EXTRACTION COEFFICIENTS FOR ^{132}I

Irradiation time (flux 6×10^{11} n cm^{-2} sec^{-1}) (hr)	Dissolution time (min)	ϕ 132	ϕ^*
1	40	0·35	0·34
2	33	0·36	0·31
2½	32	0·37	0·31
3	37	0·39	0·33
2½	80	0·35	0·46

VOL. 19 1961

also possible that reduced tellurium species, stable in the solid state, may be oxidized in solution. Observed values for the extraction coefficients of ^{132}I are listed in Table 4 for various irradiation times and dissolution times. It is notable that the observed coefficient does not appear to be sensitive to dissolution time, and that the mean value obtained, 0·37, is considerably higher than that for ^{133}I. If it is assumed that the real value for ϕ 132 is the same as that for ^{133}I, i.e. 0·18, and that all tellurium disintegrations which occur during the dissolution period lead to reduced iodine, the results expected are those listed as ϕ^* in Table 4, i.e. a marked dependence on dissolution time would be observed. If the real value for the extraction coefficient of ^{132}I was below 0·18, or alternatively if less of the ^{132}I growing from tellurium during the extraction period arose in the reduced state, then there would be more disagreement between the observed and calculated figures. The disagreement means that although ϕ 132 is not precisely determined by the present techniques, it is certain that it is greater than 0·18 and not intermediate between ϕ 131 and ϕ 133.

DISCUSSION

The increase in ϕ with overall decomposition

As previously observed, the extraction coefficient for ^{131}I appears to be constant at a value of ~0·14 over a very wide range of neutron dose. At high doses a sharp increase occurs, as shown in Fig. 1, which may be associated with the fact that a large percentage of the uranyl iodate is decomposed at these high doses. Under these conditions the fission fragments would be expected to be arrested in oxygen-depleted regions of the crystal, and a greater fraction should be in the reduced state, as is observed. A simple quantitative interpretation of this corresponds fairly closely to the observation.

Let N_0 = number of iodate ions present initially
N = number of iodate ions decomposed
b = probability that of the ^{131}I atoms which would normally arise in the oxidised state, those formed amongst fully decomposed iodate ions arise in the reduced state.
R = rate of formation of ^{131}I atoms
I = number of ^{131}I atoms formed in the reduced state
k = fraction of iodate ions decomposed per second
T = time, t, of irradiation

Then
$$\phi = \frac{\int_0^T I\,dt}{RT} \tag{1}$$

The rate at which iodate ions are decomposed will be expected to be proportional to the number of undecomposed iodate ions present, i.e.

$$\frac{dN}{dt} = k(N_0 - N) \tag{2}$$

The number of reduced ^{131}I atoms formed will be determined by the number formed when the fragments are stopped in undecomposed iodate, plus the product of the fraction of decomposed iodate ions, the number of initially oxidizable ^{131}I atoms, and the probability that the decomposed iodate will cause their reduction, i.e.

$$\phi = \phi_0 + \frac{Nb}{N_0}(1 - \phi_0) \tag{3}$$

The rate of formation of reduced ^{131}I atoms is

$$\frac{dI}{dt} = \phi R \tag{4}$$

Integrating (2), substituting in (3) and (4), and evaluating (1) over the period of the irradiation, we find that

$$\phi = \phi_0 + b(1 - \phi_0)\left(1 - \frac{1 - e^{-kT}}{kT}\right).$$

Using the values

$$\phi_0 = 0{\cdot}14 \text{ (the value in undecomposed iodate)}$$

$$k = 9{\cdot}4 \times 10^6 \text{ atoms of reduced iodine per fission}^{(2)}$$

we find that if $b = 0{\cdot}87$, ϕ would increase according to the dotted line in Fig. 1. This means that fully-decomposed iodate will cause nearly every ^{131}I atom to be reduced, over and above the number that arise in the reduced state in undecomposed iodate. The order of magnitude of b is reasonable, but as seen in Fig. 1 the number of reduced iodine atoms increases rather more steeply than the simple theory would warrant. This suggests that initially iodate decomposition has little effect on the valency state of iodine, and that as decomposition becomes more complete the valency state is affected.

Fig. 1 also suggests that the reduction of ^{132}I may increase with dose, but more results are required to substantiate this possibility.

The value of ϕ for the different isotopes of iodine

The most striking feature of Fig. 1 is that ^{131}I is found mainly in the oxidized condition, ^{133}I appears to be slightly less oxidized, while ^{135}I is radically different and is found mainly in the reduced condition. As seen in Table 1 ^{135}I differs from the other isotopes in that it is probably formed initially in the fission act, (the precursor ^{135}Te has never been firmly identified), whereas the other isotopes arise from tin or antimony precursors which undergo transformations to tellurium before giving rise to iodine. An important point arises in considering the initial fission act. Here the fragments when they are first formed are stripped of some 15–20 electrons, and they collect electrons as they slow down. It might be supposed that the fragments do not reach neutrality but tend to adopt the valency state most suited to their partially-stripped condition i.e. the fission products closest to the original fragments might be expected on this argument to be in the most oxidized condition. Amongst the iodine isotopes investigated here, the product which is closest to the original fission process, i.e. ^{135}I, is the least oxidized isotope, and this is evidence that the initial electron-stripping process has no major effect on the final valency state adopted.

VOL. 19 1961

The final valency state is probably determined by the affinities of the initially-formed elements for the surroundings in which they arise, and nothing in the findings reported here appears to contradict this supposition. There appears to be insufficient published information to warrant comparisons of the thermodynamic affinities of tin, antimony, tellurium and iodine for oxygen. Uranyl tellurates and antimonates have not been investigated, and there is insufficient information to enable inferences to be drawn from the stability of the potassium or sodium salts. However, the fission fragments arise as isolated atoms and the true thermodynamic affinities of bulk materials would not be expected to be applicable in this case. The properties of individual atoms, such as electron affinity, polarisability, and ionic radii, are more likely to be among the factors which govern the fate of the fission products. Table 5 shows the electron binding energies of the outer electrons of the elements which are genetically related to the iodine isotopes; the figures shown are for the X-ray absorption edges for the 4*d* electron shell[17]. Elements which are most easily stripped of electrons might be expected to arise mainly in the oxidized form whereas those that have higher electron binding energies might be expected to prefer the reduced condition. The order corresponds to "electropositive" or "electro-negative" character. Also shown in Table 5 are the independent fission yields of the different isobars for each mass number, expressed as fractions of the total chain yield. These have been calculated on the equal charge displacement hypothesis.[18] In the lower section of Table 5 are shown the experimental percentages of the oxidized and reduced forms for each mass number as seen in Fig. 1.

In Table 5 we see that mass 135 arises mainly as iodine, having a high electron binding-energy, so that it would be expected to be formed mainly in the reduced state, as observed. Mass 131 arises mainly as tin and antimony, which have lower electron binding-energies, and correspondingly mass 131 arises mainly in the oxidized condition. Mass 133 lies, as expected from this argument, between mass 131 and 135. However,

[17] R. D. HILL, E. L. CHURCH and J. W. MIHELICH, *Rev. Sci. Instrum.* **23**, 523 (1952).
[18] L. E. GLENDENIN, C. D. CORYELL and R. R. EDWARDS, *Radiochemical Studies: The Fission Products*, (Edited by C. D. CORYELL and N. SUGARMAN) NNES Div. IV, Vol. 9. Paper 52, McGraw-Hill, NewYork (1951).

mass 132 is not in the right order with respect to mass 133. According to the independent yields of its precursors and their electron binding-energy, the percentage reduced should fall between those for masses 133 and 131 and not between those for 133 and 135. Although, as discussed above, the precise percentage of the reduced ^{132}I formed during the irradiation is not well established, it certainly appears to be greater than 18 per cent. A possible explanation is that the independent yields shown in Table 5, as

TABLE 5.—ELECTRON BINDING ENERGIES AND INDEPENDENT FISSION YIELDS COMPARED WITH EXPERIMENTAL ϕ VALUES

Outer electron binding energy		Sn	Sb	Te	I	Xe
	eV	5	35	46	53	65
Independent yields	131	0·45	0·41	0·14	—	—
	132	0·26	0·48	0·25	0·01	—
	133	—	0·55	0·36	0·09	—
	135	—	—	—	0·95	0·05
		Oxidized		Reduced		
Mass	131	86		14		
	132	(63)		(37)		
	133	82		18		
	135	33		67		

calculated from the equal charge displacement hypothesis, are not correct. The isotopes in question lie in a region of closed nuclear shells (^{132}Sn for instance has 50 protons and 82 neutrons), and it is possible that this would influence the independent yields. This point has been discussed by PAPPAS[19] who compensates for the closed-shell effect by modifying Z_A, the value of the most probable stable charge for a given mass, in the equal charge displacement theory. THODE[20] has also considered the effect of closed shells, and modifies the values of Z_P, the most probable primary fragment charge, for isobars that include closed-shell structures. The independent yields predicted by these two modifications are shown in Table 6. The figures show that closed-shell effects increase the relative proportions of tin and antimony as precursors of ^{132}I. As these are elements with low electron binding-energies it might be expected that ^{132}I would arise in a more oxidized condition, whereas it is observed to be less oxidized than its neighbours. The nuclear shell effects therefore do not appear to explain the observations.

A possible explanation of the highly-reduced condition of ^{132}I may be seen by considering the half-lives. Reference to Table 1 shows that mass 132 will occur mainly as ^{132}Te (77 hr half-life), which is easily reduced, and will only exist for a very short time as tin and antimony, which are reduced with greater difficulty. Masses 131 and 133 spend a longer time in the more easily oxidized condition.

The effect of dose on the value of ϕ for ^{135}I

As seen in Fig. 1, the value of ϕ for ^{135}I appears to fall as the neutron dose increases. This could be due to an annealing effect caused by the irradiation, in which the fission

[19] A. C. PAPPAS, M.I.T. Technical Report No. 63, (1953).
[20] H. G. THODE, Atomic Energy of Canada Limited, Report No. 329 (CRP-642A) page 278 (1956).

fragment iodine atoms formed initially in the reduced condition tend to become oxidized and so re-form iodate ions as irradiation proceeds. This may also explain the low values of ϕ shown in Fig. 1 which were obtained in the thick glass capsule experiments, where the ratio of γ-radiation to thermal neutron flux would be much higher. Such an effect is not to be seen in the case of ^{131}I, but here mass 131 is largely present as antimony and tellurium during the irradiation and would not be expected to re-form the iodate ion.

TABLE 6.—FRACTIONAL PRIMARY FISSION YIELDS ACCORDING TO THE EQUAL CHARGE DISPLACEMENT HYPOTHESIS, AS MODIFIED BY SHELL EFFECTS ACTING ON (a) Z_A (b) Z_P

	Mass	In	Sn	Sb	Te	I	Xe
(a)	131	—	0·45	0·41	0·14	—	—
	132	—	0.36	0.41	0.22	0·01	—
	133	—	—	0·55	0·36	0·08	—
	135	—	—	—	—	0·95	0·05
(b)	131	—	0·57	0·35	0·08	—	—
	132	—	0·47	0·41	0·12	—	—
	133	—	—	0·36	0·46	0·18	—
	135	—	—	—	—	0·99	0·01

VOL. 19 1961

However, a simple quantitative treatment does not support this supposition.

If N_{ox} = number of oxidized ^{135}I atoms at time t during irradiation
N_{red} = number of reduced ^{135}I atoms at time t during irradiation
R = rate of formation of ^{135}I atoms
a = fraction of reduced atoms changed to oxidized atoms per second during irradiation
ϕ_0 = fraction of ^{135}I atoms initially in the reduced state,

the rate of formation of oxidized ^{135}I atoms equals the rate for those formed directly plus those formed from the reduced atoms i.e. neglecting radioactive decay:

$$\frac{dN_{ox}}{dt} = (1 - \phi_0)\,R + aN_{red} \tag{1}$$

$$N_{red} + N_{ox} = Rt \tag{2}$$

$$\phi_t = \frac{N_{red}}{N_{ox} + N_{red}} \tag{3}$$

Substituting (2) in (1) and integrating we obtain from (3)

$$\phi_t = \phi_0 \frac{(1 - e^{-at})}{at} \tag{4}$$

If a is given the value $5{\cdot}5 \times 10^{-4}$ sec^{-1} we obtain the dotted curve shown in Fig. 1 for the fall in the value of ϕ as irradiation proceeds. It is seen that while the simple theory will account for a reduction in ϕ, the observed reduction is a very different function of neutron dose from that predicted by the simple theory.

A further difficulty arises when the available energy is considered. In a thermal neutron flux of $1{\cdot}4 \times 10^{12}$ n/cm^2 sec in uranyl iodate the fission process produces approximately $4{\cdot}4 \times 10^{-4}$ eV per iodine atom per second. From the value of a above, the fraction of reduced ^{135}I atoms converted to the oxidized form by irradiation is $5{\cdot}5 \times 10^{-4}$ per sec. These figures imply that the G factor for the radiation-induced effect is 125 atoms of ^{135}I converted to the oxidized form per 100 eV of energy absorbed, which is a higher value than those normally observed in radiation processes. It is difficult to see how the theory could be adapted to explain the effect at the lower doses, and it would appear necessary first to obtain more precise information about the change in the extraction coefficient with dose.

J. Inorg. Nucl. Chem., 1961, Vol. 19, pp. 27 to 37. Pergamon Press Ltd. Printed in Northern Ireland

ASSOCIATED PROCESSES TO THE SZILARD–CHALMERS EFFECT IN CRYSTALS—I

HEXAMMINO-COBALTIC NITRATE. SECTION 2. THERMAL ANNEALING OF THE CRYSTALLINE DEFECTS AFTER IRRADIATION

T. COSTEA
Institute of Atomic Physics, Bucharest, Rumania

(*Received* 10 *August* 1960)

Abstract—The thermal annealing of neutron irradiated $\{Co(NH_3)_6\}(NO_3)_3$ was investigated to determine the order of the fast annealing processes, the activation energy, the fraction annealing as a function of the temperature and the effect of the history of the sample on the annealing process.

It was observed that the fast thermal annealing process formally obeys first-order kinetics. Strictly the kinetics may be explained by processes distributed in activation energy. The maximum of the activation energy spectrum is about 0·78 eV. The fraction destined to anneal is proportional to the temperature, but the saturation value of the retention for different samples heated at the same temperature, is not the same. It was observed that the radiation history of the sample has a great influence on the annealing process and a quantitative treatment of the effects is determined.

VOL. 19 1961

THE annealing of the crystalline defects produced by irradiation of hexammino-cobaltic nitrate in the reactor has been studied in a previous work.[1] It was noticed that the retention reaches a constant value after a certain time. The greater the γ dose-rate concurrent with the neutron irradiation, the higher this constant value. This effect was ascribed to an annealing process, due especially to the action of the γ quanta emitted from the reactor. It is interesting to pursue further the thermal annealing of the samples which were irradiated in the reactor.

The first to draw attention to the fact that the retention increases on heating such samples, after their irradiation, were GREEN and MADDOCK.[2] Since then, a series of works in which his effect was systematically studied have been published. Most of the authors found that the thermal annealing is described formally by first order kinetics. Another significant fact was that at each emperature the retention reaches a constant value after a certain time which increases with the heating temperature. In fact, kinetic isotherms are obtained. Experimentally it was ascertained that the fraction annealed decreases inversly in proportion to the absolute temperature.[3,4] But opinions differ as to the activation energy for this process. Another disputed point is whether the history of the sample plays a part in the annealing process or not. Thus, MADDOCK and coworkers[5,6] by heating a sample until it reaches the aforementioned constant value, and then heating it again at a higher temperature until it reaches the corresponding constant value, found the same final retention as if the sample had been

[1] T. COSTEA, *J. Inorg. Nucl. Chem.* In press (1960).
[2] I. H. GREEN and A. G. MADDOCK, *Nature, Lond.* **164**, 788 (1949).
[3] J. COBBLE and E. BOYD, *J. Amer. Chem. Soc.* **74**, 1282 (1952).
[4] A. G. MADDOCK and M. M. DE MAINE, *Canad. J. Chem.* **34**, 275 (1956).
[5] M. M. DE MAINE, A. G. MADDOCK and K. TAUGBOL, *Disc. Faraday Soc.* **23**, 211 (1957).
[6] A. G. MADDOCK and H. MÜLLER, *Trans. Faraday Soc.* **56**, 509 (1960).

heated directly at this higher temperature. On the other hand, NATH *et al.*[7] noticed that the retention in the case mentioned above, had a lower value at the end. The difference between the value of the retention obtained in a one-step treatment and that obtained in a many-step treatment was proportional to the number of heatings.

In the present work we propose to treat the irradiated samples thermally, with the following objectives:

(1) To establish the isotherms which are usually found in such cases.
(2) To determine the activation energy of the fast annealing process.
(3) To determine the fraction annealed as a function of the absolute temperature.
(4) To study the effect of the history of the sample on the annealing process.

EXPERIMENTAL

The samples were irradiated in the thermal column of the I.F.A. reactor; these irradiations were made in quartz test-tubes in air.

The heating of the samples was effected in air in an electric drying-stove, the temperature variation at a given temperature being about $\pm 0{\cdot}5°C$.

The retention was determined by the method described in detail in Section 1 of this paper,[1] i.e. by dissolving the sample in water and extracting the Co^{2+}, with chloroform in the form of a complex with pyridine and thiocyanate. The activities of the solutions were measured with immersion G. M. counters of the Vakutronik VA-Z type. The retention was computed from the percentage of activity not extracted and the total activity.

RESULTS AND DISCUSSIONS

The samples irradiated in the reactor were heated in the temperature range of 140°–170°C. The temperature interval in which the thermal treatment was pursued was, it is true, rather narrow, but we were obliged to restrict ourselves to it for the following reasons: no sample shows any annealing effects while it is being heated, even for a long time, below 140°C, whereas heating above 170°C may lead to the thermal decomposition of the hexammino-cobaltic nitrate, with the appearance of brown cobalt oxide, which is insoluble.

We tried a similar treatment to that used by NATH *et al.* in order to study the influence of the thermal history of the sample;[7] but the temperature range being limited, a sufficient number of steps could not be employed, and thus eventual variations would have been small, so that the results could not have been conclusive. In this statement we must also take into account the fact that the precision in the method of determination used was $\pm 1{\cdot}8\%$.

The isothermal treatment was applied to three categories of samples possessing substantially different initial retentions owing to the fact that they had been irradiated in the reactor under different conditions of thermal neutron flux, fast neutron flux and γ dose-rate. It must be pointed out that all these samples were irradiated in the reactor until they reached the saturation value of the retention. Thus, the initial retention of the samples is exactly the saturation retention during the neutron irradiation. The irradiation conditions and the initial retention of the samples are given in Table I.

By heating the samples, the characteristic isotherms for the process were found. As usual after a relatively short lapse of time the retention reaches a saturation value characteristic for a given temperature. The results of this thermal treatment are shown in Figs. 1–3, for three categories of samples called A, B, C. The retention R is registered on the ordinate, while on the abscissa the heating time is given in seconds.

[7] A. NATH, K. S. VENKATESWARLU and J. SHANKAR, *Proc. Indian Acad. Sci.* **46**, 29 (1957).

TABLE 1.—CONDITIONS UNDER WHICH THE SAMPLES WERE IRRADIATED IN THE REACTOR, BEFORE THE THERMAL TREATMENT

Sample	The flux of thermal neutrons ϕ_{th} ($cm^{-2}\ sec^{-1}$)	The flux of fast neutrons ϕ_f ($cm^{-2}\ sec^{-1}$)	The γ dose-rate δ_γ (rh^{-1})	The initial retention R_0 (%)
A	$6{\cdot}0 \cdot 10^{11}$	$1{\cdot}75 \cdot 10^{11}$	$1{\cdot}31 \cdot 10^{7}$	74·5
B	$1{\cdot}2 \cdot 10^{11}$	$6{\cdot}25 \cdot 10^{9}$	$3{\cdot}47 \cdot 10^{6}$	61·1
C	$8{\cdot}8 \cdot 10^{8}$	$3{\cdot}10 \cdot 10^{5}$	$5{\cdot}36 \cdot 10^{4}$	24·5

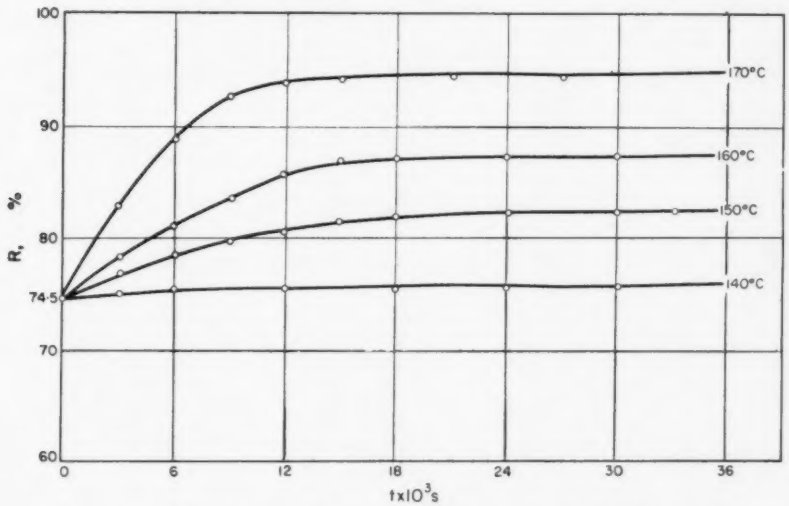

FIG. 1.—Variation with time of the retention of sample A

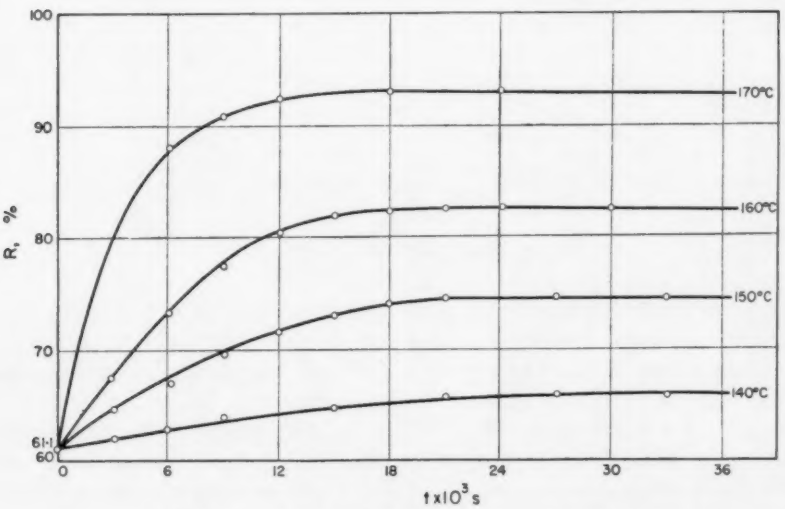

FIG. 2.—Variation with time of the retention of sample B

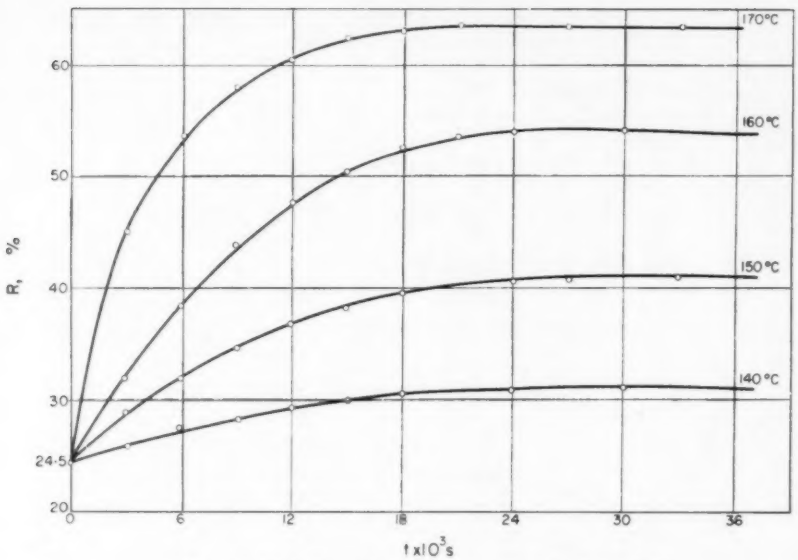

FIG. 3.—Variation with time of the retention of sample C

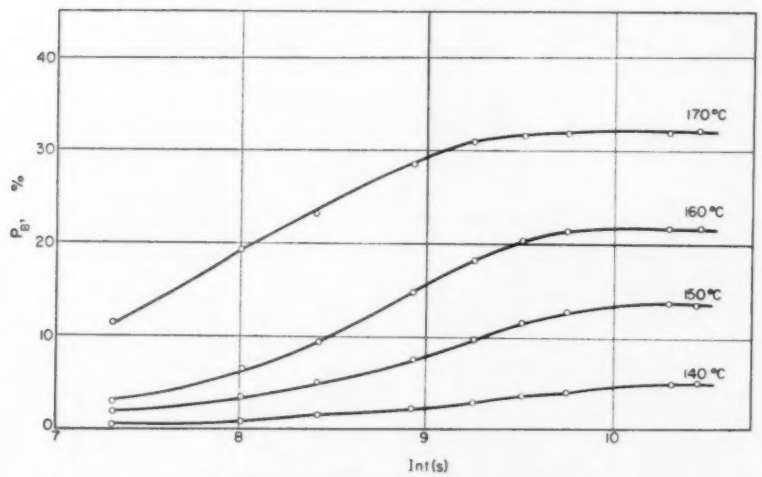

FIG. 4.—Isothermal annealing curve for sample B.

In order to determine the nature of the fast annealing process, the fraction of recoil damage annealed ($P = R - R_0$) was plotted against the logarithm of the time. The annealing curves at various temperatures, for two categories of samples, respectively B and C (see Table 1) are shown in Figs. 4 and 5.

Assuming, after FLETCHER and BROWN[8], that the annealing can be represented by an expression in which t/τ is the ultimate variable, then an equivalent annealing curve for 150°C can be composed as shown in Fig. 6. The composite annealing curve can be

[8] R. C. FLETCHER and W. L. BROWN, *Phys. Rev.* **92**, 585 (1953).

approximated by an unimolecular expression. The equation which gave the best overlap of the experimental curve is

$$P = 40\left(1 - e^{-\frac{t}{4\cdot 10^4}}\right) \tag{1}$$

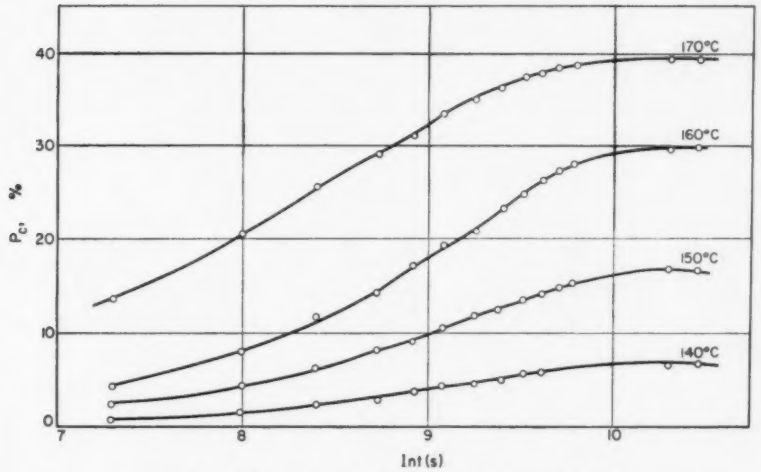

FIG. 5.—Isothermal annealing curve for sample C.

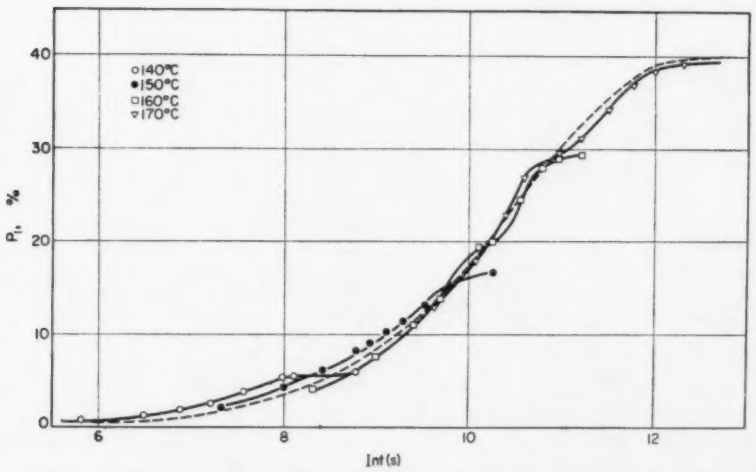

FIG. 6.—Composite annealing curve obtained by adjusting the time scales for superposition of the curves of Fig. 5 with respect to the curve at 150°C. The theoretical curve is shown by the dotted curve.

For the determination of the activation energy we have adopted VAND's concept[9] amplified by PRIMAK[10]. HARBOTTLE and SUTIN[11] have applied this treatment successfully to the potassium chromate annealing data of DE MAINE *et al.*[5]

It is seen that an approximate straight line could be drawn through the points in Figs. 4 and 5, associated with a particular temperature. If it is assumed that the

[9] V. VAND, *Proc. Phys. Soc.* **55**, 222 (1943).

kinetics can be explained by processes with distributed activation energies, the approximate initial distribution p_0 for the per cent changes in retention is given by

$$p_0 = -\frac{1}{kT}\frac{dP}{d(\ln t)} \tag{2}$$

$$E_0 = kT \ln (Bt) \tag{3}$$

where E_0 is the activation energy in eV, P is the fraction annealed at the time t, B is a constant having the dimension of frequency, k is Boltzman's constant and T, the absolute temperature.

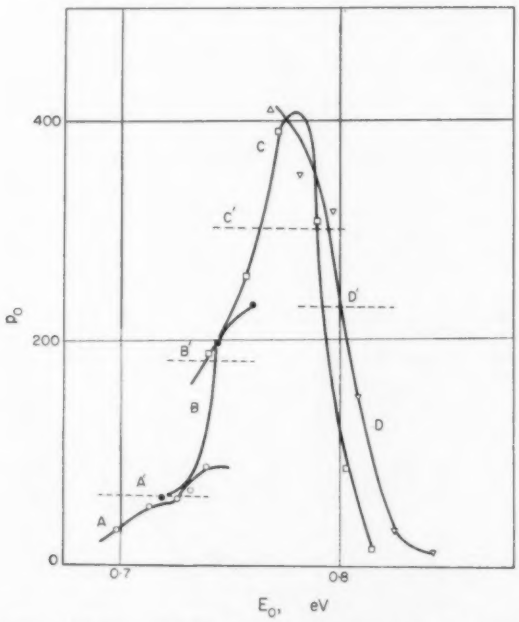

FIG. 7.—The initial distribution of activation energy for sample B. A,A′—140°C; B,B′—150°C; C,C′—160°C; D,D′—170°C.

If the initial distributions calculated for straight lines fitted to the points of Figs. 4 and 5 are plotted, it is found that a peak formed of disconnected segments is obtained, as is shown by dotted lines in Figs. 7 and 8. A second stage of refinement may be attained in which, instead of an average slope, one reads off the actual slopes point by point. One obtains a better representation of the initial spectrum as shown by the solid lines in Figs. 7 and 8. The value of the frequency factor 10^8 sec was chosen to achieve a reasonably good coincidence of the overlapping sections of the distributions obtained at different temperatures. The coincidence which has been achieved is well within the error of the results. The data seem to indicate a peak in the neighbourhood of 0·78 eV, that is, there are no processes of much higher activation energy. We shall

[10] W. PRIMAK, *Phys. Rev.* **100**, 1677 (1955).
[11] G. HARBOTTLE and N. SUTIN, *Advances in Inorganic Chemistry and Radiochemistry* (Edited by H. J. EMELEUS and A. G. SHARPE) Academic Press, New York and London. Vol. 1, p. 305 (1959).

assume that the majority of the activation energies of the annealing processes are in fact distributed between 0·70 and 0·84 eV, i.e., there is not a large range.

It is interesting that the same activation energy is found for all three categories of samples A, B and C, which were irradiated in the reactor under different conditions.

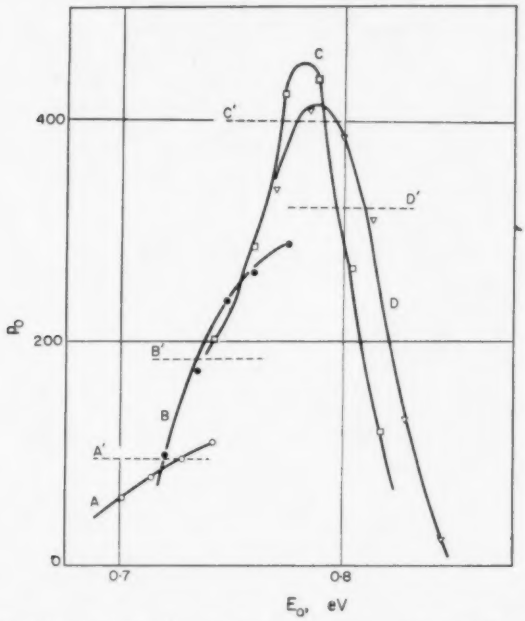

FIG. 8.—The initial distribution of activation energy for sample C. A,A′—140°C; B,B′—150°C; C,C′—160°C; D,D′—170°C.

Thus the activation energy for annealing does not appear to be a function of the number of defects present, as suggested by MARX *et al.*[12] and OVERHAUSER[13]. The classical treatment was also applied to the annealing curves shown in Figs. 1, 2 and 3. A plot of the logarithm of the fraction destined to anneal, $\Delta R = R_\infty - R$, against the time is shown in Fig. 9, for the sample of C category. In each case straight lines are obtained, their slopes increasing with the temperature at which the samples were heated. This denotes formally first-order kinetics with respect to the concentration of the fragment destined to anneal. It is possible to determine the apparent rate constants of the pseudo-unimolecular process. The values are given in Table 2.

One may observe that the rate constants are about the same for all three categories of samples at a given temperature. One can see from Fig. 10 where the logarithm of the rate constant is plotted against $1/T$, that the annealing process appears as a singular unimolecular process, characterized by a single activation energy which is constant within the given temperature range. The activation energy calculated graphically is between 0·57 and 0·74 eV with the best value of about 0·68 eV. This value is in good agreement with the value determined by VAND–PRIMAK treatment.

So far all three categories of samples behave in the same way. But it may be seen from Fig. 1–3, that if for one sample the saturation retention is characteristic for a given temperature, at the same temperature another sample that has been irradiated in

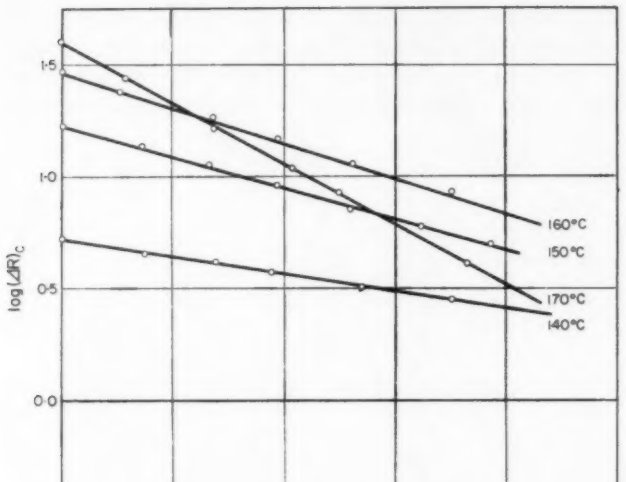

FIG. 9.—Variation with time of the logarithm of the fraction destined to anneal, for sample C.

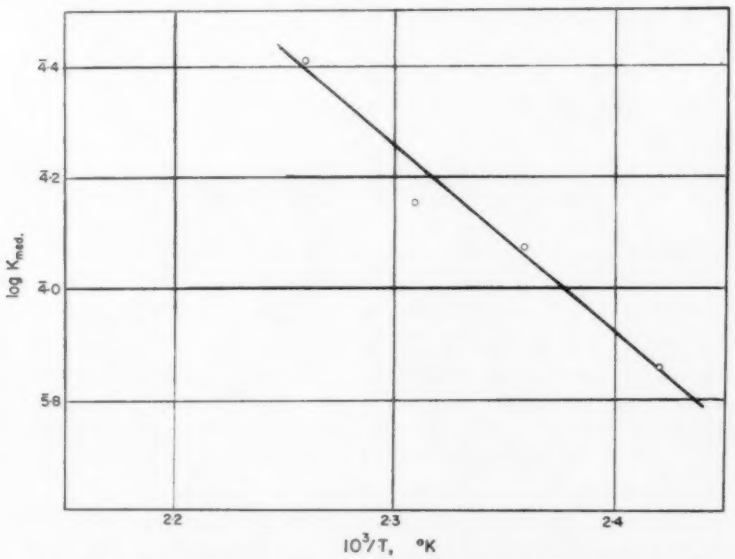

FIG. 10.—The logarithm of the apparent rate constant as a function of the absolute temperature.

the reactor under more moderate conditions may show a lower value of the saturation retention. All the same, it can be seen that the fraction destined to anneal at a given temperature is greater in the case of a sample which had received a smaller radiation dose rate in the reactor. This can be seen in Tables 3 and 4, where the values of the saturation retention R_∞ and the fraction destined to anneal $(\Delta R)_\infty$ are given at the different working temperatures.

TABLE 2.—RATE CONSTANT VALUES AT DIFFERENT TEMPERATURES, FOR THE 3 CATEGORIES OF SAMPLES

$k, 10^{-5}$ sec^{-1} / T°C	140	150	160	170
k_A	5·74	10·88	14·53	25·50
k_B	9·59	13·80	16·34	30·60
k_C	6·39	10·88	12·10	22·30
k_{med}	7·24	11·85	14·32	26·13

TABLE 3.—SATURATION RETENTION OF SAMPLES A, B, C FOR VARIOUS TEMPERATURES

Sample / R_∞ (%)	140°C	150°C	160°C	170°C
A	75·8	82·5	87·5	94·4
B	66·0	74·6	82·5	93·0
C	31·0	41·0	54·1	63·5

[12] J. W. MARX, H. G. COOPER and J. W. HENDERSON, *Phys. Rev.* **88**, 106 (1952).
[13] A. W. OVERHAUSER, *Phys. Rev.* **94**, 1551 (1954).

TABLE 4.—THE FRACTION DESTINED TO ANNEAL AT VARIOUS TEMPERATURES .

Sample / $(\Delta R)_\infty$ (%)	140°C	150°C	160°C	170°C
A	1·3	8·0	13·0	19·9
B	4·9	13·5	21·4	31·9
C	6·5	17·5	29·6	39·0

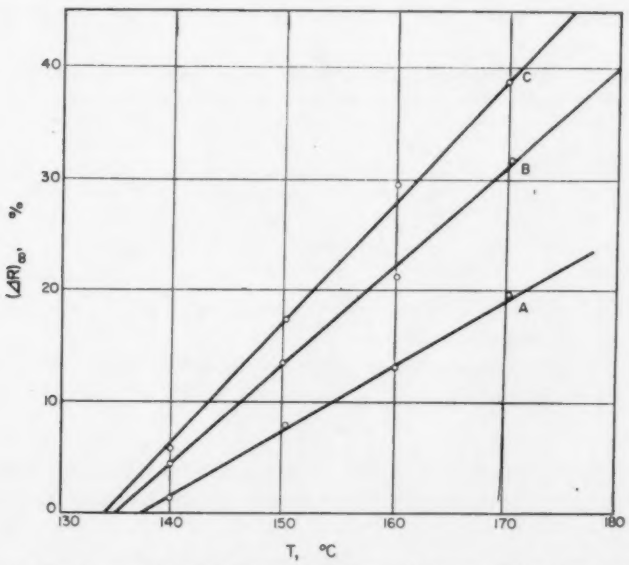

FIG. 11.—The increase in retention to the plateau, $(\Delta R)_\infty$, plotted against T, the absolute temperature, for samples A, B and C.

A linear dependence may be observed between the fraction destined to anneal at a given temperature $(\Delta R)_\infty$ and the absolute temperature T; as may be seen from Fig. 11 The less the crystals have been perturbed as a result of irradiation in the reactor, the more pronounced the slope of this straight line will be. In fact, the equation that represents this effect may be written in the form

$$(\Delta R)_\infty = a(T - T_0) \tag{4}$$

where T_0 is a constant representing the absolute temperature at which no annealing may be observed. Generally, T_0 does not vary much for different samples assuming

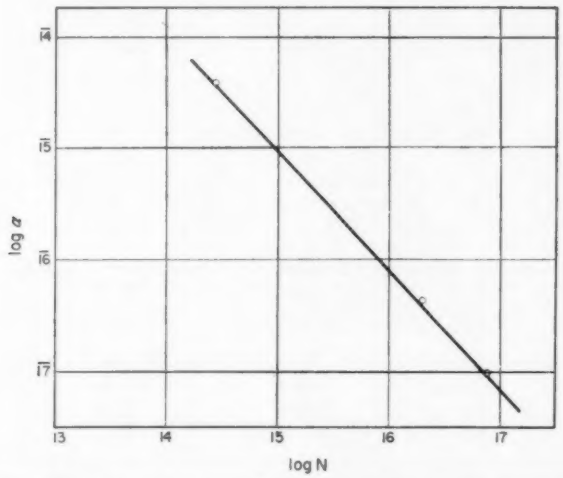

FIG. 12—The dependence of the specific annealing on the number of non-annealed atoms.

TABLE 5.—THE VALUES OF THE SPECIFIC ANNEALING AND OF THE NUMBER OF NON-ANNEALED ACTIVE ATOMS FOR THE SAMPLES A, B AND C

	A	B	C
α	$9{\cdot}70 \cdot 10^{-8}$	$4{\cdot}44 \cdot 10^{-7}$	$3{\cdot}95 \cdot 10^{-15}$
N	$6{\cdot}62 \cdot 10^{16}$	$2{\cdot}02 \cdot 10^{16}$	$2{\cdot}88 \cdot 10^{14}$

values between 134° and 138°C, as one may observe from Fig. 11. It is the constant a which varies from one sample to another.

In order to find an equation able to represent the whole family of curves, we will make the following substitution

$$a = \alpha N \tag{5}$$

where N represents the number of defects of the sample. In first approximation we consider as defects only the recoil radioactive atoms. N may be computed according to the equation

$$N = N_0 \frac{100 - R_0}{100} \tag{6}$$

where R_0 is the initial retention of the relevant sample and N_0, the number of active atoms which may be computed from the well known relation

$$N_0 = \frac{n\phi\sigma}{\lambda}(1 - e^{-\lambda t}) \tag{7}$$

here n is the number of target atoms of ^{59}Co in the sample, ϕ the thermal neutron flux, σ the activation cross-section, λ the decay constant for ^{60}Co, t the time of irradiation with neutrons. In this case α is just the percentage of annealing per atom per degree, for the particular sample. The values of α and N for the three samples are given in Table 5. Between α and N however a linear relation on a logarithmic scale may be observed, as is seen from Fig. 12. The specific annealing is greater for the samples which underwent fewer perturbations during the irradiation in the reactor. The relation between the specific annealing and the number of non-annealed atoms is of the form

$$\alpha = \alpha_0 N^{1-\beta} \tag{8}$$

where α_0 and β are constants which in this case are characteristic for a given substance, so that the relation (4) becomes

$$(\Delta R)_\infty = \alpha_0 N^{1-\beta}(T - T_0) \tag{9}$$

where the fraction which is destined to anneal is only a function of the number of non-annealed atoms and of the absolute temperature at which heating is carried out, the other quantities being characteristic constants of the substance. The values of the constants are $\alpha_0 = 92{\cdot}2$ and $\beta = 1{\cdot}128$.

In this way, at least for the case we have studied, the importance of the history, or, better still, the radiation history of the substance has been proved and an equation accounting for their effects developed.

VOL. 19 1961

J. Inorg. Nucl. Chem., 1961, Vol. 19, pp. 38 to 42. Pergamon Press Ltd. Printed in Northern Ireland

THE ELECTRONIC STRUCTURE OF URANIUM (IV) IN COMPLEX COMPOUNDS—I

COMPARISON OF THE ABSORPTION SPECTRA OF URANIUM (IV) AND PRASEODYMIUM (III) COMPOUNDS*

B. JEŻOWSKA-TRZEBIATOWSKA and K. BUKIETYŃSKA
Department of Inorganic Chemistry, Wroclaw University
Institute of Physical Chemistry,
Polish Academy of Science, Wroclaw

(*Received* 11 *August* 1960; *in revised form* 9 *September* 1960)

Abstract—The absorption spectra of U (IV) in the organic solvents: methanol, tributylphosphate, acetylacetone and tetrahydrofurane were investigated and compared with the isoelectronic praseodymium (III).

The absorption bands of U (IV) correspond to the supposed $5f^2$ electronic structure.

A much stronger influence of the ligand's field on the $5f^2$ levels than on the $4f^2$ ones was observed.

The Lande interval factor was accepted as quantitative measure, the value of which in the U (IV) depends on the type of solvent.

PREVIOUS investigations of the absorption spectra of uranium (IV) compounds have made it possible to assume the $5f^2$ electronic structure for this element.[1,2] This supposition was mainly based on a marked similarity of the U (IV) spectrum with that of other elements possessing the $5f^2$ structure. Using the Condon and Shortley theory[3] it is possible to determine the ground level as $^3H_4$, and to identify the excited states. JÖRGENSEN[1] first gave the succession of the U (IV) terms, ascribing to absorption maxima in the visible range of the spectrum the following levels: $^3P_2$ $^1I_6$, $^1G_4$, and $^1D_2$. Recently CONWAY[2] by applying another method of calculation has obtained the following succession of levels for the visible range: $^3P_1$, $^1I_6$, $^3P_2$ and $^1D_2$ or $^1G_4$. We have obtained better results using the sequence of levels given by the latter author.

Because of the stronger influence of the internal field the Lande interval factor for uranium (IV) is higher than for praseodymium (III): $\xi_{4f} = 800$ cm^{-1}—for Pr (III)[1] and $\xi_{5f} = 1870$ for U (IV) after JUDD and CONWAY[2,4]. These figures are in a rough agreement with the assumption of Sommerfield according to whom ξ_{nf} is proportional to $(Z - \sigma)^4$, where Z is the atomic number and σ the screening constant, equal to fifty-eight for $5f^2$ elements.[5]

In the present work the absorption spectra of uranium (IV) have been examined in different ligand fields, by using uranium tetrachloride dissolved in different solvents, sometimes with the addition of complexing agents. For comparison with the $4f^2$ structure analogous investigations were made with uranium tetrachloride obtained by

* This paper was presented at the XVIIth International Congress of Pure and Applied Chemistry, Section on Chemistry of actinides and lanthanides, Munchen, September 1959.

[1] C. K. JÖRGENSEN, *Kgl. Danske Videnskab. Selskab Mat. fys. Medd.* **29**, No. 7 (1955).
[2] J. G. CONWAY, U.S.A.E.C. Report UCR-8613 (1959).
[3] E. U. CONDON and G. K. SHORTLEY, *The Theory of Atomic Spectra*. Cambridge University Press (1957).
[4] J. P. ELLIOT, B. R. JUDD and W. A. RUNCIMAN, *Proc. Roy. Soc.* A **240**, 509 (1957).
[5] J. K. DAWSON, C. Z. MANDLEBERG and D. DAVIES, *J. Chem. Soc.* 2047 (1951).

chlorination of UO_2 by carbon tetrachloride[6]. The uranium content was determined cerometrically[7] as well as gravimetrically using cupferron in acidic medium. The purity of the product used was not lower than 95 per cent of UCl_4. The main impurity was UO_2 which is insoluble in organic solvents.

The absorption spectra of UCl_4 have been examined in the range 25000–12500K, on the Zeiss spectrophotometer, using the following solvents: 1M H_2SO_4 in aqueous solution, methyl alcohol, tributylphosphate (TBP), acetylacetone (Acac), and tetrahydrofuran (C_4H_8O) (Fig. 1).

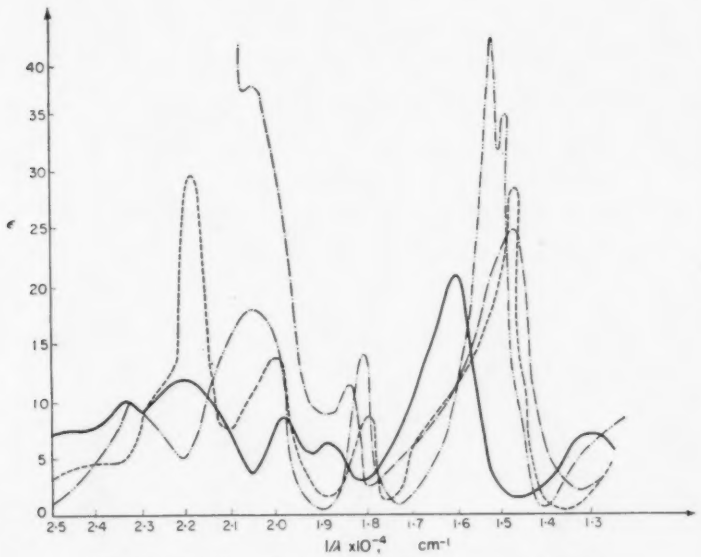

FIG. 1.—The absorption spectra of UCl_4 in various solvents.
— UCl_4 in CH_3OH
—··—·· UCl_4 in the H_2O (1M H_2SO_4)
— — — — UCl_4 in TBP
—.—. UCl_4 in Acac
UCl_4 in tetrahydrofurane.

The spectrum of the uranium tetrachloride dissolved in methanol was also examined in the presence of an excess of the complexing ligands: acetylacetone, thenoyl trifluoroacetone (TTA) and tributylphosphate (Fig. 2).

The absorption bands of uranium (IV) in different solvents are characterized by narrow and sharp maxima and relatively low intensity. These features are typical for transitions inside the *f*-shell. In the visible part of the spectrum as a rule four groups of bands occur. In organic solvents the extinction coefficients are lower than in water. A rather special picture is presented by the spectrum of uranium tetrachloride in acetylacetone. Here the *f*-transitions of uranium are not visible in the short wave range, because of overlapping with a band of high extinction coefficient. A similar band shifted toward the red is seen in the spectrum of uranium tetrachloride in methanol

[6] J. J. KATZ and G. T. SEABORG, *The Chemistry of Actinide Elements*. London, Methuen & Co. Ltd. New York, John Wiley & Sons Inc. (1957).
[7] C. J. RODDEN, Analiticeskaa khimia urana i tora Russ. transl. Izd. Innostr. Literatura Moskva (1956).
[8] M. A. ELIASEVIC, Spektry redkich zemel—Moskva (1953).

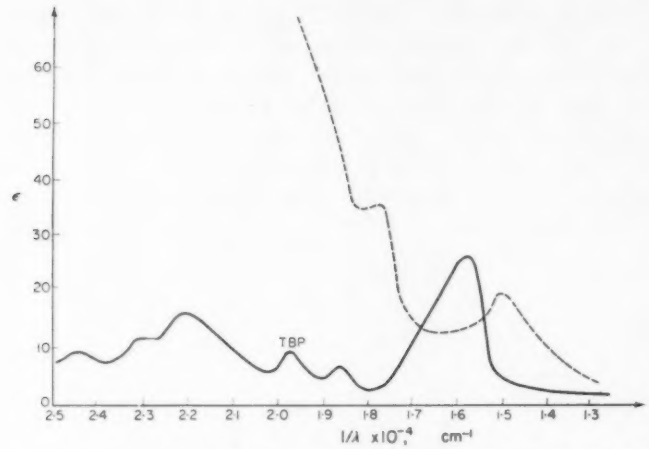

FIG. 2.—The absorption spectra of UCl_4 in methanol with excess complexing ligands.
— UCl_4 in CH_3OH with an excess of the TBP
—·—·— UCl_4 in CH_3OH with an excess of the TTA

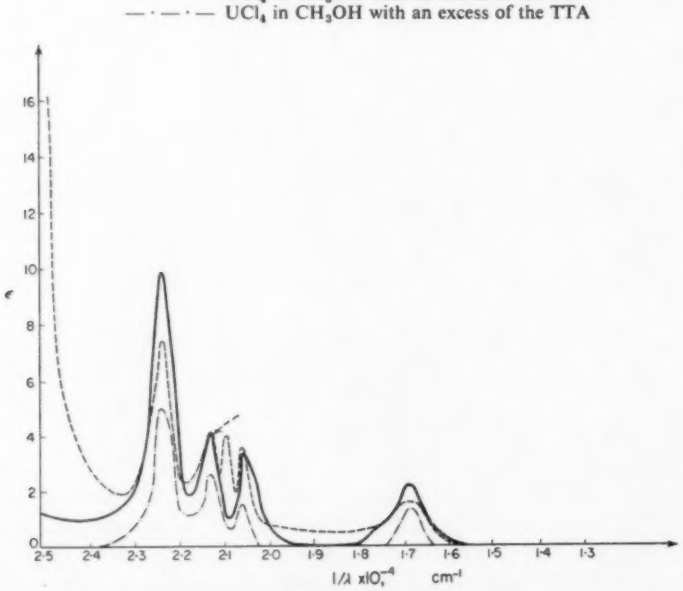

FIG. 3.—The absorption spectra of $PrCl_3$ in various solvents.
— $PrCl_3$ in water
—·—· $PrCl_3$ in CH_3OH
— — $PrCl_3$ in Acac

with an excess of thenoyltrifluoro acetone (TTA). The absorption spectra of praseodymium (III) taken over the same ranges and for the same solvents show a similarity to those of uranium (IV). The type of spectrum is generally alike, however the bands are narrower and the extinction coefficients lower. (Fig. 3). Some difference is seen as well in the influence of the solvent on the position of the absorption maxima. For uranium the maximum shift amounts to 1200 K while for the praseodymium it is 110 K.

The acceptance of the $5f^2$ structure for uranium enables one to analyze the experimental results. With this assumption and using CONWAY's results[2] the following transitions are possible here: $^3H_4$—$^3P_2$, $^3H_4$—$^1I_6$, $^3H_4$—$^3P_1$, $^3H_4$—$^1D_2$ or $^1G_4$.

TABLE 1.—THE POSITIONS OF THE ABSORPTION BANDS AND ENERGY LEVELS OF UCl_4 IN DIFFERENT SOLVENTS (CM^{-1})

Term		CH_3OH	H_2SO_4	TBP	C_4HO_8	Acac	Calc.
$^3P_2$	σ_n	22220	23860	21980	22990	—	23330
	ε_n	11·0	10·1	30·1	10·5	—	
$^1I_6$	σ_n	19800	20620	20200	21880	—	19480
	ε_n	13·4	18·6	14·2	11·5	—	
$^3P_1$	σ_n	18690	18190	18020	17860	18520	18500
	ε_n	6·4	14·6	9·0	5·7	14·5	
$^1D_2$	σ_n	16000	15440	14930	14930	14820	15664
	ε_n	21·2	42·3	29·3	22·3	25·2	

For the same range Pr (III) shows the following transitions: $^3H_4$—$^3P_2$, $^3H_4$—$^3P_1$, $^3H_4$—$^3P_0$, $^3H_4$—$^1D_2$[8]. The influence of the solvent on the position of the absorption bands of Pr (III) is negligible which points to a minute influence of the ligand field. Because the shift of the absorption maxima of $PrCl_3$ in different solvents is minute, the Lande interval factor is fairly constant and very close to the theoretical value.

TABLE 2.—THE POSITIONS OF THE ABSORPTION BANDS AND ENERGY LEVELS IN THE ABSORPTION SPECTRA OF $PrCl_3$ IN CH_3OH IN CM^{-1}

Term		$^3P_2$	$^3P_1$	$^3P_0$	$^1D_2$
Expt.	σ_n	22470	21350	20750	16810
Calc.	σ_n	22600	21400	20800	16800

The positions of the absorption maxima of UCl_4 depends on the type of solvent used. The Lande interval factor ξ was used as a measure of the influence of the ligand field. For calculation of its values, the interval between the $^3P_2$—$^3P_1$ levels was employed. This interval varied with the type of the solvent. The relation $\xi = f(\Delta\nu, J)$ was used where $\Delta\nu$ is the difference of frequencies $^3P_2$–$^3P_1$ levels, and J is the resulting quantum number.[3]

The spectrum of UCl_4 in acetylacetone cannot be discussed in these terms as the electronic transitions of uranium are here obscured by the internal π-transitions of the C═O group, because the analogous effect with TTA gives a larger shift towards the red.

The additional splittings observed in the UCl_4 spectrum are probably caused by the partial elimination of the $(2J - 1)$ fold degeneracy of the individual levels. This suggests a significant interaction with the field of the ligands.

The calculated values of ξ for the solvents discussed are the following:

$$\xi \text{ (theor)} = 1870 \text{ cm}^{-1}$$

$$\xi \ UCl_4 \text{ in } CH_3OH = 1865 \text{ cm}^{-1}$$

$$\xi \ UCl_4 \text{ in TBP} = 1980 \text{ cm}^{-1}$$

$$\xi \ UCl_4 \text{ in } C_4H_8O = 2565 \text{ cm}^{-1}$$

These values show that non-electrostatic interaction with the solvents in the case of U (IV) is considerably larger than for the isoelectronic $4f^2$ praseodymium (III), as ξ for U (IV) depends on the solvent, while for praseodymium it has a constant value. Only in methyl alcohol is ξ for U (IV) close to the theoretical value. It is somewhat higher in TBP and reaches the highest value in tetrahydrofurane. This dependence is parallel to the electron—donor properties of the solvents discussed, and points to the increasing covalent character of the UCl_4 solvent bonds. The highest proportion of covalent bonding occurs between the UCl_4 molecule and tetrahydrofuran where the formation of a bond by means of the oxygen-electron pair is realised.

The results obtained confirm the possibility of treating uranium (IV) as a $5f^2$ electron configuration. $5f^2$ orbitals being less screened than the $4f$ ones they are more easily influenced by the ligand field and therefore the energy levels of U (IV) are more changed by the ligand field than has been found in the case of the rare earths.

Acknowledgement—The authors thank Dr. K. V. NAIR for assistance with the spectrophotometric measurements.

J. Inorg. Nucl. Chem., 1961, Vol. 19, pp. 43 to 50. Pergamon Press Ltd. Printed in Northern Ireland

HYBRIDIZATION AND BOND PROPERTIES

EFFECTS OF SECOND-ORDER HYBRIDIZATION ON THE σ-BONDS IN THIONYL, SULPHURYL, PHOSPHORUS, PHOSPHORYL AND THIOPHOSPHORYL HALIDES

H. A. BENT
School of Chemistry, Institute of Technology
University of Minnesota, Minneapolis, Minnesota

(*Received* 26 *April* 1960; *in revised form* 14 *September* 1960)

VOL. 19 1961

Abstract—Effects of orbital hybridization and electronegative substituents on bond angles, bond lengths, bond moments, bond dissociation energies, force constants and proton–C^{13} coupling constants, are reviewed. It is inferred that the *s*-character of an atom tends to concentrate in orbitals directed toward electropositive substituents and that this "second-order hybridization" may account, in part, for the shapes of SOF_2, SO_2F_2, and the family of compounds PX_3, PSX_3, POX_3, X=F, Cl, Br.

THE marked effect orbital hybridization has on inter-bond angles is well known. Less well known is the suggestion that orbital hybridization may have a marked effect on other molecular properties, such as bond moments, force constants, coupling constants, bond dissociation energies, and bond lengths.

It appears well established, for example, that bond lengths decrease as the *s*-content in the bonding orbital increases.[1] For carbon–carbon single bonds, this decrease may amount to nearly 0·04 Å when the hybridization of one of the atoms participating in the bond changes from sp^3 to sp^2 or from sp^2 to sp. Thus whereas the C(sp^3)–C(sp^3) interatomic distance is typically 1·54 Å (ethane, propane, diamond), the C(sp^3)–C(sp^2) distance is typically only 1·50 Å (acetaldehyde, propene), the C(sp^3–C(sp) distance 1·46 (methyl acetylene, methyl cyanide), and so forth.[1] Bond stretching force constants may be similarly classified. The carbon–carbon stretching force constants for ethane (sp^3–sp^3), methyl acetylene and methyl cyanide (sp^3–sp), and cyanogen (sp–sp) are, respectively ($\times 10^{-5}$): 4·5, 5·3 and 5·5, and 6·7 dyne/cm.[2] Bond dissociation energies show a similar trend. Values for some C–C bonds are (in kcal/mole): CH_3–CH_3 83; CH_3–C_2H_3 92·5; CH_3–CN 103, C_2H_3–C_2H_3 104; NC–CN 112.[3]

Polar effects provide further evidence of the importance of orbital hybridization on molecular properties; for, as has been pointed out, the electronegativity of an atomic valency should increase as the *s*-character in that valency increases:[4] a carbon *sp* valency, for example, should be more electronegative than a carbon sp^2 valency, which, in turn, should be more electronegative than a carbon sp^3 valency. This prediction is in good agreement with the inductive constants that have been given

[1] M. G. BROWN, *Trans. Faraday. Soc.* **55**, 694 (1959). See, also, C. C. COSTAIN and B. P. STOICHEFF, *J. Chem. Phys.* **30**, 777 (1959); G. R. SOMAYAJULU, *J. Chem. Phys.* **31**, 919 (1959); and C. A. COULSON, *Victor Henri Commemorative Volume*, p. 15, Maison Desoer, Liege (1947–1948).
[2] J. W. LINNETT, *Quart. Revs.* **1**, 73 (1947).
[3] A. G. HARRISON and F. P. LOSSING, *J. Amer. Chem. Soc.* **82**, 519 (1960); T. L. COTTRELL, *The Strengths of Chemical Bonds*. Academic Press, New York (1954).
[4] R. S. MULLIKEN, *J. Phys. Chem.* **41**, 318 (1937); A. D. WALSH, *Disc. Faraday. Soc.* **2**, 18 (1947); W. MOFFITT, *Proc. Roy. Soc.* A **202**, 548 (1950).

recently for the cyanide, acetyl, and methyl groups (+1·30, +0·60 and −1·00, respectively, with chlorine, on this scale, at +1·10)[5] and the carbon–carbon bond moments for the pairs sp^3–sp^2, sp^2–sp, and sp^3–sp (0·68, 1·15 and 1·48 debyes, respectively, in the direction + −, with chlorine, it is found, at the positive end of the C–Cl bond moment in HC≡CCl).[6] Measurements on the intensities of the vibrational transitions in methyl acetylene[7] appear to be in essential agreement with these estimates of the polarity of the C(sp^3)–C(sp) bond.

Chemical evidence lends further support to this picture. Base strength, for example, generally increases as the *s*-character in the orbital occupied by the unshared electrons decreases. Thus ketones and aldehydes, whose unshared electrons are in oxygen sp^2-type hybrid orbitals, are generally weaker bases (poorer proton acceptors) than ethers and alcohols, whose unshared electrons are in oxygen sp^3-type hybrid orbitals; N_2 is a weaker base than pyridine, which is weaker than ammonia (the unshared electrons in these compounds are, respectively, in nitrogen *sp*-, sp^2- and sp^3-type hybrid orbitals); and acetylene, as an acid, is stronger than ethylene, and ethylene is a stronger acid than methane, which implies that the order of base strength (with the type of hybridization of the carbonion carbon atom in parentheses) is: $HC{\equiv}C{:}^-(sp) < H_2C{=}CH^- < H_3C{:}^-(sp^3)$.

The changes in bond properties described above may be ascribed largely to changes in first-order hybridization: hybridization of the type sp^3, sp^2 or *sp*. It seems likely, however, that only a relatively small fraction of all molecules contain atoms hybridized exactly sp^3, sp^2 or *sp*. The carbon atom in methane is generally described as hybridized sp^3, but other members of the isoelectronic sequence, ammonia, water and still more hydrogen fluoride, are hybridized somewhat differently; nor are the carbon atoms in ethylene hybridized exactly sp^2.[8] Numerous other examples could be cited. Departures of this type from exact sp^3-, sp^2 or *sp*-type hybridization have been termed second-order hybridization,[9] or isovalent hybridization.[10]

Familiar rules exist for determining the first-order hybridization of an atom in a molecule, particularly atoms from the first row of the periodic table. These rules are the rules of structural chemistry: e.g., the octet rule, and rules governing formal charges.[11] One may ask whether supplementary rules exist for predicting the second-order hybridization of an atom. It is suggested in the following section that second-order hybridization does follow a predictable pattern. This pattern is summarized in a rule, the evidence for which is discussed, following which the rule is used to discuss the structures of several compounds of sulphur and phosphorus.

SECOND-ORDER HYBRIDIZATION IN MOLECULES

Examination of the effect of electronegative substituents on bond angles, bond lengths, and proton–C^{13} coupling constants suggests this rule: *The s-character of an*

[5] R. W. TAFT, JR., *Steric Effects in Organic Chemistry* (Edited by M. S. NEWMAN), Ch. 13, John Wiley, New York (1956).
[6] A. J. PETRO, *J. Amer. Chem. Soc.* **80**, 4230 (1958).
[7] I. M. MILLS and H. W. THOMPSON, *Proc. Roy. Soc.* A **228**, 287 (1955).
[8] L. S. BARTELL and R. A. BONHAM, *J. Chem. Phys.* **27**, 1414 (1957); H. C. ALLEN, JR. and E. K. PLYLER, *J. Amer. Chem. Soc.* **80**, 2673 (1958).
[9] W. MOFFITT, *Proc. Roy. Soc.* A **202** 534 (1950).
[10] R. S. MULLIKEN, *J. Phys. Chem.* **56**, 295 (1952).
[11] (a) G. N. LEWIS, *J. Chem. Phys.* **1**, 17 (1933); (b) L. PAULING, *Victor Henri Commemoratif Volume* p.1. Maison Desoer, Liege (1947–1948), *J. Chem. Soc.* 1461 (1948); *J. Phys. Chem.* **56**, 361 (1952).

atom tends to concentrate in orbitals that the atom uses toward electropositive substituents. In applications of this rule, lone pair electrons are to be regarded as electrons in bonds to very electropositive atoms (atoms of zero electronegativity). Experimental evidence for this rule, which governs the direction of second-order hybridization, may be listed as follows.

Evidence from bond angles.[12] In the compounds OX_2, $X{=}CH_3$, H, and F, the XOX angles are, respectively, 111°, 105° and 103°. For NX_3, the corresponding angles are 109°, 106°46′, 102°30′. These data suggest that as the electronegativity of the substituent X increases, the central atom diverts increasing amounts of *s*-character to the orbital, or orbitals, occupied by the lone pair electrons. Additional examples have been cited by MELLISH and LINNETT.[13] It is an interesting fact that these changes in inter-bond angles are sometimes in the reverse direction from what one would expect were repulsions between nonbonded atoms the most important effect operating. One explanation for this directs attention to the electrostatic interactions that exist between substituents such as hydrogen and fluorine and the lone pair electrons on the central atom. The latter would attract protons, but repel fluorine atoms. However, this explanation appears to leave unexplained (see below) the effect of electronegative substituents on bond lengths.

Evidence from bond lengths.[12] At first sight it is surprising to find that *in the series* CH_3F, CH_2F_2, CHF_3, CF_4, *the* C–F *bond decreases monotonically in length* (and reactivity).[14] The distances are, respectively: 1·391–1·385, 1·358, 1·332–1·326, and 1·323 Å (Table 1). Similar, albeit smaller, effects are observed with chlorine[15] and bromine (Table 1). Several other examples of the shortening in the structure X—C—Y of the X—C bond when Y is replaced by an atom or group of atoms of greater electronegativity are cited in Table 1. Si—C bonds show the same trend in the series $SiMe_4$, $SiMe_3H$, $SiMe_2H_2$, $SiMe_3H$ (the distances are, respectively: 1·888, 1·873, 1·860, 1·857 Å),[16] as do the M-halogen bonds on further halogen substitution in the chlorinated and brominated silanes, the methyltin chlorides, bromides and iodides and the methylarsenic chlorides.[17] The evidence points to a definite phenomenon. Again, it is interesting to note that the effect is often in the reverse direction from what one would expect were repulsions between nonbonded atoms the important effect operating. It seems possible that shortening of adjacent bonds by electronegative substituents arises, at least in part, from the tendency of an atom to concentrate *s*-character in orbitals toward electropositive groups.

Evidence from proton–^{13}*C coupling constants.*[18] The ^{13}C nucleus has a magnetic moment. This magnetic moment can couple with the magnetic moment of a bonded proton via magnetic interactions with the magnetic moments of the intervening bonding electrons. Theory predicts that the magnitude of the magnetic interaction between a proton and an adjacent ^{13}C nucleus should depend on the probability of finding the binding electrons at the two nuclei in question. Since an electron in a pure

[12] L. E. SUTTON (Editor), *Tables of Interatomic Distances and Configuration in Molecules and Ions*, Special Publ. No 11, London (1958); also, H. A. BENT, *J. Chem. Phys.* In press.
[13] C. E. MELLISH and J. W. LINNETT, *Trans. Faraday. Soc.* **50**, 657 (1954).
[14] L. S. BARTELL and L. O. BROCKWAY, *J. Chem. Phys.* **23**, 1860 (1955); L. O. BROCKWAY, *J. Phys. Chem.* **41**, 185 (1937).
[15] H. J. BERNSTEIN, *J. Phys. Chem.* **56**, 351 (1952).
[16] A. C. BOND and L. O. BROCKWAY, *J. Amer. Chem. Soc.* **76**, 3312 (1954).
[17] T. L. COTTRELL and L. E. SUTTON, *Quart. Revs.* **2**, 260 (1948); H. A. SKINNER and L. E. SUTTON, *Trans. Faraday Soc.* **40**, 164 (1944).
[18] N. MULLER and D. E. PRITCHARD, *J. Chem. Phys.* **31**, 768, 1471 (1959).

VOL. 19 1961

p-orbital has zero probability of being found at the nucleus, whereas this quantity is finite for an electron in an *s*-orbital, it is to be expected that the coupling will depend on the state of hybridization of the carbon atom, and this appears to be the case. In methane, benzene, and methyl acetylene, the coupling constants are, respectively: 125, 159, and 248 sec^{-1}.[18] If it is taken as established by this series that the greater the *s*-character in a carbon valency toward hydrogen, and, hence, the greater the probability of finding the bonding electrons at the ^{13}C nucleus, the greater the coupling

TABLE 1.—EFFECT OF ELECTRONEGATIVE GROUPS ON THE LENGTH OF AN ADJACENT BOND

Compound	Bond	Bond length (Å)
CH_3F	C–F	1·391–1·385
CH_2F_2		1·358
CHF_3		1·332–1·326
CF_4		1·323
CH_3Cl	C–Cl	1·784–1·781
CH_2Cl_2		1·772
$CHCl_3$		1·767–1·761
CCl_4		1·766–1·760
CH_3Br	C–Br	1·939
$CHBr_3$		1·930
CH_3Cl	C–Cl	1·784–1·781
CCl_2F_2		1·775
CF_3Cl		1·751
C_2H_6	C–C	1·536
C_2F_6		1·51

constant, then the observed trend in coupling constants for the series CH_3Cl, CH_2Cl_2, $CHCl_3$ (150, 178, 209 sec^{-1})[18] supports the supposition that substitution on carbon of an electronegative atom (chlorine) for an atom (hydrogen) of lesser electronegativity causes the atom on which substitution occurred (carbon) to rehybridize slightly so as to increase the *s*-content of the orbital, or orbitals, toward the more electropositive atom(s). This second-order hybridization should cause a steady decrease in the C–H distance; the values reported for the series above are: 1·0959, 1·082, 1·07 Å.

APPLICATIONS

The shapes of several covalent molecules containing sulphur and phosphorus are examined in this section with a view to establishing in a qualitative manner the extent to which effects arising from second-order hybridization among σ-bonds may be important in determining details of molecular geometry about atoms of the second row of the periodic table.*

Thionyl and sulphuryl fluoride. . Accurate structural parameters are known for

* Additional applications to compounds of the first-row elements will be given in a subsequent publication.

thionyl[19] and sulphuryl fluoride.[20] These are given in Fig. 1 beneath the Lewis octet structures for these two molecules. Not shown in these valence-bond structures are d_π–p_π bonds between sulphur and the surrounding atoms. On formal charge grounds,[11b] it seems likely that such bonds are formed between sulphur and oxygen,[21] but not between sulphur and fluorine. Accordingly, changes in the S–F bond in passing from one compound to the other may be viewed as arising, at least in part, from changes in hybridization of the σ-orbitals of sulphur.

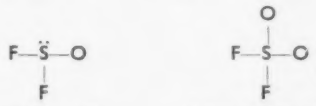

	Thionyl fluoride	Sulphuryl fluoride
S–O distance	1·412 Å	1·405 Å
S–F distance	1·585 Å	1·503 Å
FSF angle	92° 49′	96° 7′

FIG. 1.—Structures of thionyl and sulphuryl fluoride.

As shown in Fig. 1, the shapes of SOF_2 and SO_2F_2 are determined primarily by the σ-orbitals of sulphur. The two molecules differ chiefly in the fact that the lone pair on sulphur in SOF_2 is shared with an oxygen atom in SO_2F_2. In view of the strong *s*-seeking character of unshared electrons, it is to be anticipated that the S–O and S–F σ-bonds in SOF_2 will receive less *s*-character from sulphur than do the corresponding bonds in the more fully oxygenated compound. One observes that in fact the S–O and S–F interatomic distances are greater, and the FSF angle is smaller, in SOF_2 than in SO_2F_2, in agreement with the effects anticipated for second-order rehybridization of the sulphur atom.

Phosphorus, phosphoryl and thiophosphoryl trihalides. Trends similar to those observed for thionyl and sulphuryl fluoride occur in the trihalides of phosphorus and their phosphoryl and thiophosphoryl derivatives. Structural parameters[12] and Lewis structures for these molecules are given in Fig. 2. One sees that as the non-halogen

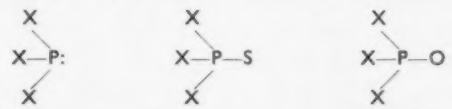

	Phosphorus trihalide		Thiophosphoryl trihalide		Phosphoryl trihalide	
	P–X	XPX	P–X	XPX	P–X	XPX
X = F	$1·53_5$	(100°)	1·53	100·3°	1·52	102·5°
Cl	$2·04_4$	99·9°	2·02	100·5°	1·99	103·6°
Br	2·23	100°	2·13	106°	2·06	108°

FIG. 2.—Structures of phosphorus, thiophosphoryl and phosphoryl trihalides.

substituent off the fourth orbital of the phosphorus atom changes from a lone pair (electrons in a bond to an atom of zero electronegativity) to a sulphur atom and, then to the still more electronegative atom oxygen, *s*-character appears to be diverted from this phosphorus orbital to the P–X bonds, causing these bonds to become shorter and the PX_3 group to become more open. Interestingly, the effects seem smallest in the

[19] R. C. FERGUSON, *J. Amer. Chem. Soc.* **76**, 850 (1954).
[20] D. R. LIDE, JR., D. E. MANN and R. M. FRISTROM, *J. Chem. Phys.* **26**, 734 (1957).
[21] W. MOFFITT, *Proc. Roy. Soc.* A **200**, 409 (1950); G. CILENTO, *Chem. Revs.* **60**, 147 (1960).

fluorine and largest in the bromine compounds. One reason for this may be that the phosphorus orbital plays a more important role in the slightly polar P–Br bond than it does in the highly polar P–F bond.

Other applications. In compounds of the type X_2YSO, there is a correlation between the length of the sulphur–oxygen bond and the electronegativities of the substituents X and Y. This correlation is in the direction that one would expect from the previous discussion: The greater the electronegativities of X and Y, the shorter the S–O bond. This is illustrated by the series Cl_2 (unshared pair)–SO, F_2 (unshared pair) SO, F_2OSO. Lewis structures and S–O bond lengths for these molecules are given in Fig. 3.

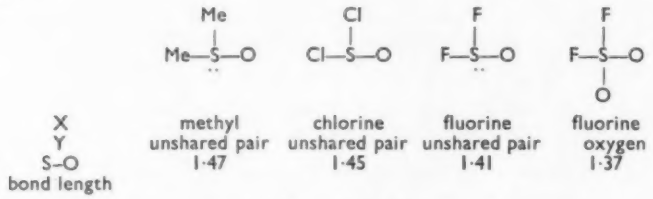

FIG. 3.—S–O bond lengths (in angstroms) in X_2YSO compounds. The series $SOCl_2$, SOF_2, SO_2F_2.

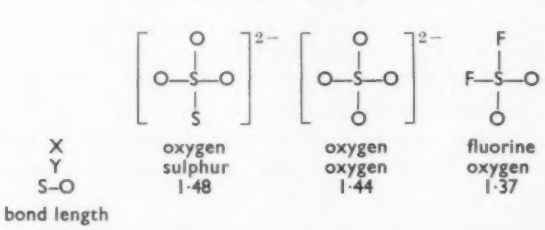

FIG. 4.—S–O bond lengths (in angstroms) in $S_2O_3^{2-}$, SO_4^{2-} and SO_2F_2.

Another series of this type, O_2SSO^{2-}, O_2OSO^{2-}, F_2OSO, is illustrated in Fig. 4.

The examples that have been discussed in this section have so far been limited to two second-row elements: sulphur and phosphorus. For these elements, we have seen in several instances that in structures of the type Y–A–X, A = S or P, the A–X bond becomes shorter as the electronegativity of Y increases. The data in Fig. 5 suggest that this rule may hold also for A = Cl (and X = O). (All structures in Fig. 5 carry a net charge of −1.)

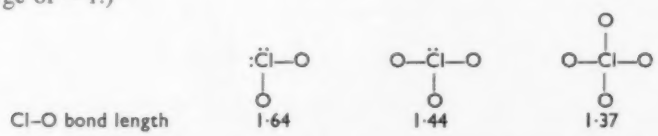

FIG. 5.—Bond lengths (in angstroms) in the ions O_n (unshared pair)$_{3-n}ClO^{-1}$, $n = 1, 2, 3$.

We may summarize this rule in the statement that for Lewis structures of the type Y–A–X, A = a first- or second-row element,

$$\frac{\delta[d(\text{A–X})]}{\delta\chi_Y} < 0.$$

Here d(A–X) is the length of the A–X bond and χ_Y is the electronegativity of Y.

Several factors might be listed as underlying causes for this rule. Of the three

(1) σ-orbital hybridization
(2) formal charges
(3) d_π–p_π bonding

it may be noted: that both the first factor (s-character tends to concentrate in orbitals toward electropositive groups; and the more s-character in a bond, the shorter that bond tends to be) and the second factor (the A–O bond tends to become shorter as the formal charge on A increases) are consistent with the trends exhibited in Figs. 3, 4, and 5; that the third factor, important though it may be in some cases, cannot explain the rule when A is a first-row element; and that of the first two factors, only one of them, the first one, is consistent with the trend in the S–S bond length illustrated in Fig. 6. (All structures in Fig. 6 carry a net charge of −2.)

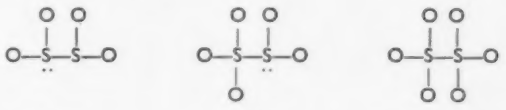

S–S bond length	2·389	2·209	2·15–2·16

FIG. 6.—S–S bond length (in angstroms) in the ions $S_2O_4^{2-}$, $S_2O_5^{2-}$, and $S_2O_6^{2-}$.

SUMMARY

The suggestion that orbital hybridization may have a marked effect on molecular properties receives support from the present review of data on bond angles, bond moments, proton–^{13}C coupling constants, and parameters generally associated with the strengths of chemical bonds: viz. bond dissociation energies, bond stretching force constants and bond lengths. As a general rule, bond strength appears to increase with increasing s-content.

For atoms from the first row of the periodic table, the s-content of a hybrid σ-orbital may be assessed in a first approximation by means of a widely used rule that consists of separating the manifold variations of hybridization that occur in practice into three classes: sp, sp^2 and sp^3. The advantages of this classification are that it is simple, that it corresponds remarkably well to the known facts, that definite and familiar rules exist whereby it can be quickly determined to which class an atom belongs, and that such a classification lends itself to a simple refinement.

This refinement states that the s-character of an atom tends to concentrate in orbitals that the atom uses toward electropositive substituents.* Evidence for this is found in the effects of electronegative substituents on bond angles, bond lengths, and proton–^{13}C coupling constants.

While much of the data presented here concerning the effects of orbital hybridization on molecular properties, and the direction of second-order hybridization, are for atoms from the first row of the periodic table free from complications of participating d-orbitals, it seems likely that data of similar accuracy for heavier atoms would reveal similar trends. Provisional verification of this conjecture has been

* It is the same thing to say that p-character tends to concentrate in orbitals toward electronegative groups.

presented here for S–F, S–O, and P–halogen bonds. S–S bonds in S_4N_4, $S_2O_4^{2-}$, $S_2O_6^{2-}$, and S_8 have been discussed recently from a similar point of view, the belief being expressed that bond lengths in these compounds are principally determined by the *s*-character of the hybrid orbitals which form the σ-bonds.[22]

[22] I. LINDQVIST, *J. Inorg. Nucl. Chem.* **6**, 159 (1958): I. LINDQVIST and M. MÖRTSELL, *Acta Cryst.* **10**, 406 (1957).

J. Inorg Nucl. Chem., 1961, Vol. 19, pp. 51 to 60. Pergamon Press Ltd. Printed in Northern Ireland

ABSORPTION SPECTRA OF SOME TETRAHALOGENOMANGANATES (II)

C. FURLANI AND A. FURLANI
Istituto di Chimica Generale, University of Rome and Istituto di Merceologia, University of Trieste

(*Received* 4 *August* 1960, *in revised form* 25 *October* 1960)

Abstract—Tetrahalogenomanganate(II) salts of onium cations exhibit in nonaqueous polar solvents a spectrum which is characteristic of tetrahedral $[MnHal_4]^{2-}$ anions, and consists of several bands grouped in three distinct absorption regions; experimental details on the measured spectra are reported. The observed form of the spectrum can be satisfactorily accounted for on the basis of ligand-field theory predictions for spin-forbidden transitions from the groundstate ^6S of Mn^{2+} to excited quartet states of d^5 arising under a field of symmetry T_d, assuming $\Delta \sim 3300\ cm^{-1}$. Absorption intensities are higher by a factor 10–100 than the intensities of octahedral Mn^{2+} complexes.

VOL. 19 1961

TETRAHALOGENOMANGANATES(II) are the most representative and well-known examples of tetrahedral complexes of Mn^{2+}. JØRGENSEN[1] reported the preparation and some data on the absorption spectra of the solid salt $[(C_2H_5)_4N]_2[MnBr_4]$ and of non-aqueous solutions supposed to contain tetrahedral complex species of Mn^{2+}. More recently GILL and NYHOLM[2] and NALDINI and SACCO[3] prepared several salts containing tetrahedral halogenated manganese(II) complexes of the general formula $[R_4A]_2[MnX_4]$, where A = N, P, As and X = Cl, Br, J; the former authors gave also a partial description of their absorption spectra in solution. A theoretical treatment of tetrahedral Mn^{2+} complexes has been given by SCHLÄFER[4]; it is however to be noticed that the well-known crystal-field interpretation of the spectra of octahedral complexes of Mn^{2+} [5–8] can be simply and directly applied also to d^5-tetrahedral complexes, since the perturbation due to the ligand field in cubic d^5 is independent of the sign of Δ, so that even the order of succession of the energy levels is equal in both cases.

We now report on a more detailed investigation of the absorption spectra of tetrahalogenomanganate(II) complexes and a systematic comparison of the experimental facts with the predictions of crystal-field theory, since we felt that such a study could still be useful and bring new results.

Adopting the procedure described by the authors already mentioned[2,3] we have prepared several new tetrahalogenomanganates(II) of onium cations, which are listed under "Experimental part". They are all more or less soluble in non-aqueous polar solvents, e.g. in nitromethane, dimethylformamide or acetonitrile. Alcohols, especially methanol and ethanol, dissolve them with partial decomposition; water hydrolyzes them instantaneously. When dissolved in polar solvents, these salts

[1] C. K. JØRGENSEN, *Acta Chem. Scand.* **11**, 53 (1957).
[2] N. S. GILL and R. S. NYHOLM, *J. Chem. Soc.* 3997 (1959).
[3] L. NALDINI and G. SACCO, *Gazz. Chim. Ital.* **89**, 2258 (1959).
[4] H. L. SCHLÄFER, *Z. Phys. Chem. N.F.* **4**, 116 (1955).
[5] C. K. JØRGENSEN, *Acta Chem. Scand.* **8**, 1502 (1954).
[6] L. E. ORGEL, *J. Chem. Phys.* **23**, 1004, 1824 (1955).
[7] Y. TANABE and S. SUGANO, *J. Phys. Soc. Japan*, **9**, 753, 766 (1954).
[8] L. J. HEIDT, G. KOSTER and A. M. JOHNSON, *J. Amer. Chem. Soc.* **80**, 6471 (1959).

behave as uni-bivalent electrolytes and exhibit a slightly yellow colour, which is due to the anions $[MnCl_4]^{2-}$ or $[MnBr_4]^{2-}$. The absorption spectra of the solutions (see Fig. 1) are independent of the cation and are practically identical in all solvents where the complex anions $[MnHal_4]^{2-}$ are stable, and are furthermore quite similar to the reflexion spectra of the solid salts. The main features of the spectra of solutions can be summarized as follows:

(1) The spectra consist of several bands, the number and type of which correspond closely to those observed for octahedral complexes of Mn^{2+}. Such bands correspond to

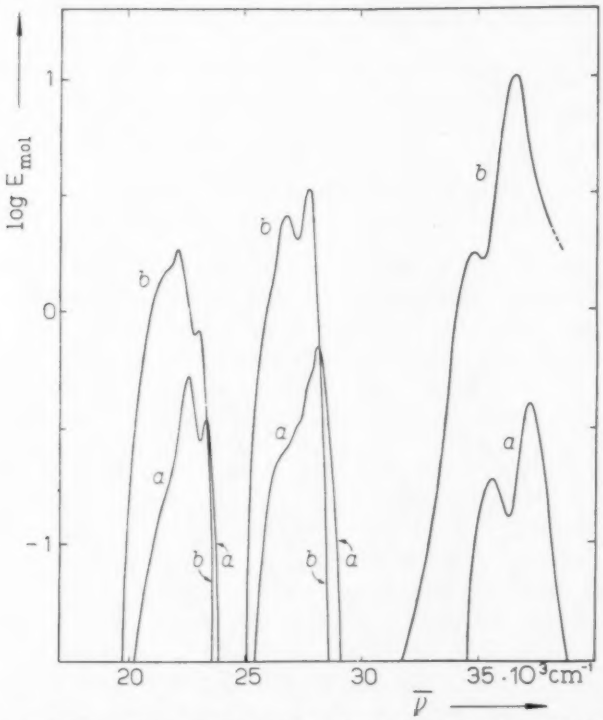

FIG. 1.—Absorption spectra of the anions $[MnCl_4]^{2-}$ (a) (0·2 M $[(CH_3)_3(C_6H_5(N_2)N]_2[MnCl_4]$ in dimethylformamide plus 0·1 M excess Cl^-) and $[MnBr_4]^{2-}$ (b) (0·2 M $[(C_2H_5)_4N]_2[MnBr_4]$ in acetonitrile plus 0·1 M excess Br^-); right hand third of both spectra extrapolated from measurements in CH_3OH.

transitions from the groundstate $^6A_1(^6S)$ to the ten levels into which the quartet terms ^4G, ^4P, ^4D and ^4F of Mn^{2+} are split under a field of symmetry T_d. The proposed assignment of the absorption peaks is given in Table 1.

(2) The maxima of the observed bands have log E_{mol} ranging from $-0{\cdot}5$ to $+1{\cdot}0$, i.e. the bands are much more intense than in octahedral Mn(II) complexes. The transitions giving rise to the observed spectrum are actually spin-forbidden, so that one would expect very low absorption intensities (log E_{mol} is ~ -1 for octahedral Mn(II) complexes), but the relatively high intensity observed here is explained by the fact that another selection rule which normally tends to lower the intensity of ligand field bands, i.e. the rule regarding the non-combinability of states of equal parity, becomes less effective in tetrahedral Mn(II) complexes, since under a field of symmetry

VOL. 19 1961

TABLE 1.—ABSORPTION SPECTRA OF $[MnCl_4]^=$ AND $[MnBr_4]^=$

Proposed assignment: transition from $^6A_1$ to	Calcd. frequency (cm^{-1}) for $\Delta = 3300$ cm^{-1} and term distances decreased by 13–18% (see text)	$[MnCl_4]^=$			$[MnBr_4]^=$			Previous works
		Observed frequency (cm^{-1})	Half-width (cm^{-1})	E_{mol}	Observed frequency (cm^{-1})	Half-width (cm^{-1})	E_{mol}	
$^4T_1(^4G)$	21000	21300(*s*)*	broad	~0·16	21600(*s*)	900(−)	1·5	7, 10
$^4T_2(^4G)$	22800	22530(*m*)	500(−)	0·54	22160(*m*)	500(+)	1·84	7, 10
$^4A_1$, $^4E(^4G)$	23180	23180(*m*) 23400(*s*)	420(+)	0·32	23040(*m*)	350(+)	0·87	7, 10
$^4T_1$, (^4P)	27200	26600(*s*)	700(−)	0·23	26750(*m*)	680(−)	2·50	10
$^4T_2(^4D)$	27360	27300(*s*) 27650(*s*)	—	~0·45				
$^4E(^4D)$	27920	28060(*m*)	450(+)	0·72	27690(*m*)	380(+)	3·32	7
$^4A_2(^4F)$	35600	35600(*m*)	750(−)	0·19	34780(*m*)	~800(−)	1·78	
$^4T_1(^4F)$	35830							
$^4T_2(^4F)$	36500	37120(*m*)	700(∓)	0·41	36450(*m*)	650(∓)	10·2	

* *s* = shoulder, *m* = maximum

T_d (i.e. hemihedral, no inversion centre) the electronic states have no longer definite g or u character. The absorption bands show therefore an increase in intensity, which is comparable to the increase observed in tetrahedral complexes of Co^{2+}[9] and of Ni^{2+}[2,10] with respect to the corresponding octahedral complexes. We deal here with a spectrum consisting of spin-forbidden but not Laporte-forbidden bands; such a situation is quite unusual, since most spectra of transition-metal complexes exhibit spin-allowed but Laporte-forbidden bands (ligand field bands), which, however, occur with intensities not higher than the intensities which we have observed in $[MnCl_4]^{2-}$ or $[MnBr_4]^{2-}$. Especially the shortest-wave band in the spectrum of $[MnBr_4]^{2-}$ ($^6A_1 \rightarrow {}^4T_2(F)$), which has $E_{mol} \sim 10$, is exceptionally intensive for a spin-forbidden band.

(3) As a consequence of the smaller intensity of the ligand field, the spectrum of tetrahedral Mn^{2+} complexes, unlike octahedral complexes, does not exhibit a succession of several bands spaced at comparable intervals, but consists of only three distinct absorption regions, where the ten expected transitions are grouped:

(a) transitions to the split terms of the level ^4G are located in the region between 21000 and 24000 cm^{-1}.
(b) transitions to the sublevels derived from ^4P and ^4D fall into the region 26000–29000 cm^{-1}.
(c) transitions to the sublevels derived from ^4F fall into the region 35000–38000 cm^{-1}.

All bands of tetrahedral Mn^{2+}-complexes are rather narrow, according to the weak intensity of the ligand field, which causes the slopes in the Orgel diagram to be very small (observed half-widths are of the order 400–600 cm^{-1}).

(4) A comparison between calculated (see Fig. 2) and observed position of the absorption bands shows that the best agreement with theory is attained if one assumes $\Delta = 3300$ cm^{-1} together with a decrease of 13–18 per cent of the term distances with respect to the free manganous ion. Remembering that Δ is 7800 cm^{-1} for the hexaaquo ion and 8–10000 cm^{-1} for other octahedral complexes of Mn^{2+}[6,8], whilst the decrease of term distances is 6–8 per cent[6,8], we can easily realize that the observed spectrum of tetrahalide complexes of Mn^{2+} corresponds very closely to the predictions of ligand field theory, since $|\Delta_{tetr.}|$ is almost exactly 4/9 of $\Delta_{oct.}$ (or even a little less, because Cl and Br are placed after water in the spectrochemical series), and the decrease of term distances is here more conspicuous, in accordance with the position of chlorine and bromine in the nephelauxetic series. Spectral differences between $[MnCl_4]^{2-}$ and $[MnBr_4]^{2-}$ are rather small, and can anyway be explained by assuming a slightly smaller Δ and a slightly larger decrease of term distances for the bromo- than for the chlorocomplex.

There are several minor details of the theoretical interpretation, such as the actual choice of parameter values, and the fact that the ^4F term apparently requires a larger decrease of electrostatic repulsion parameters, which deserve further consideration; for a discussion of them, see below under "Ligand field calculations".

The preparation of solid salts containing tetrahalogenomanganate(II) anions is

[9] C. J. BALLHAUSEN and C. K. JØRGENSEN, *Acta Chem. Scand.* **9**, 397 (1955); C. J. BALLHAUSEN and A. D. LIEHR, *Mol. Phys.* **2**, 212 (1958).
[10] D. M. GRUEN and R. L. MCBETH, *J. Phys. Chem.* **63**, 3931 (1959); C. FURLANI and G. MORPURGO. *Z. Phys. Chem.* N.F. 27 (1961) (in press).

performed best of all with large cations such as tetraalkylammonium or tetraphenylarsonium but the presence of such onium cations is not strictly necessary if we want only to form a tetrahalogenomanganate(II) anion in solution. We have observed the formation, at least in part, of these anions (revealed through the development of a yellow colour) by simply mixing alcoholic solutions of Mn(II) halides (even not

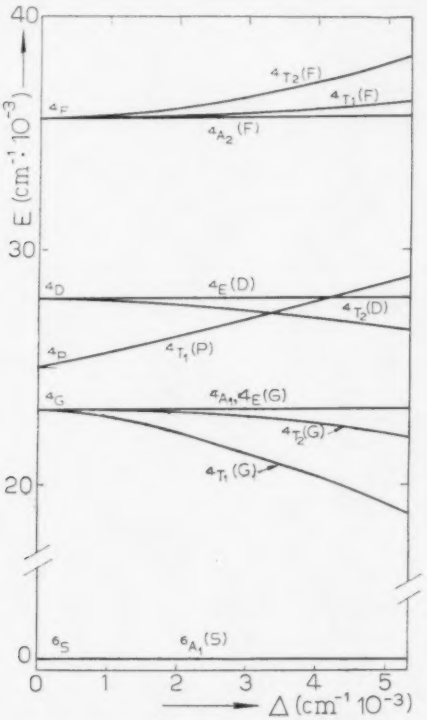

FIG. 2.—Splitting of the quartet levels of the configuration d^5 under a weak crystal field of cubic symmetry, assuming reduced term distances (see text under "Ligand field calculations")

anhydrous) with alcoholic solutions of Li or Ca halides (see Fig. 3). The formation of $[MnHal_4]^{2-}$ is under these circumstances far from being quantitative and its degree of completion depends on the amount of halide ions employed in excess; the incompleteness of the reaction is undoubtedly due to the solvent, since we have observed that appreciable decomposition (formation of octahedral alcoholates or chloride-alcoholates) occurs also on dissolving a solid tetrahalogenomanganate(II) salt in alcohol, even if anhydrous. On the other hand, tetrahedral $[MnHal_4]^{2-}$ ions are stable in other solvents already cited, e.g. in nitromethane; spectra of solutions prepared by dissolving a solid tetrahalide salt in one of such solvents show no significant variation in presence or in absence of an excess of the corresponding free halide ion. Water, on the contrary, decomposes readily and completely the tetrahalogenomanganate(II) anions; in aqueous solutions we have not been able to detect any spectral evidence of tetrahedrally coordinated manganese(II) species.

The reaction occurring in alcoholic solution and leading from pink, octahedrally coordinated Mn^{2+} complexes to the corresponding yellow tetrahedral complexes, in

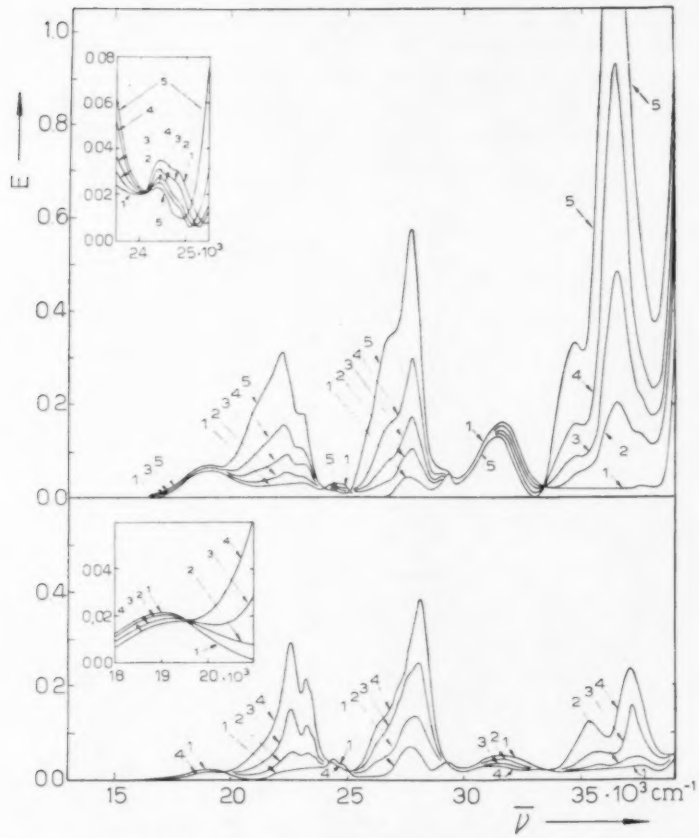

FIG. 3.—Formation of tetrahalogenomanganate(II) ions from manganese and lithium or calcium halides in methanol (room temperature); upper diagram:

(1) 0·92 M $MnBr_2$ (a) in CH_3OH
(2) 0·92 M (a) + 1·05 M $CaBr_2 \cdot 2H_2O$ (b) in the same solvent
(3) 0·92 M (a) + 1·40 M (b)
(4) 0·92 M (a) + 1·75 M (b)
(5) 0·92 M (a) + 2·10 M (b)

lower diagram:

(1) 1·06 M $MnCl_2 \cdot 4H_2O$ (c) in CH_3OH
(2) 1·06 M (c) + 1·14 M LiCl (d) in the same solvent
(3) 1·06 M (c) + 2·28 M (d)
(4) 1·06 M (c) + 3·42 M (d)

presence of excess halides, is an overall endothermic reaction: at constant concentration of all components of the solution, the formation of the tetrahedral species is significantly enhanced at higher temperatures.

LIGAND FIELD CALCULATIONS

Calculations of the term system of the configuration $3d^5$ under a ligand field of tetrahedral symmetry T_d have been carried out in the weak-field approximation,[7] where the parameter Δ occurs only in non-diagonal matrix elements, and in the final determinantal equations it appears only to the second power, i.e. the roots of the secular problem are independent of the sign of Δ, and the splittings are qualitatively

equal to those occurring under an octahedral crystal field. It is well known that the distances between the spectral terms of spin multiplicity six and four of the free manganous ion cannot be described to a very high degree of approximation by the simple Slater-Condon-Shortley theory of the Russell-Sanders coupling, and we think the same situation occurs with electrostatic complexes of Mn^{2+}. Therefore, we did not attempt to describe the position of the quartet levels with a unique choice of Racah parameters B and C, but we preferred to use in the secular equations semi-empirical values for the same distances, obtained by assuming a given per cent decrease of the term distances experimentally known for the free ion.[11] Identifying the maxima at 23200 cm^{-1} and 28100 cm^{-1} with ^4G and ^4D respectively, one gets a decrease of 13 per cent; with this value, the calculated position of the unshifted ^4P level (27000 cm^{-1}) is also in good agreement with the experimental form of the spectrum. However, if we identify ^4F with the peak at 35600 cm^{-1}, we have to admit for it an 18 per cent decrease. The reason of so large a decrease is not clear (we might think of particularly strong interactions with some higher configuration) but notwithstanding this difficulty we think our procedure of fitting the term distances with semiempirical values is still the most reasonable one, especially when the ligand field perturbation is small, as is our case, and the energy levels are expected rather close to the positions they have in the unperturbed system (typical weak field case). We feel also that it is not useful to look for a unique choice of B and C values in order to fit the term distances by means of the Condon-Shortley-Slater theory if we are not able to explain by this way the situation of the free ion, or if we do not take explicitly into account interactions with higher configurations; therefore we did not follow the procedure adopted by HEIDT *et al.*[8], who have been able to construct a term system for octahedral d^5 with one single value of B and C, only by assuming a too high position of ^4P, which leads to an inversion of the order of succession of ^4P and ^4D with respect to the experimental positions in the free ion. Our interpretation is essentially the same as already proposed by ORGEL[6] and by JØRGENSEN[1,5]; we differ however from the latter Author in the position of $^4T_1$ (^4P), which is probably shifted a little too high in the energy diagram of reference (1).

The assignment of the absorption bands is determined unequivocally by the criteria just discussed, and is summarized in Table 1. Some uncertainty of minor importance can exist e.g. in the assignment of the absorptions in the region 26–28000 cm^{-1}, where there are one main peak and three shoulders to be attributed to only three expected transitions; in Table 1 we identified tentatively the three transitions with the main peak and with the two more evident and well-formed of the three shoulders, but this is not necessarily the only assignment possible. In the region 35–38000 cm^{-1} we expect three transitions (i.e. those to the three sublevels derived from ^4F), whereas there are only two observed bands; most probably the band at 35600 cm^{-1} contains two transitions (to $^4A_2$ (F) and $^4T_1$ (F)), since these two levels are expected to lie very close (see Fig. 2). Another possible discrepancy with the calculated term system arises from the fact that about 23000 cm^{-1} there are two absorptions (a maximum at 23180 and a shoulder at ~23400 cm^{-1} in the spectrum of $[MnCl_4]^{2-}$, whereas we expect only one, corresponding to the transitions to the levels $^4A_1$ and ^4E (^4G), which should be degenerated according to the theoretical calculations. The reason of this double band is not clear, but we notice that the same splitting

[11] C. E. MOORE, *Atomic Energy Levels*, U.S. Dept. Commerce, Natl. Bureau of Standards (1953).

VOL. 19 1961

occurs also in the spectra of octahedral Mn^{2+}-complexes. In the spectra we have measured, we have found no evidence for transitions to doublet states ($\Delta S = 2$). Small variations in the intensities of the bands of bromine-containing tetrahedral complexes (see Figs. 4 and 5) occurring with different solvents are probably due to second-sphere effects.

EXPERIMENTAL

Tetrahalogenomanganates(II) of onium cations are prepared simply by mixing alcoholic solutions of manganese(II) halides and of the corresponding onium halide in 1:2 mole ratio. If the addition is performed with warm solutions the tetrahalogeno-complex salts usually precipitate on cooling to room temperature: otherwise, concentration of the alcoholic solutions is advisable; eventually, the most soluble salts can be precipitated by addition of ether or of acetone. The solid salts can be recrystallized from ethanol or methanol, but we do not recommend this procedure, since, as we have already noticed, the tetrahedral anions are decomposed to a large extent in alcoholic solution; we preferred to recrystallize them from solvents where the tetrahedral anions are more stable e.g. from nitromethane or from acetonitrile; the latter however has the drawback that it is sometimes difficult to remove the last traces of solvent from the precipitate.

Table 2 gives a survey of the compounds we prepared, together with the corresponding zinc complexes, which we used as blanks in the spectrophotometric measurements (see below); the same table contains also data on the elementary composition and preliminary remarks on their physical properties, which require little or no further comment. All manganese complexes are yellow, but some bromides or chlorobromides, which are fluorescent in the solid state, especially (5), (7) and (8), appear greenish-yellow to the eye; all tetrahalogenozincates are white. The substances behave in organic solvents as uni-bivalent electrolytes; e.g. the molar conductivities of some tetraethyl-ammonium salts in nitrometane at room temperature in approx. 0·1 M solutions are as follows: bromide (0·2 M) 67, tetrabromozincate 156 and tetrabromomanganate 158; the same salts in acetonitrile have conductivities equal to 57, 124 and 128, and in dimethylformamide 130, 236 and 226; trimethylbenzylammonium salts in nitromethane have the following values: chloride (0·2 M) 129, tetrachlorozincate 290, and tetrachloromanganate 224.

The solubilities in organic solvents depend strongly on the cation; thus the least soluble salts are those containing tetramethylammonium and their solubility does not increase appreciably with the temperature; the most soluble ones are those with tetrabutylammonium; salts of tetraphenylarsonium and of trimethylbenzylammonium have intermediate solubilities and are well more soluble at high temperatures than in the cold, i.e. they can be well recrystallized. Bromides are generally more soluble than the corresponding chlorides. All salts, of Mn as well as of Zn, are readily dissolved by water with decomposition, but are generally not deliquescent and can be dried in air. Only a few of them have sharp melting points.

We attempted also the preparation of mixed chloride-bromide complexes, and by simply mixing the appropriate halides (e.g. $(C_4H_9)_4NBr$ and $MnCl_2$ in ratio 2:1) we actually obtained precipitation of solid salts where the presence of anions like $[MnCl_2Br_2]^{2-}$ is strongly supported by the analytical data (see Table 2), but we feel that such mixed species are not very stable, since their composition varies slightly on crystallizing even from solvents where the tetrahedral anions should be stable: thus a sample of $[(CH_3)_2(C_6H_5CH_2)N]_2[MnCl_2Br_2]$ showed on recrystallizing four times from acetonitrile a constant decrease of the Br : Cl ratio from 2·03:1·97 to 1·78:2·22. A peculiar case is represented by the analogous zinc compound: even if we mix $[(CH_3)_3(C_6H_5CH_2)NCl]$ and $MnBr_2$ in ratio 2:1 (i.e. Cl:Br = 2:2), the solid salt which precipitates contains Cl and Br in ratio 3:1, and its composition does not change appreciably on recrystallization. For the compound (5) (trimethylbenzylammonium-dichloro-dibromomanganate), analytical data (especially N) support the presence of half a molecule of acetonitrile of crystallization, which is however probably lost on heating, since the observed melting point is equal to the value given by NALDINI and SACCO[2] for the same substance without solvent of crystallization.

The spectrum of the mixed dichlorodibromomanganate(II) anion is shown in Fig. 5; it does not differ appreciably from those of the tetrachloro- and of the tetrabromocomplex and its intensities are intermediate between these.

Spectrophotometric measurements. The measurements were performed with a recording Beckman DK2 instrument, mostly at room temperature (~ 23–25°C), if not otherwise specified (the spectrum

VOL. 19 1961

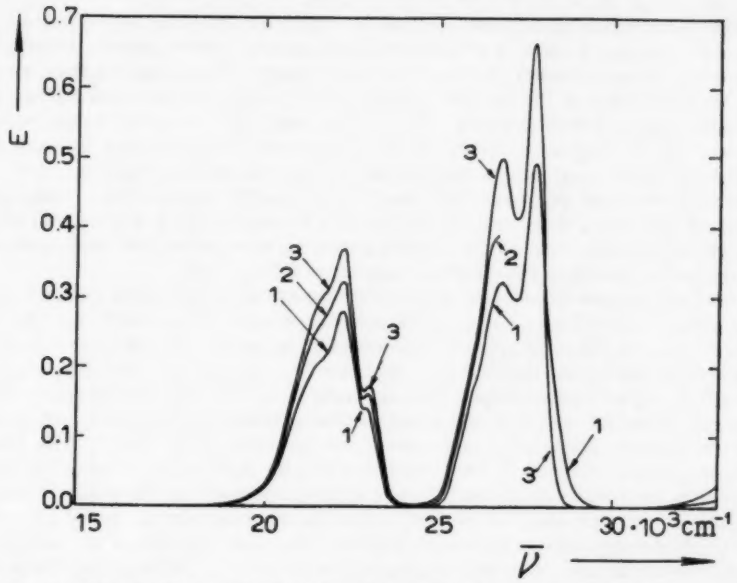

FIG. 4.—Solvent effect on the intensity of absorption bands of tetrabromomanganate(II); $[(C_4H_9)_4N]_2[MnBr_4]$ plus 0·1 M $(C_4H_9)_4NBr$ at room temperature:
(1) in dimethylformamide
(2) in nitromethane
(3) in acetonitrile

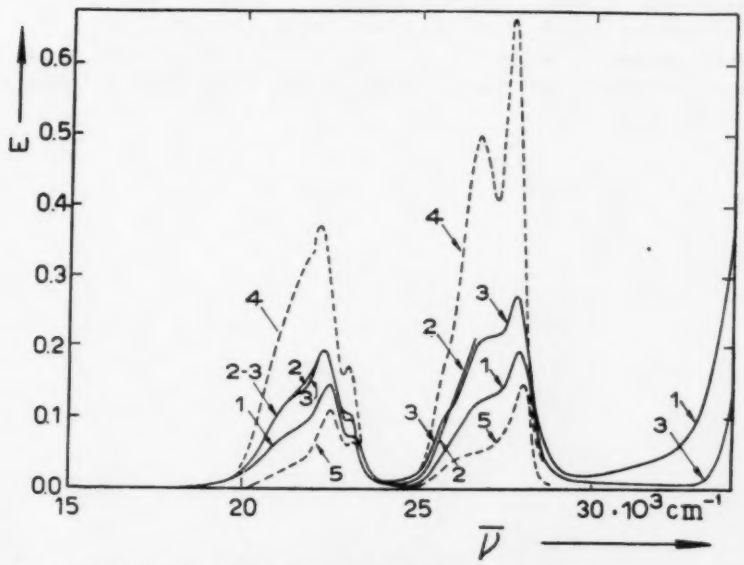

FIG. 5.—Spectrum of a mixed chloro-bromo-manganate(II); 0·2 M $[(CH_3)_3(C_6H_5(H_2)N]_2[MnBr_3Cl_2]$ (1) in dimethylformamide (2) in nitromethane (3) in acetonitrile; for comparison, spectra of 0·2 M $[MnCl_4]^{2-}$ (5) and 0·2 M $[MnBr_4]^{2-}$ (4) in acetonitrile are also shown (dotted lines).

	Substance	Formula	
1	Tetramethylammonium-tetrachloromanganate(II)	$[(CH_3)_4N]_2\,[MnCl_4]$	28·06
2	Trimethylbenzylammonium-tetrachloromanganate(II)	$[(CH_3)_3(C_6H_5CH_2)N]\,[MnCl_4]$	48·34
3	Tetraphenylarsonium-tetrachloromanganate(II)	$[(C_6H_5)_4As]_2\,[MnCl_4]$	58·86
4	Tetrabutylammonium-dichlorodibromomanganate(II)	$[(C_4H_9)_4N]_2\,[MnCl_2Br_2]$	49·13
5	Trimethylbenzylammonium-dichlorodibromomanganate(II)	$[(CH_3)_3(C_6H_5CH_2)N]_2\,[MnCl_2Br_2]\cdot 1/2CH_3CN$	41·63
6	Tetramethylammonium-tetrachloromanganate(II)	$[(CH_3)_4N]_2\,[MnBr_4]$	18·30
7	Tetraethylammonium-tetrabromomanganate(II)	$[(C_2H_5)_4N]_2\,[MnBr_4]$	30·49
8	Tetrabutylammonium-tetrabromomanganate(II)	$[(C_4H_9)_4N]_2\,[MnBr_4]$	44·88
9	Tetramethylammonium-tetrachlorozincate(II)	$[(CH_3)_4N]_2\,[ZnCl_4]$	27·90
10	Trimethylbenzylammonium-tetrachlorozincate(II)	$[(CH_3)_3(C_6H_5CH_2)N]_2[ZnCl_4]$	46·60
11	Tetraphenylarsonium-tetrachlorozincate(II)	$[(C_6H_5)_4As]_2\,[ZnCl_4]$	58·80
12	Tetrabutylammonium-dichlorodibromozincate(II)	$[(C_4H_9)_4N]_2\,[ZnCl_2Br_2]$	48·95
13	Trimethylbenzylammonium-trichlorobromozincate(II)	$[(CH_3)_3(C_6H_5CH_2)N]_2\,[ZnCl_3Br]$	43·82
14	Tetraethylammonium-tetrabromozincate(II)	$[(C_2H_5)_4N]_2\,[ZnBr_4]$	28·80
15	Tetrabutylammonium-tetrabromozincate(II)	$[(C_4H_9)_4N]_2\,[ZnBr_4]$	44·01

Abbreviations: n = nitromethane; a = acetonitrile; d = dimethylformamide; al = ethyl alcohol; *s* = soluble; *v.s* = very solu
* Data are not perfectly reproducible (see text).

TABLE 2.

Elementary composition: % found (calc. in brackets)						m.p.	Solubility	Previous references
C	H	N	Mn or Zn	Cl	Br			
28·06 (27·85)	6·85 (7·01)	7·96 (8·12)	15·96 (15·92)	40·96 (41·10)	—	—	*v.s.s.*n,a,d,al.	
48·34 (48·31)	6·46 (6·49)	5·58 (5·63)	11·17 (11·05)	28·26 (28·52)	—	156–57°	*s.a*,n,d,al(dec.)	(3)
58·86 (59·84)	3·96 (4·18)	—	5·78 (5·70)	14·57 (14·72)	—	—	*s.*a,n,d,al.	(3)
49·13 (49·87)	9·11 (9·42)	3·41 (3·63)	7·10 (7·13)	9·18 (9·20)	21·06 (20·74)	83–84°	*vs.*, *deliq.*	
41·63 (41·56)	5·54 (5·56)	5·86 (5·78)	9·20 (9·06)	11·73 (11·69)*	26·18 (26·37)	144–45°	*s.*a,n; *s.s.*d.	(3)
18·30 (18·36)	4·50 (4·62)	5·15 (5·35)	10·65 (10·50)	—	60·74 (61·14)	—	*v.s.s.*n,a,d,al.	
30·49 (30·26)	6·45 (6·35)	4·28 (4·41)	8·69 (8·65)	—	50·06 (50·33)	—	*s.*a,n,d,al.	(1) (2)
44·88 (44·71)	8·45 (8·44)	3·26 (3·26)	6·42 (6·39)	—	37·24 (37·19)	101–102°	*v.s.*, *deliq.*	
27·90 (27·03)	6·92 (6·80)	7·61 (7·88)	18·69 (18·39)	39·58 (39·89)	—	—	*v.s.s.*,a,d,al.	
46·60 (47·32)	6·35 (6·35)	5·43 (5·52)	12·66 (12·88)	27·35 (27·93)	—	184–85°	*s.s.*n,a,d.	
58·80 (59·20)	4·08 (4·14)	—	6·67 (6·71)	14·45 (14·56)	—	—	*s.*n,a,d,al.	
48·95 (49·21)	9·28 (9·29)	3·52 (3·59)	8·41 (8·37)	9·01 (9·08)	20·30 (20·46)	142°	*v.s.*, *deliq.*	
43·82 (43·48)	5·81 (5·80)	5·60 (5·07)	11·56 (11·85)	20·24 (19·29)	15·06 (14·47)	164–65°	*s.*n,a,d.	
28·80 (27·77)	6·18 (6·24)	4·35 (4·34)	9·89 (10·13)	—	49·07 (49·52)	—	*s.*n,a,d,al.	
44·01 (44·18)	8·18 (8·34)	3·22 (3·22)	7·27 (7·51)	—	34·20 (36·74)	70°	*v.s.*, *deliq.*	

soluble: *s.s.* = slightly soluble: *v.s.s.* = very slightly soluble; *deliq.* = deliquescent in air.

of trimethylbenzylammonium tetrachloromanganate in acetonitrile was taken at 70°C because of its low solubility at room temperature). Each substance was measured in three solvents (nitromethane, dimethylformamide and acetonitrile), although there were no large differences arising from the use of different solvents (see however Fig. 4); the solvent effect is in general much less marked in the spectra of chloro- than of bromocomplexes. The solutions contained an excess of halide ion (added in form of the corresponding onium halide, usually in mole ratio 0·5:1) in order to ensure better stability of the tetrahedral manganese or zinc anions, although this was not strictly necessary; only the mixed chloride–bromides were measured as such, without adding excess halides. Some spectra were measured in alcoholic solutions and a few of them are reported in Fig. 3, where it is to be noted that some of the crosspoints behave as true isobestic points, but some others (see details in upper left corner) do not, perhaps owing to the variable composition of the solvent.

Since rather high concentrations (of the order 0·1–0·2 mole/l.) were required for the spectrophotometric measurements, special care was taken in matching exactly the composition of the blank solution; to this end, we did not use the pure solvents as blank probes, but solutions containing the same excess of onium halide, and the same concentration of the corresponding zinc complex, i.e. of a transparent salt having analogous composition and similar molar volume as the manganese(II) salt being measured. Therefore we prepared also all tetrahalogenozincates(II) corresponding to the tetrahalogenomanganates studied; their composition and characteristics are listed in Table 2, besides those of their manganese analogues. Under these conditions, the matching of the optical densities of the solution and of the blank in the regions where no selective absorption occurs is quite satisfactory. Only in a couple of instances, when the solubility of the zinc compound was too low (e.g. tetrabutylammonium tetrabromozincate(II) in acetonitrile solution), the blank was made of the corresponding onium halide, in molar concentration twice as great as the concentration of Mn in the solution to be measured.

The values of the molar extinctions reported in Table 1 require some specification; for $[MnCl_4]^{2-}$ there is practically no variation in different solvents; for $[MnBr_4]^{2-}$ data reported in Table 1 refer to solutions in acetonitrile (in other solvents E_{mol} is a little lower) (see Fig. 4). Absorbance data in the third absorption region (shortest-wave bands) are extrapolated from measurements in CH_3OH. GILL and NYHOLM (reference 2) reported slightly higher absorbance values for $[MnCl_4]^{2-}$.

Absorption maxima of octahedral complexes in alcoholic solutions are located at approximately 19000, 23000, 24400, (24800), 27700, 29400, 31500 and 37600 cm^{-1} (see curves (1) in Fig. 3).

J. Inorg. Nucl. Chem., 1961, Vol. 19, pp. 61 to 64. Pergamon Press Ltd. Printed in Northern Ireland

PREPARATION AND PROPERTIES OF SOME RARE EARTH BORATES

E. J. FELTEN
Aircraft Nuclear Propulsion Department, General Electric Company, Cincinnati, Ohio

(*Received* 14 *October* 1960)

Abstract—Rare earth borates of the ABO_3 type have been prepared by the reaction of the constituent oxides in equimolar ratios between 1200 and 1400° in air. The borates of yttrium and the smaller rare earth ions (samarium through lutecium) are isostructural with vaterite ($\mu CaCO_3$). Melting points of the borates are greater than 1400° making them useful for applications at elevated temperatures.

VOL. 19 1961

THE earliest work reported on the reactions between the rare earth oxides and boric oxide indicated compound formation of the type $R_2O_3 \cdot 3B_2O_3$ or $R(BO_2)_3$. Oxides having this composition were reported for which R was lanthanum, cerium, neodymium, praseodymium, gadolinium, samarium and scandium.[1,2] More recently CANNERI[3] reported the formation of compounds of the type $R_2O_3 \cdot B_2O_3$, $R_2O_3 \cdot 2B_2O_3$ and $R_2O_3 \cdot 3B_2O_3$, where R was lanthanum, cerium, neodymium, praseodymium and yttrium.

Interest in the structures of the trivalent metal borates including those of the rare earths was stimulated by the discovery of their similarity to the divalent carbonates. For example, calcium carbonate exists in three crystalline modifications, i.e.: rhombohedral calcite, orthorhombic aragonite and the less well known vaterite. GOLDSCHMIDT and HAUPTMANN[4] showed that the borates of indium and scandium have the calcite structure while lanthanum borate is isostructural with aragonite. They reported that yttrium borate probably existed in two crystalline forms; possessing the calcite structure at high temperatures and existing in the vaterite structure at lower temperatures. The vaterite form of calcium carbonate ($\mu CaCO_3$) had been artificially prepared by GIBSON *et al.*[5] and YOSHIMURA[6] and was shown to be hexagonal by RINNE[7] and VON OLSHAUSEN.[8]

The yttrium borate phase was reported to be rhombohedral by HOJENDAHL,[9] while KEITH and ROY[10] reported finding only a single phase in the Y_2O_3–B_2O_3 system up to the melting point (1580 ± 20°). The X-ray data reported by KEITH and ROY indicates that their phase is isostructural with vaterite. LEVIN *et al.*[11] have reported the existence of a series of rare earth borates, including yttrium borate, having the vaterite structure.

(1) W. GUERTLER, *Z. Anorg. Chem.* **40**, 232 (1904).
(2) W. CROOKES, *Phil. Trans.* **210** A, 359 (1910).
(3) G. CANNERI, *Gazz. Chim. Ital.* **56**, 460-4 (1926).
(4) V. M. GOLDSCHMIDT and H. HAUPTMANN, *Nachr. Ges. Wiss. Gottingen, Math-Physk Klasse* 53 (1932).
(5) R. E. GIBSON, R. W. G. WYCKOFF and H. E. MERWIN, *Amer. J. Sci.* **10**, 325 (1925).
(6) T. YOSHIMURA, *J. Geol. Soc. Tokyo* **36**, 7 (1929).
(7) F. RINNE, *Z. Krist.* **60**, 66 (1924).
(8) S. VAN OLSHAUSEN, *Z. Krist.* **61**, 463 (1925).
(9) K. HOJENDAHL, *Kgl. Danske Videnskab. Selskab. Math.—FYS. Medd.* **16**, No. 2, 1 (1938).
(10) M. L. KEITH and R. ROY, *Amer. Min.* **39**, 1 (1954).
(11) E. M. LEVIN, R. S. ROTH and J. B. MARTIN, presented at 17th Annual Pittsburgh Diffraction Conference (1959).

It is the purpose of this report to confirm the existence of a series of rare earth borates isostructural with vaterite ($\mu CaCO_3$). Information is also presented which indicates the temperature range in which these materials might be used. The X-ray data obtained also help in the interpretation of the products from some rare earth boride preparations.

EXPERIMENTAL

The constituent oxides used to prepare samples were reagent grade B_2O_3 and rare earth oxides having a purity of 99·5 per cent or more. After mixing, the powders were compacted in a $\frac{1}{2}$ in. diameter die at about 20,000 lb/in^2 and fired in air for 2–4 hr at 1000 to 1200°. Examination by

TABLE 1.—LATTICE PARAMETERS OF RARE EARTH BORATES ISOSTRUCTURAL WITH VATERITE ($CaCO_3$)

Material	a_0(Å)	c_0(Å)
Vaterite ($CaCO_3$)	4·110	8·513[8]
YBO_3	$3·77_8$	$8·81_4$
$SmBO_3$	$3·86_2$	$8·97_8$
$EuBO_3$	$3·84_2$	$8·93_7$
$GdBO_3$	$3·83_9$	$8·90_6$
$DyBO_3$	$3·79_3$	$8·84_7$
$HoBO_3$	$3·78_4$	$8·83_6$
$ErBO_3$	$3·76_7$	$8·80_7$
$TmBO_3$	$3·75_3$	$8·78_9$
$YbBO_3$	$3·73_5$	$8·74_7$
$LuBO_3$	$3·72_7$	$8·72_3$

X-ray diffraction patterns of powders prepared in this manner showed them to be poorly crystalline. Therefore, the powders were reground, repressed and refired. During the second firing cycle temperatures between 1200 and 1400° were employed for from 5 to 40 hr. Recycling invariably increased the crystallinity of the specimens and in almost every case a single phase was obtained.

The diffraction patterns of the borates of yttrium and the smaller rare earth ions (samarium through lutecium) indicate that they are isostructural with vaterite. The borates of lanthanum, praseodymium, and neodymium do not appear to form this phase. Lanthanum borate crystallizes in the aragonite structure as shown previously.[4,10] The lattice parameters of the vaterite-type rare earth borates were obtained from the diffractometer traces using the 110 line to determine a_0 and the 004 line to determine c_0. The parameters obtained in this way are found in Table 1. While only two lines were used for the parameter determinations, good agreement was always obtained between the $\sin^2\theta$ values calculated from these parameters and the experimentally determined $\sin^2\theta$ values as seen for YBO_3 in Table 2.

The lanthanide contraction is demonstrated when the lattice constants for the borates are plotted against the atomic number of the rare earth metal present as seen in Fig. 1. Within experimental error a linear relationship is obtained. The parameters for YBO_3 are very similar to those for $HoBO_3$ as might be expected, since the ionic sizes of yttrium and holmium are very nearly the same.

DISCUSSION

From observations made during firing operations it would appear that the borates have interesting high temperature properties as indicated by KEITH and ROY[10] for YBO_3. None of the specimens fired at 1400° showed any sign of melting except when excess boric oxide was present. When two moles of B_2O_3 were mixed with one of Sm_2O_3 a melt was obtained from which the excess B_2O_3 rapidly boiled off. The density of the residue was 5·86 cm^3 which compares favorably with the theoretical density for hexagonal $SmBO_3$ (5·97 cm^3). In addition the X-ray diffraction pattern

TABLE 2.—AGREEMENT BETWEEN CALCULATED AND OBSERVED $\sin^2\theta$ VALUES FOR YBO_3

2θ	Intensity	Observed $\sin^2\theta \times 10^4$	*hkl*	Calculated $\sin^2\theta \times 10^4$
20·06	65	303	002	305
27·22	100	554	100	554
29·10	17	631	101	630
34·08	72	859	102	859
40·90	10	1221	004	1220
48·12	32	1662	110	1662
49·82	27	1774	104	1774
52·70	17	1970	112	1967
56·24	6	2221	200	2216
60·26	7	2520	202	2521
65·00	2·5	2887	114	2882
70·24	4	3310	106	3299
71·80	5	3438	204	3436
77·00	4	3875	210	3878
80·54	5	4178	212	4183

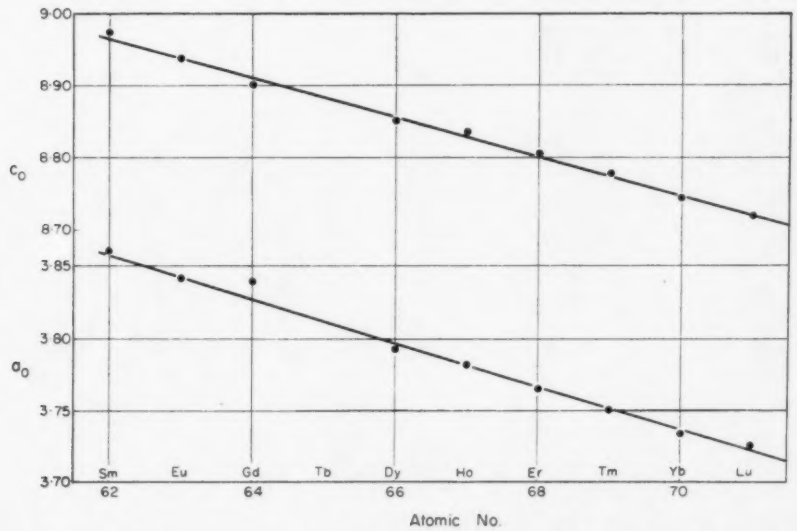

FIG. 1.—Variation of a_0 and c_0 as a function of the atomic number of the rare earth ion in the vaterite-type rare earth borates.

obtained from this reaction product was identical to that for the equi-molar preparation. Therefore, it would appear very unlikely that borates having higher B_2O_3 contents than those found in the rare earth borate compounds exist at atmospheric pressure at temperatures higher than the melting point of B_2O_3. The borates of gadolinium, samarium and europium might be useful for nuclear applications as nuclear control rod materials because of the high cross-sections of boron and the rare earth ions and their stability at elevated temperatures.

There is a marked similarity between the X-ray diffraction patterns of the rare earth borates isostructural with vaterite and the transition metal diborides. Both

types of compounds are hexagonal, and except for the presence of the relatively weak 101 line the c-axis of the rare earth borates would be halved. This would result in a cell of the size and composition that might result from the substitution of a rare earth metal atom for a transition metal atom in the AlB_2 structure. BINDER,[12] for example, attributed the presence of extra lines on the diffraction pattern of a yttrium boride preparation to the formation of YB_2. The "diboride" was reported to be hexagonal with $a_0 = 3{\cdot}78$ Å and $c_0 = 4{\cdot}40$ Å. A doubling of the c-axis would result in the YBO_3 cell. In an X-ray diffraction pattern of two or more compounds the presence of the weak 101 line might be overlooked. Since the rare earth borides are usually prepared either in vacuum or an inert atmosphere, the high stability of the borate is demonstrated. Borates of other rare earth ions have been formed in reactions in which the primary products were rare earth borides.[13]

CONCLUSION

It has been shown that the borates of yttrium and the rare earths smaller than samarium are isostructural with vaterite ($\mu CaCO_3$). The cell parameters decrease in size as the size of the rare earth ion decreases. The rare earth borates are stable to about 1400°C making them attractive for certain high temperature applications.

[12] I. BINDER, *Powder Met. Bull.* **7**, 74 (1956).
[13] I. BINDER, *J. Amer. Ceram. Soc.* **43**, 287 (1960).

J. Inorg. Nucl. Chem., 1961, Vol. 19, pp. 65 to 68. Pergamon Press Ltd. Printed in Northern Ireland

THE DENSITY OF MOLTEN THORIUM AND URANIUM TETRAFLUORIDES*

A. D. KIRSHENBAUM and J. A. CAHILL
Research Institute of Temple University, Philadelphia

(*Received* 19 *October* 1960)

Abstract—Using molybdenum crucibles and sinkers, the liquid densities of liquid uranium and thorium tetrafluorides were determined by the immersed-sinker method from 1300 to 1700°K. and are represented by the equations

$$D_{ThF_4(l)} = 7{\cdot}108 - 7{\cdot}590 \times 10^{-4}T$$

$$D_{UF_4(l)} = 7{\cdot}784 - 9{\cdot}920 \times 10^{-4}T$$

The liquid molar volumes and thermal coefficients of expansions were calculated from the liquid densities.

VOL. 19 1961

THE molten fluorides are becoming more and more useful. A check of the literature showed that very little is known of the physical properties of these molten salts at elevated temperatures. Most of the data available are on mixed fluorides and at temperatures below 1000°. The only data available on densities at higher temperatures over a temperature range were those reported by JAEGER[1] on alkali fluorides, MASHOVETZ and LUNDINA[2] on calcium fluoride and the authors[3] on alkaline earth and rare earth fluorides.

EXPERIMENTAL

Apparatus

In these studies the source of heat was the carbon tube resistance furnace in an argon atmosphere described previously.[4] Molybdenum crucibles and floats were used in these studies. The crucible, $2\frac{5}{8}$ in. high and $1\frac{1}{2}$ in. in diameter, was suspended by molybdenum wires in the centre of the furnace surrounded by a graphite chimney. A stream of dried argon entered the bottom of the chimney and engulfed the crucible. A molybdenum sinker, $\frac{1}{2}$ in. in diameter, was suspended from an analytical balance through a graphite lid into the melt by means of a molybdenum wire. In some of the runs a platinum crucible and sinker were used.

Procedure

The densities of the liquid fluorides were determined by the suspended-sinker method. The procedure consisted in measuring the weight loss of the sinker in the liquid fluoride while determining simultaneously the furnace temperature by means of a calibrated optical pyrometer. Each reading was accurate to $\pm 10°$. By taking numerous readings, however, the final temperature values had a probable error of 5° or 0·2 per cent. The readings were made on the graphite chimney at the level of the melt and were corrected for the emissivity of the graphite.

In order to prevent the reaction of water or air with the molybdenum crucible and float to form oxides of molybdenum, the density measurements were carried out in a dry argon atmosphere. This

* This work was financed by the National Science Foundation, Research Grant NSF-G6278.

[1] F. H. JAEGER, *Z. Anorg. Chem.* **101**, 1 (1917).
[2] V. P. MASHOVETZ and Z. F. LUNDINA, *Ukrain. Akad. Nauk. Inst., Proc. First All Union Conf. on Aqueous Solutions* pp. 191–212 (1935).
[3] A. D. KIRSHENBAUM, J. A. CAHILL and C. S. STOKES, *J. Inorg. Nucl. Chem.* **15**, 297 (1960).
[4] A. D. KIRSHENBAUM and J. A. CAHILL, *J. Inorg. Nucl. Chem.* **14**, 283 (1960).

procedure also prevented the formation of oxides or oxyfluorides by the reaction of water with the fluorides.

The volume of the molybdenum sinker was always corrected to the operating temperature, V_T, using the best values selected by BOCKRIS *et al.*[5] for the thermal coefficient of expansion of molybdenum. The density of the melt was calculated from the equation

$$D = \frac{W_A - W_M}{V_T},$$

where W_A and W_M are the weights of the sinker in air and in the melt, respectively. The value obtained from the above equation was always corrected for the buoyancy in air. This correction was never more than $+0{\cdot}0005$ g/cm³. The density value was also corrected for the effect of surface tension. This correction was never more than 0·5 per cent.

Materials used

Nuclear purity, anhydrous uranium and thorium tetrafluorides (Davison Chemical Co.), containing 99·5–99·9 per cent fluoride were used in these studies. The main impurities (99 per cent of the impurities) were UO_2F_2 and ThO_2, respectively. In order to eliminate the reaction of absorbed water with the fluoride forming oxides and oxyfluorides at the high temperature, the fluorides were predried by heating slowly, first to 100°C and finally to 300°C while evacuating to less than 1 mm of Hg.

Since it is difficult to remove all of the water from these fluorides, samples of the melt after use were analysed for ThO_2 and UO_2F_2. They were found to contain from 0·2 to 0·6% ThO_2 or UO_2F_2. Corrections for these impurities were made [$+0{\cdot}0006$–$+0{\cdot}0018$ g/cm³ or 0·01–0·03 per cent correction].

At the high temperatures, it was necessary to ascertain whether the molten fluoride had reacted with the molybdenum crucible. If it reacted, U or Th metal and MoF_6 and the intermediate fluorides of Mo would have formed

$$3UF_{4(l)} \rightarrow 2Mo_{(s)} \rightarrow 3U_{(l)} + 2MoF_{6(g)}.$$

No Mo in any form was found in the melt upon analysis.

The boiling and melting points of ThF_4 and UF_4 are:

	ThF_4(6)	UF_4(7)
m.p.	1383°K	1309°K
b.p.	1953°K	1723°K

RESULTS

Using the method described above, the densities of molten UF_4 and ThF_4 were determined between 1300° and 1700°K. The values obtained are tabulated in Tables 1 and 2 and fall on straight lines as shown in Fig. 1 when density is plotted against temperature. The equations of the two straight lines are

$$D_{(l)} = 7{\cdot}108 - 7{\cdot}590 \times 10^{-4}T$$

and

$$D_{(l)} = 7{\cdot}784 - 9{\cdot}920 \times 10^{-4}T$$

for liquid ThF_4 and UF_4, respectively.

Using the smoothed-density values obtained from these equations, the molar volumes for these liquid fluorides were calculated. They are summarized in Table 3

[5] J. O'M. BOCKRIS, J. L. WHITE and J. D. MACKENZIE, *Physico-Chemical Measurements at High Temperatures*, p. 347. Academic Press, New York (1959).
[6] A. J. DARNELL and F. J. KENESHEA, JR. *J. Phys. Chem.* **62**, 1143 (1958).
[7] S. LANGER and F. F. BLANKENSHIP *J. Inorg. Nucl. Chem.* **14**, 26 (1960).

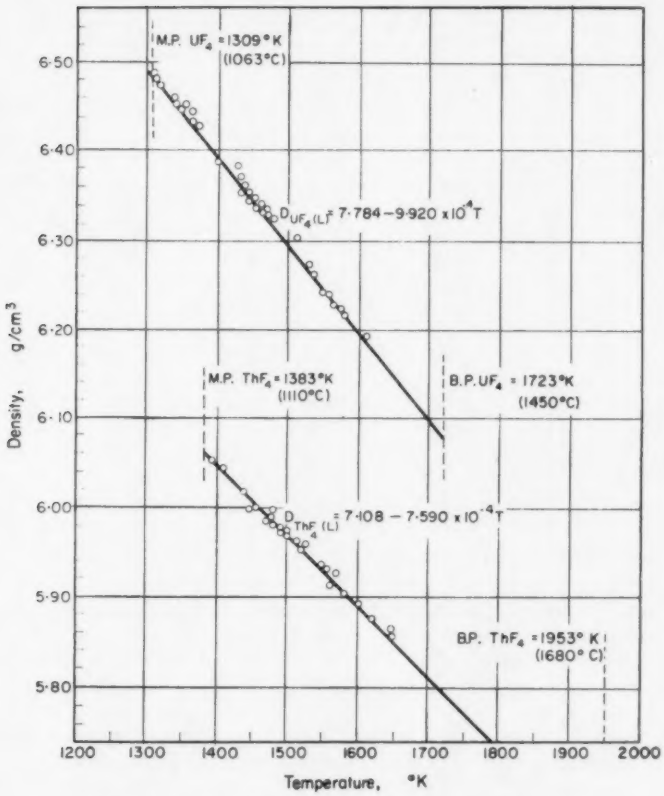

FIG. 1.—Density of molten uranium and thorium tetrafluorides.

TABLE 1.—DENSITY OF MOLTEN THORIUM TETRAFLUORIDE

Temperature (°K)	Density (g/cm³)	Temperature (°K)	Density (g/cm³)
1393	6·052	1514	5·961
1412	6·042	1519	5·953
1441	6·018	1528	5·959
1449	6·000	1551	5·935
1455	6·000	1557	5·932
1471	5·985	1557	5·931
1477	5·984	1562	5·913
1480	5·981	1573	5·926
1482	5·997	1579	5·903
1492	5·976	1603	5·893
1495	5·972	1623	5·875
1500	5·968	1647	5·863
1500	5·973	1651	5·855

VOL. 19 1961

TABLE 2.—DENSITY OF MOLTEN URANIUM TETRAFLUORIDE

Temperature (°K)	Density (g/cm³)	Temperature (°K)	Density (g/cm³)
1309	6·487	1447	6·346
1312	6·481	1449	6·343
1321	6·472	1455	6·347
1339	6·460	1455	6·338
1346	6·453	1463	6·336
1350	6·446	1465	6·331
1356	6·452	1470	6·335
1366	6·445	1475	6·327
1366	6·433	1481	6·323
1369	6·428	1512	6·303
1374	6·428	1529	6·271
1401	6·387	1538	6·262
1430	6·383	1553	6·242
1435	6·353	1558	6·238
1436	6·370	1566	6·227
1441	6·361	1577	6·222
1445	6·347	1579	6·218
1445	6·338	1614	6·191

TABLE 3.—MOLAR VOLUMES AND CUBICAL COEFFICIENTS OF EXPANSION OF ThF_4 AND UF_4

Temperature (°K)	Thorium tetrafluoride			Uranium tetrafluoride		
	Density (g/cm³) (Smoothed values)	Molar volume (cm³/mole)	Coeff. expan. $\beta \times 10^6$	Density (g/cm³) (Smoothed values)	Molar volume (cm³/mole)	Coeff. expan. $\beta \times 10^6$
1309 (m.p.)	—	—	—	6·485	48·43	153·0
1383 (m.p.)	6·058	50·86	125·3	—	—	—
1400	6·045	50·97	125·6	6·395	49·11	155·1
1500	5·969	51·62	127·2	6·296	49·88	157·6
1600	5·894	52·28	128·8	6·197	50·68	160·1

together with the cubical coefficient of expansion values calculated from the equation

$$\frac{dD}{dt} = \beta D_t$$

where dD/dt is the change in density with temperature, β is the cubical coefficient of expansion and D_t is the density at temperature t.

Acknowledgements—The authors wish to thank Dr. A. V. GROSSE for his helpful suggestions and Mrs. L. STRENG for determining the impurities in the melts.

J. Inorg. Nucl. Chem., 1961, Vol. 19, pp. 69 to 72. Pergamon Press Ltd. Printed in Northern Ireland

A GROUP OF COMPLEX METAL HALOGEN COMPOUNDS

A. G. GALINOS*
Departments of Chemistry and Chemical Engineering, New York University Heights

(*Received* 9 *September* 1960; *in revised form* 8 *December* 1960)

Abstract–A general method of preparation and some properties are reported for (a) the preparation of salts with pyridine of the strong complex simple and mixed halogen acids of the metals Sb, Cd, Zn, of the formula $(Py \ldots H \ldots Py)^+ (\overset{II}{MeX_3})^-$ or $(\overset{III}{MeX_4})^-$. (b) the preparation of complexes with the pyridine molecules inside the co-ordination sphere of the above simple and mixed acids. (c) the study of the infra-red spectra, and X-ray analysis, and other reactions are also reported.

VOL. 19 1961

THE existence of etherated mixed and simple complex halogen acids of the metals, Zn, Cd, Sb of the type $(\overset{II}{MeX_3})$ and $(\overset{III}{MeX_4})$[1,2,3] $[(C_2H_5)_2O—H—O(C_2H_5)_2]^+$, has given rise to the expectation that corresponding compounds involving protonated organic bases might be produced. Such compounds would be similar to the salts of organic bases with the common inorganic acids. In the following we report the preparation of salts of these complex halogen acids with pyridine.

Complex compounds formed by combination of metallic halides with pyridine or quinoline have been known for over one hundred years. Since the advent of the Werner theory, many authors have worked systematically to classify these salts in accordance with the requirement of the theory. They reported the preparation of compounds with pyridine and quinoline of many metals including Cd, Zn, Hg, Cu, etc.[4–8] They also prepared double salts with more than two molecules of pyridine, referring to them as di-, tri-, tetra-, penta- and hexa-pyridinium salts.

GROSSMAN, as part of his extensive work, reported the existence of complex halides and thiocyanates of cadmium containing at most two molecules of pyridine per atom of cadmium in the case of the chlorides, and up to as many as six for the bromides and iodides. All these compounds decomposed to some extent when heated above their melting points. PFEIFFER and SCHNEIDER[9] have referred to analogous compounds containing antimony. HIEBER and REINDL[10] have measured the heat of formation of these salts.

General method of preparation. A weighed quantity of freshly prepared and dried etherate of the complex halogen acid was placed in a three-necked flask equipped with a separatory funnel, a stirrer, and a vapour exit tube connected to a vacuum pump by

* Present address: Polytechnical University, Athens-Greece.

[1] A. G. GALINOS, *Z. Angew. Chem.* 69–507 (1957).
[2] A. G. GALINOS, *J. Amer. Chem. Soc.* **82**, 3032 (1960).
[3] A. G. GALINOS, *I.M. Tsangaris Chimika Chronika* **25**, 163 (1960).
[4] P. GROTH, *Lieb Ann.* **105**, 339 (1859).
[5] T. ANDERSON, *J. Chem. Soc.* (2) **7**, 406 (1869).
[6] A. HESEKIEL, *Ber. Dtsch. Chem. Ges.* **18**, 309 (1885).
[7] H. GROSSMAN, *Z. Anorg. Chem.* **37**, 568 (1904).
[8] F. HÜNSELER, *Z. Anorg. Chem.* **46**, 301 (1905).
[9] P. PFEIFFER and K. SCHNEIDER, *Ber. Dtsch. Chem. Ges.* **68** B, 50 (1935).
[10] W. HEIBER and E. REINDL, *Z. Elektrochem.* **46**, 556 (1940).

way of a weighed dry-ice acetone trap and a trap cooled by liquid nitrogen. With the use of cold water to cool the flask and with stirring, an excess of liquid pyridine was added dropwise to the contents of the flask and a reaction vigorous almost to the point of explosion ensued.

Stirring was continued to the end of reaction, all vapors evolved being collected in the traps. Analysis of the contents of the traps showed the presence only of ethyl ether in amount equal to that computed as present in the complex acid. The contents of the flask were kept in a vacuum desiccator over sulphuric acid for a period as long as seven or more days to remove the excess of pyridine.

The residue, in the form of crystals of various colours was analyzed. Precautions were always taken to exclude moisture during the preparation procedure.

Methods of analysis. Because of their sparing solubility in water, it was necessary to form solutions of these compounds in nitric acid before analysis. Standard analytical methods were used to determine the metal and halogen. The pyridine content was obtained by difference, and the H^+ was taken always as one (see Table 1).

General properties. All these compounds are crystalline and of various colors (see Table 1). They smell of pyridine and are insoluble in most of the common organic solvents, and only sparingly in water. They are soluble in acetone and especially so in a mixture of acetone with fuming concentrated hydrochloric acid. If H_2S is passed into such a solution no precipitate is noted. Dilution with much water and saturation with H_2S produces first a turbidity and then, on 10–12 hr standing, a precipitate of sulphide.

In contact with concentrated H_2SO_4 the compounds are inert. Their melting points are not very high. On heating to temperatures sufficiently above their melting points, they are chemically transformed but not decomposed, a molecule of pyridine probably entering the co-ordination sphere and displacing one of the halogen atoms. Details of these last phenomena are given in the next section.

Preparation of complexes with the pyridine in the co-ordination sphere. The thermal behaviour of the compound, $HCdBr_3 \cdot 2Py$ (Py = pyridine) was investigated. It was found to melt at 105°C and, on further heating, at 222–225°C to solidify, and form needle-like crystals easily observable with the naked eye and magnifying glass, with no observable evolution of vapour, odour of HBr or pyridine, and with no change in weight or apparent volume. These needles then melted sharply at 235° and were stable down to room temperature with no transformation to the original compound. The analytical results for the transformed product were the same as those for the starting compound. Behaviour toward organic solvents, water, H_2S, and H_2SO_4 was similar to that of the original complex salt. In general, the two compounds differed not in observable chemical properties but only in physical properties such as melting point, crystal structure and in particular, odour and colour. The high melting compounds are without odour.

Other similar thermally transformed compounds were studied (Table 1). In the case of zinc complexes, heating significantly above the first melting point has been observed to give rise to a glue-like material which, on cooling to room temperature crystallizes only after an hour or more. These crystals have a melting point different from that of the original complex.

From the study of the infra-red spectra of all these compounds, there is evidence that the low temperature form of the metalhalide-pyridine complex has an N–H

TABLE 1

Formula	Analysis	(*L*) (*H*) m.p (°C)	Colour
$H(SbCl_4)\cdot 2Py$	(*L*) 1:1 :4·05:2·07 (*H*) 1:0·98:4·01:2 .	164 182	(*L*) White (*H*)
$H(SbBr_4)\cdot 2Py$	1:1·03:3·97:2·04 1:1·04:4·04:2·1	205 226	(*L*) Yellow (*H*)
$H(SbCl_3Br)\cdot 2Py$	1:1 :3·02:0·97:1·96 1:0·96:3·01:1·04:1·98	200 226	(*L*) White (*H*) Yellow
$H(SbBr_3Cl).2Py$	1:1 :2·93:0·96:2·07 1:0·97:3·08:0·94:2·07	182 209	(*L*) Pale yellow (*H*) Deep yellow
$H(SbI_3Cl)\cdot 2Py$	1:1·02:3·04:0·97:2·08 1:1 :2·95:1·1 :2·1	190 215	(*L*) Yellow (*H*) Deep yellow
$H(SbI_3Br)\cdot 2Py$	1:1·03:3·05:0·98:2·03 1:0·97:2·90:1·1 :2·1	155 205	(*L*) Yellow (*H*)
$H(CdCl_3)\cdot 2Py$	1:1·02:3·03:1·96 1:1·01:3·05:1·98	102 280	(*L*) Yellow (*H*) Orange
$H(CdBr_3)\cdot 2Py$	1:1·05:3·02:1·94 1:1·04:2·95:2·1	105 235	(*L*) Pale yellow (*H*) Yellow
$H(CdCl_2Br)\cdot 2Py$	1:1·04:2·1 :0·95:1·94 1:1·04:1·98:1·04:2·1	155 222	(*L*) White (*H*) Gray
$H(CdBr_2Cl)\cdot 2Py$	1:1·02:2·08:0·93:1·98 1:1·05:2·02:0·98:2·1	110 236	(*L*) Orange (*H*)
$H(CdI_2Cl)\cdot 2Py$	1:1·03:1·97:1·02:2·05 1:1·08:2·03:0·95:2	115 238	(*L*) Red (*H*) Deep red
$H(CdI_2Br)\cdot 2Py$	1:0·98:1·96:1·05:2·06 1:1·01:2·02:0·99:2·1	100 226	(*L*) Yellow (*H*) Pink
$H(ZnCl_3)\cdot 3Py$	1:1 :3·01:3·03 1:1 :3·01:3·06	145 160	(*L*) White (*H*)
$H(ZnBr_3)\cdot 3Py$	1:1·02:3·04:2·97 1:1 :3 :2·98	109 158	(*L*) Pale yellow (*H*)
$H(ZnCl_2Br)\cdot 3Py$	1:1·03:2·05:0·98:3·06 1:1 :2·03:0·99:3	114 142	(*L*) White
$H(ZnBr_2Cl)\cdot 3Py$	1:1·02:1·97:1·04:3·01 1:1·02:2·03:0·95:3	125 165	(*L*) Pale yellow (*H*)

VOL. 19 1961

vibration frequency close to that of the pyridinium halides, hence suggesting that the pyridine is outside the co-ordination sphere of the central metal ion. The high temperature form, on the other hand, shows evidence of a different N–H vibration in the 3·1–3·2μ regions, which is at a significantly higher frequency. This is good evidence that there are two different bonds to pyridine species, one within the co-ordination sphere and the other outside it.

In the case of the zinc compounds, which contain three moles of pyridine per mole of metal the spectra correspond identically to those of the Cd and Sb compounds which contain two moles of pyridine. We suggest that high melting form contains only one molecule of pyridine inside the co-ordination sphere.

The appearance of pyridine molecules outside the co-ordination sphere is expected on the basis of the equation,

$$H(MeX_3)\cdot 2Et_2O + 2Pyr \rightarrow (PyrN{-}H{-}NPyr)^+ + (MeX_3)^- + 2Et_2O.$$

It may be presumed that the hydrogen ion establishes a bridge between the nitrogen of the pyridine molecules as diagramed in the formula

$$(C_5H_5N{-}H{-}NC_5H_5)^+ (MeX_3)^-$$

This bridge should be similar to the hydrogen bridge as usually formulated and should provide a certain amount of stabilization energy to the crystal.

In the case of complexes with high melting points, there probably takes place a migration of a molecule of pyridine

$$\underset{L}{H(MeX_3)}\ 2Py \rightarrow Py\ \underset{H}{H^+(MeX_2Py)X^{-*}}.$$

It is also possible that there may have been a change in the co-ordination number. It seems probable that the low melting forms of the compounds of Zn, Cd, Sb have the molecules of pyridine outside the co-ordination sphere.

The exact change in co-ordination between the low melting and the high melting forms is unknown, but many possibilities are involved, on the basis either of change in co-ordination number or of exchange between co-ordinated and non-co-ordinated groups.

X-ray powder photographs of the compounds $H(CdCl_2Br)2Pyr$, $H(CdBr_3)\cdot 2Pyr$, $H(ZnCl_2Br)\cdot 3Pyr$ show that the high and low temperature forms are distinct phases.

In an attempt to distinguish between halogen inside and outside the co-ordination sphere, an acetone solution of $AgClO_4$ was added to a solution of a weighed sample of $H(CdI_2Cl)\cdot 2Py$ of high melting point in the same solvent. A turbidity first formed and in a few seconds a precipitate of AgCl and AgI. The precipitate was filtered rapidly and was found to contain all the halogen of the compound. While there may have been a stepwise precipitation of the halide the speed of total precipitation presented separation of the steps.

Acknowledgement—The work reported in this paper was done while the author held a fellowship of the National Academy of Sciences of the United States of America under the visiting scientists' research program.

* *L* = Low temp. form. *H* = high temp. form.

J. Inorg. Nucl. Chem., 1961, Vol. 19, pp. 73 to 80. Pergamon Press Ltd. Printed in Northern Ireland

STUDIES IN CO-ORDINATION CHEMISTRY—VIII

MAGNETIC, SPECTROPHOTOMETRIC AND DIELECTRIC MEASUREMENTS ON A SERIES OF *BIS*-(N-ALKYLSALICYLALDIMINO)-COPPER(II) COMPLEXES[1]

L. SACCONI,* M. CIAMPOLINI, F. MAGGIO and F. P. CAVASINO
Institute of General Chemistry, The University of Palermo, Palermo, Italy

(*Received* 29 *October* 1960)

Abstract—Magnetic, spectrophotometric and dielectric measurements have been made with a series of tetraco-ordinated complexes of copper(II) with N-alkylsalicylaldimines, in order to account for the orientation polarization shown by these chelates in benzene and dioxane solution. The magnetic moments of these compounds measured between 90 and 400°K lie between 1·83 and 1·90 B.M. and are essentially independent of temperature. They remain practically unchanged when the solids are dissolved in benzene. This is not to be expected if the compounds have a tetrahedral structure in solution. The high values of the difference $P_{2\infty}-P_E$ found for these chelates even in "non-co-ordinating" solvents like cyclohexane and carbon tetrachloride do not support the assumption that asymmetrical pentaco-ordinated adducts with a mole of solvent are formed in solution. Such results are in accord with the hypothesis already put forward by us that in solution the above complexes have a flattened pyramidal structure.

VOL. 19 1961

IN a previous investigation of the dielectric polarization of a series of complexes of copper(II) with N-alklysalicylaldimines,[2] the difference between the total and the electronic polarization, $P_{2\infty}-P_E$, was found to be positive, increasing from 50 cm³ for the methyl derivative to 100 cm³ for the amyl derivative. These values are roughly equal to 50–75 per cent of the electronic polarization. Since the value of $P_{2\infty}-P_E$ for symmetrical planar metal chelates does not generally exceed 30 per cent of P_E,[3] one is led to assume that these high values of $P_{2\infty}-P_E$ are due, at least in part, to an orientation polarization. On the other hand, the methyl and phenyl derivatives of these copper chelates, for which X-ray data are available,[4] are *trans*-planar. One must assume therefore that on dissolving in dioxane and benzene, in which the electric polarization was measured, all these complexes take on an asymmetrical configuration.[1]

If this configuration were tetrahedral one would expect for these chelates $P_{2\infty}-P_E$ values of 500 cm³ ca. These indeed are the values for some cobalt(II) and zinc(II) complexes of this series which were found to be tetrahedral.[2,5] Even higher values of $P_{2\infty}-P_E$ should be shown by a *cis*-planar structure.

The following hypothesis can therefore be put forward:

(a) The existence of an equilibrium between *cis* and *trans*-planar forms. This hypothesis seems to be invalidated by the fact that the value of $P_{2\infty}-P_E$ increases with the length and with the hindrance of the chains, a condition that should hinder the

* Present address: Istituto di Chimica Generale dell'Università, Via Gino Capponi 9, Firenze, Italy.

[1] Part VII: L. SACCONI, R. CINI, M. CIAMPOLINI and F. MAGGIO, *J. Amer. Chem. Soc.* **82**, 3487 (1960).
[2] L. SACCONI, M. CIAMPOLINI, F. MAGGIO and G. DEL RE, *J. Amer. Chem. Soc.* **82**, 815 (1960).
[3] I. COOP and L. E. SUTTON, *J. Chem. Soc.* 1269 (1938); J. MACQUEEN and J. W. SMITH, *J. Chem. Soc.* 1821 (1956); K. A. JENSEN, *Z. Anorg. Chem.* **229**, 250 (1936).
[4] M. STACKELBERG, *Z. Anorg. Chem.* **253**, 136 (1947).
[5] E. FRASSON, C. PANATTONI and L. SACCONI, Unpublished work

formation of *cis*-forms. (The highest values of $P_{2\infty}-P_E$ are found for the amyl and the phenyl derivatives).[2]

(b) The existence of an equilibrium between tetrahedral and *trans*-planar forms, or the existence of distorted tetrahedral forms.

(c) The formation of pentaco-ordinated adducts with one molecule of solvent.

(d) Molecular deformation of the complexes from *trans*-planar in the crystal to pyramidal in solution as a result of the lack of lattice interactions.

With the aim of throwing further light on this subject the magnetic susceptibility of these complexes has been determined in the solid state above 90°K and in benzene solution. The dielectric polarization of some of the complexes dissolved in non-polar solvents, where solvent co-ordination can be considered unimportant, has also been determined. Finally, measurements have been made of the spectra of some of these complexes in solvents of different co-ordination power, such as cyclo-hexane, carbon tetrachloride, benzene, dioxane, methanol and pyridine.

EXPERIMENTAL

Preparation of compounds. The complexes of copper with N-ethyl- and N-amylsalicylaldimine were prepared as previously described.[2] The bis-(di-n-butyrylmethane)-copper(II) was prepared according to MORGAN and THOMASON.[6]

Bis-(N-methylsalicylaldimino)-copper(II). (Found: N, 8·61; Cu, 18·97. Calc. for $C_{16}H_{16}O_2N_2Cu$: N, 8·61; Cu, 19·15%).

Bis-(N-methylsalicylaldimino)-copper(II). (Found: N, 8·15; Cu, 17·77. Calc. for $C_{18}H_{20}O_2N_2Cu$: N, 7·78; Cu, 17·66%).

Bis-(N-propylsalicylaldimino)-copper(II). (Found: N, 7·63; Cu, 16·50. Calc. for $C_{20}H_{24}O_2N_2Cu$: N, 7·22; Cu, 16·38%).

Bis-(N-butylsalicylaldimino)-copper(II). (Found: N, 7·02; Cu, 15·57. Calc. for $C_{22}H_{28}O_2N_2Cu$: N, 6·73; Cu, 15·28%).

Bis-(N-amylsalicylaldimino)-copper(II). (Found: N, 6·63; Cu, 14·26. Calc. for $C_{24}H_{32}O_2N_2Cu$: N, 6·31; Cu, 14·31%).

Bis-(di-n-butyrylmethane)-copper(II). (Found: Cu, 17·02; Calc. for $C_{18}H_{30}O_4Cu$: Cu, 17·00%).

Dipole moment measurements. The dielectric contants of the solutions relative to those of the solvents were determined with a Dipolmeter DM 01 heterodyne oscillator and a cell supplied by the WTW (Wissenschaftlich-Technische Werkstätten, Weilheim Oberbayern, Germany). The precision condenser and the cell were calibrated using cyclohexane, benzene and benzene-chlorobenzene mixtures. Cyclohexane was purified according to HIEBER[7]; the density and refractive index of the fraction used were $d_4^{25} = 0{\cdot}7738$ and $n_D^{25} = 1{\cdot}4236$. Benzene was purified by the procedure described by FEW and SMITH[8] ($d_D^{25} = 0{\cdot}8738$, $n_D^{25} = 1{\cdot}4980$). The dielectric constants of cyclohexane and benzene were taken to be 2·0148 and 2·2725 respectively.[9] Chlorobenzene was washed repeatedly with concentrated sulphuric acid, potassium carbonate solution and finally with water. After it was dried over calcium chloride, it was refluxed over phosphoric oxide and distilled through a forty-plate all-glass fractionating column. The dielectric constants of benzene–chlorobenzene mixtures were taken from LE FEVRE.[10] The solvents used for the measurements were purified by standard procedures. In each case six solutions were measured. The refractive indices were determined with a Pulfrich refractometer for the sodium D line. Densities were measured with a pycnometer. The molar polarizations of the solutes at infinite dilution (P_{200}) were determined by the method of HALVERSTADT and KUMLER.[11] The plots of dielectric constants, refractive indices and densities vs. molar fractions were found to be straight lines in the concentration range used.

[6] G. T. MORGAN and R. W. THOMASON, *J. Chem. Soc.* **125**, 754 (1924).
[7] W. HIEBER, *Z. Anorg. Chem.* **287**, 223 (1956).
[8] A. V. FEW and J. W. SMITH, *J. Chem. Soc.* 753 (1949).
[9] L. HARTSHORN and D. A. OLIVER, *Proc. Roy. Soc.*, **A 123**, 664 (1929); R. MECKE and K. ROSSWOG, *Angew. Chem.* **66**, 75 (1954).
[10] R. J. W. LE FEVRE, *Trans Faraday Soc.* **46**, 1 (1950).
[11] I. HALVERSTADT and W. KUMLER, *J. Amer. Chem. Soc.* **64**, 2988 (1942).

Spectrophotometric measurements. Absorption spectra were obtained with a Beckman DU spectrophotometer using silica cells 1 cm long. The solvents were purified by the standard methods.

Magnetic susceptibility measurements. Susceptibility measurements on the complexes in the solid state as well as in benzene solution were executed using a Gouy-type magnetic balance. The apparatus previously described (Cf. Part VII of this series[1]) was equipped with an assembly for measurements at several temperatures starting from that of liquid air. A copper tube just wide enough to fit the freely suspended sample and immersed in a Dewar flask of a suitable shape was used for liquid air. The tube was surrounded by a copper jacket which was filled with little lead balls and liquid air was injected inside. Measurements were performed in a dry nitrogen atmosphere in order to avoid freezing of moisture and carbon dioxide on the sample tube. The most convenient procedure was to allow the temperature to drift upward while the field was on. The temperature was measured frequently with a thermocouple and the drift during every measurement never exceeded 1°. It is believed that errors resulting from temperature drifts are not appreciable. When working above room temperature the sample was maintained at the desired temperature by a paraffin oil bath circulating from a thermostat. The susceptibilities of the complexes in solution were determined according to the formula

$$\chi_{g(\text{complex})} = [\chi_{g(\text{solution})} - \chi_{g(\text{solvent})}(1 - x)]/x$$

where x = fraction by weight of complex in solution. After calculation of the molar susceptibilities, diamagnetic corrections for organic ligands were computed from Pascal's constants. The values are accurate within 2 per cent.

VOL. 19 1961

TABLE 1.—DIELECTRIC POLARIZATION DATA FOR SOME COPPER(II) COMPLEXES IN VARIOUS SOLVENTS AT 25°

Compound	R_D (cm³)	$P_{2\infty}$ (cm³)			
		Benzene	Dioxane	Cyclohexane	Carbon tetrachlor
Bis-(di-n-butyryl-methane)–copper(II)	100	125			
Bis-(N-ethylsalicyl-aldimino)–copper(II)	105	192	174	198	171
Bis-(N-amylsalicyl-aldimino)–copper(II)	133	232	223	246	220

RESULTS AND DISCUSSION

In order to obtain further information on the magnitude of the atomic polarization of the tetraco-ordinated copper chelates, the dielectric polarization of the complex bis-(di-n-butyrylimethane)–copper(II) was measured. This complex is presumably free from steric hindrance and should be non-polar even if tetrahedral. Moreover, its high solubility enables very accurate measurements to be made. The value of 25 cm³ found for the difference $P_{2\infty}$–P_E for this complex (Table 1), corresponding to $P_A = 25\%$ P_E, is quite reasonable in view of the values found for symmetrical tetraco-ordinated metal complexes.[2,3]

This result corroborates the hypothesis that the higher values of $P_{2\infty}$–P_E found for the bis-(N-alkylsalicylaldimino)–copper(II) complexes are to be attributed, at least in part, to a real orientation polarization.

As is well known, the PAULING's valence bond theory[12] assumed that the tetrahedral complexes of copper(II), owing to their own asymmetry, have a greater orbital

[12] L. PAULING, *The Nature of the Chemical Bond*, p. 141. Cornell Univ. Press, Ithaca, N.Y. (1940).

contribution to the magnetic moment than the square ones. RAY and SEN[13] divided the tetraco-ordinated complexes of copper(II) into two groups with values of μ_{eff} equal to 1·72–1·82 and 1·90–2·20 B.M., respectively. They attributed to the first group a planar dsp^2 structure and to the second a tetrahedral sp^3 or planar sp^2d configuration.

In terms of crystal field theory the energies of the *d*-orbitals in a square and a tetrahedral copper(II) complex can be represented by the scheme:

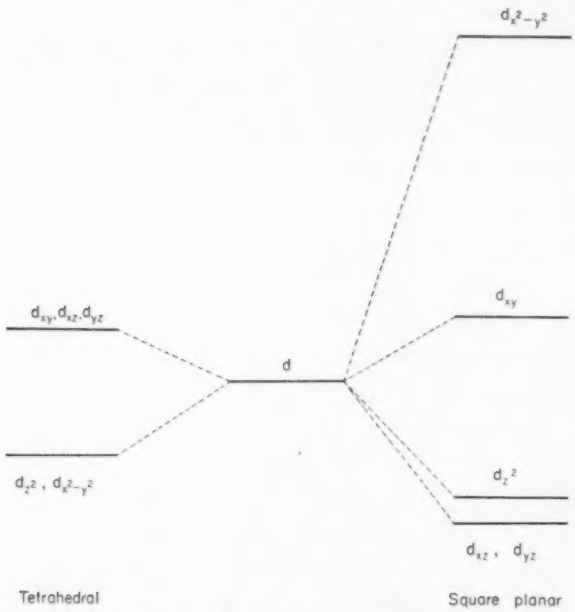

FIG. 1.—The splittings of the *d*-orbitals in the field of tetrahedral and square planar symmetry.

although an alternative scheme with δ_z^2 lying below δxz, δyz, according to the field strength, is possible for a tetragonal field.

In the ground state the nine 3*d*-electrons of the cupric ion are distributed among the five 3*d*-orbitals in such a way that the energy of the system is a mininum. The stabilization energy due to the crystal field, therefore, will be greater for a square than for a tetrahedral structure. It follows, then, that a tetraco-ordinated copper complex can take on a tetrahedral configuration only when there exist among the liagnds steric repulsions that are large enough to compensate for the diminution in Crystal Field Stabilization Energy. Such a configuration will naturally be less difficult to obtain if the ligand field is weak. Furthermore, a perfectly tetrahedral copper complex is orbitally triply degenerate, so that, by the Jahn-Teller theorem, it is unstable and must distort. These considerations account for the rarity of tetrahedral copper complexes.

Besides, the crystal field theory predicts that copper(II) complexes have a marked orbital contribution to the magnetic moment only when the ground state is orbitally degenerate.[14,15] Since, as has been shown above, a planar complex is not degenerate,

[13] P. RAY and D. N. SEN, *J. Indian Chem. Soc.* **25**, 473 (1948).
[14] J. H. VAN VLECK, *The Theory of Magnetic Susceptibilities*. Oxford Univ. Press (1932); M. KOTANI, *J. Phys. Soc., Japan* **4**, 293 (1949); H. BETHE, *Ann. Physik.* **3**, 133 (1929).
[15] K. ITO and T. ITO, *Aust. J. Chem.* **11**, 406 (1958).

it should have a value of μ_{eff} close to the "spin-only" value, 1·73 B.M. A perfectly tetrahedral copper(II) complex, instead, has a degenerate ground state and should have a large orbital contribution. In this case, the magnetic moment should vary with temperature and, at room temperature, should be about 2·20 B.M., whereas a distorted tetrahedral complex should have a lower value of μ_{eff}.[15] Thus the magnetic moment of Cs_2CuCl_4, which has been shown to have this structure,[16] is found to be 2·0 B.M. at room temperature.[17]

TABLE 2.—MAGNETIC SUSCEPTIBILITY DATA FOR BIS-(N-ALKYLSALICYLALDIMINO)-COPPER(II) COMPLEXES IN THE SOLID STATE AND IN BENZENE SOLUTION

Bis-N-alkyl–Cu complex	Concentration (mmole %)	$\frac{T}{(°K)}$	$\chi_g \times 10^6$	$\chi_A \times 10^6$	μ_{eff} (B.M.)
N-Methyl		90	13·73	4723	1·85
		200	5·84	2104	1·84
		293	3·81	1431	1·84
		413	2·61	1032	1·85
	13·00	298	3·71	1397	1·83
N-Ethyl		92	12·95	4851	1·90
		185	5·80	2278	1·84
		293	3·52	1457	1·85
		393	2·48	1083	1·85
	20·50	298	3·37	1403	1·84
	15·50	298	3·40	1414	1·84
N-Propyl		227	4·21	1846	1·84
		296	3·18	1447	1·86
		388	2·33	1117	1·87
	17·80	298	3·04	1392	1·83
	13·50	298	3·15	1435	1·86
N-Butyl		230	3·81	1822	1·84
		296	2·89	1439	1·85
		343	2·38	1227	1·84
	50·40	298	2·79	1397	1·83
	40·70	298	2·79	1397	1·83
N-Amyl		91	10·11	4751	1·87
		199	4·30	2171	1·86
		293	2·67	1446	1·85
		353	2·15	1216	1·86
	41·50	298	2·54	1389	1·83
	28·90	298	2·57	1402	1·83

If therefore there existed in solution a proportion of tetrahedral forms, possibly distorted, the bis-(N-alkylsalicylaldimino)–copper(II) complexes ought to have a higher μ_{eff} value than in the solid state.

The magnetic susceptibility of the complexes, measured between 90° and 400°K, follow the Curie-Weiss law. In Table 2 measurements at only three temperatures are reported. For each sample, however, at least ten measurements between 90° and 400°K were made (See Fig. 2). The weiss constant, Θ, is less than 5° even for the methyl complex for which a value of about—20° was reported.[18] This magnetic behaviour is in

[16] L. HELMOLZ and R. F. KRUH, *J. Amer. Chem. Soc.* **74**, 1176 (1952).
[17] B. N. FIGGIS and C. M. HARRIS, *J. Chem. Soc.* 855 (1959).
[18] M. CALVIN and C. H. BARKELEW, *J. Amer. Chem. Soc.* **68**, 2267 (1946).

accordance with a distorted octahedral or square planar arrangement of the complexes in the solid state. There is practically no change in moment when the solids are dissolved in benzene. (Table 2). This would indicate that copper chelates do not take on a tetrahedral structure when dissolved in such solvents.

The hypothesis of the formation of pentaco-ordinated addition compounds between a copper complex and a molecule of the solvent was put forward to account for the spectra of bis-(N-methylsalicylaldimino)–copper(II), salicylidene–ethylenediamino–copper(II) and other copper complexes in organic solution.[19,20] Adducts of

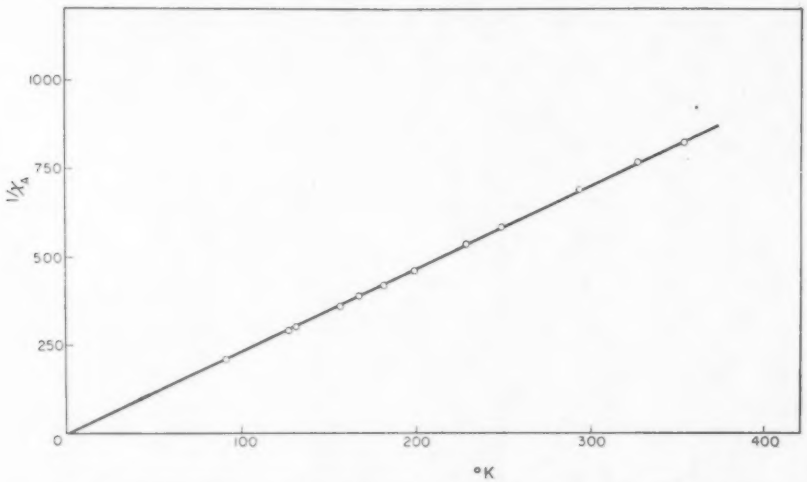

FIG. 2.—Inverse of corrected molar susceptibility of bis-(N-amylsalicylaldimino)–copper(II) complex vs. temperature.

this kind are also formed between copper(II)–acetylacetone and organic bases in solution.[21] No evidence of interaction between this complex and benzene, however, has been found.[22]

In the case of bis-(N-alkylsalicylaldimino)–copper(II) chelates dissolved in benzene or dioxane this hypothesis seems unlikely for the following reasons:

(a) because the values of $P_{2\infty}-P_E$ increases as the alkyl chain lengthens, whereas on the contrary the greater hindrance of the chains should make it more difficult for a molecule of solvent to approach a chelate molecule;

(b) because the values of P_A are higher in benzene than in dioxane, which ought instead to co-ordinate more easily.[2] To check this hypothesis, the dielectric polarization of two copper(II) chelates of this series was measured in carbon tetrachloride and cyclohexane, which are considered incapable of co-ordinating. The complexes chosen were the amyl and the ethyl derivatives, which in the solvents hitherto used showed the highest and lowest values of $P_{2\infty}-P_E$ respectively. (The solubility of the methyl complex is too low). The values of $P_{2\infty}-P_A$ shown in Table 1 are close to those found in benzene and dioxane,[2] the highest value being found in cyclohexane, to which must

[19] T. N. WATERS and D. HALL, *J. Chem. Soc.* 1200 (1959).
[20] T. TANAKA, *J. Amer. Chem. Soc.* **80**, 4109 (1958).
[21] D. P. GRADDON, *Nature, Lond.* **183**, 1610 (1959).
[22] D. P. GRADDON, *J. Inorg. Nucl. Chem.* **74**, 161 (1960).

be attributed the lowest solvating power. These results thus are against the hypothesis of a co-ordination of the complex by the solvent molecules.

The spectra of bis-(N-alkylsalicylaldimino)–copper(II) complexes in benzene, carbon tetrachloride, cyclohexane, dioxane and methanol are very simliar. These in pyridine slightly differ in the values of ε and λ_{max}. All the spectra show three bands in the 300–310, 360–370 and 600 mμ regions. In Figs. 3 and 4 the absorption curve of the amyl complex, dissolved in various solvents, is reported. The very strong absorption

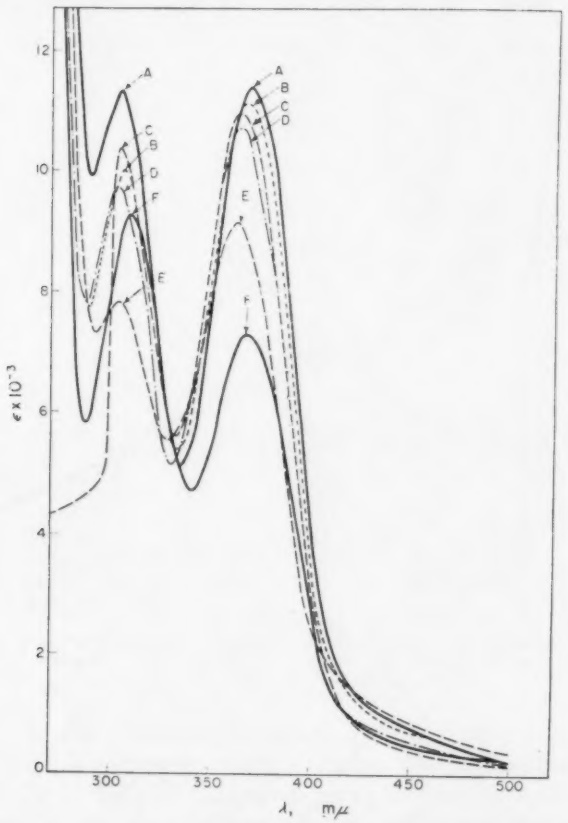

FIG. 3.—Absorption curves of the bis-(N-amylsalicylaldimino)–copper(II) complex between 280 and 400 mμ in various solvents: *A*, carbon tetrachloride; *B*, benzene; C, pyridine; *D*, dioxane; *E*, methanol; *F*, cyclohexane.

bands at 303–308 mμ (log ε = 3·9–4·1) and at 362–368 mμ (log ε = 3·9–4·1) may be attributed to intra-ligand and charge-transfer transitions, respectively.[19] The weak band at about 600 mμ (log ε = 2·1–2·2) probably not single,[23,24] can be considered as due to forbidden crystal field transitions among 3*d* levels. These spectra, with the possible exception of that in pyridine solution, can be accounted for without assuming the formation of pentaco-ordinated adducts. In fact, for these chelates, there will be a little screening of the copper(II) ion along the *z*-axis, so that the molecules of the

[33] J. BJERRUM, C. J. BALLHAUSEN and C. K. JORGENSEN, *Acta. Chem. Scand.* **8**, 1275 (1954).
[34] R. L. BELFORD, M. CALVIN and G. BELFORD, *J. Chem. Phys.* **26**, 1165 (1957).

solvents, to a greater or lesser extent according to their geometrical and electronic characteristics, will influence the ligand field acting on the copper ion.[24] Thus solvents like cyclohexane will influence the spectra, though, obviously, no real co-ordination can be invoked in this case. A similar argument was put forward in the case of the analogous planar complexes of nickel(II).[25] (Part VII of this series).

If then, one excludes the formation of pentaco-ordinated adducts with the solvents one must assume that the dipole moment of these complexes in solution is due to a distortion of the molecule, by repulsive forces of a steric nature. Since the magnetic

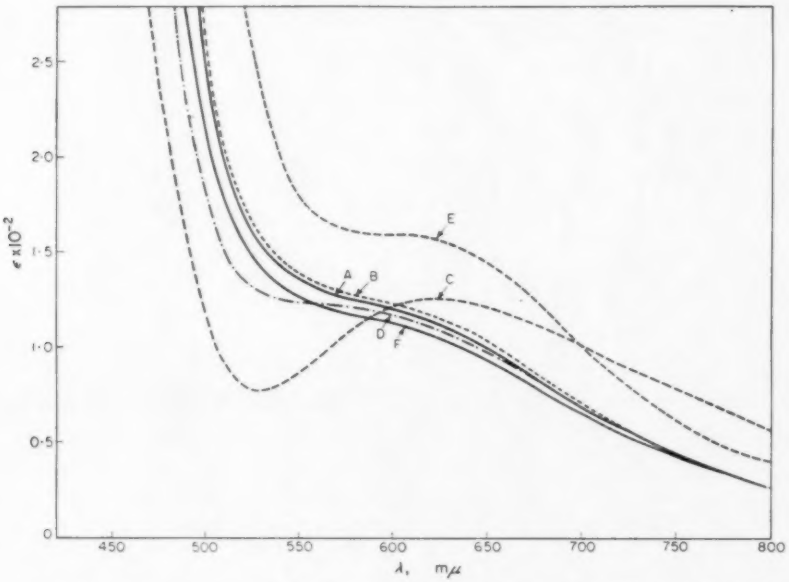

FIG. 4.—Absorption curves of the bis-(N-amylsalicylaldimino)-copper(II) complex between 450 and 800 mμ in various solvents: *A*, carbon tetrachloride; *B*, benzene; *C*, pyridine; *D*, dioxane; *E*, methanol; *F*, cyclohexane.

measurements do not support the hypothesis of tetrahedral forms, it appears reasonable to assume that in solution the molecules of the complexes take on an asymmetrical form, possibly that of flattened tetragonal pyramids, with the copper ion at the vertex, The magnetic moments, close to the "spin-only" values, are in accord with this hypothesis. In this case, in fact, the theory predicts a low orbital contribution.[14] Confirmation of this statement was given by μ_{eff} value of 1·80 B.M., measured for the copper(II)–dimethylglioxime complex ($\chi_g = 4{\cdot}23$; $\chi_M = 1243$; $\chi_A = 1369 \times 10^{-6}$ at 20°) which has been found by X-ray analysis to have a flattened pyrimadal structure.[26]

Acknowledgements—Thanks are expressed to Dr. R. CINI for assisting with some of the magnetic measurements, to the Italian "Consiglio Nazionale delle Ricerche," and to the Sicilian "Consiglio Regionale Ricerche Nucleari" for financial assistance.

[25] C. J. BALLHAUSEN and A. D. LIEHR, *J. Amer. Chem. Soc.* **81**, 538 (1959); G. MAKI, *J. Chem. Phys.* **29**, 1129 (1958).
[26] E. FRASSON, R. ZANETTI, R. BARDI, S. BEZZI and G. GIACOMETTI, *J. Inorg. Nucl. Chem.* **8**, 453 (1958); E. FRASSON, R. BARDI and S. BEZZI, *Acta Cryst.* **12**, 201 (1959).

J Inorg. Nucl. Chem., 1961, Vol. 19, pp. 81 to 93. Pergamon Press Ltd. Printed in Northern Ireland

IRIDIUMCARBONYL COMPOUNDS—V*

BROMO- AND CHLOROCARBONYLIRIDATES

L. MALATESTA and F. CANZIANI
Università di Milano, Istituto di Chimica Generale, Milano, Via C. Saldini

(*Received* 8 *August* 1960)

Abstract—The reaction of K_2IrBr_6 with carbon monoxide at high pressure yielded the previously unknown $K_2[Ir_2(CO)_4Br_5]$. From this, by condensation, cleavage and oxidation reactions, a number of halocarbonyl anions were obtained, which were isolated as tetraphenylarsonium and tetrabutylammonium salts, namely:

$$[Ir(CO)_2Br_2]^-,\ [Ir_2(CO)_4Br_3]^-,\ [Ir_2(CO)_4Br_4]^-,\ [Ir(CO)_2Br_3]^-,\ [Ir(CO)_2Br_4]^-$$

From the reaction of K_2IrCl_6 with carbon monoxide at high pressure the nonstoicheiometric salt $K_2[Ir_2(CO)_4Cl_{(5-\varepsilon)}]$ was obtained, and from this, $K[Ir_2(CO)_4Cl_4]$ and $H[Ir_2(CO)_4Cl_4]$ were prepared. The mode of formation and the possible structure of these halogenocarbonyliridates are discussed.

VOL. 19 1961

Reaction of K_2IrBr_6 *with carbon monoxide*

As was reported in a preliminary paper,[1] the reaction between potassium bromoiridate K_2IrBr_6 and carbon monoxide at high pressure in the presence of a halogen acceptor, proceeds quantitatively according to the general equation:

(a) $$2K_2IrBr_6 + 4CO + 5Cu \rightarrow \underset{I}{K_2[Ir_2(CO)_4Br_5]} + 2KBr + 5CuBr$$

With an initial pressure of 200 atm of carbon monoxide the temperature may be varied between 140 and 220°C, the corresponding reaction times being 70 and 3 hr respectively. If the time is shorter than required for the completion of the above reaction, a mixture of *I* and unreacted bromoiridate is obtained, sometimes accompanied by a small amount of K_2IrBr_5. If the reaction time is longer than required, the product consists of a mixture of *I* with $Ir(CO)_3Br$ and occasionally $Ir(CO)_4$.

Such a complex reaction as (a) very likely takes place through several intermediate steps. *I* is practically the only product isolated even if the reaction is carried out under very different conditions. It must therefore be admitted that the intermediate compounds are all highly reactive to further reaction with carbon monoxide, so that at any moment their concentration in the reaction system is very low. However, under these conditions, *I* must be relatively unreactive.

It was possible to isolate some of the intermediates formed in the first stages of the reaction, by carrying on the carbonylation without the halogen acceptor. Under these conditions iridium is not reduced beyond the trivalent state and a mixture of $K[Ir(CO)_2Br_4]$, $K_3[IrBr_6]$ and $K_2[IrBr_5]$ is obtained. Under such conditions, since the yield of K_3IrBr_6 tends to diminish on prolonging the reaction time and the yield of

* Preceding parts see references (1) to (4) in text.

[1] Part I: L. MALATESTA and M. ANGOLETTA. *J. Inorg. Nucl. Chem.* Supplement **4**, 273 (1957).

K_2IrBr_5 tends to increase, we propose the following course for the reaction:

(b) $$K_2IrBr_6 + 2CO \rightarrow K_3IrBr_6 + K[Ir(CO)_2Br_4] + Br_2$$

(c) $$K_3IrBr_6 \rightarrow K_2IrBr_5 + KBr$$

The second step of this sequence is confirmed by the fact that the previously unknown salt K_2IrBr_5 could be obtained quantitatively by heating K_3IrBr_6 in the presence of carbon monoxide at high pressure. The presence of carbon monoxide is necessary for this reaction and this suggests the existence of an intermediate carbonyl compound, probably a carbonylpentabromoiridiate(III), which however we failed to isolate:

(d) $$K_3IrBr_6 + CO \rightarrow K_2[Ir(CO)Br_5] + KBr \rightarrow K_2IrBr_5 + KBr + CO$$

The reaction sequence of the carbonylation of K_2IrBr_6 in the presence of a halogen acceptor therefore appears to be:

(e)
$$\begin{array}{ccccc} & & K[Ir(CO)_2Br_4] & \xrightarrow{Cu} & K[Ir(CO)_2Br_3] \xrightarrow{Cu} K_2[Ir_2(CO)_4Br_5] \\ K_2IrBr_6 & \nearrow & & & \uparrow Cu \\ & \searrow & K_3[IrBr_6] & \longrightarrow & K_2[Ir(CO)Br_5] \end{array}$$

In the above scheme, the salts $K[Ir(CO)Br_5]$ and $K[Ir(CO)_2Br_3]$ are hypothetical.

Under drastic conditions, *1* reacts further with carbon monoxide to give $Ir(CO)_3Br$ and $Ir(CO)_4$. Although this reduction takes place very slowly, we were unable to stop it at the stage corresponding to the univalent salt-like derivative $K_2[Ir_2^I(CO)_4Br_4]$, (*2*). However *2* is a stable compound which was prepared by us in another way, and might have been supposed to be the intermediate between *1* and $Ir(CO)_3Br$. *2* was obtained, only as a mixture with *1*, when carrying out the carbonylation at a much lower pressure (20–50 atm). The product extractable with acetone thus has a composition between *1* and *2* and can probably be considered a homogeneus mixture of the swo salts. The fact that *2* is not obtained in the carbonylation at high pressure, although it is present, as an impure phase, in the product of the carbonylation at low pressure, seems to indicate that it is very easily transformed into $Ir(CO)_3Br$ by carbon monoxide.

The remarkable difference in the reactivity of *1* and *2* towards carbon monoxide is probably due to a particularly high lattice energy of the former compound. This assumption is supported by the rather unexpected influence of the cation of the bromoiridate on the course of the carbonylation. In fact it was found that tetraphenylarsonium (Tpa) salt: $(Tpa)_2IrBr_6$, and the tetrabutylammonium (Tba) salt: $(Tba)_2IrBr_6$ give, as final stable product, derivatives of iridium (I), the composition of which corresponds to $Tpa[Ir(CO)_2Br_2]$ and $Tba[Ir(CO)_2Br_2]$ respectively.

Although the action of solvents on the crude carbonylation product does not apparently alter the nature of the original bromocarbonyliridate, still the reactivities towards carbon monoxide of the crude product and of the solvent extracted material are very different. In fact if the reaction mixture, obtained as described above at high temperature (140–220°C), is left for an additional time of 7–10 hr under high pressure of carbon monoxide at 70–100°C, another molecule of carbon monoxide per iridium atom is added and a new carbonyliridate containing 3CO per iridium is formed. This however is unstable and when dissolved in acetone immediately loses carbon monoxide and yields again *1*. On the other hand, after extraction and recrystallization from

acetone, *I* reacts with carbon monoxide under pressure at 100°C in a few hours, to give quantitatively the bromotricarbonyliridium:

(f) $$K_2[Ir_2(CO)_4Br_5] + 2CO \rightarrow 2Ir(CO)_3Br + 2KBr + \tfrac{1}{2}Br_2$$

This different behaviour must be due to some physical or chemical difference between the products before and after extraction.

Characterization of $K_2[Ir_2(CO)_4Br_5]$ *and of its hydrolysis products*

I is readily soluble in dilute hydrobromic acid, methanol, acetone and tetrahydrofurane. These solutions are readily oxidized and must not be exposed to air for a long time. From the two last solvents *I* can be recrystallized either by concentration under reduced pressure or by dilution with benzene. On concentration the colour of the solution, which at first is pale yellow, becomes gradually dark red, green and then violet, and finally the product separates in long hair-like needles with a bronze lustre. The product obtained from the solution by addition of benzene is identical with that obtained by concentration.

VOL. 19 1961

It is believed that *I* is really a potassium pentabromotetracarbonyldiiridiate (I, II) and not a 1/1 mixture of $K[Ir(CO)_2Br_2]$ and $K[Ir(CO)_2Br_3]$. Thus (i) the fractional crystallisation fails to separate *I* into crops of different composition and (ii) the solution of *I*, on addition of tetraphenylarsonium bromide, gives the salt $Tpa[Ir_2(CO)_4Br_4]$, related to *I*, and only after refluxing with dilute hydrobromic acid, the salt $Tpa[Ir(CO)_2Br_2]$ deriving from monovalent iridium.

The infra-red spectrum of *I*, could be taken only as a very dilute Nujol mull, because of the almost complete and continuous absorbance of this substance, possibly due to the metallic reflectance of the crystals. Nevertheless it was possible to detect an absorption at $\approx 2000\ cm^{-1}$ (terminal CO groups) but not at $1800\ cm^{-1}$ (bridging CO). This suggests that the two iridium atoms are linked together through bromine bridges and may be represented by the two possible formulas:

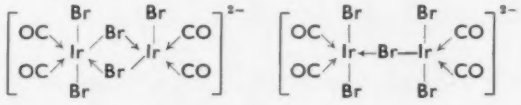

Of these, the second is preferred because of its symmetry, while the first is better in accord with the equilibrium reaction:

(g) $$[Ir_2(CO)_4Br_5]^{2-} \rightleftarrows [Ir_2(CO)_4Br_4]^- + Br^-$$

which takes place very easily in solution. This is shown by the fact that the addition of tetraphenylarsonium bromide to solutions of *I* yields the insoluble salt $Tpa[Ir_2(CO)_4Br_4]$.

Unlike *I*, the solid compound obtained by further addition of CO to the crude *I* at moderate temperature has to be considered a mixture,

(h) $$K_2[Ir_2(CO)_4Br_5] + 2CO \rightarrow K[Ir(CO)_3Br_2] + K[Ir(CO)_3Br_3]$$

unless in it the usual maximum co-ordination numbers for Ir(**I**) and Ir(**II**), five and six respectively, are exceeded. *I* is a diamagnetic substance. This behaviour, which is anomalous for a compound containing one iridium(II) atom, could be explained by assuming the presence of metal-to-metal bonds in the solid. The typical metallic lustre of this compound (and of the analogous chloroderivative) supports the above

hypothesis. This does not hold, however, for the yellow solution of *1* in acetone, which is also diamagnetic, nor for the diamagnetic salts of $[Ir(CO)_2Br_3]^-$.

The chemical investigation on *1* consisted of: (A) potentimetric oxidation; (B) cleavage reactions with amines; (C) cleavage reactions with hydrobromic acid followed by isolation of the fragments as tetraphenylarsonium salts; (D) bromine oxidation.

(A) The potentiometric oxidation of a dilute solution of *1* in dilute hydrobromic acid, using bromine as oxidizing agent, gave no definite results. However it was possible to carry out the same reaction with iodine, after addition of an excess of potassium iodide. The addition of the iodide caused the potential to drop from the initial unsteady value of +50 mV (against a saturated calomel electrode) to a constant value of −130 mV. The titration gave a sharp end point in agreement with the oxidation $Ir^{1.5+} \rightarrow Ir^{3+}$. The iridium(III) derivative thus formed was the anion $[Ir(CO)_2I_4]^-$ which was quantitatively isolated from the titrated solution as its sparingly soluble tetraphenylarsonium salt.[2]

The reaction consists therefore of two separate stages:

$$\text{(k)} \qquad \begin{aligned} K_2[Ir_2(CO)_4Br_5] + 5KI &= K_2[Ir_2(CO)_4I_5] + 5KBr \\ K_2[Ir_2(CO)_4I_5] + \tfrac{3}{2}I_2 &= 2K[Ir(CO)_2I_4] \end{aligned}$$

Although the compound $K_2[Ir_2(CO)_4I_5]$ was not isolated, its formation during the first stage of the reaction is proved by the drop of the potential from +50 mV to −130 mV, on addition of potassium iodide.

Besides confirming the average oxidation state 1·5 for iridium in compound *1*, the potentiometric oxidation with iodine shows that the stabilization of the low oxidation states of iridium, due to co-ordination of carbon monoxide, becomes much less important if the compound contains iodine instead of bromine.

(B) The reaction of *1* with amines (Am), described by ANGOLETTA[3], gives derivatives of Ir(I) and Ir(II) according to the equation:

$$K_2[Ir_2(CO)_4Br_5] + 3Am = Ir(I)(CO)_2AmBr + Ir(II)(CO)Am_2Br_2 + CO + 2KBr$$

(C) The addition of bulky anions to a cold neutral methanol solution of *1* precipitates the salts of the anion $[Ir_2(CO)_4Br_4]^-$; but in hydrobromic acid solution, hydrolysis takes place and salts derived from Ir(I) and Ir(II) may be isolated as well.

The following scheme indicates the conditions under which the various tetraphenilarsonium salts were obtained:

$K_2[Ir_2(CO)_4Br_5]$

Cold Methanol + TpaBr	5% aqueous hydrobromic ac. refluxed for 5′ + TpaBr	Methanol + 20% hydrobromic ac. + TpaBr
$Tpa[Ir_2^{1.5}(CO)_4Br_4]$	$Tpa[Ir^{I}(CO)_2Br_2]$	$Tpa[Ir^{II}(CO)_2Br_3]$

These results show the existence of the following equilibria:

$$\text{(l)} \qquad \begin{array}{ccccc} [Ir_2(CO)_4Br_5]^{2-} & \rightleftharpoons & [Ir(CO)_2Br_2]^- & + & [Ir(CO)_2Br_3]^- \\ \textit{1} \downarrow\uparrow & & \textit{2} & & \textit{4} \\ [Ir_2(CO)_4Br_4]^- & + Br^- \rightarrow & [Ir(CO)_2Br_2]^- & + & [Ir(CO)Br_3]^- + CO \\ \textit{1a} & & \textit{3} & & \textit{4a} \end{array}$$

[2] Part II: L. MALATESTA and S. SANDRONI, Special Publication No. 13 of the Chemical Society, London, p. 122 (1959).
[3] Part III: M. ANGOLETTA, *Gazz. Chim. Ital.* **89**, 2359 (1959).
[4] Part IV: M. ANGOLETTA, *Gazz. Chim. Ital.* In press.

The low solubility of the tetraphenylarsonium salts with bulky monovalent anions, is likely to be responsible of the shift in direction *1* → *1a*. The Ir(II) derivative which was isolated has a composition intermediate between *4* and *4a*, because of the tendency of *4* to lose carbon monoxide when in solution.

(D) Compound *1*, treated with an excess of bromine at low temperature, gives the salt $K[Ir(CO)_2Br_4]$, identical with the compound formed in the carbonylation of K_2IrBr_6 without halogen acceptors. This salt is rather unstable, and loses carbon monoxide readily giving first $K[Ir(CO)Br_4]$ and then $K[IrBr_4]$. The same $K[IrBr_4]$ is obtained by slow oxidation when a hydrobromic acid solution of *1* is left in the air for many hours:

(m) $$2K_2[Ir_2(CO)_4Br_5] + 6HBr + 1{\cdot}5O_2 = K[IrBr_4] + 5CO$$

The previously unknown salts $K[IrBr_4]$ and $K_2[IrBr_5]$ are very stable and nicely crystalline substances. Apparently they can be prepared only through the carbonyl-derivative. The anion $[IrBr_4]^-$ is slowly transformed into $[IrBr_5]^{2-}$ when it is boiled with excess hydrobromic acid, whereas $[IrBr_5]^{2-}$ cannot be transformed into $[IrBr_6]^{2-}$. A more detailed study of the salts of these anions will be published later.

VOL. 19 1961

The fact that on increasing the oxidation number of the metal, the carbon monoxide to metal bond becomes more labile may be related to the decreasing tendency of the metal to form π-bonds. This agrees with the observed shift towards higher frequencies of the infra-red absorption bands of the CO groups in these compounds. The CO stretching frequencies are in fact:

$Tpa[Ir^{I}(CO)_2Br_2]$	2045 cm^{-1}	1996 cm^{-1}
$Tpa[Ir^{II}(CO)_2Br_3]$	2100 cm^{-1}	2057 cm^{-1}
$Tpa[Ir^{III}(CO)_2Br_4]$	2137 cm^{-1}	2096 cm^{-1}

and for the condensed salts:

$Tpa[Ir_2^{I}(CO)_4Br_3]$	2083 cm^{-1}	2037 cm^{-1}
$Tpa[Ir_2^{1.5}(CO)_4Br_4]$	2092 cm^{-1}	2053 cm^{-1}

Reaction of K_2IrCl_6 *with carbon monoxide*

In a preliminary communication,[1] it was reported that the product of this reaction, *5*, after extraction and recrystallization from acetone, had a composition corresponding to $K_2[Ir_2(CO)_4Cl_5]$. This was assumed to be a derivative of iridium having an average oxidation state of 1·5, completely similar to the bromocarbonyliridate described above. Careful consideration of the results of a larger number of experiments have since shown that the former statement is not altogether correct. In fact the products obtained under the most varied experimental conditions, always have a chlorine content slighly lower than the value required for $K_2[Ir_2(CO)_4Cl_5]$. The analytical figures for products obtained in a number of different runs are listed in Table 2. The chlorine deficiency amounts to about 5–6 per cent of the required value, when the carbonylation is carried out at an initial pressure of 100–200 atm, with a temperature ranging between 170 and 200°C and reaction times of 8–17 hr. (the shorter times correspond to higher temperatures and vice versa). Under these conditions the reaction times do not influence the composition of the acetone extractable material. In fact for times shorter than those given above, the reaction mixture still contains some unreacted acetone insoluble chloroiridiate; while for longer times some

iridiumcarbonyl and chlorotricarbonyliridium, both insoluble in acetone, are formed. When the reaction is carried out at the highest temperature compatible with the stability of the product (240°) and at a relatively low pressure (20–30 atm), the chlorine content becomes still lower (9–10 per cent defect on the value calculated for $K_2[Ir_2(CO)_4Cl_5]$) and the composition of the product then approximately corresponds to $K_2[Ir_2(CO)_4Cl_{4\cdot5}]$. In this case too, the reaction time influences the yields more than the composition of the product.

In the carbonylation of K_2IrCl_6, the presence of the halogen acceptor has no determining influence on the type of product. Actually *5* is the only salt isolated, even if no halogen acceptor is present. The different behaviour of K_2IrCl_6 and K_2IrBr_6 in the carbonylation reaction, may be due to the fact that chlorine is likely to be eliminated as carbonyl chloride and bromine as the free element and/or to the increase of stability from the chloro to the bromocarbonyliridate(III). That the stability of the trivalent iridium carbonyl derivatives follows the above trend is indicated by the fact that the iodocompound $K[Ir(CO)_2I_4]$[2] is the only one formed quantitatively by the direct reaction of carbon monoxide on potassium iodoiridate in the presence of halogen acceptor and it is very stable.[4] The bromocompound $K[Ir(CO)_2Br_4]$ can be obtained in rather low yields only when the carbonylation is carried out without the halogen acceptor and it is an unstable substance. Finally no chlorocompound corresponding to this formula has so far been isolated. Moreover, while the addition of bromine to $K_2[Ir(CO)_4Br_5]$ readily gives the salt $K[Ir(CO)_2Br_4]$, the analogous reaction on *5* fails to give the trivalent iridium derivative. No intermediate compound could be isolated so far in the carbonylation of K_2IrCl_6. Nevertheless it can be assumed that the reaction takes place through several steps, according to the scheme:

$$K_2IrCl_6 \xrightarrow{\text{slow}} K_2[Ir(CO)Cl_5] \xrightarrow{\text{fast}} K[Ir(CO)_2Cl_4] \xrightarrow{\text{fast}} K[Ir(CO)_2Cl_3] \longrightarrow$$
$$\longrightarrow \underset{\textbf{5}}{} \xrightarrow{\text{slow}} K_2[Ir_2(CO)_4Cl_4] \xrightarrow{\text{fast}} Ir(CO)_3Cl \xrightarrow{\text{slow}} Ir(CO)_4$$

The product *5*, a non-stoicheiometric phase with a temperature dependent composition, is then to be considered as an isomorphic solution of $K_2[Ir_2(CO)_4Cl_4]$ in $K_2[Ir_2(CO)_4Cl_5]$, containing from 0·2 to 0·5 mole of univalent salt per mole of $K_2[Ir_2(CO)_4Cl_5]$. In a general way, the formula of *5* could be written as $K_2[Ir_2(CO)_4Cl_{5-\varepsilon}](\varepsilon = 0{,}2\text{–}0{,}5)$. The discussions given above for the structure of *1* are therefore valid also for *5*.

Characterization of the potassium chlorocarbonyliridate

Compound *5* is soluble in acetone, sparingly soluble in tetrahydrofurane, methanol, water and hydrochloric acid. Its solutions show a rather high electrical conductivity. Of all solvents, acetone is the most suitable for recrystallizing the salt. Attempts of fractional crystallization from this solvent failed to give different fractions. The data reported in Table 2 refer to products obtained from the crude reaction mixture by acetone extraction. When dissolved in water, or better in dilute hydrochloric acid, *5* gives a clear solution, which is pale yellow when hot and becomes deep blue on cooling. From the cold concentrated solution bronze-coloured needles separate, which have an appearance identical with *5* but are of a different composition. The yields of this new product are much higher if the solution is saturated with potassium

chloride, and the composition of the precipitate then corresponds exactly to $K[Ir_2(CO)_4Cl_4]$(*5a*). In this compound the oxidation number of iridium is 1·5, while it was lower in *5*. The crystallization of *5* from aqueous acid solutions must be accompanied either by partial oxidation or by removal, through decomposition or fractional crystallisation, of the minor component of the mixture. The anion of the salt (*5a*) must be assigned a binuclear structure, probably:

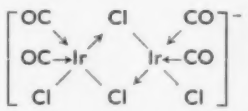

In this structure the two iridium atoms, though having formally different oxidation states, are wholly equivalent.

The anion $[Ir_2(CO)_4Cl_4]^-$ is extremely stable. The free acid, which can be prepared by treating a concentrated solution of *5* with concentrated hydrochloric acid, is also a remarkably stable substance, which crystallizes with four molecules of water $H[Ir_2(CO)_4Cl_4]\cdot 4H_2O$. The water of crystallization cannot be removed *in vacuo* at room temperature; at higher temperature complete decomposition occurs.

The free acid was transformed into the benzyltrimethylammonium (Btma) salt: (Btma) $[Ir_2(CO)_4Cl_4]$, and into the Tpa salt, (Tpa) $[Ir_2(CO)_4Cl_4]$, crystalline substances insoluble in all solvents.

The fact that *5*, like *1*, reacts with amines to give derivatives of univalent and divalent iridium[3] points out the basic similarity between the chloro and bromo dicarbonyliridiates.

Finally, the potentiometric titration of *5* is in complete agreement with the formula proposed on the basis of the analytical data. The direct oxidation of solutions of *5* in dilute hydrochloric acid, using cerium(IV) sulphate or permanganate as oxidizing agents, proceeds as if the oxidation was irreversible, and no end point can be detected. Instead reproducible results were obtained by adding an excess of potassium iodide and then titrating with iodine. On addition of potassium iodide the potential of the solution dropped from an unsteady value of +65 mV to a constant reproducible value of −130 mV (measured against a saturated calomel electrode). The titration curve showed a well marked end-point when 1·7 equivalents of iodine per iridium atom had been added. As confirmed by the isolation of the anion $[Ir(CO)_2I_4]^-$ as the tetraphenylarsonium salt, the final stage of the oxidations is the trivalent iridium derivative. The reactions which take place can be formulated as:

$$K_2[Ir_2(CO)_4Cl(5-\varepsilon)] + (5-\varepsilon)KI = K_2[Ir_2(CO)_4I(5-\varepsilon)] + (5-\varepsilon)KCl$$

$$K_2[Ir_2(CO)_4I(5-\varepsilon)] + \tfrac{1}{2}(3+\varepsilon)I_2 = 2K[Ir(CO)_2I_4]$$

The first reaction is due to the well known tendency of iodide to substitute chloride in the co-ordination compounds of metals of the platinum group, and is proved by a drop in potential upon the addition of iodide. In the second reaction, the amount of iodine required depends on the value of ε. The experimental value of 1·7 equivalents of iodine per iridium atom corresponds to a value of 0·2 for ε, in agreement with that previously assigned to compound *5* on the basis of the analysis.

VOL. 19 1961

EXPERIMENTAL SECTION

1. *Reaction of* K_2IrBr_6 *with CO in the presence of copper*

Dry $K_2[IrBr_6]$ (2–6 g) was introduced into an open glass tube, 8 mm wide and 150 mm long, with glass wool stoppers at both ends. The tube was reduced to a capillary at both sides (1·5 mm bore), introduced into a copper tube and then into the pressure vessel (stainless steel). The latter vessel was filled with dry CO at 200 atm and heated to the chosen temperature. The reaction time was varied from a few hours to several days as indicated in the Table 1. In most cases the product was a homogeneous fine crystalline powder of tobacco-like colour; a few long brown needles of $Ir(CO)_3Br$, or green-yellow prismatic crystals of $Ir(CO)_4$ could sometimes be observed.

The product was extracted with 20 ml of dry acetone for each gramme of original $K_2[IrBr_6]$. In most cases the dissolution took place without any evolution of gas and an orange solution was obtained, which was filtered and evaporated under reduced pressure. The insoluble residue from the acetone was mainly KBr, sometimes mixed with some $K_3[IrBr_6]$, K_2IrBr_5, $Ir(CO)_3Br$ and $Ir(CO)_4$.

On concentration the acetone solution became first dark-brown then deep green, until a crop of needle-like crystals of tobacco-like colour with metallic lustre separated.

This product (*1*) was recrystallized by dissolving it in a few ml of acetone and reprecipitating with benzene. It is soluble in acetone, tetrahydrofurane, methyl and ethyl alcohol giving an orange-yellow colour, and in diluite hydrobromic acid giving a deep blue color which turns yellow on warming. It is insoluble in hydrocarbons and in diethyl ether.

It does not melt and decomposes above 200°C with partial sublimation of $Ir(CO)_3Br$.

1 was analysed in the following way: 50–70 mg, weighed in a platinum boat, were introduced into a quartz tube 10 mm wide, 800 mm long. Dry hydrogen was passed through the tube while the temperature was slowly raised to 1000°C. The effluent gases were absorbed in water. Under these conditions the bromine which was not combined as potassium bromide (free bromine) was collected as hydrobromic acid.

The potassium bromide distilled from the boat to the colder part of the quartz tube. The hydrobromic acid solution was titrated, the metallic iridium left in the boat weighed, the tube rinsed and the KBr analysed for bromide. A blank test on pure $K_2[IrBr_6]$ with this method gave the following results: Found: Ir, 25·8; Br(free), 43·0; KBr, 31·7; Calc. for $IrBr_4 \cdot 2KBr$; Ir, 25·7; Br(free), 42·6; KBr, 31·7%.

In the analysis of *1* a small amount of iridium was lost owing to sublimation: the relative error is about −3 per cent.

The analysis of carbon monoxide was carried out reacting *1* with an excess of p-tolylisocyanide at about 150°C in an apparatus similar to that of Zerewitinoff. Blank tests with pure $Ir(CO)_3Br$ showed that the accuracy of the method is about ±3 per cent (relative).

The analytical results obtained for products prepared under different conditions of time, pressure and temperature are summarized in Table 1. The magnetic susceptibility of these products determined with the Gouy method varies from 205×10^{-6} to 156×10^{-6} at 20°C. The molar electric conductivity of *1* (Preparation No. 6) at 25·5° and in 1/760 M acetone solution was 300 Ω^{-1} cm² and at 1/16080 M, 310 Ω^{-1} cm².

Action of CO *on 1 at low temperature.* (1) The crude product of the carbonylation of $K_2[IrBr_6]$ at high temperature, prepared as described above, was kept for 24 hr at 70° under 200 atm CO. The product obtained was a dark mass which dissolved in acetone giving an intense blue solution. This turned orange in a few seconds with brisk evolution of CO. The substance obtained from this solution on evaporation of the solvent was identical to *1* (Ir, 38·9; CO, 11·7; Br (free), 25·0%).

The crude dark mass analysed as follows:

Ir, 30·1; CO, 13·1; Br (free), 18·5%; Ratio CO/Ir = 2·99

The solid product of the reaction

$$2K_2IrBr_6 + 6CO = 2KBr + K_2[Ir_2(CO)_6Br_5] + 5/2Br_2$$

requires Ir, 30·5; CO, 13·2; Br (free), 18·9%.

(2) *1* (2g) after extraction with acetone was kept in the pressure vessel for 12 hr at 90°C under 200 atm CO. The crude product extracted with acetone and with cold water gave as residue the pure $Ir(CO)_3Br$ (1·0 g). (Found: Ir, 54·5%; CO, 22·9. Calc. for $Ir(CO)_3Br$; Ir, 54·1; CO, 22·5%).

Potentiometric oxidation of I. The solution of *I* in dilute hydrobromic acid was titrated with 0·04 N bromine solution. A blank platinum electrode and a calomel electrode (KCl saturated) were used. The initial potential of the platinum electrode, of about +50 mV (against a calomel electrode), increased steadily on titration, but no equivalent point could be detected under these conditions.

TABLE 1.—REACTION OF K_2IrBr_6 WITH CO IN PRESENCE OF COPPER

Initial CO condition			Analysis of the compound *I* extracted with acetone					
	Pressure (atm)	Temp. (°C)	Time (hr)	Ir (%)	CO (%)	Br (free) (%)	KBr (%)	Total (%)	Yields (%)
(1)	200	140	72	38·7	11·4	25·0	23·9	99·0	80
(2)	200	160	42	39·1	11·5	24·1	23·0	99·7	82
(3)	200	210	72	39·0	11·6	25·0	23·9	99·5	75*
(4)	200	160	48	38·8	10·7	24·2	23·4	97·1	76
(5)	200	160	22	38·1	10·6	25·5	24·1	98·3	50†
(6)	200	220	6	38·9	11·6	25·0	23·9	99·4	85
(7)	50	220	18	40·5	11·3	20·7	25·4	97·9	85
(8)	30	230	18	40·8	12·0	20·6	25·6	99·0	80
(9)	10	250	18	41·0	11·7	20·8	25·0	98·5	73
$K_2Ir_2(CO)_4Br_5$ requires				39·4	11·5	24·7	24·5	100·0	
$K_2Ir_2(CO)_4Br_{4,5}$ requires				40·8	11·8	21·1	25·5	100·0	

* Impure with much $Ir(CO)_3Br$ and $Ir(CO)_4$
† Impure with much K_2IrBr_5

The titration was then carried out, after addition of an excess of KI, on 0·0380 g of *I* (0·036 mmole) in 100 ml of HBr 0·01 N. The potential of the platinum electrode changed immediately from the unstable figure of +50 mV to a very stable figure of −130 mV and a very sharp equivalent point was obtained by titrating with 0·04 N iodine:

0·00 ml	−130 mV	1·50 ml	−105 mV	2·50 ml	−75 mV
0·50	−120	1·75	−100	2·58	−60
0·75	−117	2·00	−92	2·61	+10
1·00	−115	2·25	−85	2·65	+11·5

Taking 2·60 ml as the equivalence point we have 0·104 meq iodine for 0·0362 mM of I, that is 2·9 eq/mole in comparison with the calculated figure of 3 eq/mole.

Separation of $[Ir(CO)_2I_4]^-$ *formed in the reaction of I with iodine.* Half a gramme of *I* (0·51 mmole) in 10 ml methanol were reacted with 2 g NaI and 15 ml N/10 iodine solution in methanol. A solution of 0·9 tetraphenylarsonium (Tpa) iodide (2 mmoles) in 10 ml methanol was then added. A red crystalline precipitate separated (0·9 g) which was filtered and washed with cold methanol. m.p. 210°C (Found: CO, 5·1; I, 44·6; As, 6·6; Ir, 17·0. Calc. for $C_{24}H_{20}AsIr(CO)_2I_4$; CO, 4·9; I, 44·6; As, 6·6; Ir, 16·9).

2. *Reaction of* K_2IrBr_6 *with CO without halogen acceptor*

(1) *Preparation of* $K[Ir(CO)_2Br_4]$. Five grammes of K_2IrBr_6 were enclosed in a phial with an open capillary tube of 0·1 mm internal bore and reacted with CO (initial pressure 50 atm) at 220°C for 8 hr. The crude product was extracted with tetrahydrofurane (50 ml), and the solution was evaporated under reduced pressure. The residue (1·5 g) was a yellowish crystalline powder, which did not melt. (Found: Ir, 32·0; CO, 9·0, Br, 53·5; K, 7·6. Calc. for $KIr(CO)_2Br_4$; CO, 9·0; Br, 53·5; K, 7·6%).

The same $K[Ir(CO)_2Br_4]$ was prepared from 1 g of *I* and 3 ml liquid bromine at 0°C by evaporation of the bromine in excess in the cold, and extraction with acetone. (Found: Ir, 31·9; CO, 8·92; Br, 49·3%).

(2) *Preparation of* $[As(C_6H_5)_4][Ir(CO)_2Br_4]$ *and* $[As(C_6H_5)_4][IrBr_4]$. The $K[Ir(Co)_2I_4]$ salt (1 g) was dissolved in 10 ml methanol and 10 ml 10 per cent methanolic solution of TpaBr were added. A crystalline precipitate separated (1·1 g) which was filtered, washed with cold methanol (5 ml) and dried. m.p. 190°C (dec.). (Found: CO, 5·40; Br, 33·6; Ir, 20·0. Calc. for $C_{24}H_{20}AsIr(CO)_2Br_4$; CO, 5·88; Br, 33·6; Ir, 20·3%).

The infra-red spectrum of the solid in Nujol has two intense bands in the region of the CO stretching frequency at 2135 cm^{-1} and 2095 cm^{-1}.

When the tetraphenylarsonium salt (1 g) was refluxed in 25 ml methanol for 2 hr, a new crystalline product, pink needles soluble in warm methanol and in warm 80 per cent ethanol, separated on cooling. It contains about three molecules of ethanol of crystallization, two of which are lost on heating at 200°C, m.p. 194°C. (Found: C, 35·05; H, 3·28; Ir, 19·10; Br, 31·40. Calc. for $C_{24}H_{20}AsIrBr_4{\cdot}3C_2H_5OH$: C, 35·15; H, 3·71; Ir, 18·85; Br, 31·20%).

(3) *Preparation of* $[N(C_4H_9)_4][Ir(CO)_2Br_4]$. One gram of *I* was dissolved in 50 ml of dilute hydrobromic acid (1:10), and treated with 3 ml of bromine. The excess of bromine was removed by evaporation under reduced pressure, and the residual solution treated with tetrabutylammonium bromide (TbaBr). A precipitate separated, which was crystallized from ethanol: canary-yellow plates, m.p. 190°C. (Found: Ir, 23·65; Br, 37·0; CO, 6·45; N, 1·95. Calc. for $N(C_4H_9)_4Ir(CO)_2Br_4$: Ir, 23·60; Br, 39·4; CO, 6·97; N, 1·72%).

The corresponding trimethylbenzylammonium salt, yellow prisms m.p. 192°C from ethanol of from acetone–benzene, was obtained using $(CH_3)_3(C_6H_5CH_2)NBr$ instead of $(C_4H_9)_4NBr$. (Found: Ir, 26·10; Br, 44·80; CO, 7·25. Calc. for $(CH_3)_3(C_6H_5CH_2)NIr(CO)_2Br_4$: Ir, 25·90; Br, 44·50; CO, 7·80%).

(4) *Preparation of* $[(C_4H_9)_4N][IrBr_4]$. $(Tba)Ir(CO)_2Br_4$, on prolonged boiling in ethanol, loses carbon monoxide, and gives a product which crystallizes in pink needles containing solvent of crystallization. The same salt can be obtained also from the aqueous mother liquor of Tba $Ir(CO)_2Br_4$, by concentration and recrystallization from ethanol. (Found: Ir, 22·50; Br, 37·5; C, 27·83; H, 5·34. Calc. for $(C_4H_9)_4NIrBr_4{\cdot}2C_2H_5OH$: Ir, 22·75; Br, 37·8; C, 28·4; H, 5·66%).

The solvent of crystallization is removed by heating the product just below its melting point.

(5) *Preparation of* $K_2[IrBr_5]$ *and related salts.* The product extracted with tetrahydrofurane as described in 2.(1), was dried and extracted in a Soxhelet with dry acetone. The pink acetone solution was evaporated under reduced pressure and the residue (1·5 g) recrystallized from 50 per cent ethyl alcohol. These pink crystals are soluble in acetone and very soluble in water from which they separate as dihydrate. (Found: Ir, 29·10; K, 11·7; Br, 59·5. Calc. for K_2IrBr_5: Ir, 28·80; K, 11·6; Br, 59·5%).

The same product was obtained in almost quantitative yields when K_3IrBr_6 was reacted with CO at 200 atm and 210°C for 12 hr in the absence of halogen acceptor.

No hydrolysis was observed on boiling an aqueous solution of K_2IrBr_5 for an hour. It did not react with bromine in presence of hydrobromic acid [difference from K_3IrBr_6 and $K_2IrBr_5(OH)$]. It gave insoluble precipitates with many heavy metals such as Ag^+, Tl^+, Hg_2^{2+}, Hg^{2+}. The caesium, tetraphenylarsonium and tetrabutilammonium salts, which are almost insoluble in water, were obtained by exchange and analysed. (Found: Ir, 21·55; Cs, 30·60; Br, 45·40. Calc. for Cs_2IrBr_5: Ir, 22·50; Cs, 30·80; Br, 46·70%. Found: Ir, 13·90; Br, 30·00. Calc. for $C_{48}H_{40}As_2IrBr_5$: Ir, 14·20; Br, 29·45%. Found: Ir, 17·65; Br, 36·20. Calc. for $[(C_4H_9)_4N]_2IrBr_5$: Ir, 17·90; Br, 37·00%).

When K_2IrBr_5 was reacted with CO at 200 atm initial pressure and 200°C, in the absence of a halogen acceptor, no change was observed after 20 hr. The same reaction in the presence of copper gave a 50 per cent yield of $K_2[Ir_2(CO)_4Br_5]$.

3. *Tetraphenylarsonium dibromodicarbonyliridate (I)*

(a) *Preparation from 1.* One gramme of *I* in 50 ml aqueous 5 per cent hydrobromic acid was refluxed for about 5′, filtered, and 1 g TpaBr in 10 ml methanol was then added. The yellow crystalline substance which separated at once was filtered, washed with a few ml methanol and recrystallized from ethanol. It is soluble in benzene and ethanol; m.p. 228°C. (Found: CO, 7·40; Br, 21·8; As, 8·9; Ir, 24·10. Calc. for $C_{24}H_{20}AsIr(CO)_2Br_2$: CO, 7·07; Br, 20·20; As, 9·47; Ir, 24·4%).

(b) *Preparation from* $Ir(CO)_2$(p-toluidine)Br. To 1 g $Ir(CO)_2(C_7H_7N)Br$[9] dissolved in 20 ml

warm methanol, containing a few drops of conc. aqueous hydrobromic acid, 1 g TpaBr in 10 ml methanol was added. The precipitate was filtered and washed with methanol; under the microscope it appeared to be a mixture of black needles and yellow prisms. It was then washed with a few ml acetone which dissolved the yellow crystals. The acetone was evaporated at reduced pressure and a crystalline yellow product was obtained, which, after recrystallization from ethanol, was found identical with the product of preparation (a) m.p. 227°C; m.p. in mixture with the product described in (a) 227·5°C.

(c) *Preparation by carbonylation of* $(Tpa)_2[IrBr_6]$. Tetraphenylarsonium hexabromoiridate(IV) prepared in aqueous solution from Na_2IrBr_6 and TpaBr, was carbonylated, like the potassium salt, at a pressure of 200 atm of CO and 200°C for 17 hr, in the presence of metallic copper. The crude product was extracted with acetone and crystallized from acetone–methanol. It was recognized to be identical with the product prepared as described in (a) and (b); m.p. 227°C; m.p. in mixture with the product prepared as described in (a) 227·5°C. (Found: CO, 7·7; Br, 21·3; As, 9·3. Calc. for $C_{24}H_{20}AsIr(CO)_2Br_2$: CO, 7·07; Br, 20·2; As, 9·4%).

The molar conductivity in nitrobenzene at 25°C gave the following results:

C = 1/250 M	17·5 Ω^{-1} cm^2	C = 1/2000 M	19·9 Ω^{-1} cm^2
1/500	18·9	1/4000	20·0
1/1000	19·6	1/8000	20·1

The cryoscopy in nitrobenzene at 1/240 M gave a mol. wt. of 415 (calculated 792), so that at this dilution and at 5°C, $\alpha = 0{\cdot}91$, from the conductivity data at C = 1/250 molar and at 25°C, $\alpha = 0{\cdot}88$.

4. *Tetrabutylammonium dicarbonyldibromoiridate(I)*

Tba_2IrBr_6, prepared from Na_2IrBr_6 and TbaBr by exchange reaction in water, was introduced into an open glass tube in the presence of halogen acceptor, and treated for 24 hr with carbon monoxide at 130°C and 200 atm. The crude product is a sticky mass of greenish yellow colour, readily oxidized by air. On treating with acetone, a yellow solid residue is obtained (yields about 30 per cent), which can be crystallized from ethanol to give yellow needles, m.p. 92°C. The compound is soluble in acetone, benzene, methylene chloride. (Found: Ir, 27·8; Br, 21·1; CO, 8·1; C, 33·0; H, 5·6. Calc. for $(C_4H_9)_4NIr(CO)_2Br_2$; Ir, 26·05; Br, 21·6; CO, 7·56; C, 35·5; H, 6·4%).

The same product was also obtained as in 3a, but using TbaBr instead of TpaBr.

The methanolic mother liquor, after separation of $Tba[Ir(CO)_2Br_2]$, was concentrated under reduced pressure, giving the crystalline $Tba[IrBr_4]$ described in *2* (4).

5. *Tetraphenylarsonium tetrabromotetracarbonyldiiridate(I,II)*

One gramme of *I* in 50 ml methanol were treated with 1 g TpaBr in 20 ml methanol. The crystalline product which separated, was washed with methanol, then with acetone and dried. Dark brown needles, nearly insoluble in all common solvents; m.p. 250°C. (Found: CO, 9·1; Br, 26·5; As, 6·5. Calc. for $C_{24}H_{20}AsIr_2(CO)_4Br_4$: CO, 9·3; Br, 26·6; As, 6·2%).

6. *Tetraphenylarsonium tribromocarbonyliridate(II)*

A solution of *I* (1 g) in 10 ml methanol and 5 ml conc. aqueous hydrobromic acid was refluxed for a few minutes and then a solution of 1 g TpaBr in 20 ml methanol was added. On cooling a crystalline yellow product precipitated, which was filtered and washed with cold methanol; m.p. 175°C, soluble in acetone, benzene, nitrobenzene and chloroform. (Found: CO, 5·8; Br, 28·3; As, 9·0; Ir, 23·3. Calc. for $C_{24}H_{20}AsIr(CO)_2Br_3$: CO, 6·4; Br, 28·4; As, 8·9; Ir, 22·9%).

The molar conductivity of Tpa $[Ir(Co)_2Br_3]$ in nitrobenzene at 20°C gave the following results:

C = 1/250 M	15·6 Ω^{-1} cm^2	C = 1/2000 M	18·9 Ω^{-1} cm^2
1/500	17·2	1/4000	19·3
1/1000	18·3	1/8000	19·4

Mol. Wt., by cryoscopy in 1/224 M nitrobenzene, 525 (Calc. 844).

VOL. 19 1961

7. *Tetraphenylarsonium tribromotetracarbonyldiiridate(I)*

In the reaction of $Ir(CO)_2(C_7H_7N)Br$ with TpaBr (see 3b) a mixture was obtained containing $Tpa[Ir(CO)_2Br_2]$ and $Tpa[Ir_2(CO)_4Br_3]$. The latter remained undissolved after washing with methanol and acetone. Long brown needles insoluble in all common solvents; m.p. 260°C. (Found: CO, 10·0; Br, 22·0; As, 6·8. Calc. for $(C_6H_5)_4As[Ir^I_2(CO)_4Br_3]$: CO, 10·0; Br, 21·4; As, 6·7%).

8. *Reaction of* K_2IrCl_6 *with carbon monoxide*

The carbonylation of $K_2[IrCl_6]$ was carried out as described for $K_2[IrBr_6]$ with the only difference that the action of the copper as halogen acceptor had to be limited. This was achieved by using a copper tube coated with a thin layer of CuCl, instead of a clean tube, which would have induced the formation of some $Ir(CO)_4$. The layer was mechanically removed as soon as it got thicker.

TABLE 2.—PRODUCTS OF THE REACTION OF K_2IrCl_6 WITH CO, IN THE PRESENCE OF COPPER

Initial CO conditions			Analysis of the products extracted with acetone				
Pressure (atm)	Temp. (°C)	Reaction time (hr)	Ir (%)	CO (%)	Cl (free) (%)	KCl (%)	Total (%)
(1) 200	170	12	52·0	14·8	13·5	19·5	99·8
(2) 200	200	9	51·9	14·7	13·5	20·0	100·1
(3) 200	180	17	52·4	14·7	13·3	19·6	100·0
(4) 100	200	12	51·5	14·8	13·2	18·9	98·3
(5) 100	170	27	50·5	14·7	13·5	19·1	97·8
(6) 100	210	7	53·4	14·7	13·2	18·5	99·8
(7) 200	190	10	50·0	14·5	13·0	20·4	98·9
(8) 20	240	18	51·8	14·1	11·9	22·1	99·0
(9) 200	240	3	51·6	14·4	12·3	20·6	99·0
$K_2[Ir_2(CO)_4Cl_{4.6}]$ requires			51·6	15·1	13·3	20·0	100·0
$K_2[Ir_2(CO)_4Cl_{4.5}]$ requires			52·4	15·3	12·0	20·3	100·0

Under the conditions reported in Table 2 the carbonylation reaction gave yields of 80–90 per cent. The potassium chlorocarbonyliridate was extracted with about 50 ml of warm acetone for each gramme of crude product. The dilute acetone solution is orange and becomes brown-red on concentration and finally blue-green when the first needle-like crystals separate. The evaporation was interrupted when a few ml of solution were still present, the mass was filtered by suction and washed first with a few drops of cold acetone and then with hexane. The product, *5*, was obtained as hair-like crystals with golden lustre. The analysis were carried out as described for *1*. In some cases the total chlorine was determined by the Parr bomb method. The results reported in Table 2 show that the composition of the potassium chlorocarbonyliridate *5* prepared under very different conditions is constant or almost so, and that the average values are very near to the calculated values for $K_2[Ir(CO)_4Cl_{5-\varepsilon}]$ with $\varepsilon = 0{\cdot}2$. In runs 8 and 9, at very high temperature, when a mixture of iridium-carbonyl and *5* were obtained, the latter, after extraction with acetone, had a value of ε as low as 0·5.

The electric molar conductivity of *5* (Prep. 4 of Table 2) in acetone at 25° C gave the following results:

C = 1/760 M	256 Ω^{-1} cm^2	C = 1/12160 M	314 Ω^{-1} cm^2
1/1520	298	1/24320	322
1/3040	302	1/48640	324
1/16080	308		

The reaction was repeated without the copper tube, enclosing K_2IrCl_6 in a glass tube with a long capillary. At 200°C and 200 atm. in 24 hr only the product *5* was obtained, but with much lower yield (about 30 per cent).

Potentiometric oxidation of 5. The oxidation of the solution of *5* (Prep. 4 of Table 2) in aqueous dilute (1/20 N) hydrochloric acid with N/10 cerium(IV) sulphate did not show any equivalence point whatever. The titration could however be carried out in the presence of an excess of potassium iodide. The potential of the platinum electrode which had in hydrochloric acid an unstable value of ca. +65 mV, (against a saturated calomel electrode) dropped at a stable value of −130 mV after addition of potassium iodide and a very sharp end point was obtained. The titration of 0·0392 g substance (0·053 mmole) in about 100 ml 0·01 N HCl with 0·04 N iodine solution, gave the following figures:

0·00 ml	−130 mV	2·00 ml	−105 mV	4·35 ml	+100 mV
0·40	−125	3·00	−95	4·60	+120
0·60	−120	4·00	−85	4·70	+125
1·00	−110	4·30	−80	4·90	+140

Taking 4·32 ml as the equivalent point we have 3·26 eq/mole, that is $\varepsilon = 0{\cdot}26$ in comparison to 0·2 calculated from analysis.

9. *Tetraphenylarsonium tetrachlorotetracarbonyldiiridate*

The solution of 1 g of *5* in 100 ml acetone was precipitated with excess TpaCl in methanol. The precipitate was thoroughly washed with acetone and dried. Brown needles, insoluble in all solvents; m.p. 225°C (dec.). (Found: CO, 10·75; Cl, 14·1; As, 7·30. Calc. for $C_{24}H_{20}AsIr_2(CO)_4Cl_4$; CO, 11·07; Cl, 14·03; As, 7·33).

10. *Potassium tetrachlorotetracarbonyldiiridate*

To a saturated warm solution of *5* in 50 ml 0·2 per cent hydrochloric acid, 10 g solid potassium chloride were added. On cooling, hair-like golden needles separated which were filtered, washed with a few ml ice water and dried over P_2O_5 under reduced pressure. (Found: Ir, 55·4; CO, 16·0; Cl, 20·3; K, 6·9. Calc. for $KIr_2(CO)_4Cl_4$: Ir, 56·8; CO, 16·5; Cl, 20·8 and K, 5·9%).

11. *Hydrogen tetrachlorotetracarbonyldiiridate tetrahydrate*

The warm (70–80°C) saturated solution of *5* in 30 ml 10% hydrochloric acid is filtered and cooled to 0°C. The crystalline mass is filtered by suction, washed with one ml iced water and dried under reduced pressure over P_2O_5. (Found: Ir, 52·8; CO, 15·6; Cl, 19·6; K, 1·0. Calc. for $HIr_2(CO)_4Cl_4{\cdot}4H_2O$: Ir, 53·8; CO, 15·6; Cl, 19·0; K, 0·0%).

12. *Benzyltrimethylammonium tetrachlorotetracarbonyldiiridate*

A concentrated methanol solution of the free acid was treated with an excess of benzyltrimethylammonium chloride. The brown crystalline precipitate was filtered, washed with methanol and dried under reduced pressure. (Found: CO, 14·2; Cl, 17·6; N, 3·5. Calc. for $(C_{10}H_{16}N)Ir_2(CO)_4Cl_4$: CO, 14·2; Cl, 18·0; N, 3·6%).

Acknowledgement—This research has been supported by contract No. 61(052)–83 with the Air Force Office of Scientific Research of the Air Research and Development Command, United States Air Force, through its European Office.

VOL. 19 1961

J. Inorg. Nucl. Chem., 1961, Vol. 19, pp. 94 to 100. Pergamon Press Ltd. Printed in Northern Ireland

THE STRUCTURE OF URANYL AZIDE— ITS INSTABILITY CONSTANT IN AQUEOUS SOLUTIONS

F. G. SHERIF and Miss A. M. AWAD
Faculty of Science, University of Alexandria, Alexandria, Egypt

(*Received* 14 *September* 1960)

Abstract—Aqueous solutions containing uranyl and azide ions were found to have a maximum absorption at the wavelength 420 mμ suitable for spectrophotometric studies. Spectrophotometric titrations in aqueous solutions and in water–acetone mixtures suggested the presence of complex ions containing uranyl and azide ions in the ratios 1:1 and 1:2 respectively. The slope ratio method and the continuous variation method confirmed the existence of the mono-azido uranyl complex ion $[UO_2(N_3)]^+$, the instability constant of which was found to be $4{\cdot}86 \pm 0{\cdot}4 \times 10^{-3}$. Conductimetric titrations indicated the possible stepwise formation of the mono-, di- and triazido uranyl complex ions in relatively concentrated solutions. Migration experiments indicated the existence of both positively and negatively charged complex ions.

THE study of metallic complex azides is of interest because of the analogy with the corresponding thiocyanates, and complexes between azide ions and Cu^{2+},[1] Co^{2+},[2] and Fe^{3+},[3] have been investigated. Thiocyanate produces a yellow colour with the uranyl ion, and AHRLAND[4] has reported the existence of three complexes MA^+, MA_2 and MA_3^- ($M = UO_2^{2+}$ and $A = SCN^-$). The yellow colour formed from uranyl and azide ions is apparently similar to that of the uranyl thiocyanate complexes and its importance as a means for the determination of uranium has been pointed out.[5] The intensity is proportional to the concentration of uranium in the presence of a large excess of azide ion and at a fixed hydrogen ion concentration. The nature and structure of uranyl complexes have been reviewed by COMYNS,[6] but the uranyl azide complexes do not appear to have been studied. The present studies were made in order to determine the structural formulae and stabilities of possible complexes formed in aqueous solutions.

EXPERIMENTAL

Uranyl nitrate hexahydrate (Merck analytical grade) was used. A stock solution 0·1 M was prepared and analysed gravimetrically by precipitation as ammonium diuranate and ignition to U_3O_8. Other solutions were prepared from the stock solution by appropriate dilutions. The experimental techniques have been described in a previous paper.[7] Conductivity measurements were carried out using a conductimeter equipped with a magic eye indicator; a high-wattage loudspeaker circuit replaced the headphones. The electrodes were of the dipping type with two 1 cm² platinum plates separated from each other by a distance of 1 cm. The vessel was of 50 ml capacity and was provided with a side-tube for introducing the titrating reagent without interrupting measurements.

[1] G. SAINI and G. OSTOCALI, *J. Inorg. Nucl. Chem.* **8**, 346 (1958).
[2] P. SENISE, *J. Amer. Chem. Soc.* **81**, 4196 (1959).
[3] E. K. EL-SHAMY and F. G. SHERIF, *Egypt. J. Chem.* **1**, 35; 257 (1958); **2**, 217 (1959).
[4] S. AHRLAND, *Acta Chem. Scand.* **3**, 1007 (1949); *Chem. Abstr.* **44**, 2883 (1950).
[5] H. I. FEINSTEIN, *Analyt. Chim. Acta* **15**, 288 (1956).
[6] A. E. COMYNS, *Chem. Revs.* **60**, 115 (1960).
[7] F. G. SHERIF and W. M. ORABY, *J. Inorg. Nucl. Chem.* In press.

VOL. 19 1961

RESULTS

Absorption spectrum of uranyl azide solutions

An aqueous solution was prepared containing equimolar amounts of uranyl nitrate and sodium azide, each 0·002 M, and the absorption spectrum was measured over a wavelength range from 380 to 500 mμ. The colour intensity decreased sharply with increasing wavelength to 400 mμ and then increased to a maximum at 420 mμ before decreasing again. This maximum absorption was assumed to be characteristic of the uranyl azide complex. Uranyl nitrate under the same conditions has a maximum

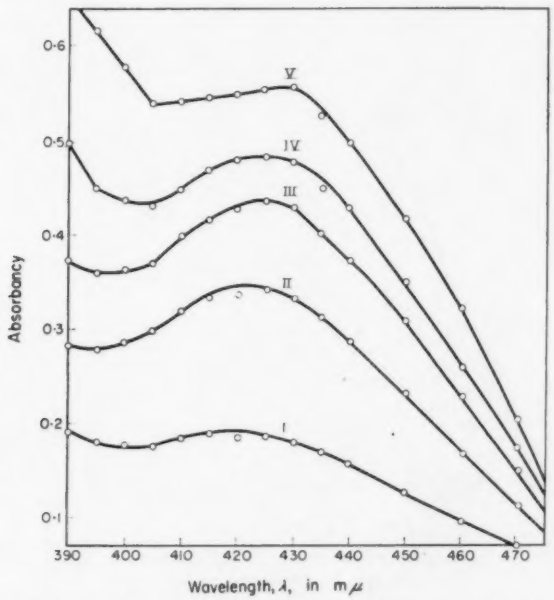

FIG. 1.—Variation in the absorbancy of uranyl azide solutions (UO_2^{2+} = 0·004 M) with increasing concentration of azide ion. N_3^- (I) 0·004 M; (II) 0·008 M; (III) 0·020 M; (IV) 0·040 M; (V) 0·080 M.

absorption at a wavelength about 10 mμ lower than that of uranyl azide, but with comparatively negligible intensity.

In one series of solutions the uranyl ion concentration was kept constant at 0·004 M while the sodium azide concentration was varied from 0·004 to 0·080 M; the absorption was measured over the same wavelength range as before. The intensity increased gradually on increasing the azide concentration, with a shift in the maximum absorption towards longer wavelengths (Fig. 1). This indicates that there is a tendency for formation of azide-rich uranyl complexes. In order to secure the most significant characteristic band for the bright yellow uranyl azide solution the ratio of the uranyl to the azide ion concentration should be 1:5. On further addition of azide ion, the intensity of the colour still increases, while the maximum absorption tends to become masked and the solution acquires an orange-yellow colour. In solutions containing a large excess of azide ions, (UO_2^{2+} : N_3^- = 1:500) the maximum absorption disappeared completely and the absorption decreased continuously with increasing wavelength.

This probably explains the failure of FEINSTEIN to observe the maximum[5], since he used solutions containing a large excess of azide ion. When the azide ion concentration was kept constant at 0·02 M while the uranyl ion concentration was varied from 0·0002 to 0·0040 M, no shift in the maximum absorption of the different curves was observed. These observations are in agreement with the assumption that the formation of the complex depends solely upon the azide concentration provided that it is present in excess.

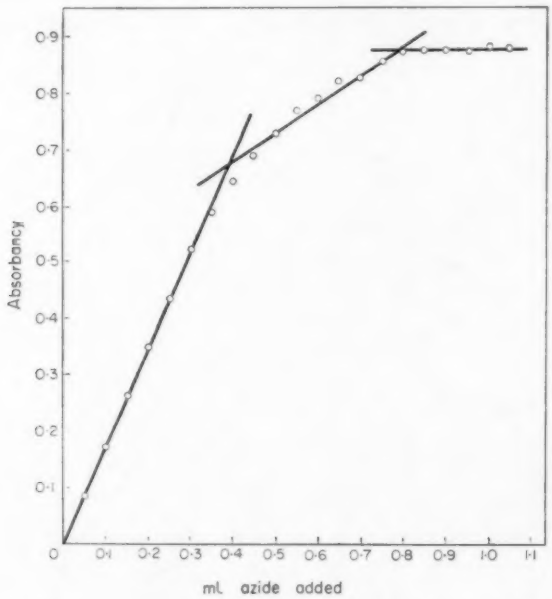

FIG. 2.—Spectrophotometric titration of uranyl nitrate solution (UO_2^{2+} = 0·008 M), with 1 M sodium azide solution at λ 380 mμ.

Structure of the azido uranyl complex

The structure of the complex was studied by applying the classical colorimetric methods:

(a) *The molar ratio method.* YOE and JONES[8] have shown that when the metal ion concentration of a coloured complex is kept constant while that of the ligand is varied systematically, then for a stable complex there is a linear relationship between the absorbancy and the ratio of the molar concentrations of the ligand to the metal ion, with a break at the molar ratio representing the composition of the complex. Spectrophotometric titrations were carried out in which 1 M sodium azide solution was added to a number of uranyl nitrate solutions varying from 0·002 to 0·008 M. The titrated solution was stirred after each addition, the glass cell was rinsed twice with the same solution and then measurements were obtained at 380 and 420 mμ. The results shown in Fig. 2 show breaks at molar ratios of 1:1 and 1:2 UO_2^{2+} to N_3^- respectively. It was noticed that the first break was more distinct at the shorter wavelength for the most concentrated solution (0·008 M UO_2^{2+}) but in dilute solutions containing less than

[8] J. H. YEO and A. L. JONES, *Industr. Engng. Chem.*, Analyt. Ed. **16**, 111 (1944).

0·004 moles of UO_2^{2+} there was only one distinct break at a molar ratio of 1 UO_2^{2+} to 2 N_3^-. Several titrations were carried out using 70 per cent by volume of acetone in water as the solvent, with different uranyl concentrations. At all dilutions, in addition to the 1:2 break, the 1:1 break was more distinct than in aqueous solutions and the mixtures acquired an orange colour at the end of the titrations. The break at the 1:1 molar ratio suggests the formation of the complex ion $[UO_2(N_3)]^+$, whereas the break at the 1:2 ratio might be due either to the existence of the complex $UO_2(NO_3)_2 \cdot 2NaN_3$

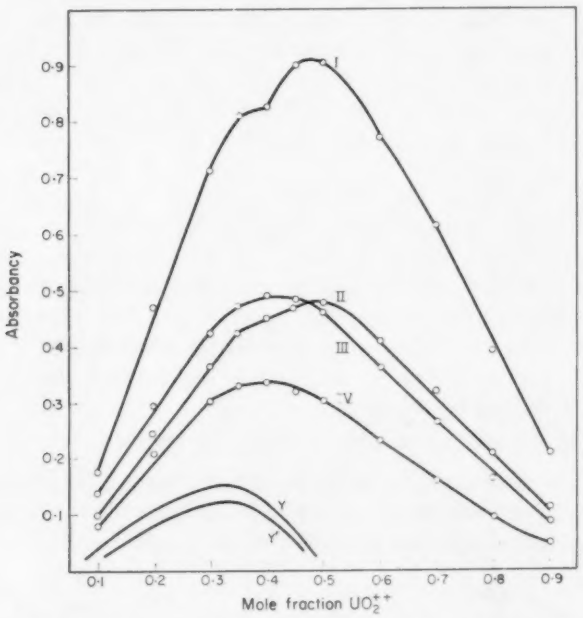

FIG. 3.—Absorbancy of uranyl azide solutions at 0·016 M total, $\mu = 0{\cdot}0448$. (I) Wavelength 380 mμ; (II) 400 mμ; (III) 420 mμ; (IV) 450 mμ. Y and Y' are the differences between the observed absorbancies and those calculated for 1 : 1 mixtures at λ 420 and λ 450 mμ respectively.

or to the dimeric form $UO_2[UO_2(N_3)_4]$. Further work is now in progress to obtain further information regarding the probable formula of the 1:2 complex.

(b) *The continuous variation method.* The existence of the uranyl azide complexes in aqueous solutions was confirmed by applying JOB's continuous variation method.[9] Several series of mixtures were prepared containing varying proportions of uranyl and azide solutions of equal concentrations and their absorbancies were measured at few arbitrary selected wavelengths. The total azide and uranyl ion concentrations varied from 0·004 to 0·016 M. The ionic strength was also adjusted to a constant value in each series by adding the appropriate amount of sodium perchlorate solution. The blank was a solution containing the same concentration of uranyl ion as that present in the test solution. The results are shown in Fig. 3. The curve at 380 mμ has a maximum at a mole fraction of UO_2^{2+} of 0·475, confirming the existence of the complex ion $[UO_2(N_3)]^+$. The shoulder at a mole fraction of 0·35 suggests the existence of a compound having a mole ratio of UO_2^{2+}:2 N_3^-. This shoulder persists at all concentrations

[9] P. JOB, *C.R. Acad. Sci., Paris* **180**, 928 (1925).

at shorter wavelengths, but slowly disappears on approaching longer wavelengths. The curve at 420 mμ has only one maximum at 0·40 mole fraction of UO_2^{2+}, equivalent to 1·5 azide ions per uranyl ion. This may be interpreted on the basis that uranyl azide solutions at these dilutions contain not only the 1:1 complex but also higher complexes such as the 1:2 complex as induced by the broad maximum in the curve, considering it unlikely that polynuclear complexes are formed at these dilutions, e.g. with a ratio of UO_2^{2+} to N_3^- ions of 2:3. The treatment of VOSBURGH and COOPER[10] was applied to the results at 420 and 450 mμ, plotting the values of Y (the difference between the observed absorbancy and that calculated on the basis that only the 1:1 complex is formed) against the mole fraction; in this way curves Y and Y′ in Fig. 3 were obtained. The maximum in this case falls at about 0·33 mole fraction UO_2^{2+}. Thus, while the presence of some $[UO_2(N_3)]^+$ cannot be denied, it appears that the solution also contains considerable amounts of a complex having a ratio of $UO_2^{2+}:N_3^- = 1:2$.

(c) *The slope ratio method.*[11] In one series of solutions the concentration of azide ion was kept constant at 0·008 M while that of the uranyl ion was varied from 0·0024 to 0·0064 M; the ionic strength was kept constant at 0·032 by adding suitable amounts of sodium perchlorate solution. In another series the uranyl ion concentration was kept constant at 0·008 M while that of the azide was varied from 0·0024 to 0·0064 M, also at ionic strength 0·032. When the absorbancies of the solutions in the two series, measured at 420 mμ, were plotted against the variable concentration, two straight lines were obtained (Fig. 4). If the reaction between uranyl nitrate and sodium azide is represented by the equation

$$mUO_2^{2+} + nN_3^- = UO_{2m}N_{3n}^{(2m-n)+} \qquad (1)$$

then the ratio of $m:n$ in the complex will be determined by the ratio of the slope of line 1 to that of line 2. This ratio was found to be 1:1, supporting the formation of the mono-azido uranyl ion in solutions at these concentrations.

Determination of the instability constant

If we assume that the values of m and n in equation 1 are equal to unity, then the equilibrium constant for this reaction can be expressed by

$$K' = \frac{x}{(a-x)(b-x)} \qquad (2)$$

where a represents the stoichiometric concentration of uranyl ions, b that of the azide and x the actual concentration of the $[UO_2(N_3)]^+$. In one series of solutions b was kept constant at 0·004 M while a was varied from 0·016 to 0·032 M; the ionic strength was adjusted to 0·096 by sodium perchlorate. Since the uranyl ion concentration is always in excess, only the mono-azido uranyl ion will be formed. The absorbancies were measured at 410, 420 and 430 mμ using 1 cm cells. If Beer's Law is obeyed, then according to the method of FRANK and OSWALT[12].

$$\frac{ab}{D} = \frac{1}{\beta}(a+b) + \frac{1}{\beta K'} \qquad (3)$$

where β is the molecular extinction coefficient of the absorbing species, at the specified wavelength. When values of ab/D were plotted against $(a+b)$, straight lines were

[10] W. C. VOSBURGH and G. R. COOPER, *J. Amer. Chem. Soc.* **63**, 437 (1941).
[11] A. E. HARVEY and D. L. MANNING, *J. Amer. Chem. Soc.* **72**, 4488 (1950).
[12] H. S. FRANK and R. L. OSWALT, *J. Amer. Chem. Soc.* **69**, 1321 (1947).

obtained at the different wavelengths. The fact that the points for each wavelength fall on a straight line confirms the expectation that at low azide ion concentration and high uranyl ion concentration, only the mono-azido uranyl ion is formed. Equations for every line were obtained by the method of the least squares. Although the straight lines at the different wavelengths have different slopes and intercepts, the ratio of the intercept to the slope is the same in every case, viz. $1/K'$. The mean value of the instability constant for the different wavelengths was found to be $4{\cdot}86 \pm 0{\cdot}4 \times 10^{-3}$. Values of the molar extinction coefficient β, calculated from these data, are 110, 88 and 78 at 410, 420 and 430 mμ respectively.

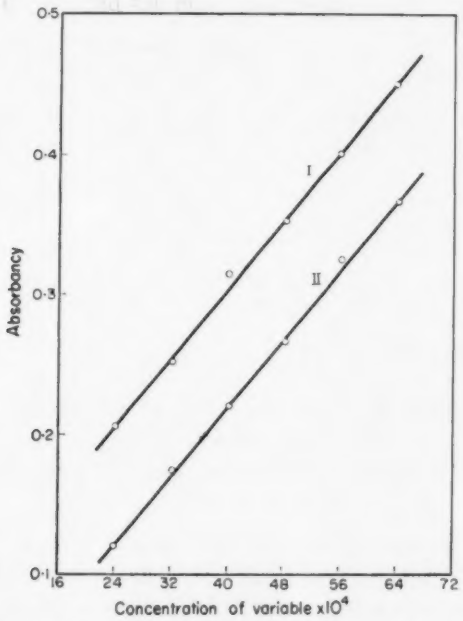

FIG. 4.—Absorbancies of uranyl azide solutions at λ 420 mμ. (I) N_3^- concentration = 0·008 M at varying uranyl ion concentration; (II) UO_2^{2+} concentration = 0·008 M at varying azide ion concentration. $\mu = 0{\cdot}032$.

Conductimetric measurements

A number of conductimetric titrations were carried out between solutions of sodium azide and uranyl nitrate. A solution of 1 M sodium azide was added systematically from a microburette to 40 ml of a 0·025 M solution of uranyl nitrate; the temperature was kept constant at 25°C ± 0·1°C and the solution was stirred gently. The relative conductance was measured after each addition, with the results shown in Fig. 5. A discontinuous curve was obtained showing three distinct breaks. The first break occurs at a molar ratio of 1:1·1 uranyl to azide respectively, and the other two at values corresponding to 1:2 and 1:3 molar ratios calculated with respect to the observed value for the 1:1 stoicheiometry. In reverse titrations where the uranyl nitrate solution was added to the azide, a discontinuous curve was also obtained with the same three breaks. These discontinuities are not very sharp, but are definitely present. The existence of the mono- and the di-azido uranyl complexes already identified was

confirmed. The third break suggests the formation of a complex with three azide ions per uranyl ion, probably $[UO_2(N_3)_3]^-$, responsible for the orange-yellow colour which appears at this concentration.

Migration experiments

These experiments were carried out in a W-shaped tube as used in previous work.[7] A deep yellow solution of uranyl azide (0·05 M), containing equal amounts of the

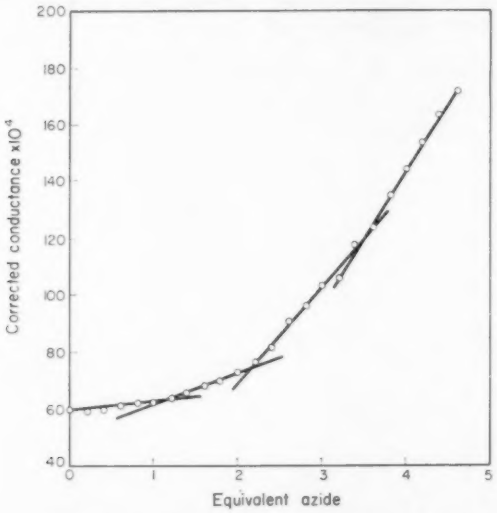

FIG. 5.—Conductimetric titration of uranyl nitrate solution (UO_2^{2+} = 0·025 M), with 1 M sodium azide solution.

components, was introduced carefully into the centre of the tube. A good boundary was formed between the uranyl azide solution and the colourless solution of sodium perchlorate on each side of the centre of the W. Reference marks were placed on the tube and the levels of the two side arms were checked to ensure that there was no change in position of the liquid as a whole. A potential gradient of about 0·5 V/cm was applied to the ends of the tube. The colour was found to migrate slightly across the boundary towards the cathode but no appreciable movement towards the anode was observed; this indicates the existence of a positively-charged coloured species, probably $[UO_2(N_3)]^+$, in solution. Another uranyl azide solution was prepared containing 0·05 M UO_2^{2+} and 0·50 M N_3^-; this solution had an orange-yellow colour. When this was introduced into the W-tube and the same current was applied the colour migrated towards the anode, indicating the presence of a negatively-charged complex ion, presumably $[UO_2(N_3)_3]^-$.

These findings prove conclusively that the yellow and orange-yellow colours of solutions containing uranyl and azide ions are to be ascribed to the stepwise formation of a number of complexes on addition of increasing amounts of sodium azide to uranyl nitrate solutions; the charge on these complexes depends on the number of azide ions in the complex.

Acknowledgement—The authors are grateful to Mr. M. G. HABASHI, of the Copper Works, Alexandria, for providing us with the conductimeter.

J. Inorg. Nucl. Chem., 1961, Vol. 19, pp. 101 to 106. Pergamon Press Ltd. Printed in Northern Ireland

OXIDATION–REDUCTION POTENTIAL OF UO_2^{2+}–U^{4+} SYSTEM IN PERCHLORIC ACID

J. SOBKOWSKI and S. MINC
Department of Electrochemistry, University of Warsaw, Warsaw, Poland

(*Received* 30 *June* 1960, *in revised form* 21 *October* 1960)

THE value of the redox potential of UO_2^{2+}–U^{4+} system is not exactly known yet, because previous workers[1–4] have taken into consideration neither the activity coefficients nor the complex formation of uranium ions with anions.

The results of previous investigations are given below:

Solution	Standard redox potential (V)	Author
H_2SO_4	0·42	LUTHER, MICHIE[1]
H_2SO_4	0·404 ± 0·012	TITLESTADT[2]
H_2SO_4	0·407 ± 0·003	CHLOPIN, GUREWICZ[3]
HCl	0·334	TAYLOR, SMITH[4]

Latimer[5] has calculated the standard potential as 0·334 V but this value is not quite correct because the values of the entropy and enthalpy of uranium ions are known only approximately. The agreement of TAYLOR's and SMITH's data[4] with the calculated value of LATIMER is quite unexpected, because these authors have not taken into account the activity coefficients of the system.

The potentials in sulphuric acid are considerably higher than in hydrochloric acid, which can be explained by relatively strong complexing of the uranium ions. The stability of U^{4+} complexes with sulphate ions[6] is considerably higher than that of UO_2^{2+}[7] and therefore the ratio of free ion concentrations UO_2^{2+}/U^{4+} is not the same as the total U(VI)/U(IV) ratio. The decrease of concentration of free ions of U^{4+} in relation to UO_2^{2+} causes the potential to shift to more positive values as compared with systems in which complex formation is not observed. The ions of U^{4+} and UO_2^{2+} bind chloride[8–10] ions more weakly than sulphate[6] and hence the value obtained by TAYLOR and SMITH[4] is considerably lower than values given by other authors.[1–3]

In order to explain the discrepancy between the half-wave potential and the standard potential of the UO_2^{2+}–U^{4+} system, HEAL[11] assumed that the value of this potential is

[1] R. LUTHER and A. C. MICHIE, *Z. Electrochem.* **14**, 826 (1908).
[2] N. TITLESTADT, *Z. Phys. Chem.* **72**, 257 (1910).
[3] W. G. CHLOPIN and A. M. GUREWICZ, *Bull. Acad. Sci URSS Classe Sci. Chim*, 271 (1943); *Chem. Abstr.* **38**, 5451 (1944).
[4] J. K. TAYLOR and E. R. SMITH, Report A 1972 Aug. 29 (1944).
[5] W. M. LATIMER, The Oxidation States of the Elements and their Potentials in Aqueous Solutions. Prentice Hall Inc. New York (1952).
[6] R. DAY, R. WILHITE and F. HAMILTON, *J. Amer. Chem. Soc.* **77**, 3180 (1955).
[7] S. AHRLAND, *Acta Chem. Scand.* **5**, 1151 (1951).
[8] S. AHRLAND and R. LARSSON, *Acta Chem. Scand.* **8**, 137 (1954).
[9] S. AHRLAND, *Acta Chem. Scand.* **5**, 1271 (1951).
[10] S. MINC and M. SIEKIERSKA, *Nukleonika* **5**, 109 (1960).
[11] H. G. HEAL, *Trans. Faraday Soc.* **45**, 11 (1949).

determined by the ratio of the concentrations of UO_2^{2+} and UO_2^{+}. The presence of U^{4+} ions influences that potential to an extent comparable with the presence of other electrolytes which do not take part in the equilibrium and only change the ionic strength of the solution. This circumstance, in HEAL's[12] opinion, explains the light sensitivity of a platinum electrode in a solution of UO_2^{2+} and U^{4+} ions, where the potential under the influence of light becomes more negative owing to reduction of the UO_2^{2+} to UO_2^{+}. The disadvantage of this interpretation is that it cannot explain the lack of influence of light on chloride solutions and—what has been established in the cited work—on perchloric acid solutions. The dependence between the light sensitivity of the system and the state of the electrode surface should be mentioned. TITLESTADT[2] noticed that the effect of light was greater on the smooth surface of a Pt electrode than on a platinized surface. Moreover, HEAL's hypothesis is weakened by the results of an investigation[13] of the exchange reaction U(IV) + U(VI) $\rightleftharpoons$ U(VI) + U(IV) with uranium labelled with the isotope ^{233}U. The rate of this exchange reaction is unaffected by light.

The marked effect of light on systems containing organic ions suggests a relation between light sensitivity and the stability of uranium complexes.

In the present work the cell has been investigated:

$$\mathrm{Pt} \mid \underset{(c_1)}{UO_2(ClO_4)_2}, \quad \underset{(c_2)}{U(ClO_4)_4}, \quad \underset{(c_3)}{HClO_4} \parallel \underset{(c_3)}{HClO_4} \mid H_2 \ (\mathrm{Pt}) \tag{1}$$

The use of perchloric acid diminishes the formation of complexes by uranium ions to a minimum. This is shown for example, by investigations of partition coefficients.[14]

In the cell (1) occurs the reaction

$$U^{4+} + 2H_2O \rightleftharpoons UO_2^{2+} + 4H^{+} + 2e^{-} \tag{2}$$

The potential of the left side of cell is

$$E_1 = E_0 + \frac{RT}{2F} \ln \frac{a_{UO_2^{2+}}}{a_{U^{4+}}} \cdot a_{H^+}^4 \tag{3}$$

and the right side (hydrogen reference electrode)

$$E_2 = \frac{RT}{F} \ln a_{H^+} + \frac{RT}{2F} \ln \frac{760}{P} \tag{4}$$

where

$$p = p_1 - p_2$$

p_1 atmospheric pressure in mm Hg,

p_2 vapour-pressure of water over $HClO_4$ (c_3) solution in mm Hg.

The electromotive force of the cell is:

$$E = E_1 - E_2 = E_0 + \frac{RT}{2F} \ln \frac{C_{UO_2^{2+}}}{C_{U^{4+}}} + \frac{RT}{2F} \ln \frac{f_{UO_2^{2+}}}{f_{U^{4+}}} \cdot f_{H_1^+}^4 + \frac{RT}{F} \ln c_{H^+} \tag{5}$$

$$- \frac{RT}{F} \ln f_{H_2^+} - \frac{RT}{2F} \ln \frac{760}{p} + E_D$$

[12] H. G. HEAL and I. G. THOMAS, *Trans. Faraday Soc.* **45**, 11 (1949).
[13] E. RONA, *J. Amer. Chem. Soc.* **72**, 4339 (1950).
[14] S. SIEKIERSKI, *J. Inorg. Nucl. Chem.* **12**, 129 (1959).

where:

$f_{H_1^+}$ is activity coefficient of H^+ ions in solution containing uranium ions,

$f_{H_2^+}$ is activity coefficient of H^+ ions in solution of reference electrode,

E_D is liquid junction potential between both solutions.

Though the concentrations of H^+ ions are equal, the activity coefficients $f_{H_1^+}$ and $f_{H_2^+}$ are different, because the ionic strengths are different in the two half-cells.

At 25°C, equation (5) may be put in the form:

$$E_0' = E_0 + 0{\cdot}02958 \log \frac{f_{UO^{2+}}}{f_{U^{4+}}} \cdot f_{H^+}{}^4 + E_D \tag{6}$$

where

$$E_0' = E - \frac{RT}{2F} \ln \frac{C_{UO_2^{2+}}}{C_{U^{4+}}} - \frac{RT}{F} \ln c_{H^+} - \frac{RT}{F} \ln f_{H_2^+} + \frac{RT}{2F} \ln \frac{760}{p} \tag{7}$$

Plotting values of E_0' against ionic strength, I, one can—by extrapolation—eliminate the unknown activity coefficients and obtain the normal potential of the UO_2^{2+}–U^{4+} system. The extrapolation is correct when the dilution is sufficient; this condition however is limited owing to hydrolysis of the U^{4+} ions.

One can take the hydrolysis into account using the hydrolysis constant of U^{4+}[15] but the precision of this correction diminishes with increasing hydrolysis. In the investigated range of concentration of H^+ ions, the hydrolysis of UO_2^{2+} does not occur.[16]

EXPERIMENTAL

Materials and apparatus. Uranyl perchlorate was prepared by two precipitations from $UO_2(NO_3)_2$ solution of uranium peroxide, which was decomposed in $HClO_4$.

Uranium (IV) perchlorate was prepared by cathodic reduction of a strongly acid solution of uranyl perchlorate on mercury. The anode compartment consisted of a glass tube ending in a sintered glass disk. The end of the reduction was indicated by the black colour of the solution, which was the result of the red colour of U(III) and green colour of U(IV). U(III) was oxidized by a brief aeration of the solution, which was then kept in a bottle under electrolytically prepared hydrogen. It was necessary to prevent oxidation of U(IV), which easily occurs in perchloric solution when air is present.[17]

The stock solution of uranyl perchlorate was analyzed gravimetrically, by precipitation of ammonium diuranate and heating at 850°C.

The concentration of U(IV) was determined by oxidation of the solution with a known quantity of $K_2Cr_2O_7$. The excess of $K_2Cr_2O_7$ was titrated potentiometrically using ferrous ammonium sulphate solution.[18]

The concentration of H^+ was determined by passing the solution containing both U(IV) and U(VI) through a column filled with Amberlite IRA 120, followed by titration of the emergent H^+. Then $C_{H^+} = C'_{H^+} - 4C_{U^{4+}} - 2C_{UO_2^{2+}}$ where C_{H^+} is the concentration of H^+ after passing the solution through the column. Before use the Amberlite was washed with dilute H_2SO_4 and then with distilled water until the acid reaction disappeared. The UO_2^{2+} ions exchange with difficulty. Therefore it was necessary to use a sufficient height of column and pass the solution slowly enough.

The solutions were prepared in such a way that $C_{UO_2^{2+}} \approx C_{U^{4+}}$ to minimize the error arising from determination of the concentration.

The vessel used is shown in Fig. 1. The two parts of the vessel were connected with a tube in which a sintered glass disk was fitted to prevent the solutions from mixing. In the right hand compartment the pure perchloric acid solution was placed, its concentration being the same as in the solution containing uranium ions, which was placed on the left hand side.

[15] K. A. KRAUS and F. NELSON, *J. Amer. Chem. Soc.* **72**, 3901 (1950).
[16] S. AHRLAND, *Acta Chem. Scand.* **3**, 374 (1949).
[17] J. HALPERN and J. G. SMITH, *Canad. J. Chem.* **34**, 1419 (1956).
[18] C. J. RODDEN, *Analytical Chemistry of the Manhattan Project*. McGraw-Hill Book Company Inc., New York (1950).

The redox electrode was platinized because the equilibrium value was reached faster than by using the smooth Pt surface.

Hydrogen was obtained by the electrolysis of a concentrated NaOH solution on nickel electrodes. It was washed in a solution of alkaline pyrogallol solution, then in H_2SO_4 and last in a $HClO_4$ solution of the same concentration as that in the cell. The values of the vapour-pressure over $HClO_4$ solutions were taken from work by PEARCE and NELSON[19].

Nitrogen was purified successively in scrubbers containing concentrated NaOH solution and active charcoal. Oxygen was removed using a column at 200°C filled with a suspension of metallic

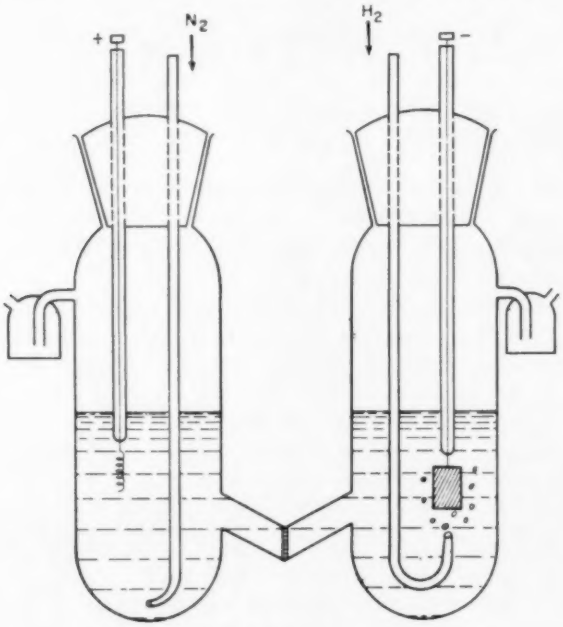

FIG. 1.

copper on infusorial earth.[20] Before coming into the cell, the nitrogen was passed through a solution of the same composition as the solution in the cell.

The cell and scrubbers were in an air thermostat, provided with a water jacket, controlled to 25 ± 0·1°C, as measured with a standard thermometer in a vessel with water of approximately the same heat capacity as the cell. The equilibrium value of the e.m.f. was reached after 3–4 hr with the most concentrated solutions, but for the most dilute solutions satisfactory results were not obtained without waiting for several days.

However, no potential mediator was used to accelerate the establishment of the redox potential.

The e.m.f.'s were measured to the nearest 0·1 mV by a RFT 0145 potentiometer using a Weston standard cell of the saturated type, and a mirror galvanometer as a current indicator.

RESULTS

It follows from equation (6) that

$$\lim_{I \to 0} E'_0 = E_0 + E_D \tag{8}$$

because all activity coefficients are then unity. The liquid junction potential E_D could

[19] I. N. PEARCE and F. NELSON, *J. Amer. Chem. Soc.* **55**, 3075 (1933).
[20] F. R. MEYER and G. RONGE, *Angew. Chem.* **52**, 637 (1939).

be estimated from the HENDERSON equation but the ionic mobilities of UO_2^{2+} and U^{4+} are not exactly known. If we assume that the mobilities of UO_2^{2+} and U^{4+} at infinite dilution are $60 \pm 10\ \Omega^{-1}\ cm^2\ eq^{-1}$ (in these limits the mobilities of majority of cations occur) we obtain $E_D = +0{\cdot}0017 \pm 0{\cdot}0002$ V. Any error in this potential should not be significant, because the concentration of H^+ is several times higher than concentration of uranium ions.

In Table 1 are given the results of the measurements and of the calculations.

TABLE 1

The acid: $HClO_4$ Temp. 25·0 ± 0·1°C

$C_{UO_2^{2+}}$ (mole l.$^{-1}$)	0·0940	0·0752	0·0563	0·0376	0·0188	0·00752	0·00376
$C_{U^{4+}}$ (mole l.$^{-1}$)	0·0970	0·0775	0·0581	0·0388	0·0194	0·00775	0·00388
C_{H^+} (mole l.$^{-1}$)	1·140	0·912	0·683	0·456	0·228	0·0913	0·0456
I (mole l.$^{-1}$)	2·391	1·910	1·435	0·955	0·478	0·191	0·0955
$K_m \cdot 10^{-2}$	2·17	2·31	2·48	2·77	3·47	4·77	5·65
$C'_{U^{4+}}$ (mole l.$^{-1}$)	0·0952	0·0757	0·0562	0·0366	0·0168	0·00509	0·00174
E (V)	0·3399	0·3323	0·3232	0·3114	0·2925	0·2717	0·2586
E'_0 (V)	0·3409	0·3402	0·3393	0·3379	0·3357	0·3334	0·3325

The activity coefficients of H^+ ions in the reference electrode were obtained by interpolation of the data of ROBINSON and BAKER[21]. The hydrolysis of U^{4+} ions was taken into account using values for the hydrolysis constant K_m for different ionic strengths from the equation given by KRAUS and NELSON[15]. The concentration of unhydrolysed U^{4+} ions is

$$C'_{U^{4+}} = \frac{C_{U^{4+}}}{1 + (K_m/C_{H^+})}$$

where $C_{U^{4+}}$ is the total concentration of U(IV). The values of E_0' are plotted against $\sqrt{I}$ in Fig. 2. To avoid uncertainty connected with extrapolation to $\sqrt{I} = 0$, the equation of the curve was calculated using the least squares method

$$E_0' = 0{\cdot}3290 + 0{\cdot}01103\sqrt{I} - 0{\cdot}0021\, I \qquad (9)$$

Because $E = 0{\cdot}0017$ V, the standard oxidation–reduction potential of UO_2^{2+}–U^{4+} system is 0·3273 V, with an error not exceeding 0·001 V. This value is about 0·007 V lower than the one obtained by TAYLOR and SMITH[4] in HCl solution, which can be explained by the formation of weak complexes of uranium ions with chloride. This

[21] R. A. ROBINSON and R. H. STOKES, *Electrolyte Solutions*. Butterworths Scientific Publications, London (1959).

assumption is uncertain however, because the result of TAYLOR and SMITH contains an unknown factor concerning the activity coefficients.

The free energy of reaction (2) is

$$\Delta G = -15{\cdot}10 \pm 0{\cdot}05 \text{ kcal/mole}$$

in good agreement with the value computed from the thermodynamic data of National Bureau of Standards,[5] ~15·4 kcal/mole.

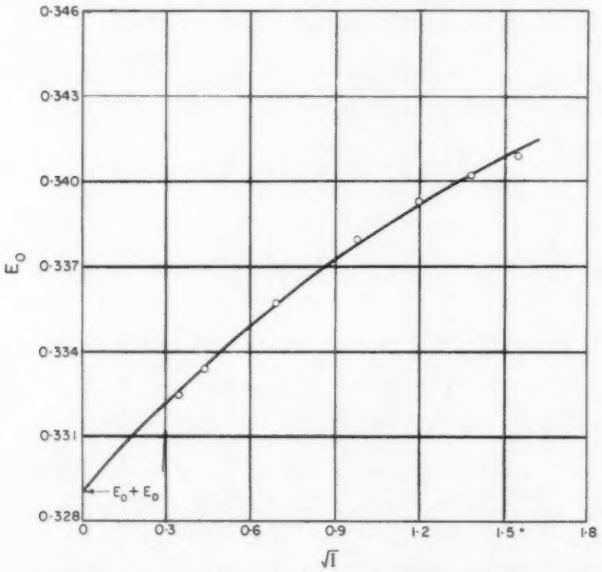

FIG. 2.—The curve is drawn according to equation (9). The points are obtained from potentiometric measurements.

Using the activity coefficients of $UO_2(ClO_4)_2$ and $HClO_4$[21] for the corresponding ionic strengths one can estimate the unknown activity coefficients of $U(ClO_4)_4$, by means of equations (6) and (9).

The results are given in Table 2.

TABLE 2

I (mole l.$^{-1}$)	0·2	0·4	0·6	0·8	1·0	1·5	2·0	2·5
$f_{\pm}$ $U(ClO_4)_4$	0·16	0·13	0·12	0·14	0·15	0·25	0·46	1·03

These values are of course only approximations because of the uncertainty in the E_0' values and the assumption that the activity coefficients of $UO_2(ClO_4)_2$ and $HClO_4$ are similiar in pure and in mixed electrolytes if the ionic strengths are the same.

J. Inorg. Nucl. Chem., 1961, Vol. 19, pp. 107 to 114. Pergamon Press Ltd. Printed in Northern Ireland

SILVER HYPONITRITE: SOLUBILITY PRODUCT AND COMPLEXES IN AQUEOUS AMMONIA

C. N. POLYDOROPOULOS and TH. YANNAKOPOULOS
National University, Laboratory of Physical Chemistry, Solonos 104, Athens

(*Received* 5 *August* 1960)

Abstract—The solubility of silver hyponitrite in aqueous ammonia has been measured over the range of concentrations 0·1–2 N NH_3. The results are compatible with the assumption that the predominant complex formed in low concentrations is $Ag(NH_3)_2^+$. By addition of sodium hyponitrite the solubility of silver hyponitrite in ammonia (at a constant concentration) decreases first, but for moderate and higher concentrations of $Na_2N_2O_2$ it increases again, showing the formation of the complex: $(NH_3)AgN_2O_2^-$. The instability constant of the latter is found to be approximately 4×10^{-3} at 25·0°, and the solubility product of $Ag_2N_2O_2$ $1{\cdot}30(\pm 0{\cdot}15) \times 10^{-19}$ at the same temperature.

VOL. 19 1961

IT has been pointed out by DIVERS[1] and many other investigators that silver hyponitrite is slightly soluble in concentrated solutions of hyponitrites and considerably soluble in aqueous ammonia. However nothing has been reported on the nature of the complexes formed, although dissolution of silver hyponitrite in ammonia and reprecipitation by mineral acids has been employed very often for purification purposes.

In view of the interesting structure of the ion $N_2O_2^{2-}$ [2] and its possible mesomeric forms some attention should be paid to its co-ordination chemistry. Apart from the complex ion $((NH_3)_5Co)_2N_2O_2^{4+}$ studied by GRIFFITH[3] and earlier workers, there seems to be in the literature very little, if any, information on the co-ordination properties of $N_2O_2^{2-}$. We present here in brief the results of some solubility and e.m.f. measurements revealing the formation of the complex $(NH_3)AgN_2O_2^-$ and we hope to be able in the future to provide some more data on the subject.

The method of investigating the composition of a complex by solubility measurements under suitable conditions was introduced by BODLÄNDER[4] who applied it to the dissolution of silver halides in ammonia. By similar arguments one would expect the equilibria

$$Ag_2N_2O_2 \rightleftharpoons 2Ag^+ + N_2O_2^{2-} \tag{1}$$

$$Ag^+ + 2NH_3 \rightleftharpoons Ag(NH_3)_2^+ \tag{2}$$

to be established in ammoniacal solutions saturated with $Ag_2N_2O_2$, with the constants

$$K_s = (Ag^+)^2(N_2O_2^{2-})$$

and

$$K_1 = (Ag^+)(NH_3)^2/(Ag(NH_3)_2^+)$$

[1] E. DIVERS, *J. Chem. Soc.* **75**, 95 (1899).
[2] L. KUHN and E. R. LIPPINCOTT, *J. Amer. Chem. Soc.* **78**, 1820 (1956); R. J. W. LE FÈVRE, W. T. OH, I. H. REECE and R. L. WERNER, *Australian J. Chem.* **10**, 361 (1957); D. J. MILLEN, C. N. POLYDOROPOULOS and D. WATSON, *J. Chem. Soc.* 687 (1960).
[3] W. P. GRIFFITH, J. LEWIS and G. WILKINSON, *J. Inorg. Nucl. Chem.* **7**, 38 (1958).
[4] G. BODLÄNDER and R. FITTIG, *Z. Phys. Chem.* **39**, 597 (1902).

respectively, where the parentheses stand for activities. Since the concentration of Ag^+ is negligible, the soluble complex can be determined analytically. If its molality is C_0, by combining the two constants and inserting $[N_2O_2^{2-}] = \frac{1}{2}[Ag(NH_3)_2^+] = C_0/2$ one obtains:

$$\log (f_{\pm} C_0) = \frac{1}{3} \log \left(\frac{2K_s}{K_1^2} \right) + \frac{4}{3} \log (NH_3) \qquad (3)$$

where $f_{\pm}$ is the mean activity coefficient of the electrolyte $(Ag(NH_3)_2)_2N_2O_2$. Therefore a plot of $\log (f_{\pm} C_0)$ against $\log (NH_3)$ is expected to be a straight line from which K_s could be evaluated.

At the same time the potential of a silver electrode immersed into the mixture is expected to drop linearly with increasing $\log (NH_3)$ according to:

$$E = E_0 + \frac{2{\cdot}3RT}{3F} \log \frac{f_{\pm}}{f_-} + \frac{2{\cdot}3RT}{3F} \log (2K_sK_1) - \frac{2 \times 2{\cdot}3RT}{3F} \log (NH_3) \qquad (4)$$

On the other hand addition of a soluble hyponitrite ($Na_2N_2O_2$) at constant ammonia concentration would reduce the silver content of the solutions, as it displaces both equilibria to the left, if there were no other reactions taking place.

As it will be seen, however, the results of the measurements can not be interpreted in terms of these two reactions only.

EXPERIMENTAL

Sodium hyponitrite was prepared by the method of Divers-Partington (discussed elsewhere[5]) with the modification that the sodium amalgam was prepared electrolytically in a cell similar to that described by ABEL[6]. The silver hyponitrite obtained by precipitation of the raw material was purified by reprecipitation from cold 0·1 N nitric acid. The solutions of sodium hyponitrite used for measurements were prepared by the action of pure silver hyponitrite (not dried) on a solution of NaI.

All solubility and e.m.f. measurements were made at 25·0 ± 0·1°C. The solutions were left to establish equilibrium with some solid $Ag_2N_2O_2$ at this temperature for about six hours. Any longer treatment might have caused serious errors due to the decomposition of hyponitrites.* Filtration (for sampling out) was effected by exerting pressure on the mixtures, being still kept in the thermostat.

The solutions contained always some NaOH (0·1–0·2 N) to avoid any considerable hydrolysis of $N_2O_2^{2-}$,[5] as well as to stabilize it as far as possible.[6]

The silver content of the samples was determined volumetrically (KSCN) after acidification with HNO_3. For the determination of the total $N_2O_2^{2-}$ in solution, silver nitrate was added (if necessary) in small excess, the solution was brought to a pH 5–6, and the precipitate ($Ag_2N_2O_2$) washed, dissolved in HNO_3 and titrated with KSCN.

The silver electrode potentials were measured by means of the set:

(—) Saturated calomel electrode ‖KNO_3‖ solution tested |Ag (+) immersed in the thermostat. The indicator electrode was silver-plated silver. It was standardized in the same cell repeatedly against 0·1 N $AgNO_3$ in which the activity coefficient of Ag^+ was taken as 0·82. The potentiometer was calibrated against a certificated Weston cell. The average uncertainty of the measurements was ±1·5 mV.†

* In a series of measurements the apparent solubility of silver hyponitrite in 0·45 M NH_3 was found to change by 2–3% between 1 and 5 hr after the preparation of the mixtures. Between 5 and 10 hr no change in the solubility was detectable. After 24 hr treatment a sample was found to have decomposed by 17 per cent.

† A higher accuracy was not attempted since, unfortunately, the accuracy in a work on hyponitrites is anyhow limited by two factors: (a) their instability and (b) lack of sufficient literature on even the most elementary points of the chemistry of hyponitrites, e.g. their quantitative determination.

[5] C. N. POLYDOROPOULOS, *Chim. Chronika* **24** A, 147 (1959).
[6] E. ABEL and J. PROISL, *Wien. Mh.* **72**, 1 (1938).

TABLE 1.—SOLUBILITY OF SILVER HYPONITRITE IN AQUEOUS AMMONIA

(NH_3)	C_0	NaOH (molal)	μ	$f_\pm$	$f_\pm C_0$	$E_0' - E$ (mV)
	$\times 10^{-2}$				$\times 10^{-2}$	
0·091	0·262	0·099	0·103	0·59	0·155	456
0·192	0·728	0·099	0·110	0·58	0·422	463
0·495	2·65	0·100	0·140	0·56	1·48	486
0·827	5·56	0·198	0·281	0·48	2·67	491
0·952	6·67	0·102	0·202	0·52	3·47	502
1·444	11·26	0·103	0·272	0·49	5·52	515

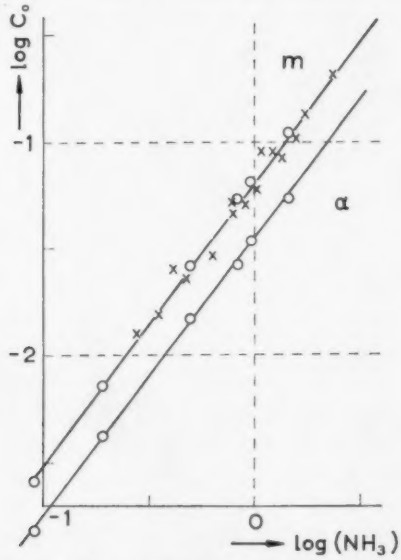

FIG. 1.—Solubility of silver hyponitrite in aqueous ammonia.
The points shown by × have been determined less accurately.

RESULTS

(a) *Variation of activity coefficients with ionic strength*

Increasing amounts of KNO_3 were added in a series of solutions saturated with $Ag_2N_2O_2$ at constant 0·45 M NH_3 and 0·1 N NaOH. The increase of the solubility with increasing ionic strength (up to $\mu = 0{\cdot}45$) showed a dependence of the form

$$-\log f_\pm = \frac{2A\sqrt{\mu}}{1 + \alpha B\sqrt{\mu}} \qquad (5)$$

(where $A = 0{\cdot}51$ and $B = 3{\cdot}29 \times 10^7$) and an effective diameter of the ions involved $\alpha = 4{\cdot}0 \times 10^{-8}$.

(b) *Solubility of silver hyponitrite in ammonia*

This is shown by table and Fig. 1 where C_0 is the total molality of silver containing soluble compounds (in equiv. of Ag) and (NH_3) is the molality of free ammonia i.e. the difference of $2C_0$ from the total ammonia according to equation (2).

In Fig. 1 curve m shows log C_0, whereas curve α shows log ($f_\pm C_0$) against log (NH_3). The latter seems to be in good agreement with equation (3). The activity coefficients where calculated by means of (5).

The slope of the experimentally found straight line α is $1{\cdot}30 \pm 0{\cdot}02$ as compared to 1·33 predicted by equation (3). Furthermore the value of the constant term in (3) is found to be $-1{\cdot}435 \pm 0{\cdot}015$. Taking $K_1 = 7{\cdot}86 \times 10^{-8}$ (RANDALL[7]) one finds* $K_s = 1{\cdot}53 \pm 0{\cdot}16 \times 10^{-19}$.

The potential of a silver electrode in aqueous ammonia saturated with silver hyponitrite should follow equation (4).

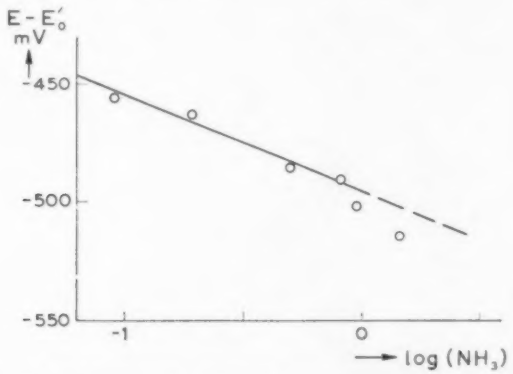

FIG. 2.—Silver electrode potential in aqueous ammonia saturated with silver hyponitrite.

Fig. 2 shows a plot of $E - E_0'$ against log (NH_3), where E_0' is the potential of the same cell for (Ag^+) = 1. For moderate concentrations the slope of the curve obtained is very near to 40 mV as expected, but it deviates at higher concentrations. This probably occurs because the ratio of the two activity coefficients involved in equation (4) does not remain constant for a wide region of ionic strengths (see Table 1)($f_\pm$ is the activity coefficient of a univalent cation, and f_- that of a bivalent anion). Besides at higher concentrations the formation of another complex ($NH_3AgN_2O_2^-$) would have to be taken into account, as shown below.

(c) *Solubility of* $Ag_2N_2O_2$ *in soluble hyponitrite at constant ammonia concentration*

The effect of the presence of sodium hyponitrite on the solubility of silver hyponitrite is shown in Table 2. [Ag] is the total molality of silver complexes in equiv. of Ag. For (NH_3) ≠ 0, C_0 is the molality of ammoniacal silver complexes, i.e. [Ag] corrected by subtraction of the solubility for the same concentration of $Na_2N_2O_2$ and (NH_3) = 0.

If only reactions (1) and (2) were to be considered, C_0 would be the molality of $Ag(NH_3)_2^+$ and

$$f_\pm C_0 = 1/K_1\,(NH_3)^2(Ag^+)$$

* A correction to allow for the formation of $AgNH_3^+$ would lie well within the limits of the experimental error since the formation constant $k_2 = (Ag(NH_3)_2^+)/(AgNH_3^+)(NH_3)$ is $7{\cdot}8 \times 10^3$ and therefore the ratio of the two complexes can not be smaller than $7{\cdot}8 \times 10^3 \times 0{\cdot}091 = 7{\cdot}1 \times 10^2$ in the region of ammonia concentrations used.

[7] M. RANDALL and J. O. HALFORD, *J. Amer. Chem. Soc.* **52**, 178 (1930).

TABLE 2.—SOLUBILITY OF $Ag_2N_2O_2$ IN $Na_2N_2O_2$ AT CONSTANT AMMONIA CONCENTRATION*

$[N_2O_2^{--}]$	[Ag]	C_0	[NaOH]	μ	$f_\pm$	$f_\pm C_0$	$E_0' - E$ (mV)
			$(NH_3) = 0$				
	$\times 10^{-2}$						
0·0311	0·055		0·270	0·364			
0·0496	0·094		0·293	0·443			
0·321	1·20		0·683	1·66			
0·673	1·96		1·231	3·28			
			$(NH_3) = 0·31$				
		$\times 10^{-2}$				$\times 10^{-2}$	
0·0069	1·38	1·37	0·100	0·121	0·75	1·03	474
0·0138	0·87	0·84	0·063	0·100	0·77	0·65	499·3
0·0303	0·97	0·91	0·069	0·151	0·74	0·67	505·8
0·0628	1·19	1·06	0·091	0·268	0·70	0·74	515·8
0·139	1·64	1·40	0·113	0·514	0·65	0·91	524·3
			$(NH_3) = 0·88$				
0·028	5·56	5·50	0·198	0·28	0·69	3·80	491
0·100	5·15	5·00	0·092	0·34	0·68	3·40	513
0·200	6·30	5·80	0·193	0·73	0·63	3·66	520
0·402	8·19	6·80	0·378	1·50	0·58	3·95	523

* C_0 = molalities and $f_\pm C_0$ = activities of silver-ammonia complexes.

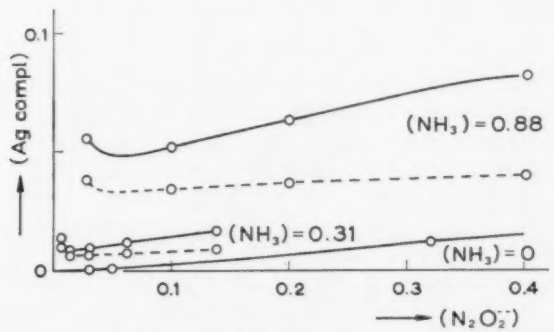

FIG. 3.—Solubility of $Ag_2N_2O_2$ in $Na_2N_2O_2$ at constant ammonia concentration. Continuous lines show molalities. Dotted lines show $f_\pm C_0$.

That the activity of free silver ions decreases is shown by the drift in the electrode potential. If $f_\pm$ is calculated from (5)for a univalent ion of $\alpha = 4·0 \times 10^{-8}$, then $f_\pm C_0$ decreases first and at higher concentrations of $Na_2N_2O_2$ it increases again, (Fig. 3). Therefore at least one more reaction apart from (1) and (2) must be considered.

(d) *The solubility product of silver hyponitrite*

To make sure that equilibrium (1) is established the silver electrode potential was measured in a series of sodium hyponitrite solutions in equilibrium with $Ag_2N_2O_2$

(Fig. 4). A small correction was made to the molality of $N_2O_2^{2-}$ to allow for the formation of silver-hyponitrito complexes according to Table 2.

E is expected to be a linear function of log $(N_2O_2^{2-})$ according to:

$$E = E_0' + \frac{2{\cdot}3RT}{2F}\log\frac{K_s}{f_-} - \frac{2{\cdot}3RT}{2F}\log(N_2O_2^{2-})$$

with a slope of 29·5 mV, provided there is no considerable variation in f_- (the activity coefficient of $N_2O_2^{2-}$).

The straight line shown in Fig. 4 was drawn at a slope 29·5 mV. The points of measurements do not seem to deviate considerably.

For $[N_2O_2^{2-}] = 0{\cdot}01$, $E - E_0'$ is found to be $-485{\cdot}8 \pm 2$ mV. Thus $K_s' = K_s/f_- = 3{\cdot}7 \pm 0{\cdot}4 \times 10^{-19}$ for $\mu \cong 0{\cdot}15$.

If $f_- = 0{\cdot}30$*, K_s would be $1{\cdot}11 \pm 0{\cdot}12 \times 10^{-19}$.

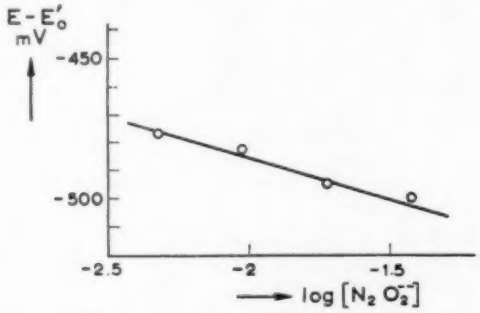

FIG. 4.—Silver electrode potential in $Na_2N_2O_2$ solution in equilibrium with $Ag_2N_2O_2$.

DISCUSSION

To draw conclusions, as to what substances are formed when silver hyponitrite dissolves in aqueous ammonia, the most characteristic of all series of measurements are those in Fig. 3. Evidently the simplest interpretation of the curves obtained is that they represent the sum of two functions, one hyperbolic and one parabolic. The hyperbola corresponds to the solubility of $Ag_2N_2O_2$ in the form of $Ag(NH_3)_2^+$, the molality of which (C_1) is expected to fall with increasing $N_2O_2^{2-}$ according to:

$$C_1 = \frac{1}{f_1} \times \frac{K_s^{\frac{1}{2}}}{K_1} \times \frac{(NH_3)^2}{(N_2O_2^{2-})^{\frac{1}{2}}}$$

where f_1 is its act. coefficient.

The parabola indicates the formation of at least one more silver complex. Its concentration seems (by Fig. 3) to be proportional to $(N_2O_2^{2-})^{\frac{1}{2}}$ (for (NH_3) = const.) and to (NH_3) (for $(N_2O_2^{2-})$ = const.). These requirements are satisfied if the reaction

$$Ag^+ + N_2O_2^{2-} + NH_3 \rightleftharpoons (NH_3)AgN_2O_2^- \qquad (6)$$

is assumed to take place together with (1) and (2). If it is so, the molality of this complex (C_2) would be:

$$C_2 = \frac{1}{f_2} \times \frac{K_s^{\frac{1}{2}}}{K_2} \times (NH_3) \times (N_2O_2^{2-})^{\frac{1}{2}}$$

* Calculated from (5) for $\alpha = 4{\cdot}0 \times 10^{-8}$ and $\mu = 0{\cdot}15$.

where K_2 is the instability constant

$$K_2 = (Ag^+)(N_2O_2^{2-})(NH_3)/(NH_3AgN_2O_2^-).$$

Thus C_0, determined volumetrically, would be the sum of the two complexes ($C_0 = C_1 + C_2$) and if it is assumed that the activity coefficients of the two complex ions are very nearly equal, and if they are replaced by f_+, it follows

$$\frac{f_\pm C_0}{(Ag^+)} = \frac{(NH_3)^2}{K_1} + \frac{(NH_3)K_s}{K_2} \times \frac{1}{(Ag^+)^2}$$

where the activity of ammonia has been substituted by its molality after RANDALL[8]. Therefore a plot of $f_\pm C_0/(Ag^+)$ against $1/(Ag^+)^2$ should be a straight line from the slope of which the ratio K_s/K_2 could be estimated. This is calculated in Table 3 from the data of Table 2 and shown by Fig. 5.

TABLE 3.

$f_\pm C_0$	$E_0' - E$ (mV)	$\frac{1}{(Ag^+)}$	$\frac{1}{(Ag^+)^2}$	$\frac{f_\pm C_0}{(Ag^+)}$
		$(NH_3) = 0{\cdot}31$		
$\times 10^{-2}$		$\times 10^{8}$	$\times 10^{16}$	$\times 10^{6}$
1·03	474	1·02	1·04	1·05
0·65	499·3	2·76	7·61	1·79
0·67	505·8	3·56	12·7	2·40
0·74	515·8	5·25	27·6	3·90
0·91	524·3	7·31	53·5	6·65
		$(NH_3) = 0{\cdot}88$		
$\times 10^{-2}$		$\times 10^{8}$	$\times 10^{17}$	$\times 10^{7}$
3·80	491	2·04	0·416	0·774
3·40	513	4·79	2·30	1·63
3·66	520	6·31	3·99	2·31
3·95	523	7·08	4·96	2·80

The slope of the functions in Fig. 5 is $4{\cdot}32 \times 10^{-11}$ for $(NH_3) = 0{\cdot}88$, and $1{\cdot}06 \times 10^{-11}$ for $(NH_3) = 0{\cdot}31$. Thus K_2/K_s is found $2{\cdot}04 \times 10^{10}$ and $2{\cdot}93 \times 10^{10}$ respectively.

From the intercept the value of K_1 is found $12{\cdot}5 \times 10^{-8}$ (for $(NH_3) = 0{\cdot}88$) and 10×10^{-8} (for $(NH_3) = 0{\cdot}31$). Its actual value is $7{\cdot}86 \times 10^{-8}$.

The inconsistency is probably due to the assumption made that $f_1 = f_2 = f_+$.

The series for $(NH_3) = 0{\cdot}31$ seems more reliable as it involves moderate ionic strengths and it yields a value for K_1 nearer to the correct one. Therefore K_2 can be taken as approximately equal to $3 \times 10^{10} K_s$, and this should not be in error by more than 30 per cent.

It seems therefore that there can be little doubt about the existence of equilibrium (6) in solutions of silver hyponitrite in ammonia. Even without addition of sodium hyponitrite, silver hyponitrite dissolves in aqueous ammonia to form $NH_3AgN_2O_2^-$ at a considerable extent as compared to the classical $Ag(NH_3)_2^+$. Thus a calculation of the ratio $Ag(NH_3)_2^+/NH_3AgN_2O_2^-$ (which must be very nearly equal to K_2/K_1K_s

[8] M. RANDALL and J. O. HALFORD, *J. Amer. Chem. Soc.* **52**, 192 (1930).

VOL. 19 1961

$(NH_3)(Ag^+)^2$) based on the dependence of E on the concentration of NH_3 (Fig. 2), shows that, even in 0·2 N NH_3, the concentration of $Ag(NH_3)_2^+$ is only twenty times as high as that of $(NH_3)AgN_2O_2^-$, and that their ratio decreases down to 1·2 in 2 N NH_3.

Thus the value $K_s = 1{\cdot}53 \times 10^{-19}$ from Fig. 1 should be considered only as an upper limit as its calculation was made with the assumption that only the complex $Ag(NH_3)_2^+$ is formed. On the other hand the value $1{\cdot}11 \times 10^{-19}$ from Fig. 4 may be

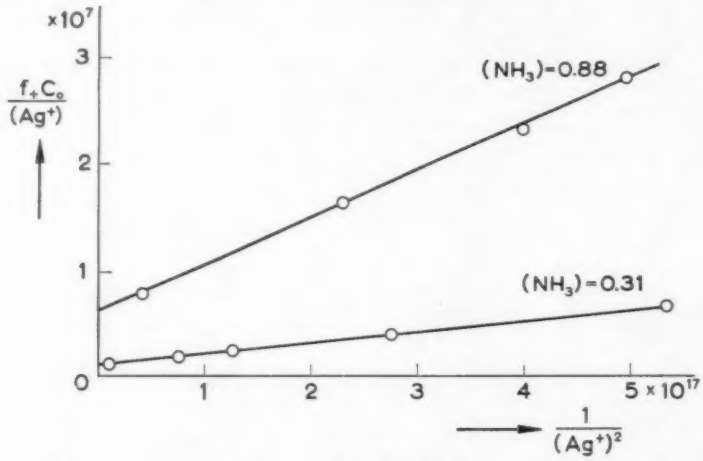

FIG. 5.—Illustration of the linear relationship between $f_{\pm}C_0/(Ag^+)$ and $1/(Ag^+)^2$.

too low as the activity coefficient of $N_2O_2^{2-}$ for $\mu = 0{\cdot}15$ was taken $f_- = 0{\cdot}30$. Higher f_- would seem more reasonable, e.g. 0·35 which would lead to a $K_s = 1{\cdot}30 \times 10^{-19}$. This is actually the mean of 1·53, 1·11 and $1{\cdot}22 \times 10^{-19}$ the last of which was calculated (as not shown here) from the measurements connected with the establishment of relationship (5). Thus we take as most reliable $K_s = 1{\cdot}30 \pm 0{\cdot}15 \times 10^{-19}$ and consequently $K_2 \cong 4 \times 10^{-9}$.

A great deal of work has been devoted to the preparation and study of silver complexes with various ligands. As a rule the ligands (usually two) coordinated to a Ag^+ are always identical or at least very similar. Comparatively, only a few cases of detection of silver complexes with different ligands have been reported, e.g. $AgNH_3PO_4^{2-}$[9], $Ag(NH_3)_2(CrO_4)_2^{3-}$ and $Ag(NH_3)_2CrO_4^-$[10], $Ag(NH_3)_2X_2^-$ where $X^- = BrO_3^-$, IO_3^-, or Cl^-[11] etc. Thus the data presented above may also be found useful to the study of the properties of silver ion.

Acknowledgement—The authors gratefully acknowledge the support of this work by the Royal Hellenic Research Foundation.

[9] H. C. SARASWAT, *Proc. Indian Acad. Sci.* **30** A, 329 (1949).
[10] M. B. SHCHIGOL and S. M. BIRNBAUM, *Zavodskaya Lab.* **15**, 1027 (1949) and *Chem. Abstr.* **44**, 1362 f (1950).
[11] M. B. SHCHIGOL, *Zh. Obshcheĭ Khim.* **22**, 721 (1952); *J. Gen. Chem. U.S.S.R.* (Engl. transl.) **22**, 787 (1952) and *Chem. Abstr.* **47**, 3167 c (1953).

J. Inorg. Nucl. Chem., 1961, Vol. 19, pp. 115 to 132. Pergamon Press Ltd. Printed in Northern Ireland

UNTERSUCHUNG DES VERHALTENS DER CHLOROKOMPLEXE DER PLATINELEMENTE IN LÖSUNG UND AN ANIONENAUSTAUSCHERN

E. BLASIUS, W. PREETZ und R. SCHMITT
Anorganisch-Chemisches Institut der Technischen Universität, Berlin

(*Received* 11 *March* 1960)

Abstract—Kinetical data have been determined for ligand exchange reactions of the chlorocomplexes of Pt(IV), Ir(III) and Ir(IV). The hydrolysis of the complexes in 10^{-3} M solution more or less rapidly gains equilibrium. Below a HCl concentration of 1 M the solution consists of partially hydrolized complexes. The original complex and the hydrolized complexes of Ir(IV) can well be recognized by spectrophotometrical measurements. The binding of the complexes to the anion exchangers takes place by exchange of the Cl^--ions of the ion exchanger by equivalent quantities of complex.

VOL. 19 1961

ÜBER das Verhalten der Chlorokomplexe der Platinelemente in wässriger Lösung sind die Angaben in der Literatur unübersichtlich und teilweise widersprechend. Bei der papierionophoretischen Trennung[1] treten oft Multispots auf, die das Vorliegen eines Gleichgewichts von mehreren Komplexen bei einem Element wahrscheinlich machen. Auch Versuche an Ionenaustauschern weisen auf diese Tatsache hin.[2] Ausserdem werden die Chlorokomplexe des Platin(IV) und Iridium(IV) extrem fest am Anionenaustauscher gebunden, eine Tatsache, die nicht mehr mit rein elektrostatischer Wechselwirkung erklärt werden kann. Die Untersuchungen erstreckten sich auf die Hydrolyse, den Ligandentausch und das Verhalten an Anionenaustauschern. Vorerst wurden die Reaktionen der Chlorokomplexe des Platins und des Iridiums unter Verwendung von ^{36}Cl als Indikator verfolgt.

Da Ligandentausch und Hydrolyse zwei zeitlich nebeneinander, aber verschieden schnell verlaufende Vorgänge darstellen, setzt die Untersuchung des einen die Kenntnis des anderen Vorganges voraus. In den meisten bisher bekannten Arbeiten wird eine strenge Unterscheidung der beiden Vorgänge nicht vorgenommen, sondern lediglich die Änderung der Aktivität verfolgt. Unter Ligandentausch wird daher in dieser Arbeit allein der Tausch von komplex gebundenen gegen in Lösung befindliche Cl^--Ionen verstanden. Die genannten Tatsachen dürften mit dazu beigetragen haben, dass anfänglich in der Literatur eine Parallelität zwischen Komplexbeständigkeit und Tauschgeschwindigkeit angenommen wurde.[3] Wie spätere Arbeiten zeigen, ist jedoch eine allgemein gültige Beziehung nicht zu erhalten.[4,5]

TAUBE[6] schlug deshalb vor, die Ordnung der Komplexionen nicht nur nach ihrer Beständigkeit, sondern auch nach ihrer Ligandentauschgeschwindigkeit vorzunehmen. Er teilte die Komplexe mit der Koordinationszahl 6 zunächst in eine "inner orbital" und eine "outer orbital" Gruppe ein, wobei die erste Gruppe hauptsächlich kovalente, die zweite dagegen elektrostatische Bindungen aufweist.

[1] E. BLASIUS und M. FISCHER, Dissert. Techn. Univ. Berlin (1959); *Z. Anal. Chem.* 177, 412 (1960).
[2] E. BLASIUS und D. REXIN, Dissert. Techn. Univ. Berlin (1959); *Z. Anal. Chem.* im Druck (1961).
[3] F. A. LONG, *J. Amer. Chem. Soc.* **63**, 1353 (1941).
[4] A. A. GRINBERG, *Einführung in die Chemie der Komplexverbindungen.* Berlin (1955).
[5] K. B. JAZIMIRSKI, *Thermochemie der Komplexverbindungen.* Berlin (1956).
[6] H. TAUBE, *Chem. Rev.* **50**, 69 (1952).

Ihr innerer Unterschied besteht in der Elektronenkonfiguration. Bei beiden Gruppen gibt es, nach Ligandentauschgeschwindigkeit geordnet, inerte und labile Komplexe. Sämtliche labilen Komplexe weisen als Charakteristikum eine unbesetzte innere *d*-Bahn auf. In dieser Klassifizierung gehören alle drei in dieser Arbeit untersuchten Komplexe zu den inerten "inner orbital"-Komplexen.

Für Tauschreaktionen gibt es grundsätzlich nur drei Reaktionsmechanismen.[7] Diese sind: erstens die reversible Dissoziation des Komplexes, zweitens Tausch durch die Bildung eines Zwischenkomplexes (Stosspaarbildung), schliesslich drittens der Übergang von Elektronen, wie er bei Redoxsystemen eine Rolle spielen kann. Der erste Mechanismus ist monomolekular, die Reaktionsgeschwindigkeit somit nur von der Konzentration des Komplexes abhängig. Dagegen spielt für den zweiten Reaktionsweg auch die Konzentration an freien Ligandionen eine Rolle. TAUBE und RICH[8] veröffentlichten bereits einige Ergebnisse zum Ligandentausch des $[PtCl_6]^{2-}$-Ions. Danach ist die Ligandentauschgeschgeschwindigkeit in starkem Masse von der Belichtung und der Anwesenheit dritter Substanzen abhängig. In dieser Arbeit wurde jedoch der zeitliche Verlauf des Tausches nicht genau untersucht. Über eine etwa stattfindende Hydrolyse wird nichts berichtet. GRINBERG[9] erwähnt, dass bei den Bromokomplexen des Pt(IV) eine autokatalytische Beschleunigung der Reaktion auftritt. Er vermutet als Zwischenstufe die Bildung von Hydrolysekomplexen. Die Ligandentauschsysteme $[IrCl_6]^{2-}/Cl^-$ und $[IrCl_6]^{3-}/Cl^-$ sind bisher noch nicht untersucht worden. Es liegen nur Angaben über die Chloro-und Bromokomplexe des Redoxsystems Ir(IV)/Ir(III) vor.[10]

Die graphische Darstellung des Ligandentausches bimolekularer Reaktionen erfolgt nach der theoretischen Beziehung[11,12]

$$R \cdot t = -\frac{(A)(B)}{(A) + (B)} \ln (1 - F) \tag{1}$$

Darin bedeuten:

R Tauschgeschwindigkeit in Mol/Liter · min

(A) Konzentration der tauschenden Ionen im Komplex (aktive und inaktive) in Mol/Liter

(B) Konzentration der tauschenden Ionen in Lösung (aktive und inaktive) in Mol/Liter

F, die getauschte Fraktion, ist definiert durch

$$F = \frac{x_t - x_0}{x_\infty - x_0} \tag{2}$$

x_0, x_t und x_∞ sind die Konzentrationen der markierten Ionen in Lösung zu den Zeiten: o, t und unendlich (völlige statistische Verteilung). Statt der Konzentrationen können bei der Berechnung die entsprechenden relativen Aktivitäten in Imp/min eingesetzt werden. Variabel sind t und F. Die Tauschgeschwindigkeit R erhält man aus der für 50% igen Tausch ($F = 0{,}5$) aus der graphischen Darstellung ersichtlichen Halbwertszeit. Die Konzentrationsabhängigkeit der Tauschgeschwindigkeit R wird für bimolekulare Reaktionen beschrieben durch

$$R = k(A) \cdot (B) \tag{3}$$

k bedeutet in dieser Gleichung die Reaktionsgeschwindigkeitskonstante (Liter/Mol · min). Die Aktivierungsenergie wurde mit Hilfe der Arrheniusschen Gleichung ermittelt.

MESSVERFAHREN UND AUSGANGSSUBSTANZEN

Als Ausgangssubstanzen dienten hauptsächlich die mit ^{36}Cl (als Cl* bezeichnet) markierten Komplexe. Bei den Platin- und Iridium-chlorokomplexen lässt sich durch Messung der Leitfähigkeit infolge der vielen durch Primärdissoziation vorhandenen Ionen die Hydrolyse nur schwer erfassen. Es ist dagegen recht einfach, abhydrolysierende Cl^{*-}-Ionen nachzuweisen. Der zeitliche Verlauf der Vorgänge konnte somit radiometrisch verfolgt werden, indem die nach der Abtrennung der Komplexe in der

[7] A. C. WAHL and N. A. BONNER, *Radioactivity Applied to Chemistry*. New York (1951).
[8] R. L. RICH and H. TAUBE, *J. Amer. Chem. Soc.* **76**, 2608 (1954).
[9] A. A. GRINBERG and G. A. SCHAGISSULTANOWA, *Nachr. Akad. Wiss. UdSSR*, 981 (1955).
[10] A. A. GRINBERG and J. A. BELOUSSOW, *Ber. Akad. Wiss. UdSSR* **111**, 599 (1956).
[11] H. MCKAY, *Nature, Lond.* **139**, 283 (1937).
[12] R. B. DUFFIELD and M. CALVIN, *J. Amer. Chem. Soc.* **68**, 557 (1946).

Lösung verbliebene Cl*-Aktivität bzw. die der gelösten Komplexe in Flüssigkeitszählrohren gemessen wurde. Mit Hilfe einer Eichkurve liessen sich die erhaltenen relativen Aktivitäten (Imp/min) auf mg Cl/ml umrechnen. Die Aktivitätswerte wurden aus mehreren Messungen als Mittelwerte erhalten. Bei den farbintensiven Iridium(IV)chlorokomplexen, die ein charakteristisches Absorptionsspektrum mit ausgeprägten Banden im sichtbaren und im UV-Gebiet geben, kann der Fortgang der Hydrolyse auch durch spektrophotometrische Untersuchungen verfolgt werden. Für die übrigen Lösungen, die nur sehr schwache Absorptionsbanden aufweisen, ist diese Methode jedoch nicht geeignet. Die entsprechenden Versuchstemperaturen hielt ein Thermostat auf ± 1°C konstant.

Als Geräte dienten das Strahlungsmessgerät FH 49 (Friesecke und Hoepfner) und das Zeiss-Spektralphotometer M4Q. Die verwendete 2 N HCl* mit einer spezifischen Aktivität von etwa 100 μc/g Cl wurde aus Amersham (England) bezogen. Als Ionenaustauscher dienten die Handelswaren Permutit *RS*, Dowex 2 $\times$ 8 (Kapazität: 2,35 mval/g lufttrocknes Harz). Die Beladung der Anionenaustauscher mit Cl^{*-} erfolgte mit HCl* über die Hydroxylform. Die Kapazitätsbestimmung geschah radiometrisch über das mit NaOH erhaltene Eluat.

Alle verwendeten Chemikalien waren "reinst"—bzw. "pro analysi"—Präparate von Merck, Darmstadt.

Darstellung von $H_2[IrCl_6^*]$. Als Ausgangsprodukt diente $H_2[IrCl_6]\cdot 6H_2O$ (Degussa, Hanau), aus dem alkali- und chloridionenfreies Iridium(IV) oxydhydrat hergestellt wurde.[13] Unter Verwendung einer geschlossenen Apparatur mit Rückflusskühler wurde der Niederschlag durch 8-stündiges Kochen in HCl* gelöst und anschliessend die überschüssige HCl* im Vakuum bei Temperaturen unterhalb von 45 C weitgehend abdestilliert, der Komplex als $Cs_2[IrCl_6^*]$ gefällt, ausgewaschen und getrocknet. Aus diesem Komplex wurde durch Behandeln mit Permutit *RS* in der H^+-Form die reine freie Säure $H_2[IrCl_6^*]$ gewonnen.

Darstellung von $H_2[PtCl_6^*]$. Als Ausgangsprodukt lag $PtCl_4$ vor, aus dem durch überschüssige HCl $H_2[PtCl_6]$ hergestellt wurde. Die Bereitung des aktiven Komplexes kann nach zwei Verfahren vorgenommen werden. Elektrolytisch abgeschiedener Platinschwamm wird in Gegenwart aktiver HCl* durch anodische Oxydation in $H_2[PtCl_6^*]$ überführt.[14] Das zweite Verfahren verwertet den im Ultravioletten sehr schnell ablaufenden Ligandentausch $[PtCl_6]^{2-}/Cl^{*-}$. Da nach einigen Stunden das statistische Gleichgewicht erreicht ist, kann dann der markierte Komplex als Cäsiumsalz abgetrennt und wie oben mit dem Kationenaustauscher in $H_2[PtCl_6^*]$ überführt werden. Zur Zurückdrängung der Hydrolyse wurde der Komplexlösung HCl* gleicher spezifischer Aktivität zugesetzt.

(1) *Ligandentausch und Hydrolyse des* $[IrCl_6^*]^{2-}$*-Komplexes*

Orientierende Ligandentauschversuche bei Zimmertemperatur mit $[IrCl_6^*]^{2-}$ ergaben, dass selbst nach Wochen kein messbarer Tausch feststellbar ist. Deshalb wurden mehrere Messreihen bei 60° und 80° durchgeführt.

Die Konzentration des indizierten Komplexes betrug 0,00134 Mol/Lit., entsprechend einer Konzentration von 0,00804 Mol/Liter komplex gebundener Cl^*-Ionen. Die freie HCl-Konzentration war bei 80 C: 1 N, 0,5 N, 0,25 N, 0,1 N, bei 60 C: 1 N und 0,3 N. Nach bestimmten Zeiten wurden jeweils 5 ml-Proben genommen und der Komplex mit $CsNO_3$ gefällt. Filtrat und Niederschlag, der sich mit Hydrazinsulfat in der Siedehitze reduzierend lösen liess,[15] wurden in Messkolben auf 25 ml aufgefüllt und der radiometrischen Messung zugeführt.

Die Abb. 1 zeigt die Aktivitätsverteilung, aufgetragen in Imp/min, zwischen der Lösung und dem Komplex in Abhängigkeit von der Zeit bei 80°C. Die aufsteigenden

[13] F. Kraus und H. Gerlach, *Z. Anorg. Chem.* **143**, 126 (1925).
[14] F. Nobis, Dissert. Techn. Hochsch. Dresden (1909).
[15] F. Mylius und A. Mazzucchelli, *Z. Anorg. Chem.* **89**, 7 (1914).

VOL. 19 1961

Kurven beziehen sich auf die Zunahme der Aktivität in der Lösung, die abfallenden auf die entsprechende Abnahme der Aktivität im Komplex. Alle Kurven streben einem Grenzwert zu, der durch das Verhältnis der molaren Konzentrationen der Tauschpartner gegeben ist. Für die weitere Auswertung wurden die genauer gemessenen Daten der Zunahme der Aktivität in Lösung zu Grunde gelegt.

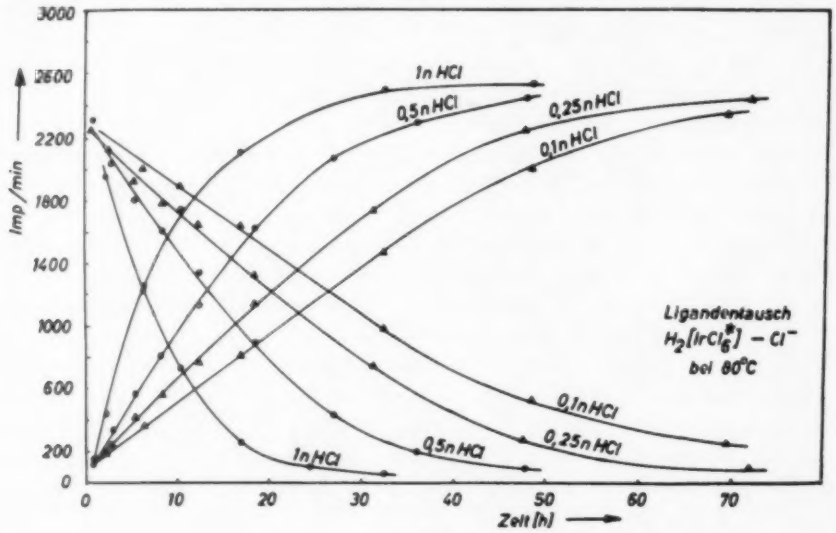

ABB. 1.

Auf der Abb. 2 sind in halblogarithmischem Massstab die Werte für $(1 - F)$ gegen die Zeit aufgetragen. Der von einer Geraden abweichende Kurvenverlauf zeigt, dass der Ligandentausch schneller verläuft, als theoretisch für bimolekulare Reaktionen zu erwarten ist. Wahrscheinlich bilden sich analog zu den Ergebnissen GRINBERGS[9] im Laufe des Versuches geringe Mengen des Iridium(III)komplexes aus, welche teilweise durch Hydrolyse in Aquo- oder Hydroxokomplexe übergehen, die dann den Ligandentausch beschleunigen. Hierfür spricht auch die Tatsache, dass in der 0,1 N HCl-Lösung nach mehreren Tagen des Erwärmens auf 80°C zum grössten Teil Iridium(III) nachgewiesen werden kann (siehe auch abweichenden k-Wert in Tabelle 1).

An den ersten Teil der Kurven lassen sich aber gut Geraden anlegen, die praktisch den idealisierten Fall der nicht beschleunigten Reaktion wiedergeben. An diesen Geraden wird die Halbwertszeit des Ligandentausches $t_{1/2}$ abgelesen und daraus die Tauschgeschwindigkeit R der Reaktion (nach 1) berechnet.

Die Tabelle 1 enthält eine Zusammenstellung der Ergebnisse.

Die Übereinstimmung der Tauschkonstanten ist recht gut und beweist den bimolekularen Charakter der Reaktion.

Unter Verwendung der k-Werte, die sich für die 1 N HCl-Lösungen bei 60° und 80°C ergaben, berechnet sich die Aktivierungsenergie nach der Arrheniusschen Gleichung zu dem recht hohen Wert von ca. 25 kcal/Mol.

Zur spektrophotometrischen Untersuchung der Hydrolysevorgänge des $[IrCl_6]^{2-}$ wurden Lösungen mit $0{,}84 \cdot 10^{-3}$ Mol/Liter $H_2[IrCl_6] \cdot 6H_2O$ in wässriger, 0,1 N,

1 N, 3 N und konz. HCl-Lösung verwendet. In den folgenden Abb. wird auf der Abszisse stets die Wellenlänge in mμ, auf der Ordinate die Absorption in % aufgetragen.

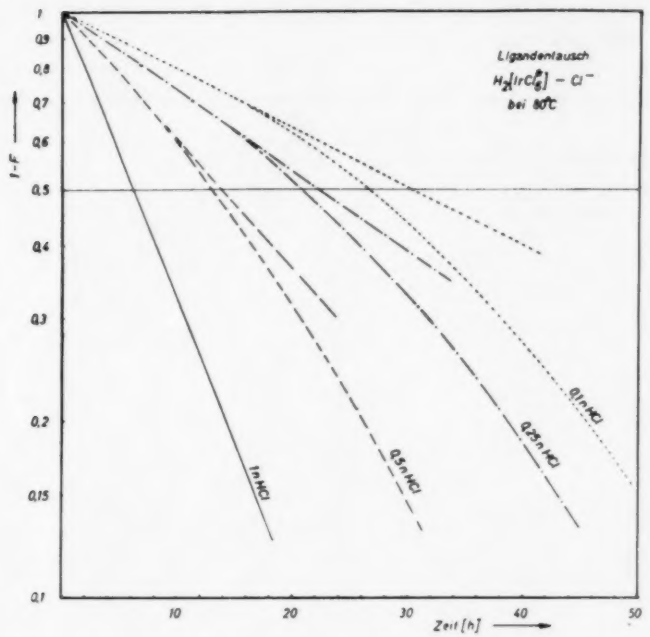

Abb. 2.

Tabelle 1.—Ligandentauschversuche $H_2[IrCl_6^*]/Cl^-$

Versuch	Temp. (°C)	Konz. HCl (N)	Konz. $[IrCl_6^*]^{2-}$ Mol/Lit.	$t_{1/2}$ (hr)	R (Mol/Lit. min)	k (Lit./Mol min)
1	80	1	0,00134	6,25	$1{,}47 \cdot 10^{-5}$	$1{,}8 \cdot 10^{-3}$
2	80	0,5	0,00134	13,5	$0{,}68 \cdot 10^{-5}$	$1{,}7 \cdot 10^{-3}$
3	80	0,25	0,00134	22	$0{,}42 \cdot 10^{-5}$	$2{,}0 \cdot 10^{-3}$
4	80	0,1	0,00134	30	$0{,}28 \cdot 10^{-5}$	$3{,}5 \cdot 10^{-3}$
5	60	1	0,00134	55	$0{,}17 \cdot 10^{-5}$	$0{,}22 \cdot 10^{-3}$
6	60	0,3	0,00134	195	$0{,}045 \cdot 10^{-5}$	$0{,}20 \cdot 10^{-3}$

Abb. 3 zeigt die Absorptionsspektren des Iridium(IV)hexachlorokomplexes in wässriger und konz. HCl-Lösung bei Zimmertemperatur. Die dazwischen liegenden Kurven für 0,1 N, 1 N, 3 N HCl wurden der besseren Übersicht halber nicht eingezeichnet. Das gleiche Kurvenbild ergibt sich nach Alterung der Lösungen um 100 Stunden und beweist die Beständigkeit des Iridium(IV)komplexes bei Zimmertemperatur im Bereich der untersuchten HCl-Konzentration. Bei Erhitzen auf 80°C hydrolysiert die wässrige Komplexlösung innerhalb von 24 Stunden vollständig. Das Iridium scheidet sich als blaues Oxydhydrat ab. Bei den salzsauren Lösungen bleibt unter diesen Bedingungen die Lage der Maxima erhalten. Sie geben alle mit $CsNO_3$

die charakteristische Fällung als $Cs_2[IrCl_6]$. Bei der 0,1 N HCl-Lösung, die gewisse Veränderungen im Absorptionsspektrum aufweist, tritt diese jedoch nur nach einiger Zeit zögernd auf. Werden die Iridium(IV)hexachlorokomplexlösungen kathodisch reduziert und nach einiger Zeit wieder anodisch oxydiert, so ergeben sich die Absorptionskurven der Abb. 4a, 4b.

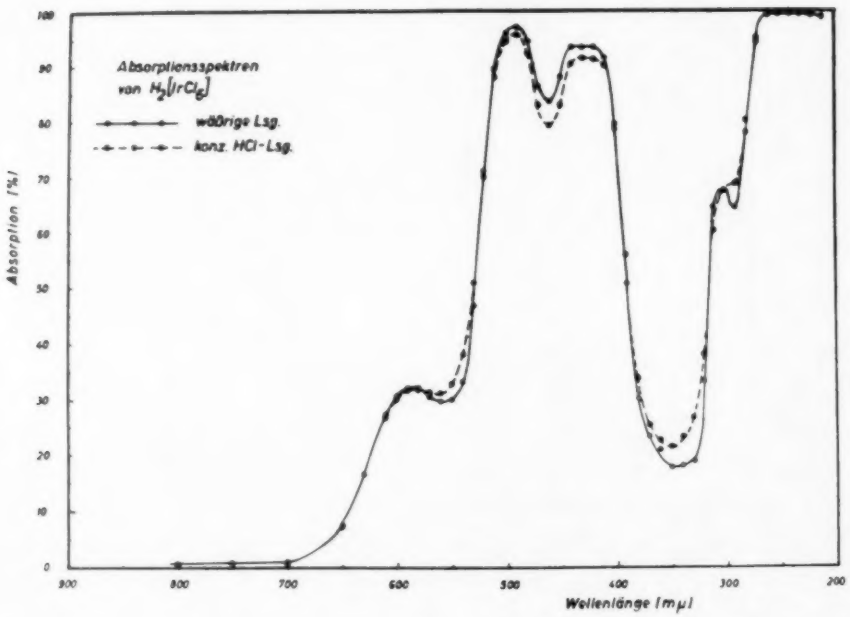

ABB. 3.

Die wesentlich veränderten Spektren der wässrigen, 0,1 N, 1 N HCl-Lösung deuten auf ein definiertes Hydrolyseprodukt hin. Die stärker salzsauren Lösungen zeigen die typische Absorptionskurve des $[IrCl_6]^{2-}$. Allerdings ist bei der 3 N HCl-Lösung noch die kleine Bande bei 360 mμ zu erkennen. Immerhin geben die stärker sauren Lösungen mit $CsNO_3$ eine Fällung, während diese bei den drei veränderten Lösungen ausbleibt und selbst nach Tagen nicht eintritt.

Erwärmt man die kathodisch reduzierten und dann wieder anodisch oxydierten Lösungen mehrere Tage auf 80°C, so hydrolysiert die wässrige Lösung vollständig. In den salzsauren Lösungen wird wieder der Iridium(IV)hexachlorokomplex gebildet, d.h. die Hydrolysekomplexe des Iridium(IV), die durch Oxydation hydrolysierter Iridium(III)komplexlösungen erhalten werden, sind in stärker salzsauren Lösungen nur metastabil (Abb. 5).

Mit $CsNO_3$ wird nunmehr aus allen Lösungen wieder die Fällung als $Cs_2[IrCl_6]$ erhalten.

Diese qualitativen spektrophotometrischen Untersuchungen zeigen, dass im Bereich der HCl-Konzentration von 0,1–3 N Hydrolyseprodukte auftreten, die durch ihr charakteristisches Absorptionsspektrum gekennzeichnet sind, sich aber von dem Hexachlorokomplex äusserlich in der Farbe nicht unterscheiden.

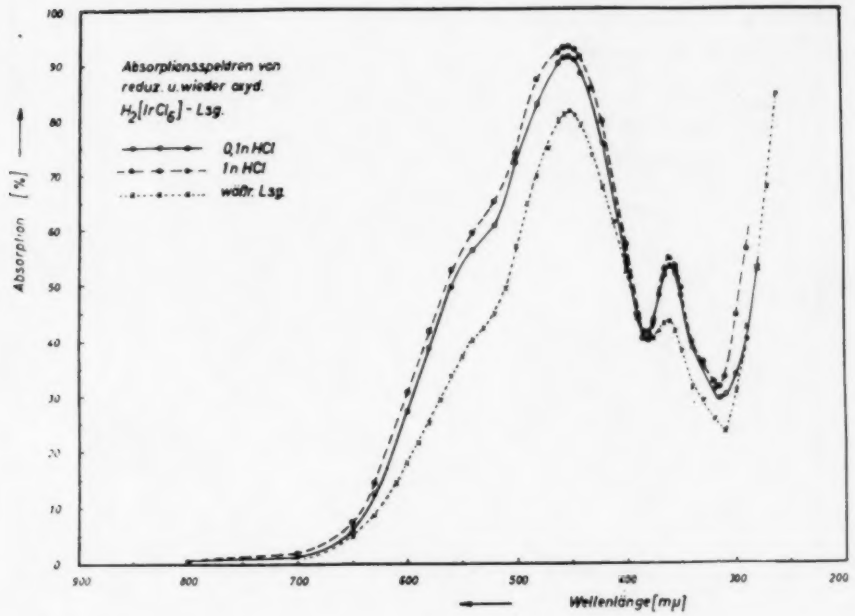
Absorptionsspektren von
reduz. u. wieder oxyd.
$H_2[IrCl_6]$ - Lsg.
0,1n HCl
1n HCl
wäßr. Lsg.
Absorption [%]
Wellenlänge [mμ]

ABB. 4a.

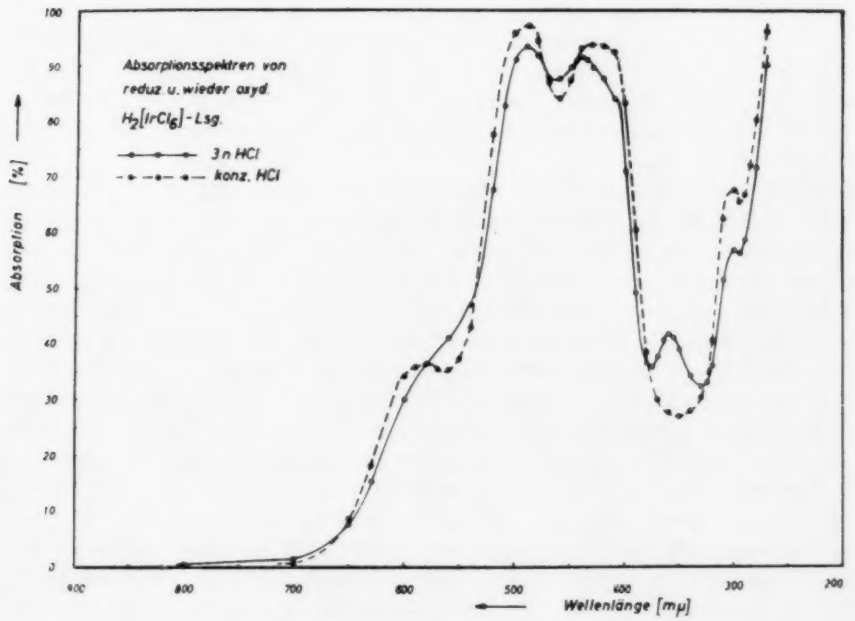
Absorptionsspektren von
reduz. u. wieder oxyd.
$H_2[IrCl_6]$ - Lsg.
3n HCl
konz. HCl
Absorption [%]
Wellenlänge [mμ]

ABB. 4b.

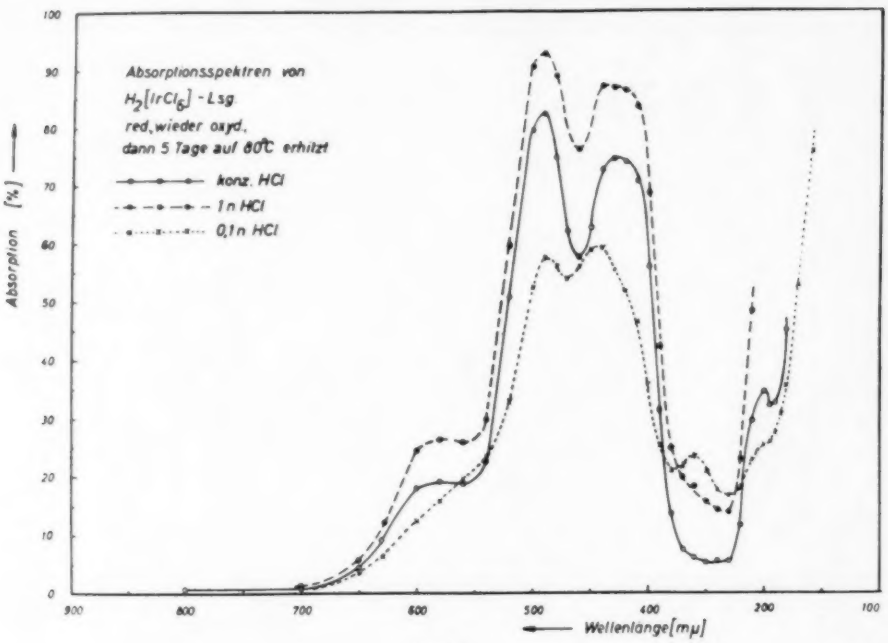

ABB. 5.

(2) *Ligandentausch und Hydrolyse des* $[IrCl_6^*]^{3-}$*-Komplexes*

Der Ligandentausch der Iridium(III)chlorokomplexe gestaltet sich durch die gleichzeitig ablaufende Hydrolyse etwas unübersichtlich. Er konnte deshalb erst nach Einstellung des Hydrolysegleichgewichtes untersucht werden, das allerdings, wie auch die spektrophotometrischen Untersuchungen ergaben, nach ziemlich kurzer Zeit erreicht ist.

Eine verdünnte wässrige Lösung des markierten Komplexes $H_2[IrCl_6^*]$ wurde während 12 Stunden an blanken Iridiumblechelektroden (1 cm^2) reduziert. Dieses Verfahren erwies sich als am geeignetesten, weil es bei Zimmertemperatur verläuft und keine störenden Fremdionen in die Lösung gelangen. Die reduzierte hellgelbe Lösung wurde aliquot auf 50 ml-Messkolben verteilt und mit inaktiver Salzsäure zu Lösungen der freien HCl-Konzentration 0,5 N, 1 N und 2 N aufgefüllt. Da für die Iridium(III)komplexe und die Hydrolyseprodukte des Iridium(IV) kein geeignetes Fällungsreagenz bekannt ist, erfolgte die Abtrennung des Komplexes aus der Lösung durch Bindung an Dowex 2 in der Cl^--Form. Da die Iridium(III)komplexe einerseits nur schwach am Anionenaustauscher gebunden werden, andererseits stark der Hydrolyse und dem Ligandentausch unterliegen, wurden zu entsprechenden Zeiten 5 ml Proben genommen und während 20 min anodisch oxydiert, wodurch die genannten Vorgänge unterbunden werden. Wie eingehende Untersuchungen an den Iridium(III)komplexen zeigten, findet durch die Oxydation keine Veränderung der Komplexzusammensetzung statt. Zu den oxydierten tiefrotbraunen Komplexlösungen wurden 20 ml eines Lösungsgemisches gegeben, so dass die Endlösung stets 0,5 N an freier HCl und 1,5 N an NaCl war. Diese Lösungen wurden dann mit 60 mg Dowex 2

30 min im "batch"-Verfahren gerührt. Nach dieser Zeit waren die Iridium(IV)-komplexe fast quantitativ am Anionenaustauscher gebunden. Die farblos erscheinende Lösung wurde nach Filtration der Messung im Flüssigkeitszählrohr zugeführt. Eine analoge Versuchsreihe wurde bei den HCl-Konzentrationen 2 N, 4 N, konz. HCl durchgeführt.

Die Abb. 6 zeigt die Aktivität in den Lösungen als Funktion der Zeit. Auf den starken Anstieg der Aktivität, bedingt durch die Hydrolyse, folgt dann ein langsamer Anstieg, der durch den Tausch der noch im Komplex verbliebenen Cl*-Liganden mit

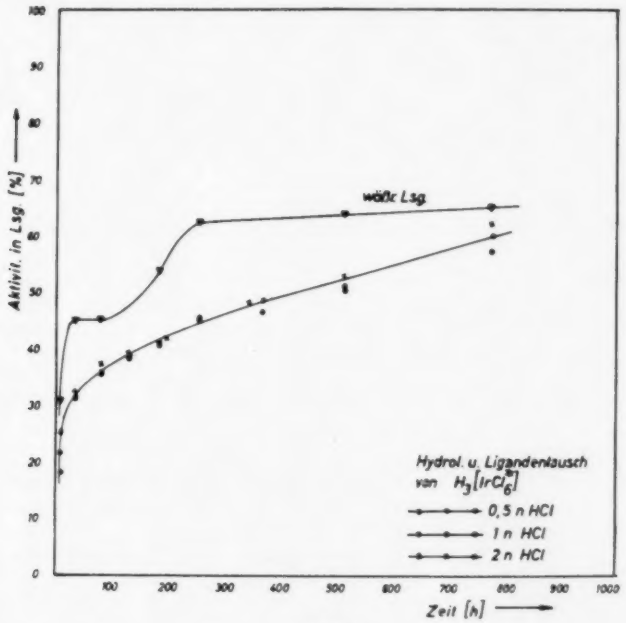

ABB. 6.

den freien Cl^--Ionen der Lösung zustande kommt. Der Ligandentausch erweist sich als unabhängig von der freien HCl-Konzentration, denn die Verhältnisse können für die 0,5 N, 1 N und 2 N HCl-Lösungen durch eine Kurve wiedergegeben werden. Auch bei höheren HCl-Konzentrationen liegt der Anstieg der Kurven in der gleichen Grössenordnung. Es handelt sich also bei dem Ligandentausch des Iridium(III)-komplexes mit den freien Cl^--Ionen um eine Reaktion 1. Ordnung, wobei anzunehmen ist, dass er über Aquo- oder Hydroxokomplexe verläuft, die unter geringer reversibler Dissoziation den Tausch bewirken. Bemerkenswert ist, dass im Gegensatz zu dem Iridium(IV)komplex hier schon bei Zimmertemperatur eindeutig ein Ligandentausch zu beobachten ist.

Bei den salzsauren Lösungen sieht man einen deutlichen Knick in der Kurve bei ca. 33% (Abb. 6). Im Bereich von 0,5–2 N HCl hydrolysieren demnach zwei Cl^--Ionen unter Bildung von Aquo- oder Hydroxokomplexen ab. Diese Hydrolysekomplexe ergeben nach der anodischen Oxydation Absorptionsspektren, wie sie bei der spektrophotometrischen Untersuchung schon festgestellt wurden (Abb. 4a). Eine Fällung mit $CsNO_3$ wird nicht erhalten.

Wie die obere Kurve zeigt, ging bei der wässrigen Komplexlösung die Hydrolyse über ein Zwischenprodukt gleich weiter zu einer Verbindung, die nur noch zwei Cl^{*-}-Ionen enthält, denn etwa 65% der Aktivität erscheinen in Lösung.

In stärker sauren Lösungen tritt keine Hydrolyse des Iridium(III)hexachlorokomplexes mehr auf.

(3) *Ligandentausch und Hydrolyse des* $[PtCl_6]^{2-}$*-Komplexes*

Im Gegensatz zu dem Iridium(IV)hexachlorokomplex wird bei dem Platin(IV)-hexachlorokomplex auch bei Zimmertemperatur Ligandentausch bemerkbar. Ausserdem tritt schon in salzsauren Lösungen Hydrolyse ein. Beide Vorgänge werden durch Lichteinwirkung stark beschleunigt.

Es wurden daher mehrere Messreihen unter Variation der Temperatur, der Belichtung und der Konzentration der Reaktionspartner durchgeführt.

Die Vorratslösung enthielt im allgemeinen 0,024 Mol/Liter $H_2[PtCl_6^*]$ und war 0,11 N an freier HCl^* gleicher spezifischer Aktivität. Zur Messung des zeitlichen Verlaufes der Vorgänge wurden nach Mischen der Reaktionspartner bzw. nach einfachem Verdünnen der Vorratslösung (im Fall der Hydrolyseversuche) nach bestimmten Zeiten Proben entnommen und der Komplex mit $CsNO_3$ gefällt. Das im Filtrat befindliche Cl^- und der durch Behandeln mit Mg-Pulver in der Siedehitze in lösliches Chlorid überführte $Cs_2[PtCl_6]$—Niederschlag wurden im Messkolben aufgefüllt und dann im Flüssigkeitszählrohr radiometrisch gemessen. Für die Versuche zur Dunkelreaktion bzw. den Hydrolysenversuch im Dunkeln wurden die Reaktionslösungen vor Licht geschützt.

Tabelle 2 gibt eine Übersicht der durchgeführten Ligandentauschversuche bei Dunkelreaktion.

TABELLE 2.—LIGANDENTAUSCHVERSUCHE $H_2[PtCl_6^*]/Cl^-$ (DUNKELREAKTION)

Versuch	Temp. (°C)	Konz. HCl (N)	Konz. $[PtCl_6^*]^{2-}$ (Mol/Lit.)	$t_{1/2}$ (hr)	R (Mol/Lit. min)	k (Lit./Mol. min)
1	20	0,047	0,0024	860	$0{,}15 \cdot 10^{-6}$	$0{,}79 \cdot 10^{-2}$
2	20	0,083	0,0024	795	$0{,}18 \cdot 10^{-6}$	$0{,}54 \cdot 10^{-2}$
3	20	0,89	0,0024	495	$0{,}34 \cdot 10^{-6}$	$0{,}94 \cdot 10^{-2}$
4	20	3,3	0,0024	370	$0{,}46 \cdot 10^{-6}$	$0{,}36 \cdot 10^{-2}$
5	20	0,052	0,0037	765	$0{,}23 \cdot 10^{-6}$	$0{,}72 \cdot 10^{-2}$
6	33	0,047	0,0024	104	$1{,}26 \cdot 10^{-6}$	$6{,}5 \cdot 10^{-2}$
7	48	0,047	0,0024	22,2	$5{,}94 \cdot 10^{-6}$	$30{,}6 \cdot 10^{-2}$

Alle Kurven für die Dunkelreaktion des Ligandentausches des $[PtCl_6]^{-2-}$Ions zeigen in der halblogarithmischen Darstellung $(1 - F)$ gegen die Zeit einen charakteristischen von der Theorie abweichenden Verlauf. Als Beispiel sind in der folgenden Abbildung 7 die Kurven für die Versuche 1 bis 4 wiedergegeben.

Abweichend von den entsprechenden Kurven des Iridium(IV)komplexes zeigt sich hier zu Beginn eine konkave Krümmung. Diese ist auf Neueinstellung des Hydrolysegleichgewichts, das durch Mischung der Komponenten gestört wird, zurückzuführen.[16] Für die Daten zur Ligandentauschreaktion wird nur der lineare Teil ausgewertet. Bei Lichteinwirkung ist der Verlauf der Kurven analog der bei dem $[IrCl_6]^{2-}$-Komplex (Tageslicht und UV-Licht; Tabelle 3 und Abb. 8).

[16] A. W. ADAMSON und R. G. WILKINS, *J. Amer. Chem. Soc.* **76**, 3379 (1954).

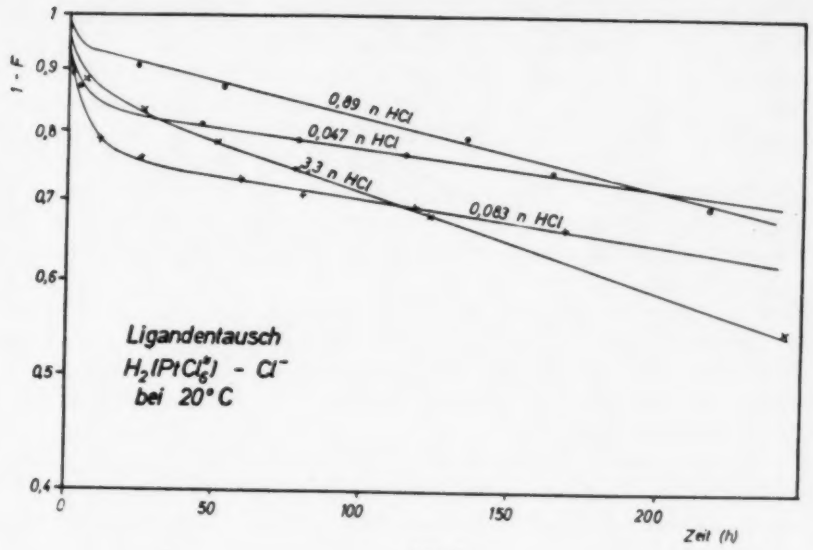

ABB. 7.

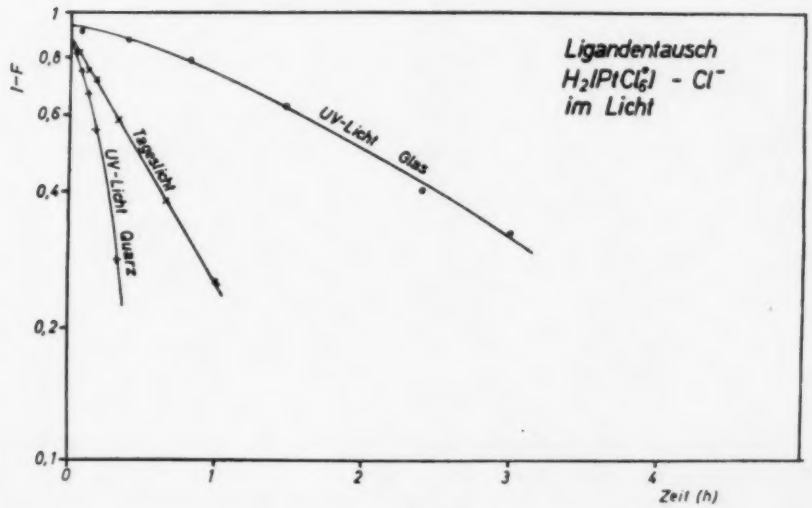

ABB. 8.

TABELLE 3.—LIGANDENTAUSCHVERSUCHE $H_2[PtCl_6^*]/Cl^-$ (HELLREAKTION)

Versuch	Temp. (°C)	Konz. HCl (N)	Konz. $[PtCl_6^*]^{2-}$ (Mol/Lit.)	$t_{1/2}$ (hr)	R (Mol/Lit. min)	k (Lit./Mol. min)
1	20	0,017	0,0053	0,55	$0{,}23 \cdot 10^{-3}$	15,1
2	20	0,021	0,0105	0,27	$0{,}67 \cdot 10^{-3}$	18,7
3	20	0,047	0,0024	3,1	$0{,}042 \cdot 10^{-3}$	2,2

VOL. 19 1961

Das Hydrolysegleichgewicht stellt sich in diesen Fällen so schnell ein, dass in der Kurve nur der reine Ligandentausch zum Ausdruck kommt.

Im Gegensatz zu den Versuchen beim Ir(IV) ist jedoch ein sogenannter "Nullpunktstausch" zu beobachten. Dieser äussert sich darin, dass die Tauschkurven unterhalb des Punktes $(1 - F) = 1$ in die Ordinate einmünden. Er ist darauf zurückzuführen, dass nach der Fällung noch Ligandentausch mit dem festen $Cs_2[PtCl_6]$-Bodenkörper stattfindet, da die Proben nach der Fällung bis zur Filtration etwa zwei Tage stehen müssen. Auch bei den Dunkelversuchen findet "Nullpunktstausch" statt; er ist aber wegen des konkaven Verlaufs der entsprechenden Kurven in der graphischen Darstellung nicht so deutlich.

Die nach Gleichung(3) ermittelten Reaktionsgeschwindigkeitskonstanten zeigen, dass es sich beim Ligandentausch des $[PtCl_6]^{2-}$-Ions tatsächlich um eine bimolekulare Reaktion handelt. Aus der Temperatur-abhängigkeit der Geschwindigkeitskonstanten ergibt sich nach der Arrheniusschen Gleichung eine Aktivierungsenergie der Tauschreaktion von ca. 27 kcal/Mol.

Die konkave Krümmung der Kurven in Abb. 8 lässt sich vermutlich ähnlich wie bei dem $[IrCl_6]^{2-}$-Komplex durch Autokatalyse erklären.[9] Als Zwischenprodukte der Reaktion treten wahrscheinlich auch hier teilhydrolysierte Komplexe auf. Ein erster Hinweis ist die gleichartige starke Beschleunigung von Ligandentausch und Hydrolyse (siehe unten) durch Licht. Weiterhin lässt auch die beobachtete Tatsache, dass der Ligandentausch bei 10 N HCl zu einem konstanten F-Wert von $\sim$0,4 führt, diesen Schluss zu.

Bei allen anderen Versuchen wird dagegen der für den Gleichgewichtszustand theoretisch geforderte F-Wert von 1 erreicht.

Bei den Hydrolyseversuchen (Tabelle 4) wurde die Vorratslösung auf das zehnfache verdünnt und die Zeit-, sowie Lichtabhängigkeit der Vorgänge untersucht.

TABELLE 4.—HYDROLYSEVERSUCHE $H_2[PtCl_6{}^*]$

Versuch	Konz. HCl (N)	Konz. $[PtCl_6{}^*]^{2-}$ (Mol/Lit.)	Anfangsaktivität des Komplexes (Imp/min)	Endaktivit t des Komplexes (Imp/min)	Hydrolyse (%)
UV-Licht	0,011	0,0024	14560	10900	25 $\pm$ 2,5
Dunkelreaktion	0,011	0,0024	14560	11070	24 $\pm$ 2,5

Aus der Anfangs- und Endaktivität des Komplexes ergibt sich der Hydrolysegrad bei Gleichgewichtseinstellung.

Die Werte für die Hydrolyseversuche sind ungenauer als die für die Ligandentauschversuche, da im Filtrat grössere Mengen an Platin als gewöhnlich nachgewiesen werden konnten. Das ist darauf zurückzuführen, dass die teilhydrolysierten Komplexe mit $CsNO_3$ etwas leichter lösliche Niederschläge bilden als das $[PtCl_6]^{2-}$-Ion selbst. Der in der Tabelle angegebene Fehler wird aus einer halbquantitativen Bestimmung des Platins im Filtrat erhalten.

In Abb. 9 ist der jeweils erreichte Hydrolysegrad (%) gegen die Zeit bei Dunkel- und U.V.-Reaktion aufgetragen. Die Hydrolysegeschwindigkeit ist somit stark von der Belichtung abhängig. Jedoch stellt sich nach genügend langer Zeit auch im Dunkeln der entsprechende Gleichgewichtszustand wie im Licht ein.

Auch einige Ergebnisse der Ligandentauschversuche (Tabelle 2) weisen auf eine wenn auch geringfügige Hydrolyse bei HCl-Konzentrationen von etwa 0,01–0,08 N hin. In diesem Bereich wurde gegenüber der Theorie durchweg etwas geringere Aktivitäten im Niederschlag gefunden, was sich in F-Werten >1 äussert.

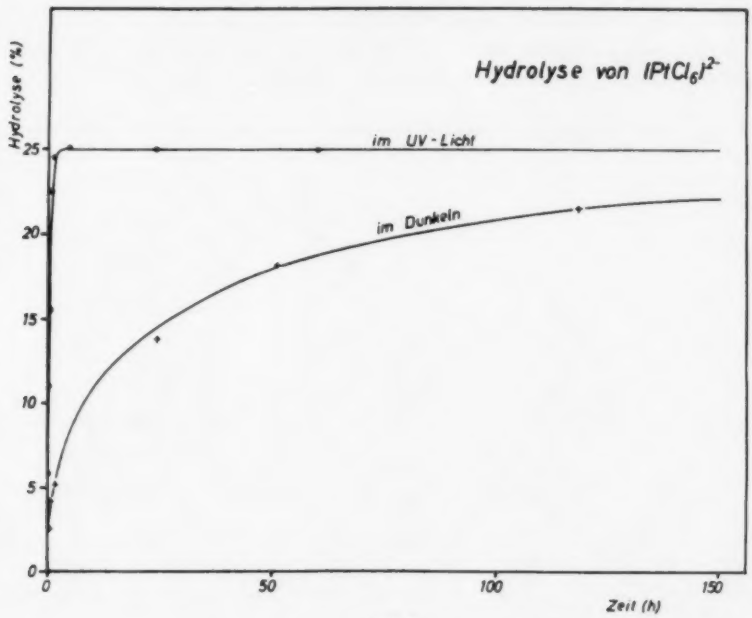

ABB. 9.

Die beobachteten Hydrolysegrade sind in der folgenden Tabelle 5 mit den zugehörigen experimentellen Daten aufgeführt.

TABELLE 5.—HYDROLYSE BEI DEN LIGANDENTAUSCHVERSUCHEN DER $H_2[PtCl_6{}^*]$

Versuch	Konz. HCl (N)	Konz. $[PtCl_6{}^*]^{2-}$ (Mol/Lit.)	Theoretische Endaktivität des Komplexes (Imp/min)	Tatsächliche Endaktivität des Komplexes (Imp/min)	Hydrolyse (%)
1	0,047	0,0024	6080	5860	3,5
2	0,083	0,0024	3820	3730	2,5
3	0,89	0,0024	430	440	—
5	0,052	0,0037	11440	11130	3

Die vorliegenden Versuche deuten darauf hin, dass die Ansicht von Archibald[17] offenbar irrig ist. Dagegen lassen sich die gefundenen Ergebnisse zwanglos den bereits von KOHLRAUSCH[18], BOLL[19] und JOB[20] angegebenen Resultaten zuordnen. Auch ein 40-facher HCl-Überschuss vermag die Hydrolyse nicht völlig zu verhindern,

[17] E. H. ARCHIBALD, *J. Chem. Soc.* 1104 (1920).
[18] F. KOHLRAUSCH, *Z. Physik. Chem.* **33**, 266 (1900).
[19] M. BOLL und P. JOB, *C. R. Acad. Sci., Paris*, **154**, 883 (1912).
[20] P. JOB und M. BOLL, *C. R. Acad. Sci., Paris*, **155**, 827 (1912).

VOL. 19 1961

wenn die Konzentration des $[PtCl_6]^{2-}$-Komplexes gering genug ist. Jedoch ist von einer HCl-Konzentration von 1 Mol/Liter an aufwärts keine Hydrolyse mehr auf radiometrische Weise nachweisbar.

(4) *Verhalten der Chlorokomplexe am Anionenaustauscher*

Die Bindung der Chlorokomplexe des Iridiums und Platins am Anionenaustauscher ist auf zweierlei Weise denkbar, und zwar durch direkten Ersatz der am Austauscher gebundenen Cl^--Ionen bzw. durch Freisetzung von zwei Cl-Liganden des Komplexes.

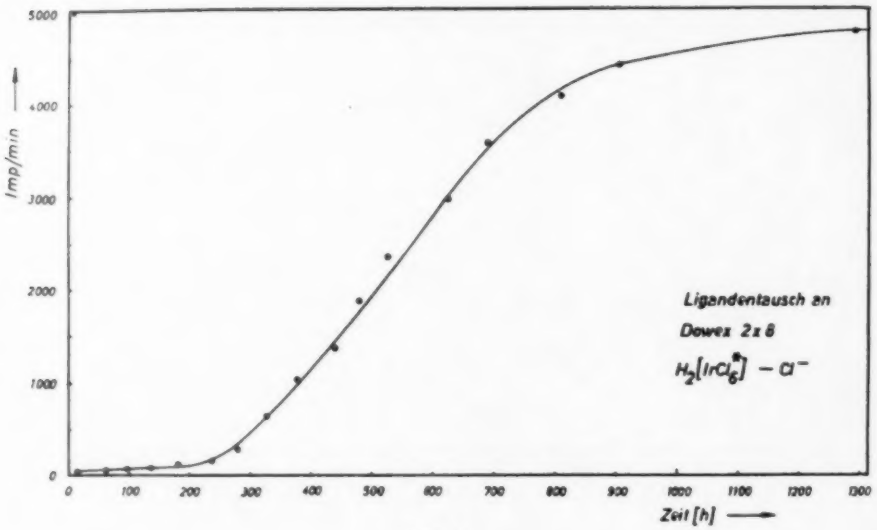

ABB. 10.

Weiterhin dürften die gebundenen Komplexe den gleichen Reaktionen hinsichtlich der Hydrolyse und des Ligandentausches unterliegen wie in homogener Lösung, wobei beim Iridium(IV)hexachlorokomplex seine leichte Reduzierbarkeit zu berücksichtigen ist.

Alle Versuche in Gegenwart von Anionenaustauschern wurden im "batch"-Verfahren durchgeführt. Die Iridium- und Platinchlorokomplexe waren nach ca. 10 min entsprechend einem Gleichgewicht, welches sehr weit auf der Seite der Komplexbindung liegt, am Anionenaustauscher gebunden. Danach erfolgte die Untersuchung des Ligandentausches des fixierten Komplexes mit den freien Ionen der Lösung. Nach bestimmten Zeiten wurden 15 ml aus der Versuchslösung abfiltriert oder abdekantiert und radiometrisch die Aktivität bestimmt. Nach der Messung wurde die Probelösung in den Kolben zurückgegeben, so dass also die Versuchsbedingungen stets gleichblieben.

Untersuchung der Iridiumchlorokomplexe. Den Ligandentausch des gebundenen markierten Iridium(IV)hexachlorokomplexes in Abhängigkeit von der Zeit zeigt Abb. 10. Um die Reduktion zurückzudrängen wurde Bromwasser hinzugefügt. Der gesamte aktive Komplex wird unter Ersatz der äquivalenten Menge inaktiver Cl^--Ionen gebunden, denn im Fall der Freisetzung von zwei Cl*-Liganden hätte sofort ca.

1/3 der Grenzaktivität in Lösung auftreten müssen. Der Iridium(IV)hexachlorokomplex zeigt auch gebunden am Anionenaustauscher keinen Ligandentausch, denn während der ersten 240 Stunden ist kein Anstieg der Aktivität in der Lösung zu beobachten. Erst nachdem das Oxydationsmittel in Form von Bromwasser langsam aufgebraucht ist, wird der Komplex auf dem Austauscher reduziert. Dabei geht die Farbe der Austauscherkörner von blauschwarz in gelb über. Der Iridium(III)komplex zeigt dann lebhaften Ligandentausch, wie man an dem starken Anstieg der Aktivität erkennt.

Angewendet wurden bei diesem Versuch 135 mg $H_2[IrCl_6{}^*]$, 2 g Dowex 2 in der Cl^--Form, 2 g NaCl und als Oxydationsmittel 5 ml gesättigte Bromwasserlösung. Das Reaktionsvolumen wurde mit Wasser auf 100 ml aufgefüllt.

Geht man von mit Cl* beladenem Dowex 2 aus, so verdrängt jedes inaktive $[IrCl_6]^{2-}$-Ion zwei Cl^{*-}-Ionen vom Austauscher. Schon nach kurzer Zeit wird die für diese Ionenaustauschreaktion theoretisch zu erwartende Aktivität von 2850 Imp/min erhalten. Nach einigen Stunden wird der Iridium(IV)hexachlorokomplex langsam reduziert und zeigt dann erheblichen Ligandentausch, was an der starken Abnahme der Aktivität in der Lösung zu beobachten ist (Abb. 11). Schliesslich stellt sich ein Endwert der Aktivität in Lösung von 1600 Imp/min ein, der die Verhältnisse bei völligem Ligandentausch wiedergibt.

VOL. 19 1961

TABELLE 6.—BERECHNETE AKTIVITÄTSENDWERTE IN LÖSUNG

Komplex	Aktivität in Lösung (Imp/min)
$H_2[IrCl_6{}^*]$	909
$H_2[IrCl_6{}^*]$	1364
$H_2[IrCl_5{}^*(H_2O)]$	1364
$H[IrCl_4{}^*(H_2O)_2]$	1364
$H_2[IrCl_4{}^*(OH)(H_2O)]$	1818

Tabelle 6 enthält eine Zusammenstellung der unter den gegebenen Versuchsbedingungen theoretisch zu erwartenden Endaktivitäten (völlige statistische Verteilung zwischen freien und komplex gebundenen Cl^{*-}-Ionen), die für eine Reihe von Komplexen zu erwarten sind.

Da keiner der hier betrachteten Verbindungen der Endwert der Aktivität in Lösung von 1600 Imp/min zukommt, ist anzunehmen, dass zwischen den verschiedenen Hydrolysekomplexen Gleichgewichte bestehen.

In dem beschriebenen Versuch kam Dowex 2 in der OH^--Form zur Anwendung, das mit einem Säureigemsch aus 9 Teilen 2,5 N inaktiver HCl und 1 Teil der radioaktiven 2,1 N HCl* beladen wurde. 1 g dieses aktiven Harzes und 478 mg $H_2[IrCl_6]$. 6 H_2O wurden in einem Reaktionsvolumen von 100 ml im "batch"-Verfahren behandelt.

Beim Eluieren der Iridiumchlorokomplexe mit verdünnter HCl wurden stets nur Komplexe in der Oxydationsstufe +3 des Iridium erhalten. Wahrscheinlich sind hierfür die reduzierenden Eigenschaften des Austauschers verantwortlich. Diese

Lösungen zeigen nach der anodischen Oxydation alle das typische Absorptionsspektrum, das die Abb. 4a wiedergibt.

Untersuchung des Platinhexachlorokomplexes. Hier wurden mehrere Versuche unter Variation der Mengenverhältnisse Anionenaustauscher-Komplex bei Lichteinwirkung durchgeführt. Bei Verwendung des Cl^{*-}-beladenen Austauschers ergeben sich bei Austauscherunterschuss bzw. äquivalenten Mengenverhältnissen analoge Kurven wie beim $[IrCl_6]^{2-}$-Komplex (Abb. 11).

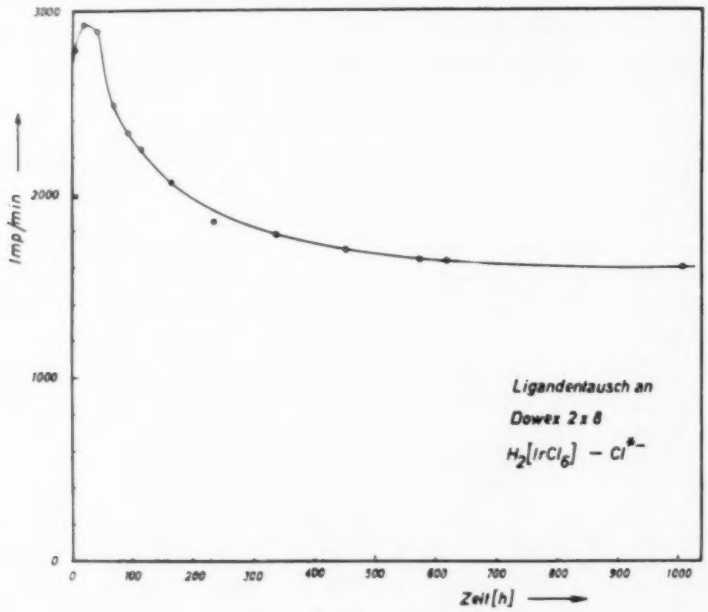

ABB. 11.

Gleich nach Beginn der Reaktion erscheint ein Maximum der Aktivität in Lösung, dessen Höhe dem Ersatz von zwei Cl^{-*}-Ionen durch ein $[PtCl_6]^{2-}$-Ion entspricht. Infolge der relativ hohen Ligandentauschgeschwindigkeit im Licht wird jedoch die Endaktivität in bedeutend kürzerer Zeit (in einigen Stunden) erreicht.

Bei grösserem Austauscherüberschuss wird der betrachtete Ionenaustausch durch den Platzwechsel der überschüssigen gebundenen Cl^{*-}-Ionen gegen die in Lösung befindlichen inaktiven Cl^--Ionen überlagert.

Eine Hydrolyse des am Anionenaustauscher gebundenen Platinkomplexes findet offenbar nicht statt; die theoretische Endaktivität in Lösung wird nämlich nicht überschritten, was bei Hydrolyse der Fall sein müsste.

ZUSAMMENFASSUNG

Die geringen Tauschgeschwindigkeiten beim $[IrCl_6]^{2-}$-und $[PtCl_6]^{2-}$-Komplex (Dunkelreaktion) sowie die hohe Aktivierungsenergie bestätigen gut die Einordnung in die Gruppe der inerten "inner orbital"-Komplexe nach TAUBE.[6] Da ein bimolekularer Mechanismus vorliegt, dürfte die Reaktion über ein Stosspaar gehen. Dagegen ist der $[IrCl_6]^{3-}$-Komplex instabiler. Der Ligandentausch verläuft schon bei Zimmertemperatur nach dem Mechanismus einer reversiblen Dissoziation. Die Ergebnisse

der Hydrolyseversuche bei ca. 10^{-3} M Komplexlösungen sind schematisch in Tabelle 7 zusammengefasst. Die Angaben über das alkalische Gebiet sind der Literatur[19,21,22] entnommen.

Beim $[IrCl_6]^{2-}$-und $[IrCl_6]^{3-}$-Komplex tritt in stärker sauren Lösungen (>3N HCl), wie die spektrophotometrischen Untersuchungen zeigen (Abb. 4b), keine Hydrolyse auf. Im Bereich der HCl-Konzentration von 0,1–3 N hydrolysieren vom $[IrCl_6]^{3-}$-Komplex zwei Cl^--Liganden ab (Abb. 6). Bei der Oxydation dieser Komplexe entstehen die entsprechenden metastabilen Ir-(IV)-hydroxokomplexe, denn bei

TABELLE 7.—IRIDIUM- UND PLATINCHLOROKOMPLEXE IN LOSUNG

	Ir(IV)		Ir(III)		Pt(IV)	
Medium	Formel	Farbe	Formel	Farbe	Formel	Farbe
>3NHCl	$[IrCl_6]^{2-}$	rotbraun	$[IrCl_6]^{3-}$	schwach gelb	$[PtCl_6]^{2-}$	gelb
0,1–3NHCl	$[IrCl_6]^{2-}$ $[IrCl_4(OH)_2]^{2-}$	oxyd.	$[IrCl_5(H_2O)]^{2-}$? $[IrCl_4(OH)_2]^{3-}$ oder $[IrCl_4(H_2O)_2]^-$	schwach gelb	$[PtCl_6]^{2-}$ Beginn der Hydrolyse	gelb
0,05 NHCl	$[IrCl_6]^{2-} \rightleftharpoons [IrCl_4(OH)_2]^{2-}$	rotbraun	$[IrCl_4(OH)_2]^{3-}$ oder $[IrCl_4(H_2O)_2]^-$	schwach gelb	20% $[PtCl_5(OH)]^{2-}$ Rest $[PtCl_6]^{2-}$	gelb–orange
0,01NHCl – neutral					0,01NHCl: $[PtCl_5(OH)]^{2-}$ $[PtCl_4(OH)_2]^{2-}$	
neutral–0,1NNaOH	$[IrCl_4(OH)_2]^{2-} \rightleftharpoons [IrCl_2(OH)_4]^{2-}$ langs. Hydrol: Endzustand: $IrO_2 \cdot 2H_2O$	oxyd.	$[IrCl_2(OH)_4]^{3-}$ oder Chloroaquo–komplexe	schwach gelb	Hydrolyse Endzustand: $[PtCl(OH)_5]^{2-}$ $[Pt(OH)_6]^{2-}$	gelb–orange
>0,1NNaOH	Red. zu Ir(III)	$+O_2$	$Ir_2O_3 \cdot xH_2O$	schwarz		

Erhitzen dieser Lösungen wird der $[IrCl_6]^{2-}$-Komplex wieder erhalten (Abb. 5). In neutraler Lösung bildet sich beim Ir-(III)-komplex unter weitergehender Hydrolyse $[IrCl_2(OH)_4]^{3-}$ bzw. ein Aquokomplex (Abb. 6). Wie in der Zwischenzeit durchgeführte Untersuchungen allerdings zeigen, liegen stets mehrere im Gleichgweicht befindliche teilhydrolysierte Komplexe vor. Bei der Oxydation erhält man die entsprechenden hydrolysierten Komplexe in der Oxydationsstufe +4, die sich wahrscheinlich auch langsam aus der neutralen $[IrCl_6]^{2-}$-Lösung bilden.

Eine radiometrisch erfassbare Hydrolyse tritt beim $[PtCl_6]^{2-}$-Komplex erst in schwächer sauren Lösungen (<1 N HCl) auf (Tabelle 4 und 5). In einer 0,05 N HCl-Lösung geht die Hydrolyse bis zu einem Zustand, der einem Anteil von 10% $[PtCl_5(OH)]^{2-}$ am im übrigen unhydrolysierten Komplex entspricht (Tab. 5). In

[21] F. MYLIUS und A. MAZZUCCHELLI, *Z. Anorg. Chem.* **89**, 14 (1914).
[22] L. WÖHLER und F. MARTIN, *Z. Elektrochem. Angew. Physik. Chem.* **15**, 769 (1909).

einer 0,01 N HCl-Lösung hydrolysieren bereits 25% der Cl^--Liganden des Komplexes ab (Tabelle 4). Dies entspricht einer summarischen Zusammensetzung von 50% $[PtCl_5(OH)]^{2-}$ und 50% $[PtCl_4(OH)_2]^{2-}$. Diese Angaben sind als Summenformeln zu verstehen. In Wirklichkeit dürften fast immer alle Ionensorten zwischen $[PtCl_6]^{2-}$ und $[Pt(OH)_6]^{2-}$ auftreten.

Sowohl der Ligandentausch als auch die Hydrolyse werden durch Lichteinwirkung stark beschleunigt.

Die bei der Papierionophorese beobachteten Multispots dürften daher einwandfrei auf Hydrolyseprodukte zurückzuführen sein.

Die Bindung der Komplexionen beim Ionenaustausch erfolgt durch Ersatz äquivalenter Mengen Cl^--Ionen des Anionenaustauschers. Die leichte Reduzierbarkeit des Ir-(IV)-hexachlorokomplexes in Gegenwart von Anionenaustauschern führt zu dem viel reaktionsfähigeren Ir-(III)-hexachorokomplex, aus dem sich ziemlich schnell mehrere im Gleichgewicht befindliche Hydrolysekomplexe bilden.

Eine besondere Wechselwirkung zwischen Chlorid und den Hexachlorokomplexen des Platins und Iridiums beim Austauschvorgang liegt nicht vor. Demnach ist die besonders feste Bindung am Anionenaustauscher auf sekundäre Einflüsse des Harzgerüstes zurückzuführen.

Die vorliegende Arbeit wurde im Anorganisch-Chemischen Institut der Technischen Universität Berlin durchgeführt. Wir danken Herrn Prof. Dr. G. JANDER, für die Unterstützung und Diskussion und der ERP—Verwaltung sowie dem Bundesatomministerium für die Bereitstellung von Mitteln und Apparaten. Die Arbeiten werden fortgesetzt.

J. Inorg. Nucl. Chem., 1961, Vol. 19, pp. 133 to 141. Pergamon Press Ltd. Printed in Northern Ireland

CATION-EXCHANGE ELUTION SEQUENCES—I

DIVALENT AND RARE-EARTH CATIONS WITH EDTA, HEDTA AND CITRATE*

D. B. JAMES,† J. E. POWELL and F. H. SPEDDING
Institute for Atomic Research and Department of Chemistry
Iowa State University, Ames, Iowa

(*Received* 20 *June* 1960)

Abstract—Ion-exchange elution sequences were established for some divalent and trivalent ions in elutions with those eluants commonly used for the separation of macroquantities of the rare-earth elements—ethylenediaminetetraacetic acid (EDTA), hydroxyethylethylenediaminetriacetic acid (HEDTA) and citric acid. The order of elution of the sequence of trivalent metal ions was found to shift with respect to the sequence of divalent metal ions when the pH of the EDTA eluant was changed and as the composition of the separating mixture changed. A theory is presented which is of qualitative value as an aid in the description of the elution of polyvalent cation mixtures with chelating eluants.

VOL. 19 1961

THE elution of mixtures of the rare earths on cation-exchange resin with chelating eluants such as citric acid and the stronger chelating aminopolyacetic acids e.g. ethylenediaminetetraacetic acid (EDTA), hydroxyethylethylenediaminetriacetic acid (HEDTA) and nitrilotriacetic acid (NTA) has proved to be an effective method for their separation.[1] When such eluants are used at low pH, so-called "elution chromatograms" result. The low-pH procedure has been used for rapid separation of microquantities of both the lanthanide and the actinide elements. However, low-pH eluants are of little value in the separation of macro-quantities of rare earths, since low-pH elution is inefficient and the sorbed rare-earth band must be displaced many times its original length (many band lengths). On the other hand, with eluants of higher pH the rare earths are displaced from the resin more efficiently, due to formation of extremely stable rare-earth complexes. Furthermore, a sharp boundary may be obtained at the front of a moving rare-earth band by use of retaining ions which form still more stable complexes. Under these conditions so-called "displacement chromatograms" result. The high-pH displacement method has been applied to the separation of half-ton quantities of rare-earth mixtures.[2]

The authors have extended the investigation of elutions of the latter type to include many common divalent and trivalent metal cations. The order of elution of these cations and rare-earth cations was investigated with eluants commonly used for separating rare earths. A theory which describes such systems has been proposed and tested.

EXPERIMENTAL

The EDTA and HEDTA used in these investigations were purchased from Geigy Industrial Chemicals, Cranston, Rhode Island, and were reputed to be at least 98 per cent pure. The rare earths

* Work was performed in the Ames Laboratory of the U.S. Atomic Energy Commission.
† Present address: Los Alamos Scientific Laboratory, Los Alamos, New Mexico.

[1] J. E. POWELL, *The Separation of Rare Earths by Ion Exchange in* F. H. SPEDDING and A. H. DAANE, *Rare Earths and Related Metals*, Chap. 5, Amer. Soc. of Metals, Novelty, Ohio (to be published ca. 1961),
[2] J. E. POWELL and F. H. SPEDDING, *Trans. Metal. Soc. Amer. Inst. Min. Metal. Engng.* **215**, 457 (1958).

were supplied by the rare-earth separation group at the Ames Laboratory of the Atomic Energy Commission. Uranyl nitrate and thorium nitrate were also supplied by the Ames Laboratory. All other chemicals were reagent grade. The cation resin (40 to 50 mesh Amberlite IR-120, approximately 8 per cent cross-linked) and the anion resin (Amberlite IR-400A) were purchased from the Rohm and Haas Company, Philadelphia, Pennsylvania.

The cation-exchange columns were assembled from flanged, 6-ft lengths of Pyrex-glass pipe having an inside diameter of 1 in. The flow was due to a 10-ft hydrostatic head of eluant and was controlled by a stopcock at the outlet end of the system. The individual columns were connected in series by Saran tubing and fittings.

The retaining ion in the HEDTA and citric acid elutions was hydrogen ion and in the EDTA elutions was cupric ion. The mixtures to be separated were prepared from appropriate oxides or salts, using one-tenth of an equivalent of each element. The mixtures were loaded from dilute aqueous solution, producing about 3 in. of sorbed band for each element loaded. In each case the total sorbed band was eluted from three to five band lengths with the chosen eluant at a flow rate of 5–10 ml per min. The eluate was collected in consecutive liter fractions.

Several runs were made for each eluant that was studied. In order not to complicate the analytical problems only five to ten metal cations were loaded in each run. In each experiment the collected fractions were boiled to dryness after the addition of nitric acid and hydrogen peroxide, and the residues were transferred to porcelain crucibles for ignition to oxide before qualitative emission-spectrographic analyses were performed.

Zinc–thulium–EDTA solutions, resulting from studies on the effect of composition, were analysed quantitatively for total zinc and total thulium. The concentration of total EDTA in these eluate solutions was assumed to be the same as the EDTA concentration of the eluant. First an aliquot of each eluate fraction was titrated with standard EDTA solution to determine the total amount of uncomplexed metal ion present. Then, after measuring the pH, a second aliquot was made two molar in hydrochloric acid and passed through an anion-exchange column, previously saturated with a two-molar hydrochloric acid solution. Under these conditions zinc was completely retained on the resin as $ZnCl_4^{2-}$. The thulium content of the sample was washed from the column with additional two-molar hydrochloric acid solution and set aside. The sorbed zinc was stripped from the resin with dilute ammonium hydroxide solution, and a subsequent titration with standard EDTA solution yielded the total zinc concentration. The total thulium concentration was assumed to be the difference between the total metal and the total zinc concentrations.

RESULTS AND DISCUSSIONS

Elution sequences

EDTA. A suitable eluant for separation of macro-quantities of the rare earths with EDTA appears to be a 0·015 M solution, adjusted to a pH of 8·4 with ammonium hydroxide. The elution sequence, determined under these conditions, is:

Co^{3+}, Bi^{3+}, Fe^{3+}, Sc^{3+}, Cu^{2+}, Ni^{2+}, Th^{4+},
Pb^{2+}, Lu^{3+}, Yb^{3+}, Zn^{2+}, Tm^{3+}, Co^{2+}, Er^{3+},
Cd^{2+}, Al^{3+}, Ho^{3+}, Dy^{3+}, Y^{3+}, Tb^{3+}, Gd^{3+},
Sm^{3+}, Fe^{2+}, UO_2^{2+}, Nd^{3+}, Pr^{3+}, Mn^{2+},
Ce^{3+}, La^{3+}, Ca^{2+}, Mg^{2+}, Be^{2+}, Sr^{2+}, Ba^{2+}.

HEDTA. The eluant used by POWELL and SPEDDING[3] for elutions with HEDTA was a 0·018 M solution, adjusted to a pH of 7·4 with ammonium hydroxide. Consequently, an elution sequence for HEDTA was determined under these conditions. Hydrogen ion was used as the retaining ion.

The ions being separated are continually redeposited at the front edge of the sorbed band when the HEDTA complexes come in contact with the hydrogen ion

[3] J. E. POWELL and F. H. SPEDDING, *Chem. Engng. Progr. Symp. Series* **55**, No. 24, 101 (1959).

sorbed on the retaining resin bed. This is due to the greater attraction of the resin for polyvalent ions and the large formation constant of the free acid HEDTA. The weak acid H_3V immediately associates with additional hydrogen ions, sorbed on the resin, to form the resin species $\overline{H_5V^{2+}}$, where V represents the HEDTA anion, and the bar indicates a species sorbed in the resin phase. JAMES[4] has shown that two sites tend to be occupied by each HEDTA molecule at eluant concentrations between 0·006M and 0·08M. With lower concentrations of HEDTA less than two sites are occupied; with higher concentrations some $\overline{H_4V^+}$ is present. The band of sorbed $\overline{H_5V^{2+}}$ grows as an elution proceeds, and the initial eluate consists of pure water. When the growing band of $\overline{H_5V^{2+}}$ passes off the column, the eluate becomes an aqueous solution of pure HEDTA which is twice the concentration of the eluant. By adjusting the pH and the concentration, this solution can be reused as eluant. Sorption on ion-exchange resin in the hydrogen-ion form provides an excellent method for purifying HEDTA.

When a mixture which contains copper and/or nickel is eluted with this eluant, these ions are not retained by the $\overline{H_5V^{2+}}$ band. Their HEDTA complexes pass over this band and remain intact until they strike the free hydrogen-ion-form resin ahead of the growing band of $\overline{H_5V^{2+}}$:

$$HCuV + \overline{4H^+} \rightarrow \overline{H_5V^{2+}} + \overline{Cu^{2+}}$$

A band, which is a mixture of $\overline{Cu^{2+}}$ and/or $\overline{Ni^{2+}}$ and $\overline{H_5V^{2+}}$, forms ahead of the pure $\overline{H_5V^{2+}}$ band. After all the copper and nickel have been removed from the separating mixture which is retained by the $\overline{H_5V^{2+}}$ band, they separate from each other with copper preceding nickel in separate, constant-length bands ahead of the growing $\overline{H_5V^{2+}}$ band.

The elution sequence obtained with 0·018 M HEDTA at a pH of 7·4 is:

Co^{3+}, Bi^{3+}, H^+, Cu^{2+}, Ni^{2+}, H_5V^{2+},
Fe^{3+}, Cr^{3+}, Zn^{2+}, Pb^{2+}, Co^{2+}, Cd^{2+},
Lu^{3+}, Yb^{3+}, Th^{4+}, Tm^{3+}, Al^{3+}, Er^{3+},
Ho^{3+}, Dy^{3+}, Tb^{3+}, Gd^{3+}, Eu^{3+}, Sm^{3+},
UO_2^{2+}, Y^{3+}, Nd^{3+}, Pr^{3+}, Ce^{3+}, Mn^{2+},
La^{3+}, Ca^{2+}, Mg^{2+}, Be^{2+}, Sr^{2+}, Ba^{2+}.

Citric acid. For a separation of a mixture of all the rare earths with citric acid an effective eluant is a 0·0052 M solution, raised to a pH of 8·0 with ammonium hydroxide.[5] The elution sequence, determined under these conditions, is:

H^+, Fe^{3+}, Cr^{3+}, UO_2^{2+}, Th^{4+}, Be^{2+}, Al^{3+}, Cu^{2+},
Lu^{3+}, Yb^{3+}, Tm^{3+}, Er^{3+}, Ho^{3+}, Ni^{2+}, Dy^{3+}, Y^{3+},
Tb^{3+}, Gd^{3+}, Eu^{3+}, Sm^{3+}, Nd^{3+}, Zn^{2+}, Pr^{3+}, Co^{2+}, Ce^{3+},
Pb^{2+}, La^{3+}, Mn^{2+}, Cd^{2+}, Mg^{2+}, Ca^{2+}, Sr^{2+}, Ba^{2+}.

Separation factor. For the ion-exchange separation of a divalent metal cation, D^{2+},

[4] D. B. JAMES, Ph.D. Thesis, Ames, Iowa, Library, Iowa State University of Science and Technology (1960).
[5] F. H. SPEDDING and J. E. POWELL, *Chem. Engng. Progr. Symp. Series* **50**, No. 14, 7 (1954).

VOL. 19 1961

from a trivalent rare earth, R^{3+}, the separation factor may be defined as,

$$\alpha = \frac{\bar{X}_D[R_T]}{\bar{X}_R[D_T]}; \quad (1)$$

where $\bar{X}_D$ and $\bar{X}_R$ are the mole fractions of the components R and D in the resin phase, and R_T and D_T are the total concentrations of R and D in the aqueous phase. If α is unity, no separation can occur. The larger the absolute difference of α from unity, the smaller will be the number of band lengths that a binary mixture must be eluted before a steady-state condition is reached. If α is greater than unity, R^{3+} will precede D^{2+}; if α is less than unity, D^{2+} will precede R^{3+}.

The present discussion will be confined to elutions with EDTA, and only one-to-one metal–EDTA complexes will be considered significant in the aqueous phase. Therefore, in the pH range of the eluate (2·0–3·5) equations (2) and (3) apply.

$$[R_T] = [R^{3+}] + [RY^-] + [HRY]; \quad (2)$$

$$[D_T] = [D^{2+}] + [DY^{2-}] + [HDY^-] + [H_2DY], \quad (3)$$

where Y^{4-} represents the EDTA anion.

In subsequent discussions many reactions of the form,

$$M + N \rightleftharpoons MN,$$

will be considered. Stability constants for such associations will be written in the form,

$$K^M_{MN} = \frac{[MN]}{[M][N]},$$

in order to distinguish one from another. JAMES[4] has determined all these constants at an ionic strength of 0·015 (potassium nitrate solution).

By substitution of the appropriate stability constants, equations (2) and (3) become

$$[R_T] = [R^{3+}]\{1 + K^R_{RY}[Y^{4-}](1 + [K^H_{HRY}H^+])\} \quad (4)$$

and

$$[D_T] = [D^{2+}]\{1 + K^D_{DY}[Y^{4-}](1 + K^H_{HDY}[H^+] + K^H_{HDY}K^H_{HDY}[H^+]^2)\} \quad (5)$$

JAMES has shown that the cation-exchange relationship,

$$K^D_R = \frac{[D^{2+}]^3\bar{X}_R^2}{[R^{3+}]^2\bar{X}_D^3}, \quad (6)$$

is virtually constant for the case of zinc and thulium at a constant ionic strength. Combinations of equations (1), (4), (5) and (6) yields

$$\alpha = \sqrt{\frac{[D^{2+}]}{K^D_R\bar{X}_D}}\ \frac{1 + K^R_{RY}F_R(H)[Y^{4-}]}{1 + K^D_{DY}F_D(H)[Y^{4-}]}, \quad (7)$$

where the functions,

$$F_R(H) = 1 + K^H_{HRY}[H^+] \quad (8)$$

and

$$F_D(H) = 1 + K^H_{HDY}[H^+] + K^H_{HDY}K^H_{HDY}[H^+]^2, \quad (9)$$

are dependent only upon the stability constants and the pH of the eluate. Consequently, they are dependent upon the pH of the eluant. Equation (7) indicates that

the separation factor and, therefore, the elution order should depend upon the pH of the eluant and the composition of the separating mixture. Because $K^{R}_{RY}F_{R}(H)[Y^{4-}]$ and $K^{D}_{DY}F_{D}(H)[Y^{4-}]$ are much larger than unity, changes in the concentration of Y^{4-}, which occurs in numerator and denominator, should not effect α to any large degree. The separation factor should depend only slightly upon the concentration of the chelating agent in the eluant.

The pH effect. A mixture composed of one-tenth of an equivalent of each of the

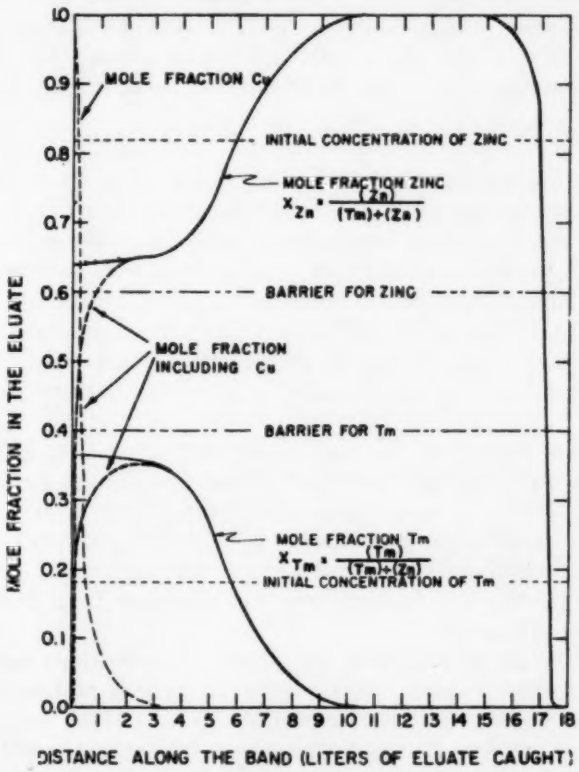
MOLE FRACTION Cu
INITIAL CONCENTRATION OF ZINC
MOLE FRACTION ZINC
$X_{Zn} = \frac{(Zn)}{(Tm)+(Zn)}$
BARRIER FOR ZINC
MOLE FRACTION INCLUDING Cu
BARRIER FOR Tm
MOLE FRACTION Tm
$X_{Tm} = \frac{(Tm)}{(Tm)+(Zn)}$
INITIAL CONCENTRATION OF Tm
MOLE FRACTION IN THE ELUATE
0.0 0.1 0.2 0.3 0.4 0.5 0.6 0.7 0.8 0.9 1.0
0 1 2 3 4 5 6 7 8 9 10 11 12 13 14 15 16 17 18
DISTANCE ALONG THE BAND (LITERS OF ELUATE CAUGHT)

FIG. 1.—The separation of a mixture of zinc and thulium containing 82 mole per cent zinc.

elements, ytterbium, thulium, erbium, holmium, dysprosium, zinc, cobalt and cadmium, was eluted with 0·015 molar EDTA, adjusted to a pH of 8·0 with ammonium hydroxide; an identical charge was eluted with the same eluant, raised to a pH of 8·65 with ammonium hydroxide. The lower-pH eluant effected a separation with the order,

$$Yb^{3+}, Zn^{2+}, Tm^{3+}, Co^{2+}, Er^{3+}, Cd^{2+}, Ho^{3+}, Dy^{3+},$$

which is identical with the order given earlier. The higher-pH eluant gave the order,

$$Yb^{3+}, Tm^{3+}, Zn^{2+}, Er^{3+}, Co^{2+}, Ho^{3+}, Cd^{2+}, Dy^{3+}.$$

In these elutions the order of the trivalent rare earths was always that predicted by

POWELL and SPEDDING[3]; and, in spite of the changes in pH, the order for the divalent ions was always:

$$Zn^{2+}, Co^{2+}, Cd^{2+}.$$

Only a shift of the divalent sequence relative to the trivalent sequence was observed. This result would be expected if the ratio, $F_R(H)/F_D(H)$, is much less dependent upon the identity of D^{2+} and R^{3+} than upon the hydrogen-ion concentration. A major portion of the pH dependence of $F_R(H)/F$ (H) is undoubtedly due to $F_D(H)$; because HRY is generally a much stronger acid than HDY^-, and HRY is almost completely dissociated at the pH's of these eluates. When HEDTA was used as the eluant, no comparable pH dependence was observed. In this case $F_R(H)$ is unity, and

$$F_D(H) = 1 + K^H_{HDV}[H^+]$$

is nearly unity. The acid HDV, like HRY, is almost completely dissociated. Consequently, a pH dependence is not to be expected in elutions with HEDTA.

The effect of composition. Four separations of mixtures of zinc and thulium were made with a 0·01703M EDTA solution, three at a pH of 8·00 and the fourth at a pH of 8·65. The first mixture, which contained 82 mole per cent zinc, gave the results shown in Fig. 1. The separation factor, as defined in equation (1), must have been greater than unity, because thulium preceded zinc. There was some pure zinc at the rear of the band, but the mole fraction of thulium at the front was only four-tenths.

The second mixture contained 50 mole per cent zinc and gave the results shown in Fig. 2. The separation factor must have been less than unity in this case, because zinc preceded thulium. There was pure thulium at the rear, but the front portion of the band contained the same inseparable mixture ($\bar{X}_{Zn} = 0{\cdot}6$, $\bar{X}_{Tm} = 0{\cdot}4$).

The third mixture contained 60 mole per cent zinc, and showed no signs of separating after being eluted over sixty band lengths. The separation factor must have been very nearly unity in this case.

With dilute EDTA eluant at a pH of 8·00 there is a composition barrier beyond which separation cannot proceed. As the composition in a portion of the band approaches the barrier, the separation factor in this portion of the band approaches unity. According to equation (7) this composition barrier should be pH dependent. A fourth mixture, which also contained 60 mole per cent zinc, was separated with 0·01703 M EDTA, raised to a pH of 8·65. The results, which are shown in Fig. 3, indicate that the composition of the barrier was lowered to approximately 44 mole per cent zinc and 56 mole per cent thulium.

CONCLUSIONS

The sequence found for EDTA suggests some alternate retaining ions for the rare earths. For separating all the lanthanides by elution with EDTA the possibilities include Bi^{3+}, Ni^{2+} and Pb^{2+}, in addition to the Cu^{2+} and Fe^{3+}. For separating the light rare earths alone, Zn^{2+}, Co^{2+}, or Cd^{2+} might also be used. It does not appear practical on a theoretical basis to add a large amount of a common element to a rare-earth mixture in order to improve the separation. While a common ion may wedge between two rare earths, the separation factor between the individual rare earths is not changed. Hence, the number of band lengths required for separation does not decrease. Since

the addition of another species increases the length of the sorbed band, the total elution distance is actually increased considerably. Furthermore, the common ion itself may not separate completely from either or both of the rare earths after a steady state is reached due to a "concentration barrier". The separation factor and the elution order of hetero-polyvalent cation mixtures appears to depend upon the pH of the eluant and the composition of the particular mixture. Neither of these factors controls the separation of a mixture which contains rare earths alone.

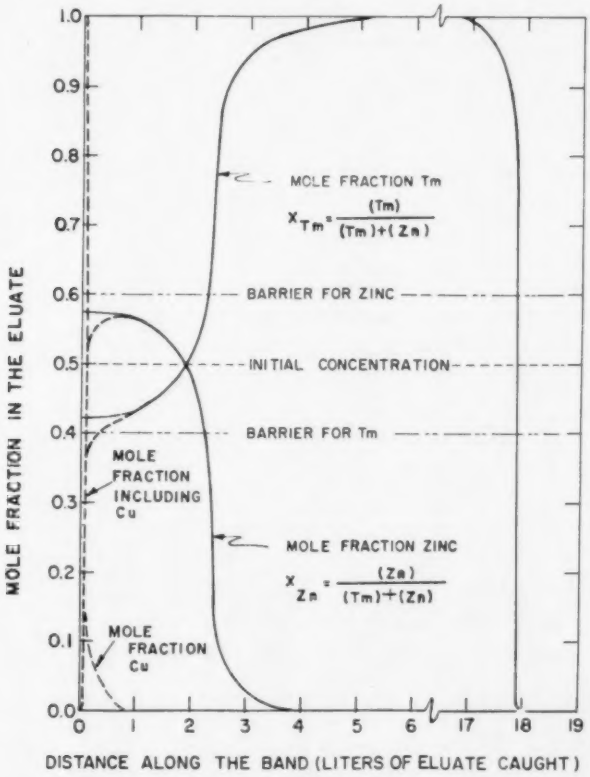

FIG. 2.—The separation of a mixture of zinc and thulium containing 50 mole per cent zinc.

In a static, batch experiment, where it is possible to analyze for the factors on the right of equation (1), α could be calculated. However, it is not easy to duplicate in a batch operation the self-adjusting, constantly-changing conditions which occur in a column as a result of an arbitrary choice of eluting conditions. It would be just as difficult to analyse infinitesimal segments of a resin bed and the interstitial eluate solution associated with these segments in experiments of a kinetic nature. One prime difficulty lies in the disparity of concentrations in the aqueous and resin phases. Coupled with this disparity in concentrations there is the problem of simultaneously removing both resin and aqueous phase from a column in thin enough segments to permit a valid correlation of $\bar{X}_D/\bar{X}_R$ and $[D_T]/[R_T]$, in view of the fact that the individual mole fractions at points along the resin bed vary in a non-linear fashion.

Theoretically, either equation (1) or (7) would also permit the determination of the separation factor from a knowledge of the magnitude of ten constants (K^{D}_{R}, K^{R}_{RY}, K^{D}_{DY}, K^{H}_{HDY}, $K^{H}_{H_2DY}$, K^{H}_{HRY}, K^{H}_{HY}, $K^{H}_{H_2Y}$, $K^{H}_{H_3Y}$ and $K^{H}_{H_4Y}$) and measurements of $[R_T]$, $[D_T]$,

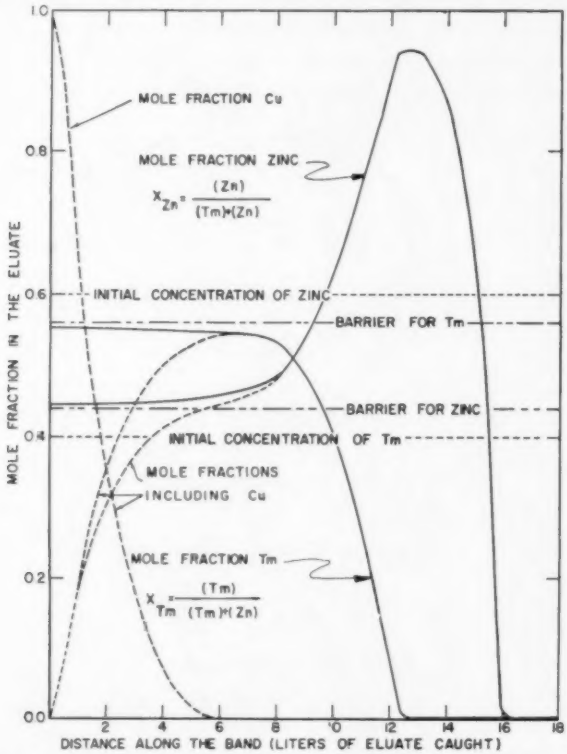

FIG. 3.—The separation of a mixture of zinc and thulium containing 60 mole per cent zinc.

$[Y_T]$ and $[H^+]$ in the aqueous phase only. Then $[Y^{4-}]$, $[D^{2+}]$ and $[R^{3+}]$ can be computed from the equations:

$$[Y_T] + \{([Y_T] - [D_T])K^{D}_{DY}F_D(H) + ([Y_T] - [R_T])K^{R}_{RY}F_R(H) - Y(H)\}[Y^{4-}] + \{([Y_T] - [R_T] - [D_T])K^{D}_{DY}K^{R}_{RY}F_D(H)F_R(H) - Y(H)(K^{D}_{DY}F_D(H) + K^{R}_{RY}F_R(H)\}[Y^{4-}]^2 - K^{D}_{DY}K^{R}_{RY}F_D(H)F_R(H)\,Y(H)[Y^{4-}]^3 = 0, \quad (10)$$

$$[D^{2+}] = \frac{[D_T]}{1 + K^{D}_{DY}F_D(H)[Y^{4-}]}, \quad (11)$$

and

$$[R^{3+}] = \frac{[R_T]}{1 + K^{R}_{RY}F_R(H)\,[Y^{4-}]}; \quad (12)$$

where,

$$Y(H) = 1 + K^{H}_{HY}[H^+] + K^{H}_{HY}K^{H}_{H_2Y}[H^+]^2 + K^{H}_{HY}K^{H}_{H_2Y}K^{H}_{H_3Y}[H^+]^3 + K^{H}_{HY}K^{H}_{H_2Y}K^{H}_{H_3Y}K^{H}_{H_4Y}[H^+]^4, \quad (13)$$

and $F_R(H)$ and $F_D(H)$ are functions defined in equations (8) and (9). Once $[D^{2+}]$ and $[R^{3+}]$ are known, $\bar{X}_D$ and $\bar{X}_R$ can be obtained using equation (6) and the assumption that $\bar{X}_D + \bar{X}_R = 1$. However, the coefficients of the cubic equation (10) contain differences between measured quantities ($[R_T]$, $[D_T]$, $[Y_T]$ and $[H^+]$). Some of these differences are extremely small and have a magnitude less than the accuracy with which the totals can be measured. The coefficients of equation (10) are also quite sensitive to errors in the magnitudes of the ten constants listed above. The methods currently used for determining stability constants, such as K^D_{DY} and K^R_{RY}, may permit cumulative errors as high as 50 per cent in their absolute magnitude. Thus, while this calculation is theoretically possible, it cannot be expected to yield accurate separation factors until the required concentrations and constants can be measured with much greater accuracy than at present.

However, if the extremely dilute concentrations of the simple ions, D^{2+}, R^{3+}, Y^{4-} and H^+, which play a dominant role in these calculations, could be measured directly, then the theoretical equations could be used to calculate reasonable separation factors. The concentrations of these ions are precisely determined by the true values of the stability constants associated with the various species. It is the marked differences in the various stability constants of divalent and trivalent ions which cause changes in the concentrations of these ions and therefore the separation factor during elution.

VOL.
19
1961

J. Inorg. Nucl. Chem., 1961, Vol. 19, pp. 142 to 155. Pergamon Press Ltd. Printed in Northern Ireland

THE INFRA-RED SPECTRA OF URANIUM SPECIES IN CARBON TETRACHLORIDE SOLUTIONS OF URANIUM (VI), DIBUTYL PHOSPHORIC ACID AND TRI-*n*-OCTYL PHOSPHINE OXIDE

J. KENNEDY and A. M. DEANE
Atomic Energy Research Establishment, Harwell, Berks, England

(*Received* 15 *July* 1960)

Abstract—Comparisons of the infra-red spectra of uranyl dibutyl phosphate polymer $[UO_2(DBP)_2]_n$, tri-*n*-octyl phosphine oxide (TOPO), and dibutyl phosphoric acid (HDBP), for both the separate reagents and in combination in carbon tetrachloride, are consistent with the formation of $UO_2(DBP)_2 \cdot 2TOPO$, $UO_2(DBP)_2HDBP \cdot TOPO$ and $UO_2(DBP)_2 \cdot 2HDBP$. The data imply that extraction of UO_2^{+2} from aqueous solutions by combinations of tri-*n*-octyl phosphine oxide and dibutyl phosphoric acid dimer may be represented by the equations

$$UO_2^{2+} + 2(HDBP)_2 + TOPO \rightleftharpoons UO_2(DBP)_2 \cdot HDBP \cdot TOPO + \tfrac{1}{2}(HDBP)_2 + 2H^+$$

$$UO_2^{2+} + (HDBP)_2 + 2TOPO \rightleftharpoons UO_2(DBP)_2 2TOPO + 2H^+.$$

Considerable hydrogen bonding between TOPO and HDBP occurs when these reagents are together in solution. The evidence for previously-postulated structural formulae for the uranium species is not conclusive, but the data are consistent with the equivalence of three DBP ligands in uranium species containing HDBP.

EXTRACTION of uranyl nitrate from aqueous solutions by non-ionic phosphorylated reagents N (where $N = A_3PO$, and A is alkyl or alkoxy) occurs via the equation.[1,2]

$$UO_2^{2+} + 2NO_3^- + 2N \rightleftharpoons UO_2(NO_3)_2 \cdot 2N \quad (1)$$

Dialkyl phosphoric acids HX ($X = (RO)_2POO$) extract uranium by a similar ($[NO_3^-]$-dependent) mechanism from solutions >3M in nitric acid and give an extracted species of probable stoichiometry $UO_2(NO_3)_2 2HX$,[2,3,4] but from low aqueous acid concentrations HX, which is dimeric in the inert diluents in which it is usually dissolved, extracts U(VI) via the mechanism[5,6]

$$UO_2^{2+} + 2(HX)_2 \rightleftharpoons UO_2X_2 \cdot 2HX + 2H^+. \quad (2)$$

HARDY and SCARGILL[7] have estimated the dissociation constant (K_D) of dibutyl phosphoric acid dimer $(HDBP)_2$ and the association constant (K_A) of the monomer with tri-*n*-butyl phosphate (TBP) in kerosene, and give them as

$$K_D = \frac{[HDBP]^2}{[(HDBP)_2]} \simeq 1{\cdot}6 \times 10^{-6} \quad (3)$$

$$K_A = \frac{[HDBP \cdot TBP]}{[HDBP][TBP]} \simeq 6{\cdot}8 \times 10^2 \quad (4)$$

[1] R. L. MOORE, U.S.A.E.C. Report, AECD-3196 (1951).
[2] T. V. HEALY and J. KENNEDY, *J. Inorg. Nucl. Chem.* **10**, 128 (1959).
[3] J. KENNEDY, R. V. DAVIES, H. SMALL and B. K. ROBINSON, *J. Appl. Chem.* **9**, 32 (1959).
[4] C. J. HARDY, UKAEA Report, AERE-R 3267 (1960).
[5] C. F. BAES JR., R. A. ZINGARO and C. F. COLEMAN, *J. Phys. Chem.* **62**, 129 (1958).
[6] D. DYRSSEN and F. KRASOVEC, *Acta Chem. Scand.* **13**, 561 (1959).
[7] C. J. HARDY and D. SCARGILL, *J. Inorg. Nucl. Chem.* **11**, 128 (1959).

From equations (3) and (4) the overall association constant (K_O) between the dimer $(HDBP)_2$ and TBP may be estimated as follows:

$$K_O = K_A^2 \cdot K_D = \frac{[HDBP{\cdot}TBP]^2}{[(HDBP)_2][TBP]^2} \simeq 7{\cdot}4 \times 10^{-1} \quad (5)$$

The extraction coefficients $D_u^N \left(D_u = \frac{\text{U organic}}{\text{U aqueous}}\right)$ for N are negligible compared with those for HX ($D_u^{HX}/D_u^N \simeq 10^3$–$10^4$)[8]. As a result of the reduction in $(HX)_2$ activity due to its association with N (equation 5), a reduction in D_u (anti-synergic effect) would be expected when N and HX are combined. If the dissociation and TBP association constants are the same for di-2-ethyl hexyl phosphoric acid (D2EHPA) as for HDBP (equations 3 and 5), then it can be readily estimated from these equations and the data ($D_u^{D2EHPA} \simeq 3{\cdot}0$)[8] that D_u^{N+HX} would be about 2·3 for a system consisting of 0·1 M TBP and 0·1 M D2EHPA. The magnitude of the reduction in D_u would be expected to follow the order of increasing hydrogen-bonding tendencies for N, i.e. $(RO)_3PO < (RO)_2RPO < (RO)R_2PO < R_3PO$. A reduction in the extraction of Fe^{3+}, Th and Ti with HX is actually observed and at least in the case of Fe^{3+} the order of reduction is $(RO)_3PO < (RO)_2RPO$.[9] In the absence of N, extraction of polyvalent cations from dilute acids occurs as in equation (2) for UO_2^{2+} [10,8].

$$M^{n+} + n(HX)_2 \rightleftharpoons MX_n{\cdot}nHX + nH^+. \quad (6)$$

A slight but significant reduction in D_u is also observed on adding TBP to a dialkyl phosphinic acid R_2POOH.[8] Much larger reductions in the extraction of U(VI),[8] Th and Np(IV)[11] occur on the addition of TBP to monoalkyl phosphoric acids (RO)PO$(OH)_2$, and PEPPARD *et al.*[11] have exploited this effect to aid the back-extraction of metals into an aqueous phase.

In view of the expected repression of D_u, the large enhancement of the latter (synergic effect) which occurs with combinations of N and HX[8] is surprising and of considerable interest. It has been suggested[12] that a probable extraction mechanism when HX and N are in combination is

$$UO_2^{2+} + (HX)_2 + 2N \rightleftharpoons UO_2X_2{\cdot}2N + 2H^+. \quad (7)$$

If such a reaction takes place, then the addition of N to an organic solvent containing $UO_2X_2{\cdot}2HX$ should result in a displacement of HX, viz.

$$UO_2X_2{\cdot}2HX + 2N \text{ — } UO_2X_2{\cdot}2N + (HX)_2. \quad (8)$$

Supporting evidence for equation (8) and by implication for equation (6) was found in the case where N in the form of a phosphonate $[(RO)_2RPO]$ polymer was contacted with a benzene solution of $UO_2(DBP)_2{\cdot}2HDBP$.[13] In this case approximately 2HDBP were liberated into the benzene phase per mole of adsorbed $UO_2(DBP)_2$. In view of the inhomogeneity of the organic phase in this system the experiment was not considered to be fully conclusive. It was therefore decided that examination of

[8] C. A. BLAKE JR., C. F. BAES, JR., K. B. BROWN, C. F. COLEMAN and J. C. WHITE, *Proceedings of the Second Conference on the Peaceful Uses of Atomic Energy, Geneva*, 15/P/1550 (1958).
[9] C. A. BLAKE, JR., D. E. HORNER and J. M. SCHMITT, U.S.A.E.C. Report, ORNL–2259 (1959).
[10] D. F. PEPPARD, G. W. MASON, W. J. DRISCOLL and R. J. SIRONEN, *J. Inorg. Nucl. Chem.* **7**, 276 (1958).
[11] D. F. PEPPARD, G. W. MASON and R. J. SIRONEN, *J. Inorg. Nucl. Chem.* **10**, 117 (1959).
[12] J. KENNEDY, UKAEA Memo., AERE C/M 369 (1958).
[13] J. KENNEDY, F. BURFORD and P. G. SAMMES, *J. Inorg. Nucl. Chem.* **14**, 114 (1960).

the infra-red spectra of homogeneous systems consisting of monomeric N, HX and UO_2X_2 (separately and in combination) might provide information on the stoicheiometry of the uranium species in the organic phase under extracting conditions. A preliminary account of the results of these experiments has already been published.[14]

EXPERIMENTAL

Materials

To facilitate interpretation of infra-red data, dibutyl phosphoric acid (HDBP = HX), uranyl dibutyl phosphate [$UO_2(DBP)_2 = UO_2X_2$], and tri-*n*-octyl phosphine oxide (TOPO = N) were chosen as reagents in these experiments. TBP was not used in these experiments as it tends to precipitate $UO_2(DBP)_2$ from solution in organic media, and its infra-red spectrum would interfere with that of HDBP. Carbon tetrachloride (AR grade) was used as diluent. HDBP and TOPO were obtained from Albright and Wilson Ltd., Birmingham. After vacuum drying at 60°C for 3 hr their infra-red spectra in CCl_4 (Fig. 1) correspond to those of pure anhydrous laboratory samples, and further purification was considered unnecessary.

Infra-red measurements

Absorption spectra were obtained using a Hilger H-800 infra-red spectrometer with NaCl prism and linear wavelength cams. The solvent (CCl_4) was compensated in all spectra, and in some instances the difference spectra for two solutions were obtained. Cell thicknesses of 0·05 mm and 0·25 mm are denoted in figures by continuous and broken lines respectively. The results from some intensity measurements based on areas under absorption bands are included in the tables. Spectra of solid $UO_2(DBP)_2$ were obtained in Nujol mull and KBr disc.

Preparations

Deuterated dibutyl phosphoric acid (DDBP). Dry HDBP (44 g) was shaken with heavy water (20 ml, 99·8% D_2O) for 3 hr at room temperature, followed by vacuum drying (3 mm) at 60°C for 1 hr. The dry product was subjected twice more to this treatment. Conversion to DDBP, based on the infra-red spectrum (Fig. 5c), was >95 per cent.

Uranyl dibutyl phosphate [$UO_2(DBP)_2$]. This was prepared as previously described[15] except that a solution of $UO_2(NO_3)_2$ (1000 ml, 0·24 M) was added to NaDBP (1000 ml, 0·6 M) instead of to a solution of NH_4DBP. The light yellow precipitate was washed with water at 60°C and dried *in vacuo*. Analyses of product (yield 120 g) were consistent with the formula $UO_2(DBP)_2$. Like previous preparations it appeared to be amorphous on microscopic examination. To avoid photocatalytic reduction to U(IV) and the production of butyric acid it must be stored in dark bottles.[2] Similar changes occur in solutions containing $UO_2(DBP)_2$ on prolonged exposure to light. The uranyl di-2-ethyl hexyl phosphate analogue—prepared by saturating a toluene solution of the phosphoric acid with U(VI) followed by evaporation of solvent—is described as a yellow waxy solid[16] (cf. also BAES *et al.*).[5] UO_2X_2 compounds are polymerized in solution.[2,5]

0·25 *and* 0·125 M HDBP/CCl_4, 0·25 M DDBP/CCl_4, 0·25 *and* 0·125 M TOPO/CCl_4. These were prepared by dissolving the requisite amounts of the reagents in CCl_4.

0·0625 M $UO_2(DBP)_2/CCl_4$. In contrast to benzene, in which $UO_2(DBP)_2$ is very soluble at room temperature,[2,15] heating is necessary to dissolve the latter in CCl_4. $UO_2(DBP)_2$ (2·15 g) was shaken at 60°C with CCl_4 (ca. 40 ml) until the solid had dissolved. On cooling, the solution was diluted to 50 ml with CCl_4. A scaly deposit of $UO_2(DBP)_2$ begins to separate on the walls of the container after 6–8 days at room temperature. Separation from solution is, however, incomplete after four months.

0·0625 M $UO_2(DBP)_2 \cdot 2HDBP/CCl_4$. This was prepared by adding 0·25 M HDBP/CCl_4 (25 ml) to $UO_2(DBP)_2$ (2·15 g). After dissolution, which takes place on shaking at room temperature, the solution was diluted to 50 ml with CCl_4. Results of infra-red examinations (see below) are consistent with the complete chemical combination of the reagents.

Other solutions in CCl_4. The following systems containing 0·0625 M $UO_2(DBP)_2$ were similarly prepared by dissolution of the latter (2·15 g) in the requisite amount of a CCl_4 solution of the

[14] A. M. DEANE, J. KENNEDY and P. G. SAMMES, *Chem. Industr.* 443 (1960).
[15] J. KENNEDY and S. S. GRIMLEY, UKAEA Memo., AERE CE/M 48 (1953).
[16] D. F. PEPPARD and J. R. FERRARO, *J. Inorg. Nucl. Chem.* **10**, 275 (1959).

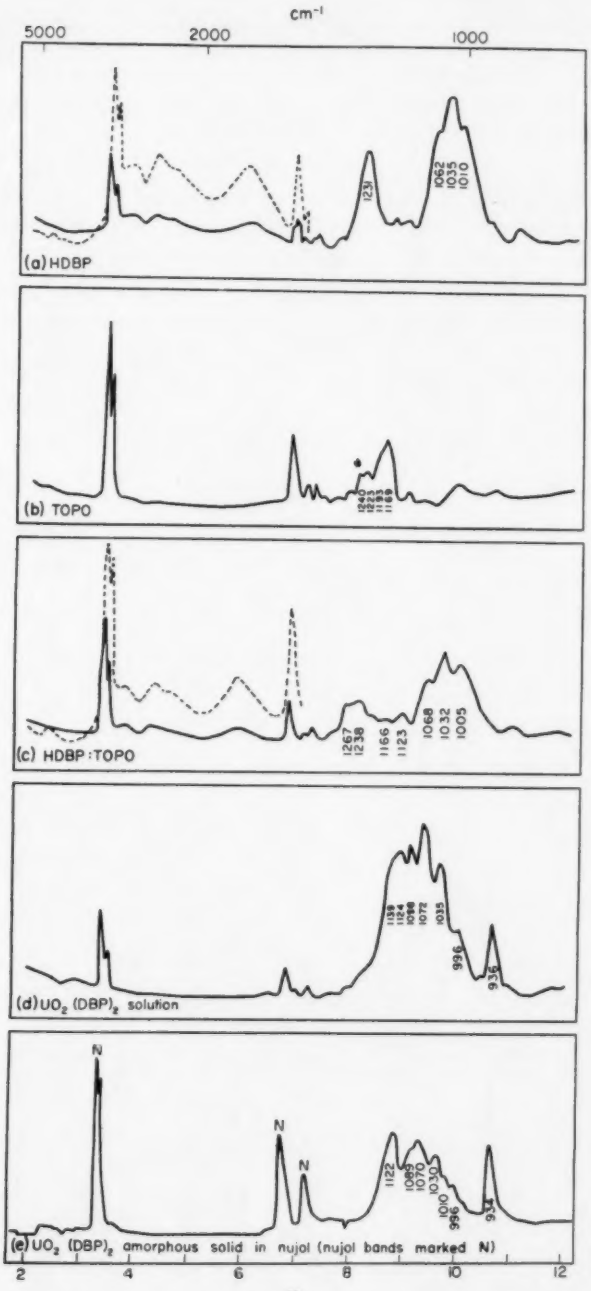

FIG. 1.—Infra-red spectra in CCl_4 of (a) 0·125 M HDBP, (b) 0·125 M TOPO (c) 0·0625 M HDBP and 0·0625 M TOPO combined (d) 0·0625 M $UO_2(DBP)_2$. Spectra of solid $UO_2(DBP)_2$ in Nujol mull (e).

phosphorylated reagent or mixtures of reagents, followed by dilution to 50 ml with CCl_4. The figures indicate the relative mole ratios of reagents present: $UO_2(DBP)_2$:2TOPO; $UO_2(DBP)_2$:4TOPO; $UO_2(DBP)_2$:4HDBP; $UO_2(DBP)_2$:DDBP:TOPO; $UO_2(DBP)_2$:HDBP:TOPO; $UO_2(DBP)_2$:2HDBP:2TOPO; $UO_2(DBP)_2$:2HDBP:4TOPO. No deposition of solid from these solutions occurred after standing for four months at room temperature.

RESULTS

The absorption spectra of CCl_4 solutions consisting of 0·125 M HDBP, 0·125 M TOPO, an equimolar mixture (0·0625 M in each component) of HDBP and TOPO, and $UO_2(DBP)_2$ (solid and 0·0625 M solution) are given in Fig. 1, band assignments

TABLE 1.—BAND ASSIGNMENTS IN cm^{-1} OF SPECTRA OF HDBP, TOPO, HDBP:TOPO AND $UO_2(DBP)_2$ POLYMER. Underlined P → O indicates further oxygen bonding

Assignment	HDBP	TOPO	HDBP:TOPO	$UO_2(DBP)_2$ solution	$UO_2(DBP)_2$ solid
H Bond	3000–1700		3200–1700		
P → O of DBP			1267		
P → O of DBP	1231		1238		
unassigned		1223/40/64			
$\nu_{POO(a)}$ of DBP				1139/24	1122
$\nu_{POO(s)}$ of DBP				1098	1089
P → O of TOPO		1195/69	1166		
P → O of TOPO			1123		
P—O—(Bu)	1062		1068	1072	1070
Bu—O—(P)	1035		1032	1035	1030
P—O—(H)	1010		1005	—	1010
ν_a of UO_2				936	934
Unassigned				996	996

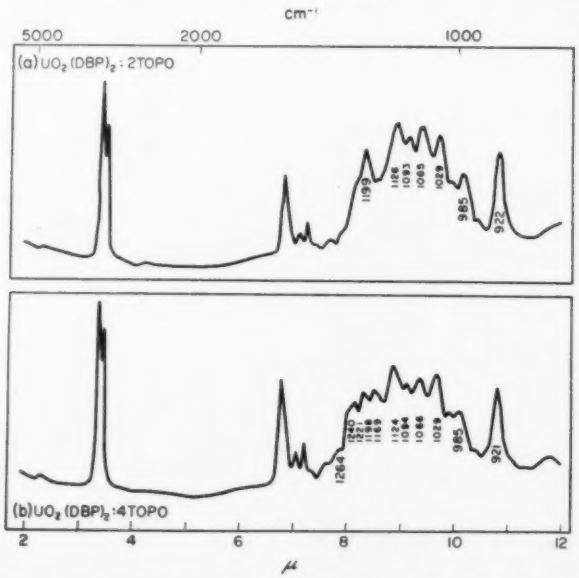

FIG. 2.—Infra-red spectra in CCl_4 of combinations of (a) 0·0625 M $UO_2(DBP)_2$ and 0·125 M TOPO; (b) 0·0625 M $UO_2(DBP)_2$ and 0·25 M TOPO.

TABLE 2.—BAND ASSIGNMENT IN cm^{-1} OF SPECTRA OF $UO_2(DBP)_2$/TOPO SYSTEMS

Assignment	$UO_2(DBP)_2$:2TOPO	$UO_2(DBP)_2$:4TOPO
$\nu_{POO(a)}$ of DBP	1199 (~2 bonds)	1198
$\nu_{POO(s)}$ of DBP	1093	1094
P → O of TOPO		1169
P → O of TOPO	1126 (~2 bonds)	1124
P—O—(Bu)	1065	1066
Bu—O—(P)	1029	1029
ν_a of UO_2	922	921
Unassigned	985	985
Unassigned TOPO bands.		1264, 1240, 1221

are given in Table 1. Spectra of $UO_2(DBP)_2$:2TOPO and $UO_2(DBP)_2$:4TOPO in CCl_4 are given in Fig. 2, with band assignments in Table 2. Spectra of $UO_2(DBP)_2$: 2HDBP, $UO_2(DBP)_2$:4HDBP and their differences spectrum are given in Fig. 3,

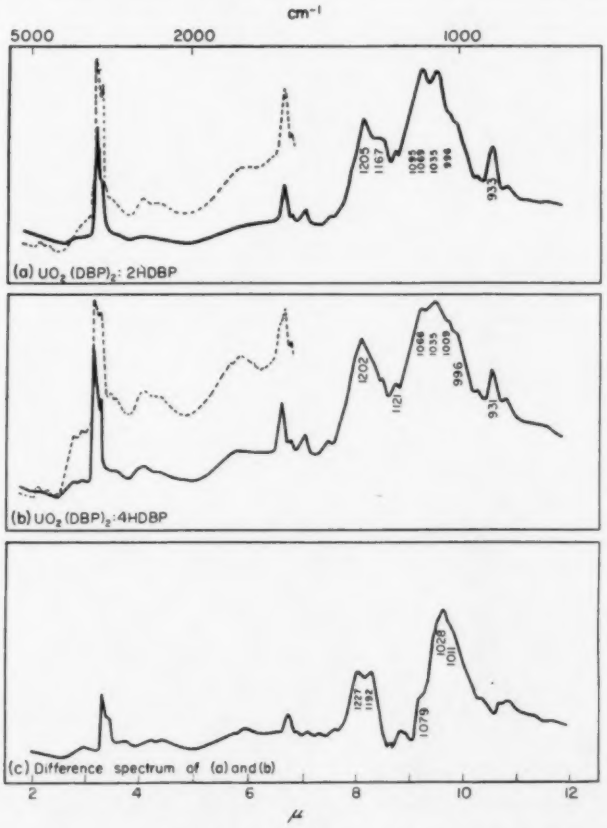

FIG. 3.—Infra-red spectra in CCl_4 of a combination of (a) 0·0625 M $UO_2(DBP)_2$ and 0·125 M HDBP (b) 0·0625 M $UO_2(DBP)_2$ and 0·25 M HDBP. Difference spectra for solutions (a) and (b) are given in (c).

TABLE 3.—BAND ASSIGNMENTS IN cm^{-1} OF SPECTRA OF $UO_2(DBP)_2$/HDBP SYSTEMS

Assignment	$UO_2(DBP)_2$:2HDBP	$UO_2(DBP)_2$:4HDBP
H bond	3400–2000	3400–2000
	1800–1400	1800–1400
$\nu_{POO(a)}$ of DBP	1205 (~3 bonds)	1202/27
$\nu_{POO(s)}$ of DBP	1095 inflexion (hidden)	hidden
P → O of HDBP	1167	uncertain
P—O—(Bu)	1069	1066
Bu—O—(P)	1035	1035
P—O—(H)	ca. 1010 ? (hidden)	1009
ν_a of UO_2	933	931
Unassigned	996	996

with band assignments in Table 3. Spectra of $UO_2(DBP)_2$:HDBP:TOPO: $UO_2(DBP)_2$:2HDBP:2TOPO, and $UO_2(DBP)_2$:2HDBP:4TOPO are given in Fig. 4; difference spectra for these systems are shown in Fig. 5, and band assignments are given in Table 4.

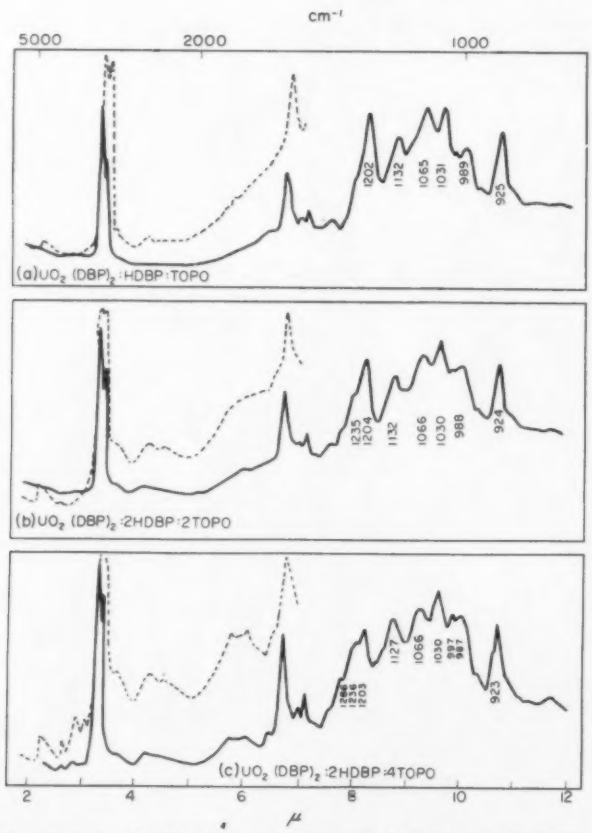

FIG. 4.—Infra-red spectra in CCl_4 of a combination of (a) 0·0625 M $UO_2(DBP)_2$, 0·0625 M HDBP and 0·0625 M TOPO, (b) 0·0625 M $UO_2(DBP)_2$, 0·125 M HDBP and 0·125 M TOPO, (c) 0·0625 M $UO_2(DBP)_2$, 0·125 M HDBP and 0·25 M TOPO.

VOL. 19 1961

DISCUSSION

An extensive investigation of the infra-red spectra of $M(D2EHP)_n$ species, (D2EHP = di-2-ethyl hexyl phosphate) has been carried out by PEPPARD and co-workers[16]

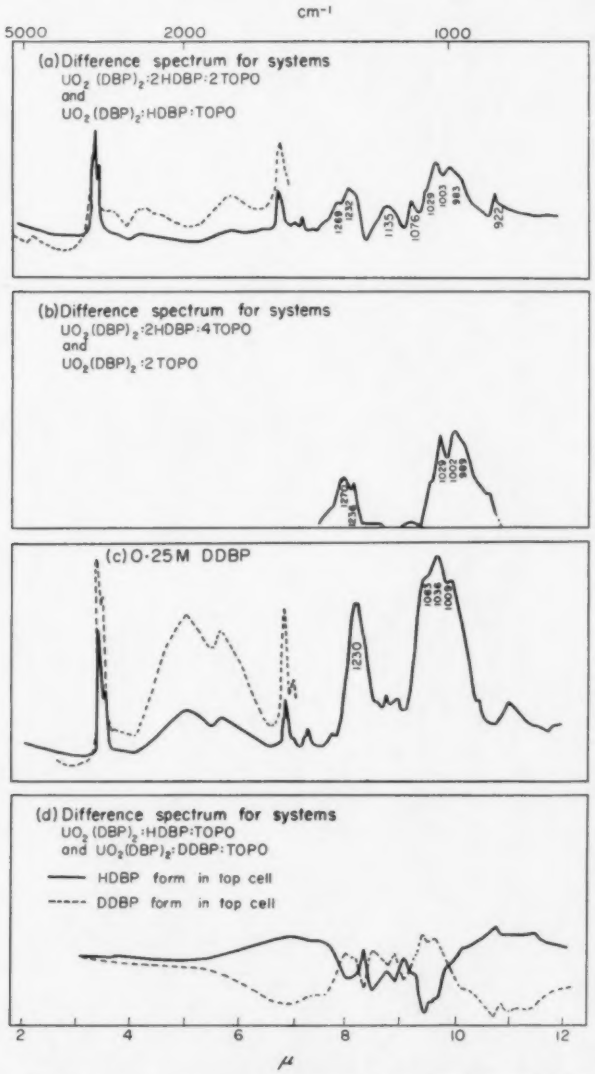

FIG. 5.—Infra-red difference spectra of (a) and (b) $UO_2(DBP)_2$/HDBP/TOPO systems, (c) the spectrum of 0·25 M DDBP and (d) difference spectrum using 0·1 mm cells for the systems $UO_2(DBP)_2$: HDBP: TOPO and $UO_2(DBP)_2$: DDBP: TOPO.

for one- to four-valent cations. Solid $UO_2(D2EHP)_2$ was included in their studies, but spectra of solutions of this or of other UO_2X_2 analogues or of mixtures of MX_n, HX and N have not to our knowledge been published.

TABLE 4.—BAND ASSIGNMENTS IN cm^{-1} OF $UO_2(DBP)_2$/HDBP/TOPO SYSTEMS

Assignment	$UO_2(DBP)_2$:HDBP:TOPO	$UO_2(DBP)_2$:2HDBP:2TOPO	$UO_2(DBP)_2$:2HDBP:4TOPO
H bond	Normal bond absent 1800–1200	3200–1550 1800–1400	3200–1550 —
P → O of DBP	—	1269	1266
$\nu_{POO(a)}$ of DBP	1202 (~3 bonds)	1204/35	1203/36
$\nu_{POO(s)}$ of DBP	1095 inflexion (hidden)	hidden	hidden
P → O of TOPO	absent	absent	absent
P → O of TOPO	1132	1132	1127
P—O—(Bu)	1065	1066 (shoulder)	1066 (shoulder)
Bu—O—(P)	1031	1030	1030
P—O—(H)	—	1003 (Fig. 5a)	997
ν_a of UO_2	925	924	923
Unassigned	989	988	987

VOL. 15 1967

HDBP *and* $UO_2(DBP)_2$ *solid and solution systems.*

PEPPARD *et al.*,[16] and others[17–20] have assigned bands in the regions 1080–1100 cm^{-1} for $M(D2EHP)_n$ to the $PO\overline{O}$ symmetrical vibrations, ν_s, and other bands at 1160–1200 cm^{-1} [probably at 1130 cm^{-1} with solid $UO_2(D2EHP)_2$[16]] to the $PO\overline{O}$ anti-symmetrical vibrations, ν_a. The corresponding ν_s and ν_a bands for the $CO\overline{O}$ anion are 1300–1400 and 1500–1610 cm^{-1} respectively.[19] For convenience ν_a and ν_s

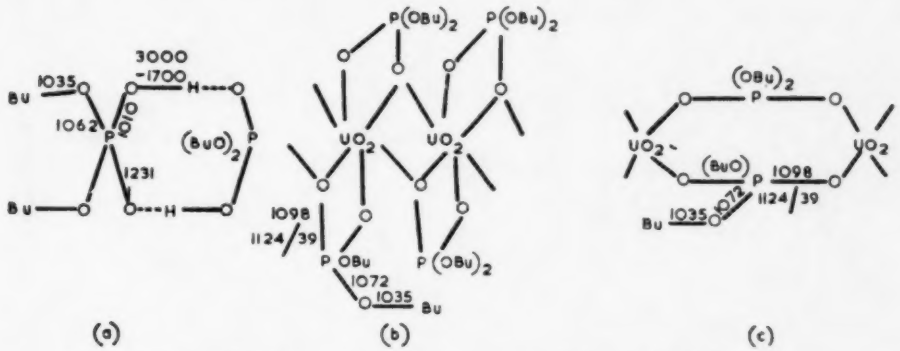

FIG. 6.—Assignment of frequencies to bonds in postulated structures for (a) $(HDBP)_2$ dimer, (b) and (c) $UO_2(DBP)_2$ polymer (see references 2 and 5). U(VI) is octa- and hexa-coordinated in (b) and (c) respectively.

of the POO group are referred to below and in the tables as $\nu_{POO(a)}$ and $\nu_{POO(s)}$ respectively.

Our spectra for solid $UO_2(DBP)_2$ show structure in the 900–1100 cm^{-1} region which is absent in PEPPARD's spectra[16] for solid $UO_2(D2EHP)_2$, possibly due to the simpler aliphatic groups in $UO_2(DBP)_2$. Both the solid and solution spectra of the latter were almost identical, except for the expected broadening of the bands in the mulls in the case of the solid. The large shifts in $\nu_{POO(a)}$ from ca. 1200 cm^{-1} for the alkali metal–D2EHP species to ca. 1130 cm^{-1} for $UO_2(D2EHP)_2$[16] and $UO_2(DBP)_2$ is (as pointed out by PEPPARD *et al.*[16]) probably indicative of considerable covalent character in the UO_2–O bonds in these species.

The assignments in Table 1 are fitted to bonds of previously-proposed or possible structures for the $(HDBP)_2$ dimer and $UO_2(DBP)_2$ polymer in Fig. 6. Fig. 6a shows the generally-accepted structure for $(HX)_2$ dimers,[5,21,22] while 6b and c have been suggested for repeating units in the polymer $[UO_2X_2]_n$[2,5].

The frequency assignments in $(HX)_2$ dimers (6a) have been discussed by BELLAMY[19] and others,[16,22,23] and our measurements are in agreement with theirs. The data do not permit us to decide in favour of (6b) or (6c) unless one regards the large movement of the $\nu_{POO(a)}$ band from about 1130 cm^{-1} in the polymer to about 1200 cm^{-1} in the presence of two molar equivalents of TOPO or HDBP (see below) as being more

[17] H. GERDING and J. W. MAARSEN, *Rec. Trav. Chim.* **76**, 431 (1957).
[18] D. E. CORBRIDGE and E. J. LOWE, *J. Chem. Soc.* 4555 (1954).
[19] L. J. BELLAMY, *The Infra-red Spectra of Complex Molecules* Methuen, London (1954).
[20] J. W. MAARSEN, *Rec. Trav. Chem.* **76**, 724 (1957).
[21] G. M. KOSOLAPOFF and J. S. POWELL, *J. Chem. Soc.* 3535 (1950).
[22] D. F. PEPPARD, J. R. FERRARO and G. W. MASON, *J. Inorg. Nucl. Chem.* **7**, 231 (1958).
[23] L. W. DAASCH and D. C. SMITH, *Analyt. Chem.* **23**, 853 (1951).

VOL. 19 1961

consistent with a structure such as (6b) for the polymer, containing a triple-bonded oxygen in the POO group.

TOPO, HDBP:TOPO, $UO_2(DBP)_2$:2TOPO *and* $UO_2(DBP)_2$:4TOPO *systems*

The band at 1169 cm^{-1} in the spectrum of TOPO is assigned to the P → O stretching vibration (Table 1), compared with 1176 cm^{-1} for Me_3PO.[23] The data for HDBP:TOPO (Fig. 1; Table 1) indicate considerable interaction via hydrogen-bonding between the reagents. BAKER and BAES[24] have obtained infra-red data for a mixture

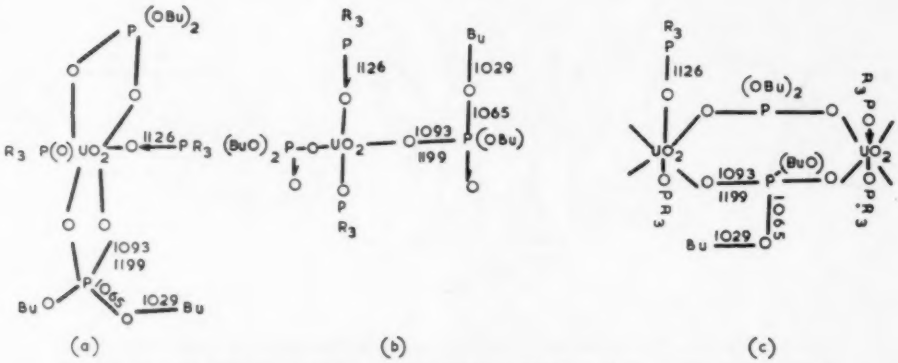

FIG. 7.—Possible structures for species $UO_2(DBP)_2$·2TOPO: (a) monomer with 8-co-ordinated U(VI), (b) monomer with 6-coordinated U(VI), (c) polymer with 8-co-ordinated U(VI).

of dioctyl phosphoric acid and TOPO, and conclude that interaction occurs via the equations

$$N \text{ and/or } 2N + (HX)_2 \rightleftharpoons N(HX)_2 \text{ and/or } 2NHX.$$

The 1267 cm^{-1} band assigned to a free phosphate P → O in the HDBP:TOPO system (Table 1) is probably due to the species $(BuO)_2PO^*OH..OP(OR)_2OH..TOPO$ i.e. $N(HX)_2$, with the asterisk depicting the unbonded P → O. As we have not had access to the full report (reference 24), we cannot adequately compare our results with those of Baker and Baes.

The addition of reagents containing donor atoms to a solution of the polymer $[UO_2(DBP)_2]_n$ gives rise to a marked reduction in viscosity and was thought to result in formation of the monomeric species $UO_2(DBP)_2$·2L[2] where L is a monodentate ligand. No experimental evidence was available at the time to support this stoicheiometry, which was mainly based on the ligand requirements of octa-co-ordinated U(VI). In the spectrum of $UO_2(DBP)_2$:2TOPO (Fig. 2, Table 2), the P → O frequency has shifted completely from 1169 cm^{-1} in free TOPO to 1126 cm^{-1}, consistent with complete reaction of the species, while in the $UO_2(DBP)_2$:4TOPO spectrum, the reappearance of the 1169 cm^{-1} band and its intensity (approx. 2 mole equivalents of TOPO) is consistent with the presence of the species $UO_2(DBP)_2$·2TOPO, and free TOPO. Structures for $UO_2(DBP)_2$·2TOPO, or the polymeric species $[UO_2(DBP)_2$·2TOPO$]_n$ which could be formed from (6b) and (6c) are given in Fig. 7, and bands assigned in Table 2 are fitted to these structures. Again the infra-red evidence for any particular structure is not conclusive, but as mentioned in the preceding section the rise

[24] H. T. BAKER and C. F. BAES, U.S.A.E.C. Report, ORNL-CF-58-5-93 (1958), quoted in Ref. 31.

in $\nu_{POO(a)}$ from 1124–39 cm^{-1} in $[UO_2(DBP)_2]_n$ (Fig. 6b) to 1199 cm^{-1} for $UO_2(DBP)_2 \cdot 2TOPO$ (Fig. 7a) might be due to breaking of the polymerizing bond in the former. The absence of a band at about 1270 cm^{-1} corresponding to the free P → O group of a phosphate indicates that the structure shown in Fig. 7b (6-co-ordinated U(VI)) is absent. The polymeric structure (7c) involving 8-co-ordinated U(VI) is also very improbable, since considerable reduction in viscosity occurs when TOPO is added to solutions of $[UO_2(DBP)_2]_n$ polymer. This effect is observed with a number of reagents containing atoms (O or heterocyclic N) which have strong donor tendencies towards hexavalent uranium.[2]

Bands in the region 909–950 cm^{-1} in the spectra of U(VI) compounds have been assigned by various authors to the antisymmetric vibration ν_a of the uranyl group[25–27]. This occurs at 936–933 cm^{-1} in spectra of $[UO_2(DBP)_2]_n$ and $UO_2(DBP)_2 \cdot 2HDBP$, (Tables 1 and 3), but a slight drop in frequency (10–15 cm^{-1}) to about 923 cm^{-1} occurs in all systems containing $UO_2(DBP)_2$ and TOPO (Figs. 2, 4 and 5, Tables 2 and 4). Another weak band whose origin is uncertain moves similarly in the range 996 to 985 cm^{-1}. An intensity anomaly is also noted in that the intensities of both bands are approximately doubled in the presence of TOPO.

VOL. 19 1961

$UO_2(DBP)_2$:2HDBP *and* $UO_2(DBP)_2$:HDBP:TOPO *systems*

In the spectra of $UO_2(DBP)_2$:2HDBP (Fig. 3, Table 3) the 1231 cm^{-1} band assigned to the P → O group in the $(HDBP)_2$ dimer (Table 1) has disappeared, and there are no bands at about 1270 cm^{-1} which could be attributed to a free phosphate P → O group. This indicates a reaction between $UO_2(DBP)_2$ and $(HDBP)_2$ to give the species $UO_2(DBP)_2 \cdot 2HDBP$, with $\nu_{POO(a)}$ band at 1205 cm^{-1} and another band at 1167 cm^{-1} which could probably be assigned (see below) to a combined P → O group in HDBP. No free P → O bands (1195–69 cm^{-1}) for TOPO are evident in the spectrum of the system $UO_2(DBP)_2$:HDBP:TOPO (Fig. 4, Table 4), and no bands characteristic of free $(HDBP)_2$ or of species formed in the HDBP:TOPO system (Fig. 1, Table 1) are present. This is consistent with the reaction of the three reagents to form the complex $UO_2(DBP)_2 \cdot HDBP \cdot TOPO$. Measurements of the intensities of the $\nu_{POO(a)}$ band at about 1205–1202 cm^{-1} in the spectra of the latter and $UO_2(DBP)_2 \cdot 2HDBP$, are consistent with the presence of three identical POO groups and therefore three identical DBP ligands in these species. The fact that the 1167 cm^{-1} band and the normal H bond pattern (3400–2000) in the spectrum of $UO_2(DBP)_2 \cdot 2HDBP$ are absent in the spectrum of $UO_2(DBP)_2 \cdot HDBP \cdot TOPO$, as well as the intensities of these bands, suggests that they are associated with one HDBP molecule in the former complex. We can only assign the 1167 cm^{-1} band to a P → O frequency in this HDBP molecule, as none of the other groups would be expected to absorb in this region. These facts suggest the molecular arrangements $UO_2(DBP)_3H \cdot HDBP$ and $UO_2(DBP)_3H \cdot TOPO$. The nature of the bonding of H in the $UO_2(DBP)_3H$ portion of these molecules is not known. The band starting at 1800 cm^{-1} and continuing underneath the bands above 1400 cm^{-1} is however associated with this bonding, as is seen in the difference spectrum between $UO_2(DBP)_2$:HDBP:TOPO and $UO_2(DBP)_2$:DDBP:TOPO (Fig. 5d). Here the H-form has a band maximum at 1470 cm^{-1} while the

[25] E. RABINOWITCH, U.S.A.E.C. Report, ANL-5122 (1953).
[26] L. SACCONI, G. GAROTI and P. PAOLETTI, *J. Chem. Soc.* 4257 (1958).
[27] A. E. COMYNS, B. M. GATEHOUSE and E. WAIT, *J. Chem. Soc.* 4655 (1958).

D-form has its maximum at about 1140 cm^{-1}, the frequency ratio (ca. 1·3) being that normally found for deuterium substitution. Small frequency and intensity changes between 1250 and 1000 cm^{-1} prevent exact compensation in this region.

$UO_2(DBP)_2$:4HDBP, $UO_2(DBP)_2$:2HDBP:2TOPO *and* $UO_2(DBP)_2$:2HDBP:4TOPO systems.

Partition data for UO_2–HX systems have shown that the only uranium species formed under low loading conditions is $UO_2X_2 \cdot 2HX$.[5,6] The difference spectrum for $UO_2(DBP)_2$:2HDBP and $UO_2(DBP)_2$:4HDBP (Fig. 3c) should on this account be identical with that obtained for $(HDBP)_2$ (Fig. 1). Although they are not exactly identical, the difference can be attributed to a shift in the $\nu_{POO(a)}$ peak from 1205 cm^{-1} in $UO_2(DBP)_2$:2HDBP to 1202 cm^{-1} in $UO_2(DBP)_2$:4HDBP. Otherwise the difference spectrum is consistent with the presence in this system of approximately one mole equivalent of unreacted $(HDBP)_2$ dimer.

Comparison of the spectrum of the system $UO_2(DBP)_2$:2HDBP:2TOPO with that of the species $UO_2(DBP)_2 \cdot HDBP \cdot TOPO$, together with the equal intensity of the $\nu_{POO(a)}$ bands (1202–1204 cm^{-1}) in both cases, and comparison of their difference spectrum (Fig. 5) with that of the HDBP:TOPO mixture (Fig. 1), suggest that the system is mainly composed of the species $UO_2(DBP)_2 \cdot HDBP \cdot TOPO$ and hydrogen-bonded HDBP–TOPO reaction products. $UO_2(DBP)_2 \cdot 2TOPO$ was not detected in this system.

The absence of the 1169 cm^{-1} band (Table 1) for free TOPO in the spectrum of the system $UO_2(DBP)_2$:2HDBP:4TOPO (Table 4), indicates that all the TOPO is combined in this system. In addition the difference spectrum between this system and $UO_2(DBP)_2$:2TOPO shows bands at 1236 cm^{-1} and 1266 cm^{-1}, suggesting the presence of HDBP–TOPO reaction products. The intensities and positions of the bands are consistent with most of the uranium being present as $UO_2(DBP)_2 \cdot 2TOPO$.

CONCLUSIONS

The infra-red data do not exclude the possibility of other species such as $UO_2(DBP)_2 \cdot 2HDBP \cdot x TOPO$, ($x = 1$[8] and/or 2) being present in systems consisting of $UO_2(DBP)_2$, HDBP and TOPO. With the ratios of these reagents chosen for examination the spectra are however best interpreted on the basis of TOPO displacing one or two mole equivalents of HDBP from the species $UO_2(DBP)_2 \cdot 2HDBP$. The formation of the species $UO_2(DBP)_2 \cdot HDBP \cdot TOPO$ as well as $UO_2(DBP)_2 \cdot 2TOPO$ as a result of this displacement, suggests that the partition of U(VI) between an aqueous phase and an organic phase containing a combination of N and HX can occur via the mechanism

$$UO_2^{2+} + 2(HX)_2 + N \rightleftharpoons UO_2X_2 \cdot HX \cdot N + \tfrac{1}{2}(HX)_2 + 2H^+ \qquad (9)$$

as well as via that previously postulated (equation 7). As hydrogen-bonding between TBP and HX (equation 5) is less effective than was previously implied,[12] the partition data of BLAKE *et al.*[8] do indicate, as these authors suggested, that only one mole equivalent of TBP partakes in the extraction of uranium from concentrations of D2EHPA = 0·1 M and TBP < 0·05 M; IRVING and EDGINGTON[28] have made a similar observation with combinations of TBP and di-*n*-octyl phosphoric acid.

[28] H. IRVING and D. EDGINGTON, *J. Inorg. Nucl. Chem.* **15**, 158 (1960).

DYRSSEN and KUČA[29] following exhaustive studies of the HDBP–TBP system[30,31] have concluded from partition data that extraction of UO_2^{2+} by the latter takes place via equation (9) alone, for concentrations of HDBP between 0·0003 and 0·06 M and TBP $\leq$ 0·1 M. TOPO is a much more powerful donor than TBP and, as is apparent from the infra-red spectra, succeeds when present in excess in displacing 2HDBP from the species $UO_2(DBP)_2 \cdot 2HDBP$. A similar displacement ($>$1·8 HDBP) is also

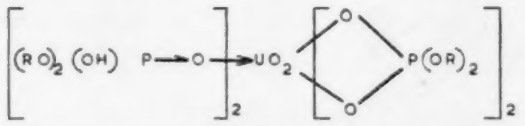

FIG. 8.—Structure[12] previously proposed for $UO_2X_2 \cdot 2HX$. The infra-red data are not consistent with this.

evident when N in the form of a phosphonate polymer $[(RO)_2RPO]_n$ is reacted with $UO_2(DBP)_2 \cdot 2HDBP$ in benzene.[13] In this instance N was also in large excess (3 meq/g $\simeq$ 1 meq/ml of swollen resin) compared with the HDBP present (ca. 2×10^{-2} meq/ml) in the benzene phase, and the phosphonate, although a weaker donor than TOPO, may also be stronger than TBP. The structure proposed previously for $UO_2(DBP)_2 \cdot 2N$ (Fig. 7a)[2] is consistent with the infra-red data, but that for $UO_2X_2 \cdot 2HX$[12] (Fig. 8), is not consistent with the data as interpreted by us in the previous sections. The intensity of the $\nu_{POO(a)}$ band (1205–1202 cm^{-1}) remains unchanged in the spectra of $UO_2(DBP)_2HDBP \cdot TOPO$, $UO_2(DBP)_2 \cdot 2HDBP$ and even in the spectrum of the system $UO_2(DBP)_2$:2HDBP:2TOPO. The spectra in all these cases are consistent with a configuration depicting three rather than two DBP ligands in equivalent association with the uranium, suggesting the formation of the entity $UO_2(DBP)_3H$, but the mode of combination of this with either TOPO or the additional HDBP in the above species is at present uncertain. Anionic uranyl species of the type $[UO_2A_3]^{z-}$ are of course well known,[32] and we are examining the species $Bu_4N\ UO_2(DBP)_3$* formed from Bu_4N DBP and $UO_2(DBP)_2$. In the light of present knowledge of the magnitude of the TBP–HX interaction (equation 5), assuming as before[12] that the phosphoryl oxygen of TBP has the same donor strength as that of HX in Fig. 8, it is easily shown that the extraction of uranium via equations 7 or 9) with combinations of TBP and HX would be much greater than that observed.[8] This indicates that the species $UO_2X_2 \cdot 2HX$ is more stable than was previously supposed. The extra stability might to some extent be conferred if the OH groups of HDBP in Fig. 8 were associated via H bonds with the uranyl and/or DBP oxygens in the remainder of the complex. Though the data (Fig. 3, Table 3) indicate a normal H bond in the species $UO_2(DBP)_2 \cdot 2HDBP$, there is no evidence to suggest that uranyl oxygens are involved in this bonding.

* *Note added in proof:*—Infra-red data for this species and comparison with that for the species $UO_2(DBP)_2 \cdot HDBP \cdot TOPO$, inclines us to the view that the latter is the oxonium salt $TOPO \cdot H^{1+}[UO_2(DBP)_3]^{1-}$. *J. Inorg. Nucl. Chem.* In press (1960).

[29] D. DYRSSEN and L. KUČA, *Acta. Chem. Scand.* **14**, 1945 (1960).
[30] D. DYRSSEN, *Acta Chem. Scand.* **11**, 1771 (1957).
[31] D. DYRSSEN and D. H. LIEM, *Acta Chem. Scand.* **14**, 1091 (1960).
[32] A. E. COMYNS, *Chem. Revs.*, **60**, 115 (1960).

J. Inorg. Nucl. Chem., 1961, Vol. 19, pp. 156 to 159. Pergamon Press Ltd. Printed in Northern Ireland

INORGANIC SALTS DISSOLVED IN NON-AQUEOUS OR IN MIXED SOLVENTS—X

CONDUCTANCE STUDIES AT 20 AND 45°C FOR HYDRATED TIN CHLORIDES IN METHANOL AND IN METHANOL–CARBON TETRACHLORIDE

P. A. D. DE MAINE* and E. J. WALSH
Chemistry Department, New York State College for Teachers,
State University of New York, 135 Western Avenue,
Albany 3, N.Y.

(*Received* 14 *April* 1960)

Abstract—Here are reported conductance values at 20 and 45°C for $SnCl_2 \cdot 2H_2O$ and $SnCl_4 \cdot 5H_2O$ dissolved separately in methanol and for $SnCl_4 \cdot 5H_2O$ in methanol–carbon tetrachloride. The ratio, R (= molar conductance at 45°/molar conductance at 20°) is a constant for a wide range of tin (II) and tin (IV) salt concentrations at a given solvent composition. For the tin (IV) system the value for R decreases from 1·450 (±0·010) to 1·020 (±0·010) in passing from pure methanol to a solvent with a 6·92 moles/l methanol concentration. Relations between specific conductance and salt concentration are also reported.

INTRODUCTION

CONDUCTOMETRIC[1] and spectrophotometric[2] studies for $SnCl_2 \cdot 2H_2O$ and $SnCl_4 \cdot 5H_2O$ dissolved separately in methanol and in methanol–carbon tetrachloride at 25°C have been reported. Empirical relations between specific conductance and salt concentration with constant solvent composition were given for salt concentrations between 0·002 and 0·520 M in both separate[1] and mixed[3] salt systems.

More recent conductometric and spectrophotometric studies of the iron-group halides dissolved in methanol[4] and of $CoCl_2 \cdot 2H_2O$[5] and $NiCl_2 \cdot 2H_2O$[6] dissolved in methanol–carbon tetrachloride have shown that R (= molar conductance at 45°C/molar conductance at 20°C) is independent of the salt concentration and of the number of waters of crystallization for each salt; but is dependent on the solvent composition. Here R values are determined for systems containing $SnCl_2 \cdot 2H_2O$ and $SnCl_4 \cdot 5H_2O$.

EXPERIMENTAL

Purities of chemicals and experimental techniques used have been reported elsewhere.[1,2] Electrical resistance measurements at 20 and 45°C, made with the General Radio Impedance Bridge,[7] were reproducible to within two per cent. No measurable changes in the resistance were effected with time or by alternate heating and cooling of the samples.

* Present address: Department of Chemistry, University of Mississippi, University, Miss.

[1] P. A. D. DE MAINE, M. M. DE MAINE, and G. E. MCALONIE, *J. Inorg. Nucl. Chem.* **14**, 268 (1960).
[2] M. M. DE MAINE and P. A. D. DE MAINE, *J. Inorg. Nucl. Chem.* **11**, 13 (1959).
[3] P. A. D. DE MAINE, G. E. MCALONIE, and M. M. DE MAINE, *J. Inorg. Nucl. Chem.* **14**, 273 (1960).
[4] Part VII: P. A. D. DE MAINE and G. E. MCALONIE, *J. Inorg. Nucl. Chem.* In press.
[5] Part VIII: P. A. D. DE MAINE and G. D. HOWARD.
[6] Part IX: P. A. D. DE MAINE and P. J. SANTIAGO.
[7] P. A. D. DE MAINE and E. KOUBEK, *J. Inorg. Nucl. Chem.* **11**, 329 (1959).

In the present work conductance measurements at 20 and 45°C were made for solutions of $SnCl_2 \cdot 2H_2O$ in methanol at twenty-five different concentrations between 0·041 and 1·021 M; and for solutions of $SnCl_4 \cdot 5H_2O$ in methanol and nine methanol–carbon tetrachloride combinations at sixteen different concentrations (subject to two-phase formation[8]) between 0·0041 and 0·899 M.

RESULTS

For both salts at both temperatures, plots of molar conductance versus the square root of the salt concentration for a fixed solvent composition, show the normal deviations from linearity reported for weak polyelectrolytes.[1] Plots of specific conductance versus salt concentration for $SnCl_2 \cdot 2H_2O$ dissolved in methanol show two straight portions with a sharp inflexion point at a salt concentration equal to 0·262 M at 20°

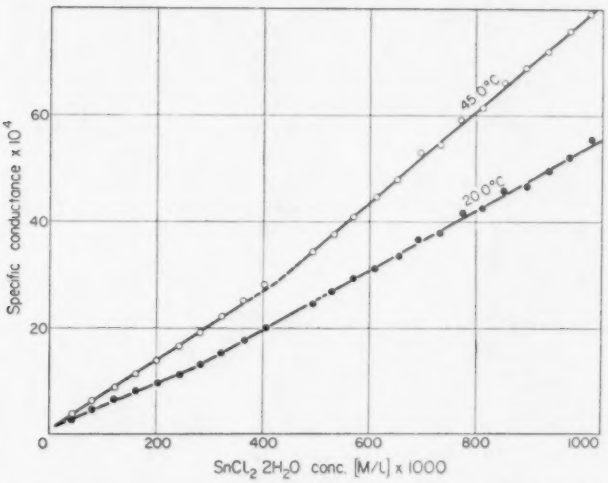

FIG. 1.—Plots of specific conductance vs. salt concentration for $SnCl_2 \cdot 2H_2O$ dissolved in methanol at the temperatures indicated.

and 0·420 M at 45°C (Fig. 1). The ratio, R (molar conductance at 45°/molar conductance at 20° is independent of salt concentration in the range studied, 0·041 to 1·021 M (Table 1).

For $SnCl_4 \cdot 5H_2O$ solutions plots of specific conductance versus salt concentration at fixed solvent composition, are linear for two concentration ranges at both temperatures (reported previously[1] for 25°). At salt concentrations greater than 0·520 M a marked negative curvature shows in these plots for solvents with higher methanol concentrations (Fig. 2). For each solvent composition, *R* is independent for a wide range of salt concentrations. The value of *R* does increase for the high salt concentrations in the solvents of higher methanol concentration (Table 2).

DISCUSSION

These new data confirm that the linear relation between specific conductance and salt concentration found earlier[1] at 25° also applies at 20° and 45° over the same concentration ranges. The constant *R* values for both salts in fixed solvent compositions cannot be explained on assuming that only binary ionization occurs because heats of ionization calculated with the van't Hoff equation are much lower than

[8] P. A. D. DE MAINE and M. M. DE MAINE, *J. Inorg. Nucl. Chem.* **14**, 142 (1960).

TABLE 1.—THE MOLAR CONDUCTANCE AT 20°C (M) AND $R\left\{=\frac{\text{MOLAR CONDUCTANCE AT 45°C}}{\text{MOLAR CONDUCTANCE AT 20°C}}\right\}$ FOR THE INDICATED CONCENTRATIONS OF $SnCl_2 \cdot 2H_2O$ IN PURE METHANOL

Salt conc. in (mole/l)	M	R	Salt conc. in (mole/l)	M	R
0·082	54·5	1·381	0·572	51·1	1·410
0·124	50·5	1·426	0·613	51·2	1·421
0·163	50·5	1·380	0·653	51·5	1·423
0·204	46·5	1·475	0·694	53·3	1·427
0·286	45·9	1·466	0·735	51·6	1·428
0·327	47·7	1·430	0·776	53·9	1·423
0·368	47·7	1·443	0·817	52·1	1·436
0·408	48·8	1·429	0·858	53·8	1·444
0·449	—	1·453	0·899	51·9	1·477
0·490	49·9	1·408	0·939	52·2	1·464
0·531	50·7	1·408	1·021	54·7	1·419
	Arithmetic mean for twenty four solutions				1·434
	Square-root-mean-square deviation				0·028

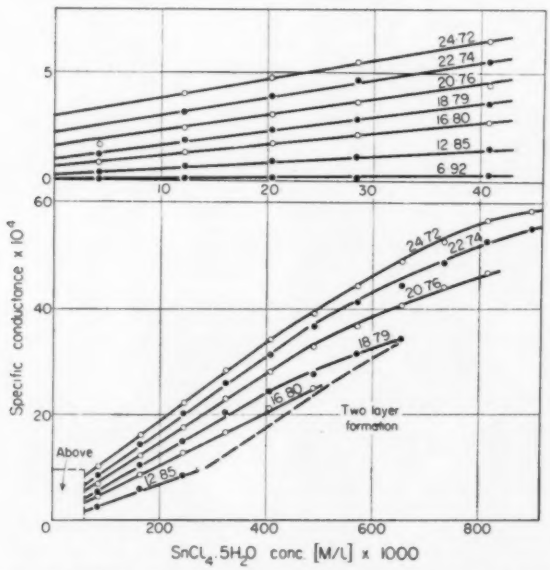

FIG. 2.—Plots of specific conductance vs. salt concentration for $SnCl_4 \cdot 5H_2O$ dissolved in methanol and in methanol–carbon tetrachloride at 20°C. Methanol mole fractions are indicated.

expected (Table 3). An explanation is that specific complex formation between methanol and salt species (exothormic process) actually precedes ionization (endothermic process). The calculated heats of ionization (Table 3) would then be the algebraic sum of the heats evolved in the two processes.

The negative curvature found in plots of specific conductance versus $SnCl_4 \cdot 5H_2O$ concentration for high methanol and high salt concentrations (Fig. 2) cannot be due to

TABLE 2.—$R\left\{=\frac{\text{MOLAR CONDUCTANCE AT 45°C}}{\text{MOLAR CONDUCTANCE AT 20°C}}\right\}$ VALUES FOR THE INDICATED CONCENTRATIONS OF $SnCl_4 \cdot 5H_2O$ IN PURE METHANOL OR IN METHANOL–CARBON TETRACHLORIDE. METHANOL CONCENTRATIONS ARE INDICATED

Salt conc. (mole/l.)	24·72	22·72	20·76	18·79	16·87	14·83	12·85	10·88	8·90	6·92
	Methanol concentration (mole/l.)									
0·0041	1·444	1·448	1·437	1·403	—	1·364	1·285	1·231	1·103	—
0·0123	1·438	1·443	1·438	1·412	1·402	1·352	—	1·226	1·155	1·021
0·0204	1·442	1·461	1·426	1·415	1·352	1·346	1·295	1·214	1·136	1·011
0·0286	1·453	1·451	1·435	1·396	1·368	1·330	1·278	1·189	1·129	1·013
0·0408	1·467	1·445	1·414	1·368*	1·371	1·319*	1·272	1·199	1·098	1·036
0·0817	1·435	1·454	1·384	1·382	1·372	1·351	1·300	1·218	1·164	—
0·163	1·460	1·423	—	1·380	1·354	1·354	1·310	—	—†	—†
0·245	1·452	1·433	1·416	1·394	1·379	1·360	—	—†	—†	—†
0·327	1·461	1·433	1·411	—	1·393	1·368	—†	—†	—†	—†
0·408	1·451	1·442	1·419	1·424*	1·413	—†	—†	—†	—†	—†
0·490	1·480*	1·467	1·424	1·468*	1·447*	—†	—†	—†	—†	—†
0·572	1·490*	1·466	1·452*	1·468*	—†	—†	—†	—†	—†	—†
0·653	1·490*	1·488*	1·473*	1·477*	—†	—†	—†	—†	—†	—†
0·735	1·509*	1·526*	1·481*	—†	—†	—†	—†	—†	—†	—†
0·817	1·533*	1·531*	1·503*	—†	—†	—†	—†	—†	—†	—†
0·899	—	1·546*	—	—†	—†	—†	—†	—†	—†	—†
Average	1·450	1·442	1·424	1·397	1·374	1·353	1·291	1·213	1·131	1·020
S-R-M-S deviation	0·010	0·011	0·011	0·013	0·016	0·011	0·013	0·015	0·024	0·010

* Values not included in average.

† Two-layer formation observed at 25° (P. A. D. DE MAINE and M. M. DEMAINE, *J. Inorg. Nucl. Chem.* **14**, 142 (1960)).

TABLE 3.—THE APPARENT HEAT OF IONIZATION (ΔH) FOR BINARY IONIZATION OF $SnCl_4 \cdot 5H_2O$ AND $SnCl_2 \cdot 2H_2O$ IN METHANOL–CARBON TETRACHLORIDE MIXTURES WITH THE INDICATED ALCOHOL CONCENTRATIONS. ΔH WAS CALCULATED WITH VAN'T HOFF'S EQUATION AND AVERAGE VALUES FOR R(TABLES 1 AND 2). VALUES IN BRACKETS BELOW ARE THE ± SQUARE-ROOT-MEAN-SQUARE DEVIATIONS

Salt	MeOH conc. (M)	ΔH(kcal/mole)	Salt	MeOH conc. (M)	ΔH(kcal/mole)
$SnCl_2 \cdot 2H_2O$	24·72	5·40 (0·28)	$SnCl_4 \cdot 5H_2O$	14·83	4·52 (0·12)
$SnCl_4 \cdot 5H_2O$	24·72	5·56 (0·16)	$SnCl_4 \cdot 5H_2O$	12·85	3·80 (0·12)
$SnCl_4 \cdot 5H_2O$	22·74	5·48 (0·12)	$SnCl_4 \cdot 5H_2O$	10·88	2·88 (0·16)
$SnCl_4 \cdot 5H_2O$	20·76	5·28 (0·12)	$SnCl_4 \cdot 5H_2O$	8·90	1·84 (0·32)
$SnCl_4 \cdot 5H_2O$	18·79	5·00 (0·16)	$SnCl_4 \cdot 5H_2O$	6·92	0·28 (0·16)
$SnCl_4 \cdot 5H_2O$	16·87	4·76 (0·20)			

changes in electrical properties of the solution for no such effects are observed for the $SnCl_2 \cdot 2H_2O$ system (Fig. 1). Partial, reversible polymerization of covalent tin (IV) species at salt concentrations greater than 0·520 M can explain both the negative curvature and the increase in R (Table 2).

Detailed mathematical examinations of the possible models for these systems are in progress and the results will be published later.[9]

Acknowledgement—A grant from the Research Corporation is gratefully acknowledged.

[9] Part XII: P. A. D. DE MAINE and R. T. WIGGIN.

VOL. 19 1961

J. Inorg. Nucl. Chem., 1961, Vol. 19, pp. 160 to 169. Pergamon Press Ltd. Printed in Northern Ireland

GEL-LIQUID EXTRACTION—II

THE SEPARATION OF METALLIC SPECIES USING ION EXCHANGE RESINS IN CONJUNCTION WITH WATER-IMMISCIBLE ORGANIC EXTRACTANTS

H. SMALL
Physical Research Laboratory, The Dow Chemical Company
Midland, Michigan

(*Received* 7 *September* 1960)

Abstract—A number of new metal separation techniques have been developed which employ water swollen ion exchange resins in conjunction with water immiscible extractants. The application of these processes to the problem of rare earth separation is illustrative of their general principles. The work has brought to light some of the problems attendant on using incompatible phases of this type and introduced means whereby their influence on separation efficiency may be minimized.

IN the very extensive area of ion exchange chromatography, as applied to the separation of metallic species, by far the majority of methods employ an aqueous electrolyte solution as the mobile phase. In contrast, there are relatively few examples of separations which embody the use of organic solvents. Moreover, the choice of solvent has generally been made from a group which displays the common property of having a high degree of miscibility with water rather than from those solvents of low water compatibility.

It is now well-known that certain water immiscible organic solvents and solutions of water insoluble species in non-polar solvents can absorb metallic species from aqueous solution and in many cases exhibit considerable discrimination for one species over another.[1] Liquid–liquid extraction techniques have been developed to exploit these phenomena but the intrinsic selectivity of the system is somewhat negated by certain inherent inefficiencies in the liquid–liquid extraction process. These particular inefficiencies were discussed in a previous paper[2] and it was demonstrated how they might be minimized to a degree by incorporating one of the liquids in a gel which could in turn be used as the immobile phase in a chromatographic type process (gel–liquid extraction). The work of the earlier paper was primarily concerned with the means of immobilizing the organic phase but it became apparent that the separation efficiency of the liquid–liquid process might also be enhanced by the alternate device of immobilizing the aqueous phase and having the organic phase mobile. In essence, of course, this is partition chromatography but the combinations of immobile aqueous phase and organic "developer" which have been used are somewhat unique.

It was anticipated that the general scheme for carrying out such a separation might be one wherein the first step would involve loading of a solution of the metallic species in the organic solvent through a bed of aqueous gel. This would be followed by elution with the solvent to obtain a separation of the absorbed species. For such a

[1] G. H. MORRISON and H. FREISER, *Solvent Extraction in Analytical Chemistry*. J. Wiley, New York (1957).
[2] H. SMALL, *J. Inorg. Nucl. Chem.* In press.

process to be an effective means of resolution it is, of course, essential that the aqueous gel phase be capable of rapidly absorbing and desorbing the metallic species. In this respect, the immobilizing matrix might be called upon to act merely as a convenient support for water or in some cases to provide a source of exchangeable ions. As to which function is demanded of the gel, it may be said that this will be determined entirely by the extraction mechanism which prevails in the analogous liquid–liquid system. It may, however, be more pertinent to discuss the stripping mechanism since the first step in any proposed gel–liquid extraction (GLX) process involves removal of the metal species from the organic phase by the aqueous gel phase. When the metals exist in the organic feed as neutral salts, which would be the case if the solvent is of the neutral coordinating type (e.g. tri-butyl phosphate, ether and certain water insoluble ketones), then the immobilizing matrix need only support water. In those cases, however, where the metal in the organic phase is bound to a chelating extractant (e.g. 8-quinolinol, alkyl phosphoric acids and acetyl acetone) it is essential that the aqueous gel phase supply cations capable of exchanging with the metal ions of the organic phase.

VOL. 19 1961

Ion exchange resins, since they are capable of holding relatively large amounts of water and of supplying exchangeable ions, seemed a natural choice for the immobile aqueous phase. Consequently a number of separation schemes were devised using ion exchange resins and certain water immiscible metal extractants. The separations are illustrative of cases wherein the ion exchange function of the resin may be said to be primary while in others where it is used as a support for water its ion exchange function may be regarded as secondary.

RESULTS AND DISCUSSION

A. *Ion exchange function primary—the separation of rare earths using di(2-ethyl hexyl) phosphoric acid and Dowex* 50*

Dialkyl phosphoric acids extract rare earths from aqueous solution by a mechanism which may be most simply described as ion exchange between the organic and aqueous phases.

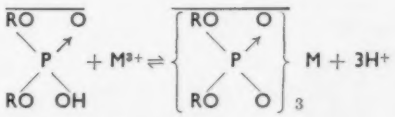

[Barred symbols denote the organic phase]

PEPPARD and co-workers[3] have shown that when R = di(2 ethyl hexyl), the extractant exhibits a selectivity between adjacent rare earths which is surpassed by few known rare earth complexing agents. There is a monotonic increase in extractability from lanthanum to lutetium with the logarithm of the distribution coefficient showing a linear dependence on atomic number. The extractabilities of lanthanum and lutetium differ by a factor of $3{\cdot}5 \times 10^5$ while the separation factor for any pair of adjacent rare earths is approximately 2·5. Normally one would exploit these differences by employing counter current extraction techniques but on the basis of earlier arguments[2] it seemed that application of a GLX process would result in more efficient utilization of

* Trade name of the Dow Chemical Company.

[3] D. F. PEPPARD, G. W. MASON, J. L. MAIER and W. J. DRISCOLL, *J. Inorg. Nucl. Chem.* **4**, 334 (1957).

this unique extractant. A process was therefore devised in which the aqueous mineral acid normally used to strip rare earths from the organic phase would be replaced by a fixed bed of water-swollen strong-acid ion exchange resin. The reactions envisaged as taking place in such a process are illustrated in Fig. 1. On loading the rare earth phosphates [$M(DEHP)_3$] to a column of hydrogen form resin, exchange of hydrogen ion for metal in the complex would force the rare earths onto the resin bed. At the

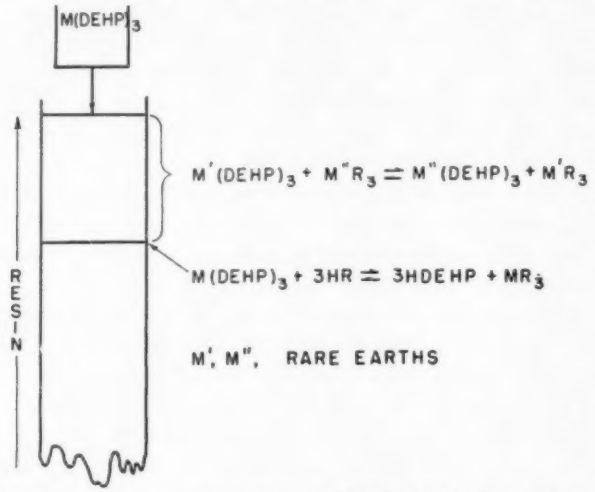

FIG. 1.—Column farctionation of rare earths on Dowex 50, Di(2-ethyl hexyl) phosphoric acid (HDEHP) eluant.

same time, percolation of organic phase through the resin–metal zone thus formed would lead to a resolution of the rare earths with the order of their appearance being determined by their relative affinities for the DEHP species. As a result, the heavier rare earths would advance to the leading edge of the band and appear first in the effluent on exhaustion of the resin absorption capacity.

The result of an actual separation attempted in this manner is illustrated in Fig. 2. A solution of rare earth DEHP complexes in toluene was loaded onto a column of water swollen Dowex 50X4: 50–100 mesh (see Section C, however). The volume of the bed (V_B) was 47 ml. The concentrations of the various components of the solution were as follows: [DEHP] = 0·97 M; [RE^{3+}] = 0·1 M; [H^+] = 0·67 M. The interstitial void space between the resin particles was initially filled with toluene. It is evident from Fig. 2A, which shows the composition of the effluent, that the hydrogen form resin acted as an efficient stripping agent for the bulk of the rare earths. From an examination of Fig. 2B, it is also to be concluded that, qualitatively at least, the expected resolution of rare earths was achieved with the heavier species appearing first in the effluent. The concentrations of rare earths in the effluent are expressed as a fraction of their concentration in the feed solution. The analyses for individual rare earths in the effluent wave (Cuts 1–6) are presented in Table 1 with the results normalized with respect to yttrium which was the major component. Although this frontal analysis operation has led to a separation of rare earths, it is noticeably inefficient in that holmium dysprosium and terbium break through in a fashion which is far from the ideal square wave. This could be an equilibrium phenomenon, but on the basis

of other observations it may be reasonably attributed to a high mass transfer resistance at the solvent resin interface. This feature of the problem will be discussed in more detail in Section C.

Under the conditions of this experiment, the resin showed another aspect of inefficiency in that it did not effectively retain the heaviest rare earth, lutetium, which

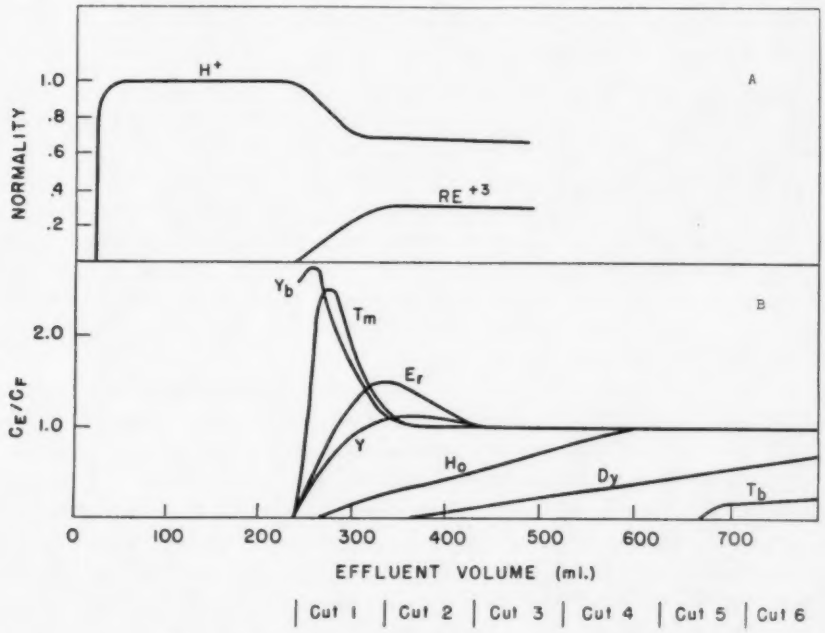

FIG. 2.—Separation of rare earths on Dowex 50–HDEHP eluant.

TABLE 1.—ANALYSES OF CUTS FROM EXPERIMENT OF FIG. 2

Cut number	Y	Yb	Tm	Er	Ho	Dy	Tb	Gd	Eu	Nd	Ce	La
Feed	100	1·4	0·36	4·8	2·9	19·5	2·5	7·3	0·05	0·18	0·36	0·35
1	100	2·6	1·0	8·8	1·0	1·0	—	—	—	—	—	—
2	100	0·9	0·24	6·8	1·3	2·3	—	—	—	—	—	—
3	100	0·5	?	6·0	2·0	4·5	—	—	—	—	—	—
4	100	0·5	?	6·0	2·7	6·7	—	—	—	—	—	—
5	100	0·5	?	6·2	3·1	11·0	0·44	—	—	—	—	—
6	100	0·5	?	5·6	3·7	17·5	0·62	0·25	—	—	—	—
Resin	100	—	—	5·0	2·5	29·0	5·0	17·5	0·1	2·3	0·25	0·5

appeared quite early as a contaminant in the HDEHP wave. This, in contrast to the case of Ho, Dy and Tb, is undoubtedly an equilibrium effect arising out of the fact that the organic phase has apparently a greater affinity for lutetium than does the resin phase. There is not a great deal of latitude in which to change the affinity of the resin phase for rare earths, but the affinity of the organic phase may be lowered by the simple expedient of decreasing the concentration of the alkyl phosphoric acid.[3]

An appropriate dilution of the organic phase, would therefore have rendered the resin an effective absorbent for all of the rare earths. It will be obvious that the concentration of phosphate in the organic phase is an important consideration where elution analysis of rare earths is the main aim.

B. *Ion exchange function secondary—the separation of rare earths using tri butyl phosphate and Dowex* 1 (NO_3^-)

There has been considerable work done to show that tri butyl phosphate (TBP) extracts rare earth nitrates selectively from aqueous solution. PEPPARD[4] and MCKAY[5] have studied the extraction of trace levels as a function of nitric acid concentration in the aqueous phase and found separation to be most favored by a high acid level. The work of the SPEDDING group, on the other hand, has indicated that rare earths may also be extracted selectively by the same solvent from concentrated solutions of rare earths.[6] On the basis of this latter work, a GLX process was devised which utilizes the water holding properties of an anion exchange resin, the ability of such a resin to extract rare earth nitrates from TBP and the selective extraction properties of this solvent.

The preconceived method of operation was as follows. A concentrated solution of rare earth nitrates in TBP or in TBP diluted with an inert solvent to reduce viscosity, would be loaded to a column of a strong base quaternary resin, water swollen and in the nitrate form. It was the expectation that the rare earths would be extracted by the aqueous gel phase and could be subsequently resolved by an elution with TBP. The function of the resin would therefore be secondary in that it would be used merely as a support for water, although it should be added that, being analogous to a nitrate solution, it would exert a salting out effect on the rare earth nitrates tending to force them into the mobile phase.

Prior to an actual column separation, a brief study was made of the distribution of a typical rare earth nitrate, yttrium nitrate between Dowex 1X4 (NO_3) and tri-butyl phosphate. A solution of yttrium nitrate in 80% TBP. (toluene diluent) was equilibrated with water swollen Dowex 1 (NO_3^-) and from the analyses of the equilibrium solvent phase the distribution behaviour determined. The results are shown in Fig. 3. It is clear that the water swollen resin was an effective stripping agent for the yttrium nitrate. An absorption elution experiment was then carried out in which a volume of yttrium nitrate in 80% TBP was loaded onto a column of Dowex 1X4 (NO_3^-) 50–100 mesh (see section C, however) and the column eluted with 80% TBP. The nature of the elution wave (Fig. 4) was found to agree with the results of the equilibration experiments in that the position of the concentration maximum was compatible with the magnitude of the distribution coefficient and the shape of the wave could be attributed to the concentration dependence of the distribution which favors the resin phase at lower concentrations of yttrium nitrate.

Having shown that the resin solvent combination was a successful partitioning system, it remained to demonstrate its application to an actual rare earth separation. A small volume of a saturated solution of mixed "heavy" rare earth nitrates in 80%

[4] D. F. PEPPARD, W. J. DRISCOLL, R. J. SIRONEN and S. MCCARTY, *J. Inorg. Nucl. Chem.* **4**, 326 (1957).
[5] D. SCARGILL, K. ALCOCK, J. M. FLETCHER, E. HESFORD and H. A. C. MCKAY, *J. Inorg. Nucl. Chem.* **4**, 304 (1957).
[6] J. BOCHINSKI, M. SMUTZ, and F. H. SPEDDING *Industr. Engng. Chem.* **50**, 157 (1958).

TBP was passed through a column of water swollen Dowex 1 (NO_3^-) and followed by an elution with TBP . The volume of the feed was equal to $0{\cdot}25V_B$.

In this first experiment no significant resolution of the rare earths was obtained; although, during the loading it was evident that neodymium nitrate (blue) was concentrating at the top of the band. The SPEDDING group has shown that the successful

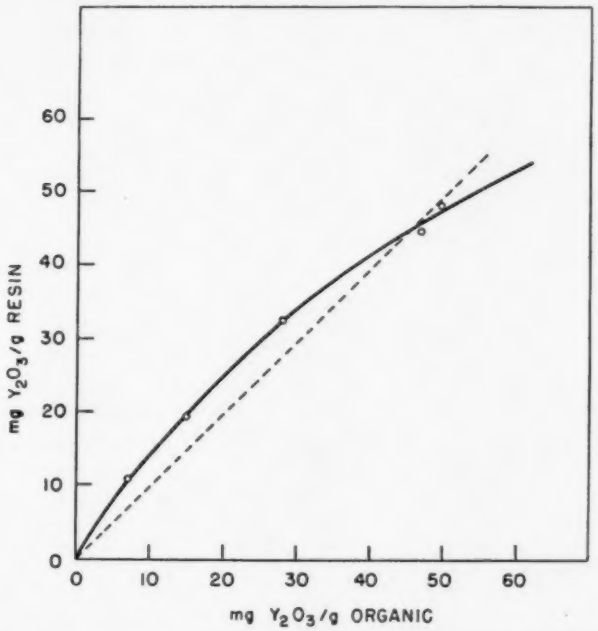

FIG. 3.—Distribution of $Y(NO_3)_3$ between 80% TBP and Dowex 1X4 (NO_3^-)

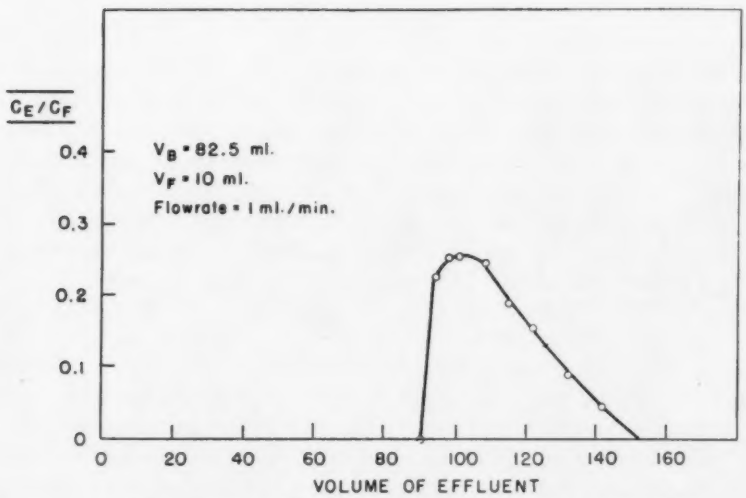

FIG. 4.—Elution of $Y(NO_3)_3$ from Dowex 1X4 (NO_3^-) by 80 %TBP.

separation of rare earths from concentrated solutions of same, depends in great part upon maintaining the concentration in both phases close to saturation.[6] In the type of column operation just described, there is an inevitable dilution of rare earths in the organic phase during loading and elution. It was reasoned that this dilution was the cause of the poor separation and further argued that this drawback might be overcome by loading a larger feed volume to the column. The result of such an experiment in which the feed volume to bed volume ratio was unity, is shown in Fig. 5 where it is

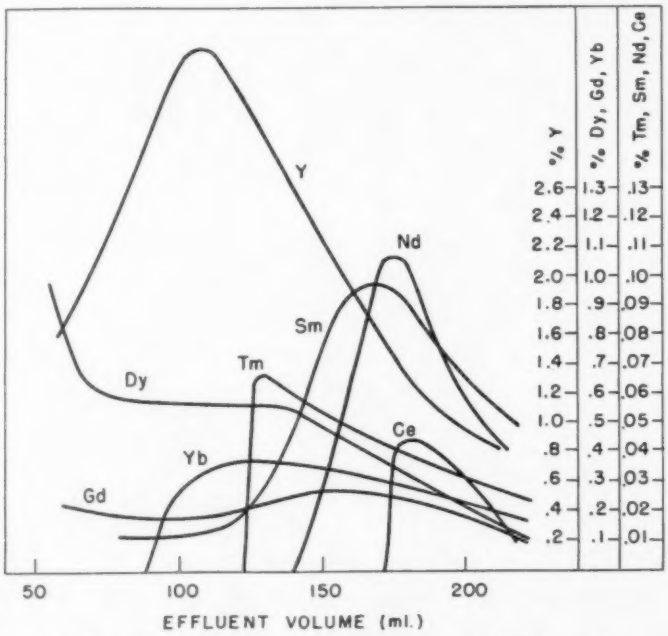

FIG. 5.—Separation of rare earths on Dowex 1 (NO_3^-)–TBP eluant.

now evident that some separation has been obtained. The position and nature of elution of some of the rare earths is not without interest, since the order of elution does not dispay any simple dependence on atomic number, as witness the case of ytterbium and thulium. Moreover, the manner of elution of the various species is in some cases quite different. Whereas Yb, Tm, Nd, Sm and Ce break through quite sharply, gadolinium on the other hand trails throughout the whole elution wave. Since it is reasonable to expect the size of all the distributing species to be approximately the same and hence to have similar transfer rates, this type of behaviour seems to be most readily explained on the basis of the complex equilibria which must exist in this system and in this respect the work of others may provide clarification.

A separation of a "light" rare earth fraction was attempted and is illustrated in Fig. 6. Separations of this type (Figs. 5 and 6) could be improved by the use of smaller resin particle sizes and slower flow rates and show promise as a means of separating groups of rare earths. In view of the high concentrations of rare earths employed in the feed, this GLX process has the advantage of a high production rate with a small volume of equipment. Moreover, the operation of such a process may surpass in

simplicity that required for a conventional liquid–liquid process, in which scale-up might prove to be a problem in itself. The scale-up of fixed bed absorption processes, on the other hand, has the reputation of being notably straightforward. The relative efficiencies of the two techniques are still however matters of conjecture which can only be resolved by a detailed analysis of the two processes as applied to a given separation.

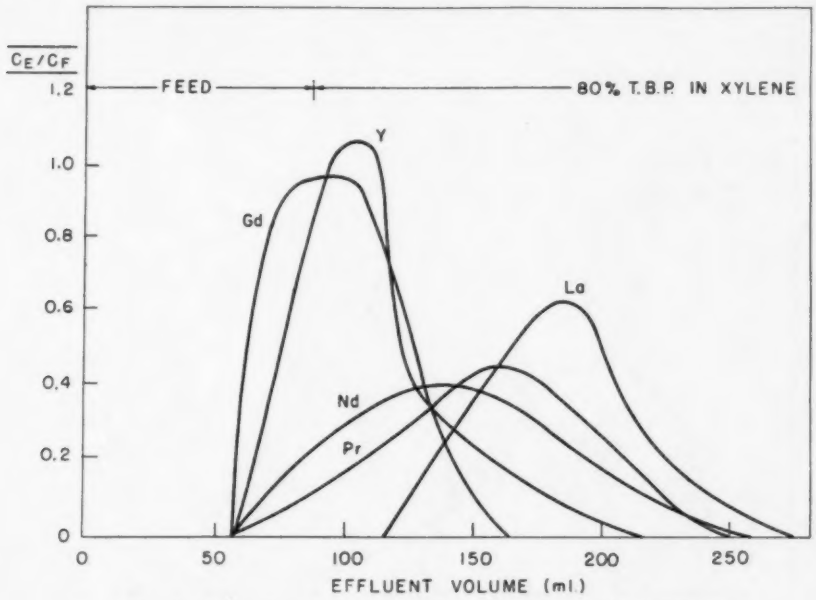

FIG. 6.—Separation of "light" rare earths on Dowex 1 (NO_3^-) TBP eluant.

Where the affinities of the solute components for TBP show a greater difference than that which exists for adjacent rare earths, it is expected that more efficient separations will be attainable. Such a case, namely the separation of thorium nitrate from rare earth nitrates, is illustrated by Fig. 7.

C. *The nature of the resin–solvent interface and its effect upon the efficiency of separations*

A problem which might be said to be a universal feature of the use of water swollen resins with non-polar solvents arises out of the incompatibility of the two phases. This may show itself merely as a tendency for the resin to agglomerate when placed in the solvent, but in other cases it can apparently lead to a high interfacial resistance to mass transfer. The separation of rare earths, using HDEHP and Dowex 50, provided an example of the latter type of behaviour. It was found that when a mixture of rare earth phosphate in toluene was loaded to a fully water swollen Dowex 50 column, little or no retention of rare earths took place. Since the exchange of ions between the solvent and the resin depends on the ability of rare earth phosphate complexes to make intimate contacts with the resin functional groups, it is evident that a thin film of water around the resin particles could effectively eliminate these

contacts. This is so, since unlike an aqueous acid solution, the acid species, in this case the resin functional group, has no mobility beyond the particle boundary and the rare earth phosphates have an extremely low solubility in water. It seemed possible that the failure of the fully swollen resin could be attributed to its having this surface barrier to exchange. On this basis, the use of partially dehydrated resin was investigated as a possible solution. Accordingly the separation of Fig. 2 was obtained on such a resin, namely Dowex 50X4 (H^+) containing 50 per cent water as compared to

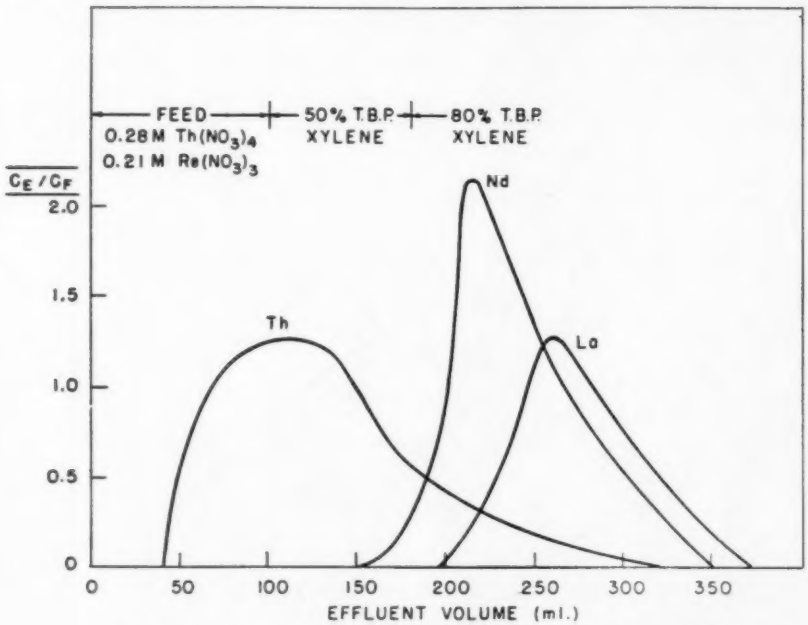

FIG. 7.—Separation of thorium and rare earths on Dowex 1 (NO_3^-) TBP eluant.

its fully swollen water content of 67 per cent. Although the use of this partially dehydrated resin led to retention of rare earths, it nevertheless showed poor resolution. This could quite possibly be due to a water barrier effect, if one takes into account the fact that a resin saturated with rare earth ions has less demand for water than a resin in which the counter ions are hydrogen ions. It is therefore conceivable that the water content of the resin used exceeded the demands of the absorbed rare earth ions and that as loading proceeded the resin "oozed" water to form an impermeable film, thus accounting for the diffuse break through of Ho, Dy and Tb. Further work is being carried out in an attempt to discover the exact nature of these interfacial phenomena in the hope that more efficient means may be devised for exploiting this potentially powerful rare earth separation scheme.

The main disadvantage of water films in the Dowex 1/TBP/$RE(NO_3)_3$ system was their aggravation of the resin's tendency to agglomerate. The presence of a water film on the Dowex 1 (NO_3) resin would not be expected to lead to high interfacial resistances since the rare earth nitrates are quite soluble in water. Various devices were employed to increase resin solvent compatibility including: (1) partial dehydration (2) treatment of the interface with long chain acids e.g. oleic acid (3) surface

etherification. Surface etherification describes a process wherein lipophilic ether groups are introduced onto the surface of the anion exchange resin particles thereby rendering them wettable by non-polar solvents. Such a modified resin was used in the separations illustrated by Fig. 5–7; although it should be added that partial dehydration of a resin appeared equally effective. The details for preparing a surface etherified resin are supplied in the Experimental section.

CONCLUSION

The main aim of this work has been to devise some possible new uses for ion exchange resins by extending their application into the area of water immiscible solvents. Demonstrating the feasibility of new separation techniques has consequently taken precedence over a study of the optimum conditions for any specific separation, particularly since the rules for improving the efficiency of ion exchange chromatographic processes are by now almost axiomatic. When using incompatible phases of the type studied, the problem of interfacial resistance to mass transfer can apparently become important. In this connection, the work has revealed some possible origins of this "barrier" and introduced methods for its removal. These uses of ion exchange resins with water immiscible extractants promise to add a new dimension to the related fields of ion exchange, solvent extraction and gel-liquid extraction.

VOL. 19 1961

EXPERIMENTAL

(A) *Preparation of a solution of rare earth phosphates in toluene*

The feed solution used in the experiment of Fig. 2 was prepared by dissolving a mixed rare earth carbonate directly in a one molar solution of di(2-ethyl hexyl) phosphoric acid in toluene. The small amount of water formed in the organic phase was removed by passage through a plug of absorbent paper.

(B) *Analysis of the effluent in the experiment of Fig.* 2

The total concentration of rare earths in any effluent fraction was calculated from a knowledge of the concentration of phosphate in the solution and from a measurement of the exchangeable hydrogen ion concentration. Such a measurement could be made by diluting a sample solution with methanol and titrating with aqueous sodium hydroxide using methyl red as the end point indicator. The concentration of individual rare earths in effluent cuts was determined by X-ray fluorescence.

(C) *Surface etherification*

A quantity (75 g) of dry chloromethylated styrene divinyl benzene beads[7] (4 per cent crosslinked) was refluxed for 3 hr with a 4 per cent solution of sodium hydroxide in ethanol. Since ethanol does not swell chloromethylated polymer, alcoholysis of $—CH_2Cl$ groups to produce $—CH_2OC_2H_5$ groups was confined to a thin surface shell. The surface modified polymer was subsequently aminated with tri methyl amine to yield a strong base anion exchange resin which was poorly wetted by water but easily wetted by non-polar solvents.

[7] G. D. Jones, *Industr. Engng. Chem.* **44**, 2686 (1952).

J. Inorg. Nucl. Chem., 1961, Vol. 19, pp. 170 to 193. Pergamon Press Ltd. Printed in Northern Ireland

NOTES

Aluminium hydride etherate formed from ether–pentane solution

(*Received* 1 *December* 1960)

THE PREPARATION of non-solvated aluminium hydride by treatment of an ether solution of the hydride with n-pentane has been described by GIBB *et al.*[1] Investigations carried out here indicate that aluminium hydride free of ether cannot be prepared by this method. Various means of mixing the ether aluminium hydride solutions with n-pentane were tried but in all cases an etherated hydride solid was formed. The table below details the results of various preparations

Sample	Aluminium Content	Empirical Formula
1. White solid	43·04%	$(AlH_3)_{2\cdot30}Et_2O$
2. White solid	40·69%	$(AlH_3)_{2\cdot05}Et_2O$
3. White solid further evacuated for 6½ hours	42·62%	$(AlH_3)_{2\cdot27}Et_2O$

On standing, the hydride samples decomposed, turning grey in colour. Nevertheless, the hydride is deposited in a particularly active form, undergoing decomposition shortly after preparation and reacting vigorously with water. This is in contrast to the etherate formed by evaporation of an ether solution followed by high vacuum pumping where the hydride obtained is stable on standing.[2]

The most unreactive form of aluminium hydride may be assumed to approximate to the structure proposed by LONGUET-HIGGINS[3] in which the aluminium atom achieves a co-ordination number of six and where all the hydrogen atoms are involved in bridging of the type Al—H—Al; this structure will not be achieved in the etherated forms since the ether competes for co-ordination with the aluminium such that some of the hydrogen atoms form Al—H bonds. It is possible that the conditions of formation of the solid hydride from an ethereal solution may influence the occurrence of Al—H groupings and that under the conditions of rapid formation from n-pentane more of such Al—H groups are formed than would be allowed by evaporation of the ether solution. No quantitative data is available on the rate of polymerisation of aluminium hydride in ether solution and it is possible that the persistent ether accompanying the hydride is due to ether soluble polymers of the hydride formed during the course of the preparation and being deposited by addition of n-pentane. In the extreme case where co-ordination with nitrogen is involved as in trimethylamine derivatives a complete breakdown of the bridged structure occurs to yield monomeric, sublimable products.[4]

Experimental

Ether solutions of aluminium hydride were prepared as outlined by SCHLESINGER *et al*,[2] the solutions being filtered through a No. 4 glass sinter immediately before use. The solutions were treated with n-pentane as described by GIBB *et al.*,[1] using 100 ml of n-pentane per gram of aluminium hydride, followed by high vacuum pumping for at least 12 hours. Various means of mixing the ether solution with n-pentane were tried and the aluminium and hydrogen content of the resulting hydrides estimated. The presence of ether in the samples was confirmed by the infra-red spectra of the samples,

[1] G. CHIZINSKY, G. Y. EVANS, T. R. P. GIBB and M. J. RICE, *J. Amer. Chem. Soc.* **77**, 3164 (1955).
[2] A. E. FINHOLT, A. C. BOND and H. I. SCHLESINGER, *J. Amer. Chem. Soc.* **69**, 1199 (1947).
[3] H. C. LONGUET-HIGGINS, *J. Chem. Soc.* 139 (1946).
[4] H. GRAF, R. V. LACAL, M. SCHMIDT and E. WIBERG, *Z. Naturforsch* **9**, 51 (1952).

recorded in Nujol. In order to compare the reactivity of the hydrides obtained by this method, etherates were obtained by evaporation of the original ether solutions.[2] In all cases the reactivity of the hydride obtained by rapid precipitation was greater than that obtained by direct evaporation.

Acknowledgement—The authors wish to express their gratitude to the Ministry of Aviation for a grant in support of this work.

I. McLure
T. D. Smith

Department of Chemistry
University College of North Wales,
Bangor, Caernarvonshire

Non-dispersive X-ray fluorescence analysis of uranium-containing solutions

(*Received* 19 *October* 1960)

VOL. 19 1961

X-ray fluorescence methods are being applied in an ever-increasing degree to the measurement and control of component concentrations in chemical plants. In most cases, continuous readings on the process stream are not attempted, but even so, the rapidity and accuracy with which analyses of samples can be obtained show great advantages over previous chemical techniques.

Work on the analysis of uranium in solution has been described by Wilson and Wheeler[1] and others. They have employed conventional X-ray generators, with crystal spectrometers to perform the energy discrimination. Typical of their results is the detection of 100 p.p.m. of uranium in tributyl phosphate, with an accuracy of 3 per cent on a 30-minute count.[2] At lower levels of detection, improved accuracy can be achieved by absorbing the solutions on to filter paper; levels of 1 p.p.m. have been measured thus.

Disadvantages associated with this form of analysis are the cost of the initial equipment, the expense of maintenance, the bulk of the instruments and the necessity for highly stabilised power supplies. The efficiency of the system is extremely low; less than 1 per cent of the electric power consumed appears as X-rays, and only a minute fraction (10^{-7}) of the fluorescent radiation excited is detected, mainly because of the effect of collimation and crystal reflection.

The use of a non-dispersive method of analysis in place of the crystal spectrometer clearly has much to offer, though available techniques do not have the high resolution of the crystal spectrometer.

The use of radioactive sources, particularly low-energy-gamma emitters, instead of X-ray generators confers the additional benefits of simplicity, economy, compactness and stability.[3] In the work described here, some success has been achieved with an americium-241 source.

EXPERIMENTAL

The experimental arrangement comprised the source, which was contained in a shielded capsule; a sample cell; and the detector and its associated counting equipment. Fluorescent X-rays excited in the sample were detected by a xenon-filled proportional counter, the output of which is proportional to the energy of the radiation detected. Electronic analysis of the amplified signal enabled the energy spectrum to be scanned.

The choice of the actual source to be used was made on the basis of the problem being studied.[4] With solutions containing uranium alone, the primary question was whether to attempt to excite the K (98 keV) or the L_{α_1} (13·6 keV) X-ray lines. Photo-electric absorption is much higher at the L-level, where Compton scattering also forms a less serious proportion of the total γ-attenuation, and accordingly it was decided to excite the L-level. The source thus required radiation energy of at least 17·2 keV (L_{III} absorption energy), but rather less than 70 keV, at which fluorescence efficiency is poor and shielding a problem. A long half-life was another desirable feature, in order to eliminate day-to-day

[1] H. M. Wilson and G. V. Wheeler, *Appl. Spectroscopy*, **11**, 128 (1957).
[2] H. M. Davis and H. I. Shalgosky, U.K.A.E.A. Report AERE C/R 2394 (1957). *A preliminary investigation of the analytical potentialities of the Philips X-ray Spectrograph.*
[3] G. B. Cook, C. E. Mellish and J. A. Payne, *Proceedings of the Second United Nations Conference on the Peaceful Uses of Atomic Energy*, **19**, 127 (1958) (A/Conf. 15/P/285). Geneva: United Nations.
[4] K. J. H. Mackay and R. P. Thorne, U.K.A.E.A. DEG Report 134 (CA) (1960). *The application of X-ray fluorescence methods to the in-line determination of uranium and plutonium concentrations.*

corrections for changes in source intensity and to avoid frequent replacement. High specific activity would ensure the most compact source of a given strength. Americium-241, which was chosen, has a principal γ-energy of 60 keV, a half-life of 470 years, and a specific activity of 1 mc/mg. A source of intrinsic strength 700 μc was prepared by the Chemistry Division, A.E.R.E., Harwell. This represented a 60 keV γ-source strength of 300 μc.

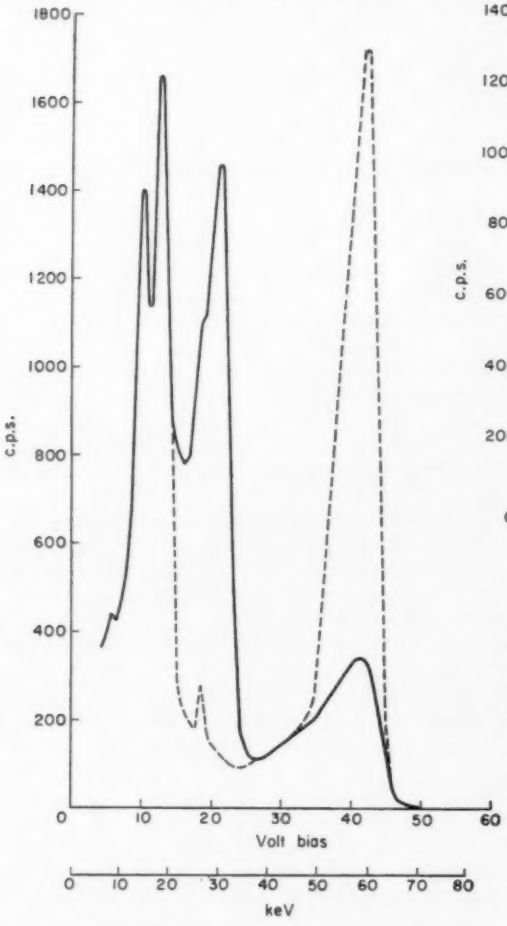

FIG. 1.—Observed spectrum of americium–241 source, with escape peak at 29 keV. Dashed graph shows corrected spectrum (escape peak contribution transferred to true position at 60 keV). Other peaks are Np L_α at 13·5 keV, Np L_β at 17·3 keV and ^{241}Am γ at 26·4 keV.

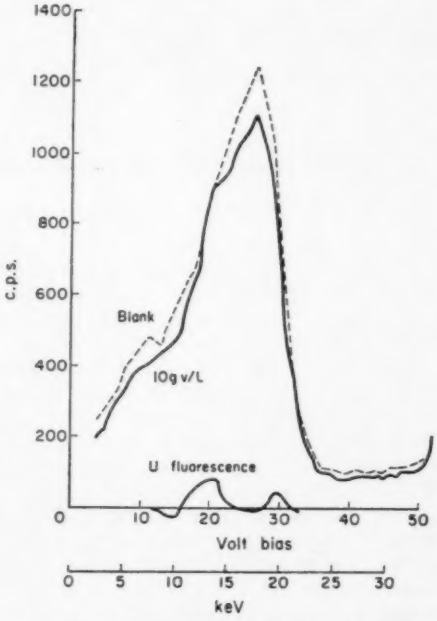

FIG. 2.—Comparison of observed spectra from solution containing 10 g uranium per litre and from blank (2 N HNO_3). (The uranium fluorescence response is found by subtracting the blank reading, corrected for absorption, from that of the solution.)

A proportional counter was preferred to the scintillation type because of its better theoretical energy resolution (at 14 keV, 12 per cent instead of 51 per cent), although at this energy the detection efficiency of the xenon-filled counter used (PX 130A, Twentieth Century Electronics, Ltd.) was only 70 per cent of that of a scintillation counter.

Reflection geometry was chosen in preference to transmission, since slight variations in sample thickness and position may be tolerated, and interference by scattered radiation from the source is reduced. The sample cells were constructed of Perspex, the windows being of 200-gauge Melinex, sealed in position with Araldite cold-setting cement, and a range of samples was prepared, containing uranium in concentrations from 10 g/l. down to 1 mg/l.

VOL.
19
1961

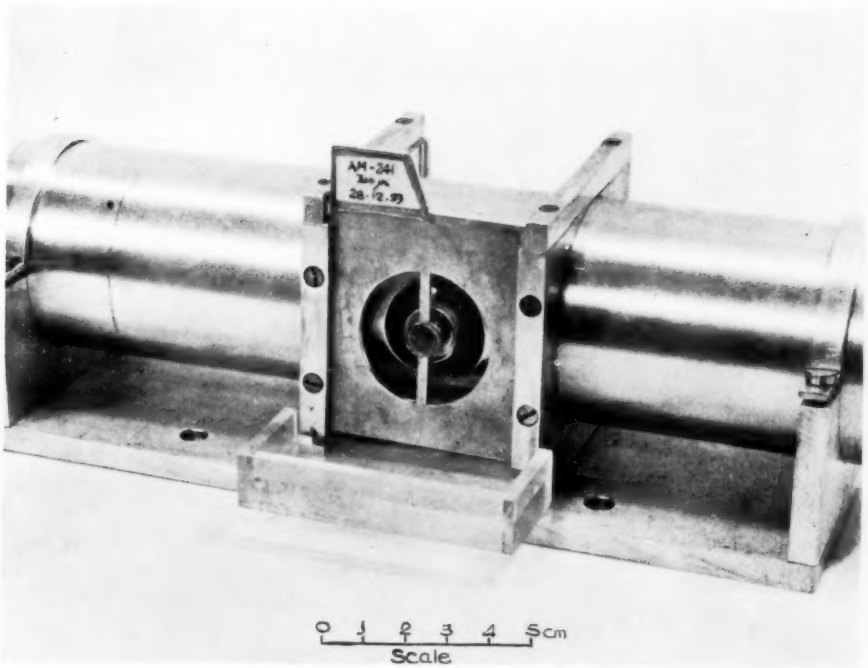

FIG. 3.—Modified americium source in position on counter.

RESULTS AND DISCUSSION

Examination of the spectrum of the americium source (Fig. 1) showed that, apart from a prominent "escape" peak in the region of 30 keV, the spectrum agreed satisfactorily with the published spectrum.[5] The escape peak is caused by fluorescence in the xenon gas filling the counter, the resulting radiation leaving the counter without being absorbed. This proved particularly troublesome when examining the fluorescence from uranium solutions. The energy of the exciting radiation had become degraded by scattering in the solution, and a broad escape peak, recorded at 18 keV, almost completely masked the uranium response (Fig. 2).

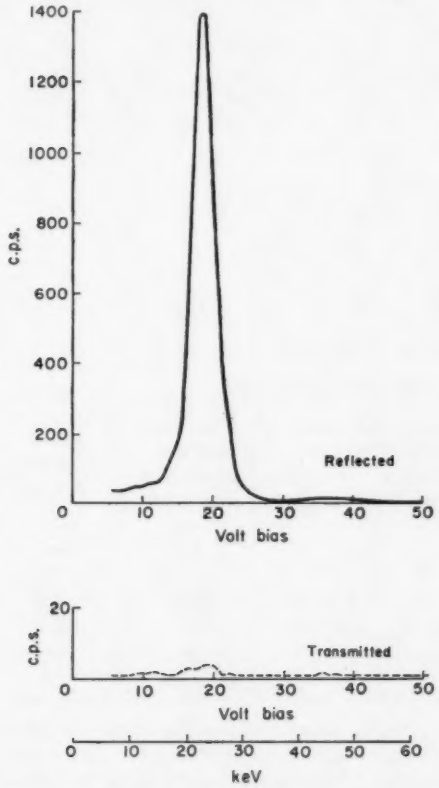

FIG. 4.—Reflected and transmitted spectra from 3 mm cadmium, excited by americium source.

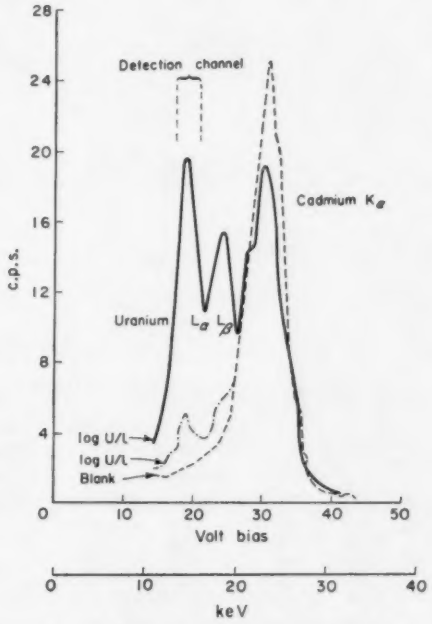

FIG. 5.—Spectra of fluorescence excited in uranium solutions.

A simple way of avoiding this is to use an intermediate target of a material whose K X-ray energy is less than that of xenon, but greater than 17·2 keV. Silver (22·2 keV) and cadmium (23·2 keV) are suitable materials, and cadmium was successfully used. In the form of a 3 mm thick cup, fixed over the source (Fig. 3), this was found to produce a simple excitation spectrum of good intensity, and with low general background and transmission (Fig. 4). With this modified source, the fluorescent spectrum of a 1 per cent uranium solution clearly showed the two prominent L-lines (Fig. 5).

Analyses of uranium as a single component in 1·0 N nitric acid solution were performed by irradiating each of the sealed standard samples, alternately with a blank, for a period of 10 minutes, the cycle being repeated 10 times. The results are shown in Table 1, and in graphical form in Fig. 6. Taking the limit of detection nominally as one-tenth of background, the present method has a detection limit in the region of 50 p.p.m.

The development of an in-line instrument will require further investigation of several factors. An

[5] D. STROMINGER, J. M. HOLLANDER and G. T. SEABORG, *Rev. Mod. Phys.*, **30**, no. 2, pt. 2 (1958).

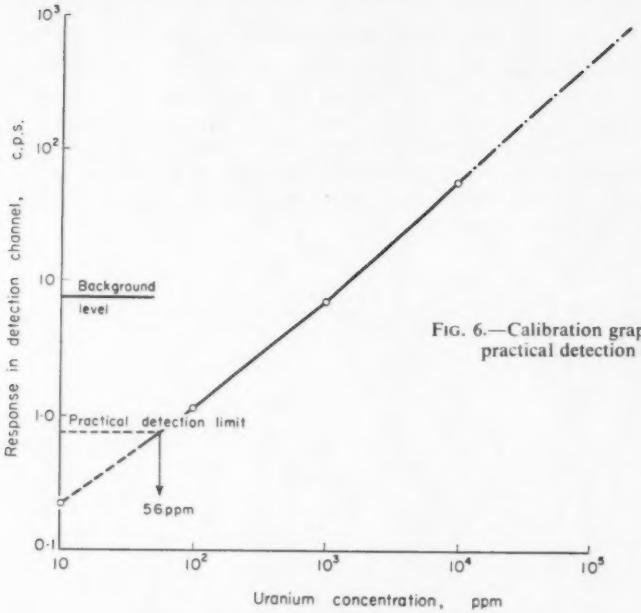

FIG. 6.—Calibration graph, showing practical detection limit.

TABLE 1.—RESULTS OF CALIBRATION EXPERIMENTS

Uranium concentration (p.p.m.)	Average total counts in 10 min (over ten runs) (background subtracted)	Standard deviation for ten runs	Coefficient of variation (per cent)	Theoretical coefficient of variation (per cent)	Mean count-rate (c.p.s.)
10^4	32911·9	±416	1·26	0·63	54·85
10^3	4180·5	±203	4·86	2·7	6·97
10^2	691·5	±126·3	18·25	15·0	1·153
10	131·4	±159·9	121·7	72·0	0·219
Blank	4516·5	±69·7	1·54	1·5	7·52

annular source design, for instance, would permit a higher source strength and at the same time leave clear the counter window. This would enable a higher accuracy to be obtained in a given time, though it would not be expected to lower the detection limit. Other useful features would be a device whereby alternate counts on sample and blank could be performed automatically, and a means of determining and allowing for the effect of other components in solution. Finally, by taking advantage of differential absorption in material such as gold, platinum and lead, it should be possible to measure the concentrations of uranium and plutonium in the process streams of a plutonium separation plant.

Acknowledgements—The work was directed by Mr. R. P. THORNE, of Research and Development Branch, Capenhurst, who provided helpful discussion. Mrs. K. M. GLOVER, of Chemistry Division, A.E.R.E., Harwell, prepared the americium source. This Note is published by permission of Sir WILLIAM COOK, Managing Director, and Dr. H. KRONBERGER, Director of Research and Development, of the U.K.A.E.A. (Development and Engineering Group).

K. J. H. MACKAY*

United Kingdom Atomic Energy Authority
(Development and Engineering Group)
Research and Development Branch
Capenhurst, Chester.

* Present address: *Tube Investments Research Laboratory, Hinxton Hall, Saffron Walden, Essex.*

VOL. 19 1961

The thermal annealing of ^{60}Co in irradiated *tris*-(ethylenediamine)-cobalt(III) nitrate*

(*Received* 25 *November* 1960; *in revised form* 18 *January* 1961)

SEVERAL attempts have been made to interpret the rate of thermal annealing of ^{60}Co in irradiated *tris*-(ethylenediamine)-cobalt(III) nitrate.[1,2,3] These attempts have been handicapped by a lack of information concerning the values of the retentions reached on prolonged annealing. On prolonged annealing the retentions may either reach the same plateau-value, regardless of the actual annealing temperature, or they may reach different plateau-values depending on the particular annealing temperature employed. We have investigated the annealing of ^{60}Co in irradiated *tris*-(ethylenediamine)-cobalt(III) nitrate and have found that true temperature-dependent plateaus do not exist in this system.

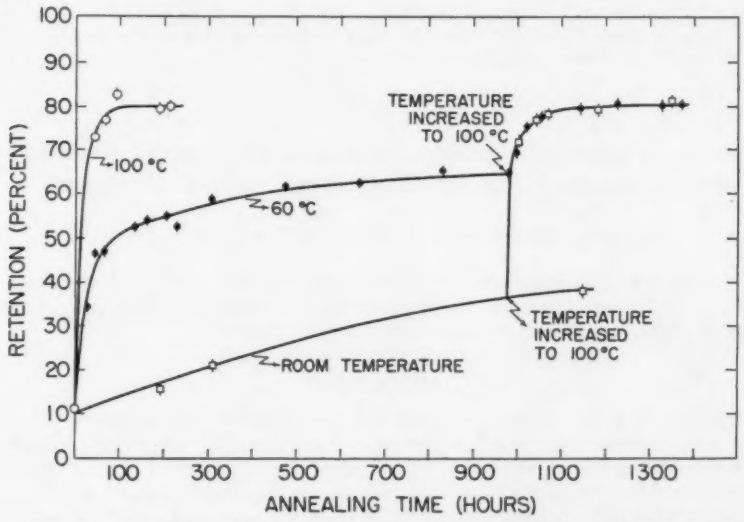

FIG. 1.—Rate of annealing of ^{60}Co in irradiated *tris*-(ethylenediamine)-cobalt(III) nitrate.

Samples of *tris*-(ethylenediamine)-cobalt(III) nitrate were irradiated for five minutes in the Brookhaven reactor at a thermal neutron flux of $1{\cdot}1 \times 10^{13}$ neutrons cm^{-2} sec^{-1}. After irradiation the percentage of ^{60}Co as Co^{++} was determined by extracting an aqueous solution of the irradiated salt with a 1% solution of 8-hydroxyquinoline in chloroform. The percentage of the total activity as the parent form, the retention, was determined by recrystallizing the irradiated salt to constant specific activity. The rate of annealing of the ^{60}Co was studied by heating samples of the irradiated salt for various lengths of time in an oven at 60° or 100° before analysis.

The results of the annealing experiments conducted at room temperature, 60° and 100° are shown in Fig. 1. It will be seen that the retention of samples annealed at room temperature or at 60° and then annealed at 100° reaches the same value as that of a sample annealed at 100° throughout. This suggests that competing annealing reactions do not occur in this system and thus that the retentions of all irradiated samples would reach the same plateau-value on prolonged annealing, regardless of the annealing temperature. It is also apparent from Fig. 1 that on increasing the temperature to 100° the rates of annealing of the samples initially annealed at room temperature or 60° are the same and very similar to the rate of annealing of the sample which had been annealed at 100° throughout.

* Research performed under the auspices of the U.S. Atomic Energy Commission.

[1] A. ZUBER, Thesis, *Columbia University, New York* (1954).
[2] G. HARBOTTLE and N. SUTIN, *Advances in Inorganic and Radiochemistry*, **1**, 369. Academic Press, New York (1959).
[3] H. E. RAUSCHER, N. SUTIN and J. M. MILLER, *J. Inorg. Nucl. Chem.*, (in press).

Using a value of 82·0 per cent for R_∞, the plateau-value for the retention at all three annealing temperatures, it was found that plots of log $(R_\infty - R)$ *vs* time could be resolved into two components. The intercepts of these components vary with the annealing temperature, a result which is difficult to reconcile with the absence of temperature-dependent plateaus.[2,3,4,5] We thus conclude that the annealing of ^{60}Co in *tris*-(ethylenediamine)-cobalt(III) nitrate cannot be readily described in terms of two first order reactions. It may still be possible, however, to describe the annealing processes in those systems in which temperature-dependent intercepts and temperature-dependent plateaus are observed in terms of competing first order reactions.[3,4]

Department of Chemistry
Brookhaven National Laboratory
Upton, L.I., N.Y.

L. L. WILLIAMS†
N. SUTIN
J. M. MILLER‡

† *Summer Student from Hollins College, Virginia.*
‡ *Visiting Chemist from Columbia University, New York.*

[4] A. ZUBER, H. E. RAUSCHER, J. M. MILLER and N. SUTIN, *paper presented at the International Atomic Energy Agency Symposium on Chemical Effects of Nuclear Transformations, Prague, Czechoslovakia* (1960).
[5] M. M. DE MAINE, Thesis, *Cambridge University, England* (1955).

Determination of zirconium in presence of common metals using 2:5 dihydroxy *p*-benzoquinone and the nature of metal complexes with this reagent

(*Received* 4 *January* 1961; *in revised form* 30 *January* 1961)

Abstract—2:5 Dihydroxy *p*-benzoquinone precipitates only zirconium from 1 N hydrochloric acid solution in presence of a large number of common metals. The insolubility of the metal chelates in common organic solvents indicates that these are polymeric in character.

INTRODUCTION

IN a previous communication[1] we have reported that 2:5 dihydroxy p-benzoquinone precipitates thorium in presence of cerium (IV and III), lanthanum and uranium (VI); and zirconium in presence of titanium but in absence of iron (III) from 1 N hydrochloric acid solution. In another paper[2] we have reported that cerium (III and IV), lanthanum and yttrium are precipitated at pH 2·5–3·0; uranium (VI) in presence of ammonium chloride at pH 2·8–7·0 and titanium (IV) at pH 0·8–1·5. The precipitate in each case is ignited to oxide. The present communication describes the precipitation of zirconium in presence of common metals. The nature of the metal chelates with 2:5 dihydroxy *p*-benzoquinone is also discussed.

DETERMINATION OF ZIRCONIUM

2:5 Dihydroxy *p*-benzoquinone was prepared by the oxidation of hydroquinone with hydrogen peroxide in the presence of sodium hydroxide.[3]

After the addition of different amounts of foreign ions to the zirconium solution, its volume was made to 150–200 ml and its acidity adjusted to about 1 N with hydrochloric acid. 0·5–1 g of the solid reagent was then added and the resultant solution boiled for 1–2 minutes. The solution was then cooled to room temperature and filtered through Whatman No. 40 filter paper. The precipitate was washed with about 200 ml 0·2% aqueous solution of the reagent which had been made 1 N with hydrochloric acid. On drying the precipitate at 120°, the filter paper became brittle and before incineration it was encased in another filter paper (slightly bigger in size) and finally ignited to oxide at 900°. When zirconium was estimated in the presence of about 50 times its weight of iron (II) and about five times its weight of aluminium, vanadium (V and IV), uranium (VI), cerium (IV), copper (II), cadmium, nickel (II), cobalt (II), chromium (III), manganese (II), zinc, beryllium, calcium barium and magnesium, none of the additives made more than 0·1 mg differ on 20·4 mg weight of ZrO_2 recorded.

[1] B. D. JAIN and S. P. SINGHAL, *Talanta*, **4**, 178 (1960).
[2] B. D. JAIN and S. P. SINGHAL, *J. Sci. Ind. Res.* (India) **19B**, 494 (1960).
[3] R. G. JONES and H. A. SHONLE, *J. Amer. Chem. Soc.*, **67**, 1034 (1945).

NATURE OF METAL COMPLEXES WITH 2:5 DIHYDROXY *p*-BENZOQUINONE

Chelates of 2:5 dihydroxy *p*-benzoquinone with a large number of common metals have been described to be insoluble in water, alcohol, acetone, ether and pyridine.[4] The insolubility of the zirconium, thorium, rare earth, uranium and titanium chelates in water and in common organic solvents indicates their polymeric nature.[2] This inference is also supported by the fact that 2-hydroxy 1–4 naphthoquinone has a five membered chelated ring —C(=O)—C(OH)= similar to that present in 2:5 dihydroxy *p*-benzoquinone and because of the absence of a second chelating centre in the same molecule its metal chelates are soluble in dilute alcohol.

The great stability of the zirconium and thorium chelates of 2:5 dihydroxy *p*-benzoquinone towards mineral acids[1] also indicates that probably these chelates are polymeric. The small size of 2:5 dihydroxy *p*-benzoquinone molecule facilitates polymerisation of its chelates with metals.

A bivalent ion like copper may form a linear polymer with 2:5 dihydroxy *p*-benzoquinone, but with a trivalent ion like cerous, having a coordination number six or a tetravalent ion like zirconium with a coordination number eight, three dimensional cross-linked structures are possible. The stability of these compounds is a result both of the increase in the strength of the bonding arising from chelate ring formation, and of the way in which the chelating groups pack around the central ion making reactions with other substances sterically difficult.

Acknowledgements—Our thanks are due to Prof. T. R. SESHADRI, F.R.S. for his keen interest and helpful discussions and to the Department of Atomic Energy, Government of India, for financial assistance.

B. D. JAIN
S. P. SINGHAL

Department of Chemistry
University of Delhi
Delhi, India.

[4] R. L. FRANK, G. R. CLARK and J. N. COKER, *J. Amer. Chem. Soc.*, **72**, 1827 (1950).

On the structure of antimonates

(*Received* 10 *January* 1961)

Abstract—A pure solution of antimonic acid has been prepared. It has been shown that the acid is monobasic and corresponds to the structure $HSb(OH)_6$. The pH-titration shows that it is a strong acid.

THERE is a lot of confusion regarding the chemical structure of antimonates. They have been wrongly classified with the pyrophosphates and arsenates. Even to this day in some of the important text books and reference books, the antimonates are supposed to be the salts of non-existent pyro-antimonic acid and the formula given to the salts is $M_2^IH_2Sb_2O_7, xH_2O$. The water of crystallization (xH_2O) has offered a lot of difficulty in the interpretation of the structure of these salts.

TOMULA[1] in 1921 was the first to conclude from the conductivity measurements of the potassium salt that the anion could not be tetravalent and the results could be explained only if the anion is assumed to be monovalent. PAULING[2] in 1933, on the grounds of atomic sizes pointed out that we should expect the salts to have a structure corresponding to that of the tellurates and periodates. Pauling predicted that antimony, unlike phosphates and arsenates, where P and As are co-ordinated tetrahedrally, should be co-ordinated octahedrally. He ventured to represent antimonic acid as $H(Sb(OH)_6)$. He also pointed out that the representative salts in the new formulation could be represented as $M^I(Sb(OH)_6)$. The majority of the antimonates described in literature contain just enough water so as to correspond to the formula $M^I(Sb(OH)_6)$, though some contain additional

[1] H. REMY, *Treatise on Inorganic Chemistry*–Amsterdam (1956).
[2] L. PAULING, *J. Amer. Chem. Soc.* **55**, 1895 (1933).

VOL. 19 1961

water of crystallization. PAULING's predictions have been confirmed by BEINTEMA[3,4] and SCHREWELIUS,[5] who determined the crystal structure of antimonates. The new formula also falls in line with the predictions of TOMULA on the basis of the conductivity measurements of the potassium salt.

We in the present work have prepared the solution of the free acid and found it to be monobasic. This provides an independent evidence that the structure of the acid must be $H(Sb(OH)_6)$. As far as we know this is the first time that the pure acid solution has been prepared free from all kind of extra electrolytes.

The acid was prepared by passing a saturated solution of the Merck sample of the so called potassium hydrogen antimonate through an ion exchange column packed with the hydrogen form the Amberlite I.R. 120 ion exchange resin. Since the solubility of potassium salt is not much at the room temperature, therefore, acid solutions of relatively lower strength (0·0127 N) could be obtained. The acid thus prepared has a pH of about 2·6 and the freshly prepared sample is quite stable. However, if left for some time (2–3 days) a white substance is precipitated which is most probably antimony oxide or a polymer of $(Sb(OH)_6)^-$. When hydrogen sulphide is passed through the solution of antimonic acid there is a light orange colouration, showing some of the antimony is in the cationic form. This may be due to the dissociation of the complex acid according to the following reaction:

$$Sb(OH)_6^- = Sb(OH)_{6-n}^{+(n-1)} + nOH^-$$

The potentiometric and conductometric titrations were also carried out against potassium hydroxide (Merck quality).

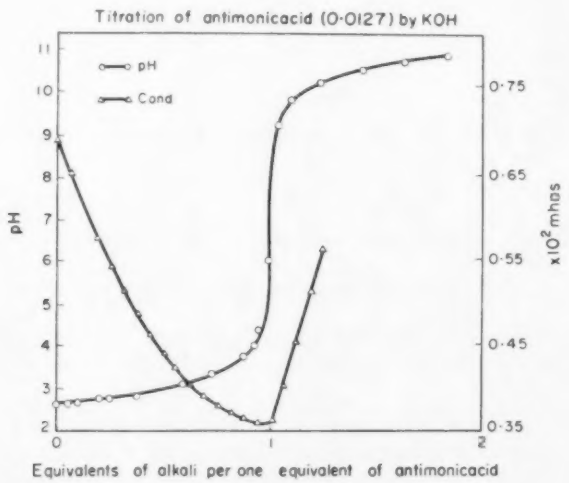

Both the titration curves are given in the above diagram. The pH titration curve is that of a typical strong monobasic acid and the rise in the pH at the end point is very sharp. The conductometric titration curve is not the one, we generally get for a strong monobasic acid. The fall in the conductivity is not only due to the replacement of hydrogen ion by potassium ion but it is quite likely that some other processes (e.g. the polymerisation or depolymerisation of $Sb(OH)_6^-$) is superimposed on the neutralisation process. G. JANDER[6] has shown that antimonate ions are condensed in aqueous solution if the concentration of hydrogen ions is increased. The rise in specific

[3] J. BEINTEMA, *Proc. K. Akad. Amst.* **38,** 1015 (1935).
[4] J. BEINTEMA, *Proc. K. Akad. Amst.* **39,** 652 (1936).
[5] N. SCHREWELIUS, *Z. Anorg. Chem.* **238,** 241 (1938).
[6] See Ref. (1), page 666.

conductivity after the break corresponds to the addition of the alkali showing no neutralisation process is taking place after the break.

Acknowledgement—The authors express their sincere gratitude to Professor R. P. MITRA for his interest in this work.

Department of Chemistry
University of Delhi
Delhi, India

D. V. S. JAIN
A. K. BANERJEE

Reduction of permanganate by iodide in a neutral medium

(*Received* 12 *December* 1960; *in revised form* 30 *January* 1961)

VOL. 19 1961

IODIDE acts as a strong reducing agent[1] towards permanganate in an alkaline medium with reduction from Mn(VII) to Mn(VI); in a neutral medium reduction is to Mn(IV). Analytical measurements have been made to determine the oxidation state of iodine which is formed in the latter case. Potassium permanganate and potassium iodide were allowed to react until manganese dioxide separated, leaving a colourless supernatant liquid. The precipitate was filtered and washed in a measuring flask; 25 ml aliquots of the filtrate were analysed for iodate and iodide.[2] Manganese dioxide was determined iodometrically. 25 ml samples were also titrated against a standard solution of oxalic acid to determine the liberated alkali. Table 1 shows the results obtained.

It was found that manganese was in the Mn(IV) state, retaining only two fifths of its original

TABLE 1.—$KMnO_4$ = 0·2 N; KI = 0·2 N; TOTAL VOLUME = 50 ml

$KMnO_4$ ml	KI ml	MnO_2 found as ml of $KMnO_4$	Oxidant in filtrate as ml of $KMnO_4$	Remaining KI, found ml	Remaining KI, calculated ml
10	1	4·05	5·98	0	0
10	2	4·04	5·98	1·017	1·00
10	4	4·04	5·97	3·007	3·00
10	6	4·05	5·98	4·948	5·00
10	8	4·07	5·96	—	—
5	0·5	1·98	3·00	0	0
5	1·0	1·98	3·00	0·508	0·500
5	1·25	1·99	3·00	0·766	0·75
5	2·50	1·99	3·00	2·014	2·00
5	5·00	1·99	3·00	—	—
2·5	0·25	0·995	1·502	0	0
2·5	0·50	0·995	1·502	0·266	0·25
2·5	0·75	0·995	1·51	0·508	0·50
2·5	1·25	0·995	1·50	1·017	1·00

oxidising capacity; three fifths of the latter is imparted to the filtrate. The latter is colourless and contains no iodine, hydrogen peroxide or potassium hypoiodite, but responds to tests for potassium iodate.[3] The minimum concentration of iodide required for the reduction of permanganate is 0·1 equivalent per equivalent of permanganate, and determination of the unused iodide in the filtrate

[1] Y. K. GUPTA, *Bull. polon. Sci.* (Poland), **8**, 79 (1960).
[2] W. W. SCOTT, *Standard Methods of Chemical Analysis*, 454, D. Van Nostrand and Co., Inc., New York (1958).
[3] A. I. VOGEL, *A Textbook of Macro- and Semimicro Quantitative Inorganic Analysis*, p. 372, Longmans Green and Co., London, 4th Edition, 1959.

shows that in all the experiments 0·1 equivalent of iodide is oxidised by one equivalent of permanganate according to the equation $2MnO_4^- + I^- + H_2O = IO_3^- + 2MnO_2 + 2OH^-$. This estimation of iodide in presence of the oxidant, assumed to be iodate, provides strong support for the presence of iodate in the filtrate; the amount of iodide was calculated on the basis of the reaction, $IO_3^- + 5I^- + 6H^+ = 3I_2 + 3H_2O$. The amount of alkali determined was found to be irregular and to decrease with time.

Experiments were also performed using amounts of iodide less than 0·1 equivalent of the original permanganate, and the excess permanganate was estimated colorimetrically at 524 mμ after separating the manganese dioxide by centrifuging. The results are tabulated in Table 2.

TABLE 2.—REACTION MIXTURE 50 ML

$KMnO_4$ N	KI N	Optical density of remaining $KMnO_4$ (10 times diluted)	$KMnO_4$ from Beer's law graphically N	Remaining $KMnO_4$ N	Expected remaining $KMnO_4$ N
0·05	0·004	0·48	0·001	0·01	0·01
0·05	0·002	1·39	0·00297	0·0297	0·03
0·05	0·001	1·90	0·00405	0·0405	0·04
0·04	0·002	0·93	0·00197	0·0197	0·02
0·04	0·001	1·42	0·00302	0·0302	0·03
0·02	0·001	0·48	0·001	0·01	0·01

The results obviously point to the formation of iodate when permanganate is reduced to manganese dioxide by potassium iodide.

Y. K. GUPTA

Department of Chemistry
D.S.B. Government College
Nainital, India

Der Reaktionsdruck des Indium(I)sulfids

(*Received* 30 *January* 1961)

DAS Zustandsdiagramm des Systems Indium/Schwefel[1] enthält keine Hinweise für die Existenz des festen oder geschmolzenen Indium(I)sulfids. Es ist jedoch bekannt,[2] dass sich bei der Einwirkung von Schwefelwasserstoff auf Indium-Metall bei 1000°C gasförmiges In_2S bildet, welches sich im Vakuum absublimieren lässt und im kühleren Teil der Apparatur als schwarzer Spiegel erscheint. In Zusammenhang mit unseren früheren Untersuchungen über Gallium(I)sulfid[3] schien es uns von Interesse, den Reaktionsdruck von In_2S über Schmelzen der Bruttozusammensetzung InS + In und In_2S_3 + 4 In zu messen. Die Ergebnisse der Messungen zwischen 1000° und 1200°C zeigen die Tab. 1 und 2.

Innerhalb des untersuchten Temperaturintervalles zeigen die Messwerte der Tab. 1 im $\lg p - T^{-1}$ Diagramm keine merkliche Abweichung von einer Geraden, d.h. ΔH_R ist in diesem Bereich im Rahmen der Messgenauigkeit temperaturunabhängig. Es ist daher gerechtfertigt, die Messungen durch eine Dampfdruckgleichung mit nur zwei Parametern zu beschreiben. Nach der Methode der kleinsten Fehlerquadrate erhält man

$$\lg p_{In_2S}(\text{Torr}) = -\frac{9\,320{\cdot}3}{T} + 7{\cdot}9212 \qquad (1)$$

Der Gleichgewichtsdruck von In_2S über Indiumsulfid-Phasen mit hinreichend grosser Indiumaktivität ist unabhängig von der Art der ursprünglich eingesetzten festen Indiumsulfide. Der Reaktionsdruck von In_2S über Schmelzen der Bruttozusammensetzung In_2S_3 + 4 In stimmt also überein

[1] M. F. STUBBS, J. A. SCHUFLE, A. J. THOMPSON and J. M. DUNCAN, *J. Amer. Chem. Soc.* **74**, 1441 (1952)
[2] E. GASTINGER, *Z. Naturf.* **10B**, 115 (1955)
[3] H. SPANDAU und F. KLANBERG, *Z. anorg. allg. Chem.* **295**, 300 (1958)

TABELLE 1.—REAKTIONSDRUCK VON In_2S ÜBER $InS_{fl.} + In_{fl.}$

t°C	T°K	p(Torr)	lg p_{exp}	lg p_{ber}	% In im Sublimat
986	1259	3·1	$0{\cdot}49_1$	$0{\cdot}51_8$	
1008	1281	4·5	$0{\cdot}65_3$	$0{\cdot}64_5$	
1038	1311	6·6	$0{\cdot}81_9$	$0{\cdot}81_2$	87·0
1060	1333	8·5	$0{\cdot}92_9$	$0{\cdot}92_9$	87·6
1079	1352	11·1	$1{\cdot}04_5$	$1{\cdot}02_8$	88·0
1110	1383	15·4	$1{\cdot}18_7$	$1{\cdot}18_2$	87·4
1139	1412	21·3	$1{\cdot}32_8$	$1{\cdot}32_0$	87·6
1158	1431	24·4	$1{\cdot}38_7$	$1{\cdot}40_8$	87·4
1176	1449	30·3	$1{\cdot}48_1$	$1{\cdot}48_9$	87·4
1198	1471	37·9	$1{\cdot}57_9$	$1{\cdot}58_5$	87·5

lg p_{ber} nach Gleichung (1)
In_2S ber.: 87·74% In
Mittlerer Fehler der Einzelmessung: $f_m = 1{\cdot}5$ Prozent.

VOL. 19 1961

mit dem Druck über Schmelzen der Ausgangszusammensetzung InS + In. Einige Messwerte der Versuchsreihe In_2S_3 + 4 In zeigt Tab. 2.

TABELLE 2.—REAKTIONSDRUCK VON In_2S ÜBER In_2S_3 + 4 In

t°C	T°K	p(Torr)	lg $p_{exp.}$	lg $p_{ber.}$	% In im Sublimat
1010	1283	4·6	$0{\cdot}66_3$	$0{\cdot}65_7$	
1110	1383	15·3	$1{\cdot}18_5$	$1{\cdot}18_2$	87·4
1143	1416	22·0	$1{\cdot}34_2$	$1{\cdot}34_9$	87·0

Die Auswertung der Messergebnisse ergibt für die Reaktionen

$$\frac{1}{3}\,In_2S_{3fl.} + \frac{4}{3}\,In_{fl.} \rightarrow In_2S_{gas}\ (1300-1500°K) \qquad (2)$$

$$InS_{fl.} + In_{fl.} \rightleftharpoons In_2S_{gas}\ (1250\text{–}1500°K) \qquad (3)$$

Reaktionsenthalpie: $\Delta H_R = 42{\cdot}6 \pm 0{\cdot}6$ kcal/mol

Reaktionsentropie: $\Delta S = \dfrac{\Delta H_R - \Delta G_R}{T} = 23{\cdot}1$ cal/gradmol

Die Umrechnung dieser Werte auf die Normalbildungsenthalpie von In_2S_{gas} ist nur näherungsweise möglich, da Daten über die Molwärmen der Indiumsulfide bisher fehlen. Die beiden in der Literatur[4–5] vorhandenen Werte für die Normalbildungsenthalpie des InS($\Delta H_f = -39{\cdot}3$ kcal/mol bzw. $\Delta H_f = -33{\cdot}6$ kcal/mol) weichen relativ stark voneinander ab. Wir haben dem kalorimetrisch bestimmten Wert $\Delta H_f = -33{\cdot}6$ kcal/mol von BUROW[5] den Vorzug gegeben. Die Werte für $\Delta H_f(In_2S_3)$ der beiden Autorengruppen[4–5] stimmen recht gut miteinander überein. Die übrigen für die Rechnung benutzten thermochemischen Grössen wurden dem NBS Circular 500 entnommen oder aus analogen Verbindungen geschätzt. Auf diese Weise erhält man

$$\Delta H_f^{298}(In_2S_{gas}) = +6{\cdot}5 \pm 8 \text{ kcal/mol}$$

Für die Reaktion $2In_{gas} + S_{gas} = In_2S_{gas}$ ergibt sich daraus

$$\Delta H_R^{298} = -162 \pm 12 \text{ kcal/mol}$$

[4] A. J. THOMPSON, M. F. STUBBS und J. A. SCHUFLE, *J. Amer. Chem. Soc.* **76**, 341 (1954)
[5] H. HAHN und F. BUROW, *Angew. Chem.* **68**, 382 (1956); F. BUROW, Dissertation Universität Kiel (1956)

EXPERIMENTELLES

Die experimentelle Durchführung unserer Versuche auf der Grundlage der Mitführungsmethode ist bereits an anderer Stelle beschrieben.[6] Die Strömungsgeschwindigkeit des als Trägergas benutzten Stickstoffs betrug im Mittel 20 ml/min, was zur Einstellung eines quasistatischen Gleichgewichtes ausreicht.

In_2S_3 wurde durch Fällung dargestellt und bei 500°C im H_2S-Strom getrocknet; InS wurde durch Synthese aus den Elementen im Quarzrohr[7] erhalten; das verwandte Indium war 99·999 Prozent. Die Analysen der Verbindungen entsprachen den berechneten Werten.

Das aus der Gasphase kondensierte In_2S schied sich in Form eines feinen grauen bis schwarzen Pulvers ab, das ausserordentlich fest an den Quarzrohren der Apparatur haftete. Dieses Pulver erleidet beim Aufbewahren an der Luft keine merkliche Veränderung; es löst sich leicht in oxidierenden Säuren. Das Pulverdiagramm (CuK_α-Strahlung) zeigt nur die Linien des InS. Nach diesem Befund und dem Zustandsdiagramm[1] sollte man daher annehmen, dass In_2S_{fest} instabil ist und gemäss dem Schema

$$In_2S_{gas} \rightarrow In_2S_{fest} \rightarrow InS_{fest} + In_{fl.} \qquad (4)$$

disproportioniert. Wir konnten jedoch im Debye–Scherrer–Diagramm des aus der Gasphase erhaltenen Produktes der Bruttozusammensetzung In_2S auch nach längerem Aufbewahren keine Linien des metallischen Indiums entdecken. Worauf dies zurückzuführen ist, ist noch nicht geklärt.

Anerkennungen—Wir danken den Unterharzer Berg- und Hüttenwerken, Oker am Harz, für die Überlassung reinsten Indiums.

F. KLANBERG
H. SPANDAU

Eduard-Zintl-Institut fur anorganische und physikalische Chemie der Technischen Hochschule, Darmstadt, Germany.
Anorganisches-chemisches Institut der Technischen Hochschule, Braunschweig, Germany.

[6] H. SPANDAU und F. KLANBERG, *Z. anorg. allg. Chem.* **295**, 291 (1958)
[7] W. KLEMM und H. U. VON VOGEL, *Z. anorg. allg. Chem.* **219**, 45 (1934)

Search for an antimony isotope with a 30 days half-life

(*Received* 20 *January* 1961)

A fission product isotope of antimony which decays with a half-life around 30 days has been reported by several authors.[1,2,3] As in previous work at our laboratory with the heavy isotopes of antimony we had never observed such a half-life, some experiments were performed to determine its existence and nuclear properties.

EXPERIMENTAL

0·5 grams of UO_2 were irradiated for 8 hours in the RA1 reactor. 30 days after the end of the irradiation the antimony fraction was separated chemically and purified by reduction with zinc to form volatile stibine.[4]

Radioactivity measurements were performed with a thin end-window G.M. counter, over approximately 8 months. Because of the low intensity of the source available, the gamma spectrum could not be measured.

The analysis of the curve showed a half-life of approximately 4 days corresponding to Sb^{127}, which had not completely decayed, and a much longer half-life, of over one year, which may be due to Sb^{125}.

In another experiment UO_2 was irradiated for 8 hours with 28 MeV deuterons from the Buenos Aires synchrocyclotron. The antimony fraction was separated 31 days after the end of irradiation. A series of gamma spectra of the source obtained were taken at from 32 to 200 days after the end of irradiation with a single channel scintillation spectrometer with a $2'' \times 2''$ NaI(T1) crystal. These spectra show the more important rays of Sb^{124} (60 days), Sb^{125} (2 years), Sb^{126} (11 days) and Sb^{127}

[1] E. W. GRUMMITT and G. WILKINSON, *Nature, Lond.* **158**, 163 (1946).
[2] J. W. BARNES and A. J. FREEDMAN, *Phys. Rev.* **84**, 365 (1951).
[3] T. T. SUGIHARA P. J. DREVINSKY E. J. TROIANELLO and J. M. ALEXANDER, *Phys. Rev.* **108**, 1264 (1957).
[4] H. BOSCH and H. MUNCZEK, *Phys. Rev.* **106**, 983 (1957).

(4 days). The peaks of the Sb^{127}, as was expected, were only found in the first spectrum taken. In the spectra taken after 190 days only the peaks belonging to Sb^{125} were left.

The same source was beta-counted without absorber and with a 270 mg/cm² aluminium foil absorber. The decay curve without absorber showed four half-lives: 4 days (Sb^{127}), 12 days (Sb^{126}), 60 days (Sb^{124}) and a residual activity of half-life over one year which may be due to Sb^{125}. The analysis of the curve taken with aluminium absorbers shows only the 12 days and 60 days half-lives.

In earlier work at our laboratories and in other centres[5] no 30 day activity was found on irradiating the enriched heavy isotopes of tellurium with fast neutrons. In order to confirm these results enriched Te^{126} (80 per cent), Te^{128} (85 per cent) and Te^{130} (78 per cent) were irradiated once more with fast neutrons produced by 28 MeV deuterons on beryllium in the Buenos Aires synchro cyclotron. Some gamma spectra were taken at different times from the end of the irradiation and the decay curves were followed in a gamma-ray spectrometer. In no case could a 30 day activity be seen.

DISCUSSION

In the antimony fraction obtained from thermal fission 30 days from the end of the irradiation we only observed the half-lives of Sb^{127} and Sb^{125}, which were known already. The Sb^{124} and Sb^{126} half-lives were not seen because both isotopes are shielded and their independent yields in thermal fission are small.

In fission induced by 28 MeV deuterons, as was expected under our working conditions, all the isotopes with half-lives longer than 30 days were found. As the energy of the bombarding particles increases, Z_p (most probable charge in a fission chain) shifts towards Z_A (most stable charge), so that the independent fission yield of isotopes close to Z_A increases rapidly.

Both disintegration curves show no sign of a 30 days half-life.

The series of gamma spectra show only peaks belonging to isotopes already known, even though a complete analysis of the spectra was not possible because there were too many isotopes present with complex disintegration schemes.

The decay curves of the gamma activity were obtained by integration of several parts of the spectra taken at different times and no 30 day half-life was observed.

From our experiments we may conclude that in thermal fission and fission induced by 28 MeV deuterons on natural uranium no antimony isotope of 30 days half-life is formed. If such nuclide should exist, its mass number would be over 125. The only mass numbers possible would then be 126, 128 or 130, because the isotopes with odd A are known and do not admit isomers. Two isomers are known for each mass number for masses 126, 128 and 130, but a third isomer could exist as in the case for Sb^{124}. However, the experiments with enriched isotopes of tellurium of masses 126, 128 and 130 did not show any half-life of approximately 30 days.

Acknowledgement—The authors wish to express their appreciation to the crew of the synchro-cyclotron and the RA1 for the irradiations performed and to the Electronics Department for maintenance of the equipment.

M. C. PALCOS
R. RADICELLA
J. RODRIGUEZ

Radiochemistry Division National Atomic Energy Commission
Buenos Aires, Argentine Republic

[5] H. BOSCH. Private communication (1960).

Formation of antimony orthophosphate, $SbPO_4$

(*Received* 24 *December* 1960; *in revised form* 4 *February* 1961)

THERE are very few references in the literature to the preparation of antimony phosphates: standard reference sources[1,2,3] all quote identical early original sources and include only one or two more recent references.

[1] GMELIN, "*Handbuch der anorganische chemie*", System nummer 18, Teil B, Lieferung 3 (1949).
[2] P. PASCAL, "*Nouveau traité de chimie minéral*", Tome XI, p. 641, Masson et Cie, Paris (1958).
[3] J. MELLOR, "*Inorganic and Theoretical Chemistry*", Vol. IX, p. 585, Longmans Green and Co., London (1933).

Most of the methods described have been based on solution and precipitation techniques; this present note describes a thermogravimetric investigation into the formation of antimony orthophosphate $SbPO_4$, from antimony trioxide and orthophosphoric acid and shows that this compound can be conveniently prepared.

EXPERIMENTAL

Antimony trioxide (B.D.H., specially low in lead) and orthophosphoric acid (B.D.H., A.R. Grade, minimum 88 per cent H_3PO_4) were mixed together in suitable proportions to provide a range of Sb_2O_3:P_2O_5 ratios between 5:1 and 1:2, sufficient distilled water being added to give the mixture the consistency of a thin cream. The suspension was transferred to a porcelain ball mill containing a suitable charge of porcelain balls and then rolled for sixteen hours, after which it was transferred to a Pyrex basin and evaporated to dryness in an air oven at 130°C. The resulting white solid was easily ground and sieved except in the case of the mixture Sb_2O_3:P_2O_5 = 1:2, where the product had a putty-like consistency.

Samples of 1·500 gm were heated at a linear rate of temperature increase of approximately 5·5°C/min on a Stanton Model HT-M Thermobalance up to 1200°C using sintered alumina crucibles.

Thermograms of mixtures having an Sb_2O_3:P_2O_5 ratio greater than one show a weight gain due to oxidation of antimony trioxide between about 450°C and 550°C and a weight loss due to decomposition of antimony pentoxide and volatilisation of antimony trioxide from 1000°C upwards. Fig. 1 shows, as an example, a graph derived from a thermogram and showing the weight change of

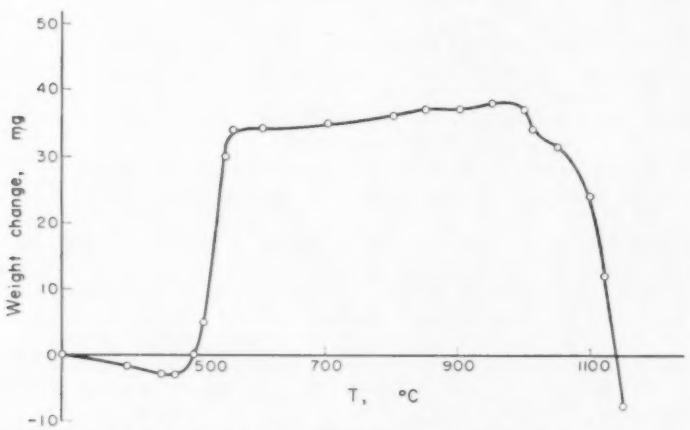

FIG. 1.—Weight changes in mixture Sb_2O_3: P_2O_5 = 3:1.

a sample of the mixture Sb_2O_3:P_2O_5 = 3, plotted against temperature. If the quantity of Sb_2O_3 in the mixtures in excess of that required to form $SbPO_4$ with the available P_2O_5 is calculated, and then plotted against the weight increase on oxidation, a straight line is obtained (Fig. 2); the line passes through the origin, confirming the thermogram of the mixture Sb_2O_3:P_2O_5 = 1, which shows no definite oxidation step nor volatilisation at 1000°C.

Expressed as a percentage of the excess antimony trioxide, the oxidation corresponds to a weight increase of 4·21 ± 0·38 per cent over the range of mixtures studied. When heated alone on the thermobalance, antimony trioxide shows a weight gain of 4·5 per cent over the range 520°C to 680°C agreeing closely with the value of 4·6 per cent obtained in a thermogravimetric study by Wanmaker and Verheyke.[4] Oxidation to Sb_4O_8 (or, $Sb_2O_3 \cdot Sb_2O_5$)[5] would require a weight increase of 5·5 per cent.

[4] W. L. WANMAKER and M. L. VERHEYKE, *Philips Res. Rep.*, 1956, **11**, 5.
[5] *Ann. Reports*, 1938, **35**, 119.

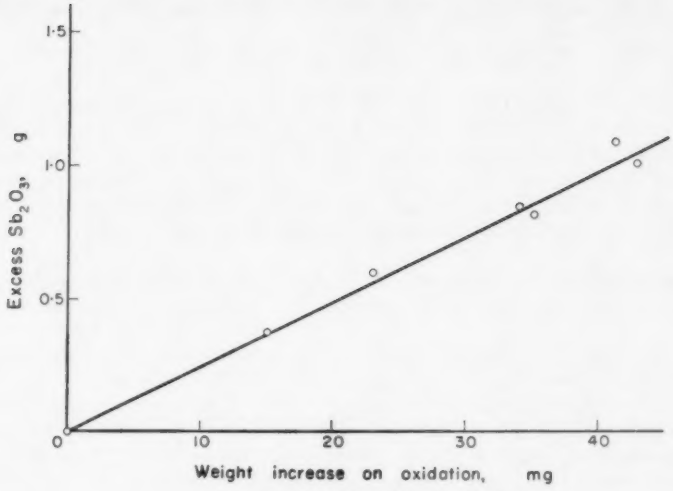

FIG. 2.—Oxidation of excess Sb_2O_3.

Except in the case of the 1:2 mixture, the thermograms did not show the marked loss of water which was expected to arise from the decomposition of phosphoric acid, thus suggesting that the antimony trioxide and phosphoric acid had interacted in the cold or, at least, in the drying stage This hypothesis is supported by the analytical data of Table 1, which shows the dried material to have a composition close to the theoretical composition. The mixtures were analysed by conventional methods, antimony being determined by titration with potassium bromate and phosphate volumetrically after precipitation as quinoline phosphomolybdate.

TABLE 1

Theoretical		Found at 130°C	
$\%Sb_2O_3$	$\%P_2O_5$	$\%Sb_2O_3$	$\%P_2O_5$
91·12	8·88	89·64	8·66
89·15	10·85	88·20	10·37
86·03	13·97	86·03	12·16
84·96	15·04	83·08	14·48
80·42	19·58	79·44	17·95
75·50	24·50	75·88	22·24
67·25	32·75	65·59	27·42
50·67	49·33	46·57	36·68

Further confirmation of this has been obtained by X-ray analysis; the standard powder diffraction technique, using CuKα radiation, was applied to the 1:1 ratio material taken after drying at 130°C, as described above, and to samples furnaced at temperatures up to a maximum of 800°C. All the samples gave the same diffraction pattern, presumably that of $SbPO_4$, and showed a slight increase in crystalline perfection with temperature increase. Antimony trioxide not detected.

Antimony orthophosphate is quite stable when heated in air; thermograms covering the ignition from room temperature to 1200°C show no apparent decomposition or volatilisation.

A.E.I. Lamp and Lighting Co. Ltd.
Head Office, Melton Road
Leicester, England

D. ROBBINS

12A—(4 pp.)

VOL. 19 1961

Production of carrier-free I-131 from telluric acid by an adsorption method

(*Received* 12 *September* 1960; *in revised form* 15 *March* 1961)

IN ALL wet processes[1–5] used for the production of I-131, iodine is separated from the irradiated tellurium or a telluric compound by distillation. Elementary tellurium is dissolved under strong oxidizing conditions, and the distillation process leads to samples containing impurities and the yield is rather low. With telluric acid as a target, the I-131 samples are of higher purity and the process is more efficient.[6] Distillation, however, involves some contamination by inactive material (e.g. NaOH, KOH, Na_2SO_4), because the distillate is trapped in an alkaline medium to prevent the escape of iodine.

Studies of the adsorption[7] and electrolytically-induced desorption of I-131 on a platinum surface have lead to a new technique for the preparation of chemically and radiochemically pure I-131.

The adsorption of I-131 onto platinum metal in solutions of varying pH has been studied by suspending a platinum disc in the solutions; the activity on the disc is measured by Geiger counting. Equilibrium adsorption is attained in about 30 min, and the adsorption rate is increased by increasing the hydrogen ion concentration. The adsorption equilibrium is considerably affected by the quality of the platinum surface, e.g. treatment of the platinum by chloro-nitric acid, annealing in an oxygen flame, or an anodic polarisation treatment, lead to small amounts of adsorbed iodine. The most satisfactory surface to give maximum adsorption was obtained by thorough polishing with a fine abrasive paper and after cathodical polarization. Iodine may be removed almost completely from the platinum by treatment with a strong oxidising reagent, or by making the platinum the anode of an electrolytic cell in which the cathode is also platinum but of much smaller surface area (presumably due to formation of an oxide layer).

Experiments to study the removal of iodine from solutions containing telluric acid have been carried out, and the following results obtained.

Telluric acid was irradiated in a quartz capsule, sealed in an aluminium can, at a neutron flux of 10^{13} n/cm²/sec. The activated telluric acid was then dissolved in 50 ml N sulphuric acid contained in a 50 ml platinum vessel. This vessel was agitated for 40 min and, after removing the telluric acid solution, was repeatedly rinsed with redistilled water. It was then filled with 50 ml redistilled water, into which a 6 cm² surface platinum disk was suspended, and a terminal voltage of 2–3 volts was applied to the vessel as anode, and the platinum disc as cathode, to initiate electrolytic polarization. Eighty-five per cent of the I-131 adsorbed on the platinum surface passed into the solution in 90 min; the results are as follows.

Experiment	Telluric acid dissolved in platinum vessel	I-131 activity in telluric acid	I-131 activity adsorbed on platinum surface	
	Grams	*mc*	*per cent*	*mc*
1.	1	5·7	74	2·2
2.	2·16	12	56	6·72
3.	4·32	24	56	13·44
4.	8·0	44	52	22·8
5.	18·2	180	48	86·0

[1] W. J. ARROL, J. CHADWICK and J. EAKINS, Progress in Nuclear Energy Series III. *Process Chemistry*, Vol. I. pp. 356–362 (1956).
[2] H. SELIGMAN, *Angew. Chem.* **66**, 95 (1954).
[3] K. TAUGBOL and U. BLIX, *Jener Report* No. 18 (1953).
[4] W. M. GARRISON and J. G. HAMILTON, *Chem. Rev.* 49 (1951).
[5] L. G. STANG, W. D. TUCKER, R. G. DOERING, A. J. WEISS, M. W. GREENE and H. O. BANKS, *UNESCO Report* NS/RIC/110.
[6] R. CONSTANT, *J. Inorg. Nucl. Chem.* **17**, 133 (1958).
[7] G. TÓTH, *KFKI Közlemények* **7**, 59 (1959).

The active and inactive impurities of the sample were analysed by gamma spectroscopy and optical spectroscopy.* The gamma spectrum showed no activity other than I-131 and a decay curve followed for ten half-lives showed not more than 0·05 per cent of contamination. This small contamination is attributed to long-lived I-129 produced from Te-128. By using a platinum vessel of suitable dimensions (surface of about 200–300 cm^2) the method can be used for producing I-131 in quantities of the order of 1 Curie.

Observations on the adsorption and electrolytic recovery of I-131 on platinum surface will be published in a subsequent paper.

G. Tóth

Hungarian Academy of Sciences
Central Research Institute for Physics
Budapest 114, *P.O. Box.* 49
Hungary

* The results showed no more impurities than in the redistilled water used.

VOL. 19 1961

Some experiments on the use of the chelating ion exchanger Dowex A-1 in nuclear chemistry

(*Received* 29 *September* 1960; *in revised form* 20 *March* 1961)

The chelating ion exchanger Dowex A-1[2] is, to our knowldege, the first commercially available material of this type. It has been shown in this laboratory[1] that divalent cations in the presence of complex-forming sodium triphosphate were strongly absorbed by the resin. Since hitherto no literature data concerning the behaviour of trivalent ions in this resin are known to the authors, it seemed interesting to extend the studies to this region. So far two preliminary experiments have been performed.

EXCHANGE BETWEEN La AND Cu IN Cu-SATURATED RESINS

A solution containing 25 ml of 0·3 C $CuCl_2$ solution, pH-buffer, 20 mg inactive $La(NO_3)_3 \cdot 6\,H_2O$ (corresponding to 3 per cent of the resin capacity), and radioactive La^{140} (produced by irradiation in the Danish high flux reactor DR 2) were mixed in a beaker together with Cu-saturated, 50–100 mesh, Dowex A-1 chelating resin at room temperature.

The activity of the solution was measured in a double-mantled GM-tube both before and at the end of different times of contact with the resin. At the end of the experiment, the resin was separated from the solution and washed with distilled water. The copper in the resin phase was displaced with

Table 1.—Copper-lanthanum equilibrium on A-1 resin

pH	3·08 (acetate-buffer)		2·28 (biphtalate-buffer)
Contact time	1 and 3·5 h	25 h	0·5 h
$\frac{Cu_r}{Cu_s}$	0·30	0·30	0·31
$\frac{La_r}{La_s}$	0·4*	0·57	0·5*

* Somewhat less accurate than the other figures.

[1] S. Forberg and S. Lundgren *Anal. Chem.* **32**, 1202 (1960).
[2] "Dowex Chelating Resin A-1", January 1959, The Dow Chemical Company, Technical Service and Development, Midland, Michigan.

1 N HCl and the amount of copper in both the solution and the resin was then determined by titration with EDTA using murexide as indicator. The resin capacity was found to be about 0·3 mmoles Cu/ml Na-form in agreement with Dow's brochure.[2] The ratio of the amounts of copper in the resin and solution is denoted by Cu_r/Cu_s and the analogous quantity for lanthanum by La_r/La_s. If A_I is the radioactivity in the solution before and A_{II} the activity after contact with the resin, then

$$\frac{La_r}{La_s} = \frac{A_I - A_{II}}{A_{II}}$$

The volume of the supernatant liquid was not influenced by the activity measurements. Table 1 shows the results obtained.

The experiment shows that the affinity of Dowex A-1 is slightly higher for La^{3+} than for Cu^{2+} under the experimental conditions employed here.

SEPARATION OF La^{3+} AND Lu^{3+} ON A COLUMN OF Ca-SATURATED RESIN

A solution containing 1·2 mmol inactive dysprosium (as a carrier and proposed, in addition, as a spacing medium), radioactive La^{140} and Lu^{177} (produced in the Danish DR 2 reactor), and acetate-buffer of pH 4·6 was sorbed on a column of the Dowex A-1 resin (50–100 mesh) in the Ca^{2+}-form. The amounts of La^{140} and Lu^{177} were chosen so that La^{140} gave the same β-counting rate as Lu^{177} when distributed over the same volume (30 ml) and measured in a flow-cell. The Ca^{2+}-form of the resin was chosen in order to prevent too great a shrinkage of the resin upon elution with acid[2] and to give a sharp borderline with respect to the rare earths (according to the previously determined distribution La-Cu and the selectivity scale in Dow's brochure[2]). The length of the column was 68 cm and it contained 62 ml of resin. Measuring the activity from outside with an end-window GM-counter showed no separate peaks in the band and no special colours could be seen.

The sorbed band was displaced with 0·1 N HCl at room temperature at a rate of 1·5 ml/min and the β-activity in the effluent was measured in a 0·25 ml flow cell with a thin window. The counting rate from a GM tube placed directly over the cell was continuously registered on an Esterline–Angus recorder. When the activity appeared after about 700 ml of effluent, the electrical conductivity was also measured continuously and the effluent was taken up in fractions in test-tubes. These fractions were analysed in a γ-spectrometer and the ratio of the areas under the 0·21 MeV photopeak of Lu^{177} and the 0·48 MeV photopeak of La^{140} was determined. The results are given in Table 2, and in Fig. 1 the β-counting rate and the electrical conductivity are plotted versus the effluent volume.

TABLE 2.—THE PHOTOPEAK RATIO OF Lu/La IN THE EFFLUENT

Lu/La	2·2*	2·7*	3·4	2·9	2·4	1·2	0·5	0·5
ml effluent	702	745	807	852	898	926	935	944

* Somewhat uncertain values.

DISCUSSION

The front of the β-activity curve in Fig. 1 does not exhibit a sharp boundary between Ca^{2+} and and R^{3+} (R = rare earth) as was expected. It might be possible that the lanthanide ions react slowly with the resin (perhaps due to the fact that the functional groups are divalent).

However, the rear of the activity curve shows a sharp front against the hydrogen ions, which is in good agreement with the rapid increase in the electrical conductivity, also shown in Fig. 1. Both the conductivity curve and the rear of the activity curve have a normal shape.

These facts and also the fact that the photopeak ratio Lu/La, shown in Table 2, is definitely lower at the end of the eluation, indicate that the high atomic number lutecium is eluted first and that further

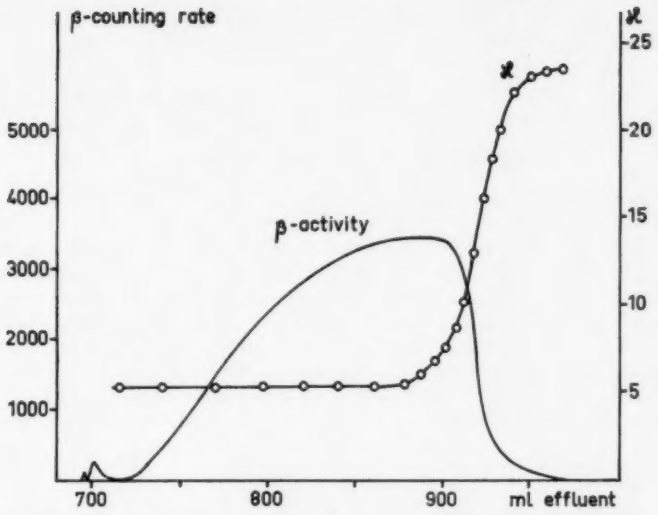

FIG. 1.—Plots of the β-counting rate and the electrical conductivity versus the effluent volume.

studies might provide a selective separation method for lanthanides which in some respects might be simpler than the successful methods used at present[3,4].

R. CHRISTELL*
S. FORBERG
T. WESTERMARK

Division of Physical Chemistry
The Royal Institute of Technology
Stockholm 70, Sweden

* Present address: Isotope Techniques Laboratory, Stockholm Ö.

[3] J. E. POWELL and F. H. SPEDDING, *Transactions of the Metallurgical Society of Aime*, Vol. 215, June 1959-457.
[4] J. E. POWELL and F. H. SPEDDING, *Chem. Eng. Progr.* Symposium Series, No. 24, **55**, 101 (1959).

(Contribution from the George Herbert Jones Laboratories of the University of Chicago)

The exchange reaction between uranyl ion and water in perchloric acid solution

(*Received* 9 *February* 1961, *in revised form* 30 *March* 1961)

RESULTS have been published on the uranium(V) catalysed exchange reaction between uranyl ion and water using a method whereby uranyl ion was precipitated directly.[1] This paper presents the results obtained in a continuation of these studies in which the intrinsic exchange between uranyl ion and water is shown to proceed at a reasonable rate.

EXPERIMENTAL

All of the chemicals used in this work were reagent grade. Uranyl perchlorate pentahydrate was prepared from uranyl nitrite.[1] Exchange experiments were done by adding perchloric acid solutions, which were enriched H_2O^{18} and through which chlorine gas had been passed, to weighed samples of $UO_2(ClO_4)_2 \cdot 5H_2O$. Lithium perchlorate was used to maintain constant ionic strength. After mixing, the samples were kept in a constant temperature bath at 25°C and chlorine gas was passed through the solution every 200–300 hr to insure removal of uranium(V).[1] Aliquots of UO_2^{++} solution were

[1] G. GORDON and H. TAUBE, *J. Inorg. Nucl. Chem.* **16**, 272 (1961).

VOL. 19 1961

removed as a function of time, and uranyl ferrocyanide was precipitated from them as described earlier.[1] The dried samples of $(UO_2)_2Fe(CN)_6$ were heated to 400°C with $HgCl_2$. The carbon dioxide formed was purified for analysis over zinc amalgam at 200°C. The isotopic composition of the CO_2 thus prepared was read directly on the mass spectrometer. Duplicate samples were usually taken and chlorine gas was bubbled through the solution after each set of samplings.

RESULTS AND DISCUSSION

Two sets of exchange experiments were carried out. One set at 0·939 M $HClO_4$ and a second set at 0·0939 M $HClO_4$. In all experiments the ionic strength was 3·79 and T = 25°C. Samples were collected over a total time period of 3200 hrs. Samples were taken at $t = 0$ and 25 hr to learn whether removal of uranium(V) by chlorine gas was complete. Subsequent samples were taken at ~400–600 hr intervals. The McKay[2] plots for the data obtained from the solutions which were 0·939 M in $HClO_4$ are not strictly linear, the initial points corresponding to a succession of half-lives which decrease as time increases, but the points after 500 hr conform to linear McKay plots. The deviation from linearity is not large as can be judged from the fact that the linear portion extrapolates to a value for $\log(1-f)$ only 4 per cent lower than the true value. Data for the series in 0·939 M H^+ were treated analytically to compute the reported half-lives, using the following relation.

$$t_{1/2(\text{computed})} = \frac{0{\cdot}30103\Delta t}{\Delta \log(1-f)}$$

derived from the McKay equation,[2] where f is the fraction of sample which has exchanged. Values of 700 hr or greater for Δt were chosen so as to minimize the scatter and the initial points were not included. From a total of 12 individual points, 31 half-lives were computed for each run. These results were averaged and they are presented along with the standard deviation in Table 1. The data for the experiments in 0·0939 M $HClO_4$ resulted in linear McKay plots and are also presented in Table 1.

Values for the rate of exchange for each experiment were calculated using data given in Table 1. The data on the exchange of uranyl ion and water establish the kinetic law for the principal path under the condition of our experiments to have the form $k[UO_2^{++}][H^+]^{-1}$, as the constancy of the coefficient k reported in Table 1 shows. The assumption made in calculating $t_{1/2}$ for experiments 3 and 4 appears to be valid since no apparent deviation from simple and reasonable kinetic behavior appears in the results. However, it must be admitted that the reason for the departure from linearity in the McKay plots of the data at 0·939 M $HClO_4$ is not known. It is possible that the half-life of UO_2^+ even in the presence of Cl_2 becomes very long when UO_2^+ is at extremely low concentration and the acidity is high.

TABLE 1.—THE EXCHANGE OF URANYL ION AND WATER IN PERCHLORIC ACID SOLUTION AT $\mu = 3{\cdot}79$ AND $t = 25°C$.

Experiment No.	M UO_2^{++}	M H^+	M H_2O^*	$t_{1/2}$ (hr)	k (M hr^{-1})
1	0·401	0·0939	55·4	$3{\cdot}57 \times 10^3$	$1{\cdot}81 \times 10^{-5}$
2	0·950	0·0939	55·4	$3{\cdot}55 \times 10^3$	$1{\cdot}80 \times 10^{-5}$
3	0·400	0·939	53·2	$3{\cdot}62 \pm 0{\cdot}07 \times 10^4$	$1{\cdot}78 \times 10^{-5}$
4	0·950	0·939	53·2	$3{\cdot}66 \pm 0{\cdot}13 \times 10^4$	$1{\cdot}75 \times 10^{-5}$

* Calculated from the density of $HClO_4$ and assuming that $LiClO_4$ can be substituted for $UO_2(ClO_4)_2$ to maintain constant ionic strength.

The dominant path for the exchange of UO_2^{++} with water presumably takes place through the ion UO_2OH^+. The present evidence,[1] which is admittedly incomplete, is that the rate of exchange of UO_2^+ with water is linear in H^+, and this conclusion is in accord with the observations of MASTERS and SCHWARTZ[3] on U exchange between U(IV)–U(V)–U(VI). The difference between the exchange behavior of UO_2^{++} and UO_2^+ is interesting but the reason for it is not understood.

[2] H. A. McKAY, *Nature, Lond.* **142**, 997 (1938).
[3] B. J. MASTERS and L. L. SCHWARTZ, *J. Amer. Chem. Soc.* In press.

Acknowledgements—The authors wish to thank the National Science Foundation for support of this work under Contract No. N.S.F. G-5411, and Richard Thompson for purification and analysis of the uranium compounds.

G. GORDON*
H. TAUBE

Department of Chemistry
University of Chicago
Chicago 37, *Illinois*

* Present address: *Department of Chemistry, University of Maryland, College Park, Maryland.*

Hexa-*n*-Alkylamino triphosphonitriles, $[NP(NHR)_2]_3$

(*Received* 9 *March* 1961)

VOL. 19 1961

ALTHOUGH the reactions of trimeric phosphonitrilic chloride have been explored extensively,[1,2] no quantitative correlation of the observed physical properties of a series of related derivatives of the compound has been attempted. In evaluating the characteristics of a series of aminolysis products of the type $[NP\{NH(CH_2)_nCH_3\}_2]_3$, where $n = 0$–5, the authors have noted trends in melting point and frequency of the P–N ring stretching mode that lend themselves to interpretation in terms of structural factors.

EXPERIMENTAL

All derivatives were prepared by aminolysis

$$[NPCl_2]_3 + 12\,RNH_2 \rightarrow [NP(NHR)_2]_3 + 6RNH_3Cl$$

in refluxing benzene and purified by recrystallization as previously described for the tetrameric analogues.[3] Pertinent details relating to synthesis, analysis, and properties are summarized in Table 1. All infra-red spectra were measured with a Model 21 Perkin–Elmer instrument, using a sodium chloride prism.

DISCUSSION

The melting point of a crystalline substance is a function of the molecular (dispersion forces) present, the shape of the molecules, and the type of crystal lattice. The influence of these factors is indicated by deviations from linearity among the melting points of homologous paraffin hydrocarbons, fatty acids, glycols, and diamides of alkyl dicarboxylic acids.[6]

For the phosphonitrilic compounds in question, these factors may be considered in terms of the lattice energy (U) and the intermolecular forces (E) of the crystals. Melting point can be expected to vary directly with the lattice energy. As n increases in compounds of the type $[NP\{NH(CH_2)_nCH_3\}_2]_3$, steric repulsions increase, and decreases in lattice energy and melting point are reasonable. On the other hand, alteration in intermolecular forces by changes in polarizability of the alkyl group[7] is also important. Although differences in inductive effects among alkyl groups are small, differences in polarizability are sufficient to modify London dispersion forces (E) significantly.[8] As n increases,

[1] N. L. PADDOCK and H. T. SEARLE, *Advances in Inorganic Chemistry and Radiochemistry*, (H. J. Emeléus and A. G. Sharpe, Eds.), Vol. 1, pp. 347–383. Academic Press, New York (1959).
[2] L. F. AUDRIETH, *Rec. Chem. Progr.*, **20**, 57 (1959).
[3] K. JOHN, T. MOELLER, and L. F. AUDRIETH, *J. Amer. Chem. Soc.* **83**, (1961). In press.
[4] M. BECKE-GOEHRING, K. JOHN, and E. FLUCK, *Z. Anorg. Allgem. Chem.* **302**, 103 (1959).
[5] S. K. RAY and R. A. SHAW, *Chem. Ind.* p. 53 (1959).
[6] J. A. LEERMAKERS and A. WEISSBERGER, *Organic Chemistry, An Advanced Treatise*, (H. Gilman, Ed.) Vol. II, p. 1727. John Wiley and Sons, New York (1947).
[7] T. L. BROWN, *J. Amer. Chem. Soc.* **81**, 3232 (1959).
[8] T. L. BROWN, *J. Amer. Chem. Soc.* **81**, 3229 (1959).

increase in polarizability thus increases intermolecular forces and should result in an increase in melting point. It is apparent that counterbalance of the opposing lattice energies and dispersion forces is reached with the *n*-butyl derivative, the first of these being predominant at $n < 3$ and the second at $n > 3$. An extension of these considerations to melting-point data for the corresponding octa-substituted aminolysis products of tetrameric phosphonitrilic chloride[3] would predict a minimum at $n > 5$. X-ray data permitting evaluation of unit-cell dimensions would provide supporting evidence for postulated variations in lattice energy.

TABLE 1.—SYNTHESIS AND PROPERTIES OF $[NP(NHR)_2]_3$

Compound	Yield per cent	Analysis				Melting point (°C)	P–N Frequency (Ring) (cm^{-1})
		P per cent	C (%)	H (%)	N (%)		
$P_3N_3(NHCH_3)_6$[4]	85					258	1175 (KBr disk or Nujol mull)
$P_3N_3(NHCH_2CH_3)_6$[5]	—					119	—
$P_3N_3[NH(CH_2)_2CH_3]_6$	80	Calcd. 19·22	44·70	10·01	26·07	56	1195 (5 per cent in CH_3CN)
		Found 18·84	44·56	10·06	26·02		1183 (KBr disk)
$P_3N_3[NH(CH_2)_3CH_3]_6$	84	Calcd. 16·37	50·77	10·65	22·21	30	1195 (5 per cent in CH_3CN)
		Found 16·02	50·49	10·66	22·53		
$P_3N_3[NH(CH_2)_4CH_3]_6$	82	Calcd. 14·26	55·27	11·13	19·34	38	1190 (10 per cent in CS_2)
		Found 13·96	54·84	11·26	19·41		1183(KBr disk)
$P_3N_3[NH(CH_2)_5CH_3]_6$	87	Calcd. 12·63	58·74	11·50	17·13	49	1192 (5 per cent in CH_3CN)
		Found 12·70	58·47	11·15	16·86		1185(KBr disk)

The P–N ring frequency is influenced by coupling of this vibration to vibrations of the substituents on the phosphorus atom.[9] It is thus of interest to attempt to relate the electron-donor ability of an amine to the observed frequency of the P–N vibration of its aminolysis product. The data in Table 1 reveal little variation in this frequency where $n > 0$, suggesting comparable inductive and steric influences by all these alkyl groups regardless of size. The substantially lower frequency for the methylamino derivative ($n = 0$) is significant. It might be inferred that the necessity for using potassium bromide- and mull-techniques for measurement, because of the reduced solubility of the compound, could enhance lattice interactions and thus alter the P–N frequency sufficiently so that these data could not be compared with those for solutions of the other derivatives. However, differences between disk and solution values for other derivatives are not significant (Table 1).

Contributing resonance forms for compounds of this type include

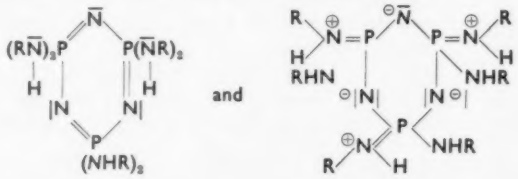

I II

The more extensive the contribution by II, the greater the single-bond character of the ring and the lower the ring P–N frequency. Highly electronegative substituents such as fluorine and chlorine should favour I because of the difficulty of their assuming positive charges. That the observed ring

[9] H. J. BECHER and F. SEEL, *Z. Anorg. Allgem. Chem.* **305**, 148 (1960).

P–N frequencies are 1287 cm^{-1} and 1218 cm^{-1} for $(NPF_2)_3$ and $(NPCl_2)_3$, respectively,[1] supports the concept of favouring I by electronegative substitution. Indeed, Paddock has pointed out that among the trimeric methyl and halo phosphonitriles the P–N frequency increases regularly with increasing electronegativity of the substituent.[10] Although it would then follow that II might be favoured by the much less electronegative amine-type substituents, steric hindrance by the R groups must be considered also. Where little or no steric hindrance can exist, e.g., with $[NP(NHCH_3)_2]_3$ or $[NP(NH_2)_2]_3$,[11] the ring P–N frequency is 1175 cm^{-1}, and II must contribute significantly. Increasing steric hindrance by increasing the size of the alkyl substituent then favours I and is reflected in frequencies in the 1190 cm^{-1} range. It is significant both that a value of 1195 cm^{-1} has been reported for $[NP\{N(CH_3)_2\}_2]_3$[5] and that a structural analysis of $[NP\{N(CH_3)_2\}_2]_4$ reveals that one dimethylamino group on each phosphorus atom is planar and contains a shorter P–N bond.[12] The latter suggests some double bond character in the exo P–N linkage, as demanded by II for the analogous trimer. Again detailed structural determinations are essential to provide a complete answer to this problem.

It is of interest that the same trends as regards canonical forms of types I and II are noted for octa-substituted tetrameric derivatives.[3] Thus the ring P–N frequency is 1305 cm^{-1} for $[NPCl_2]_4$[1], 1262 ± 3 cm^{-1} for *n*-alkylamino derivatives where $n = 1$–5,[3] 1240 cm^{-1} for $[NP(NH_2)_2]_4$[11], and 1215 cm^{-1} for $[NP(NHCH_3)_2]_4$.[3]

Acknowledgement—This investigation was supported by Contract AF-33(616)-5486 with the Materials Laboratory of Wright Air Development Command, Wright–Patterson Air Force Base, Ohio. Reproduction of this communication in whole or in part is permitted for any purpose of the United States Government.

S. G. KOKALIS
K. JOHN
T. MOELLER
L. F. AUDRIETH

Noyes Chemical Laboratory
University of Illinois
Urbana, Illinois

[10] N. L. PADDOCK, Paper presented at 135th National Meeting of the American Chemical Society, Boston (1959).
[11] L. F. AUDRIETH and D. B. SOWERBY, *Chem. Ind.* 748 (1959).
[12] G. J. BULLEN, *Proc. Chem. Soc.* 425 (1960).

VOL. 19 1961

J. Inorg. Nucl. Chem., 1961, Vol. 19, p. 194. Pergamon Press Ltd. Printed in Northern Ireland

BOOK REVIEW

S. DOCKX: **Théorie Fondamentale du Système Périodique des Eléments.** Office International de Librairie, Brussels 1959, 183 pp. No price stated. (Archives de l'Institut International des Sciences Théoriques, Volume 10).

The original idea of a periodic classification of the elements derives from Béruger de Chancourtois in France (1862) and Newlands in England (1864). But the classic exposition is due to Mendeléeff in 1869. Until the rise of Bohr's quantum theory, this classification was purely empirical, being based solely on similarity of chemical behaviour. But first Bohr and more recently the wave mechanics of Schrodinger have shown the underlying reason for the existence and nature of a periodic table. In the present book the author, who is Director of the Institut International des Sciences Théoriques proposes a modification of this table. He is concerned because the various shells (K, L, M . . .) do not always get completely filled before electrons start forming the next outer shell. Notable examples of this are the transition elements of the first and second long periods, where the 4s and 5s sub-shells are completed before the 3d and 4d orbits are used. The rare earths with their 4f sub-shell and the actinides with their 5f sub-shell, are other examples.

In order to rationalise this, the author defines a new series of periods, the first seven of which are, in sequence;

$$1s^2;\ 2s^2;\ 2p^6,\ 3s^2;\ 3p^6,\ 4s^2;\ 3d^{10},\ 4p^6,\ 5s^2;\ 4d^{10},\ 5p^6,\ 6s^2;\ 4f^{14},\ 5d^{10},\ 6p^6,\ 7s^2.$$

It is asserted that in the ground states of the atoms, each period is completely filled before the next one is started. A group of five theorems relate to the order of filling within any one period. In a formal way this may be correct—though even now there appear to be some exceptions. But this mathematical regularity is achieved at the expense of grouping together the six p-electrons of one of Mendeléef's shells with the two s-electrons of the next. If the author had paid more attention to the observed and calculated charge distributions and mean radii for s and p orbitals, and the expected variations of the Hartree–Fock parameters for s, p and d orbitals as the atomic number was increased; and if he had recognised more clearly that even to speak of orbitals (with no mention of configuration interaction) is a serious oversimplification, and that the total energy of any atomic configuration depends critically on the electron-interaction as well as on the sum of the Hartree–Fock parameters (or ionization potentials), the present reviewer believes that he would have hesitated before abandoning a scheme which, although it may not possess the same mathematical regularity as the one here being proposed, yet does more justice to our physical knowledge of the nature and size of atomic orbitals.

C. A. COULSON

J. Inorg. Nucl. Chem., 1961, Vol. 19, p. 195. Pergamon Press Ltd. Printed in Northern Ireland

ANNOUNCEMENT

An informal conference, organized jointly by the European Organization for Nuclear Research (CERN) and the Max Planck Institute at Heidelberg, entitled:

CONFERENCE ON FISSION & SPALLATION PHENOMENA AND THEIR APPLICATION TO COSMIC RAYS

will take place at the CERN Laboratories, Meyrin (Geneva) from September 26 to 29. Attendance will be by invitation only.

VOL.
19
1961

For further information, please apply to:

Scientific Conference Secretariat:

(E. W. D. Steel)

CERN

Geneva 23, Switzerland.

J. Inorg. Nucl. Chem., 1961, Vol. 19, pp. 197 to 203. Pergamon Press Ltd. Printed in Northern Ireland

NEW ISOTOPES OF EMANATION AND FRANCIUM: ^{223}Em, ^{224}Em and ^{224}Fr*

A. V. BELLIDO
Universidad Nacional San Agustin de Arequipa, Peru

(*Received* 12 *September* 1960; *in revised form* 11 *November* 1960)

Abstract—An examination of the products of the interaction of thorium with 230 MeV protons has revealed evidence for the existence of the neutron-excess isotopes: ^{223}Em, ^{224}Em and ^{224}Fr.

The existence of these three new isotopes was confirmed by identification of their decay products: ^{223}Ra and ^{224}Ra.

VOL. 19 1961

THE purpose of this research work, carried out in the Radiochemistry Laboratories at Liverpool University, was to try to find new isotopes of emanation in the neutron excess region, particularly ^{223}Em and ^{224}Em. As a result of this work it is possible to point out the existence of the three new isotopes: ^{223}Em, which has been previously indicated by BAERG[1] in measurements of the cross-section of ^{222}Em for slow neutron capture in a reactor; also ^{224}Em and ^{224}Fr, neither of which have been reported up to this moment.

The β^- decay energies, calculated by FOREMAN and SEABORG,[2] for these isotopes are:

$$^{223}\text{Em} = 1{\cdot}91 \text{ MeV}$$
$$^{224}\text{Em} = 0{\cdot}70 \text{ MeV}$$
$$^{224}\text{Fr} = 3{\cdot}09 \text{ MeV}.$$

Using this data and the graphs given by GLASS *et al.*,[3] the half-lives for these isotopes are:

$$^{223}\text{Em} = 12 \text{ min}$$
$$^{224}\text{Em} = 4{\cdot}9 \text{ hr}$$
$$^{224}\text{Fr} = 2 \text{ min}.$$

Since it is difficult to assign the correct value of (log ft) to these transitions, the calculated half-lives are only approximate, but they give an order of magnitude value.

It was thought possible to prepare these isotopes by bombarding thorium targets in the synchrocyclotron with high energy protons.

Although it is easy to separate emanation gas from the bombarded thorium target, direct counting of the radioactive gas was not possible for the following reasons:

(i) in a spallation of thorium, practically all known isotopes of emanation are formed. with half-lives ranging from a few minutes to several days and the decay curve would be exceedingly complex and impossible to resolve;

* Research work carried out in Radiochemistry Laboratories at Liverpool University 1959-60.

[1] A. P. BAERG, *Phys. Rev.* **90**, 1121 (1953).
[2] B. M. FOREMAN, JR. and G. T. SEABORG, *J. Inorg. Nucl. Chem.* **7**, 305 (1958).
[3] R. A. GLASS, S. G. THOMPSON and G. T. SEABORG, *J. Inorg. Nucl. Chem.* **1**, 3 (1955).

(ii) in addition to emanation, neutron excess isotopes of krypton and xenon are also formed in high yield by the high energy fission of ^{232}Th, and these will also make the gross decay curve, of the separated rare gases, more complex.

In these circumstances, the experimental problem was faced in the following way:

If we assume that these unknown isotopes decay by β^- emission, the ^{223}Em will decay into ^{223}Fr (22 min) which in turn decays into ^{223}Ra (11·6 days), and the ^{224}Em will decay into ^{224}Fr (unknown) which almost certainly will β^- decay into ^{224}Ra (3·64 days). (Figs. 1–2.) Therefore, if after bombardment we quickly extract emanation

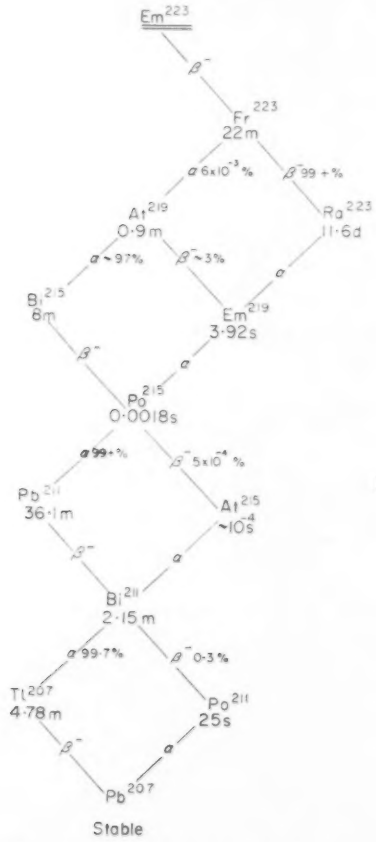

FIG. 1.—Decay scheme of ^{223}Em.

and allow the isotopes ^{223}Em and ^{224}Em to decay, a separation of radium from the decay products and, an identification of the ^{223}Ra and ^{224}Ra, α-emitters, will provide a definite proof that the emanation ancestors were formed by spallation reaction on thorium.

The identification of the ^{223}Ra and ^{224}Ra was carried out:

(i) by chemical separation of radium and determination of the half-lives by direct counting of samples; and

(ii) by chemical separation and half-life determination of ^{211}Pb (36·1 min) and ^{212}Pb (10·64 hr), products of the radioactive decay of ^{223}Ra and ^{224}Ra respectively. (See Figs. 1–2.)

VOL. 19 1961

Finally, in order to verify that the radium had not been carried directly, by the gas stream, during the separation of emanation, a special test was performed.*

The content and results of this research work is described in the following sections:

A. *Target and type of bombardment*

$^{232}Th_{90}$ in its compound ThO_2, was chosen as the most suitable target for bombardment, and sealed in a silica tube. The weight of ThO_2 used in each bombardment was about 0·2 g.

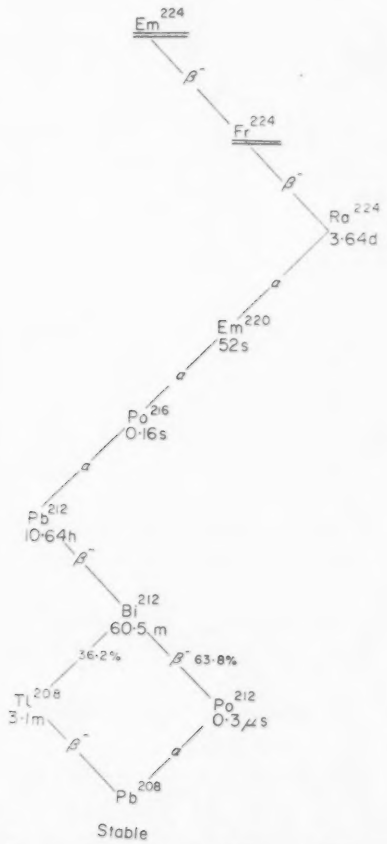

FIG. 2.—Decay scheme of ^{224}Em and ^{224}Fr.

The bombardments were carried out in the Nuclear Physics Research Laboratory's 156 in. synchrocyclotron, at Liverpool University. The internal beam was used at 51 in. corresponding to 230 MeV protons and the duration of bombardment was 30 min.

* It is necessary to point out that in different experiments a trial was made to isolate francium from the decay products of emanation in order to determine the half-lives of the ^{223}Em and ^{224}Em by milking experiments, but these attempts were thwarted by caesium which appeared in a high yield as fission product of thorium. In fact, a chemical procedure was devised to isolate francium as silicotungstate which gave a sample quite clean from all elements except caesium, since the β^- activity was shown to correspond to a nuclide 31 min half-life. This activity can be identified with ^{138}Cs.

B. *Extraction of emanation*

After 14 min from the end of bombardment, the targets were broken in a special opening tube attached to the apparatus (Fig. 3) and the extraction of the gas was performed as follows:

The target dropped, from the opening tube *C*, into a round-bottomed flask *A*, containing hot concentrated nitric acid and ammonium fluosilicate in 0·01 M solution.

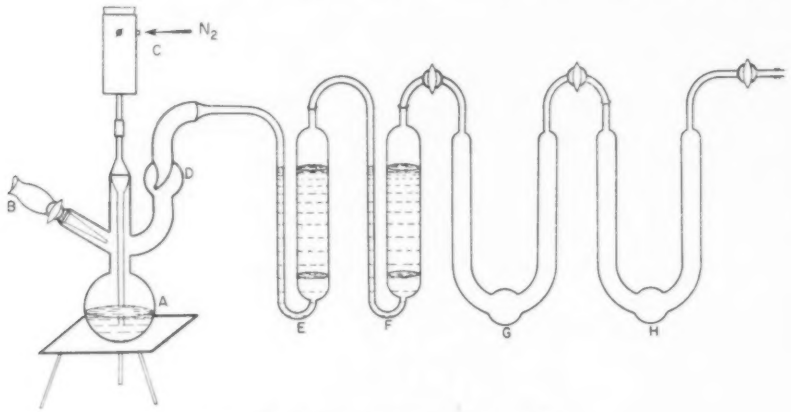

FIG. 3.—Apparatus for extraction of Em.

The gases liberated, as the solid dissolved, were swept by a slow current of nitrogen through a splash-head *D*, through the trap *E*, containing concentrated sodium hydroxide solution (in order to trap astatine) then, through the trap *F*, containing concentrated sulphuric acid (to trap water and to eliminate all possibilities of radium contamination), and, finally, the emanation was collected in two cold traps *G* and *H* cooled with liquid oxygen.

The traps *E* and *F* had a sintered disk at the bottom in order to break the gas stream into fine bubbles to improve the efficiency of the traps.

C. *Separation of radium; identification of radium daughter products*

The emanation, which was collected in the traps *G* and *H*, was allowed to decay for 8 hr and after this time a separation of radium was carried out.

The following chemical procedure was used to separate radium:

(1) The decay products of emanation were taken up in 20 ml 0·3 N HNO_3 solution, using 10 ml for each trap, and the solution transferred to a 50 ml centrifuge tube;

(2) To the solution, in the centrifuge tube, 1 ml barium nitrate solution (5 mg/ml Ba^{2+}) was added as holdback carrier for Ra. In addition, 1 ml lead nitrate solution (3 mg/ml Pb^{2+}) and 1 ml bismuth chloride solution (6 mg/ml Bi^{3+}) were added as carriers for the decay products of emanation;

(3) Hydrogen sulphide was passed through the solution to precipitate lead, bismuth and polonium as sulphides. These sulphide precipitates also act as scavenger for astatine and any other activities, which may be present. The suspension was centrifuged, filtered and the precipitate discarded;

(4) Further, 1 ml portions of lead and bismuth carriers were added to the

centrifugate and precipitated again with hydrogen sulphide. The suspension was centrifuged, filtered and the precipitate discarded;

(5) Step 4 was repeated;

(6) Four ml 6 N H_2SO_4 solution was added to the clear solution to precipitate $BaSO_4$ which carried the radium activity by coprecipitation. The $BaSO_4$ precipitate was separated by centrifugation;

(7) The precipitate was washed, first with 10 ml of water and 1 ml 6 N H_2SO_4, centrifuged, and then washed with 5 ml of acetone and centrifuged off;

(8) The precipitate was mounted on a planchet for α-counting, with the help of a few drops of acetone and dried under an infra-red lamp.

The α-activity of the radium was measured with an α-scintillation counter for a period of 1–2 months. The decay curve (Fig. 4) has two components which decay with half-lives of 3·4 days and 11·2 days giving a definite identification of ^{223}Ra and ^{224}Ra

VOL. 19 1961

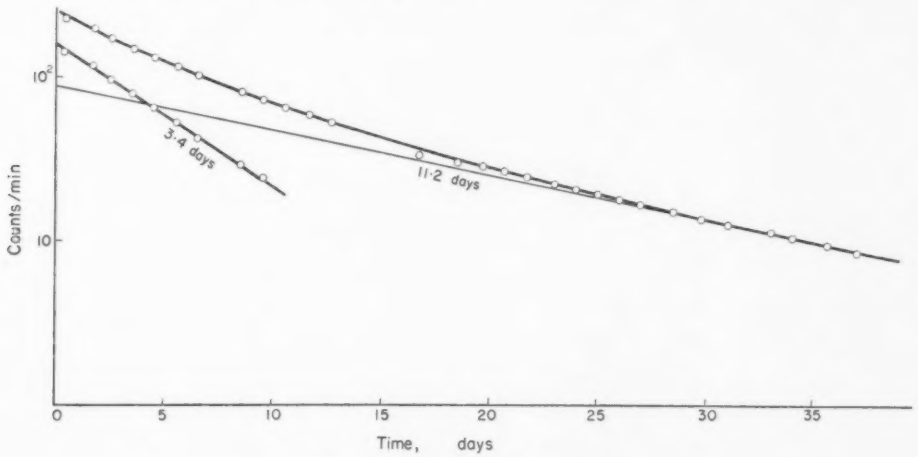

FIG. 4.—α-activity in a Ra sample.

and indicating that ^{223}Em and ^{224}Em were formed in the bombardment and then decayed into above mentioned radium isotopes.

No strontium and barium isotopes, which may be present in the sample, due to decay of krypton and xenon isotopes, would have been detected by the α-scintillation counter, since they are beta emitters. The counter is comparatively insensitive to beta activity and accurate alpha measurements can be made in the presence of β-particles of up to 10^9 disintegrations/min.

D. *Separation of lead; identification of* ^{211}Pb *and* ^{212}Pb

In order to be quite sure about the identity of ^{223}Ra and ^{224}Ra, separations of lead were carried out from the radium isolated from the decay products of emanation, according to the procedure described in the preceding section.

It can be seen, from Figs. 1 and 2, that ^{211}Pb (36·1 min) and ^{212}Pb (10·64 hr) are present as members of the decay chains of ^{223}Ra and ^{224}Ra respectively. Therefore, isolation and identification of these isotopes would provide convincing proof of the identity of the radium parents.

The separation of lead from radium was performed using the following chemical procedure:

(1) The $BaSO_4$ precipitate was transferred to a 100 ml beaker, and 10 ml 50% K_2CO_3 solution was added. The suspension was boiled for 5 min to convert the Ba, Ra SO_4 to Ba, Ra CO_3. Ten ml of water was added and the suspension transferred to a 50 ml centrifuge tube, centrifuged and the solution discarded;

(2) The precipitate was washed with 10 ml of water, centrifuged off and then dissolved in about 10 ml of 0·3 N HNO_3 and 2 ml lead nitrate solution (3 mg/ml Pb^{2+}) and 1 ml bismuth chloride solution (6 mg/ml Bi^{3+}) were added, as carriers.

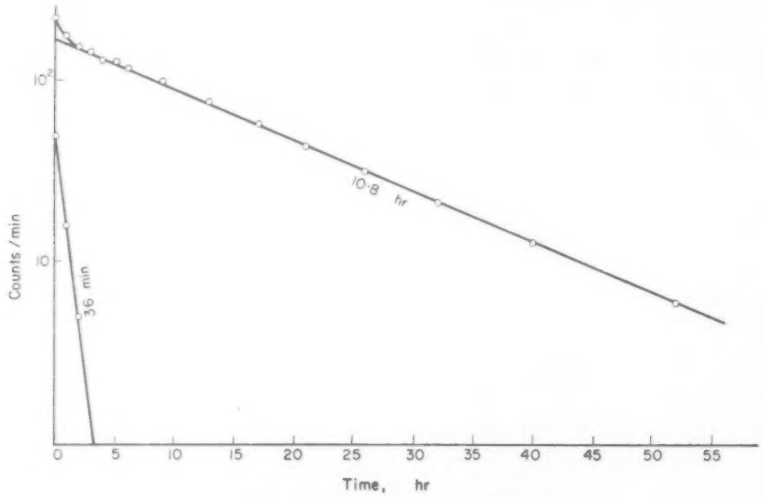

FIG. 5.—β-activity in a Pb sample.

(3) Hydrogen sulphide was passed through the solution in order to precipitate lead and bismuth as sulphides. The precipitate was centrifuged off and the solution retained for further separations of lead;

(4) The precipitate was washed twice with 10 ml of water, centrifuged off, and then washed with 5 ml of acetone and centrifuged off;

(5) The precipitate was mounted on a planchet for β-counting, using a few drops of acetone and dried under an infra-red lamp. Finally, the precipitate was fixed with five drops of collodion in acetone (1:25) and dried.

The β^- activity was measured by counting the samples with an end-window Geiger–Müller counter and the radioactive decay was followed for 4 days. The number of counts per minute was plotted against time on semilogarithmic paper.

The graphs (Fig. 5) confirmed that the lead isotopes separated were daughters of ^{223}Ra and ^{224}Ra since they show two components which decay with half-lives of 36 min and 10·8 hr, in good agreement with the half-lives reported for the ^{211}Pb and ^{212}Pb, respectively.

E. *Test for contamination*

There was a possibility that the separated isotopes ^{223}Ra and ^{224}Ra had been directly carried, by the gas stream, into the traps from the target solution through the

apparatus for extraction of emanation, since it is very probable that these radium isotopes are formed in high yield in thorium spallation.

In order to eliminate any doubt on this matter a test for contamination was performed in the following way:

The target solution from a bombardment was kept and, after 6 days—sufficient time for the decay of all ^{223}Em and ^{224}Em which may have remained in the solution—it was placed in the round-bottomed flask of the apparatus for extraction of emanation (Fig. 3) and using all the complete set, as in other experiments, a nitrogen stream was passed through the target solution and apparatus.

After working for about six times the usual operating time, i.e. $1\frac{1}{2}$ hr, the traps *G* and *H* were taken out of the liquid oxygen Dewars and a separation of radium was carried out.

The radium sample was counted on the α-scintillation counter and gave 3 counts per min, i.e. less than 1 per cent of the counting rate observed in the other experiments. This shows that the obtained results are not due to contamination from the target solution.

VOL.
19
1961

Conclusions

As a result of this research work it is possible to indicate the existence of the three new isotopes, in the neutron excess region, which decay by β^- emission: ^{223}Em, ^{224}Em and ^{224}Fr.

Acknowledgements—I wish to express my sincere gratitude to F. D. S. Butement, Head of the Radiochemistry Laboratories at the University of Liverpool, who suggested the subject for this work and gave me assistance whilst it was carried out; and, also, to G. B. Briscoe and V. J. Robinson, for their valuable help and advice.

I wish to thank too the crew of the Nuclear Physics Research Laboratory's 156 in. synchrocyclotron and especially Mr. B. S. Halliday, for help with the bombardments.

I am deeply indebted to the British Council for a grant whilst this research was in progress.

J. Inorg. Nucl. Chem., 1961, Vol. 19, pp. 204 to 207. Pergamon Press Ltd. Printed in Northern Ireland

INFLUENCE OF CARBON DIOXIDE ON THE YIELDS OF HYDROGEN ON IRRADIATION OF AQUEOUS SOLUTIONS OF ORGANIC COMPOUNDS WITH ^{60}Co γ-RAYS

J. T. ALLAN, N. GETOFF, H. P. LEHMANN, K. E. NIXON,
G. SCHOLES and M. SIMIC
King's College, University of Durham, Newcastle upon Tyne.

(*Received* 5 *December* 1960)

IN some studies of the effects of ^{60}Co γ-rays on deaerated aqueous solutions of certain aliphatic alcohols, e.g. methanol, ethanol, t-butanol, it has been noticed that the yields of hydrogen gas obtained from solutions irradiated in the pH range ~4 to ~7 were somewhat irreproducible. With methanol solutions, in particular, the measured hydrogen yields in this pH range were considerably lower than anticipated from stoichiometric considerations of the measured radiolysis products.[1] It was suspected that this irreproducibility and the low values of the hydrogen yields may be associated, at least in part, with the presence of small amounts of carbon dioxide (or bicarbonate) in the irradiated solutions, since carbon dixoide (or bicarbonate) is known to react with the "hydrogen atom" species produced in the radiolysis of aqueous systems.[2] Normally, the irradiations were carried out after evacuation of solutions which had been previously adjusted to the required pH by either Sorensen phosphate buffer (10^{-3} M) for pH values in the range pH ~5 to pH ~8, or by sulphuric acid for lower pH's. To test whether adventitious quantities of carbon dioxide were responsible for the discrepancies, a modified experimental technique was used to eliminate, to a greater or lesser extent, any carbon dioxide from the solutions prior to irradiation. This consisted of evacuation of solutions acidified with sulphuric acid (pH ~3) and then adjustment to the required pH by the addition of solid buffer contained in a side-arm of the irradiation vessel (final buffer concentration $= 7 \times 10^{-3}$ M).

Table 1 shows some values of the hydrogen yields obtained on irradiation of solutions of methanol, ethanol and of t-butanol after using the "normal" and "modified" evacuation techniques. It can be clearly seen that with the latter technique higher gas yields were consistently obtained.

Some experiments have also been carried out with aqueous solutions of various organic substances saturated with carbon dioxide (1 atm; pH 3–4). It was found in all the systems examined that carbon dioxide substantially depressed the yield of hydrogen on irradiation. Table 2 shows some results obtained from solutions of oxalic acid, t-butanol, formaldehyde and formic acid. Lowering the pH reduced the effect of added carbon dioxide until, in 0·8 N sulphuric acid solutions, this was essentially zero. The pH-dependence was studied in greater detail with ethanol solutions (Fig. 1).

[1] J. LYON, Thesis, University of Durham (1960).
[2] W. M. GARRISON and G. K. ROLLEFSON, *Discussion Faraday Soc.* **12**, 155 (1952); N. GETOFF, G. SCHOLES and J. WEISS, *Tetrahedron Let.* No. 18, 17, (1960); G. SCHOLES, M. SIMIC and J. WEISS, *Nature, Lond.* **188**, 1019 (1960).

In several of these systems irradiated in the presence of carbon dioxide small quantities of carbon monoxide were detected among the gaseous products. At pH ~3, $G(CO)$ values varied from 0·02 for the t-butanol and oxalic acid solutions to 0·1 for the formaldehyde and formic acid solutions (G = molecules/100 eV).

TABLE 1.—YIELDS OF HYDROGEN FROM DEAERATED AQUEOUS SOLUTIONS OF VARIOUS ALIPHATIC ALCOHOLS IRRADIATED WITH ^{60}Co γ-RAYS, USING DIFFERENT EVACUATION TECHNIQUES PRIOR TO IRRADIATION

Solution	Evacuation technique*	Yields of hydrogen† (G)
10^{-2} M Methanol; pH = 7·6	Normal	1·1
	Modified	2·0
2×10^{-2} M Ethanol; pH = 7·25	Normal	1·3
	Modified	1·5
10^{-1} M t-Butanol; pH = 5·0	Normal	1·1
	Modified	1·7

* See text for description.
† Average values using doses up to 2×10^{18} eV/ml.

TABLE 2.—INFLUENCE OF CARBON DIOXIDE (1 ATM) ON THE INITIAL YIELDS OF HYDROGEN FROM DEAERATED SOLUTIONS OF VARIOUS ORGANIC SUBSTANCES IRRADIATED WITH ^{60}Co γ-RAYS

Solution	Initial yields of hydrogen (G)	
	In the absence of CO_2	In the presence of CO_2 (1 atm)
10^{-3} M Oxalic acid; pH 3·0	1·26	0·45
10^{-3} M Oxalic acid; pH 0·5	1·54	1·54
10^{-2} M t-Butanol; pH 4·0	1·5*	0·45
10^{-2} M Formaldehyde; pH 3·5	2·93	1·33†
10^{-2} M Formic acid; pH 0·5	2·50	2·50
10^{-2} M Formic acid; pH 1·9	3·10	2·03
10^{-2} M Formic acid; pH 2·95	3·25	1·22

* Average value using doses up to 2×10^{18} eV/ml.
† pH = 2·9, dose = $4·6 \times 10^{18}$ eV/ml.

The influence of carbon dioxide in these aquo-organic systems has been ascribed to the reaction,[3]

$$(H_2O)^- + CO_2 \rightarrow CO_2^- + H_2O \qquad (1)$$

where $(H_2O)^-$ is the electron in water, (or "polaron"[4]), assumed to be one of the two "hydrogen atom" species produced in the primary radiolytic decomposition of water.

The polarons normally react with hydrogen ions to form hydrogen atoms, viz.,

$$(H_2O)^- + H_3^+O \rightarrow H + 2H_2O \qquad (2)$$

leading in certain systems (e.g. methanol, ethanol, formic acid) to dehydrogenation of

[3] J. T. ALLAN and G. SCHOLES, *Nature, Lond.* **187**, 218 (1960).
[4] J. WEISS, *Nature, Lond.* **186**, 751 (1960).

VOL. 19 1961

the organic solute, $H + RH \rightarrow H_2 + R$, or in certain other systems to the formation of molecular hydrogen by the recombination reaction, $H + H \rightarrow H_2$. Hence it can be seen that the influence of carbon dioxide on the hydrogen gas yields is dependent upon pH, the dependence being determined by the competition of reactions (1) and (2). From the data given in Fig. 1, assuming that $G(H_2O)^- = 2{\cdot}3$ and that the increased extent of water decomposition in solutions irradiated at pH's below about 3 does not involve the formation of more polarons, it is found that $k_1/k_2 \sim 3$.

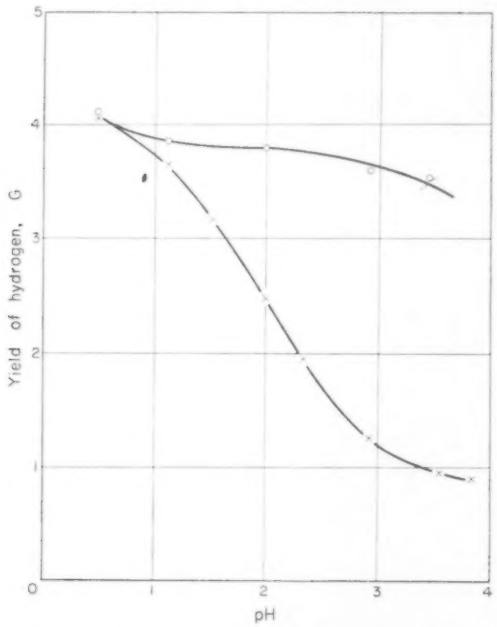

FIG. 1.—pH-Dependence of the initial yields of hydrogen on irradiation of aqueous solutions of ethanol (2×10^{-2} M) with ^{60}Co γ-rays.
○—*in vacuo*
×—in the presence of carbon dioxide (1 atm)

The yield of hydrogen ($G = 0{\cdot}45$) obtained on irradiation of solutions of t-butanol and also of oxalic acid in the presence of carbon dioxide in the pH range 3–4 (Table 2) is essentially the "molecular" hydrogen yield.[5] We may conclude, therefore, that in addition to reaction with the polarons, carbon dioxide can also react with the second hydrogen atom species which is produced in the primary radiolysis act ($G = 0{\cdot}6$ in neutral solutions) and which is possibly a hydrogen atom or an excited water molecule.[3,6]

All of these experiments show that the radiation yields from deaerated solutions of methanol, ethanol and t-butanol in the pH range ~4–~7 can be governed to some extent by the presence of small amounts of carbon dioxide. This situation, however, does not arise in all aquo–organic systems; for example, with isopropanol solutions perfect reproducibility was obtained over this particular pH range. The reason for this difference is as follows: In isopropanol solutions the pH dependence of the radiation

[5] H. A. SCHWARZ, J. P. LOSEE JR. and A. O. ALLEN, *J. Amer. Chem. Soc.* **76**, 4693 (1954).
[6] F. S. DAINTON and D. B. PETERSON, *Nature, Lond.* **186**, 878, (1960).

yields is associated with a competition involving reaction (2) and reaction of the polarons with the radiation-produced acetone. The amount of acetone produced and its reactivity is sufficient to suppress interference by adventititious amounts of carbon dioxide according to reaction (1). On the other hand, no carbonyl compounds are produced in the radiolysis of t-butanol solutions, only very small amounts of formaldehyde in methanol solutions and insufficient amounts of acetaldehyde in ethanol solutions; in these systems, therefore, reaction (1) can take place under suitable pH conditions and can lead to the observed irreproducibility and to the effects noted in Table 1.

Acknowledgements—We wish to express our thanks to Professor J. J. WEISS for his encouragement of this work and to the Northern Council of the British Empire Cancer Campaign for financial support. Two of us (N. G. and M. S.) are indebted to the British Council for maintenance grants.

VOL.
19
1961

J. Inorg. Nucl. Chem., 1961, Vol. 19, pp. 208 to 211. Pergamon Press Ltd. Printed in Northern Ireland

AN INFRA-RED SPECTROSCOPIC INVESTIGATION OF THE NATURE OF THE HYDROGEN HALIDE IN *TRANS*-DICHLORO *BIS* ETHYLENEDIAMINE COBALT (III) CHLORIDE, HYDROCHLORIDE DIHYDRATE; AND THE BROMIDE ANALOGUE

N. F. CURTIS
Chemistry Department, Victoria University of Wellington

(*Received* 7 *November* 1960)

Abstract—Comparison of the infra-red spectra of *trans* dichloro *bis* ethylenediamine cobalt (III) as the chloride and as the chloride hydrochloride dihydrate, and of *trans* dibromo *bis* ethylenediamine cobalt (III) as the bromide and as the bromide hydrobromide dihydrate indicates the presence of the hydroxonium ion in the hydrohalides, showing that the hydrogen halide is present in the ionized form H_3O^+, X^-.

JÖRGENSON described several transition-metal amine complexes with hydrogen-chloride and hydrogen bromide "of crystallization". Thus the dichlorobisethylene-diamine cobalt (III) ion crystallizes from a solution containing hydrochloric acid as *trans* dichloro *bis* ethylenediamine cobalt (III) chloride hydrochloride dihydrate A.[1] This readily loses hydrogen chloride and water to form the simple chloride B. The bromide analogue, *trans* dibromo *bis* ethylenediamene cobalt (III) bromide hydro-bromide dihydrate C[2] is similarly prepared, and is readily converted to the simple bromide D. JÖRGENSON also reported the formation of a hydrochloride of dichloro tetrapyridineo rhodium (III) chloride and a hydrobromide of *trans*-dichloro *bis* ethy-lenediamine cobalt (III) bromide, although attempts to prepare the latter by his method, during this investigation, were unsuccessful.

A	*trans*-[Co en_2 Cl_2]Cl.HCl 2 H_2O
B	*trans*-[Co en_2 Cl_2]Cl
C	*trans*-[Co en_2 Br_2]Br HBR. 2 H_2O
D	*trans*-[Co en_2 Br_2]Br

Formulation of (A) as the ammonium salt complex, $[Co\ en.(enH^+)Cl_3]^+$,[3] was shown to be incorrect by ETTLE and JOHNSON,[4] who proved that the chloride of the hydrochloride was distinct from the two co-ordinated chlorides using chlorine-36, and suggested that the hydrogen chloride was present as hydrogen chloride molecules, similar to water of crystallization. DREW and PRATT[3] report that they were able to prepare an anhydrous form of (A), but not the dihydrate. In this study, all attempts to prepare this anhydrous compound were unsuccessful; the dihydrate crystallized under conditions as diverse as evaporation of a solution of (B) in hot concentrated hydro-chloric acid, saturation of an ice-cold aqueous solution of (B) with hydrogen chloride

[1] S. M. JÖRGENSEN, *J. Prakt. Chem.* **39**, 16 (1889).
[2] S. M. JÖRGENSEN, *J. Prakt. Chem.* **41**, 440 (1890).
[3] H. D. K. DREW and N. H. PRATT, *J. Chem. Soc.* 506 (1937).
[4] G. W. ETTLE and C. H. JOHNSTON, *J. Chem. Soc.* 1490 (1939).

gas, or precipitation by the addition of acetone to a solution of (B) in hydrochloric acid. In view of the conclusions reached in this paper as to the nature of the hydrochloride, it seems unlikely that the anhydrous form could exist.

INFRA-RED SPECTRA

A comparison of the infra-red spectra of the pairs of compounds (A) and (B), and (C) and (D) was made in the region 700–4000 cm^{-1}.

The spectrum of (A) is similar to that of (B) described by MORRIS and BUSCH,[5] but contains in addition a weak band at about 2130 cm^{-1}, a sharp band at 1680 cm^{-1}, and a broad band 750–1400 cm., maximum about 950 cm^{-1}. This latter is overlaid by

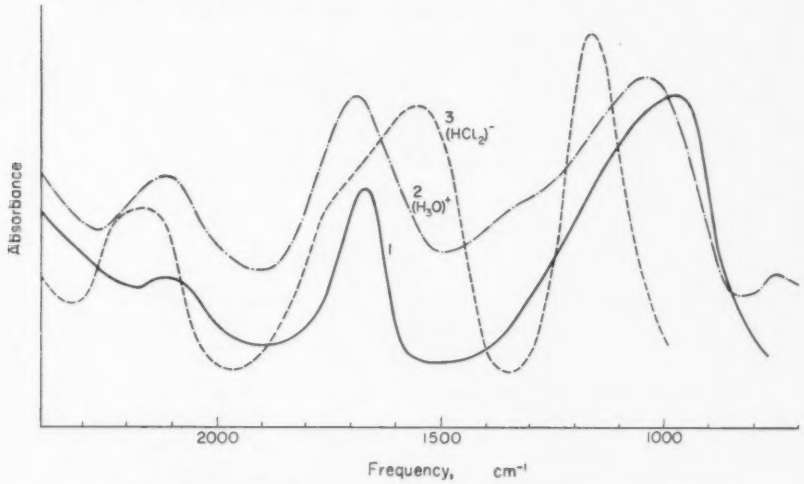

FIG. 1.—Infra-red spectra. 1. Spectrum of *trans* [Co en_2Cl_2] $(H_3O).2Cl.H_2O$ with that of *trans*-[Co en_2Cl_2] subtracted. 2. H_3O^+ [10] 3. HCl_2^- [8]

the spectrum of the *trans* dichloro *bis* ethylenediamine cobalt (III) ion, and the shape is difficult to determine, but the asymmetry suggests the presence of a weaker band on the higher frequency side.

The spectra of (C) and (D) are similarly related. Thus in the case of (C), the spectrum of (D) (very similar to that of (B)) is present, together with the same additional bands present in the spectrum of (A).

The most likely forms in which the hydrogen halide of (A) and (C) could exist are considered to be (a) as hydrogen halide of crystallization; (b) as the ion HX_2^- or (c) as the ionized hydroxonium halide $H_3O^+.X^-$.

The fact that the additional bands present in (A) and (B) are the same suggests (c) as the most probable case. Because of the strong absorption of the dihalide *bis* ethylenediamine cobalt (III) ion, absorption in the hydrogen stretching region is difficult to distinguish, but there are no bands present at 2840 cm^{-1} or 2450 cm^{-1}, as expected for molecular hydrogen chloride[6] or hydrogen bromide.[7] In the table and

[5] M. L. MORRIS and D. H. BUSCH, *J. Amer. Chem. Soc.* **82**, 1521 (1960) also M. E. BALDWIN, *J. Chem. Soc.* 4369 (1960).
[6] W. WEST, *J. Chem. Phys.* **7**, 795 (1939).
[7] J. ZUNINO, *Z. Physik* **100**, 335 (1936).

figure, the observed spectrum is compared with that reported for the HCl_2^- ion,[8] and the H_3O^+ ion.[9–14]

Observed	2130(*w*)	1680(*s*)	(?)	950(*s*) broad
H_3O^+[10]	2109(*m*)	1700(*s*)	1150,	1060(*s*) broad
HCl_2^-[8]	2180(*m*)	1560(*s*)	1180(*s*)	sharp

The absorption of the remaining water molecule at 1616 cm^{-1}[15] is obscured by the NH_2 deformation vibration of the dihalide *bis* ethylenediamine cobalt (III) ion at the same frequency[5], but the relative intensities of this band, compared with the C—N or C—C stretching band at 1050 cm^{-1} [5] is greater for A and C than for B and D, indicating that absorption by H_2O at this frequency is probably present.

From the foregoing it is concluded that the hydrogen halide in (A) and (C) exists as the ionized hydroxonium halide, and (A) and (C) are respectively dichloro *bis* ethylenediamine cobalt (III) hydroxonium chloride monohydrate, and dibromo *bis* ethylenediamine cobalt (III) hydroxonium bromide monohydrate. The hydroxonium ion in solid compounds has previously been reported in the hydrates of the hydrogen halides,[9,10] and in the hydrates of perchloric,[13,14] nitric[11,12] and other acids.[17]

Note added in proof—From X-ray crystallographic studies on A[18], C[19], and the Cr(III) analogue of A[20], it has been suggested that these compounds contain the symmetrical ion $[H_2O—H—OH_2]^+$. The similarity of the infra-red spectra observed to that of the H_3O^+ ion, together with the probable H_2O absorption at 1616 cm^{-1} support the alternative asymmetric arrangement $[H_2O–H—OH_2]^+$, with a hydrogen bond between the H_3O^+ ion and the H_2O molecule.

EXPERIMENTAL

Trans-dichloro *bis* ethylenediamine cobalt (III) hydroxonium chloride monohydrate (A) was prepared by a standard method,[18] and recrystallized by saturating an ice-cold aqueous solution with hydrogenchloride. The crystals were filtered, washed with hydrochloric acid and acetone, and dried in a desiccator containing hydrogen chloride, over concentrated sulphuric acid. (Found: Co, 16·5; C, 13·6; H, 6·0; N, 15·5; Cl, 39·7; loss on heating at 110° 19·7. Calc. for $[Co\ en_2Cl_2]$. $H_3O.2Cl.H_2O$. Co, 16·5; C, 13·4; H, 5·9; N, 15·5; Cl, 39·7; loss on heating (—$HCl.2H_2O$) 20·2%).

Trans-dibromo *bis* ethylenediamine cobalt (III) hydroxonium bromide monohydrate (C) was prepared by passing an aqueous solution of (B) through a strong base anion exchange column (amberlite IRA400) charged with hydroxide ions. The resultant solution of dihydroxy (or hydroxy-aquo) *bis* ethylene-diamine cobalt (III) hydroxide was rendered just acid with hydrobromic acid,

[8] T. C. WADDINGTON, *J. Chem. Soc.* 1708 (1958).
[9] D. F. FERRISO and C. C. HORNIG, *J. Amer. Chem. Soc.* **75**, 4113 (1953).
[10] D. F. FERRISO and C. C. HORNIG, *J. Chem. Phys.* **23**, 1464 (1955).
[11] D. E. BETHELL and N. SHEPPARD, *J. Chim. Phys.* **50**, C. 72 (1953).
[12] D. E. BETHELL and N. SHEPPARD, *J. Chem. Phys.* **21**, 1421 (1953).
[13] J. T. MULLHAUPT and D. F. HORNIG, *J. Chem. Phys.* **24**, 169 (1956).
[14] G. L. VIDALE and R. C. TAYLOR, *J. Amer. Chem. Soc.* **78**, 294 (1956),
[15] P. J. LUCCHESI and W. A. GLASSON, *J. Amer. Chem. Soc.* **78**, 1347 (1956).
[16] *Inorg. Synth.* II, 222.
[17] R. E. RICHARDS and J. A. S. SMITH *Trans. Faraday Soc.* **47**, 1261 (1951).
[18] AKITSUGU NAKAHARA, YOSHIHIKO SAITO and HISAO KUROYA *Bull. Chem. Soc. Japan* **25**, 331 (1952)
[19] SCHUN'ICHIRO OOI, YOSCHIMICHI KOMIYAMA, YOSHIHIKO SAITO and HISAO KUROYA, *Bull. Chem. Soc. Japan* **32**, 263 (1959).
[20] SCHUN'ICHIRO OOI, YOSCHIMICHI KOMIYAMA and HISAO KUROYA *Bull. Chem. Soc. Japan* **33**, 355 (1960).

evaporated to dryness under reduced pressure, and then crystallized from hot 45 per cent hydrobromic acid, pale green plates depositing on cooling. These were filtered and washed with acetone (in a dry atmosphere, as the crystals are very hygroscopic) and dried in a desiccator filled with hydrogen bromide, over sulphuric acid. (Found: Co, 11·0; C, 8·6; H, 2·8; Br, 59·6; loss on heating at 110°, 21·5. Calc. for [Co en_2Br_2]. $H_3O.2Cl.H_2O$. Co, 11·0; C, 9·0; H, 3·9; Br, 59·6; loss on heating (—$HBr.2H_2O$) 22·0%).

Analysis. C and H by combustion, N by DUMAS, Cl and Br by mixing with anhydrous sodium carbonate, moistening, drying and then heating strongly to decompose the complex. Halide finally determined gravimetrically as AgCl or AgBr. Co; complex decomposed by boiling with peroxydisulphate. Cobalt determined gravimetrically as the pyridine thiocyanate complex.

Infra-red spectra. The infra-red spectra were measured on a Perkin-Elmer model 221 infra-red spectrophotometer, in "Nujol" and hexachlorobutadiene mulls. The samples of (B) and (D) were prepared by heating (A) and (C) respectively at 110° for an hour. Microscopic examination showed that the mulls of (A) and (C) were stable indefinitely, although an exposure to the air crystals of (A) change to (B) over a period of hours, and crystals of (C) rapidly deliquesce, but do not change to (D).

Acknowledgements—The author thanks Dr. C. J. WILKINS of the University of Canterbury for the infra-red spectra measurements, Dr. A. D. CAMPBELL of the University of Otago for the microanalysis, and Mr. W. E. DASENT of this University for helpful discussions.

VOL. 19 1961

J. Inorg. Nucl. Chem., 1961, Vol. 19, pp. 212 to 222. Pergamon Press Ltd. Printed in Northern Ireland

HIGH-PRESSURE HIGH-TEMPERATURE INVESTIGATION OF THE URANIUM–OXYGEN SYSTEM

W. B. WILSON
Battelle Memorial Institute, 505 King Avenue, Columbus, Ohio

(*Received* 22 *August* 1960; *in revised form* 14 *November* 1960)

Abstract—An investigation was made of the effects of combined ultrahigh pressure and high temperature on the oxides of uranium with particular emphasis on U_3O_8. A new polymorph of U_3O_8, designated γ-U_3O_8, occurs at pressures in excess of 16,000 atm at temperatures above 400°C. At 60,000 atm the gamma U_3O_8 coexists with a cubic U_4O_9-like phase.

These results, although of a preliminary nature, show that the uranium–oxygen phase diagram is greatly modified by the effects of pressure.

THE determination of the effects of ultrahigh pressure and temperature on uranium oxides was undertaken as a prerequisite to the study of the effects of pressure on reactions of uranium oxides with other oxides. The phase relationships of the uranium–oxygen system at ambient pressure have been studied by various investigators.[1–6] While the results of these and other investigations differ in certain details, there appears to be general agreement on the broad features of the phase diagram. The work of GRONVOLD[7] and that of HOEKSTRA and SIEGEL[8] and other workers, given in Fig. 1, may be used to depict the normal-pressure behaviour of the uranium–oxygen system, between UO_2 and U_3O_8. The results of the recent work of HOEKSTRA and SIEGEL,[9] for the region from U_3O_8 to UO_3, are not included, since they are beyond the compositional range of the present investigation.

In the present work, emphasis was placed on the determination of the effects of pressure on U_3O_8, from those related to possible reactions between U_3O_8 and other metal oxides. The structure of U_3O_8, as described in the literature, has been the subject of some controversy. For this reason, a review of structural studies of U_3O_8 appears warranted for comparison to the high-pressure results.

U_3O_8

The crystal structure of U_3O_8 was determined by ZACHARIASEN[10] and later by GRONVOLD[11] to be orthorhombic with cell dimensions of $a = 6{\cdot}70$ Å, $b = 3{\cdot}98$ Å and

[1] W. BLITZ and H. MULLER, *Z. Anorg. Chemie* **163**, 257 (1927).
[2] R. E. RUNDLE, N. C. BAENZIGER, A. S. WILSON and R. A. MCDONALD, *J. Amer. Chem. Soc.* **70**, 99 (1948).
[3] K. B. ALBERMAN and J. S. ANDERSON, *J. Chem. Soc.* **5**, 303 (1949).
[4] H. HERING and P. PERIO, *Bull. Soc. Chim.* 351 (1952).
[5] P. PERIO, *Bull. Soc. Chim.* 256 (1953).
[6] F. GRONVOLD and H. HAROLDSEN, *Nature, Lond.* **112**, 69 (1948).
[7] F. GRONVOLD, *J. Inorg. Nucl. Chem.* **1**, 357 (1955).
[8] H. HOEKSTRA and S. SIEGEL, *J. Phys. Chem.* **59**, 136 (1955).
[9] H. R. HOEKSTRA and S. SIEGEL, *Proceedings of the Second International Conference on Peaceful Uses of Atomic Energy Geneva* (1958) Paper A/Conf. 15/P/1548.
[10] W. H. ZACHARIASEN, Manhattan Project Reports CN–2689, 3053 (1944).
[11] F. GRONVOLD, *Nature, Lond.* **162**, 70 (1948).

$c = 4{\cdot}14$ Å. Independent work by RUNDLE and BAENZIGER[12] established that the b dimension should be tripled to explain certain weak reflexions. BAENZIGER[13] subsequently proposed that small x and y parameters were required for certain uranium positions to explain observed intensities. These results were obtained by powder X-ray diffraction techniques.

Single crystals of two allotropic modifications of U_3O_8 were examined by WILSON[14,15] using Weissenberg and precession techniques. The normal or α-form of U_3O_8 was obtained by vaporizing U_3O_8 in air at 1400°C.[14] Deposition and growth from the vapour occurred at lower temperatures.

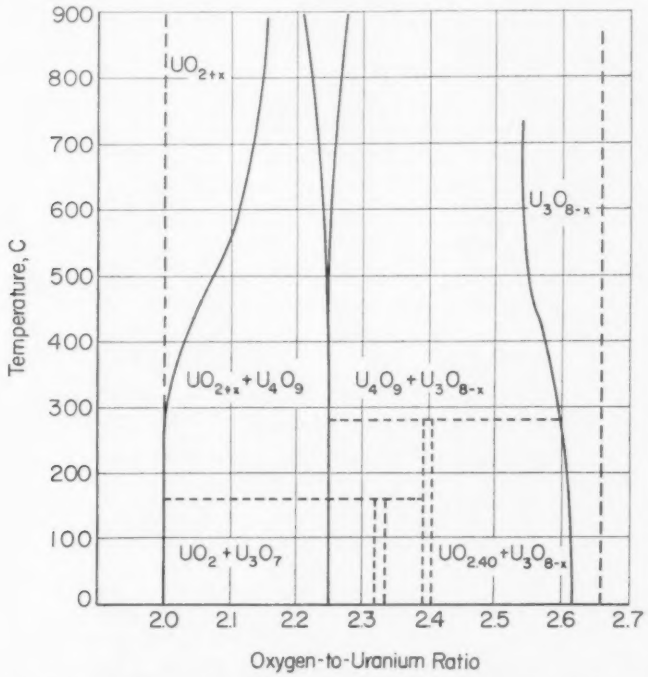

FIG. 1.—The Gronwold tentative phase diagram of the uranium–oxygen system between UO_2 and U_3O_8.

Details of the mechanism by which the U_3O_8 single crystals are formed has been given recently by ACKERMANN *et al.*[16] It is shown that such U_3O_8 crystals result from the two step process:

$$\tfrac{1}{3}U_3O_8(s) + \tfrac{1}{6}O_2(g) \xrightarrow{T_1} UO_3(g)$$

$$UO_3(g) \xrightarrow{T_2} \tfrac{1}{3}U_3O_8(s) + \tfrac{1}{6}O_2(g)$$

where $T_2 < T_1$.

X-ray analysis of these crystals gave an orthorhombic unit cell with $a = 6{\cdot}70$ Å, $b = 11{\cdot}91$ Å and $c = 4{\cdot}144$ Å. Although the crystals exhibited the tripled b axis and

[12] R. E. RUNDLE and N. C. BAENZIGER, Report CC, 1980 (1944).
[13] N. A. BAENZIGER, AECD 3237 (1948).
[14] W. B. WILSON, General Electric Company Aircraft Nuclear Propulsion Project APEX–202 (1955).
[15] W. B. WILSON, General Electric Company Aircraft Nuclear Propulsion Project, APEX–187, (1955).
[16] R. J. ACKERMANN, R. J. THORN and C. A. ALEXANDER, *J. Phys. Chem.* **64**, 350 (1960).

VOL. 19 1961

were otherwise nearly identical to the orthorhombic structure determined by BAENZIGER,[13] pronounced reciprocal lattice streaking of some reflexions was observed to occur for certain crystallographic directions. These streaks were analyzed as being produced by faulting in the crystal structure, which was related to the small x parameter for certain uranium positions as described by BAENZIGER. The effect of the repetitive faulting is to produce an apparent monoclinic cell with β of the cell $\sim$35′ off orthorhombic.

Nearly identical results for U_3O_8 have recently been reported by CHODURA and MALY.[17] They found unit cell dimensions of $a = 11{\cdot}93$ Å, $b = 6{\cdot}72$ Å and $c = 8{\cdot}29$ Å with pronounced lattice streaking.* The streaking is explained in their paper as a combination of alternating orthorhombic and monoclinic cells with the β angle of the monoclinic cell 1° to 1°30′ off orthorhombic. The use by WILSON[14] of half the c axis value of CHODURA and MALY is due to the possibility that the weak reflections requiring the larger c dimension may also arise from faulting.

In view of these results, the two hexagonal cells proposed by MILNE[18] for U_3O_8 appear invalid. As CHODURA and MALY have suggested, these results probably arise through the use of crystals with multiple twins around the c axis of U_3O_8. The two-cell hypothesis is also considered invalid by GRONVOLD.[7]

Single crystals of a second allotropic modifications of U_3O_8 were also examined by WILSON.[15] These crystals, designated β-U_3O_8, were truly orthorhombic—unfaulted—with $a = 11{\cdot}58 \pm 0{\cdot}02$ Å, $b = 7{\cdot}06 \pm 0{\cdot}02$ Å and $c = 8{\cdot}30 \pm 0{\cdot}02$ Å. This unit cell is very closely related by symmetry to the α-form of U_3O_8 and contains nearly equal unit-cell volume. The composition of these crystals was analysed to be $UO_{2{\cdot}62}$ using thermal balance techniques. Independent confirmation of the existence of the β-U_3O_8 structure was obtained by HOEKSTRA and SIEGEL[8] for crystals produced under different conditions having a composition of $UO_{2{\cdot}66}$.

Although the existence of β-U_3O_8 is confirmed, the conditions required for its formation have not been clearly established. A recent attempt by WILSON (unpublished) to form β-U_3O_8 by a method similar to that of HOEKSTRA and SIEGEL was not successful. However, it has been obtained in several instances when uranium oxide is heated in excess of 1000°C at oxygen pressures of 750 mm or more. This suggests that β-U_3O_8 may result when the loss of oxygen from U_3O_8, which occurs at high temperatures, is offset by higher oxygen pressures. The resulting structure appears to be a metastable high-temperature phase which reverts to normal U_3O_8 upon heating in air.[8]

The high-temperature behaviour of the uranium–oxygen system has been investigated by BILTZ and MULLER[1] who showed that above 600°C, U_3O_8 tends to dissociate toward lower O/U ratios. On the basis of these studies BILTZ and MULLER estimated that at 1350°C and 10 mm Hg oxygen partial pressure U_3O_8 should decompose to an O/U ratios of $UO_{2{\cdot}25}$. At higher oxygen pressures, such as 150 mm, the temperature required for the dissociation to U_4O_9 is in excess of 1450°C.[19]†

* CHODURA and MALY have interchanged the a and b axes normally used to describe U_3O_8.

† LEBEAU[20] has indicated that the compound U_3O_7 is obtained by "fusion" of any of the oxides of uranium in air, using a solar furnace.

[17] B. CHODURA and J. MALY, *Proceedings of the Second International Conference on the Peaceful Uses of Atomic Energy, Geneva*, (1958). Paper A/Conf. 15/P/2099.

[18] I. H. MILNE, *Amer. Mineralo.* **36**, 415 (1951).

[19] C. ALEXANDER. Unpublished work. Battelle Memorial Institute (1958).

[20] P. LEBEAU, *C. R. Acad. Sci., Paris* (1953).

More recent work dealing with the oxygen decomposition pressures of the uranium–oxygen system has been given by BLACKBURN,[21] ARONSON and BELLE,[22] ACKERMANN and THORN[23] and BUDNAKOV.[24]

EXPERIMENTAL

The investigation of the effects of combined pressure and temperature on the uranium oxides was performed using two types of high-pressure high-temperature equipment. A Bridgman "anvil" unit as modified to permit external heating,[25] was used in the pressure and temperature range of its capabilities. For this unit, the sample, such as U_3O_8 powder, is placed between two abutting tungsten carbide anvils and compacted to form a disk of the order of 0·010 in. thick by $\frac{1}{4}$ in. diameter. Friction between the sample and the carbide prevents the expulsion of the sample, and pressures of the order of 200,000 atm (at low temperature) may be obtained. Temperature is obtained by use of an external furnace which surrounds both carbide pistons and the sample. The compresive strength of the tungsten carbide is reduced by high temperatures permitting only modest pressures at elevated temperature.[18]

In order to extend the range of pressure and temperature beyond that of the Bridgman "anvil", an internally heated apparatus, called the "Girdle"[26] was constructed. The calibration of this equipment for pressure and temperature was accomplished by the methods described by HALL[27] who, in other work,[27–30] has discussed various aspects of high-pressure high-temperature research.

In this apparatus, the sample configuration was prepared by compaction of the uranium oxide into the center portion of a thin-walled platinum tube. Platinum foil was placed over each end of the uranium oxide and a thermal insulator (such as unfired Grade A Lava*) was inserted in each end to fill the tube. The heater tube was subsequently inserted into the pressure transmitting medium (which is also the thermal insulation) consisting of either Lava or pyrophyllite. Heating is accomplished in the high-pressure apparatus by passing current through the heater tube.

Experimental difficulties associated with the insertion of thermocouples into the high-pressure apparatus prevented the determination of temperature for each individual experiment. In practice, a temperature versus power input curve was established for a given sample configuration, after which power input was used to obtain a desired temperature. This technique leads to an uncertainty of temperature for individual tests. In addition, temperature gradients exist in the sample and heater region, further contributing to temperature errors. Such inherent errors and corrective techniques have been discussed elsewhere.[26,31]

In the present work a repetitive approach was employed to obtain reproducible results, in which the probable behaviour at a given temperature and pressure was determined from many samples subjected to similar conditions. Unfortunately, identical conditions were not possible since both the pressure equipment and sample configurations were subject to necessary modifications during the work.

The dependency of reactions on rate processes[28] has led in the present work to the use of varying times for subjecting the sample to temperature and pressure. For instance, at room temperature pressure was maintained for periods ranging from 4 to 16 hr. Two hour periods were used in the range near 400°C with a decrease to 1 hr at temperatures near 600°C and higher. The internally heated apparatus was commonly used for periods of 1 hr since higher temperatures were employed. Following

* Product of the American Lava Corporation, Chattanooga, Tennessee.

[21] P. E. BLACKBURN, *J. Phys. Chem.* **62,** 897 (1958).
[22] S. ARONSON and J. BELLE, *J. Chem. Phys.* **29,** 151 (1958).
[23] R. J. ACKERMANN and R. J. THORN. Paper presented at the 133rd National Meeting, American Chemical Society, San Francisco, April (1958).
[24] T. P. BUDNAKOV, S .G. TRESVETSKII, V. I. KUSHAKOVSHII, *Technical Physics, Dokl. Acad. Nauk.* (AEC–TR–4035) SSSR–**128,** 85–8 (1959).
[25] D. T. GRIGGS and G. C. KENNEDY, *Amer. J. Sci.* **254,** 722–735 (1956).
[26] W. B. WILSON, *Rev. Sci. Instrums.* **31,** 331 (1960).
[27] H. T. HALL, *Rev. Sci. Instrum.* **29,** 267 (1958).
[28] H. T. HALL. Article in Proceedings of the Stanford Symposium on High Temperature, Stanford Research Institute, Menlo Park, California (1956).
[29] H. T. HALL, *Rev. Sci. Instrum.* **31,** 402, 125 (1960).
[30] H. T. HALL. Article in High Temperature Technology, Stanford Research Institute, 145 (1959).
[31] W. B. WILSON, Battelle Memorial Institute Report BMI–1328. (1959).

exposure to temperature and pressure, the samples were analysed for constituent phases by X-ray diffraction techniques.

RESULTS

The results of the investigation are given in the diagram of Fig. 2. α-U_3O_8, obtained by air oxidation of Mallinckrodt UO_2 at 750°C, was subjected to various conditions of pressure and temperature. The results obtained by use of the Bridgman anvil are indicated in parentheses.

Samples examined at room temperature at pressures up to 100,000 atm indicated a

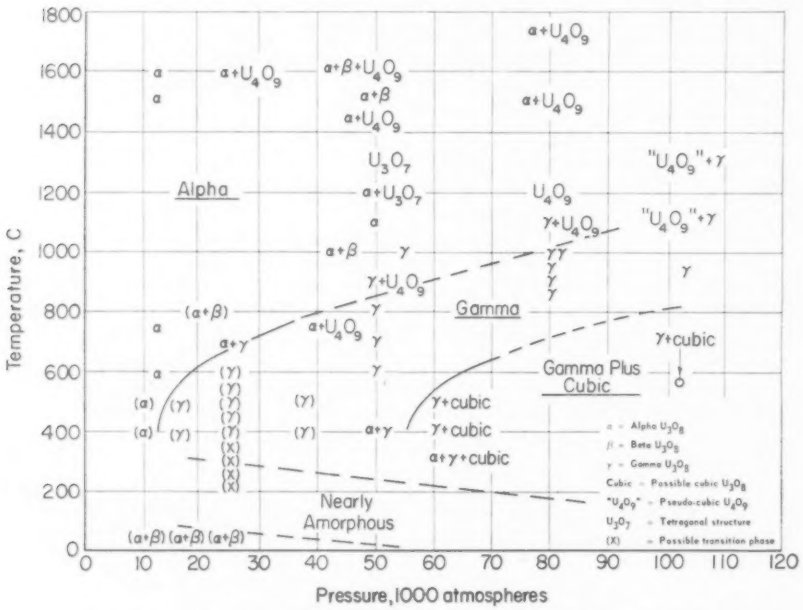

FIG. 2.—X-ray diffraction analysis of U_3O_8 subjected to temperature and pressure.

progressive change to a nearly "amorphous" state with increasing pressure. The amorphous nature, as judged by the diffraction pattern, may arise from residual stresses and particle size effects as well as a lack of crystallinity. After 16 hr at 100,000 atm, the diffraction pattern was almost entirely devoid of coherent diffraction maximum (this suggests that the amorphous nature of some pitchblende minerals, known to be "metamict" minerals,[32] possibly arises from the combined effects of high pressure and low temperature as well as from the effects of oxidation and autoirradiation). At lower pressures, near 25,000 atm, spurious reflexions occur, the strongest of which are essentially those associated with the β-form of U_3O_8.

At pressures of 25,000 atm at 200–300°C the observed diffraction pattern for U_3O_8 also assumes amorphous characteristics. A new modification of U_3O_8, designated γ-U_3O_8, appears at 400°C and above. This form did not occur at 10,000 atm, and the minimum pressure at which this modification was observed was 16,000.

Since the general effect of temperature is to offset the effects of pressure, it was of interest to determine if the γ-U_3O_8 transformed back to the α-structure at higher

[32] E. J. BROOKER and E. W. NUFFIELD, *Amer. Mineralogist* **37**, 363 (1952).

temperatures. This was observed to occur at 800°C and 20,000 atm. The resulting diffraction pattern, however, again showed weak reflexions previously associated with β-U_3O_8. The diffraction pattern obtained from the high-pressure γ-modification of U_3O_8 is given in the appendix.

When the pressure is increased to 60,000 atm at 400°C and slightly higher, γ-U_3O_8 was found to coexist with the U_4O_9 structure. At 100,000 atm and 500°C the gamma plus U_4O_9 phases were still evident.

It can be seen from Fig. 2 that the general effect of increasing temperature beyond about 750°C is to produce oxide structures usually associated with lower oxygen–uranium ratios. Increasing the pressure tends to lower the temperature at which the "suboxides" (O/U $<2{\cdot}66$) may be found, for example, the cubic U_4O_9 is found as low as 400°C at 60,000 atm and beyond. Thus, it was desirable to establish if these structures had suffered oxygen decomposition under pressure or represented a transformation of U_3O_8 to the crystal morphology associated with the lower oxides. In order to establish the compositional variation occurring with temperature and pressure, selected samples were analysed by microbalance techniques to determine their O/U ratios. The results of the analysis are given in Table 1.

VOL. 19 1961

The microbalance analysis of Table 1 shows that the compositions of the gamma, high pressure, form of U_3O_8 is essentially identical to that of normal U_3O_8 and does not constitute a lower oxide of uranium. In addition, it also shows that at lower

TABLE 1.—MICROBALANCE DETERMINATION OF COMPOSITION OF SAMPLES SUBJECTED TO PRESSURE AND TEMPERATURE

Sample no.	Pressure (Atm)	Temp. (°C)	Phases present	Composition X in UO_x
		Group I*		
	1	25	α-U_3O_8	2·64
58	16,600	400	γ-U_3O_8	2·66
59	16,600	500	γ-U_3O_8	2·66
60	25,000	550	γ-U_3O_8	2·65
62	37,000	450	γ-U_3O_8	2·65
112	60,000	450	γ + cubic	2·63
114	60,000	300	$\alpha + \gamma$ + cubic	2·65
97	50,000	1300	U_3O_7	2·38
80	80,000	1500	$\alpha + U_4O_9$	2·64
75	80,000	1750	$\alpha + U_4O_9$	2·48
83	80,000	1200	U_4O_9	2·49
		Group II†		
	1	25	αU_3O_8	2·70
163	100,000	500	γ + cubic	2·72
164	100,000	900	γ	2·73
165	100,000	1100	cubic + γ	2·69
167	100,000	1300	"U_4O_9" + γ	2·68
142	1	25	U_4O_9	2·26

* Heated in vacuum at 0·05 mm Hg to 750°C then oxidized in air to stoicheiometric U_3O_8.
† Dried at 110°C, reduced to UO_2 with H_2 at 900°C, then oxidized to U_3O_8 with dry air at 750°C.

pressures at temperatures above approximately 1000°C some dissociation of U_3O_8 possibly occurs, apparently by the loss of oxygen from the high-pressure apparatus. Thus, although U_3O_8 was used as the starting material to determine the results of Fig. 2, it should not be concluded that the diagram represents a pressure–temperature phase diagram of constant composition.

While Table 1 does indicate that decomposition of U_3O_8 occurs at high temperatures, the results also show that the cubic U_4O_9-like structure was also observed in substantial amounts in samples having O/U ratios of 2·63 and greater. These results suggest that the cubic structure can be obtained in two distinct ways. It may be produced at intermediate pressures by decomposition of U_3O_8 to form U_4O_9 and it also may be formed as the result of very high pressure. In the latter case the composition of the cubic phase definitely appear equivalent to that of U_3O_8.

Table 1 also shows that at 100,000 atm at all temperatures up to 1300°C the O/U ratios were in excess of that of U_3O_8, yet phases related to the cubic U_4O_9 were produced and retained. At temperatures above 1100°C further structural changes were observed to occur. The diffraction pattern of samples subjected to these conditions may be described as being related to the fluorite U_4O_9 structure but of lower symmetry. Thus the individual reflexions of the fluorite structure of U_4O_9 were split into multiple reflexions. It appears possible that the structure might possibly have been cubic at pressure and temperature but changed to lower symmetry upon release of pressure or temperature.

Although the present results suggest that the cubic U_4O_9 structure may be retained with abnormally high oxygen composition, the decrease in lattice parameter shown by PERIO[33] for the extrapolation of the cubic UO_{2+x} structure to U_3O_8 was not observed. A slight decrease appears possible, from 5·44 to 5·42 Å. (The conditions of high pressure and low temperature produce diffuse diffraction patterns making parameter measurements uncertain).

The conclusion that a cubic U_3O_8 structure exists, is supported to some extent by results of studies of the mineral pitchblende. Results given by BERMAN[34] show that pitchblendes have compositions near that of U_3O_8, yet produce cubic diffraction patterns. The lattice parameters of the pitchblendes, examined by BERMAN both before and after annealing, are smaller than those observed in the present work and agree more nearly with the extrapolated values of PERIO.[33]

A brief comparison of the present high pressure results with the study of pitchblende by BERMAN[34] and BROOKER and NUFFIELD[32] is of interest. The most striking difference of such a comparison is the very greatly amplified pressure scale in the present work over that known to be operative in the geological formation of pitchblende.[35] While pressures of the order of perhaps 1000 atmospheres are involved in the formation of cubic U_3O_8 as pitchblende, the present results show that it does not form readily at 100,000 atm. While an exact analogy between the two formative methods of producing cubic U_3O_8 is not possible, it appears that two factors are significant to explain the large pressure differences.

First, the formation of cubic U_3O_8 in nature is known to be a hydrothermal process.[32] By analogy, HALL[28] has shown that for Coesite, the high-pressure polymorph of SiO_2, pressures in excess of 100,000 atmospheres at 2000°C are required

[33] P. PERIO. Thesis, University of Paris (1955).
[34] R. M. BERMAN, *Amer. Mineralogist* **42**, 705 (1957).
[35] C. B. SCLAR. Private communication, Battelle Memorial Institute (1959).

for direct formation from quartz, and MACDONALD[36] has shown that less than 20,000 atms at 450°C are required to form it hydrothermally from silicic acid ($SiO \cdot nH_2O$).[30]

The second significant difference to explain the pressure discrepancy is in the manner of formation and the time difference between laboratory formation and that which occurs in nature. Thus, the production of cubic U_3O_8 in the laboratory attempts to duplicate in an hour that which occurs over geological time in nature. In addition the formation is attempted directly from U_3O_8 in the present work as opposed to perhaps a very gradual oxidation process for pitchblende.*

On the basis of the present work, an explanation appears possible for the amorphous nature of pitchblende in some mineral deposits and the crystallinity that occurs in others.[32] From Fig. 2, it may be seen that at slightly elevated temperatures over a wide range of pressures U_3O_8 assumes amorphous characteristics. This appears to be a consequence of the fact that alpha U_3O_8 is metastable with respect to the γ-modification under these conditions of temperature and pressure but the temperature is too low to provide the activation energy needed for transformation. Thus, the material at 25,000 atm is crystalline α-U_3O_8 at room temperature and virtually amorphous at 300°C. When the temperature increased to 400°C, the gamma U_3O_8 appears in crystalline form.

VOL. 19 1961

In view of the existing similarities of the present high-pressure work and the mineralogical studies of pitchblende, it is of interest to question why γ-U_3O_8 has not been reported as a mineral. Aside from previously discussed differences existing between laboratory and natural processes, it appears probable that the temperature and pressure required for the formation of γ-U_3O_8 are not usually obtained where uranium deposits occur. Nevertheless, the reported "X" phase of BROOKER and NUFFIELD[32] does bear some similarity to reflexions associated with the γ-form of U_3O_8. It appears possible that the phase may have been present and was altered by the very high annealing temperatures which they used.

DISCUSSION

It is generally assumed in nearly all of the recent investigations of the uranium–oxygen system that excess oxygen is incorporated interstitially in the UO_2 fluorite structure, even up to and including such excess compositions as occur for pitchblende.[34] It is difficult to believe that an excess oxygen ion can be retained in either cubic[33] $(\frac{1}{2},\frac{1}{2},\frac{1}{2})$ or octahedral $(\frac{1}{2},0,0)$ positions[34] without expanding the lattice parameter, even considering the corresponding change from U^{4+} to the smaller U^{6+} ion.† The conclusion that oxygen is interstitial has been based, to date, almost exclusively upon density measurements.

A plot of the most reliable density measurements for the uranium–oxygen system is given in Fig. 3. For comparison purposes, the theoretical density variations to be expected for a cubic fluorite structure, containing oxygen interstitials, uranium vacancies, and uranium sites containing oxygen are superimposed. The densities

* FRONDEL[37] has stated that the fluorite structure may form directly in the oxidized state (as uraninite) by hydrothermal means.

† The size consideration given here would not necessarily be valid if the additional oxygen is incorporated, as a complex such as O_2^{-} or O_2^{2}. Under these circumstances U_4O_9 would become $U_4^{4+}(O_2)^{2-}O_7^{2-}$.

[36] G. J. F. MACDONALD, *Amer. J. Sci.* **254**, 713–721 (1956).
[37] C. FRONDEL, *Amer. Mineralogist* **42**, 131 (1957).

obtained by GRONVOLD[7] for his uranium oxide samples, investigated by high-temperature diffraction show a monotonic increase to U_4O_9, followed by a density decrease for the two-phase region of U_4O_9 plus U_3O_8.

The densities of UO_2 and U_4O_9 determined by PERIO[5] and those obtained by ANDERSON[38] for several O/U compositions also show density increases with increasing oxygen. The latter, however, shows the density still increasing beyond the U_4O_9 composition. In an earlier work GRONVOLD[39] also determined densities for $UO_{2\cdot33}$ and

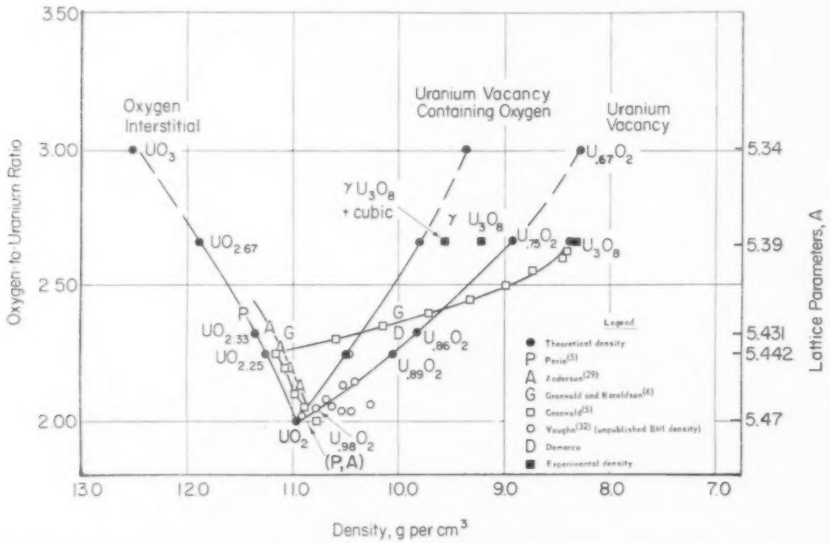

FIG. 3.—Theoretical and experimental densities of uranium oxides from UO_2 to UO_3 assuming defect fluorite structure.

$UO_{2\cdot40}$, as shown, in which the $UO_{2\cdot40}$ density was best explained by GRONVOLD by assuming the composition to be $U_{0\cdot88}O_{2\cdot12}$. This corresponds to the uranium vacancy model with the excess oxygen occupying the uranium vacancy positions.

In contrast (except for the GRONVOLD $UO_{2\cdot40}$) to the high density results of the annealed samples of ANDERSON, PERIO, and GRONVOLD, the recent work of DEMARCO *et al.*,[40] yielded density of 10·01 g/cm³ for the composition U_3O_7. This density was obtained by the helium compression method on oxides formed by low-temperature oxidation. Although DEMARCO supports the interstitial oxygen hypothesis, his experimental value agrees better with the theoretical density assuming uranium vacancies.

As shown in Fig. 3, if pressure is capable of producing a cubic phase of U_3O_8 composition its density would be 12 g/cm³ for the oxygen interstitial model, 9·8 g/cm³ for uranium vacancies containing oxygen and 8·9 g/cm³ for uranium vacancies alone. The measured density of the γ-U_3O_8 was 9·2 g/cm³. A further increase in density to 9·6 g/cm³ appears possible with the appearance of the cubic "U_4O_9" like phase in samples subjected to 70,000 atm pressure at 450°C.

[38] M. J. S. ANDERSON, *Bull. Soc. Chim.* 781 (1953).
[39] F. GRONVOLD, *Nature, Lond.* **162**, 70 (1948).
[40] R. E. DEMARCO, H. A. HELLER, R. C. ABBOTT and W. BURKHARDT, *Bull. Amer. Cer. Soc.* **38**, 360 (1959).

The precision of the density determination was of the order of ±10 per cent because of the limited quantity of the sample material available. This coupled with the fact that the samples produced at 70,000 atms were in the two-phase region of γ-U_3O_8 plus the cubic phase, makes it difficult to determine whether the interstitial oxygen or uranium vacancy model is operative. The answer to this question will apparently require the production (and retention) of a sufficient quantity of cubic phase U_3O_8 from which more accurate density determinations are possible.

Additional density values are shown in Fig. 3 for uranium oxides of oxygen composition up to U_4O_9. The values, previously unpublished, were obtained from the work of VAUGHAN *et al.*[41] The oxides were prepared by air oxidation of UO_2 at 180°C. The product was subsequently homogenized at 450°C for 100 hr in sealed capillaries. The density determination was made by the helium compression method.

Although the X-ray results of GRONVOLD were largely confirmed by VAUGHAN, it may be seen from Fig. 3 that the density values obtained tend to follow the uranium vacancy models more closely. An initial density of 10·9 g/cm³ was obtained by VAUGHAN for the composition U_4O_9. Since this material was used in the present work a redetermination of the density was undertaken. A vacuum pycnometric density of 10·33 g/cm³ and a helium density of 10·489 ± 0·033 g/cm³ were obtained. A redetermination of the O/U ratio by microbalance technique yielded a composition of $UO_{2\cdot26}$. It may be seen from Fig. 3 that the latter density determination agrees better with the model of the uranium vacancy containing oxygen and is well below those given by GRONVOLD.

Although these results do not conclusively demonstrate which defect model is predominant they do suggest that additional work should be performed to establish the validity of the interstitial oxygen model.

The U_4O_9 material, described above, was subjected to pressures up to 100,000 atm at temperatures to 1000°C. No significant change was observed to occur in its structure or lattice parameter of $a = 5{\cdot}44$ Å. The same general results were obtained for UO_2 with the lattice parameter of 5·47 Å. Broadening of the X-ray reflexions from samples of both compositions was observed. This in all probability, results during the release of pressure from the non-hydrostatic components of pressure known to exist in the pressure devices.

Acknowledgement—The writer would like to acknowledge the assistance of P. B. ROBBINS, B. G. KOEHL and A. F. GERDS of the Battelle staff. Mr ROBBINS contributed to the high-pressure work and B. G. KOEHL and A. F. GERDS performed the microbalance and density determinations. This work was performed under AEC Contract W-7405-ENG-92.

ADDENDUM

The pressures used herein are based upon the calibration scheme assuming the validity of the Ba II–III transition at 80,000 atms, determined by BRIDGMAN, and that of the Bi VI–VIII transition at 121,000 atm determined by BUNDY. It has recently been suggested by KENNEDY at the Lake George Conference on Ultra-High Pressure that this pressure scale is in error, and should be correspondingly reduced by a factor of $\frac{1}{3}$ for all pressures above 25,000 atm. Should the latter scale ultimately prove to be correct, the pressures herein would be modified by this factor.

[41] D. A. VAUGHAN, J. R. BRIDGE and C. M. SCHWARTZ, Battelle Memorial Institute Report BMI–1241 (1957).

VOL. 19 1961

APPENDIX A

The observed d values of the high-pressure γ-modification of U_3O_8 are given in Table 2. Limited work to determine the structure of the phase has given a tentative indexing on an hexagonal (rhombohedral) cell with $a = 8{\cdot}78$ Å and $c = 9{\cdot}18$ Å. On the basis of this cell a computed density of 9·15 g/cm³ was obtained assuming four molecules per unit cell. The agreement with the measured density of 9·2 g/cm³ is

TABLE 2.—OBSERVED INTERPLANAR SPACINGS FOR THE GAMMA, HIGH PRESSURE MODIFICATION OF U_3O_8

d	I*	d	I
4·68	*vf*	1·240	*m*
3·48	*vs*	1·225	*f*
3·35	*m*(†)	1·215	*f*
3·05	*s*	1·195	*mf*
2·92	*s*	1·170	*mf*
2·70	*ms*	1·162	*m*
2·53	*m*	1·150	*mf*
2·40	*m*	1·127	*f*
2·25	*vf*	1·122	*mf*
2·20	*vf*	1·103	*vf*
2·11	*vf*	1·098	*mf*
2·04	*vf*	1·086	*f*
1·95	*s*	1·080	*f*
1·91	*f*	1·074	*f*
1·85	*ms*	1·061	*mf*
1·83	*f*(†)	1·049	*vf*
1·79	*m*	1·041	*f*
1·77	*ms*	1·035	*mf*
1·74	*m*	1·029	*mf*
1·69	*mf*	1·020	*mf*
1·65	*m*	1·016	*mf*
1·59	*m*	1·004	*mf*
1·53	*s*	1·000	*mf*
1·46	*m*	0·998	*f*
1·40	*f*	0·997	*f*
1·36	*f*	0·991	*mf*
1·33	*f*	0·979	*m*
1·32	*vf*	0·977	*m*
1·27	*vf*	0·975	*m*
1·26	*f*		

* Intensities estimated visually.

† These reflexions appear when gamma is first formed at lower temperatures but are not observed at the higher temperatures.

fortuitous in view of the uncertainty of both the indexing and the density measurements.

The oxygen analyses of Group I appear low apparently as a result of the vacuum treatment. The Group II analyses, undertaken to check these results, show higher oxygen/uranium ratios than that corresponding to U_3O_8. It is probable that the starting U_3O_8, originally stoicheiometric, had chemisorbed oxygen. During the high-pressure experiments this would tend to be incorporated into the structure. It is not believed, however, that the small shift from stoicheiometric U_3O_8 would materially affect the present results.

J. Inorg. Nucl. Chem., 1961, Vol. 19, pp. 223 to 228. Pergamon Press Ltd. Printed in Northern Ireland

THE INDIUM(I) BROMIDE–INDIUM(III) BROMIDE SYSTEM

P. H. L. WALTER*, J. KLEINBERG and E. GRISWOLD
Department of Chemistry, University of Kansas, Lawrence, Kansas

(*Received* 11 *October* 1960; *in revised form* 15 *November* 1960)

Abstract—A cryoscopic phase study of the system indium(I) bromide–indium(III) bromide has been made. Evidence has been found for the existence of three intermediate compounds: In_2Br_3, In_4Br_7 and $InBr_2$. The results of the phase study have been verified by X-ray powder patterns and by an extraction experiment.

In the light of Pauling's "radius ratio theory" and previous work on indium halides, it is postulated that In_2Br_3 exists as $In^I_3[In^{III}Br_6]$ and that $InBr_2$ exists as $In^I[In^{III}Br_4]$. No structure is proposed for In_4Br_7.

VOL. 19 1961

THE valence relationships among the metals of representative group III have been a source of debate for many years. The 1+ and 3+ states are unambiguously shown by all the metals: aluminium, gallium, indium and thallium. In addition, examples of an apparent dipositive state were provided by the gallium and indium dihalides. However, gallium dichloride has been shown[1–3] to be gallium(I) tetrachlorogallate(III), and therefore it does not contain dipositive gallium. Because of this work, a re-examination of the indium halides seemed worthwhile to determine whether they, too, might be explained without invoking the divalency of indium. Up to this time, phase studies had been reported on only the indium–iodine system.[4,5] These studies confirmed the existence of compounds with stoicheiometries InI, InI_2 and InI_3. Following the gallium dichloride work, CLARK *et al.*[6] undertook a phase study of the indium monochloride-indium trichloride system. They found no evidence for a compound with the stoicheiometry $InCl_2$. Rather, they found a congruently melting "sesquichloride", In_2Cl_3 and two incongruently melting compounds, in addition to the monochloride and the trichloride. The stoicheiometry of the stable iodides and chlorides was explained in light of the gallium work, by assuming that indium exists only in unipositive and tripositive states and that the co-ordination number of tripositive indium changes from four for iodide to six for chloride, in accordance with the formulations

$$InI_2 = In^I[In^{III}I_4]$$

$$In_2Cl_3 = In_3^I[In^{III}Cl_6]$$

This change in co-ordination number is in agreement with Pauling's radius ratio theory.[7] Since this theory is based on a simplified form of the binding energy

* Present Address, Central Research Dept., E. I. du Pont de Nemours and Co., Inc., Wilmington 98, Delaware.

[1] J. D. CORBETT and R. K. MCMULLEN, *J. Amer. Chem. Soc.* **78**, 2906 (1956).
[2] L. A. WOODWARD, G. GARTON and H. L. ROBERTS, *J. Chem. Soc.* 3723 (1956).
[3] G. GARTON and H. M. POWELL, *J. Inorg. Nucl. Chem.* **4**, 84 (1957).
[4] A. THIEL and H. KOELSCH, *Z. Anorg. Chem.* **66**, 288 (1910).
[5] E. A. PERETTI, *J. Amer. Chem. Soc.* **78**, 5745 (1956).
[6] R. J. CLARK, E. GRISWOLD and J. KLEINBERG, *J. Amer. Chem. Soc.* **80**, 4764 (1959).
[7] L. PAULING, *The Nature of the Chemical Board* (3rd Ed.). pp. 540–543. Cornell University Press, Ithaca (1960).

equation, it is not applicable to "borderline cases". Neither iodide nor chloride creates a borderline case with indium, but bromide does. Since the theory does not give an unambiguous co-ordination number for indium(III) toward bromide, we undertook this study of the indium(I) bromide–indium(III) bromide system to determine what phases do exist.

In(III)/X^-

Halide	Radius ratio	Expected C.N.
Cl	0·447	6
Br	0·415	4 or 6
I	0·375	4

EXPERIMENTAL

Because of the moisture sensitivity of the halides studied, all the materials were prepared and handled by conventional vacuum and dry-box techniques.

Preparations. Indium(III) bromide was prepared by passing bromine vapour (B & A, Reagent Grade), diluted with dry, oxygen-free nitrogen, over indium metal (Fairmount Chemical Company, 99·97 per cent pure) and resubliming the product twice under nitrogen. A typical analysis of the product gave In, 32·37; Br, 67·55% (Calculated for $InBr_3$: In, 32·37; Br, 67·63%).

The indium-rich indium–bromide compositions were prepared by reducing indium(III) bromide with a calculated amount of indium metal. The materials were placed in a dry, outgassed Pyrex tube which was then evacuated, sealed and heated to 350° to form a homogeneous melt. While the samples were molten, the tubes were shaken from time to time to insure reaction. After overnight heating the tubes were removed from the furnace and rapidly cooled in a stream of compressed air. Since the melts readily supercooled, phase separation at this point did not occur. The samples were then stored in the tubes until needed.

Cooling curves. Cooling curves were obtained on each sample. The cooling-curve cell consisted of a vacuum-jacketed 16 mm Pyrex tube. The outer jacket was fashioned from 32 mm Pyrex tubing. The upper end of the cell consisted of a 34/45 standard taper joint into which fit a 34/45 standard taper-top containing a thermocouple well, a nitrogen inlet and outlet and a stirrer. The cell was heated in an aluminium block and the samples were brought to about 30° above their melting points and then were allowed to cool at the rate of 2–4° per min. The temperature was recorded every 0·5 min.

Analyses. Indium was determined by the method of DANIEL *et al.*[8] using a complexiметric titration with EDTA followed by a back titration with standard Zn^{2+} using Eriochrome Black T as the indicator.

Bromine was determined by the Volhard method.

Powder pattern. Diffraction patterns were taken on a North American Philips X-ray Unit using a Debye-Scherrer powder camera of 114·57 mm diameter.

The samples were prepared for X-ray analysis by grinding them in a sapphire mortar and screening to 200 mesh. The powder was loaded in 0·3 mm capillaries and exposed to CuK_α radiation for from 2 to 6 hr.

Extraction experiment. The behaviour of $InBr_3$ toward ether extraction was determined. Samples of $InBr_2$ were sealed in nitrogen-filled, Pyrex tubes containing 2–10 ml of anhydrous diethyl ether. The tubes were then equilibrated at 30° for varying lengths of time. After removing the samples from the bath, the liquid and solid were separated and each was analysed for indium and bromine.

RESULTS AND DISCUSSION

Phase study. The results of the phase study on the system, indium monobromide-indium tribromide, are presented in Fig. 1. The phase diagram is more complex than

[8] S. S. DANIEL, J. P. REDFERN, J. E. SALMON and J. G. L. WALL, *Lab. Pract.* **7**, 15 (1958).

that obtained for the indium–iodine system,[5] or the indium–chlorine system.[6] It is clear from the diagram that there are no intermediate compounds in the indium–bromine system as high melting as indium monobromide or indium tribromide. Three other compounds do appear on the diagram. These have the empirical formulas, In_2Br_3, In_4Br_7 and $InBr_2$.

In_2Br_3 appears to be just on the borderline between a congruently melting and an incongruently melting compound. It is not possible to determine from our data whether a eutectic point at about 232° appears slightly to the left of the 25 mole % $InBr_3$ line, or whether a transition point occurs at the same temperature and very slightly to the right of the 25 mole % $InBr_3$ line. The change in slope of the liquidus line at the composition corresponding to this compound was negligible. Indeed, were it not for the large change in solidus temperature (35°C), this compound could have been missed. In addition to the change in solidus temperature at 25 mole per cent indium tribromide, there was also a change in colour at this point. All the compositions richer in indium than In_2Br_3 (to the left of this compound on the diagram) were a deep red in colour. All the compositions poorer in indium than In_2Br_3, however, were white with more or less a trace of green. The red colour was probably due to the presence of indium monobromide which by itself is almost black. A similar observation was made by CLARK *et al.*[6] in the indium–chlorine system at the composition corresponding to In_2Cl_3.

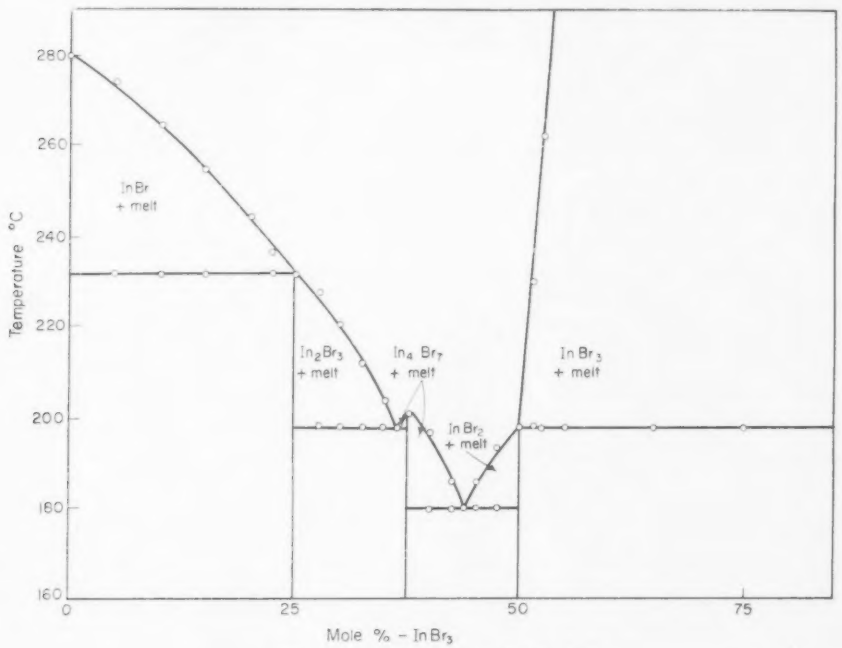

FIG. 1.—Phase diagram of $InBr$–$InBr_3$.

A second compound appears at 37·5 mole per cent indium tribromide. This corresponds to a composition, In_4Br_7. While this compound possesses a limited range of stability, it was quite clearly congruently melting. An incongruently melting

compound reported in the indium–chlorine system by CLARK *et al.*[6] was in the composition range which includes In_4Br_7 and so was possibly In_4Cl_7. CLARK *et al.* were unable to determine its exact composition.

The remaining compound appears at 50 mole per cent indium tribromide, corresponding to the composition $InBr_2$. This, like In_2Br_3, was just on the borderline between a congruently melting and an incongruently melting compound. At the compositions richer in bromine than indium dibromide, the liquidus temperature rapidly increased and indium tribromide began to sublime from the samples. Again, a corresponding observation was made by CLARK *et al.*[6] at a similar point in the indium–chlorine system, although in that system no indium dichloride was observed.

X-ray study. X-ray powder patterns were taken of all the apparent compounds and at one composition between each pair of compounds. The purpose of the X-ray work was not to determine structures but was rather to verify the phase diagram with additional evidence. In Table 1 are presented the lines with *d*-values greater than 1·85 for each composition examined.

If the phase diagram (Fig. 1) is correct, and the intermediate compositions consist of mixtures of two pure compounds, one would expect that each line of an intermediate composition could be identified with a line of one of its components. Since, however, the concentration of the "line-producing", pure compound is lower in the mixture than in the pure compound itself, the intensity of the line in the mixture cannot be greater than its intensity in the pure compound. In Table 1 it can be seen that all the lines produced by the intermediate compositions can indeed be correlated with the lines of the pure compounds. In all the cases, the intensities of the lines of the mixtures are equal to or less than the intensities of the same lines in the pure compounds.

Furthermore, if the phase diagram is correct, lines characteristic of a given phase should not appear in compositions beyond the boundaries of that phase. For example, a line characteristic of "In_2Br_3" should appear only within the range $1{\cdot}0 < x < 1{\cdot}75$. While in patterns such as these, certain lines may appear coincidentally over a wide range of compositions, this should not be generally so. Table 1 shows that these restrictions, too, are satisfied.

Thus, while the X-ray patterns do not in themselves prove the existence of compounds at In_2Br_3, In_4Br_7 and $InBr_2$, when taken in conjunction with the cryoscopic phase diagram already obtained, they provide verification for the conclusions drawn.

Extraction experiment. It was observed that ether caused "indium dibromide" to dissociate completely into indium monobromide and indium tribromide. This reaction was so rapid that even ether vapour changed the colour of "indium dibromide" from a faintly greenish white to red. In no ether extraction was any intermediate compound obtained. This result tends to confirm the phase diagram which shows no compound of high stability between indium monobromide and indium tribromide. The results can be described by the equation:

$$2InBr_2 \xrightarrow{\text{Ether}} InBr_3 + InBr.$$

SUMMARY

The cryoscopic phase study and the X-ray powder patterns are in agreement and can be easily interpreted. There exist in the indium monobromide–indium tribromide

TABLE 1.—A COMPARISON OF THE X-RAY LINES FOR VARIOUS In-Br COMPOSITIONS*

Composition of $InBr_x$						(Figures below are *d*-Values)		
InBr		In_2Br_3		In_4Br_7		$InBr_2$		$InBr_3$
$x = 1{\cdot}0$	1·2	1·5	1·6	1·75	1·9	2·0	2·4	3·0
	10·51	9·92(*s*)	10·00					9·38
				8·11(*w*)				
				7·37(*w*)		7·19(*w*)		7·02
			6·80	6·75(*m*)	6·72			
	6·29	6·41(*vw*)					6·23	6·28
						6·19(*w*)		
			5·82	5·90(*m*)	5·80			5·79
				5·60(*w*)				
			5·20	5·24(*m*)	5·21			
					5·22	5·21(*m*)	5·18	
			4·68	4·74(*m*)	4·62			
	4·57	4·64(*vw*)						
4·19	4·15			4·07(*w*)				
					3·99	3·98(*vs*)	3·96	
			3·80	3·80(*s*)	3·80			
3·75				3·72(*vw*)				
					3·67	3·69(*m*)	3·63	
	3·43	3·39(*w*)	3·41	3·45(*m*)	3·46	3·48(*m*)	3·43	3·50
			3·18	3·20(*s*)	3·20			
						3·16(*m*)	3·14	3·14
3·13	3·12		3·10	3·13(*m*)				
3·08	3·09	3·08(*s*)	3·07					
	3·00	2·99(*s*)	3·00					
			2·96	2·97(*vs*)	3·00			
					3·02	3·01(*vs*)	2·99	
	2·90	2·90(*m*)	2·89					
		2·82(*w*)						
		2·76(*vw*)		2·72(*m*)	2·72	2·61(*m*)	2·61	
2·58	2·58							
	2·53	2·54(*w*)			2·53	2·53(*s*)	2·54	
						2·50(*m*)	2·51	
						2·47(*vw*)	2·46	
						2·40(*vw*)		
2·37	2·35			2·35(*ms*)		2·34(*s*)	2·31	
		2·30(*w*)						
2·23	2·21			2·21(*m*)		2·22(*vw*)		
2·16	2·14			2·11(*w*)		2·17(*vw*)		
						2·13(*w*)		2·14
						2·09(*m*)	2·07	2·10
	2·01	2·01(*s*)	2·02	2·02(*m*)	2·00	2·00(*s*)		2·01
1·97								1·95
1·88		1·89(*m*)		1·90(*s*)		1·88(*m*)		
						1·84(*m*)		1·85

* Relative intensities of the lines are indicated by the symbols: *vs* = very strong; *s* = strong; *ms* = moderately strong; *m* = medium; *w* = weak; *vw* = very weak. Not all the lines which were observed are listed, the main purpose of the table being to indicate the approximate ranges of existence of the various phases.

VOL. 19 1961

system three intermediate compounds, with empirical formulas In_2Br_3, In_4Br_7 and $InBr_2$. Only one of these compounds, In_4Br_7, is stable at its melting point.

The oxidation states of indium in InBr and $InBr_3$ are well-accepted as 1+ and 3+ respectively. While the structure of In_2Br_3 is unknown, it clearly must contain indium in two different valence states. It seems most likely that it contains both 1+ and 3+ indium and that it probably exists as indium(I) hexabromoindate(III), $In_3^I[In^{III}Br_6]$. Furthermore, since there is no direct evidence for a 2+ oxidation state in indium, it seems probable that $InBr_2$ exists as indium(I) tetrabromoindate(III), $In^I[In^{III}Br_4]$. These formulations are analogous to those proposed by CLARK *et al.*[6] with regard to In_2Cl_3 and InI_2.

CLARK *et al.* observed that when "$InCl_2$" was extracted with ether, the results varied, depending on the length of time the sample was extracted. With a single extraction, the products were always In_2Cl_3 and $InCl_3$, while on continuous extraction, InCl and $InCl_3$ was obtained. Since no compound having the empirical formula $InCl_2$ exists in the indium–chlorine system, the composition $InCl_2$ consists of a mixture of In_2Cl_3 and $InCl_3$. It was proposed that the single extraction merely separated the mixture because of solubility differences, the $InCl_3$ dissolving in the ether while the In_2Cl_3 remained behind. Since In_2Cl_3 was shown to have considerable stability, it reacted only slightly with ether. However, in a continuous extraction over a long period of time, the ether being a stronger Lewis base than chloride ion is able to replace chloride ion. Remembering that $In_2Cl_3 = In_3^I[In^{III}Cl_6]$, the reaction with ether can be written:

$$In_3^I[In^{III}Cl_6] + xEt_2O = \underline{3InCl} + InCl_3 \cdot xEt_2O$$

Similar reasoning can be used to explain the rather different results obtained with $InBr_2$. Here the only products obtained are InBr and $InBr_3$ even after a short single extraction. In this case, however, there are no intermediate compounds with stability comparable to In_2Cl_3, so while the equilibrium in the reaction above is far to the left, that in the reaction below is much to the right:

$$In^I[In^{III}Br_4] + xEt_2O = \underline{InBr} + InBr_3 \cdot xEt_2O$$

Acknowledgements—The authors wish to acknowledge the financial support given this research by the Atomic Energy Commission. One of us (P. H. L. W.) also wishes to thank the Monsanto Chemical Company for a fellowship which he received during part of this work.

J. Inorg. Nucl. Chem. 1961 Vol. 19, pp. 229 to 236. Pergamon Press Ltd. Printed in Northern Ireland

THE MnTe–GeTe PHASE DIAGRAM

W. D. JOHNSTON and D. E. SESTRICH
Chemistry Department, Research Laboratories Westinghouse Electric Corporation, Pittsburgh

(*Received* 26 *September* 1960; *in revised form* 17 *November* 1960)

Abstract—The phase diagram of the pseudo-binary MnTe–GeTe has been developed. At elevated temperatures there is a continuous range of solid solution between GeTe and MnTe having NaCl symmetry. The thermal expansion characteristics of the NiAs form of MnTe have been examined and the transformation of MnTe from NiAs to NaCl symmetry has been established by X-ray and thermal analysis.

VOL. 19 1961

PHASE diagram studies of the Ge–Te system revealed that the only compound in this system was GeTe with a melting point of 725°.[1] This material has a rhombohedrally distorted NaCl crystal structure at low temperatures. The structure becomes NaCl cubic at temperatures above 440°C. Until the recent work of MCHUGH and TILLER,[2] it was not clear whether GeTe decomposed peritectically or melted congruently. These workers showed that the GeTe phase melts congruently as $GeTe_{1\cdot025}$ at 724°C which is very close to the eutectic composition $GeTe_{0\cdot994}$, having a melting point of 723·7°C.

Very little is known about the Mn–Te system. FURBERG[3] in particular showed that the phases formed in this binary include only MnTe which has the NiAs structure and $MnTe_2$ which has the pyrite structure. The magnetic data of UCHIDA[4] are in agreement with this representation in the MnTe–$MnTe_2$ region. JOHANSEN[5] has shown that MnTe is also a tellurium excess material, as would be expected from its p type behaviour, with a composition range of $MnTe_{1\cdot002}$ to $MnTe_{1\cdot013}$. Beyond this information nothing is reported on the phase diagram of the MnTe system.

No mention has been made in the open literature of any materials within the ternary system Mn–Ge–Te. CORNISH[6] examined $Mn_{0\cdot5}Ge_{0\cdot5}Te$ and found it to solidify at 1000°. This material had a NaCl structure. DONAHOE,[7] in attempting to zone refine this material, succeeded only in separating GeTe from MnTe. From DONAHUE's experiment it became immediately obvious to us that $Mn_{0\cdot5}Ge_{0\cdot5}Te$ cannot melt congruently.

This preliminary work prompted this survey of the MnTe–GeTe pseudobinary systems. Arbitrarily, the pseudo-binary has been examined in such a way that the metal to nonmetal ratio is one, i.e., $Mn_xGe_{1-x}Te$. This decision was made in spite of the fact that the end members of the system are slightly anion excess since there was no assurance that this excess would be constant throughout the pseudo-binary.

[1] M. HANSEN, *Constitution of Binary Alloys*. McGraw-Hill, New York (1958).
[2] J. P. MCHUGH, W. A. TILLER, *Trans. Met. Soc. AIME* **218**, 187 (1960).
[3] S. FURBERG, *Acta Chem., Scand.* **7**, 693 (1953).
[4] E. UCHIDA, H. KONDOH and N. FUKOUOKA, *J. Phys. Soc. Japan* **11**, 27 (1956).
[5] H. A. JOHANSEN, *J. Inorg. Nucl. Chem.* **6**, 344 (1958).
[6] A. J. CORNISH, Westinghouse Research Laboratories, Private communication (1959).
[7] R. DONAHOE, Westinghouse Materials Engineering, Private communication (1959).

EXPERIMENTAL

Preparation

MnTe was prepared from triply vacuum distilled manganese and American Smelting and Refining Company 99·99 per cent tellurium. The elements were crushed to $-20 + 40$ mesh and placed in a graphite crucible which had previously been fired in vacuum. The crucible and sample were then placed in a Vycor tube which was evacuated and sealed off. The sample was heated slowly to 900° in order to avoid a violently exothermic reaction and held there for 24 hr. To ensure the reaction had progressed to completion, the sample was crushed, returned to the graphite crucible and melted for 10 min in an argon-filled bell jar by using r.f. power. The several MnTe stock materials used in this work were dissolved for analysis in 1:1 nitric acid contained in a covered three litre beaker and then the excess oxides of nitrogen were boiled off. An excess of ethylenediaminetetraacedic acid (EDTA) was added to complex the manganese in the solution. The solution was made alkaline and the excess EDTA was titrated with a standard magnesium solution giving the manganese content by difference. Tellurium was found by adding sulphuric and phosphoric acids and then an excess of potassium dichromate to oxidize the Te^{4+} to Te^{6+}. The solution was heated to reduce any Mn^{3+} which may have been formed and then the excess dichromate titrated with ferrous ammonium sulphate. Found: Mn, 30·4 ± 0·4; Te, 69·7 ± 0·3; C, 0·08% maximum in any sample. Calc. Mn, 30·1; Te, 69·9; C, 0%).

GeTe was prepared from $-4 + 20$ mesh semiconductor grade germanium and 99·99 per cent tellurium according to the proecdure developed by MCHUGH and TILLER.[2] The materials were sealed off under vacuum in an Aquadag lined Vycor tube which was heated rapidly to 800° under vacuum and held at this temperature for 3 hr. The tube was shaken occasionally to promote mixing. Aquadag has been found by these authors[2] to be inert to GeTe.

Materials in the $Mn_xGe_{1-x}Te$ system were prepared from -200 mesh MnTe and GeTe. These materials were manipulated in an argon-filled glove box although this precaution is probably not necessary. Weighed amounts of the powders were mixed and pressed together and placed in graphite crucibles which were sealed off in Vycor tubes under a partial argon pressure. The samples were fired for 24–48 hr at 700° or 800°C. Although the pellets were homogeneous at this point, they were not mechanically strong, so they were reground to -200 mesh, pressed at 100,000 lb/in² and refired. In this way densities of 85 per cent of theoretical could be obtained. In certain cases quenching was performed by dropping small samples contained in Aquadag-coated Vycor tubes from a vertical furnace into water. These samples were not analysed chemically since the use of sealed tubes and graphite crucibles precludes any change of composition.

X-ray measurements

Room temperature X-ray measurements were made using a Phillips 11·54 cm diameter powder camera with cobalt radiation $\lambda K_{\alpha 1} = 1{\cdot}78892$ and $\lambda K_{\alpha 2} = 1{\cdot}79278$ Å. The high temperature X-ray studies were performed using a Unicam 19 cm diameter high temperature camera and copper radiation $\lambda K_{\alpha 1} = 1{\cdot}54051$ and $\lambda K_{\alpha 2} = 1{\cdot}54433$ Å. In this case a rotating anode X-ray tube designed and built by Dr. A. TAYLOR was used in order to minimize the time at temperature. Aquadag coated silica capillaries were used to prevent reaction of the sample with glass. In all cases the lattice parameters were determined using the extrapolation function $(\cos^2\theta/\sin\theta + \cos^2\theta/\theta)/2$.

Repeated attempts failed to give high temperature X-ray patterns with a measurable back reflexion region. Since the front reflexion region is not nearly so sensitive to variations in lattice parameter as the back reflexion region, it was not possible to obtain the accuracy that is normally expected of X-ray methods. At the highest temperatures the possible error of lattice parameter measurements was estimated to be nearly ±0·1 per cent. Temperatures were measured by a platinum 10 per cent rhodium thermocouple placed within ¼ in. of the sample. Corrections to the measured temperatures were provided by Dr. A. TAYLOR who calibrated the apparatus by measuring the thermal expansions of a number of standard samples.

Compression test

This test was performed using a tensile tester designed and built by Mr. E. WESSEL. A ¼ in-diameter by ½ in. pellet was placed in compression under a 200 lb load. The temperature was increased and the point at which the load could no longer be supported was taken as the solidus.

Temperatures were measured by chromel–alumel thermocouples placed at the top and bottom block compressing the sample and beside the sample. In many cases, due to sample softening and thermal gradients, the point at which the load could not be supported was ill defined and could only be determined to $\pm 12°$.

Thermal analysis

A sample of 15–20 g was placed in either of two types of crucibles. One crucible was fabricated from boron nitride which was fitted with a threaded cap of boron nitride which closed tightly by the use of matched tapers. The other crucible was made of graphite sealed in quartz. Both crucibles had reentrant tubulations in the bottoms for chromel–alumel thermocouples.

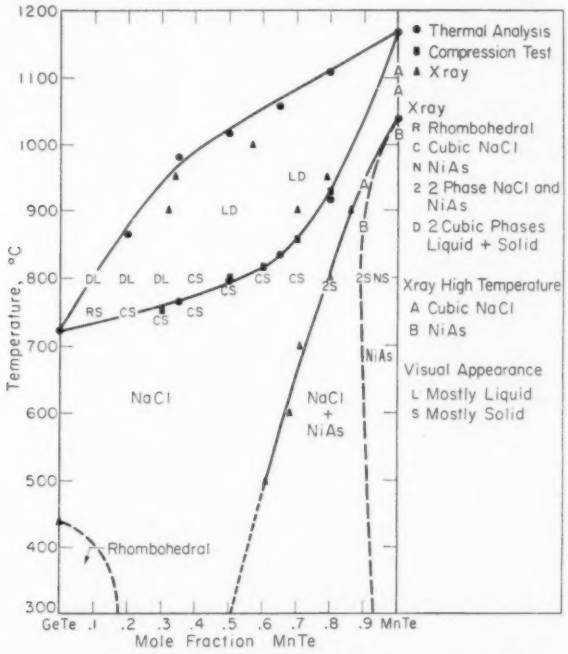

FIG. 1.—Phase diagram for MnTe–GeTe system.

A normal cooling curve was satisfactory for MnTe. For other compositions the liquidus and solidus region was so broad that thermal effects were much less pronounced and differential thermal analysis was used. The differential curves were run against mullite for samples contained in boron nitride and against graphite enclosed in quartz for samples in graphite and quartz containers.

Solidus arrests could be found from the first heating of a homogeneous sample prepared by powder metallurgy. Liquidus points could be determined repeatedly during cooling cycles and were generally within $\pm 2°$, although in two cases the error was considerably larger presumably due to supercooling.

RESULTS AND DISCUSSION

A preliminary survey of the system was made on pellets prepared at 700° and 800° from MnTe and GeTe. The results of visual and X-ray examinations are included in the final phase diagram which is shown in Fig. 1. The X-ray data obtained are tabulated in Table 1 and certain of the data plotted in Fig. 2.

Fig. 2 shows that the rhombohedral distortion in GeTe decreases rapidly with Mn and vanishes at $x \sim 0{\cdot}18$. Beyond this point the structure is of undistorted NaCl symmetry with the lattice parameter decreasing with Mn content. The decrease in

VOL. 19 1961

volume with Mn content is much more rapid in the rhombohedral structure than in the cubic structure. Fig. 2 also shows that in the cubic region the graph of a vs. composition is linear to $x = 0{\cdot}7$ suggesting a single phase region throughout this range of composition. Between $x = 0{\cdot}8$ and $x = 0{\cdot}9$ a two phase region consisting of phases of NiAs and NaCl symmetry was found. Where $x = 0{\cdot}8$ the lines of the NaCl phase were strongest while where $x = 0{\cdot}9$ the NiAs lines were strongest. Where $x = 0{\cdot}95$ and $1{\cdot}0$ only the NiAs structure could be detected. Again the data in Table 1 indicate that the size of the unit cell, this time NiAs, decreases with the Mn content.

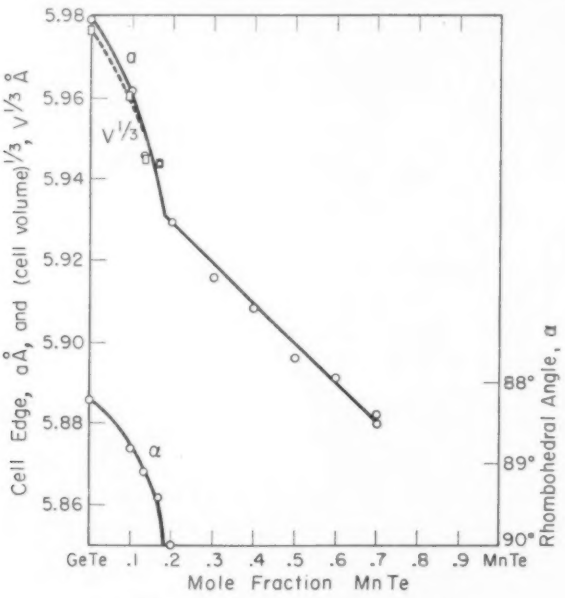

FIG. 2.—Lattice parameter vs composition.

Since GeTe has been found to transform from rhombohedral to cubic at ~440°,[8] it is therefore clear that at temperatures in excess of ~440° the overall phase diagram consists of two single phase regions, one of NaCl and the other of NiAs symmetry, and the two phase region separating them. Presumably the transformation temperature of GeTe from rhombohedral to cubic is lowered by the introduction of Mn and is below room temperature beyond $x \sim 0{\cdot}18$. This is indicated by the dotted line in the phase diagram.

Certain of the survey samples prepared at 800° ($x = 0{\cdot}1$–$0{\cdot}4$) appeared to be at least partially liquid according to both visual and X-ray inspection. The X-ray patterns of these materials consisted of two phases. One phase was characterized by sharp lines that could be indexed on a NaCl unit cell and is identified as the solidus. The parameter of this cell is approximately that of the composition where $x = 0{\cdot}5$. Therefore $Mn_{0{\cdot}5}Ge_{0{\cdot}5}Te$ is approximately the solidus composition at 800°. The other X-ray lines were very broad and believed to be of rhombohedral symmetry and probably result from the liquidus. In order to get a quick survey of the shape of the solidus and liquidus, samples were quenched from 900°, 950° and 1000°C and the

[8] K. SCHUBERT and H. FRICKE, *Z. Metal.* **44**, 459 (1953).

parameters resulting from the X-ray examination used to establish points along both the solidus and liquidus lines as shown in Fig. 1. The data resulting from the quenching experiments are given in Table 2. In the samples quenched from 900 and 1000° the solidus and the liquidus separated partially. X-ray examination of these separated phases validated the interpretation that has been applied. However, this entire

TABLE 1.—ROOM TEMPERATURE X-RAY DATA FOR SINGLE PHASE PRODUCTS

	a(Å)	c(Å)	$\alpha°$	c/a
GeTe	5·979		88·22	
$Mn_{0·1}Ge_{0·9}Te$	5·962		88·83	
$Mn_{0·133}Ge_{0·867}Te$	5·946		89·19	
$Mn_{0·166}Ge_{0·834}Te$	5·944		89·40	
$Mn_{0·2}Ge_{0·8}Te$	5·930			
$Mn_{0·3}Ge_{0·7}Te$	5·916			
$Mn_{0·4}Ge_{0·6}Te$	5·909			
$Mn_{0·5}Ge_{0·5}Te$	5·896			
$Mn_{0·6}Ge_{0·4}Te$	5·892			
$Mn_{0·7}Ge_{0·3}Te$	5·882 5·880			
$Mn_{0·9}Ge_{0·1}Te$ (2 phase)	4·152	6·737		1·622
$Mn_{0·95}Ge_{0·05}Te$	4·153	6·735		1·622
MnTe	4·148	6·710		1·618
$Mn_{0·9}Ge_{0·1}Te$ 875°	4·222	6·900		1·634
935°	6·003			

TABLE 2.—X-RAY DATA OF TWO PHASE MATERIALS

Sample composition	Quenching temp. (°C)	a(Å)	Composition (x) liquidus and solidus
$Mn_{0·7}Ge_{0·3}Te$	1000	5·893	0·57 liquidus
$Mn_{0·7}Ge_{0·3}Te$	950	5·872	0·79 solidus
		5·915	0·34 liquidus
$Mn_{0·5}Ge_{0·5}Te$	900	5·880	0·70 solidus
		5·917	0·32 liquidus
			Solid-solid boundary
$Mn_{0·8}Ge_{0·2}Te$	500	5·889	0·61
$Mn_{0·8}Ge_{0·2}Te$	600	5·882	0·68
$Mn_{0·8}Ge_{0·2}Te$	700	5·879	0·71
$Mn_{0·88}Ge_{0·12}Te$	800	5·87	0·80
$Mn_{0·92}Ge_{0·08}Te$	900	5·865	0·86

procedure is qualitative at best, particularly in the case of the liquidus where rapid reaction between the liquidus and solidus might occur on quenching resulting in liquidus and solidus points being obtained that are actually within the liquidus–solidus region. As can be seen from the diagram, this is indeed the case although the general location of the solidus and liquidus lines are revealed.

The boundary between the solid NaCl symmetry region and the two phase NaCl + NiAs symmetry region was determined by comparing the X-ray parameters of samples quenched from various temperatures with Fig. 2. The data for this determination are listed in Table 2. The boundary between the two phase region and solid NiAs

VOL. 19 1961

symmetry region is dotted since the small range of solution prevented the X-ray technique from being applied with any assurance.

Both the liquidus and solidus curves were determined by thermal analysis. This method is thought to be the most accurate of the methods used. The solidus was determined from the thermal arrest during the first heating of a homogeneous sample prepared by powder metallurgy. The liquidus could be determined repeatedly from cooling experiments. Additional solidus points were obtained by noting the temperature at which a homogeneous single phase pellet would not support a load. As can be

TABLE 3.—THERMAL ANALYSIS

	Liquidus (°C)	Solidus (°C)	Solid transformation (°C)	Compression test solidus °C
MnTe	1167 ± 0		1039 ± 4 1004 ± 4	
$Mn_{0.8}Ge_{0.2}Te$	1107 ± 15*	915		927
$Mn_{0.7}Ge_{0.3}Te$				856
$Mn_{0.65}Ge_{0.35}Te$	1057 ± 9*	833		
$Mn_{0.6}Ge_{0.4}Te$				816 ± 12
$Mn_{0.5}Ge_{0.5}Te$	1016 ± 2	800 ± 2		804 ± 12
$Mn_{0.35}Ge_{0.65}Te$	981 ± 3	766		
$Mn_{0.3}Ge_{0.7}Te$				754
$Mn_{0.2}Ge_{0.8}Te$	863 ± 2	—		
GeTe[2]	724			

* supercooling present—took average of heating and cooling points.

seen from the figure, the data obtained from the various methods are in general agreement. In most of the compounds only thermal arrests corresponding to the onset and completion of solidification were observed. In $Mn_{0.8}Ge_{0.2}Te$ and $Mn_{0.65}Ge_{0.35}Te$ there were additional thermal arrests centering about 875 and 863°C respectively. These are believed to be due to the solid phase transformation of some of the first material to solidify from the single phase to the two phase region.

The cooling curve of MnTe showed several arrests. In addition to the sharp melting point at 1168°, there was a strong arrest at 1039° and a weak arrest at 1004°.

The nature of the arrests in MnTe was examined using high temperature X-ray diffraction. The results of this study are shown in Fig. 3. It will be seen that MnTe maintains NiAs symmetry to 1018°C. Within experimental error the lattice parameters are a linear function of temperature. Thermal expansion data and the coefficients of thermal expansion are given in Table 4. At 1080° and above the symmetry is NaCl cubic. Thus the 1039° arrest is connected with the NiAs to NaCl transformation. No reason for the weak arrest at 1004°C was discovered.

At this point several observations might be made with respect to the crystallographic transformation. The transformation is very similar to the aragonite-calcite transition since the atomic arrangements in aragonite and calcite are similar to NiAs and NaCl respectively. Furthermore, aragonite structures are found at low temperatures while calcite structures are found at high temperatures. The differences between NaCl and NiAs is merely one of stacking anion and cation layers alternately according

to *ABC ABC* vs. *ABAC ABAC*. For cubic symmetry the *c*/*a* ratio measured with *c* taken along the cubic [111] is 1·633. The figure shows that the *c*/*a* for NiAs actually increases somewhat beyond this value before the transformation takes place. This transformation is further associated with an increase in volume/molecule. An increase in volume is also associated with the aragonite to calcite transformation.[9] Hexagonal coordinates may be calculated for the NaCl structure at 1080° and 1106° and compared

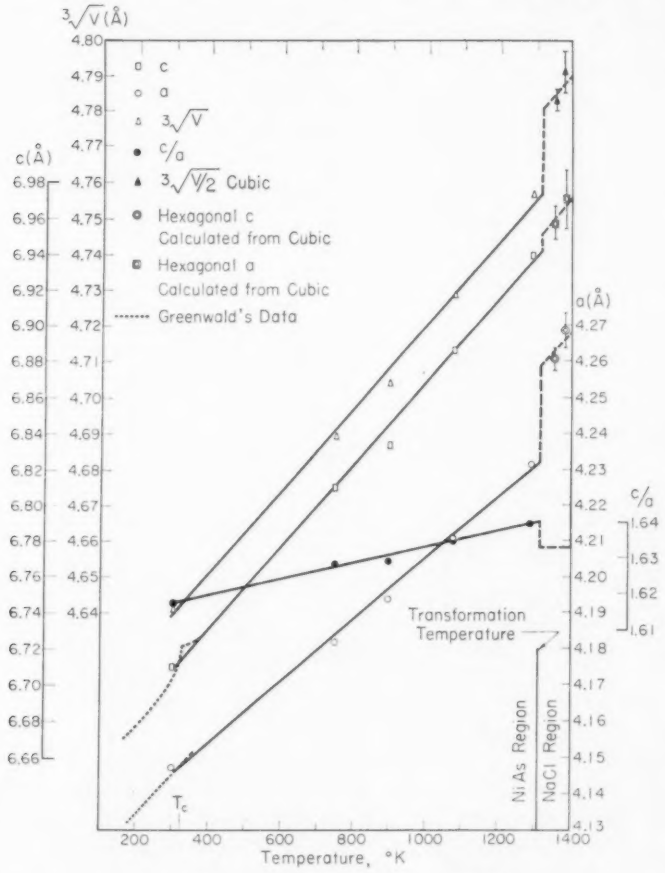

FIG. 3.—Thermal expansion of MnTe.

with hexagonal co-ordinates which may be extrapolated to those temperatures. This comparison gives good agreement of the *c* parameter but a large increase is found the *a* parameter which results in the increased volume.

The slope of the thermal expansion curve in the NiAs region is somewhat different from that obtained by GREENWALD[10] at low temperatures. GREENWALD'S data are given by the broken line on the curve. This is not at all surprising since most of her data are obtained below the antiferromagnetic Curie temperature at 323°K while the data presented here were obtained mainly above this temperature.

[9] J. J. LANDER, *J. Chem. Phys.* **17**, 892 (1949).
[10] S. GREENWALD, *Acta Cryst.* **6**, 396 (1953).

VOL. 19 1961

In order to confirm that the phase diagram is as pictured in Fig. 1, high temperature X-ray pictures were taken of $Mn_{0.9}Ge_{0.1}Te$. At 935° the X-ray picture showed only a NaCl phase validating the diagram. At 875° the pattern was pure NiAs, suggesting that this phase field is wider at high temperatures than at low temperatures. The dotted phase boundary qualitatively indicates this effect. The parameters of the

TABLE 4.—THERMAL EXPANSION OF MnTe

T°K	a(Å)	c(Å)	c/a	V(Å^3)	$V^{\frac{1}{3}}$(Å)
298	4·1475	6·710	1·618	100·0	4·641
744	4·182	6·810	1·628	103·1	4·690
892	4·194	6·834	1·630	104·1	4·704
1071	4·211	6·887	1·636	105·8	4·729
1291	4·232	6·94	1·640	107·6	4·757
					$\left(\frac{V}{2}\right)^{\frac{1}{3}}$
1353	6·026 ± 0·004			218·8	4·783
1379	6·037 ± 0·007			220·0	4·792

Coefficient of linear expansion using straight line through all points in NiAs region	
Plot used	α(/°C)
$V^{\frac{1}{3}}$	$24·5 \times 10^{-6}$
a	$20·6 \times 10^{-6}$
c	$33·7 \times 10^{-6}$

NiAs phase at 875° are almost identical to those of pure MnTe. Further the parameter of the NaCl phase is quite close to the parameter of MnTe which may be calculated using the assumption that MnTe remained cubic to 935° and that the coefficient of expansion is independent of symmetry (6·003 Å measured vs. 6·007 Å calculated). However, the large experimental error inherent in the high temperature X-ray work combined with the lack of any large amount of data at these temperatures excludes any discussion of these similarities beyond the general statement that the sizes of the cells are reasonable.

Acknowledgements—The authors wish to thank Mr. N. DOYLE and Mr. R. HOVAN who contributed to various aspects of this work. The chemical analysis technique was developed by Mr. E. BEITER. Useful discussions were also contributed by Drs. R. C. MILLER and R. MAZELSKY.

This work was done in connexion with U.S. Navy Buships. Contract No. NOBS-78365, *W.* G.O No. WG-79150-CE.

J. Inorg. Nucl. Chem., 1961 Vol. 19, pp. 237 to 244. Pergamon Press Ltd. Printed in Northern Ireland

STRUCTURAL EVIDENCE ON THE BERYL–SODIUM FLUOROSILICATE REACTION

K. R. HYDE, P. L. ROBINSON, M. J. WATERMAN and J. M. WATERS
Atomic Energy Research Establishment, Harwell, Didcot, Berks.

(*Received* 25 *November* 1960)

Abstract—An X-ray examination has been made of the products of the reaction of beryl with sodium fluoride, silicon tetrafluoride and sodium fluorosilicate. The evidence, in conjunction with that from chemical analysis, has enabled certain stages in the reaction of beryl with sodium fluorosilicate to be recognized. The first of these leads to a soluble fluoroberyllate, cryolite and cristobalite, and the second to the felspar albite. The third stage, occurring when all the beryl has been destroyed, produces albite, sodium fluoride and silicon tetrafluoride by a reaction between cryolite and cristobalite. The albite incorporates beryllium ions in its lattice and these cease to be extractable by water.

VOL. 19 1961

SINCE it was advocated in 1919, the Copaux process,[1] sometimes in a modified form, has been used for the extraction of the beryllium from beryl; a recent instance is by Murex Ltd.[2] We have described an investigation of the beryl–fluorosilicate reaction on which the Copaux extraction is based, directed to establishing conditions furnishing a product which gave the maximum proportion of beryllium extractable by aqueous leaching.[3] Here we deduce something of the mechanism of this reaction, largely from an X-ray identification of certain intermediate and final products.

The beryl was ground material from the U.K.A.E.A. Milford Haven factory, almost entirely free from other minerals and, judged by the proportion of beryllium (BeO = 11·9 per cent), of high quality. Thus the reaction can be considered as occurring between two well-characterised chemical compounds, an aluminosilicate, empirically $3BeO{\cdot}Al_2O_3{\cdot}6SiO_2$, and sodium fluorosilicate, Because more or less pure beryl has generally been used and because the reaction is remarkably specific in that water extracts from the reaction products almost exclusively the elements sodium, beryllium and fluorine and leaves silicon and aluminium in the leached residue, rather precise courses for the reaction have been advanced, such as:

$$3BeO{\cdot}Al_2O_3{\cdot}6SiO_2 + 3Na_2SiF_6 \rightarrow 3BeF_2 + 2AlF_3 + 9SiO_2 + 6NaF$$

or $$3BeO{\cdot}Al_2O_3{\cdot}6SiO_2 + 6Na_2SiF_2 \rightarrow 3Na_2BeF_4 + 2Na_3AlF_6 + 9SiO_2 + 3SiF_4$$

or $$2(3BeO{\cdot}Al_2O_3{\cdot}6SiO_2) + 6Na_2SiF_6 \rightarrow 6Na_2BeF_4 + 2Al_2O_3 + 15SiO_2 + 3SiF_4$$

There does not appear to have been much stoicheiometric justification for any of these equations, or even identification of the compounds. The mechanism is certainly complex and recognition of individual products not always possible, but a combination of chemical and X-ray observations has given us some insight into the course of the reaction. First a non-crystalline sodium fluoroberyllate glass is formed along with

[1] H. COPAUX, *C.R. Acad. Sci., Paris* **168,** 610 (1919).
[2] P. S. BRYANT, Beryllium production at Milford Haven. *Extraction and refining of the rarer metals* (London: Inst. Min. Metall., 1957) 310.
[3] K. R. HYDE, P. L. ROBINSON, M. J. WATERMAN and J. M. WATERS, *Trans. Inst. Min. Metall.*, **70,** 397, (1960–61).

insoluble, crystalline cryolite, Na_3AlF_6, and α-cristobalite, SiO_2. This is followed by a re-arrangement of the ions Al^{3+}, Si^{4+} and O^{2-} and their combination with Na^+ to produce crystalline albite, $NaAlSi_3O_8$. Finally there is a reaction between α-cristobalite and cryolite to form more albite. Some of the beryllium is incorporated in the albite lattice and ceases to be soluble. There is reason to suppose the α-cristobalite is derived from the silicon of the fluorosilicate.

The structure of beryl and its behaviour when heated

Beryl has a structure[4] consisting of sheets of hexagonal rings of six silicon-oxygen tetrahedra bound to one another in the individual sheets and to rings in contiguous sheets by bridging aluminium and beryllium ions, the former being hexa-coordinated and the latter tetra-co-ordinated to the oxygen ions. Although the arrangement appears layered in a diagram, the bonding is so uniform that in place of a marked basal cleavage there is a poor and irregular subconchoidal fracture. The mineral has a hexagonal unit cell with fifty eight atoms ($a_0 = 9{\cdot}215$ Å, $c_0 = 9{\cdot}192$ Å) and a sharp X-ray diffraction pattern; the latter is useful both for detecting structural differences and for recognising its presence, even in low proportions, in mixtures. The structure remains unchanged after the crystal has been heated to 800° and rapidly cooled. Extra, unascribed lines appear, however, when the temperature has been to 1100°, and beryllia is detected when it has reached 1200°. The amount of beryllia is larger at 1400°, and the beryl has lost much of its crystallinity when it has been heated to 1600°.

Within the temperature range employed for the fluorosilicate reaction, the expansion of beryl is slight up to about 300° and somewhat greater in both a and c directions between that point and 800°. The change is completely reversible and there is no evidence of structural alteration that might facilitate chemical attack.

Sodium fluorosilicate

The effect of heat on sodium and other fluorosilicates has been examined by CAILLAT[5] who gives dissociation pressures for the sodium salt. Although some of Caillat's results have been questioned,[6] we have our own evidence that liberation of silicon tetrafluoride occurs at 500°, a temperature at which a reaction with beryl is barely detectable after 24 hr, and that it becomes very considerable at 600°, a temperature at which most of the mineral is consumed in 4 hr. Thus the question arises of the respective parts played by sodium fluoride, silicon tetrafluoride and undissociated sodium fluorosilicate in the attack on beryl. When heated in an open system, the salt loses silicon tetrafluoride without melting and leaves mixtures in which the proportion of sodium fluoride increases with the time of heating. The reaction is reversed in an atmosphere of silicon tetrafluoride. Thus the reactant always contains a certain proportion of sodium fluoride, a proportion which depends not only on time, but also upon the atmosphere over the solid.

[4] W. L. BRAGG and J. WEST, *Proc. Roy. Soc.* A**111**, 691 (1926); N. V. BELOV and R. G. MATVEENA, *Dokl. Akad. Nauk* SSSR **73**, 299 (1950).

[5] R. CAILLAT, *Ann. Chim.* **20**, 368, (1945).
Atomic Energy Commission.

[6] I. G. RYSS, *The Chemistry of Fluorine and its Inorganic Compounds* Moscow (1956). Translated from a publication of the State Publishing House for Scientific, Technical and Chemical Literature, Moscow, (1956). AEC-tr-3927 (Pt. 1) and (Pt. 2). United States Atomic Energy Commission, Technical Information Service (1960).

Sodium fluoride and beryl

Sodium fluoride melts about 990° at which temperature the vapour-pressure is low. With beryl:fluoride ratios less than 1:4, the mixture melts below 700° and leaves, on cooling, a hard slag. At 600° all mixtures form a frit; with a 1:3 ratio about 90 per cent of the beryl is consumed in 4 hr, but the proportion of beryllium rendered soluble in water is low. The crystalline products which have been identified show that at 600° the reaction proceeds mainly with the formation of albite, very little α-cristobalite is produced, and cryolite is not detected. Clearly there is a fluorine attack on some of the silicon atoms co-ordinated with oxygen which leads to a release of the four ions Be^{2+}, Al^{3+}, Si^{4+} and O^{2-} and allows the last three to rearrange with Na^+ as albite, $NaAlSi_3O_8$. The plagioclase felspar lattice can accommodate beryllium ions and the low extraction of beryllium from the roast compacts by water is, in part at least, due to this cause. But neither sodium fluoride nor fluoride ion appear to convert the aluminium to fluoride and there may be a similar difficulty with beryllium. The failure to produce aluminium fluoride accounts for the absence of cryolite. The absence of α-cristobalite is significant and suggests that this compound, when formed, is derived from the silicon of the fluorosilicate; for this we have other evidence.

VOL. 19 1961

Silicon tetrafluoride and beryl

Silicon tetrafluoride boils at −65° and the gas does not react with beryl below 800°. At 900°, however, interaction produces α-cristobalite in appreciable quantity, and also, though less evidently, aluminium fluoride. The appearance of α-cristobalite suggests a fluorine oxygen interchange:

$$SiF_4 + 2O^{2-}\ (\text{beryl}) \rightarrow SiO_2 + 4F^-,$$

followed by the formation of aluminium fluoride;

$$3F^- + Al^{3+}\ (\text{beryl}) \rightarrow AlF_3.$$

It is pertinent that reactions similar to these, at least as regards their products, take place at a temperature 200° lower when sodium fluorosilicate or sodium fluoride and silicon tetrafluoride are present.

Silicon tetrafluoride and beryl mixed with sodium fluoride

Sodium fluoride and silicon tetrafluoride react to give mixtures of the former with sodium fluorosilicate. Accordingly the behaviour of sodium fluoride and silicon tetrafluoride when together with beryl might be expected to resemble that of sodium fluorosilicate itself rather than of either of the reactants separately. This proves to be true. In 4 hr at 700° all the beryl is consumed, much α-cristobalite is produced, cryolite is formed but, significantly, only a trace of albite is found. With lower proportions of sodium fluoride, the aluminium appears in the alternative fluoroaluminate chiolite, $Na_5Al_3F_{14}$, rather than in cryolite. In effect, these conditions are equivalent to maintaining a higher concentration of Na_2SiF_6 during the whole period of heating, with a consequentially greater replacement of oxygen by fluorine.

Sodium fluorosilicate and beryl

Reaction in this mixture between 500 and 600° produces, according to the conditions, albite, cryolite, α-cristobalite and an unidentified, soluble fluorine compound of

beryllium. Albite is formed at 600° in mixtures with beryl:fluorosilicate ratios up to 1:3. But at the higher ratio of 1:4, albite is absent because more time is required for an equivalent dissociation of the fluorosilicate and thus the proportion of sodium fluoride is lower in the earlier stages. However, at 800°, where a more rapid dissociation of the fluorosilicate increases the concentration of sodium fluoride, albite persists in mixtures with ratios up to 1:4·5. Always, longer heating periods encourage the formation of albite.

Cryolite is the first crystalline phase, other than residual beryl, to be detected at 500°. Although at 500 and 600° the cryolite formed does not increase with the proportion of sodium fluorosilicate, at 800° it does; probably because there is a partial conversion of cryolite to chiolite at the lower temperature where the concentration of fluorosilicate is higher.

Silica, an early product is found at all temperatures. It appears in X-ray photographs as α-cristobalite—the term used for it throughout this paper—but is probably produced in the β form and remains as such down to about 300°. We believe the silicon for it comes from the fluorosilicate. In a separate study of the reaction of beryl with sodium fluoroferrate, Na_3FeF_6, in a 1:3 molecular ratio at 700°, the first products were sodium fluoroberyllate, α-ferric oxide and cryolite which were followed, later, by albite. It is notable that α-cristobalite, or other form of crystalline silica, is absent and reasonable to assume that its place has been taken by α-ferric oxide also derived from the anion of the sodium salt, this time FeF_6^{3-}.

The results of operating with a beryl:sodium fluorosilicate ratio of 1:3 at temperatures above 600° are, briefly, that all the beryl is consumed in 2 hr at 700°, in 1 rh at 750°, and in 15 min at 800°. Cryolite and α-cristobalite are invariably produced.

Under suitable conditions, namely a 1:3 ratio of reactants, a temperature of 700°C and a heating time of 4 hr, 96 per cent of the beryllium in beryl is rendered soluble. With shorter periods, the release of beryllium is incomplete and, with even an hour longer, it has fallen to 94 per cent. After 19 hr heating there is a further fall to ca. 80 per cent. This fall coincides with the appearance of more albite and, as some natural plagioclase felspars are known to carry beryllium, the incorporation of Be^{2+} ions in the albite lattice is understandable.

Of the nature of the soluble beryllium compound only indirect evidence has been obtained. Both $NaBeF_3$ and γ-Na_2BeF_4 are known. These compounds and also $NaBe_2F_5$ and BeF_2 have been prepared and X-ray diffraction photographs have been taken; but none of the lines characteristic of any of these substances has been observed in our reaction products. Furthermore, the diffraction pattern of the residue after leaching is identical with that of the virgin material which suggests that the compound in question occurs as a glass. As, however, only a trace of sodium fluoride, which is readily identified, is found in the roast material before leaching, and, as sodium, beryllium and fluorine in leach liquors, giving maximum extraction of beryllium, are present in a ratio corresponding to $NaBeF_3$, it is possible that this fluoroberyllate is formed,[3] but glassy mixtures of Na_2BeF_4 and BeF_2 are not excluded.

DISCUSSION OF THE BERYL–FLUOROSILICATE REACTION AT 750°

The presence of undissociated sodium fluorosilicate appears to be necessary in an attack on beryl which is to release soluble beryllium, although it most probably operates through the agency of the sodium fluoride produced in its thermal

decomposition. Silicon tetrafluoride, so long as it remains within the system, serves the reaction by maintaining the concentration of fluorosilicate; otherwise it seems to take no part.

It is possible to give a tentative picture of the main course of this complex reaction as it occurs in compacts heated to about 750° under conditions not especially designed to conserve the silicon tetrafluoride liberated. Three consecutive, somewhat overlapping, stages may be recognized.

In the first, during which little silicon tetrafluoride has been lost, the proportion of sodium fluoride to fluorosilicate in the reacting mass remains low. The product species first to be formed are sodium fluoroberyllate glass, cryolite, Na_3AlF_6, and α-cristobalite, SiO_2. A remarkable feature is that more than half the beryllium is rendered soluble in as short a period as 15 min.

During the second stage the proportion of sodium fluoride to fluorosilicate is higher and, as would be expected from our examination of the reaction of fluoride with beryl, the change is accompanied by the appearance of albite, $NaAlSi_3O_8$. It is possible that some albite is formed earlier, but, if so, then in quantities insufficient for recognition. It seems reasonable to suppose that most, if not all, the albite formed at this stage is derived from fluoride and beryl because, so long as the later remains available, there is no evidence of a reduction in the amounts of cryolite and α-cristobalite.

VOL. 19 1961

The third stage, however, is marked by a decrease in the amounts of cryolite and α-cristobalite and an increase in the amount of albite. Notably, there is a progressive fall in the proportion of beryllium which can be extracted by water, although none of it has been lost from the roast. We have shown that cryolite and silica, when heated together at the process temperature, give albite and sodium fluoride and, furthermore, that when this reaction occurs in the presence of beryllium ions some of these become incorporated in the albite crystals. Thus the third stage is entirely disadvantageous. Indeed, it is probable that albite formed at any time during the complex reactions of beryl with sodium fluorosilicate includes beryllium in its lattice and thereby hinders the aqueous extraction of the element.

These three stages, which must all include other less important reactions and which undoubtedly overlap one another to a certain extent, are shown schematically.

First stage (with low sodium fluoride)

$$Na^+ + Be^{2+} + 3F^- \rightarrow NaBeF_3 \text{ (glass)}$$

$$3Na^+ + Al^{3+} + 6F^- \rightarrow Na_3AlF_6 \text{ (crystalline)}$$

$$Si^{4+} + 2O^{2-} \rightarrow SiO_2 \text{ (crystalline)}$$

Second stage (with higher sodium fluoride)

$$Na^+ + Al^{3+} + 3Si^{4+} + 8O^{2-} \rightarrow NaAlSi_3O_8 \text{ (crystalline)}$$

Third stage (in the absence of beryl)

$$Na_3AlF_6 + 4SiO_2 \rightarrow NaAlSi_3O_8 \text{ (crystalline)} + 2NaF \text{ (crystalline)} + SiF_4$$

Although the chemical changes involved are more numerous and mechanistically of greater complexity than has been indicated, it is not unreasonable, on the evidence, to speculate about the steps in the first stage. The ready fritting of sodium fluoride

and beryl, at temperatures as low as 500°, suggests the early formation of a molten or semi-molten film of fluoride–beryl flux round the mineral particles. Through this film Na^+ and F^- ions pass inwards and O^{2-} ions outwards. The first two take part in the formation of $NaBeF_3$ and Na_3AlF_6 and the O^{2-} ion reacts with the SiF_6^{2-} ion of the fluorosilicate to produce SiO_2 and F^-. This implies that the α-cristobalite is derived from silicon in the fluorosilicate rather than from that in the beryl. The suggestion is consonant with the implications of the behaviour of sodium fluoroferrate with beryl where we have shown α-cristobalite is not formed, its place being taken by ferric oxide which must originate in the FeF_6^{3-} ion. Further attack on the mineral by fluorosilicate may be assumed to proceed by the interfacial film moving inwards on the surface of a diminishing core of residual beryl.

The bearing of these findings on the commercial extraction of beryllium from beryl by the Copaux process have been discussed elsewhere.[3]

EXPERIMENTAL

Materials. The beryl was crushed, good quality material of sieve-size −200 mesh, from the U.K.A.E.A. agency factory at Milford Haven. Microscopic and X-ray inspection did not disclose any other mineral present. It was dried at 110°C for 24 hr, but no attempt was made to remove combined water and the reactions described must be assumed to have occurred in the presence of some moisture. The sodium fluorosilicate, from two commercial sources, was dried at 110°C for 24 hr. The sodium fluoride was AR salt. The silicon tetrafluoride was made by heating dried sodium fluorosilicate.

Chemical operations. The components were weighed-out into a screw-capped glass bottle and mixed by rolling. About 2·5 g of the mixture was compressed in a Millen press at 3000 lb/in². to give a ½ in. × ½ in. cylindrical compact. This was weighed in a silica boat and introduced into a silica furnace-tube which was long enough to allow the boat to be drawn into a cold zone for cooling. The tube was protected from atmospheric moisture and could be provided with the required atmosphere, either streaming or stagnant. It was heated by a Variac-controlled electric furnace. Heating times were defined as the period in the hot zone, the temperature of which was measured by a thermocouple.

After cooling and reweighing, the sample was transferred to a glovebox, crushed and ground to −200 mesh. Some of the powder was mounted for X-ray examination and a 1 g portion was subjected to the standard extraction. This consisted of stirring with 10 ml cold water in a centrifuge tube for 15 min, filtering the extract through a weighed, fritted-glass crucible, and washing and drying the residue at 110°. The residue was weighed; the beryllium in it was determined by chemical analysis and sometimes an X-ray photograph was taken. The filtrate was analysed for sodium, beryllium and fluorine. The chemical work has been already described in detail.[3]

X-ray examination. For the X-ray photographs of beryl at high temperatures a Unicam S-150 camera and CuK_α radiation were used. The capillaries holding the specimens were coated with metallic platinum, the thermal expansion of which allowed the temperature attained by the specimen to be calculated. The diffraction patterns for beryl had sharp but weak lines where sin θ was large.

The X-ray photographs of the powdered sinters and the extracted residues, used for the identification of crystalline phases produced in the various reactions, were taken with monochromatised CuK_α radiation on a Guinier focusing camera. The specimens were prepared by sprinkling a very shallow layer of powder on cellotape supported by means of a small brass disc with a hole in the centre. To avoid health hazard through the powder becoming detached from the cellotape, it was covered with a thin film of a non-scattering adhesive, Bostikote, before removal from the glove-box.

Most of the photographs given by these solids had a great number of lines varying widely in sharpness and reflecting a great range of crystallinity among the product compounds. Despite the presence of glassy material among them, the background scatter was, in general, not high. The complexity of the patterns encountered is illustrated by the typical one given in Table 1; this shows the observed and calculated values of $\sin^2\theta$ for several phases.

Action of heat on beryl. The lattice constants of beryl were derived by the least-squares refinement of $\sin^2\theta$, with the assumption that the systematic errors would be expressed by the Nelson-Riley

function, from diffraction lines of general indices *hkl*. A plot of the cell constants against temperature showed that the thermal expansion in the direction of both (*c*) and (*a*)-axes occurred in two stages; it is very slight up to about 250° and greater from that temperature up to 800°.

A least squares treatment of the data gave $a = a_0(1 + xt)$ where x is the average linear expansion coefficient between the temperatures; (i) 20–250°: $a = 9{\cdot}181(1 + 1{\cdot}7 \times 10^{-6}\,t)$; $c = 9{\cdot}208(1 + 1{\cdot}4 \times 10^{-6}\,t)$; (ii) 250–800°: $a = 9{\cdot}175(1 + 4{\cdot}7 \times 10^{-6}\,t)$; $c = 9{\cdot}193(1 + 6{\cdot}5 \times 10^{-6}\,t)$. Of these (i) is derived from results at three temperatures and (ii) from those at six, the mean standard deviations being 0·001 for *a* and 0·002 for *c*.

Values for *a* and *c* at 20° derived for the higher temperature measurements are 9·176 Å and 9·194 Å which are close to those found at 20° for a specimen of beryl which had been previously heated to

TABLE 1.—TYPICAL DIFFRACTION PATTERN OF A REACTION PRODUCT
(Compact beryl–sodium fluorosilicate in molecular ratio 1 : 3, heated at 600° for 24 hr)

$\sin^2\theta$ (observed)	I*	Compounds present	$\sin^2\theta$ (calculated)
0092	*w*+	beryl	0093
0140	*w*−	albite	0145
0279	*w*	beryl	0280
0290	*w*	cryolite	0290
0303	*w*	cryolite	0302
0362	*s*	α-cristobalite, albite	0364, 0365
0374	*w*−	beryl	0372
0396	*w*+	cryolite, albite	0393, 0399
0429	*w*	albite	0437
0459	*w*	albite	0442
0496	*w*−	cryolite	0490
0563	*m*−	beryl	0559
0584	*w*+	albite	0581
0596	*w*	α-cristobalite	0606
0656	*w*+	beryl	0653
0725	*m*−	beryl, α-cristobalite, albite	0723, 0731, 0723
0768	*w*	cryolite, albite	0763, 0763
0795	*w*+	cryolite	0786
0818	*w*	cryolite	0810
0936	*w*−	beryl	0933
0964	*w*+	α-cristobalite, cryolite	0965, 0964
1011	*w*	cryolite	1001
1071	*w*	cryolite	1064
1098	*w*	cryolite	1089
1113	*w*+	beryl	1117
1166	*w*	cryolite	1155
1217	*w*	beryl	1213
1293	*w*	beryl	1286
1315	*w*	α-cristobalite, albite	1332, 1314
1368	*w*	cryolite, albite	1360, 1376
1405	*w*−	beryl	1399
1451	*w*−	α-cristobalite	1454
1495	*w*−	beryl	1494
1588	*m*−	cryolite, α-cristobalite	1574, 1592
1641	*w*−	cryolite	1646
1851	*w*−	beryl	1846
1971	*w*	beryl	1961

* *w* = weak, *m* = medium, *s* = strong.

VOL. 19 1961

1500°, namely 9·175 Å and 9·194 Å. Probably the alkali metals known to be present in this beryl expand the lattice and give a false coefficient at lower temperatures. The alkalis are removed by heating and normal values are then observed. Of the extrapolated a_0 and c_0 values, namely 9·183 and 9·205 Å, that for a_0 is shorter than the reported values 9·200 and 9·215 Å, but that for c_0 agrees with FRANK-KAMENETSKII and SOSEDKO's[7] 9·209 Å for beryl which contained alkali metal.

Acknowledgements—We are indebted to Dr. R. W. M. D'EYE for X-ray facilities and other help, to Dr. E. WAIT for preparing the Mercury Computer Programme for cell-constant calculations and useful discussion, and to Mr. R. S. STREET who took the high-temperature X-ray photographs.

[7] V. A. FRANK-KAMENETSKII and T. A. SOSEDKO, *Dokl. Akad. Nauk S.S.S.R.* **118,** (4), 815 (1958).

J. Inorg. Nucl. Chem., 1961, Vol. 19, pp. 245 to 250 Pergamon Press Ltd. Printed in Northern Ireland

A DIFFERENTIAL THERMAL ANALYSIS STUDY OF THE DEHYDRATION OF THE RARE-EARTH (III) SULPHATE HYDRATES. THE HEATS OF DEHYDRATION

W. W. WENDLANDT and T. D. GEORGE
Department of Chemistry, Texas Technological College, Lubbock, Texas

(*Received* 25 *October* 1960; *in revised form* 30 *November* 1960)

Abstract—The dehydration of the rare-earth sulphate hydrates, $M_2(SO_4)_3 \cdot nH_2O$, was studied by the methods of differential thermal analysis (DTA). The lighter rare-earths, lanthanum through samarium, all gave three endothermic dehydration peaks, while with the heavier elements, with the exception of ytterbium, only two peaks were observed. The lighter rare-earths were completely dehydrated below 350°C while for the heavier rare-earth salts, the dehydration process was completed below 300°C. The heats of dehydration were determined by integration of the DTA curve peaks. The heats of dehydration ranged from 68 to 152 kcal/mole^{-1}; the former for $Ce_2(SO_4)_3 \cdot 5H_2O$, and the latter for $Yb_2(SO_4)_3 \cdot 11H_2O$.

VOL. 19 1961

THE dehydration and thermal decomposition of the rare-earth (III) metal sulphate hydrates has been studied by a number of investigators. Early workers found that dehydration of the hydrated salts readily took place in the temperature range from 200 to 650°C[1–3] and that the anhydrous metal sulphate began to decompose in the 800–1020°C temperature range.[1–5] More recently, the thermal decomposition of the rare-earth metal sulphate hydrates was studied by thermogravimetric analysis[6–8] and differential thermal analysis.[8]

Since the above investigations were incomplete as far as differential thermal analysis is concerned, it is the object of this investigation to study all of the rare-earth metal sulphate hydrates, with the exception of promethium, by this method. Since the heats of hydration are known, or can be calculated, for only several of the rare-earth sulphates,[9–10] these data were also evaluated by the above technique.

EXPERIMENTAL

Chemicals. The rare-earth compounds were obtained as the oxides or chlorides of 99·9 per cent purity from the Lindsay Chemical Co., West Chicago, Ill., and Research Chemicals, Inc., Burbank, Calif. All other chemicals used were of C.p. quality.

Rare-earth sulphates hydrates. The compounds used were prepared as previously described.[7] The water contents of the salts were determined by ignition on a thermobalance to 350°C. The amount of water found agreed to within 0·5 per cent of that required by theory.

Differential thermal analysis apparatus. The differential thermal analysis (DTA) apparatus

[1] J. W. MELLOR, *A Comprehensive Treatise on Inorganic and Theoretical Chemistry*, Vol. 5, Chapt. 3. Longmans, Green, London (1924).
[2] B. BRAUNER and F. PAVILICEK, *J. Chem. Soc.* **81**, 1243 (1902).
[3] S. H. KATZ and C. JAMES, *J. Amer. Chem. Soc.* **36**, 779 (1914).
[4] L. WOHLER and M. GRUNZWEIG, *Ber. Dtsch. Chem. Ges.* **46**, 1726 (1913).
[5] J. J. PITHA, A. L. SMITH and R. WARD, *J. Amer. Chem. Soc.* **69**, 1870 (1947).
[6] G. R. HALL and T. L. MARKIN, *J. Inorg. Nucl. Chem.* **4**, 137 (1957).
[7] W. W. WENDLANDT, *J. Inorg. Nucl. Chem.* **7**, 51 (1958).
[8] L. A. ALEKSEENKO, A. F. LEMENKOVA and V. V. SEREBRENNIKOV, *Zh. Neorg. Khim.* **4**, 1382 (1959).
[9] R. L. MONTGOMERY, *U.S. Bur. Mines, Rept. Invest.* No. 5445, (1959); *Ibid.* No. 5468 (1959).
[10] F. D. ROSSINI *et al.*, *Nat. Bur. Stand.*, Circular No. 500 (1952).

consisted of a furnace and sample chamber similar to that previously described [11,12] and a strip-chart microvolt recorder.[13] A "sandwich" type sample packing was employed which consisted of the following layers: 100 mg of alumina; 150 mg of sample; and 300 mg of alumina. Each layer was uniformily tamped into place with a glass rod as the sample chamber was filled. The reference chamber contained 550 mg of alumina. A furnace heating rate of 10°C per min was employed with an air atmosphere in contact with the sample.

Calibration of DTA *apparatus.* The DTA apparatus was calibrated for the heat of dehydration

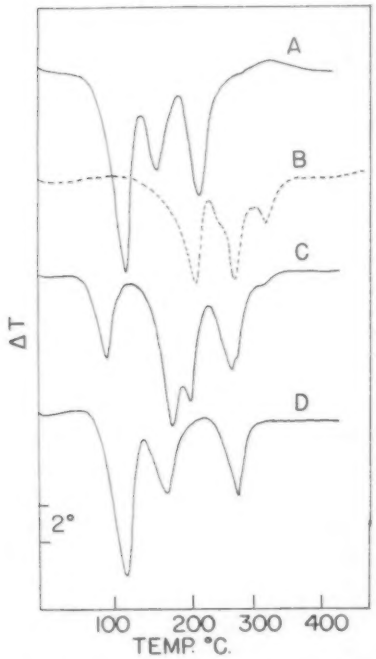

FIG. 1.—DTA curves of rare-earth sulphate hydrates.
A. $La_2(SO_4)_3 \cdot 9H_2O$
B. $Ce_2(SO_4)_3 \cdot 5H_2O$
C. $Pr_2(SO_4)_3 \cdot 8H_2O$
D. $Nd_2(SO_4)_3 \cdot 8H_2O$

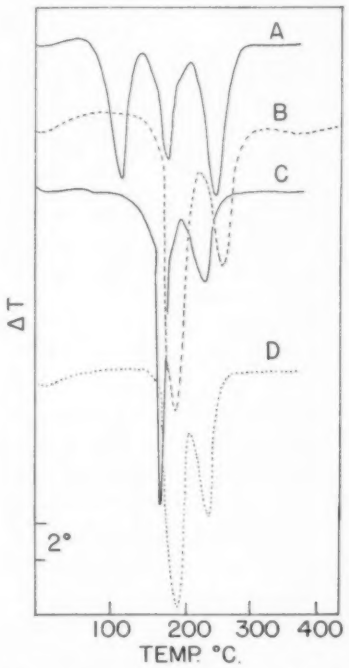

FIG. 2.—DTA curves of rare-earth sulphate hydrates.
A. $Sm_2(SO_4)_3 \cdot 8H_2O$
B. $Eu_2(SO_4)_3 \cdot 8H_2O$
C. $Gd_2(SO_4)_3 \cdot 8H_2O$
D. $Ho_2(SO_4)_3 \cdot 8H_2O$

studies by the use of metal salt hydrates having known heats of dehydration. The calibration compounds were $CuSO_4 \cdot 5H\text{-}O$, $CaSO_4 \cdot 2H\text{-}O$, and $BaCl_2 \cdot 2H_2O$.[14] The endothermic dehydration peaks were integrated by tracing the curves onto good quality tracing paper, cutting out the peaks, and weighing them on a semi-micro analytical balance. The calibration factors obtained were: 29·5 cal/0·1 g of paper for $CuSO_4 \cdot 5H_2O$; 32·2 cal/0·1 g of paper for $BaCl_2 \cdot 2H_2O$; and 35·5 cal/0·1 g of paper for $CaSO_4 \cdot 2H_2O$; an average value of 32·4 $\pm$ 2·0 cal/0·1 g of paper was used to determine the heat of dehydration of the rare earth sulphate hydrates. Duplicate, and in some cases, triplicate, samples were run for each compound. The average of three curve integrations was used to determine each heat of dehydration value. The areas of the curves for the same sample could be reproduced to within $\pm$2 per cent while for different samples of the same compound, the areas could be reproduced to within $\pm$5 per cent.

[11] W. LODDING and L. HAMMEL, *Rev. Sci. Instrum.* **30,** 885 (1959).
[12] W. LODDING and L. HAMMEL, *Analyt. Chem.* **32,** 657 (1960).
[13] W. W. WENDLANDT, *J. Chem. Educ.* **37,** 94 (1960).
[14] *International Critical Tables*, Vol. 7, 263 (1926); *Selected Values of Chemical Thermodynamic Properties*, U.S. Bureau of Standards, Series 1, Vol. 1, Tables 87-5, 89-2, 3, 4 (1949).

RESULTS AND DISCUSSION

The DTA curves of the rare-earth metal sulphate hydrates are given in Figs. 1–4.

The difficulties and problems arising in the interpretation of the dehydration peaks found in inorganic salt hydrates has been discussed by BORCHARDT and DANIELS[15] and REISMAN and KARLAK.[16] The interpretation of the curves is difficult because the DTA curve obtained depends on the furnace heating rate, ambient

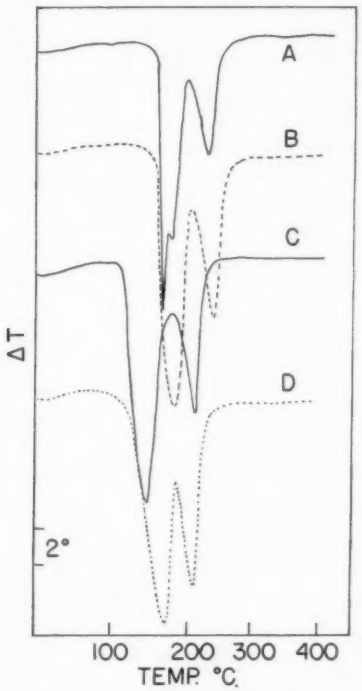

FIG. 3.—DTA curves of rare-earth sulphate hydrates.
A. $Tb_2(SO_4)_3 \cdot 8H_2O$
B. $Dy_2(SO_4)_3 \cdot 8H_2O$
C. $Er_2(SO_4)_3 \cdot 8H_2O$
D. $Tm_2(SO_4)_3 \cdot 8H_2O$

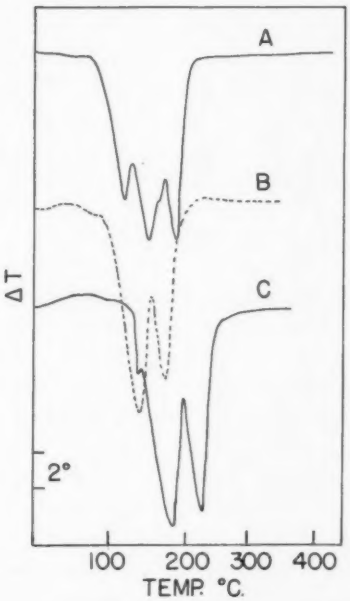

FIG. 4.—DTA curves of rare-earth sulphate hydrates.
A. $Yb_2(SO_4)_3 \cdot 11H_2O$
B. $Lu_2(SO_4)_3 \cdot 8H_2O$
C. $Y_2(SO_4)_3 \cdot 8H_2O$

aqueous tension, particle size, vapour-pressure–temperature curve of the hydrate system, the latent heats of hydration and vaporization, instrumentation factors, sample purity, sample packing, and so on.[16] It is further complicated by the fact that certain salt hydrate transitions involve the formation of $H_2O(l)$ which subsequently vaporizes to $H_2O(g)$, giving rise to additional endothermic peaks.[15] The conditions for the latter type of phenomena have been thoroughly discussed by the above investigators. With these considerations in mind, the dehydration peaks found in the rare-earth sulphate hydrate systems can only be discussed in an approximate fashion since additional evidence, such as X-ray data, are not available at the present time.

[15] H. J. BORCHARDT and F. DANIELS, *J. Phys. Chem.* **61**, 917 (1957).
[16] A. REISMAN and J. KARLAK, *J. Amer. Chem. Soc.* **80**, 6500 (1958).

The lighter rare-earth salts, lanthanum through samarium, all gave three endothermic dehydration peaks, while with the heavier rare-earth compounds, with the exception of ytterbium, only two peaks were observed. The lighter rare-earth salts were completely dehydrated below about 350°C while for the heavier rare-earth compounds, the dehydration process was completed below 300°C. This is in fair agreement with previous thermogravimetric analysis (TGA)[7] data although the dehydration temperatures were somewhat higher in this study, due perhaps to the faster heating rate employed.

The results obtained in this study were not in agreement with previous studies on the DTA of the lighter rare-earth salts.[8] The latter investigators found three peaks in the curve for lanthanum and cerium, one peak for praseodymium and neodymium, while two peaks were found for samarium. The peak maxima temperatures that were found by the above authors were lower than those reported here but this may be due to the lower heating rate, 2–3°C per min., that was employed. ALEKSEENKO *et al.*[8] claimed that the metal sulphates containing rare-earth ions of odd atomic number gave sharper and greater endothermic peaks than those of even numbered ions. However, in this study, gadolinium, $Z = 64$, and terbium, $Z = 65$, both gave very sharp peaks while for the other salts, the peaks were of about the same symmetry.

The peak maxima temperatures for the first dehydration peak shifted to higher temperatures as the atomic number of the rare-earth ion increased, although there were several anomalies. This is in agreement with the work of ALEKSEENKO *et al.*[8] who found that the temperatures at which four, six, and eight molecules were lost shifted to higher values as the atomic number of the lighter rare-earth ions increased. However, as previously emphasized,[8] it is difficult to use thermal stability data as criteria for evaluation of the metal ion–water bonding because the DTA curve is the result of water loss as well as the rearrangement of the crystal lattice. A relative comparison could only be made if the heat of crystalline rearrangement did not vary greatly with the different rare-earth salts.

It is of interest to compare the DTA curves with those obtained by TGA.[7] The lighter rare-earth compounds, lanthanum through samarium, as well as erbium, exhibited inflexions in the weight-loss curves which were due to the formation of a 5-hydrate and in some cases, possibly a 2-hydrate. These same compounds, with the exception of erbium, exhibited three endothermic DTA peaks, while praseodymium, a fourth, shoulder peak at 200°C was also observed. Ytterbium, which gave evidence for a 2-hydrate on the TGA curve, also gave three DTA peaks. A possible interpretation of the peaks is as follows:

(a) For La, Pr, Sm:
Peak (1): $M_2(SO_4)_3 \cdot 8 \text{ or } 9H_2O(s) \rightarrow M_2(SO_4)_3 \cdot 5H_2O(s) + 3 \text{ or } 4H_2O(g)$
Peak (2): $M_2(SO_4)_3 \cdot 5H_2O(s) \rightarrow M_2(SO_4)_3 \cdot 2H_2O(s) + 3H_2O(g)$
Peak (3): $M_2(SO_4)_3 \cdot 2H_2O(s) \rightarrow M_2(SO_4)_3(s) + 2H_2O(g)$

(b) For Eu through Lu (except Yb):
Peak (1): $M_2(SO_4)_3 \cdot 8H_2O(s) \rightarrow M_2(SO_4)_3 \cdot 2H_2O(s) + 6H_2O(g)$
Peak (2): $M_2(SO_4)_3 \cdot 2H_2O(s) \rightarrow M_2(SO_4)_3(s) + 2H_2O(g)$

(c) For the shoulder peaks, perhaps the transition: $H_2O(l) \rightarrow H_2O(g)$ is also involved in the dehydration process.

In general, compete dehydration is accomplished at lower temperatures as the atomic weight of the rare-earth ion increases.

Heats of dehydration. Under specific experimental conditions, DTA can be used to determine the heat of reaction involved in a chemical change by integration of the differential curve peak or peaks. From the theories of SPEIL *et al.*[17] and others,[18,19] the area of the curve peak is

$$\text{peak area} = \int_{t_1}^{t_2} \theta \, dt = \frac{\Delta HM}{g\lambda}$$

where t_1 and t_2 are the temperature limits of the peak, θ is the differential temperature,

TABLE 1.—HEATS OF DEHYDRATION OF RARE EARTH METAL SULPHATE HYDRATES

Compound	ΔH (kcal mole^{-1})	$\Delta H_{H_2O(g)}$ (kcal mole^{-1})	$\Delta H_{H_2O(l)}$ (kcal mole^{-1})
$CuSO_4 \cdot 5H_2O$*	71·17		
$CaCO_4 \cdot 2H_2O$*	28·03		
$BaCl_2 \cdot 2H_2O$*	26·83		
$La_2(SO_4)_3 \cdot 9H_2O$		128 ± 13	34 ± 3
$Ce_2(SO_4)_3 \cdot 5H_3O$		68 ± 7	16 ± 2
$Pr_2(SO_4)_3 \cdot 8H_2O$		110 ± 11	26 ± 3
$Nd_2(SO_4)_3 \cdot 8H_2O$		91 ± 9	7 ± 1
$Sm_2(SO_4)_3 \cdot 8H_2O$		103 ± 10	19 ± 2
$Eu_2(SO_4)_3 \cdot 8H_2O$		113 ± 11	29 ± 3
$Gd_2(SO_4)_3 \cdot 8H_2O$		104 ± 10	20 ± 2
$Tb_2(SO_4)_3 \cdot 8H_2O$		112 ± 11	28 ± 3
$Dy_2(SO_4)_3 \cdot 8H_2O$		116 ± 12	32 ± 3
$Ho_2(SO_4)_3 \cdot 8H_2O$		128 ± 13	44 ± 4
$Er_2(SO_4)_3 \cdot 8H_2O$		119 ± 12	35 ± 3
$Tm_2(SO_4)_3 \cdot 8H_2O$		126 ± 13	42 ± 4
$Yb_2(SO_4)_3 \cdot 11H_2O$		152 ± 15	37 ± 4
$Lu_2(SO_4)_3 \cdot 8H_2O$		119 ± 12	35 ± 3
$Y_2(SO_4)_3 \cdot 8H_2O$		112 ± 11	28 ± 3

* Calibration values; based on the dehydration reactions:

$CuSO_4 \cdot 5H_2O(s) \rightarrow CuSO_4(s) + 5H_2O(g)$
$CaSO_4 \cdot 2H_2O(s) \rightarrow CaSO_4(s) + 2H_2O(g)$
$BaCl_2 \cdot 2H_2O(s) \rightarrow BaCl_2(s) + 2H_2O(g)$

ΔH is the heat of reaction, M is the mass of reactive sample present, λ is the thermal conductivity of the sample, and g is a constant dependent on the furnace and sample holder geometry. In practice, the apparatus is calibrated by studying reactions of known thermal effects. In this manner, the constants g and λ are evaluated.

Table 1 gives the heats of dehydration, $\Delta H_{H_2O(g)}$, and $\Delta H_{H_2O(l)}$, as represented by the following reactions:

$$(1)\ M_2(SO_4)_3 \cdot nH_2O(s) \rightarrow M_2(SO_4)_3(s) + nH_2O(g) — \Delta H_{H_2O(l)}$$

$$(2)\ M_2(SO_4)_3 \cdot nH_2O(s) \rightarrow M_2(SO_4)_3(s) + nH_2O(l) — \Delta H_{H_2O(l)}$$

[17] S. SPEIL, L. H. BERKELHAMER, J. A. PASK and B. DAVIS, *U.S. Bur. Min. Tech. Paper* **664**, (1945).
[18] M. J. VOLD, *Analyt. Chem.* **21**, 683 (1949).
[19] S. L. BOERSMA, *J. Amer. Ceram. Soc.* **38**, 281 (1955).

The latter heat of dehydration, $\Delta H_{H_2O(l)}$, was calculated by subtracting the heat of vaporization of water.,

(3) $H_2O(1) \rightarrow H_2O(g)$ - - - - - $\Delta H = 10{\cdot}49$ kcal mole^{-1} (25°C) from reaction (1).

As a check on the accuracy of the method, the $\Delta H_{H_2O(l)}$ of lanthanum sulphate 9-hydrate was compared against that determined by a calorimetric method.[9] The latter obtained a value of $32{\cdot}5 \pm 3{\cdot}5$ kcal mole^{-1} at 25°C, in fair agreement with that presented in Table 1. Taking into account the various factors of sample particle size, calibration errors and determination of the curve areas, a limit of error of ± 10 per cent was assigned to the $\Delta H_{H_2O(g)}$ and $\Delta H_{H_2O(g)}$ values. For the $\Delta H_{H_2O(l)}$ values, the error is probably greater than this because of the heat of vaporization of water at 25°C was used, which in reality is not the case.

The $\Delta H_{H_2O(g)}$ values ranged from 68 to 152 kcal mole^{-1}. The former for $Ce(SO_4)_3 \cdot 5H_2O$ and the latter for $Yb_2(SO_4)_3 \cdot 11H_2O$. For the 8-hydrate compounds, the values ranged from 91 kcal mole^{-1} for neodymium to 128 kcal mole^{-1} for holmium. The values for neodymium and samarium appear to be abnormally low. However, three different sample preparations of each, prepared by three different methods, gave the same values to within ± 5 per cent. Apparently the thermal conductivity of these compounds differs considerably from that of the others, causing a change in calibration constants of the system.

J. Inorg. Nucl. Chem., 1961, Vol. 19, pp. 251 to 261. Pergamon Press Ltd. Printed in Northern Ireland

NEGATIVE CHELATE COMPLEXES OF LANTHANIDE AND ACTINIDE ELEMENTS

L. W. HOLM
Research Institute of National Defense, Dept. 4, Stockholm 80, Sweden
G. R. CHOPPIN and D. MOY
Department of Chemistry, Florida State University, Tallahassee, Florida

(*Received* 13 *October* 1960; *in revised form* 21 *November* 1960)

Abstract—Ion exchange and electrophoretic studies of the glycolic, lactic and α-hydroxy isobutyric acid-lanthanide and actinide systems have shown the presence of negative mononuclear complexes in solutions at ligand ion concentrations above 0·1 M. These negative complexes are monovalent with four ligands attached to the central atom.

VOL. 19 1961

STUDIES of the complexes of the trivalent lanthanide and actinide ions with α-hydroxy carboxylic acids have been conducted to investigate the possibility of the formation of negative complex ions in such systems. This paper is an extension of the preliminary studies carried out in 1956 by HOLM.[1]

Solutions of these α-hydroxy carboxylic acids have been used extensively to separate the ions of the lanthanide and actinide elements by ion exchange techniques. The use in such separations of glycolic, lactic and α-hydroxy isobutyric acid with Dowex-50, a strong acid cation exchange resin, has been summarized in two recent papers.[1,2] However, no attention has been given to the possibility of using anion exchange resins with these systems until recently. Our approach has been to utilize the data from both types of resin systems, anion and cation, to obtain more definitive information on the complexes present than can be deduced from either resin system alone.

If the logarithm of the elution position from a cation exchange resin column of a trivalent lanthanide or actinide is plotted vs. the logarithm of the concentration of α-hydroxy isobutyrate ion, a straight line with a negative slope whose value is close to four is obtained.[3] To understand the implications of this fact, it is necessary to consider the possible reactions in this system. The possible reactions in the solution phase are:

$$M^{3+} + B^- = MB^{2+} \qquad \beta_1 = \frac{(MB)}{(M)(B)} \tag{1}$$

$$MB^{2+} + B^- = MB_2^+ \qquad \beta_2 = \frac{(MB_2)}{(M)(B)^2} \tag{2}$$

$$MB_2^+ + B^- = MB_3 \qquad \beta_3 = \frac{(MB_3)}{(M)(B)^3} \tag{3}$$

$$MB_3 + B^- = MB_4^- \qquad \beta_4 = \frac{(MB_4)}{(M)(B)^4} \tag{4}$$

[1] G. R. CHOPPIN, *J. Chem. Educ.* **36**, 462 (1959).
[2] D. C. STEWART, *Proceedings of International Conference Peaceful Uses Atomic Energy, Geneva* 1955, **7**, 321 United Nations (1956).
[3] H. L. SMITH and D. C. HOFFMAN, *J. Inorg. Nucl. Chem.* **3**, 243 (1956).

where M = trivalent lanthanide or actinide ion,
B = α-hydroxy isobutyrate ion and
β_i = the equilibrium constant for the ith complex.
The possible reactions in the resin (NR) phase are:

$$M^{3+} + 3NR = MR_3 + 3N^+ \qquad K_1 = \frac{(MR_3)(N)^3}{(M)(NR)^3} \tag{5}$$

$$MB^{2+} + 2NR = MBR_2 + 2N^+ \qquad K_2 = \frac{(MBR_2)(N)^2}{(MB)(NR)^2} \tag{6}$$

$$MB_2^+ + NR = MB_2R + N^+ \qquad K_3 = \frac{(MB_2R)(N)}{(MB_2)(NR)} \tag{7}$$

The cation resin-solution distribution coefficient K_d^c is defined by

$$K_d^c = \frac{\Sigma(M)\text{ resin}}{\Sigma(M)\text{ solution}} = \frac{(MR_3) + (MBR_2) + (MB_2R)}{(M) + (MB) + (MB_2) + (MB_3) + (MB_4)} \tag{8}$$

When this equation is combined with those given for the resin and solution reaction equilibria, it may be derived that

$$K_d^c = \frac{\dfrac{K_1(M)(NR)^3}{(N)^3} + \dfrac{K_2\beta_1(M)(NR)^2(B)}{(N)^2} + \dfrac{K_2\beta_2(M)(NR)(B)^2}{(N)}}{(M) + \beta_1(M)(B) + \beta_2(M)(B)^2 + \beta_3(M)(B)^3 + \beta_4(M)(B)^4} \tag{9}$$

In these systems N is usually ammonium ion and the pH is between 4·0 and 4·5. Under this latter condition and provided that M is present only in tracer concentrations (N) ≃ (B) and (NR) is constant. Equation (9) can then be rearranged to

$$K_d^c = \frac{K_1(NR)^3(B)^{-3} + K_2\beta_1(NR)^2(B)^{-1} + K_3\beta_2(NR)(B)}{1 + \sum_{n=1}^{4} \beta_n(B)^n} \tag{10}$$

If the assumption is made that one species is predominant in each phase, then it is possible to calculate values for the slope $d(\log K_d^c)/d(\log B)$ for various combinations of species in the two phases. Values obtained in this fashion are listed in Table 1.

TABLE 1.—VALUES OF $d(\log K_d^c)/d(\log B)$ FOR COMBINATIONS OF IONIC SPECIES

		Species in the resin phase		
		M^{3+}	MB^{2+}	MB_2^+
Species in the solution phase	M^{3+}	−3	−1	+1
	MB^{2+}	−4	−2	0
	MB_2^+	−5	−3	−1
	MB_3	−6	−4	−2
	MB_4^-	−7	−5	−3

From Table 1, it is seen that the experimental slope of −4 is predicted by two solution–resin phase combinations, MB_3–MB^{2+} and MB^{2+}–M^{3+}. However, the assumption of

the predominance of a single species, particularly for the solution phase, does not seem realistic. Also, the relative insensitivity of a log–log plot gives rise to doubts as to the value of a rigorous interpretation of the slope value. Consequently, from cation exchange data, it is not possible to draw definite conclusions concerning the species in the solution phase.

Potentiometric investigations have been used to measure the stability constants of the lanthanide complexes with glycolate,[4] lactate[5] and isobutyrate.[5] Evidence for the existence of a tetra-ligand complex was obtained. However, the relative errors of the higher constants were too great to allow use of the latter to calculate the relative concentrations of the higher complex species as a function of ligand concentration.

EXPERIMENTAL

Chemicals. Glycolic acid was purified by recrystallization from aqueous solution. α-hydroxy isobutyric acid was obtained commercially as light brown crystals. The crystals were dissolved in water and the solution passed through a bed of hydrogen form cation exchange resin (Dowex-50) until a water clear solution is obtained. Commercial lactic acid often exists partially as a lactone dimer.[6] To convert it completely to the free acid form, an aqueous solution of the lactic acid is neutralized with sodium hydroxide. To regenerate the acid, the solution is passed through a bed of hydrogen form cation exchange resin where the sodium ions are replaced by hydrogen ions.

Aqueous solutions of glycolic, lactic and α-hydroxy isobutyric acid were adjusted to a pH value between 4·6 and 4·7 by addition of concentrated ammonium hydroxide. Mold growth in these solutions may be inhibited by addition of sufficient phenol to make the solution 0·01 M in phenol. Without phenol, these solutions may be kept free of mold for periods of more than a month by storage in glass stoppered bottles. The resin used was Dowex-1 (10% DVB), 200–400 mesh with a capacity of 3·2 milliequivalents per gramme. It was supplied by the Dow Chemical Co. A fraction with a settling rate in water of 0·25–0·50 cm/min was selected for the column elutions. The total resin batch was washed alternately with water and 1, 3 and 9 M HCl, then with 3 M NaOH and water and finally with ethyl alcohol and water before use. The purified resin was converted to the desired anionic form (e.g. glycolate, etc.) by treatment with a solution of the proper acid. It was washed with distilled water, air dried and stored in a dessicator over sodium nitrite for later use. Storage over $NaNO_2$ was used as it maintained the relative humidity at 63 per cent at 25°C—approximately equal to the average humidity in our laboratory. This minimized weight changes due to moisture gain or loss between weighings.

Tracers. The lanthanide tracers used were ^{144}Ce, ^{147}Pm, ^{152,154}Eu, ^{160}Tb and ^{170}Tm. ^{22}Na and ^{91}Y were also used. All of these tracers were obtained from the Oak Ridge National Laboratory and were counted by either thin window Geiger-Müller tubes or windowless proportional counters. ^{244}Cm and ^{250,252}Cf were obtained through the generosity of Dr. S. G. Thompson of the Lawrence Radiation Laboratory, University of California. These α-emitting nuclides were counted in windowless proportional counters and in an alpha grid chamber connected to a fifty-channel pulse height analyser.

Equilibrium studies. The expression used to determine the distribution coefficient for the anion exchange resin system, K_d^a, is

$$K_d^a = \frac{A_0 - A_s}{A_s} \cdot \frac{\text{ml of solution}}{\text{g of resin}} \tag{11}$$

where A_0 and A_s are the activity of the solution phase before and after equilibration with the resin. To minimize the error in K_d, it is desirable to have $(A_0 - A_s)/A_s$ as close to unity as possible. Proper selection of the ratio of resin weight to solution volume is necessary to approach this situation. However, a limiting ratio of 2·0 ml solution per 0·5 g resin was found to be experimentally practical for low values of K_d. A sample of resin in the proper anionic form was sealed in a tube with 2 ml of solution of the acid (pH 4·6) containing approximately 10^5 counts/minute of the tracer ion. The tubes were agitated for 12 hr in a constant temperature bath at 25°C or in an oven at 87°C. Duplicate

[4] A. Sonesson, *Acta Chem. Scand.* **13**, 998 (1959).
[5] G. R. Choppin and J. A. Chopoorian. Submitted for publication (*J. Inorg. Nucl. Chem.*)
[6] G. R. Choppin and R. Silva, *J. Inorg. Nucl. Chem.* **3**, 153 (1956).

VOL. 19 1961

aliquots of the solution before and after equilibration were prepared and counted to 0·1 per cent probable error. The pH and concentration of the solution were checked after equilibration to allow for correction due to solvent or electrolyte uptake by the resin. Unfortunately, it was not feasible to use solutions of constant ionic strength in these runs as addition of perchlorate, etc., would change the chemical composition of the resin phase.

Column elutions. For elutions at 87°C, a jacketed column of the type described previously[7] was used. The resin bed dimensions varied from 5–15 mm in length and 1–3 cm in diameter, depending on the value of the K_d^a for the particular eluting solution. The void volume (free column volume) of the columns were determined by passage of ^{22}Na and was found to be very close to 30 per cent of the total resin bed geometric volume. This is lower than the 40–50 per cent value reported by many groups previously.

The activities were dissolved in 10–25 μl of the eluting solution and transferred to the top of the resin bed. After this volume had run into the resin bed, an additional drop of eluting solution was used to wash all the activity into the resin bed before the bulk of the eluting solution was added to the reservoir above the resin bed. Elution was performed at a flow rate of approximately 0·25 ml cm^{-2} min^{-1}. The drops from the column were collected individually, evaporated to dryness and counted. Aluminium absorbers were used in counting, when feasible, to resolve overlapping elution curves. From the volume (V) for the maximum in the elution curve, the free column volume (v) and weight of the resin in the column (w), the K_d^a could be calculated by

$$K_d^a = \frac{V - v}{w} \tag{12}$$

The K_d^a's for the lactate and isobutyrate systems were so small that it was necessary to perform the elutions at 87°C where the K_d^a-values are greater than at 25°C.

Electrophoretic studies. The apparatus used for the electromigration studies consisted of two polyethylene cups for the solution into which the ends of a paper strip were dipped. A polyethylene bridge was placed midway between the two cups to allow the paper strip to be placed in an inverted V position during the experiment. The cell was covered with a glass jar to minimize evaporation of water from the solution. The paper strip (Whatman No. 1) was placed in position and after the strip had become saturated with solution, the power supply was turned on and the same current to be used in the tracer experiment passed for an hour to ensure that any subsequent ionic movement would not be due to a siphoning effect. ^{170}Tm or a combination of ^{170}Tm and ^{22}Na were placed along a thin line on the paper strip at the apex of the inverted V and the electromigration carried out for 12–36 hr. At the end of the run, the paper strip was dried under a heat lamp and the profile of the band of activity ascertained by counting successive sections of the strip through a slit in a lead shield with a thin window G.M. tube.

RESULTS

The results of the batch equilibrations and column elutions are shown in Figs. 1–5. A typical set of K_d^a data are shown in Table 2 to indicate the experimental quantities as well as the average deviation for a set of measurements. The concentration of the glycolate ion in the equilibration experiments was determined by a conductometric titration with a standard solution of HCl. For lactate and isobutyrate the K_d^a values were too low to allow accurate measurement by batch equilibration, therefore the points in Figs. 3, 4 and 5 are calculated from column elution data. Fig. 5 shows the data for Cm, Cf, Y, Pm and Tm obtained by column elution with isobutyrate from anion resin of a different batch. The difference in absolute K_d^a-values is not inconsistent with that observed between different resin batches. It was found difficult to perform successful elutions at concentrations below 0·01 M. Possibly at these low concentrations of the complexing ligand, hydrolysis occurs in the resin phase causing tailing of the elution peaks. Separation factors for lanthanides and actinides using

[7] S. G. THOMPSON, B. G. HARVEY, G. R. CHOPPIN and G. T. SEABORG, *J. Amer. Chem. Soc.* **76**, 6229 (1954).

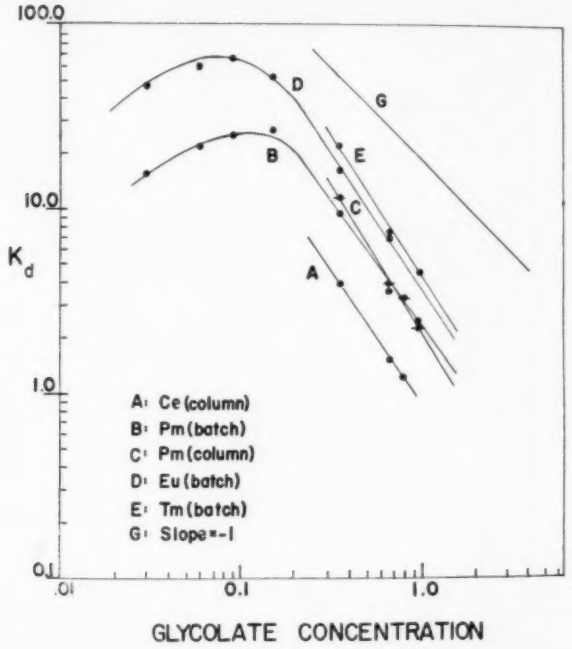

FIG. 1.—Log K_d^a vs. log (glycolate ion concentration) for several lanthanide ions at 25°C.

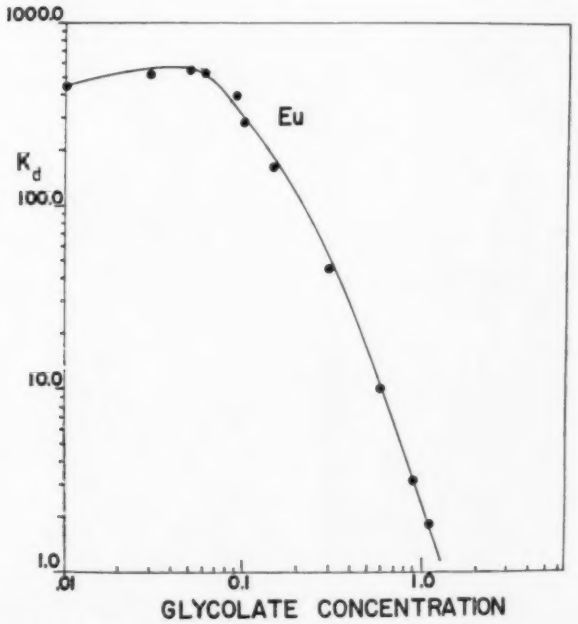

FIG. 2.—Log K_d^a vs. log (glycolate ion concentration) for europium at 87°C.

VOL. 19 1961

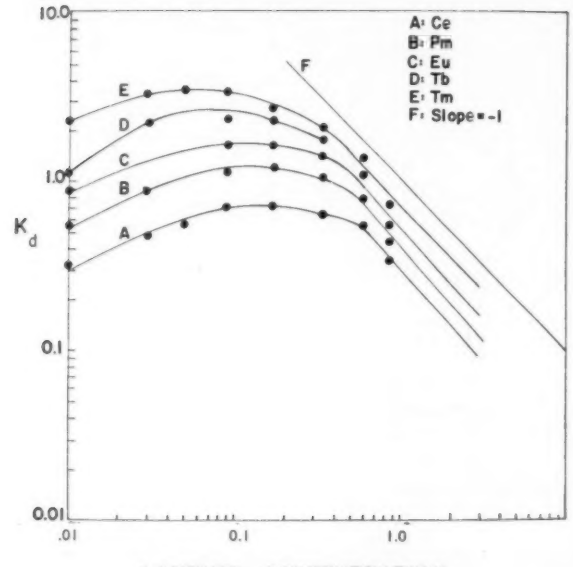

FIG. 3.—Log K_d^a vs. log (lactate ion concentration) for several lanthanide ions at 87°C.

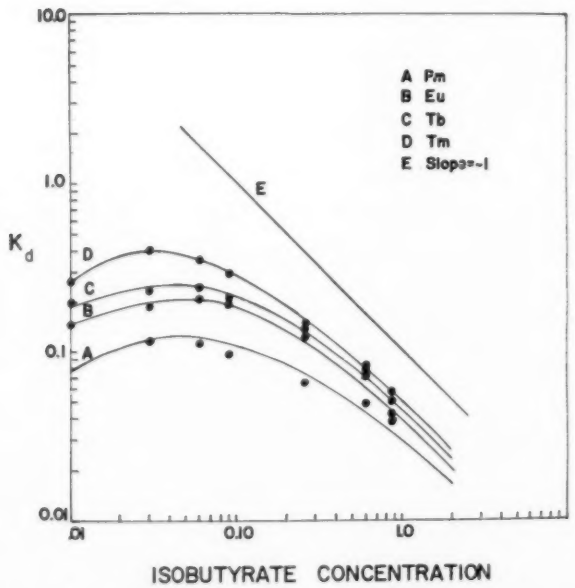

FIG. 4.—Log K_d^a vs. log (isobutyrate ion concentration) for several lanthanide ions at 87°C.

solutions of these acids as eluants with anion exchange resin columns has been reported previously.[8]

Table 3 summarizes the results of the electromigration studies. ^{22}Na was included in two runs with lactate solution and ^{170}Tm to determine whether the direction of movement of the ^{170}Tm was truly an electromigration effect. Since the ^{22}Na moved to the cathode in both cases, whereas the ^{170}Tm moved to the cathode in the 0·01 M

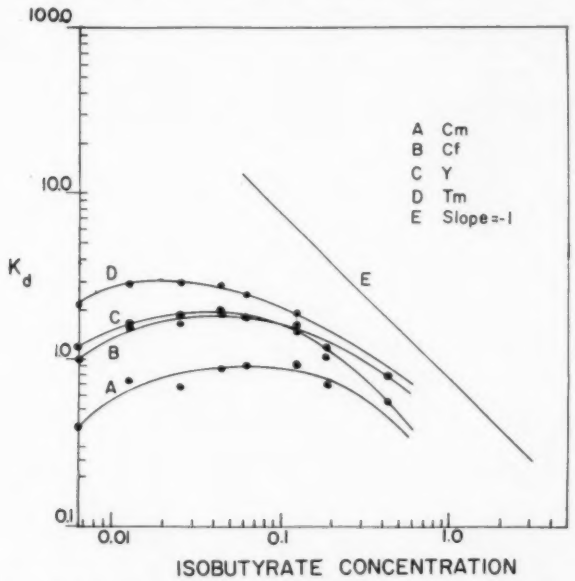

FIG. 5.—Log K_d' vs. log (isobutyrate ion concentration) for Cm, Cf, Y and Tm at 87°C.

solution and to the anode in the 0·03 M solution it was concluded that the movement of thulium was due to electromigration and not an experimental artifact. These measurements are only semi-quantitative due to the difficulties encountered in maintaining constant and reproducible operating conditions.

A similar investigation of the lanthanide glycolate system with anion exchange resin has been reported by SONESSON[9].

DISCUSSION

In order that the anion exchange resin (RB) systems may be treated in a manner analogous to that of the cation exchange resin system, it is useful to express the anion exchange reaction for trivalent metal ions in the following general fashion, assuming only mononuclear complexes:

$$MB_n^{3-n} + (m-3)RB = R_{m-3}MB_m + (n-3)B^- \tag{13}$$

Thus the exchange equilibrium constant for this reaction becomes

$$K_{ex} = \frac{(R_{m-3}MB_m)(B)^{n-3}}{(MB_n)(RB)^{m-3}} \tag{14}$$

[8] G. R. CHOPPIN, D. MOY and L. W. HOLM, IAEA Conference on the Use of Radioisotopes in the Physical Sciences and Industry, Paper 282, Copenhagen (1960).
[9] A. SONESSON, *Acta Chem. Scand.* **13**, 1437 (1959).

TABLE 2.—K_d^e FOR EUROPIUM VS. CONCENTRATION OF GLYCOLATE ION

Conc. (M)	A_0 (cpm)	A_s (cpm)	Weight of resin (g)	Volume of soln. (ml)	K_d^e	Average K_d^e	Deviation (%)
0·97	16590	8803	0·4858	2·00	3·77	3·59	3·62
	16590	8825	0·4791	2·00	3·67		
	13420	7291	0·4858	2·00	3·46		
	13420	7348	0·4791	2·00	3·45		
0·67	16556	8002	0·3209	2·00	6·66	6·89	1·31
	14160	6680	0·3209	2·00	6·97		
	16556	8371	0·2793	2·00	6·99		
	6003	2977	0·2957	2·00	6·94		
	6003	2765	0·3433	2·00	6·89		
0·36	15674	7740	0·1361	2·00	15·44	16·21	4·75
	15874	7631	0·1271	2·00	16·98		
0·15	15802	4975	0·0883	2·00	49·30	52·45	4·23
	14044	4036	0·0883	2·00	56·18		
	15802	4840	0·0873	2·00	51·86		
	14044	4108	0·0873	2·00	55·39		
	6468	1802	0·0999	2·00	51·83		
	6468	1924	0·0949	2·00	50·14		
0·09	15842	4146	0·0828	2·00	68·17	65·74	3·70
	13984	3825	0·0828	2·00	64·16		
	15842	4570	0·0750	2·00	65·74		
	13984	4260	0·0750	2·00	60·84		
	8163	2258	0·0749	2·00	69·78		
	8163	2090	0·0907	2·00	64·08		
0·06	15191	3930	0·0958	2·00	59·81	60·38	2·21
	13385	3403	0·0958	2·00	59·68		
	15191	4123	0·0899	2·00	60·73		
	13385	3671	0·0899	2·00	58·83		
	6326	1185	0·1466	2·00	59·17		
	6326	1427	0·1072	2·00	64·05		
0·03	16131	3185	0·1684	2·00	48·27	47·18	2·50
	14100	2920	0·1684	2·00	45·76		
	16131	3760	0·1385	2·00	47·51		
	14100	3306	0·1385	2·00	47·25		
	7522	1279	0·2167	2·00	45·48		
	7522	1295	0·1957	2·00	49·13		

where $n \geq 0$ and $m \geq 4$ to include any complex in the solution phase and any negative complex in the resin phase. It is easily seen from equation (14) that the total concentration of metal ion in the resin is

$$\Sigma(\mathrm{M})_{\mathrm{resin}} = \mathrm{R}_{m-3}\mathrm{MB}_m = \mathrm{K}_{\mathrm{ex}}(\mathrm{RB})^{m-3}\beta_n(\mathrm{M})(\mathrm{B})^3 \qquad (15)$$

Since tracer concentrations of metal ion have been used, (RB) is constant.

Therefore

$$K_d^a = \frac{\Sigma(\mathrm{M})_{\mathrm{resin}}}{\Sigma(\mathrm{M})_{\mathrm{solution}}} = \frac{(\mathrm{const.})(\mathrm{B})^3}{1 + \sum_{n=1}^{m} \beta_n(\mathrm{B})^n} \tag{16}$$

This equation is independent of the charge of the negative ion in the resin phase and if the assumption is made that only one species is predominating in the solution phase

TABLE 3.—ELECTROMIGRATION DATA: THULIUM(III) IN GLYCOLATE, LACTATE AND α-HYDROXY ISOBUTYRATE SOLUTIONS AND SODIUM IN LACTATE SOLUTION

Ligand	Concentration (M)	Voltage (V)	Current (mA)	Time (hr)	Direction of migration	Distance moved (cm)
					For ^{170}Tm	
Glycolate	0·50	100	2	23	Anode	5·1
	0·10	200	2	20	Anode	4·8
	0·05	200	1	22	Anode	2·8
	0·03	200	0·5	33	Anode	0·5
	0·01	200	0·5	12	Cathode	5·3
Lactate	1·00	100	3	14	Anode	2·8
	0·10	200	2	23	Anode	3·0
	0·03	400	1	24	Anode	2·3
	0·01	450	0·5	13	Cathode	5·1
Isobutyrate	0·10	200	1	23	Anode	3·3
	0·05	200	0·8	20	Anode	3·3
	0·03	200	0·5	28	Anode	2·5
	0·01	200	0·3	36	Cathode	1·3
					For ^{22}Na (run with ^{170}Tm)	
Lactate	0·03	400	1	24	Cathode	7·6
	0·01	450	0·5	13	Cathode	4·1

it is possible to calculate the corresponding value of the slope $d(\log K_d^a)/d(\log \mathrm{B})$ as is listed in Table 4. Since the slopes of the log K_d^a vs. log B curves in Figs. 1–5 approach or exceed a value of -1 at higher ligand concentrations, Table 4 shows that at least one negatively charged complex is present in the solution phase at ligand concentrations above 0·1 M. From Table 4 it is further seen that $d(\log K_d^a)/d(\log \mathrm{B}) = 0$ for MB_3 predominating in the solution. It is easily shown that this corresponds to a maximum in K_d^a.[10] From equation (16) we find that at the maximum

$$\frac{\sum_{n=1}^{m} n\beta_n(\mathrm{B})^n}{1 + \sum_{n=1}^{m} \beta_n(\mathrm{B})^n} = 3 \tag{17}$$

i.e. the maximum in K_d^a or log K_d^a corresponds to an average ligand number in the

[10] S. FRONAEUS, *Svensk Kem. Tidskr.* **65**, 1 (1953).

solution of 3. Therefore, the position of the maxima in the curves of the Figs. 1–5. indicate the concentration of ligand for which the average complex composition *in the solution* is MB_3. For thulium it was found that this condition is attained at a lactate concentration of 0·05 M at 87°C; below this concentration ($n < 3$) there should be a net positive charge for the mixture of complexes while above it ($n > 3$), a net negative charge should exist. The electromigration results for this system confirm this as the movement was towards the cathode at 0·01 M lactate and towards the anode for concentrations of 0·03 M and above. Since the electromigrations were performed at 25°C and the column elutions at 87°C, the agreement would seem to be acceptable. From our data we conclude that the anionic solution phase species is MB_4^-. The

TABLE 4.—VALUES OF $d(\log K_d^a)/d(\log B)$ FOR ANION EXCHANGE. (THIS VALUE IS INDEPENDENT OF THE CHARGE OF THE NEGATIVE ION IN THE RESIN PHASE).

Species in the solution phase	M^{3+}	MB^{2+}	MB_2^+	MB_3	MB_4^-	MB_5^{2-}	etc.
Value of $d(\log K_d^a)/d(\log B)$	+3	+2	+1	0	−1	−2	etc.

deviation of the slopes from −1 is not surprising when it is recalled that in this experimental analysis, activity coefficients in both the solution and the resin phase have been neglected, very probably a serious omission for such a wide range in ionic strengths in this concentration region. We have excluded the possibility of the doubly charged complex MB_5^{2-} from a consideration of steric factors ruling out the grouping of so many large organic ligands around these central metal atoms. In the case of the cation exchange resin system for routine separations, solutions of isobutyrate of 0·3–0·5 M concentration are used. Our anion exchange resin results indicate that the negative complex, MB_4^-, is predominant in this concentration range although a significant fraction of the metal ion will still be in the form of the neutral complex, MB_3. The experimental slope of −4 discussed above for the cation exchange resin systems implies according to Table 1 that the resin phase species is a mixture of the complex ions MB^{2+} and MB_2^+ if the solution phase is a mixture of MB_3 and MB_4^-. A recent investigation[11] has shown that at isobutyrate concentrations of 0·014 M the predominating species in the resin phase is MB^{2+}. Since our anion exchange resin data show that the neutral species, MB_3, is predominant in the solution phase at these concentrations, Table 1 also indicates that MB^{2+} is the predominant species in the resin phase. At an isobutyrate ion concentration of 0·25 M, analyses of the experimental slopes by the methods used to derive Tables 1 and 4 give for californium the following results:

Cation Resin Phase	Solution Phase
$40\%CfB^{2+}$—$60\%CfB_2^+$	$20\%CfB_3$—$80\%CfB_4^-$

These results are of course approximate and may be quite different from the "true" values that would be obtained using activities rather than concentrations. However, this serves to demonstrate the value of knowing accurate distribution curves for *both* anion and cation exchangers. The fact that the K_d^a-values for the glycolate complexes

[11] S. BJORNHOLM, M. JORGENSEN and B. KLINKEN. Private communication. See also, A347, Abstracts of the XVII International Congress of Pure and Applied Chemistry.

are quite a bit larger than those for the lactate and isobutyrate complexes may be interpreted to mean that the larger size of the latter two anions give rise to a steric hindrance effect. Also it seems probable that the mechanism of the exchange reaction is more properly represented by

$$MB_3 + RB \rightleftharpoons RMB_4 \tag{18}$$

rather than

$$MB_4^- + RB \rightleftharpoons RMB_4 + B^- \tag{19}$$

the reason being the larger diffusion coefficient in the resin phase of the smaller, neutral species MB_3 as compared to the larger, negatively charged MB_4^-. This is of course independent of the B^- concentration in the solution as long as the latter is below the magnitude at which an excess of free electrolyte is forced into the resin by osmotic effects.

Hitherto we have assumed the presence of only simple, mononuclear complexes, e.g. for the negative complex the composition MB_4^-. This latter formula is based on the assumption that the organic ligands are monovalent in the complex, i.e. the hydroxyl group is not protolysed upon complex formation. If it were, complexes such as MB_2^- and MB_3^- would be formed, however this possibility is ruled out by the fact, that our results indicate that the negative complex is MB_4^-. As mentioned earlier the potentiometric determination of stability constants also showed the existence of a complex with ligand number of four. In the potentiometric studies no evidence was found for polynuclear complex formation in these systems. Two possibilities can be seen from the existence of the complex MB_4^-. First, the trivalent metal ion could possess a co-ordination number of six, requiring two of the ligands to be doubly co-ordinated and two to be singly co-ordinated. Alternately, all the ligands may be chelating, requiring the central atom to have a co-ordination number of eight. The possibility of a co-ordination number of eight for such complexes is a subject of continuing study.

Acknowledgements—The authors thank Mrs. D. McKenon, J. Tatum, J. Chopoorian and R. Dinius for their assistance with these experiments. One of the authors (L. W. H.) wishes to express his gratitude for the hospitality shown him at the Lawrence Radiation Laboratory when the initial work was done in 1956. We also wish to acknowledge the financial assistance of the U.S. Atomic Energy Commission.

VOL. 19 1961

J. Inorg. Nucl. Chem., 1961, Vol. 19, pp. 262 to 271. Pergamon Press Ltd. Printed in Northern Ireland

THE REACTION OF TRICHLOROIODOMETHANE WITH SOME ORGANOMETALLIC COMPOUNDS OF GROUP VB ELEMENTS

B. J. PULLMAN and B. O. WEST
Department of Physical and Inorganic Chemistry, University of Adelaide, South Australia

(*Received* 14 *November* 1960)

Abstract—Trichloroiodomethane reacts with a number of alkyls and aryls of Group VB elements forming 1:1 adducts, $R_3M.CCl_3I$. The compounds are unstable in the presence of moisture. Conductimetric titrations show that the compounds are not quaternary salts similar to the di-iodo derivatives of the organometallic compounds. The failure of carbon tetrachloride to react in a similar way to trichloroiodomethane indicates that an M—I bond is most probably formed.

POLYHALOGENO-ALIPHATIC compounds are known to react with amines and organometallic compounds of Group VB elements in a variety of ways. Thus methylene dibromide reacts with trimethylamine to form the diquaternary compound, $[(CH_3)_3N\text{-}CH_2\text{-}N(CH_3)_3]Br_2$ via the intermediate $[(CH_3)_3N\text{-}CH_2Br]Br$.[1,2] A similar reaction has been observed by RAMIREZ and MCKELVIE[3] when triphenylphosphine reacts with bromoform to give $[(C_6H_5)_3PCHBr_2]Br$. Alternatively, the hydrogen halide derivative of an organic base has been obtained by the reaction of tetrabromoethane,[4] pentachloroethane[5] or bromoform[6] with the base.

In many cases direct compound formation has been observed where the product contains the reactants in a 1:1 or other ratio and does not behave as a salt. Thus amines such as quinoline, pyridine and ethylamine react under anhydrous conditions with carbon tetrabromide to give compounds such as $C_9H_7N\cdot CBr_4$, $C_5H_5N\cdot(CBr_4)_2$ and $(C_2H_5NH_2)_4\cdot CBr_4$.[7] Iodoform forms a variety of such adducts with primary amines containing one, two or three amine molecules per molecule of iodoform.[6] HANTZSCH and HIBBERT[8] have reported a violent reaction between triethylphosphine and carbon tetrachloride giving a compound reputed to be $Cl\text{-}C\text{-}[P(C_2H_5)_3Cl]_3$.

An unusual exchange reaction occurs when trifluoroiodomethane reacts with trimethylphosphine, trimethylarsine or trimethylstibine at low temperatures.[9] A trifluoromethyl group is exchanged for a methyl group forming dimethyltrifluoromethylphosphine, -arsine or -stibine. Methyl iodide will also react at higher temperatures with fluoromethyl-phosphines and -arsines to give the reverse exchange reaction.[10] Trifluoroiodomethane will also react directly with a number of elements to form

[1] F. M. LITTERSCHIED, *Liebigs Ann.* **337**, 67 (1904).
[2] W. C. DAVIES, E. B. EVANS and F. L. HULBERT, *J. Chem. Soc.* 412 (1939).
[3] F. RAMIREZ and N. MCKELVIE, *J. Amer. Chem. Soc.* **79**, 5829 (1957).
[4] W. M. DEHN, *J. Amer. Chem. Soc.* **34**, 286 (1912).
[5] W. H. C. RUEGGEBERG and M. M. FALKOF, *J. Amer. Chem. Soc.* **67**, 2052 (1945).
[6] W. M. DEHN and R. B. CONNOR, *J. Amer. Chem. Soc.* **34**, 1409 (1912).
[7] W. M. DEHN and A. H. DEWEY, *J. Amer. Chem. Soc.* **33**, 1588 (1911).
[8] A. HANTZSCH and H. HIBBERT, *Ber. Dtsch. Chem. Ges.* **40**, 1508 (1907).
[9] R. N. HASZELDINE and B. O. WEST, *J. Chem. Soc.* 3631 (1956).
[10] R. N. HASZELDINE and B. O. WEST, *J. Chem. Soc.* 3830 (1957).

trifluoromethyl organometallic derivatives.[11] NESMEIANOV *et al.*[12] have recently reported the preparation of stable trichloromethylmercury halides by the action of mercury on trichlorobromomethane or trichloroiodomethane. The tris (trichloro-derivatives of Group VB elements are however, unknown.

In this paper the interaction of trichloroiodomethane with a number of GroupVB alkyls and aryls is reported. Group exchange, such as occurs between trifluoroiodomethane and the trimethyl derivatives of phosphorus, arsenic and antimony does not occur, but 1:1 adducts are formed at low temperatures.

EXPERIMENTAL

Preparation of trichloroiodomethane

The compound was prepared by a modification of the method due to BESSON.[13] Aluminium tri-iodide[14] was freshly prepared before each experiment and finely ground in a dry-box. Carbon tetrachloride and carbon disulphide were reagent grade solvents dried and distilled before use. It was found to be essential that oxygen and water were excluded from the reaction mixture and the apparatus used was constantly swept with a current of dry nitrogen from which oxygen was removed by a train of chromous chloride–zinc amalgam bubblers.

In a typical preparation a mixture of carbon tetrachloride (3850 g, 25 mole) and carbon disulphide (380 g, 5 mole) was cooled to −10° and solid aluminium tri-iodide (205 g, 0·5 mole) added in small portions. The mixture was stirred vigorously and its temperature kept below 0° by controlling the rate of addition of aluminium tri-iodide. The temperature was then allowed to rise spontaneously to room temperature and then again lowered to −10°. Sodium hydroxide solution (1 l, 1 N) was added slowly with vigorous stirring at a rate sufficient to keep the temperature below 0°. This decomposed the aluminium halides. The organic layer was separated, washed with water, dried and fractionally distilled at 760 mm to yield trichloroiodomethane (90 g, 0·37 mole, 25 per cent based on AlI_3) as a fraction boiling in the range 140–142°. A sample was analysed for total halide by the Carius method. The silver halide mixture was treated with ammonia and the residue of silver iodide determined. (Found: Cl + I, 95·3; I, 51·6. Calc. for CCl_3I: Cl + I, 95·1; I, 51·7%).

When first prepared trichloroiodomethane was a viscous, highly coloured (red) liquid with a choking odour. The colouration was due mainly to iodine since the compound decomposes at its boiling point thus

$$2CCl_3I \rightarrow C_2Cl_6 + I_2.$$

Shaking the liquid with sodium thiosulphate solution removed the colour leaving pale orange coloured trichloroiodomethane. The liquid was stored under a layer of water and in the dark. Both conditions served to lessen decomposition of the compound. The substance slowly decomposed to give red products when pure or in solution in a number of solvents. The reaction seemed inhibited in the absence of light. The infra-red spectrum of trichloroiodomethane which had been kept under nitrogen failed to show the presence of a carbonyl band in the region of 1700–1800 cm^{-1}, but after exposure of the compound to air such a band was detected. The red colour on decomposition may not solely be due to free iodine but to coloured iodinated hydrocarbons[15] which could form as a result of substitution reactions involving the fragments of initial decomposition.

Preparation of adducts

The reaction vessel used consisted of a glass tube sealed at one end and fitted with a standard taper socket at the other. It was connected to a conventional all-glass vacuum system by a vacuum-tap adaptor fitted with standard taper cones. The vessel was evacuated and flamed to aid the removal

[11] J. LAGOWSKI, *Quart. Revs.* **13**, 233 (1959).
[12] A. N. NESMEIANOV, R. KH. FREIDLINA and G. K. VELICHKO, *Bull. Acad. Sci. U.S.S.R. Div. Chem. Sci.* 36 (1958), Consultants Bureau Inc., New York (Izvest. Akad. Nauk S.S.S.R. Otdel. khim. Nauk).
[13] A. BESSON, *Bull. Soc. Chim.* **9**, [3], 179 (1880).
[14] W. WATT and J. L. HALL, *Inorganic Syntheses*, Vol. 4, p. 117. McGraw-Hill, New York (1953).
[15] W. M. DEHN, *J. Amer. Chem. Soc.* **31**, 1225 (1909).

of moisture. A weighed amount of a Group VB compound was placed in the vessel, or if volatile condensed into it from the vacuum system, followed by known weights of a trichloroiodomethane and a solvent (if used), both being introduced from the vacuum system. The vessel was then surrounded by a low temperature bath and evacuated continuously until no further volatile products were recovered from the reaction mixture. The product sealed in the reaction tube could be weighed as a check on the ratio of reactants. Halogen analyses were carried out by the Carius method, weighed samples of the solid adducts being prepared in a dry-box. Melting points and decomposition temperatures were determined on small samples directly prepared in glass tubes sealed under vacuum. The decomposition temperature (d.t.) was taken as the temperature at which an intense colouration was produced in the substance.

The molecular weights of volatile products were measured by Regnault's method.

Immediately before use trichloroiodomethane was separated from the water layer under which it was stored, dried over anhydrous magnesium perchlorate and finally purified by trap-to-trap distillation in the vacuum system, being collected in a trap cooled to −46°.

Ammonia (1·00 g, 59 mmole) and trichloroiodomethane (1·25 g, 5 mmole) produced a deep magenta colour on warming the mixture from −196° to −78°. The colour disappeared at room temperature but was regained on cooling. The colour was apparently due to traces of iodine in the trichloroiodomethane since dilute solutions of iodine in liquid ammonia showed a similar colour. All the ammonia could be removed from CCl_3I at −46°.

Methylamine (1·04 g, 34 mmole) and trichloroiodomethane (1·14 g, 4·6 mmole) failed to react at −46°. The volatile material was methylamine (Found: mol. wt. 31. Calc. mol. wt. 31) and the residue CCl_3I (1·14 g).

Dimethylamine (1·9 g, 42·3 mmole) and trichloroiodomethane (1·04 g, 4·2 mmole) reacted at −78° for 15 hr then the vessel was pumped out at −46°. A white crystalline solid remained (1·28 g, 4·2 mmole), m.p. 33°; d.t. 110°. (Found: Cl + I, 80·5. Calc. for $(CH_3)_2NH{\cdot}CCl_3I$: Cl + I, 80·4%).

Trimethylamine (1·50 g, 25 mmole) and trichloroiodomethane (1·25 g, 5 mmole) formed at liquid phase at −46° which rapidly deposited white crystals (1·55 g, 5 mmole), m.p. 100°, 100° (dec). (Found: Cl + I, 76·7. Calc. for $(CH_3)_3N{\cdot}CCl_3I$: Cl + I, 77·6%).

The solid was converted to a red oil on exposure to moist air. A sample of the adduct (1 g) was heated in a sealed tube at 180° for 4 hr giving volatile products and a black tar. The volatile products were fractionated in the vacuum system, practically the entire product condensing at −46°. The substance was 1:1:1-trichloroethane. (Found: mol. wt. 133; Cl, 80·0. Calc. for $C_2H_3Cl_3$: mol. wt. 133·5; Cl, 79·8%). The infra-red spectrum of the substance showed no C—N or C—O bonds to be present.

A molecular weight determination of the adduct was carried out in benzene by the freezing point method with dry nitrogen continuously passing through the system. In 50·0 ml of benzene 0·2004 g of adduct gave a depression of 0·849° corresponding to a mol. wt. = 275. The variation from the calculated value for $(CH_3)_3N{\cdot}CCl_3I$, viz., 304·5, may be accounted for in terms of some dissociation of the complex into its constituents due to traces of moisture being taken up by the solid when being transferred from a reaction vessel into the freezing point apparatus. This contamination was found to be unavoidable despite the use of a dry-box for most of the operations involved. The solution did show a faint red colour indicating that dissociation and probably some decomposition had occurred. The result indicates that dimers do not exist however in benzene solution. Similar experimental difficulties led to a low mol. wt. being obtained for the triphenylphosphine–trichloroiodomethane adduct in benzene.

Action of oxygen on $(CH_3)_3N{\cdot}CCl_3I$.

(a) A sample of the adduct was prepared and dry gaseous oxygen admitted at −196°. The mixture was then allowed to warm to room temperature (20°) and remained at that temperature for 2 hr. No red colouration appeared in the solid during this time as appeared in the presence of air.

(b) Sufficient benzoyl peroxide was added to a solution of the adduct in dry ether to give a ratio of one labile oxygen atom per mole of adduct. No colouration was produced at room temperature. Addition of methyl iodide to this solution did not precipitate any tetramethyl-ammonium iodide hence no dissociation had occurred at this stage.

Action of water on $(CH_3)_3N{\cdot}CCl_3I$

(a) A sample of pure water condensed onto the solid adduct in the absence of oxygen caused a deep red colouration to appear on the surface of the solid at room temperature. The volatile products of reaction were fractionated in the vacuum system through traps cooled to −23°, −46° and −196°. The fraction condensing at −196° was trimethylamine. (Found: mol. wt. 59. Calc. for $(CH_3)_3N$: mol. wt. 59).

(b) Water added to an ether solution of the adduct caused a brown-red colour to develop which deepened rapidly to violet. Methyl iodide was then added to the solution and tetramethyl-ammonium iodide crystals were deposited. (Found: C, 24·2; H, 5·7; N, 7·02; I, 63·4. Calc. for $(CH_3)_4NI$: C, 23·9; H, 5·78; N, 6·98; I, 63·2%).

Triethylamine (1·73 g, 17 mmole) reacted with trichloroiodomethane (1·25 g, 5 mmole) at −20° to give a pale yellow, crystalline solid (1·76 g, 5 mmole), m.p. 45°; d.t. 80°. (Found: Cl + I, 67·4. Calc. for $(C_2H_5)_3N{\cdot}CCl_3I$: Cl + I, 67·8%). Exposure of the solid to laboratory air caused discolouration and eventual formation of a red, viscous product. The odour of CCl_3I was noticed.

When the reaction was carried out in a vessel open to the air at 0° a vigorous reaction resulted and a white crystalline product was formed mixed with tarry material. At higher temperatures the reaction was so vigorous that only black tarry products were obtained. The reaction carried out in ether or benzene gave a similar white crystalline product which was found to be triethylamine hydrochloride (derived picrate m.p. 174°; $(C_2H_5)_3N$ picrate, m.p. 175°). (Found: C, 52·4; H, 11·6; N, 10·1; Cl, 25·8. Calc. for $(C_2H_5)_3N{\cdot}HCl$: C, 52·4; H, 11·6; N, 9·8; Cl, 25·6%).

VOL. 19 1961

Pyrolysis of the adduct in a sealed tube at 180° for 20 hr gave a volatile product which was identified as chloroform by its infra-red spectrum. (Found: mol. wt., 120; Cl, 89·4. Calc. for $CHCl_3$: mol. wt. 119·5; Cl, 89·1%).

Aniline (0·438 g, 4·68 mmole) reacted with trichloroiodomethane (1·15 g, 4·68 mmole) in dry ether (20 ml) at −78° for 10 hr. Removal of the solvent at −78° gave a pale yellow solid (1·59 g). The adduct liquefied at −50° and decomposed to a red viscous product above +10°. This made sampling for analysis difficult and a weighed sample was therefore completely decomposed with concentrated sodium hydroxide solution to give ionic halides. This solution was made to a known volume and halogen determined on an aliquot. (Found: Cl + I, 69·1. Calc. for $C_6H_5N{\cdot}CCl_3I$: Cl + I, 69·4%).

Ethylenediamine (0·124 g, 2·07 mmole) and trichloroiodomethane (1·02 g, 4·15 mmole), dissolved in ether (25 ml), were allowed to react at −15° for 4 days. The ether was then removed at −23° by pumping and CCl_3I could also be slowly removed at this temperature. No stable adduct appeared to be formed at this temperature.

Triphenylamine (0·24 g, 1 mmole) and trichloroiodomethane (1·72 g, 7 mmole) were allowed to react at temperatures from −196° to +20°. No apparent reaction occurred and all the CCl_3I could be removed by pumping at room temperature. Similarly the reactants were recovered unchanged after being in contact in dry ether for 20 hr at −20°.

Pyridine (0·11 g, 1·5 mmole) failed to react with trichloroiodomethane (1·47 g, 6 mmole) at temperatures between −196° and −23°. After 10 hr at −23° the entire amount of CCl_3I was recovered unchanged. A similar reaction mixture in dry ether could be separated at room temperature.

Trimethylphosphine (4·40 g, 58 mmole) reacted smoothly with trichloroiodomethane (2·45 g, 10 mmole) in dry ether (50 ml) at −78°. A white solid was deposited and the supernatant liquid removed by pumping. The solid appeared indefinitely stable at temperatures below about −46° but decomposed rapidly with the production of considerable heat at or near room temperature. For analysis a sample of the adduct was allowed to decompose inside a reaction tube at room temperature. The products were weighed, then dissolved in concentrated sodium hydroxide solution made to a standard volume and an aliquot analysed for halogen. (Found: Cl + I, 72·3. Calc. for $(CH_3)_3P{\cdot}CCl_3I$: Cl + I, 72·6%). The reaction between trimethylphosphine and trichloroiodomethane at temperatures above −78° was violent and accompanied by great heat. There was a great deal of decomposition evident by the heterogeneous appearance of the product which contained a highly coloured viscous liquid and orange to red coloured solids. No attempt was made to examine these products in detail.

Triphenylphosphine (0·53 g, 2 mmole) was mixed with trichloroiodomethane (0·5 g, 2 mmole) in dry ether at −46° and the solvent removed at −23°. A pale yellow crystalline product (1·03 g,

2 m mole) remained, m.p. 72°; d.t. 110°. (Found: mol. wt. (0·3020 g in 50·0 ml benzene gave a F.P. depression of 0·768°), 458; Cl + I, 46·3. Calc. for $(C_6H_5)_3P{\cdot}CCl_3I$: mol. wt. 507; Cl + I, 46·1%). The solid was stable at room temperature in the absence of air and water but decomposed in the presence of moist air giving a red viscous product.

Trimethylarsine (0·78 g, 6·5 mmole) reacted with trichloroiodomethane (1·42 g, 5·8 mole) at −46°. The excess arsine was removed to the vacuum system leaving a white solid (2·1 g), m.p. 39°; d.t. 90°. The solid was stable when air and moisture were excluded but rapidly decomposed in the presence of moist air giving red-orange viscous products. (Found: Cl + I, 63·9. Calc. for $(CH_3)_3As{\cdot}CCl_3I$: Cl + I, 63·9%).

Triphenylarsine (0·61 g, 2 mmole) and trichloroiodomethane (0·5 g, 2 mmole) reacted in ether (20 ml) at −46° to give a white crystalline product, m.p. −30°; d.t. 100°. (Found: Cl + I, 42·1. Calc. for $(C_6H_5)_3As{\cdot}CCl_3I$: Cl + I, 42·3%). The compound was stable in the absence of air and moisture but rapidly decomposed in air. It decomposed more rapidly than the triphenylphosphine compound.

Trimethylstibine (1·6 g, 9·6 mmole) and trichloroiodomethane (1·50 g, 6·1 mmole) reacted in dry ether (20 ml) at −46° and white crystals were formed. Ether was removed at −78° and pumping continued at −46° until no more volatile material was removed. The resulting compound (2·52 g, 6·1 mmole) was a liquid at room temperature, m.p. 5°; d.t. 82°. (Found: Cl + I, 56·5. Calc. for $(CH_3)_3Sb{\cdot}CCl_3I$: Cl + I, 56·6%). The compound rapidly decomposed to red oily products on contact with moist air.

Triphenylstibine was not found to react with trichloroiodomethane in dry ether at any temperature between −78° and +20°.

Boron trifluoride (1·23 g, 18·8 mmole) and trichloroiodomethane (1·1 g, 4·48 mmole) were allowed to react in a sealed tube at 20°. The reactants could be separated at −78° indicating no reaction.

Solubilities. The compounds with $(CH_3)_3N$, $(C_2H_5)_3N$, $(C_6H_5)_3P$, $(CH_3)_3As$, $(C_6H_5)_3As$ all dissolved readily in benzene, nitrobenzene, chloroform, diethylether, pyridine, acetone or ethyl alcohol. Traces of moisture in the solvents led to rapid formation of red coloured solutions indicating decomposition. All experiments were conducted in an inert atmosphere box.

Carbon tetrachloride (3·1 g, 20 mmole) was condensed onto trimethylamine (1·9 g, 30 mmole) at −196° and the mixture allowed to warm to room temperature. No reaction was observed. The volatile materials were removed at −63° and separated into the original reactants in the vacuum system. A similar experiment failed to show any reaction with trimethylphosphine. Heating carbon tetrachloride with trimethylamine, triphenylamine, aniline, trimethylamine, or ethylenediamine in sealed tubes for 48 hr at 200° produced black solids. The solutions obtained by boiling these solids with water gave tests for chloride ions.

Exchange reactions

(i) *Trimethylamine* (0·23 g, 3·9 mmole) was condensed onto a sample of *trimethylphosphine–trichloroiodomethane* (1·28 g, 3·9 mmole). The mixture stood at −63° for 3 hr then the volatile materials fractionated in the vacuum system. The fraction condensing at −78° (0·1 g) was trimethylamine (Found: mol. wt., 61. Calc. for $(CH_3)_3N$: mol. wt., 59) and that at −46° was trimethylphosphine (0·02 g) (Found: mol. wt., 75. Calc. for $(CH_3)_3P$: mol. wt., 76). The latter fraction gave a red compound with carbon disulphide whereas the −78° fraction did not,[16] thus confirming the separation. The solid remaining in the reaction vessel gave a qualitative test for nitrogen after decomposition with metallic sodium.

The reverse reaction was demonstrated by reacting *trimethylamine–trichloroiodomethane* (1·07 g, 3·5 mmole) with *trimethylphosphine* (2·7 g, 3·55 mmole) at −23° for 4 hr. The volatile material was then fractionated in the vacuum system. The mixture could not easily be separated into pure components and molecular weight determinations indicated an approximately equimolar mixture of trimethylamine and trimethylphosphine (fraction 1, −46°; mol. wt., 65; fraction 2, −78°, mol. wt., 67·7).

(ii) *Trimethylarsine–trichloroiodomethane* (2·22 g, 6·08 mmole) was prepared and *trimethylphosphine* (0·46 g, 6·05 mmole) condensed onto it. The mixture stood at −46° for 4 hr then the volatile materials were removed and fractionated in the vacuum system showing the presence of trimethylarsine with a small proportion of trimethylphosphine.

[16] H. C. BROWN and R. H. HARRIS, *Amer. Chem. J.* **71**, 2751 (1949).

(iii) Dry ether (20 ml) and methyl iodide (0·466 g, 3·28 mmole) were condensed onto trimethylamine-trichloroiodomethane (1·0 g, 3·28 mmole). At 20° no precipitate or colouration had appeared in the solution after 2 hr indicating no dissociation of the adduct. A trace of water was admitted to the system resulting in an immediate red colouration appearing in the solution followed rapidly by the precipitation of white needle-like crystals. The mixture was partitioned between ether and water to remove the red product and the aqueous extract was treated with mercuric iodide in potassium iodide solution. The resulting white solid was tetramethylammonium tri-iodomercurate, m.p. 244°, mixed m.p. 243°, indicating that tetramethylammonium iodide had been formed on the dissociation of the adduct. The weight of iodomercurate recovered (2·05 g, equivalent to 3·13 mmole of quaternary iodide) indicated that almost quantitative decomposition of the adduct had occurred.

Conductimetric titrations

All titrations were performed under nitrogen at 20° and extreme precautions were taken to avoid the entrance of water vapour into the cell. A magnetic stirrer was used to ensure thorough mixing of the reactants. The cell constant was 0·02. Resistances were measured with a Philips Bridge (PR9500). To prepare solutions of trichloroiodomethane a sample of the compound sufficient to give an approximately 0·1 M solution was purified as described previously and then distilled from a vacuum system directly into a calibrated vessel, dry nitrogen was then admitted and purified, oxygen free solvent added.

VOL. 19 1961

RESULTS AND DISCUSSION

The compounds that are formed between trichloroiodomethane and Group VB alkyl and aryl derivatives are stable at room temperature for varying periods of time in the complete absence of water and oxygen. The trimethylphosphine compound is unstable at room temperature even in the absence of water and oxygen and decomposes readily. The direct reaction between this alky derivative and CCl_3I is violent at temperatures close to room temperature, leading to decomposition of the product. The trimethylamine–trichloroiodomethane reaction is also violent at room temperature but the reaction is moderated in both cases by working at lower temperatures. Similar strongly exothermic reactions are known between alkyl phosphines or amines and halogens.[17]

On exposure to moist air the compounds all decompose readily forming red viscous products. Oxygen alone does not cause decomposition since neither pure oxygen nor an organic peroxide caused the trimethylamine–trichloroiodomethane compound to decompose. Water, however, added to the solid compound caused an immediate red colour to appear throughout the solid even in the absence of oxygen. The addition of water to an ether solution of the compound also caused the red decomposition products to appear and methyl iodide added to the mixture precipitated tetramethylammonium iodide. A solution of pure trimethylamine–trichloroiodomethane in anhydrous ether shows no reaction with methyl iodide.

It appears that dissociation of the compound is the first stage in the decomposition of the trichloroiodomethane adducts and this is caused by the attack of water molecules thus

$$R_3M{\cdot}ICl_3 + H_2O \rightarrow [R_3MH]^+OH^- + ICl_3$$

The presence of hydroxide ions may then catalyse decomposition of the trichloroiodomethane molecule to iodine and other coloured substitution products. The detection of an infra-red carbonyl band in a sample of the trichloroiodomethane that had been

[17] J. F. Norris, *Amer. Chem. J.* **20**, 51 (1898); G. Kosolapoff, *Organophosphorus Compounds*, p. 24. Wiley, New York (1950).

exposed to the air supports the view that the following reaction may occur, aided by light.

$$CCl_3 + \tfrac{1}{2}O_2 \rightarrow COCl_2 + ICl$$

The iodine monochloride may further substitute unreacted CCl_3I molecules to give higher substituted iodo derivatives which are coloured, e.g. CCl_2I_2.[15] Decomposition of trichloroiodomethane by a base can explain why triethylammonium chloride was isolated from the reaction of triethylamine and trichloroiodomethane in wet ether.

The fact that trichloroiodomethane itself decomposes in the presence of light and air but is protected by covering with a water layer may be explained by assuming that the water layer prevents oxygen reaching the liquid and forming phosgene, in a light catalysed reaction similar to that undergone by chloroform.[18]

Nature of the compounds

The following alternative formulae may be considered for these compounds

$$[R_3MCCl_3]^+I^- \quad (1)$$

$$[R_3MI]^+CCl_3^- \quad (2)$$

$$R_3M \rightarrow ICCl_3 \quad \text{or} \quad R_3M \rightarrow Cl{\cdot}CCl_2I \quad (3)$$

Conductimetric titration of trichloroiodomethane with triethylamine, triphenylamine or triphenylarsine in nitrobenzene shows no evidence for the formation of salt-like compounds in solution (Fig. 1). On the other hand, the titration curves of iodine with triethylamine, triphenylphosphine or triphenylarsine (Fig. 2) show a marked break in the slope of the curves at the points corresponding to the formation of 1:1 compounds, indicating that the compounds $[R_3MI]I$ have been formed

HANTZSCH[19] first suggested the quaternary formula for amine–halogen compounds and conductivity measurements by BOHME and KRAUSE[20] of the Me_3N–Br_2 system support this view. ISSLIEB and SEIDEL[21] have similarly shown that trialkylphosphine di-iodides act as quaternary compounds in acetonitrile or nitrobenzene.

The conductimetric evidence eliminates formulae (1) and (2) from consideration as structures for the trichloroiodomethane compounds and suggests either of the structures (3). The failure of carbon tetrachloride to react with Me_3N, Me_3P or $(C_6H_5)_3P$ (Fig. 1, curve E) at low temperatures indicates that there is probably an M-I bond in the adducts with trichloroiodomethane rather than an M-Cl bond. The solid state structures of a number of amine-halogen compounds have been examined by HASSEL[22] and his coworkers who have found that a halogen molecule is bonded to a nitrogen atom to form the linear arrangement N-X-X. The trimethylamine-iodine compound examined by STRØMME[23] has this structure with a N-I-I arrangement. A similar configuration may be suggested for the CCl_3I compounds, viz., R_3M-I-CCl_3. The apparent contradiction of the quaternary view of HANTZSCH[19] raised by these crystal structure determinations of R_3NX_2 compounds is overcome by considering that heterolysis of the halogen–halogen link can occur readily in polar solvents. The conductimetric titration of triphenylphosphine with trichloroiodomethane shows a definite

[18] P. KARRER, *Organic Chemistry*, p. 182. Elsevier, Amsterdam (1950).
[19] A. HANTZSCH, *Ber. Dtsch. Chem. Ges.* **38**, 2161 (1905).
[20] H. BOHME and W. KRAUSE, *Ber. Dtsch. Chem. Ges.* **84**, 170 (1957).
[21] K. ISSLIEB and W. SEIDEL, *Z. Anorg. Chem.* **288**, 201 (1956).
[22] O. HASSEL, *Proc. Chem. Soc.* 250 (1957); *Molec. Phys.* **1**, 241 (1958).
[23] K. O. STRØMME, *Acta Chem. Scand.* **13**, 268 (1959).

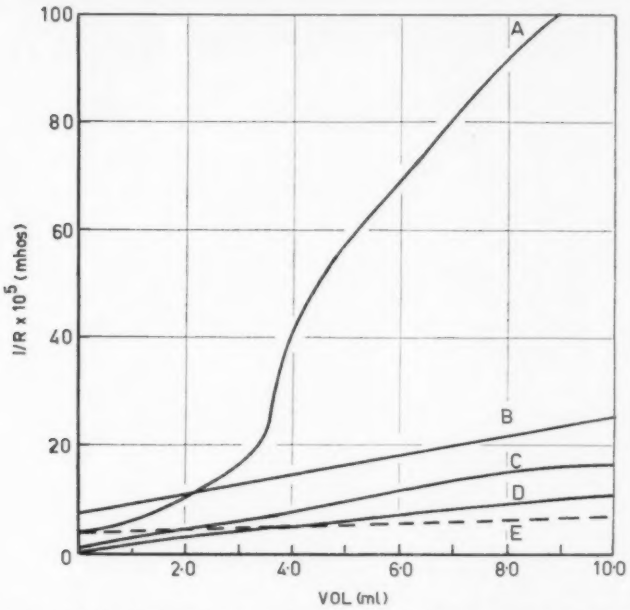

FIG. 1.—Trichloroiodomethane conductimetric titration curves in nitrobenzene at 20°.
A—0·01 M $(C_6H_5)_3P$, 0·12 M CCl_3I, theoretical equivalence point for 1:1 compound at 4·15 ml.
B—0·01 M $(C_6H_5)_3As$, 0·09 M CCl_3I, theoretical equivalence point for 1:1 compound at 5·39 ml.
C—0·01 M $(C_2H_5)_3N$, 0·114 M CCl_3I, theoretical equivalence point for 1:1 compound at 4·5 ml.
D—0·01 M $(C_6H_5)_3N$, 0·12 M CCl_3I, theoretical equivalence point for 1:1 compound at 4·15 ml.
E—0·01 M $(C_6H_5)_3P$, 0·10 M CCl_4, equivalence point for 1:1 compound at 5·0 ml.

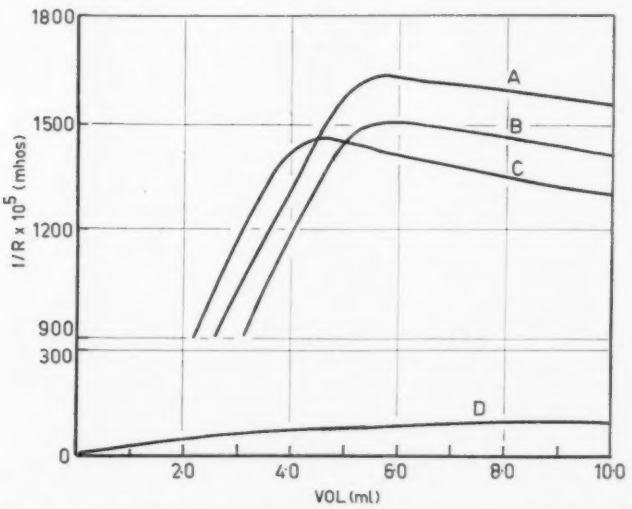

FIG. 2.—Iodine conductimetric titration curves in nitrobenzene at 20°. Solutions each 0·10 M.
A—50 ml $(C_2H_5)_3N$ solution, theoretical end point 5·0 ml.
B—50 ml $(C_6H_5)_3P$ solution, theoretical end point 5·0 ml.
C—45 ml $(C_6H_5)_3As$ solution, theoretical end point 4·5 ml.
D—50 ml $(C_6H_5)_3N$ solution, theoretical end point 5·0 ml.

VOL. 19 1961

TABLE 1.—REACTIONS OF TRICHLOROIODOMETHANE WITH ORGANOMETALLIC COMPOUNDS

Compound	Conditions	Nature of product	m.p. (°C)	d.t. (°C)
1. Amines				
NH_3	−78°–−46° in excess NH_3	None	—	—
CH_3NH_2	−78°–−46° in excess CH_3NH_2	None	—	—
$(CH_3)_2NH$	−78° in excess $(CH_3)_2NH$	1:1 adduct	33	110
$(CH_3)_3N$	−46° in excess $(CH_3)_3N$	1:1 adduct	100	100
$(C_2H_5)_3N$	(a) −46° in excess $(C_2H_5)_3N$	1:1 adduct	42	80
	(b) 0° in air	$(C_2H_5)_3N{\cdot}HCl$	—	—
$NH_2{\cdot}C_2H_4{\cdot}NH_2$	−78°–+20°	None	—	—
$(C_6H_5)NH_2$	−46°	1:1 adduct	−50	10
$(C_6H_5)_3N$	−46°–+20° with or without $(C_2H_5)_2O$	None	—	—
C_5H_5N	−46°–+20°	None	—	—
2. Phosphines				
$(CH_3)_3P$	−78° in $(C_2H_5)_2O$	1:1 adduct	—	10
$(C_6H_5)_3P$	−78° in $(C_2H_5)_2O$	1:1 adduct	72	110
3. Arsines				
$(CH_3)_3As$	−46° in excess $(CH_3)_3As$	1:1 adduct	39	95
$(C_6H_5)_3As$	−78° in $(C_2H_5)_2O$	1:1 adduct	5	100
4. Stibines				
$(CH_3)_3Sb$	−46° in excess $(CH_3)_3Sb$	1:1 adduct	5	82
$(C_6H_5)_3Sb$	−78°–+20° in $(C_2H_5)_2O$	None	—	—

inflexion point at a ratio of reactants of 1:1 although the curve in Fig. 1 has not the appearance of those obtained in the iodine titrations. This may indicate that slight dissociation occurs with the triphenylphosphine–trichloroiodomethane compound.

Boron trifluoride does not co-ordinate with trichloroiodomethane so that the primary bond in the compounds with Group VB organometallic compounds must be a co-ordinate link involving donation of an electron pair from the Group V atom to the iodine of CCl_3I. The exchange reactions observed with several of the compounds which must involve breaking and making this bond are similar to those which have been studied for other donor–acceptor systems involving Group VB methyl derivatives, e.g., with Me_3Al,[24] and Me_3Ga.[25]

The relative donor character of the Group VB elements has been found to lie in the order $N > P > As > Sb$[26] for donor–acceptor reactions involving non-transition elements. A comparison of the exchange reactions, decomposition temperatures and resistance to hydrolysis of the trichloroiodomethane compounds indicates that the order of stability of adducts is $Me_3N > Me_3As > Me_3Sb$. The position of Me_3P is unclear, however, because of the highly exothermic nature of its reaction with CCl_3I contrasted with the rapid decomposition of the CCl_3I adduct at room temperature.

Basicity considerations alone cannot be used in predicting the formation or otherwise of the trichloroiodomethane derivatives. Thus trimethylamine forms a stable adduct with trichloroiodomethane although being of lower basicity with respect to proton attachment than methylamine which does not form an adduct. It would appear that the inductive effects of successive methyl groups outweigh their steric effect on basicity in these instances.[27] The formation of a compound by aniline, a weaker base than ammonia (which fails to react), is difficult to explain on basicity grounds.

The Group VB triaryl derivatives show a more distinct pattern of behaviour based on basicity considerations. The aryl derivatives are expected to be weak bases because of the electron withdrawing nature of the aromatic rings. Triphenylamine is known to have virtually no basic properties and fails to show any reaction with either iodine or trichloroiodomethane (Figs. 1 and 2). Triphenylphosphine which would be expected to be a weak base like triphenylamine forms the most stable derivative prepared with trichloroiodomethane and must owe its strong bonding character to p_π–d_π bonding[26] between iodine and phosphorus being superimposed upon the ordinary $P \rightarrow I$ co-ordination. This type of bonding can occur with arsenic and antimony derivatives but as the primary σ-bonding due to the unshared pair on the metal becomes weaker the overall bonding ability will decrease in the order $P > As > Sb$. Nitrogen is unable to participate in π-bonds of this kind since it does not possess any suitable vacant orbitals to receive electrons from iodine.

Acknowledgements—The authors are indebted to Mr. M. O'Connor who conducted the preliminary investigations into the preparation of trichloroiodomethane and its reaction with trimethyl-phosphine and -arsine.

[24] H. C. Brown and W. R. Davidson, *J. Amer. Chem. Soc.* **64**, 316 (1942).
[25] G. E. Coates, *J. Chem. Soc.* 2203 (1951).
[26] S. Ahrland, J. Chatt and N. R. Davies, *Quart. Revs.* **12**, 265 (1958).
[27] H. C. Brown, H. Bartholomay and M. D. Taylor, *J. Amer. Chem. Soc.* **66**, 435 (1944).

J. Inorg. Nucl. Chem., 1961, Vol. 19, pp. 272 to 277. Pergamon Press Ltd. Printed in Northern Ireland

THE URANIUM(IV) COMPLEXES WITH 8-QUINOLINOL AND 5,7-DIHALO-8-QUINOLINOLS

W. W. WENDLANDT and G. R. HORTON
Department of Chemistry, Texas Technological College, Lubbock, Texas

(*Received* 30 *August* 1960; *in revised form* 1 *November* 1960)

Abstract—The preparation of the 5:1 uranium(IV) complexes of 8-quinolinol, 5,7-dibromo-, and 5,7-dichloro-8-quinolinol is presented. By the use of thermogravimetric analysis, differential thermal analysis, and ultraviolet, visible, and infrared absorption spectroscopy, it was shown that the resulting complexes were similar to the thorium(IV) analogues of these chelating agents. It does not appear to be possible to prepare the unsolvated, 4:1, uranium(IV) complexes.

ALTHOUGH the uranium(VI) complexes with 8-quinolinol and its derivatives have been extensively investigated,[1–15] nothing is known about the uranium(IV) complexes with these well known chelating agents. Stoicheiometrically, complexes of the general formula, $M(Ox)_4$, where Ox is the ionic chelating molecule, would be expected. On the other hand, since the chemistry of uranium(IV) compounds is similar to that of thorium(IV), perhaps complexes of the solvated type, $U(Ox)_4 \cdot HOx$, would be obtained. The results of this investigation confirm the latter case. In this study, the uranium(IV) complexes with 8-quinolinol, 5,7-dichloro-, and 5,7-dibromo-8-quinolinol were prepared and characterized by thermogravimetric analysis (TGA), differential thermal analysis (DTA), and ultra-violet, visible, and infra-red absorption spectroscopy.

EXPERIMENTAL

A. *Apparatus*

The automatic recording thermobalance and the differential thermal analysis apparatus have previously been described.[16] Sample sizes ranged in weight from 55 to 65 mg for the TGA studies and 100 mg for the DTA studies.

The heating rate for the DTA studies was 10°C per min, while for the TGA studies, 8° and 4°C per min, was employed.

B. *Absorption spectra studies*

The ultra-violet and visible absorption spectra were determined with a Beckman Model DU spectrophotometer, using 5·00 cm quartz windowed cells. Chloroform was employed as the solvent

[1] J. F. FRERE, *J. Amer. Chem. Soc.* **55,** 4362 (1933).
[2] F. HECHT and W. REICH-ROHRWIG, *Monatsch.* **53–54,** 596 (1929).
[3] H. R. FLECK, *Analyst* **62,** 378 (1937).
[4] H. GOTO, *Sci. Repts. Tohoku Imp. Univ.*, First Ser. **26,** 391 (1937).
[5] T. MOELLER and D. H. WILKINS, *Inorganic Syntheses*, Vol. 4, p. 101. McGraw-Hill, New York (1953).
[6] C. DUVAL, *Anal. Chim. Acta.* **3,** 335 (1949).
[7] W. W. WENDLANDT, *Analyt. Chem.* **28,** 499 (1956).
[8] T. MOELLER and M. V. RAMANIAH, *J. Amer. Chem. Soc.* **75,** 3946 (1953).
[9] N. ESWARANARAYANA and BH. S. V. RAGHAVA RAO, *Anal. Chim. Acta*, **11,** 339 (1954).
[10] K. S. VENKATESWARLU and BH. S. V. RAGHAVA RAO, *Anal. Chim. Acta*, **12,** 554 (1955).
[11] J. H. VAN TASSEL and W. W. WENDLANDT, *J. Amer. Chem. Soc.* **81,** 813 (1959).
[12] E. P. BULLWINKEL and P. NOBLE, *J. Amer. Chem. Soc.* **80,** 2955 (1958).
[13] W. W. WENDLANDT, *Anal. Chim. Acta*, **17,** 274 (1957).
[14] J. P. PHILLIPS, J. F. EMERY and H. P. PRICE, *Analyt. Chem.* **24,** 1033 (1952).
[15] J. H. VAN TASSEL and W. W. WENDLANDT, *J. Amer. Chem. Soc.* **82,** 4821 (1960).
[16] W. W. WENDLANDT, T. D. GEORGE, G. R. HORTON, *J. Inorg. Nucl. Chem.* 17, (1961).

and was purified by first washing out the 0·5 per cent ethanol preservative with water, drying over anhydrous calcium chloride for 24 hr, and then collecting the fraction that distilled off from 60·5 to 61·5°C. The concentrations of the solutions were 0·00744 g U per l. and 0·00534 g Th per l.

The infra-red absorption spectra were determined on a Perkin-Elmer Model 137B spectrometer using the KBr pellet technique. Sample size was 5 mg in a total weight of 400 mg of KBr.

C. *Reagents*

The uranium(VI) nitrate 6-hydrate was obtained from the Mallinckrodt Chem. Works, St. Louis Mo.; 8-quinolinol, 5,7-dichloro-, and 5,7-dibromo-8-quinolinol, were obtained from Eastman Organic Chemicals, Rochester, N.Y. The latter reagents were purified by repeated crystallization from water–acetone mixtures.

All other chemicals used were of C.p. quality.

D. *Preparation of uranium(IV) complexes*

Uranium(VI) was reduced to uranium(IV) with sodium dithionite as previously described by MARCHI[17]. The resulting uranium(IV) solution was used immediately to prepare the complexes.

The 8-quinolinol uranium(IV) complex, $U(C_9H_6NO)_4 \cdot C_9H_6NOH$, was prepared as follows. To 100 ml of a solution containing 0·3 g of uranium(IV) ion, was added 1·8 g of 8-quinolinol in 50 ml of glacial acetic acid (50 per cent excess). The pH of the resulting solution was about 1·9. To this mechanically stirred solution, 6 N ammonium hydroxide was added dropwise. The first precipitate appeared at pH 4·82, with the ammonium hydroxide being added until the pH was 5·30. The resulting brownish-yellow coloured precipitate was filtered off into a sintered porcelain crucible, washed repeatedly with water, and then washed twice with small portions of acetone. It was then dried in a vacuum desiccator over anhydrous calcium chloride for 24 hr. Analysis of the compound for uranium content by ignition in a muffle furnace at 900°C gave the following results. (Found: U, 25·08, 25·09, Theor. U, 24·80%). The 8-quinolinol content was determined by a bromometric titration.[18] (Found: 75·16, 75·90. Theor. 75·20%.)

The 5,7-dichloro-8-quinolinol complex, $U(C_9H_4Cl_2NO)_4 \cdot C_9H_4Cl_2NOH$, was prepared by a method similar to that given above. To 100 ml of a solution containing 0·3 g of uranium(IV) ion, was added a solution of 1·40 g of 5,7-dichloro-8-quinolinol dissolved in a mixture of 25 ml of 2 N hydrochloric acid and 100 ml of glacial acetic acid. To this stirred solution, 6 N ammonium hydroxide was added dropwise until the pH was 3·24. The gold coloured precipitate was filtered off into a sintered porecelain crucible, washed once with water, and then washed repeatedly with a 30 per cent acetone–70 per cent water mixture. The precipitate was dried in a vacuum desiccator over anhydrous calcium chloride for 24 hr. Analysis of the complex for uranium gave: Found: U, 19·04, 19·06 Theor. U, 18·25%.

The 5,7-dibromo-8-quinolinol complex, $U(C_9H_4Br_2NO)_4 \cdot C_9H_3Br_2NOH$, was prepared in the same manner as the 5,7-dichloro-8-quinolinol complex. Precipitation was completed at a pH of 2·30. On analysis for uranium, the gold coloured precipitate gave: Found: U, 14·39, 14·22: Theor. U, 13·73%.

All of the uranium complexes appeared to be stable to oxidation in that after two weeks, there was no apparent decomposition. They were soluble in chloroform but only slightly soluble in acetone and ethyl alcohol.

The 8-quinolinol complex, when heated at 190°C at a pressure of 20 mm of Hg, gave a sublimate which melted at 74–76°C (8-quinolinol, m.p. 74–76°C). A small portion of the residue was dissolved in 6 N hydrochloric acid and gave a greenish coloured solution, indicating the presence of the uranium(IV) ion.

RESULTS AND DISCUSSION

The TGA curves for the uranium(IV) complexes are given in Fig. 1. The 8-quinolinol complex (curve *A*) began to lose weight at about 130°C, giving a pronounced

[17] L. E. MARCHI, *Inorganic Syntheses* (Edited by L. F. AUDRIETH) Vol. 3, p. 166. McGraw-Hill, New York (1950).

[18] I. M. KOLTHOFF and E. B. SANDELL, "Textbook of Quantitative Inorganic Chemistry," 3rd Edition, Macmillan, New York, 1952, p. 607.

VOL. 19 1961

break in the curve at 235°C. On the basis of weight-loss data, the composition of the curve at 235°C approximated that for the 4 : 1 complex, $U(C_9H_6NO)_4$; (weight-loss: Found: 15·7. Theor: 15·12%). However, this may be fortuitous since a horizontal weight level was not obtained. After a range of slow weight-loss, the complex began to decompose rapidly beginning at 530°C. The oxide, U_3O_8, was obtained at 625°C.

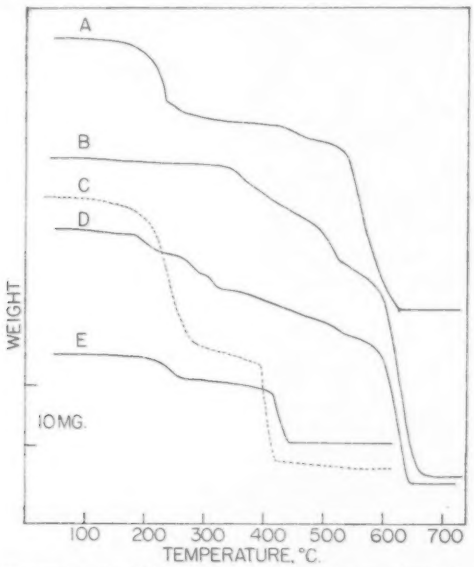

FIG. 1.—Thermogravimetric analysis curves of the uranium(IV) complexes.
A. Uranium(IV) 8-quinolinol complex
B. Uranium(IV) 5,7-dibromo-8-quinolinol complex
C. Uranium(IV) 8-quinolinol complex (4°C per min)
D. Uranium(IV) 5,7-dichloro-8-quinolinol complex
E. Residue from sublimation experiment

From the above curve, it is apparent that the uranium(IV) complex behaves differently than the thorium(IV) analogue. In the case of the latter, the extra molecule of 8-quinolinol began to come off at 80°C, resulting in a horizontal weight level of the 4 : 1 thorium complex which was stable up to 250°C.[7]

At a slower heating rate, 4°C per min, a totally different curve was obtained for the uranium(IV) 8-quinolinol complex (curve *C*). Although the first weight-loss began at about 100°C, the remainder of the complex decomposed at a much faster rate. The explanation for this is not known.

Of the 5,7-dichloro- and 5,7-dibromo-8-quinolinol uranium(IV) complexes (curves *D* and *B*), the latter was by far the most stable. Again, there was no evidence for the formation of the 4 : 1 complexes, although for the 5,7-dichloro-complex, breaks were observed in the 295°–320°C temperature range which approximated this composition. The oxide levels were obtained at 640° and 660°C, respectively.

The residue from the sublimation experiment (curve *E*) gave a markedly different curve than the other two 8-quinolinol complexes (curves *A* and *C*). However, the residue was not the 4 : 1 uranium complex since the amount of uranium present was far too high (Found: 57·19. Theor: 29·22%). This composition does not correspond to any known stoicheiometry.

The DTA curves are given in Fig. 2. For the uranium(IV) 8-quinolinol complex (curve *A*), exothermic peaks were found with maxima at 225° and 365°C, respectively, and an endothermic peak with a maximum at 275°C. In DTA, exothermic peaks are usually caused by oxidation or crystalline inversion reaction while such phenomena as reduction, decomposition, sublimation, fusion, and so on, cause endothermic peaks. Thus, there is little evidence from the curve that the extra molecule of 8-quinolinol is lost by a sublimation process. However, the rearrangement reaction of the 4 : 1

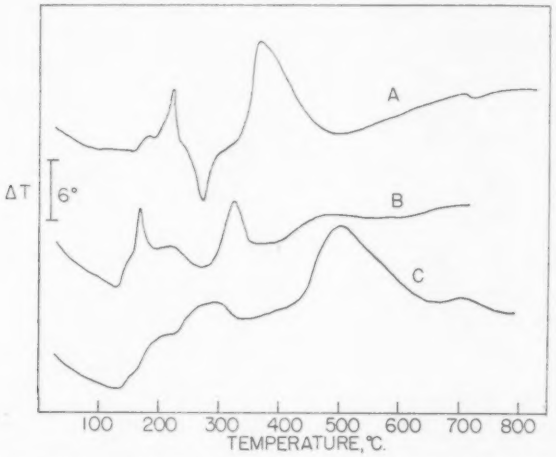

FIG. 2.—Differential thermal analysis curves of the uranium(IV) complexes.
A. Uranium(IV) 8-quinolinol complex
B. Uranium(IV) 5,7-dichloro-8-quinolinol complex
C. Uranium(IV) 5,7-dibromo-8-quinolinol complex

complex during the evolution of the solvate molecule may be an exothermic reaction which may mask the endothermic sublimation reaction. Outside of the loss of solvate molecule from the complex, an interpretation of the peaks is not possible except that they represent the decomposition and oxidation of the complex to uranium oxide, U_3O_8, or possibly a mixture of metal oxides.

The uranium(IV) 5,7-dichloro-8-quinolinol complex (curve *B*) gave a broad endothermic peak with a maximum at 135°C and two exothermic peaks with maximas at 165° and 325°C, respectively. The 5,7-dibromo-8-quinolinol complex (curve *C*) was different from the corresponding 5,7-dichloro-analog in that after a broad exothermic peak with a maximum at 135°C, broad exothermic peaks were found in the 200–400°C region, as well as a broad exothermic peak with a maximum at 500°C.

The ultra-violet and visible absorption spectra curves for the uranium(IV) and thorium 8-quinolinol complexes are given in Fig. 3. The thorium curve, in agreement with MOELLER and RAMANIAH,[8] gave a peak at 324 mμ (320 mμ previously reported). For the uranium(IV) complex, the peak maximum was at 325 mμ with $E = 10{,}000$. However the peak shoulder at 370 mμ was more pronounced in the case of the uranium curve. It is thus seen that the absorption spectra of these two compounds are almost identical.

Similarly, the infra-red spectra for the uranium and the thorium compounds were almost identical, as shown in Fig. 4. The 5,7-dichloro- and 5,7-dibromo-8-quinolinol

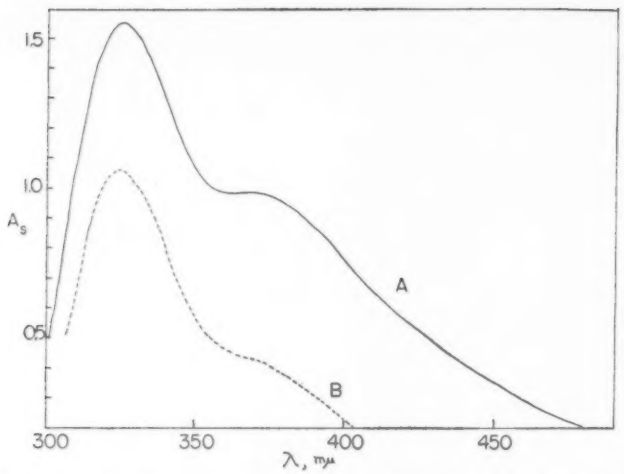

FIG. 3.—Absorption spectra curves of the uranium(IV) and thorium complexes.
A. Uranium(IV) 8-quinolinol complex
B. Thorium 8-quinolinol complex

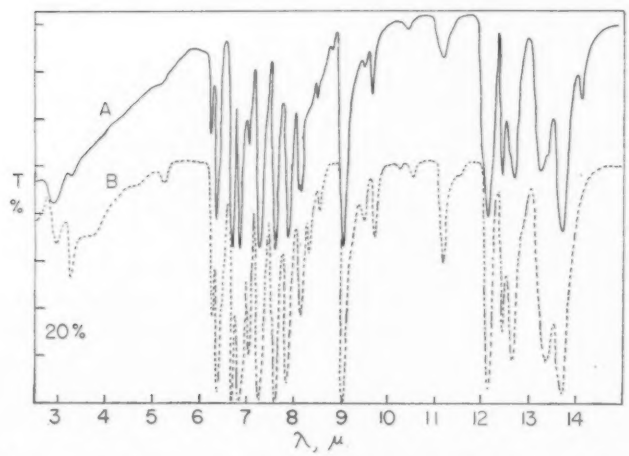

FIG. 4.—Infra-red absorption spectra curves of the uranium(IV) and thorium complexes.
A. Uranium(IV) 8-quinolinol complex
B. Thorium 8-quinolinol complex

chelates of these two ions also exhibited similar spectra (not reproduced). The strong absorption at about 9·0 μ, which has been attributed to vibrations of the M—O—C$\diagdown\!\!\diagup$ —bond,[19] was present in all of the metal chelates.

From the evidence presented here, it may be concluded that the uranium(IV) and the thorium 8-quinolinol and 5,7-dihalo-8-quinolinol complexes possess identical structures. However, just what this structure is remains unknown. A structure for the 4 : 1 thorium 8-quinolinol complex has been proposed by DYRSSEN[20] which

[19] R. G. CHARLES, H. FREISER, R. FRIEDEL, L. E. HILLIARD and W. D. JOHNSTON, *Spectro. Acta* **8**, 1 (1956).
[20] D. DYRSSEN, *Svensk Kem. Tidskrift* **68**, 212 (1956).

consisted of having the O and N donor atoms in a square Archimedian antiprism about the thorium ion. The structure for the 5 : 1 complex still remains unknown. It is interesting to note that if all of the chelating group's donor atoms are attached to the uranium(IV) ion in the 5 : 1 complex, a co-ordination number of ten would be obtained. This would be the first example of tenfold co-ordination for uranium(IV).[21]

Acknowledgement—The assistance of Mr. T. D. GEORGE is gratefully acknowledged. This work was supported by the U.S. Atomic Energy Commission through contract no. AT-(40-1)-2482.

[21] A. E. COMYNS, *Chem. Rev.* **60**, 115 (1960).

VOL.
19
1961

J. Inorg. Nucl. Chem., 1961, Vol. 19, pp. 278 to 285. Pergamon Press Ltd. Printed in Northern Ireland

A STUDY OF TRANSFERENCE AND SOLVATION PHENOMENA—IV

POTASSIUM CHLORIDE IN WATER AND WATER–ETHANOL SOLVENTS

J. O. WEAR, C. V. MCNULLY and E. S. AMIS
Chemistry Department, University of Arkansas, Fayetteville, Arkansas

(*Received* 12 *August* 1960; *in revised form* 14 *October* 1960)

Abstract—Transference and solvation phenomena for the ions of potassium chloride in water and water–ethanol solvents have been studied. The transference numbers of the anion as a function of salt concentration and solvent composition are presented graphically. The sine-like curve for the solvent transferred from anode to cathode has been discussed in relation to the relative solvation and the nature of solvation of the potassium and chloride ions.

IN this series of studies, transport and solvation phenomena have been investigated for the ions of uranyl chloride, of silver perchlorate, and of lithium chloride in water, water–ethanol, and ethanol solvents.[1,2,3] This additional study involves the transport and solvation phenomena of the ions of potassium chloride in water and water–ethanol. This study could not be carried above 75 weight per cent ethanol because of solubility of the salt. The study of the transport and solvation phenomena for potassium chloride seemed of special interest since the potassium ion and chloride ion are of almost equal size. Any change in grammes of solvent in an electrode portion should be due to a difference in solvation of univalent positive and negative ions since there is little difference in ionic radii.

The method chosen for the determination of transport and solvation data involved the use of an inert reference substance in a Hittorf transference measurement as in our previous studies.[1,2,3]

EXPERIMENTAL

The potassium chloride was Fisher Certified Reagent. The absolute ethanol used was 99·7 vol % ethanol. The inert reference substance, α-methyl-D-glucoside, was prepared by Nutritional Biochemical Corporation. The silver wire and all other chemicals were of reagent quality.

The experimental procedure used was the same as used previously.[3]

TREATMENT OF DATA

The symbols used in this paper are the same as were used in the lithium chloride study.[3]

Using methods already described,[1,2] the Hittorf transference numbers of the anion and cation, respectively, and the grammes of solvent transferred per faraday of electricity were calculated using the following equations:

$$t_c = \left(\frac{P_s{}^m}{100 - P_s{}^m} - \frac{P_s{}^a}{100 - P_s{}^a}\right)\left(\frac{W(100 - P_s{}^a)A_{Ag}}{100\, W_{Ag} M_s}\right) \quad (1)$$

$$t_a = 1 - t_c \quad (2)$$

[1] D. M. MATHEWS, J. O. WEAR and E. S. AMIS, *J. Inorg. Nucl. Chem.* **13**, 298 (1960).
[2] W. V. CHILDS and E. S. AMIS, *J. Inorg. Nucl. Chem.* **16**, In press (1960).
[3] J. O. WEAR, C. V. MCNULLY and E. S. AMIS, *J. Inorg. Nucl. Chem.* In press.

and

$$\Delta G^{F}_{sol} = \frac{\left[\alpha_a \frac{d_m}{d_a} - \alpha_m\left(\frac{1 - f_s{}^a}{1 - f_s{}^m}\right)\right] W}{F\alpha_m} \tag{3}$$

In pure water, the moles of water transported per faraday could be calculated by dividing equation (3) by the molecular weight of water. This could not be done in the case of mixed solvents since no molecular weight could be calculated for the solvent in the solvation sheath.

In Table 1 are recorded the data used to calculate the transference and solvation numbers at various salt concentrations in water. Figs. 1 and 2, respectively, are the

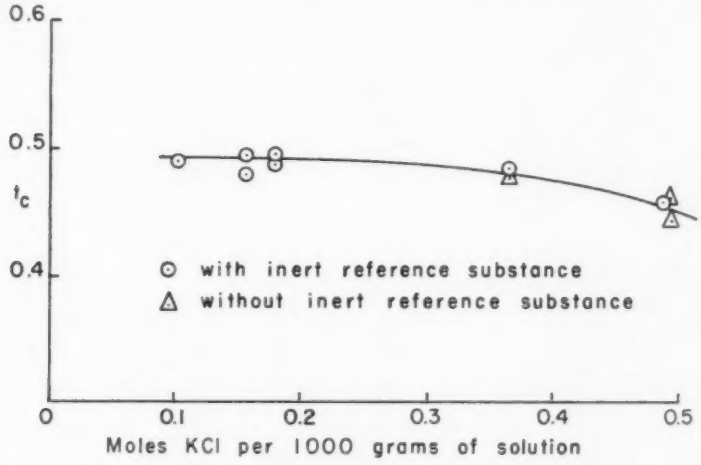

FIG. 1.—Cation transference number against moles of KCl/1000 g of solution in water.

transference numbers and grammes of water transferred per faraday from anode to cathode plotted against concentration of potassium chloride in moles per 1000 g of solution. The transference numbers agree well with those recorded in the literature[4] except for the values at 0·487 m and 0·490 m. The deviation from MacInnes and Dole's value is about eight per cent which is outside the experimental error of this method. The data in columns 8 and 9 of Table 1 were taken with the inert reference substance present, but the data in columns 10 and 11 of Table 1 were obtained without the presence of an inert reference substance. This shows that our low value could not be due to the inert reference substance's not being inert, i.e. the inert reference substance did not influence the value of the transference number at this concentration of KCl.

In Fig. 1 it is observed that the transference number of the cation, t_c, remains almost constant up to about 0·362 moles/1000 g of solution. After this point there is a smooth curving to a lower value. This could be due to the formation of a complex such as KCl_2^-. Although such a complex would explain this drop in t_c since some potassium would be moving in the opposite direction than normal, it is a very unlikely complex since the alkali metals form very few complexes. Another explanation might be that as the salt concentration increases the solvation of the ions decreases with the

[4] D. A. MACINNES and M. DOLE, *J. Amer. Chem. Soc.* **53**, 1357 (1931).

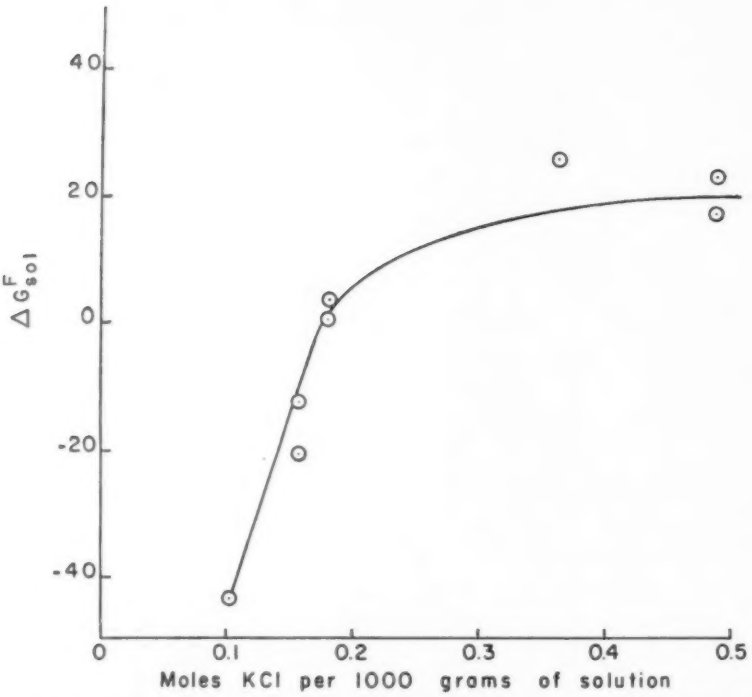

FIG. 2.—Calculated grammes of solvent transferred from anode to cathode per faraday of electricity plotted against moles KCl/1000 of solution.

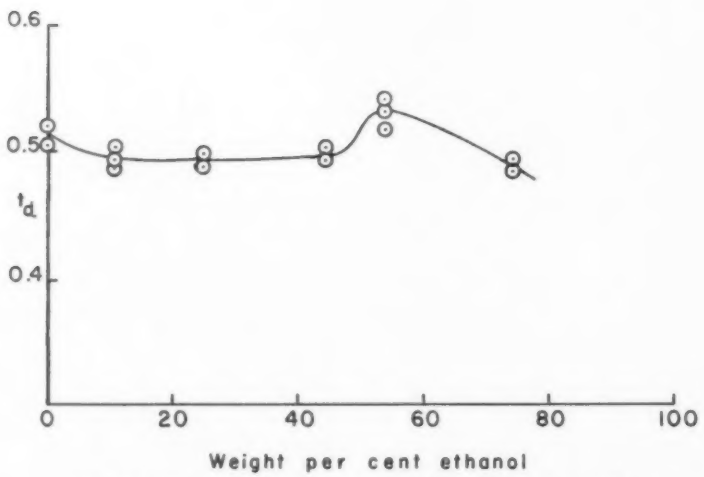

FIG. 3.—Anion transference number against weight per cent ethanol at ~0·15 moles KCl/1000 g of solution.

VOL. 19 1961

TABLE 1.—HITTORF TRANSFERENCE NUMBERS AND GRAMMES OF SOLVENT TRANSPORTED FROM THE ANODE TO THE CATHODE FOR KCl SOLUTE IN WATER

Temperature 25·00 ± 0·05°C

Conc. KCl moles 1000 g of solution	0·1004	0·1559	0·1559	0·1786	0·1786	0·3624	0·3624	0·4870	0·4870	0·4904	0·4904
α_m	13·4444	13·3360	13·3360	14·2552	14·2552	—	13·4696	13·5876	13·5876	—	—
α_a	13·4347	13·3365	13·3343	14·2655	14·2672	—	13·4869	13·5992	13·5986	—	—
W_{Ag_1}	0·67617	0·78562	0·78647	0·81953	0·78973	0·78898	0·81246	0·69147	0·69746	0·80142	0·82581
W_{Ag_2}	0·67605	0·78575	—	0·81934	0·78709	0·78890	0·81293	0·69074	0·69759	0·80212	0·82690
$F \times 10^3$	6·267	7·283	7·290	7·596	7·308	7·313	7·533	6·406	6·466	7·432	7·660
$P_s{}^m$	0·74580	1·16223	1·16223	1·33146	1·33146	2·70184	2·70184	3·63201	3·63021	3·65571	3·65571
$P_s{}^a$	0·65060	1·05041	1·05116	1·21442	1·22173	2·59471	2·59263	3·54284	3·54232	3·54545	3·53143
W	238·0632	230·4645	240·2230	236·7269	238·5044	238·0152	241·2957	238·9748	241·5006	214·6053	213·3990
t_c	0·489	0·480	0·497	0·496	0·487	0·481	0·482	0·454	0·457	0·443	0·460
t_a	0·511	0·520	0·503	0·504	0·513	0·519	0·518	0·546	0·543	0·557	0·540
d_m	1·00846	1·01120	1·01120	1·01226	1·01226	—	1·02095	1·02691	1·02691	—	—
d_a	1·00791	1·01047	1·01048	1·01197	1·01200	—	1·02030	1·02622	1·02625	—	—
ΔG^E_{sol}	−43·4	−12·1	−20·3	3·9	0·5	—	25·8	23·1	17·3	—	—

chloride solvation decreasing more rapidly than that of the potassium ion. Looking at Fig. 2 eliminates this argument since the solvation difference changes greatest at less than 0·200 moles KCl/1000 g of solution.

In Fig. 2 it can be seen that the ΔG^F_{sol} goes from −43·4 g of solvent to about +24 g of solvent as the concentration of KCl goes from 0·100 to 0·487 moles KCl/1000 g of solution. This indicates that in low salt concentrations where total solvation is large[5] that the chloride ion is more solvated than the potassium ion. As the salt concentration increases and the ions lose solvation sheath, the chloride ion loses more

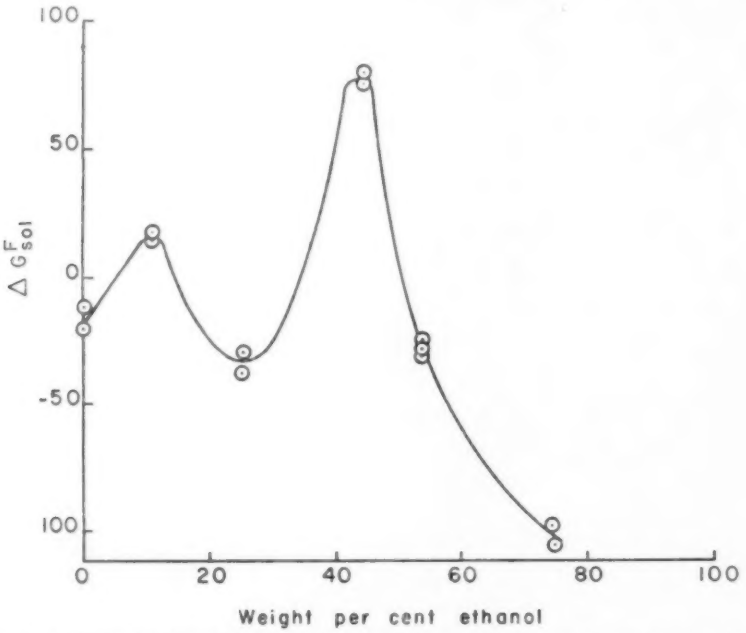

FIG. 4.—Calculated grammes of solvent transferred from anode to cathode per faraday of electricity at ~0·15 moles KCl/1000 g of solution plotted against weight per cent ethanol.

molecules of solvent than the potassium ion. This would be expected since positive metallic ions hold solvent more tightly.[6]

The data used for Figs. 3 and 4 are listed in Table 2. In Fig. 3 a plot of the transference number of the chloride ion, t_a, vs. weight per cent ethanol at 0·15 moles KCl 1000 g of solution is given. The t_a values decrease from water to 10·9 weight per cent ethanol, then reach a maximum value at 53·6 weight per cent ethanol, and again decrease to 74·3 weight per cent ethanol.

While t_a is to some extent dependent on the composition of the solvent, as seen from Fig. 3, the explanation of this slight dependence is rather difficult. The dependence arises perhaps from a combination of the relative solvation of cation and anion the lack of inertness of the reference substance[3,7] and the change in the viscosity of the solvent with change of solvent composition. (See Fig. 5.)

[5] H. ULICH, *Z. Phys. Chem.* **A168**, 141 (1934).
[6] S. GLASSTONE, *Textbook of Physical Chemistry* p. 921. Van Nostrand, New York (1948).
[7a] L. G. LONGSWORTH, *J. Amer. Chem. Soc.* **69**, 1288 (1947); [b] C. H. HALE and T. DEVRIES, *Ibid.* **70**, 2473 (1948); [c] F. Z. FISHER and T. E. KOVAL, *Bull. Sci. Univ. Kiev.* No. 4, 137 (1939).

TABLE 2.—HITTORF TRANSFERENCE NUMBERS AND GRAMMES OF SOLVENT TRANSPORTED FROM THE ANODE TO THE CATHODE FOR KCl SOLUTE

Ethanol (Wt. %)	10·9	10·9	10·9	10·9	10·9	24·8	24·8	24·8
Conc. KCl moles/ 1000 g of solution	0·1432	0·1432	0·1519	0·1522	0·1522	0·1340	0·1456	0·1529
α_m	13·306	—	13·462	—	13·359	—	13·587	15·429
α_a	13·324	—	13·475	—	13·368	—	13·573	15·453
W_{Ag_1}	0·81768	0·79426	0·78892	0·83047	0·82464	0·77946	0·84150	0·99969
W_{Ag_2}	0·81820	0·79381	0·78870	—	0·82501	0·77919	0·84239	0·99950
$F \times 10^3$	7·582	7·360	7·312	7·698	7·646	7·224	7·804	9·266
P_s^m	1·06756	1·06756	1·13241	1·13465	1·13465	0·99897	1·08545	1·1399
P_s^a	0·94977	0·95349	1·01388	1·01164	1·01463	0·88342	0·95871	0·9870
W	236·3360	233·0266	233·8774	231·7259	233·4803	227·3604	227·1055	228·6039
t_c	0·498	0·490	0·514	0·503	0·497	0·493	0·500	0·512
t_a	0·502	0·510	0·486	0·497	0·503	0·507	0·500	0·488
d_m	0·99091	—	0·99236	—	0·99082	—	0·97230	0·97071
d_a	0·99036	—	0·99168	—	0·99010	—	0·97136	0·97200
ΔG^F_{sol}	21·1	—	14·3	—	16·0	—	−38·6	−30·4

Ethanol (Wt. %)	44·1	44·1	53·6	53·6	53·6	74·3	74·3
Conc. KCl. moles/ 1000 g of solution	0·1522	0·1547	0·1589	0·1589	0·1538	0·1564	0·1564
α_m	6·849	6·901	7·015	7·015	7·2720	6·519	6·495
α_a	6·865	6·921	7·009	7·009	7·2788	6·496	6·475
W_{Ag_1}	0·82263	0·78453	0·79790	0·79850	0·80298	0·78984	0·79471
W_{Ag_2}	0·82278	0·78444	0·79786	0·79853	0·80282	0·78923	0·79515
$F \times 10^3$	7·626	7·272	7·396	7·402	7·443	7·319	7·369
P_s^m	1·1347	1·15329	1·18460	1·18460	1·14658	1·16596	1·16596
P_s^a	1·0072	1·02954	1·06607	1·06756	1·02283	1·03103	1·02879
W	218·9141	219·4767	214·0673	213·3876	214·0856	202·8367	204·1647
t_c	0·497	0·507	0·466	0·458	0·483	0·507	0·516
t_a	0·503	0·493	0·534	0·542	0·517	0·493	0·484
d_m	0·93171	0·93277	0·90942	0·90942	0·90926	0·86731	0·86731
d_a	0·93089	0·93192	0·90844	0·90861	0·90981	0·86637	0·86645
ΔG^F_{sol}	75·5	79·0	−28·1	−32·3	−26·6	−106·3	−98·5

Fig. 4 shows a maximum in ΔG^F_{sol} at 10·9 and 44·1 weight per cent ethanol. This curve is very similar to the one obtained for lithium chloride,[3] but this curve has only two maxima while the lithium chloride curve has three; however, the potassium chloride data only goes to 74·3 weight per cent ethanol. The third lithium chloride maximum was found at 94·0 weight per cent ethanol.

At the salt concentration used the chloride ion carried more solvent than the potassium ion in water. At 10·9 weight per cent ethanol the potassium ion was solvated with

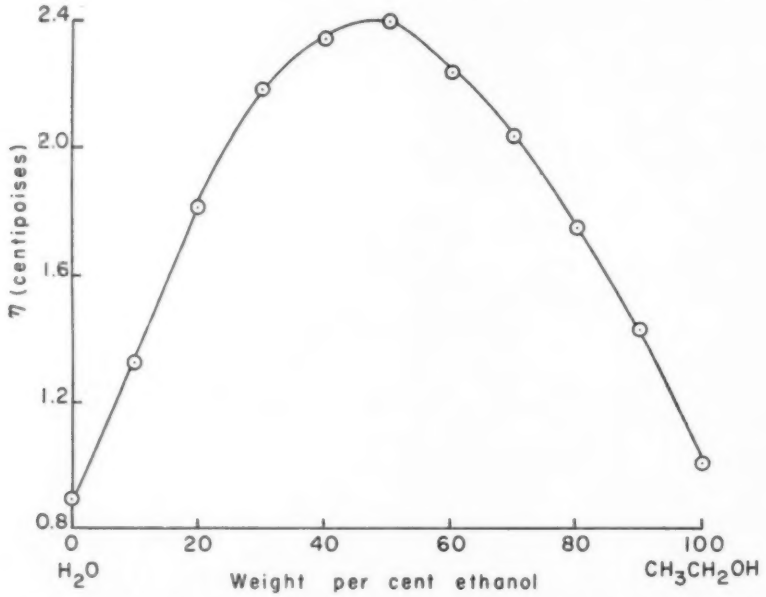

FIG. 5.—A plot of viscosity of water–ethanol mixtures against weight per cent ethanol. [Viscosity values from *Handbook of Chemistry* (Edited by N. A. LANGE) p. 1667. Handbook Publishers, Sandusky, Ohio (1956)]

a greater mass of solvent than the chloride ion. This increase in ΔG^F_{sol} can be explained by the outer layer of solvated water on the potassium ion being replaced by ethanol molecules.

A minimum value of ΔG^F_{sol} appears in the curve at 24·8 weight per cent ethanol. At this point the chloride ion is again solvated with a greater mass of solvent than the potassium ion. This can be explained as the outer layer of water molecules around the chloride ion being replaced by ethanol molecules.

A maximum occurs at 44·1 weight per cent ethanol where the potassium ion is again solvated with a greater mass of solvent than the chloride ion. This could be where all the solvation of the potassium ion is ethanol. After this point there is a decrease to negative ΔG^F_{sol} values.

At 58·6 and 74·3 weight per cent ethanol the chloride ion is solvated with a greater mass of solvent than the potassium ion. This can be explained as the rest of the water molecules in the solvation sheath of the chloride ion being replaced by ethanol. Since the values of ΔG^F_{sol} are so far negative, another contributing factor could be the potassium ions being partly solvated by the inert reference substance.

ACCURACY AND PRECISION

From comparing transference numbers at equal salt concentrations in Tables 1 and 2 the average deviation for t_a and t_c is 0·9 per cent which is well within the 2 per cent accuracy of the method. The average deviation of the grams of solvent transferred is about 20 per cent from comparison of Tables 1 and 2.

Acknowledgement—The authors wish to thank the Atomic Energy Commission for Contract AT-(40-1)-2069 which supported this research financially.

VOL.
19
1961

J. Inorg. Nucl. Chem., 1961, Vol. 19, pp. 286 to 297. Pergamon Press Ltd. Printed in Northern Ireland

A STUDY OF THORIUM–IODATE COMPLEXING IN AQUEOUS SOLUTIONS*

R. W. STOUGHTON, A. J. FRY† and J. E. BARNEY, II‡
Chemistry Division, Oak Ridge National Laboratory, Tennessee

(*Received* 16 *August* 1960)

Abstract—Thorium–iodate complexing at 25°, ionic strength of 0·5 and pH ca. 2·6 was studied by means of solubility measurements. While the solid phase showed no evidence of crystal structure and under some conditions varied somewhat in composition with solution composition, the observed solubilities were reproducible. The data have been interpreted in terms of the species $Th(IO_3)_5^{4-}$, $Th(IO_3)_6^{2-}$, $Th(IO_3)_3^{+}$, $Th(IO_3)_2^{2+}$, $ThIO_3^{3+}$, $ThOH(IO_3)_2^{+}$ and $ThOHIO_3^{2+}$, and the corresponding stability quotients derived. There was no evidence for the existence of the intermediate species $Th(IO_3)_7^{3-}$, $Th(IO_3)_5^{-}$ and $Th(IO_3)_4$.

THE formation quotients for the positive thorium–iodate complexes $ThIO_3^{3+}$, $Th(IO_3)_2^{2+}$ and $Th(IO_3)_3^{+}$ have been determined by DAY and STOUGHTON[1] using a solvent extraction method involving a benzene–thenoyltrifluoroacetone (TTA) phase. They found no evidence for complexes of more than three iodate ligands per Th(IV) in IO_3^- concentrations up to 0·01 M.

In precipitating thorium or zirconium with iodate ion in dilute acid solutions[2] it was found that the solubility of the thorium or zirconium salt did not continue to decrease monotonically with increasing iodate ion concentration. Rather when the latter exceeded some few hundredths molar further increases caused an increase in the solubility. This behavior indicated the formation of negative complex ions.

The current work was undertaken to determine the solubility of thorium iodate and to elucidate complex formation over wide Th(IV) and iodate ion concentration ranges. Constant ionic strength of 0·5 and essentially constant pH of 2·6 were used. The value 2·6 was selected to minimize simultaneously effects of association of IO_3^- with hydrogen ion and of Th^{4+} hydrolysis. The dissociation constant of HIO_3 is reported to be about 0·16 at 25°C.[3] The initial hydrolysis of Th(IV) according to KRAUS and HOLMBERG[4] can be represented by the three equilibria

$$Th^{4+} + H_2O = ThOH^{3+} + H^+$$

$$Th^{4+} + 2H_2O = Th(OH)_2^{2+} + 2H^+$$

$$2Th^{4+} + 2H_2O = Th_2(OH)_2^{6+} + 2H^+$$

The highest Th^{4+} concentration in this study was about 10^{-2} M. At this concentration and the pH existing in solution the total Th(IV) in the form of the above hydrolysis

* This paper is based upon work performed for the United States Atomic Energy Commission at the Oak Ridge National Laboratory operated by Union Carbide Corporation.

† Present address; Chemistry Department, University of Arkansas, Fayetteville, Arkansas.

‡ Present address: Spencer Chemical Company, Research Center, 9009 W. 67th St., Merriam, Kansas.

[1] R. A. DAY, JR., and R. W. STOUGHTON, *J. Amer. Chem. Soc.* **72**, 5662 (1950).

[2] R. W. STOUGHTON. Unpublished work (1946).

[3] E. ABEL, O. REDLICH and P. HERSCH, *Z. Phys. Chem.* A **170**, 112–22 (1934); S. NAIDLICH and J. E. RICCI, *J. Amer. Chem. Soc.* **61**, 3268–73 (1939); N. C. C. LI and YING-TU LO, *J. Amer. Chem. Soc.* **63**, 397–9 (1941).

[4] K. A. KRAUS and R. W. HOLMBERG, *J. Phys. Chem.* **58**, 325 (1954).

products should be about 2 per cent, on the assumption that the quotients for the above reactions found by KRAUS and HOLMBERG in perchlorate media at ionic strength 1·0 are valid for the nitrate–iodate media used here. If 0·16 is used for the dissociation quotient of HIO_3, the ratio HIO_3/IO_3^- is also about 2 per cent at pH 2·6.

EXPERIMENTAL

Method of measurement. Stock $Th(NO_3)_4$, $LiIO_3$, and $LiNO_3$ solutions at ionic strength 0·5 were adjusted to pH 2·6 by addition of NaOH or HNO_3 solution. In the region of high iodate concentration stock thorium nitrate was added slowly to a mixture of the $LiIO_3$ and $LiNO_3$ solutions until a permanent precipitate was obtained. In the region of high Th(IV), stock $LiIO_3$ was added slowly to a mixture of the $Th(NO_3)_4$ and $LiNO_3$ solutions until a permanent precipitate formed.

The reaction vessels were placed in a constant-temperature bath at 25·0 ± 0·1°C, and the Th(IV) and total iodate concentrations were followed as a function of time. Some were not stirred until analysed; others were stirred once or twice a day until analysed. At various intervals, the solids were analysed for Th(IV) and iodate and in some cases for other substances. Many of the solids were examined by X-ray analyses and with a microscope to determine if they were amorphous or crystalline.

VOL. 19 1961

Methods of analysis. Thorium in solution was usually determined radiometrically, UX_1 (Th-234) being added as tracer; actually only the UX_2 (1·14 min Pa-234) beta is counted when a 25 mg/cm² aluminium absorber is inserted between the sample and counter. In some cases thorium analyses were conducted gravimetrically using oxalate precipitation and ignition to ThO_2. Iodate was determined by reduction to I_3^- with KI in HCl solution and titration with thiosulphate. The pH was measured with a glass electrode using either a Beckman Industrial Model M or a Beckman Model H-2 pH meter.

The solids were washed with small volumes of dilute HNO_3 at the pH of the solution and filtered through a small Hirsch funnel under vacuum. Thorium analyses were conducted gravimetrically and iodate analyses volumetrically as described above. Nitrate analyses were conducted by a modified Kjeldahl method. In cases where the iodate/Th(IV) ratios were greater than four, the solids were also analysed for lithium and other alkalis.

Materials. C.P. $Th(NO_3)_4$, $LiNO_3$, NaOH and HNO_3 were used without further purification since analyses for fluoride, phosphate and sulphate showed them to be below the limits of detection by the methods used (i.e., less than 10, 5 and 100 p.p.m., respectively). The $Th(NO_3)_4$ was analysed for thorium, water and nitrate; the NO_3/Th(IV) ratio was found to be 4·06 ± 0·05 and the H_2O/Th(IV) ratio was 4·34 ± 0·10. The weight remaining after straight ignition to ThO_2 agreed very well with that expected from the gravimetric analysis. The $LiIO_3$ was made by heating solutions of weighed stoichiometric quantities of C.P. Li_2CO_3 and HIO_3 to boiling, cooling, filtering and adjusting to pH 2·6.

RESULTS

The solubility data obtained in two typical runs after optimum conditions had been worked out in advance are presented in Fig. 1. The data represent solubilities under as wide a set of concentrations of Th(IV) and iodate as possible at ionic strength 0·5, i.e. from nearly 0·5 M $LiIO_3$ to nearly 0·05 M $Th(NO_3)_4$. The solubility decreased from $1{\cdot}5 \times 10^{-3}$ M at 0·5 M $LiIO_3$ to $1{\cdot}7 \times 10^{-6}$ M at the minimum with respect to Th(IV) in 0·05 M IO_3^-. With further lowering of iodate concentration the solubility increased, then went through another minimum (with respect to iodate) of 7×10^{-4} M, after which it increased to 0·0042 M in 0·05 M $Th(NO_3)_4$. For purposes of discussing the results the curve in Fig. 1 has been divided into three regions: *A*, *B* and *C*.

1. *Region A—high iodate concentration*

1.1 *Solid phase.* Within the first few weeks the solids forming in this region appeared to be dense with no evidence of crystallinity (either by microscopic observation or X-ray analysis) and they usually showed an IO_3/Th(IV) ratio of 4·0 ± 0·1. In a few instances during this period amorphous solids were found which had

IO_3/Th(IV) ratios as high as 4·5 ± 0·1; in these cases the solubilities were found to be lower than the usual values.

On long standing (i.e. many weeks) some precipitates converted to a bulky gelatinous form and some to a needle crystalline form; some converted first to the gelatinous and then to the crystalline form. Other investigators[5] have found other thorium salts to precipitate in a dense form which slowly converted to a gel without change in pH; namely the arsenate, phosphate and molybdate.

The needle crystals showed an IO_3/Th(IV) ratio of 4·5 ± 0·1. Both the crystalline

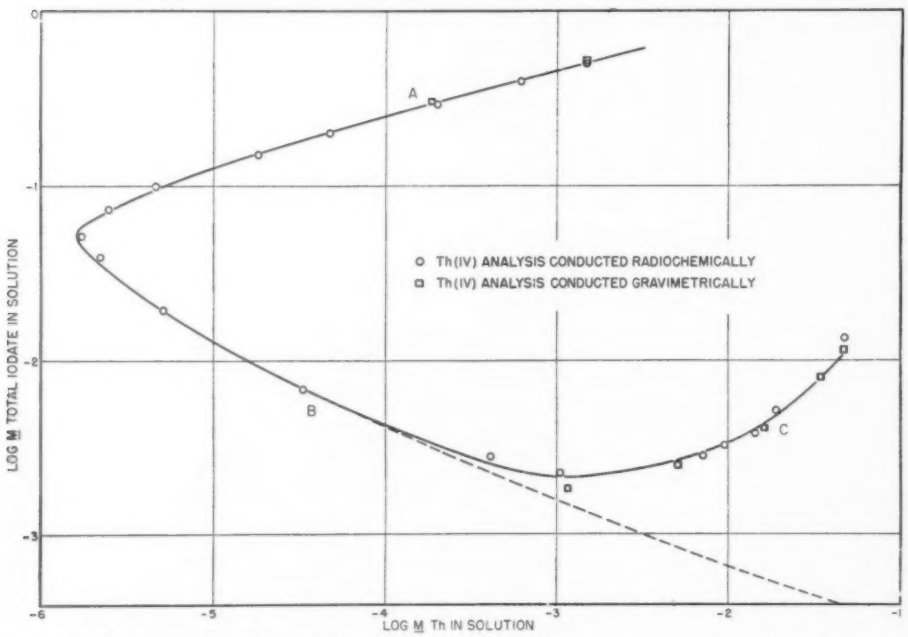

FIG. 1.—Solubility of thorium iodate at ionic strength 0·5 and pH 2·6 (except in region *C*). Calculated curve with experimental points. Dotted line gives concentration of IO_3^- where different from total iodate.

and amorphous precipitates showing ratios of 4·5 were found to have a Li/Th(IV) ratio of less than 0·1 and only a trace of sodium. It was consequently concluded that when the IO_3/Th(IV) ratio was greater than four, the other cation was hydrogen.

1.2 *Solution.* In this region the short time solubilities measured (i.e. about a day to a few weeks) were consistent and reproducible, showing a marked decrease with decreasing iodate concentration. After a few weeks, and usually when the solid changed visibly, erratic and considerably lower thorium concentrations were often observed. In the presence of the gelatinous precipitate the observed solubility values were often an order of magnitude lower than in the presence of the dense amorphous form. When the needle crystals formed the Th(IV) concentration was often an order of magnitude or so lower still. It was not found possible, within three or four months

[5] M. U. PARWAR, S. M. MEHTA and M. PRASAD, *Proc. Indian Acad. Sci.* **3** A, 107–18 (1936); *Chem. Abstr.* **30**, 47427; also M. PRASAD and D. M. DESAI, *J. Univ. Bombay* **7**, Pt. 3, 132–56 (1948); *Chem. Abstr.* **33**, 44932.

at least, to get constant solubilities in the presence of either the gelatinous or crystalline precipitate. Seeding a newly formed amorphous precipitate with the crystals caused rapid and erratic lowering of the Th(IV) concentration below the usual short time value.

2. *Region B—between minimum solubilities with respect to* Th(IV) *and with respect to iodate*

2.1 *Solid phase.* In this region the long time stability of the solid varied with solution composition. The visual appearance of the precipitate during the first few

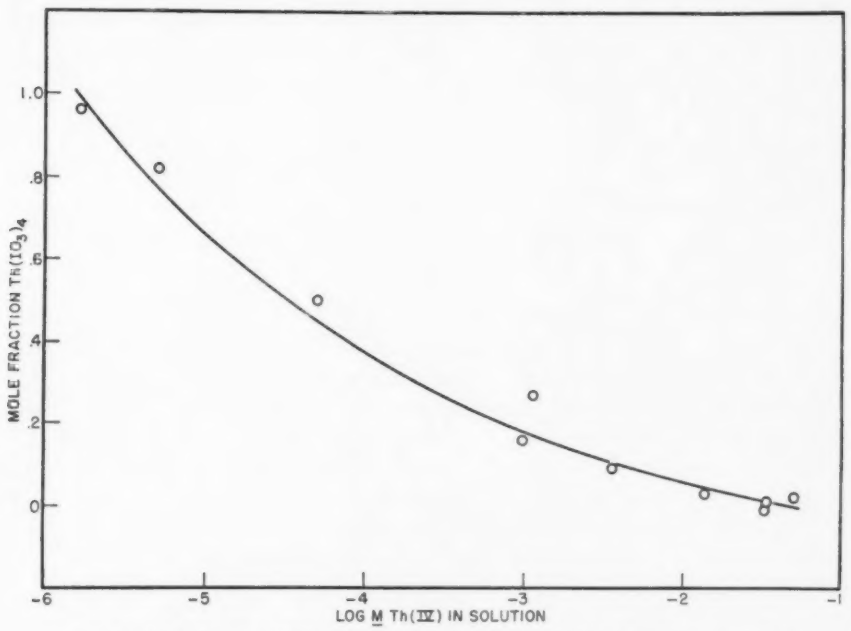

FIG. 2.—Mole fraction of $Th(IO_3)_4$ in solid $Th(IO_3)_4$–$ThOH(IO_3)_3$ equilibrium mixture.

weeks was the same as that in region *A*; also as in region *A* some of the solids formed under conditions near the point of minimum solubility with respect to Th(IV) (see Fig. 1) on long standing converted to either a bulky gelatinous or crystalline form. Seeding recently formed precipitates with the needle crystals caused a more rapid conversion to the latter. Under conditions nearer to and at those obtaining for minimum solubility with respect to iodate, the solids did not change with time from the dense amorphous form even if they were seeded with the crystals.

The composition of the solid changed continuously from an IO_3/Th(IV) ratio of $4{\cdot}0 \pm 0{\cdot}1$ to about $3{\cdot}2 \pm 0{\cdot}1$ at the point of minimum solubility with respect to iodate (see Fig. 2). These analyses were time independent except when the appearance of the solids changed. Analyses of the solids showed that under no conditions was the NO_3/Th(IV) ratio greater than $0{\cdot}1 \pm 0{\cdot}1$. It was consequently assumed that when the IO_3/Th(IV) ratio was less than 4·0, the other anion was hydroxide.

2.2 *Solution.* As in region *A* the short term solubilities were consistent and

reproducible throughout this region. At the high iodate end of region *B* long term erratic decreases in Th(IV) concentration were observed, and these could be related to changes in the solid phase. At the low iodate end of this region the solubilities were time independent for at least a few months. Seeding with the needle crystals did not affect the solution concentrations. At the right hand end of region *B* and in region *C*, the solubility may be calculated by dividing the iodate concentration by the IO_3/Th(IV) ratio in the solid.

3. *Region C—between minimum solubility with respect to iodate and* 0·05 *M* $Th(NO_3)_4$

3.1 *Solid phase.* As in the low iodate concentration end of region *B*, the solid phase in region *C* was dense amorphous and time independent in appearance and composition. The IO_3/Th(IV) ratio continued to decrease from about 3·2 to 3·0 in the presence of nearly 0·05 M $Th(NO_3)_4$.

3.2 *Solution.* As the IO_3/Th(IV) ratio varied from 3·2 to 3·0, the pH in solution decreased continuously from 2·6 to about 2·2 (see Fig. 4). There was no indication of a time change within several months; i.e. the solubilities were constant to within the estimated experimental error (±15 per cent).

4. *Reliability of results*

While the dense precipitate which was present within the first few weeks after mixing the solutions was amorphous and while it varied somewhat in composition (in regions *B* and *C*) depending on solution conditions, consistent and reproducible solubilities could be obtained. Table 1 shows solubility data from 2 to 75 days after initial precipitation for four different initial solution concentrations: (1) (2) (3) and (4). The results of two separate runs are shown for conditions (1) and (4). Under conditions (1) and (2), consistent results were obtained within the first two or three weeks, after which erratic and low solubilities were frequently found, e.g., (1b) shows a relatively small decrease while (1a) and (2) show large decreases after 15 days. Under conditions (3) and (4) no time variations were observed within the estimated experimental error.

In order further to confirm the consistency of the results of this study, precipitations were carried out at 5° and 95° where the solubilities were appreciably different from the 25° values. For example, the short time solubilities at 95° were lower in region *A* and higher in region *B* by as much as a factor of three, while at 5° they were higher in region *A* and lower in region *B* by nearly a factor of two. Less variation was found in region *C*. When the vessels were kept at 25° the solubilities slowly attained the usual 25° values (within the experimental error of about ±15 per cent) over a period of a couple weeks.

5. *Thorium–iodate titrations*

Since the pH decreased systematically from 2·6 to 2·2 in region *C* an attempt was made to correlate these changes with acid liberated on mixing $Th(NO_3)_4$ and $LiIO_3$ solutions. Solutions at ionic strength 0·5 and containing 0·01, 0·02 and 0·05 M $Th(NO_3)_4$ were titrated with 1 M $LiIO_3$, and pH readings were made after each incremental addition. To convert the pH readings to H^+ concentrations at ionic strength 0·5, conversion factors were established through potential measurements of $Th(NO_3)_4$–$LiNO_3$ solutions containing known quantities of additional HNO_3.

VOL. 19 1961

TABLE I.—TYPICAL THORIUM AND IODATE MOLARITIES AS A FUNCTION OF TIME AFTER INITIAL PRECIPITATION

Run*	Days After Initial Precipitation											
	2		7		15		37		42		51		75	
	$-\log M_{IO_3^-}$	$-\log M_{Th(IV)}$	$-\log M_{IO_3^-}$	$-\log M_{Th(IV)}$	$-\log M_{IO_3^-}$	$-\log M_{Th(IV)}$	$-\log M_{IO_3^-}$	$-\log M_{Th(IV)}$	$-\log M_{IO_3^-}$	$-\log M_{Th(IV)}$	$-\log M_{IO_3^-}$	$-\log M_{Th(IV)}$	$-\log M_{IO_3^-}$	$-\log M_{Th(IV)}$
1a					1·31	5·77			1·31	6·68	1·31	6·80		
1b	1·29	5·77					1·28	5·88					1·26	5·84
2	2·16	4·48	2·15	4·44	2·15	4·45	2·15	5·20					2·14	5·48
3	2·53	2·09	2·55	2·07	2·54	2·07	2·54	2·14					2·57	2·10
4a			1·92	1·32	1·92	1·31			2·00	1·35	2·00	1·33	1·99	1·33
4b	1·85	1·32	1·87	1·31	1·87	1·30	1·87	1·29					1·88	1·30

* Initial conditions:
(1) 0·05 M $LiIO_3$, 0·45 M $LiNO_3$ plus sufficient $Th(NO_3)_4$ to form a ppt.
(2) 0·0075 M $LiIO_3$, 0·4925 M $LiNO_3$ plus sufficient $Th(NO_3)_4$ to form a ppt.
(3) 0·01 M $Th(NO_3)_4$, 0·4 M $LiNO_3$ plus sufficient $LiIO_3$ to form a ppt.
(4) 0·05 M $Th(NO_3)_4$ plus sufficient $LiIO_3$ to form a ppt.

After correcting for expected changes in hydrolytic species[4] and estimating by trial and error the conversion factor at the highest pH value in each case, the results shown in Table 2 were obtained. (The estimated uncertainty here is larger by a factor of three or more than the standard error calculated from the treatment of the data).

TABLE 2.—pH TO (H^+) CONVERSION FACTORS FOR $Th(NO_3)_4$–$LiNO_3$ MEDIA

Medium	[Antilog (−pH)]/(H^+)
0·05 M $Th(NO_3)_4$	0·68 ± 0·1
0·02 M $Th(NO_3)_4$–0·3 M $LiNO_3$	0·82 ± 0·1
0·01 M $Th(NO_3)_4$–0·4 M $LiNO_3$	0·87 ± 0·1
0·5 M $LiNO_3$	1·06 ± 0·1

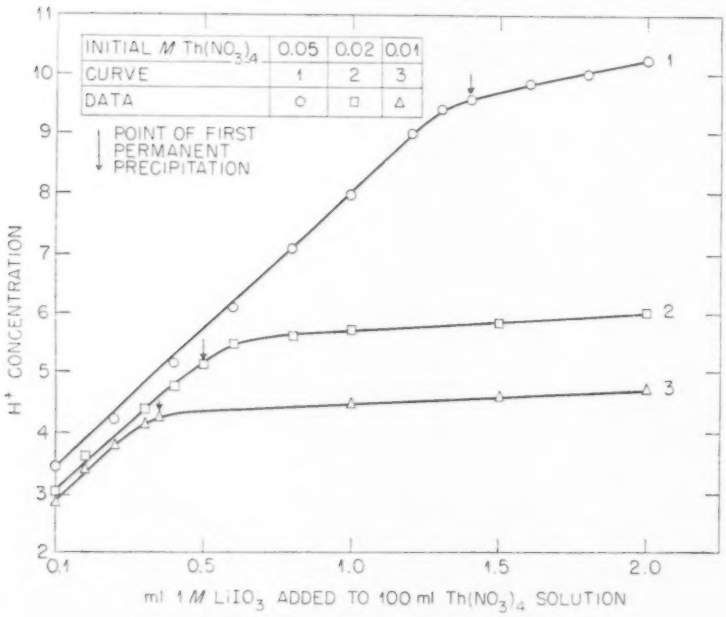

FIG. 3.—H^+ liberated on titrating $Th(NO_3)_4$ solutions with $LiIO_3$.

By the use of these results along with the further assumption that the conversion factors were independent of the presence of a small amount of iodate, the H^+ concentrations in the above Th(IV)–iodate titrations were calculated from the pH values; see Fig. 3. In a similar manner the variation in H^+ concentration in region *C* was determined, as seen in Fig. 4.

INTERPRETATION OF DATA

1. *Region A*

The large increase in solubility with increase in iodate ion concentration (see Fig. 1) implies the existence of negative Th(IV)–IO_3^- complexes in solution; and the negative of the slope should give the average charge[6] of the complex species, or

[6] K. A. KRAUS. Private communication (1960).

the difference between the IO_3/Th(IV) ratio in the average complex species and that obtaining in the solid. At the highest iodate ion concentrations the slope is four; hence since the solid is $Th(IO_3)_4$, the principal species must be $Th(IO_3)_8^{4-}$.

The following two equilibria explain the data in this region:

$$ThX_4 + 4X^- = ThX_8^{4-} \qquad K_{48} \tag{1}$$

$$ThX_4 + 2X^- = ThX_6^{2-} \qquad K_{46} \tag{2}$$

where X^- represents iodate ion and the K's are the concentration quotients, i.e.,

$$K_{4i} = (ThX_i^{(4-i)+})/(X^-)^{i-4}$$

VOL. 19 1961

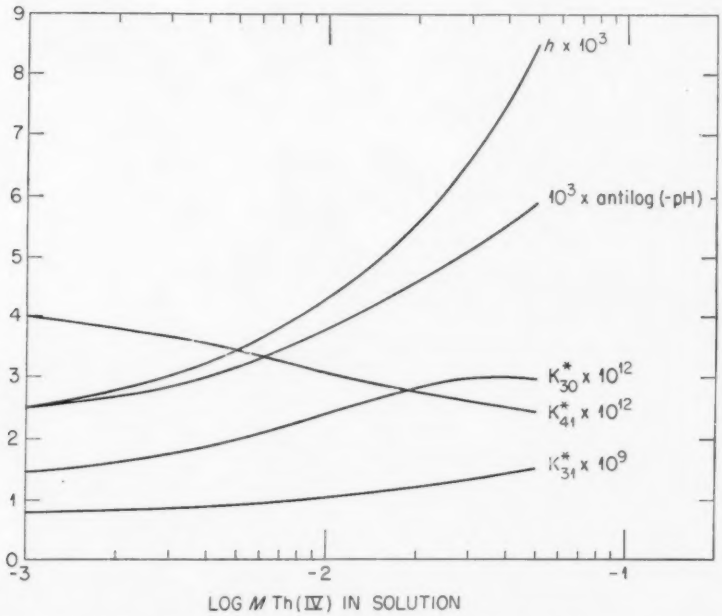

FIG. 4.—Variation of H^+ concentration, K^*_{30}, K^*_{31} and K^*_{41} in region *C*.

The values of K_{48} and K_{46} were evaluated by a graphical method. Straight lines of slopes four and two, respectively, were drawn on a plot like that shown in Fig. 1, and then the lines were moved vertically until a best-fit was obtained. At any iodate ion concentration the values given by the lines represent the logs of the ThX_8^{4-} and ThX_6^{2-} concentrations, or the sum of the antilogs should give the total Th(IV) concentration on the assumptions made. When optimum fit is made the intercepts at $(X^-) = 1$ give the values of the quotients K_{48} and K_{46}. These are shown in Table 3.

There was no advantage in the fitting to assume the existence of any of the species ThX_7^{3-}, ThX_5^- or ThX_4 in solution. Further, if any of these species was assumed to be the predominate one under any conditions, the agreement was poorer regardless of the values of the K's corresponding to the other species.

2. *Regions B and C*

The complexes ThX_3^+, ThX_2^{2+}, ThX^{3+} and $ThNO_3^{3+}$ have been shown to exist[1] at nitrate and iodate concentrations obtaining in these regions. The data in Fig. 3 indicate that complexes of thorium containing both hydroxide and iodate should be present here; these were assumed to be $ThOHX^{2+}$ and $ThOHX_2^+$. The solid in these regions was assumed to be an ideal solution of ThX_4–$ThOHX_3$ where the mole fraction S_4 of ThX_4 is given by the analytical IO_3/Th(IV) ratio less three. See Fig. 2. With these assumptions, relations can be given for the molarity of total thorium in solution M Th(IV) and total iodate M IO_3^- in terms of the equilibrium quotients for the following equilibria.

$$ThX_4 = ThX_n^{+(4-n)} + (4-n)X^- \qquad K_{4n} \qquad (3)$$

$$ThX_4 + H_2O = ThOHX_n^{+(3-n)} + (4-n)X^- + H^+ \qquad K_{4nh} \qquad (4)$$

$$ThOHX_3 + H^+ = ThX_n^{+(4-n)} + (3-n)X^- + H_2O \qquad K'_{3n} \qquad (5)$$

$$ThOHX_3 = ThOHX_n^{+(3-n)} + (3-n)X^- \qquad K'_{3nh} \qquad (6)$$

$$Th^{4+} + NO_3^- = ThNO_3^{3+} \qquad k_N = 4{\cdot}7^{[1]} \qquad (7)$$

The equations for thorium and iodate then become

$$\text{M Th(IV)} = K_{48}X^4 + K_{46}X^2 + S_4\sum_{n=0}^{3} K^*_{4n}/X^{4-n} + (1-S_4)\sum_{n=0}^{3} K^*_{3n}/X^{3-n} \qquad (8)$$

$$\text{M } IO_3^- = 8K_{48}X^4 + 6K_{46}X^2 + X + S_4\sum_{n=1}^{3} nK^*_{4n}/X^{4-n} + (1-S_4)\sum_{n=1}^{3} nK^*_{3n}/X^{3-n} \qquad (9)$$

where

$$K^*_{4n} = K_{4n} + K_{4nh}/h, \quad n = 1, 2, 3$$

$$K^*_{3n} = hK'_{3n} + K'_{3nh}, \quad n = 1, 2, 3$$

$$K^*_{40} = K_{40}(1 + k_N(NO_3^-)),$$

$$K^*_{30} = hK'_{30}(1 + k_N(NO_3^-)),$$

$$h = H^+ \text{ concentration},$$

and where K_{43h} and K'_{33h} are equal to zero according to the assumptions made. Also while equations (8) and (9) were written to hold in all regions, the terms in K_{48} and

TABLE 3.—SOLUBILITY QUOTIENTS AT IONIC STRENGTH 0·5

Symbol	Value	Symbol	Value
K_{48}	$2{\cdot}2 \times 10^{-2}$	K_{41h}	$5{\cdot}5 \times 10^{-15}$
K_{46}	$2{\cdot}5 \times 10^{-4}$	K'_{32h}	$3{\cdot}6 \times 10^{-8}$
K_{43}	$3{\cdot}5 \times 10^{-8}$	K'_{31h}	$4{\cdot}4 \times 10^{-10}$
K_{42}	$1{\cdot}6 \times 10^{-10}$	K'_{33}	$2{\cdot}4 \times 10^{-3}$
K_{41}	$1{\cdot}8 \times 10^{-12}$	K'_{32}	$1{\cdot}0 \times 10^{-5}$
K_{40}	$2{\cdot}4 \times 10^{-15}$	K'_{31}	$1{\cdot}2 \times 10^{-7}$
K_{42h}	$6{\cdot}0 \times 10^{-13}$	K'_{30}	$1{\cdot}6 \times 10^{-10}$

K_{46} are completely negligible in regions *B* and *C* except for the extreme left hand end of region *B* (Fig. 1), where they are small at most.

As seen above, the values of the K^*'s should be approximately constant in region *B* since the solution is to a good approximation a 0·5 M $LiNO_3$ solution at constant *h*. Further, as in region *A*, the M $LiIO_3$ is nearly equal to X^- throughout much of region *B*. In region *C* on the other hand *h*, the NO_3^- concentration and the medium are all varying and hence corrections had to be made in evaluating the solubility quotients. In addition (X^-) had to be evaluated by trial and error. The dotted curve in Fig. 1 shows the computed (X^-) where it is different from the molarity of the total iodate.

In evaluating the various *K*'s use was made of Fig. 3. It was assumed that up to the point of inception of precipitation the iodate added (less a small correction for uncomplexed X^-) formed ThX^{3+} and $ThOHX^{2+}$, while the H^+ liberated was equal to the $ThOHX^{2+}$ formed. By the use of this assumption and the value of the stability quotient

$$Th^{4+} + 2X^- = ThX_2^{2+} \qquad k_{02} = \frac{K_{42}}{K_{40}} = \frac{K'_{32}}{K'_{30}} = 6{\cdot}2 \times 10^4$$

from previous work[1], all the solubility quotients were evaluated from the solubility data. Actually in the process slight adjustments were made in obtaining the best fit to the data after which the two ratios did not give identical values for k_{02}. The final values are given in Table 3.

The calculated variations in K^*_{30}, K^*_{31} and K^*_{41} in region *C* are shown in Fig. 4. These are the only K^*'s whose variations are of any importance in fitting equations (8) and (9). K^*_{40} is of some importance in the left hand part of region *C*; however it varies only with NO_3^- (not with *h*) which varies significantly only at the extreme high Th(IV) end of the region, and here the value of S_4 is essentially zero.

3. *Stability quotients for species in solution*

Stability quotients for the various species assumed to exist in solution were evaluated by taking ratios of the appropriate solubility quotients. The former are presented in Table 4. In some cases two different ratios could be used to evaluate the stability quotients.

4. *Self-consistency and comparison with other methods*

4.1 *Stability quotients* The stability quotients for the equilibria

$$Th^{4+} + X^- = ThX^{3+} \qquad k_{01} \tag{10}$$

$$Th^{4+} + 3X^- = ThX_3^+ \qquad k_{03} \tag{11}$$

were each calculated from two ratios of solubility quotients

$$k_{01} = K_{41}/K_{40} = K'_{31}/K'_{30}$$

$$k_{03} = K_{43}/K_{40} = K'_{33}/K'_{30}$$

as seen in Table 4. The two values for each quotient were close together in each case and close to the values obtained by DAY and STOUGHTON[1] by a solvent extraction method. This agreement lends support to the interpretation given here, although the closeness of the values obtained by the two methods was fortuitous in view of the relative inaccuracy of the solubility method and the difference in media.

VOL. 19 1961

TABLE 4.—STABILITY QUOTIENTS FOR THE VARIOUS IONIC SPECIES AT IONIC STRENGTH 0·5

Equations		Equilibrium quotients			Quotients from Solvent Extraction[1]
		From ratios	Values	Av. values	
$Th^{4+} + IO_3^- = ThIO_3^{3+}$	k_{01}	K_{41}/K_{40} K'_{31}/K'_{30}	$7{\cdot}5 \times 10^2$ $7{\cdot}8 \times 10^2$	$7{\cdot}6 \times 10^2$	$7{\cdot}6 \times 10^2$
$Th^{4+} + 2IO_3^- = Th(IO_3)_2^{2+}$	k_{02}	K_{42}/K_{40} K'_{32}/K'_{30}	$6{\cdot}7 \times 10^4$ $6{\cdot}2 \times 10^4$	$(6{\cdot}2 \times 10^4)$*	$6{\cdot}2 \times 10^4$
$Th^{4+} + 3IO_3^- = Th(IO_3)_3^+$	k_{03}	K_{43}/K_{40} K'_{33}/K'_{30}	$1{\cdot}45 \times 10^7$ $1{\cdot}50 \times 10^7$	$1{\cdot}5 \times 10^7$	$1{\cdot}4 \times 10^7$
$Th^{4+} + H_2O + IO_3^-$ $= ThOHIO_3^{2+} + H^+$	k_{01h}	K_{41h}/K_{40} K'_{31h}/K'_{30}	2·3 2·7	2·5	
$Th^{4+} + H_2O + 2IO_3^-$ $= ThOH(IO_3)_2^+ + H^+$	k_{02h}	K_{42h}/K_{40} K'_{32h}/K'_{30}	$2{\cdot}5 \times 10^2$ $2{\cdot}3 \times 10^2$	$2{\cdot}4 \times 10^2$	
$Th^{4+} + 6IO_3^- = Th(IO_3)_6^{2-}$	k_{06}	K_{46}/K_{40}	$1{\cdot}04 \times 10^{11}$	$1{\cdot}04 \times 10^{11}$	
$Th^{4+} + 8IO_3^- = Th(IO_3)_8^{4-}$	k_{08}	K_{48}/K_{40}	$9{\cdot}2 \times 10^{12}$	$9{\cdot}2 \times 10^{12}$	

* Value taken from solvent extraction results of DAY and STOUGHTON[1].

4.2 *Equilbrium between the two solids* ThX_4 *and* $ThOHX_3$. The equilibrium quotient K_s for the equilibrium

$$ThX_4 + H_2O = ThOHX_3 + H^+ + X^- \qquad K_s \qquad (12)$$

may be evaluated by taking ratios of the various solubility quotients and these should all give about the same value at ionic strength 0·5. See Table 5A. Also K_s may be evaluated at any point in region *B* from the analyses of the solid and the calculated (X^-), since

$$ThX_4/ThOHX_3 = S_4/(1 - S_4).$$

Such values are shown in Table 5B. The overall consistency is as good as could be expected.

TABLE 5A.—COMPARISON OF THE K_s VALUES DETERMINED FROM DIFFERENT PAIRS OF SOLUBILITY QUOTIENTS

Ratio	$K_s \times 10^5$
K_{43}/K'_{33}	1·46
K_{42}/K'_{32}	1·60
K_{41}/K'_{31}	1·44
K_{40}/K'_{30}	1·50
K_{42h}/K_{32h}	1·67
K_{41h}/K_{31h}	1·25
	Average 1·48

TABLE 5B.—VALUES OF K_8 FROM SOLUBILITY AND MOLE FRACTION CURVES AT $h = 2{\cdot}5 \times 10^{-3}$

Molarity Th(IV)	$(1 - S_4)/S_4$	$(X^-) = (IO_3^-)$ Molarity	$K_8 \times 10^5$
3×10^{-6}	0·15	$2{\cdot}8 \times 10^{-2}$	1·05
1×10^{-5}	0·52	$1{\cdot}3 \times 10^{-2}$	1·69
3×10^{-5}	0·92	$7{\cdot}4 \times 10^{-3}$	1·70
1×10^{-4}	1·63	$4{\cdot}2 \times 10^{-3}$	1·71
3×10^{-4}	2·57	$2{\cdot}6 \times 10^{-3}$	1·67
1×10^{-3}	4·56	$1{\cdot}6 \times 10^{-3}$	1·82
		Average	1·61

Acknowledgements—We wish to express our appreciation to Dr. M. A. BREDIG of the ORNL Chemistry Division for investigations concerning crystallinity of solids by X-ray analyses; to P. F. THOMASON and co-workers of the ORNL Analytical Chemistry Division for conducting some of the chemical analyses; to Raymond Jensen, a part-time employee of the ORNL Chemistry Division, for conducting pH measurements on $Th(NO_3)_4$–$LiNO_3$ mixtures; and to Dr. K. A. KRAUS for numerous interesting discussions concerning this work.

VOL. 19 1961

J. Inorg. Nucl. Chem., 1961, Vol. 19, pp. 298 to 303. Pergamon Press Ltd. Printed in Northern Ireland

EXCHANGE PROPERTIES OF AMMONIUM SALTS OF 12-HETEROPOLYACIDS—II

SEPARATION OF RUBIDIUM AND CAESIUM ON AMMONIUM PHOSPHOTUNGSTATE

J. KRTIL
Institute of Nuclear Research, Czechoslovak Academy of Sciences, Řež u Prahy

(*Received* 4 *November* 1960)

Abstract—The separation of rubidium and caesium on a column of freshly-precipitated ammonium phosphotungstate and asbestos carrier has been investigated; rubidium may be eluted with 1 N ammonium nitrate and caesium with 6 N ammonium nitrate. The exchange capacity of NH_4PW* for caesium and rubidium corresponds to two thirds of the theoretical ammonium content, and the exchange of ammonium for caesium and rubidium is quantitatively expressed by the mass action law at micro-levels.

THE use of heteropolyacids which are stable in strong acid and oxidizing media and which precipitate the heavy alkali metals selectively offers the possibility of isolating rubidium and caesium from fission product solutions arising from the processing of nuclear fuels. Some processes[1] and analytical methods[2] are known which use silicotungstic and phosphotungstic acids for Cs and Rb isolation.

The exchange properties of the ammonium salts of heteropolyacids were first mentioned by BAXTER and GRIFFIN,[3] who demonstrated the reversible exchange of potassum for ammonium ion in ammonium phosphomolybdate precipitates when determining phosphorus analytically. THISTLETHWAITE[4] reported approximately two NH_4 ions to be exchangeable in the ammonium molybdophosphate molecule. MEIER and TREADWELL[5] studied the exchange of K, Rb, and Cs for NH_4 in the NH_4PMo precipitate, and found that the sorption increased in the order $K < Rb < Cs$ and with increasing amount of sorbent. Recently BUCHWALD and THISTLETHWAITE[6] studied the sorption of K, Rb, Cs, Tl and the alkaline earths on NH_4PMo and found that exchange between NH_4 ion and other cations is isomorphous and involves ammonium and hydrogen ions in the molecule. SMIT and co-workers[7] described the preparation of the ammonium heteropolyacid salts and measured distribution coefficients for the sorption of alkali metals in trace concentrations. In further experiments[8,9] they applied the exchange properties of NH_4PMo to the separation of

* HPW stands for phosphotungstic acid, and NH_4PW for its ammonium salt; HPMo represents phosphomolybdic acid.

[1] A. RAGGENBASS, M. QUINEY, J. FRADIN and J. DUFRENE, *Proceedings of the Second International Conference on the Peaceful Uses of Atomic Energy, Geneva*, 1958 Paper 1179 (U.N.).
[2] W. J. O'LEARY and J. PAPISH, *Industr. Engng. Chem.* (Analyt. Ed.) **6**, 107 (1934).
[3] G. P. BAXTER and R. C. GRIFFIN, *J. Amer. Chem. Soc.* **34**, 204 (1905).
[4] W. P. THISTLETHWAITE, Analyst **72**, 531 (1947).
[5] D. MEIER and W. D. TREADWELL, *Helv. Chim. Acta* **34**, 155 (1951).
[6] H. BUCHWALD and W. P. THISTLETHWAITE, *J. Inorg. Nucl. Chem.* **5**, 341 (1958).
[7] J. VAN R. SMIT, J. J. JACOBS and W. ROBB, *J. Inorg. Nucl. Chem.* **12**, 95 (1959).
[8] J. VAN R. SMIT, *Nature* (Lond.) **181**, 1530 (1958).
[9] J. VAN R. SMIT, W. ROBB and J. J. JACOBS, *J. Inorg. Nucl. Chem.* **12**, 104 (1959).

Na, K, Rb, Cs in micro and macro-amounts. Other authors have used NH_4PMo[10] or TlPMo[11] for the analytical determination of ^{137}Cs in waste waters.

Our previous communication[12] described the sorption of Cs on NH_4PMo and NH_4PW precipitates under static conditions, and in this paper we report on the dynamic sorption and elution of Cs and Rb using columns of NH_4PW. The aim was to find convenient conditions for Cs and Rb isolation, to determine the exchange capacity of the sorbent and to examine whether the mass action law applies to the exchange.

EXPERIMENTAL

Columns were of 0·6 cm diameter and 12 cm height; the height of the active charge was 3–5 cm. Ammonium phosphotungstate freshly precipitated on asbestos served as the column filling.* Columns were prepared as follows: a weighed amount of asbestos was mixed with an excess of 1 N NH_4NO_3 and transferred into the column together with the appropriate volume of 0·1 M phosphotungstic acid,† care being taken to avoid channeling. The flow rate was regulated to 1 drop in 25–35 sec. The weight ratio of asbestos to HPW was between 1:1 and 1:2. The column was washed with 0·3 N NH_4NO_3 followed by 0·4 N $NaNO_3$ to remove the excess of NH_4 ions, which would lower the Cs and Rb sorption. The washing of the column with salt solutions also prevents peptization of NH_4PW. Tracer methods were used for analysis, with radiochemically pure ^{134}Cs, ^{86}Rb and ^{137}Cs as tracers. All chemicals used were of analytical grade.

VOL. 19 1961

RESULTS

(a) Rb *and* Cs *separation*

Experiments were carried out as follows to study the sorption and elution of Rb and Cs separately: a trace amount of ^{134}Cs or ^{86}Rb ($\sim 10^{-6}$ mole) was absorbed on the column; the latter was washed with 0·4 N $NaNO_3$ and then eluted with NH_4NO_3 solutions of different concentrations. The drops from the column were evaporated on an aluminium strip, dried, and their activity measured by means of a GM-counter with a mica window. The dependence of Cs or Rb activity in the filtrate on the number of drops was plotted (Figs. 1 and 2).

The position of the elution peak depends upon the NH_4NO_3 concentration. Cs is only slowly eluted with 0·3 N NH_4NO_3, and between 6 N and 10 N NH_4NO_3 there is no substantial difference in the position of the peak, whereas Rb is eluted appreciably with 0·3 N NH_4NO_3, and with 1 N and 3 N NH_4NO_3 there is little variation in the position of the maximum. From these data we proceeded to separate trace amounts of ^{134}Cs and ^{86}Rb, using 1 N and 6 N NH_4NO_3 respectively to elute Rb and Cs (Fig. 3a). Radiometric measurements showed the two peaks to correspond to Rb and Cs; the activity between the peaks does not decrease to background level, and analysis of the curve shows that minor amounts of Cs are present in the tail of theRb peak, owing to slight elution of Cs by 1 N NH_4NO_3 (cf. Fig. 1). Separation is improved by using lower flow-rates on longer beds. Macro-quantities were also separated under optimum conditions of elution (see Fig. 3b), with results similar to those of SMIT[9] using NH_4PMo.

The use of 1 N NH_4NO_3 for Rb elution is preferable to 3 N NH_4NO_3 since it leads to only half the amount of ammonium salts in the eluate. Elution of Rb and Cs absorbed on NH_4PW with HNO_3 at various concentration gave negative

* Analytical asbestos (serpentine type), thoroughly washed with hydrochloric acid and sodium hydroxide, was used.

† Commercial phosphotungstic acid was purified by the etherate process.

[10] R. W. C. BROADBANK, S. DHABANANDANA and R. D. HARDING, *Analyst* **85**, 365 (1960).

[11] H. TADASHI, *Bull. Chem. Soc. Japan* **31**, 635 (1958).

[12] J. KRTIL and V. KOUŘÍM, *J. Inorg. Nucl. Chem.* **12**, 367 (1960).

results, because HNO_3 eluates Cs and Rb only slightly. The washing is affected by two factors, viz. lowering of the solubility of caesium ammonium salts in presence of mineral acid and ion exchange between caesium and hydrogen ions, of which the first

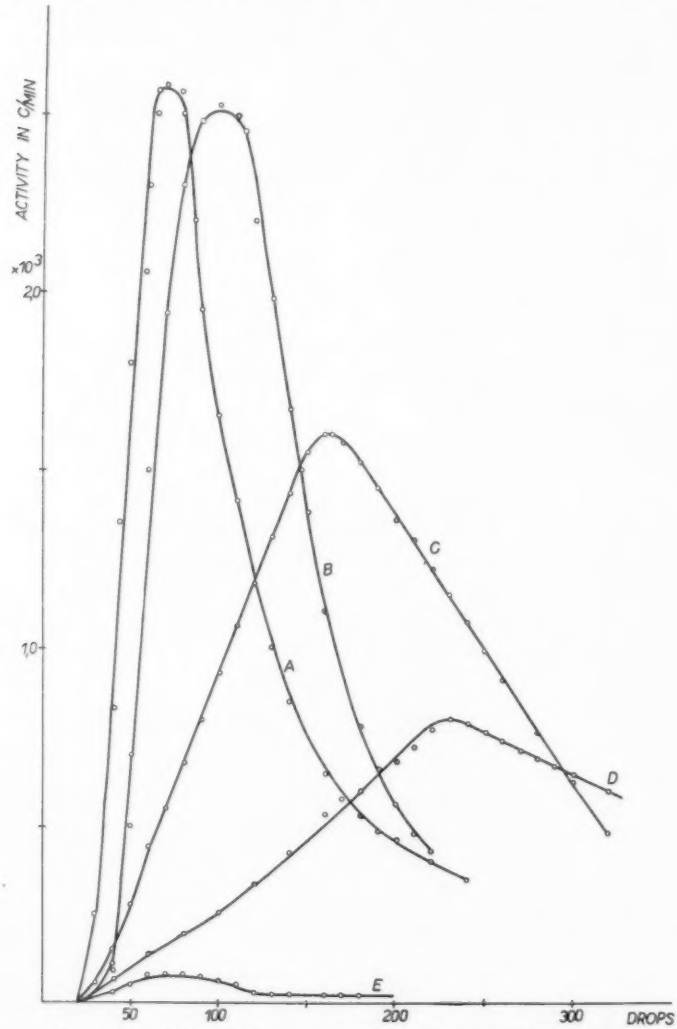

FIG. 1.—The elution of ^{134}Cs with ammonium nitrate of various concentrations. 3 cm bed (0·2 g NH_4... PW + 0·2 g asbestos); drop interval 20 sec. *A*... 10 M NH_4NO_3, *B*... 6 M NH_4NO_3, *C*... 3 M NH_4NO_3, *D*... 1 M NH_4NO_3, *E*... 0·3 M NH_4NO_3.

influence apparently predominates. Elution with $HNO_3 + NH_4NO_3$ showed no difference in comparison with NH_4NO_3 of the same concentration. Since sodium ions are not absorbed, $NaNO_3$ is suitable for washing excess ions out of the column.

(b) *Exchange capacity of* NH_4PW *for* Cs *and* Rb

The capacity was determined by passing through the column excess of Cs or Rb solution of known concentration labelled with ^{137}Cs or ^{86}Rb; after washing with 0·4 N

$NaNO_3$ to remove the excess Rb or Cs from the column, the amount of absorbed cation was found from the difference between the initial and final activities. The column charge (NH_4PW) was determined, after displacing all of the Cs or Rb with 10 N NH_4NO_3, by dissolving in 3 N NH_4OH, and collecting in a weighed crucible.

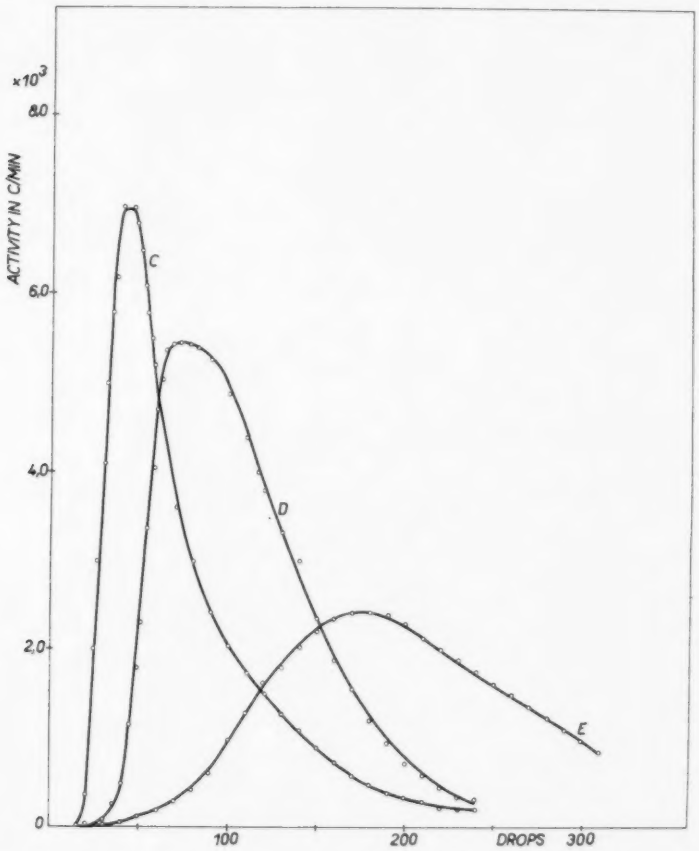

FIG. 2.—The elution of ^{86}Rb with ammonium nitrate of various concentrations. 3 cm bed (0·2 g NH_4PW + 0·2 g asbestos); drop interval 20 sec. *E*...0·3 N NH_4NO_3, *D*...1 N NH_4NO_3, *C* 3 N NH_4NO_3.

The oxides were estimated and the capacity calculated after drying with an infrared lamp and igniting to 550°C. The capacity was found to be 0·70 mmol/g of oxides for Cs and 0·8 mmol/g for Rb, corresponding to two atoms Cs/Mol NH_4PW and 2·38 atoms Rb/Mol NH_4PW. These values are in agreement with those previously quoted for NH_4PMo.[9,10]

(c) *Application of the mass action law to the* Cs *exchange with* NH_4PW

If the exchange between Cs and NH_4 is written

$$Cs^+ + NH_4PW = CsPW + NH_4^+, \quad (1)$$

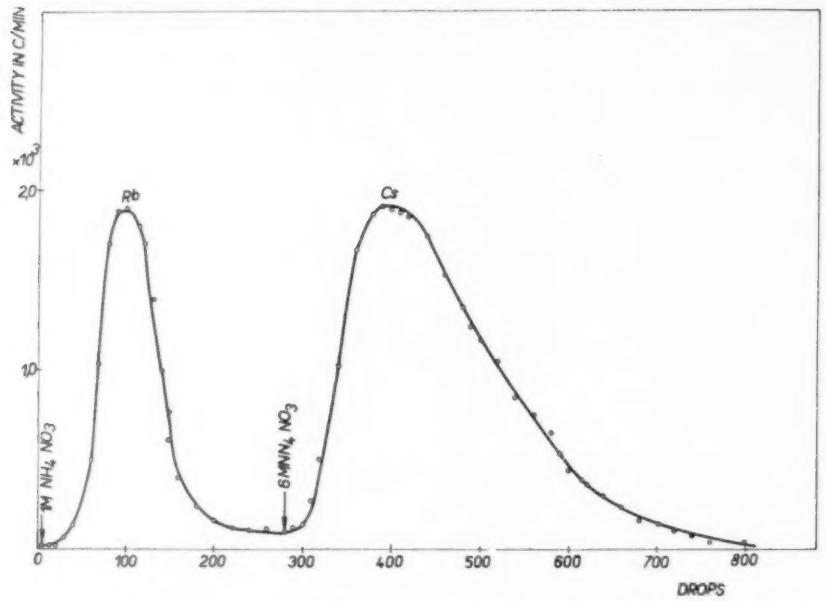

FIG. 3a.—Separation of trace ^{86}Rb from trace ^{134}Cs. 3 cm bed (0·2 g NH_4PW + 0·2 g asbestos); drop interval 25 sec.

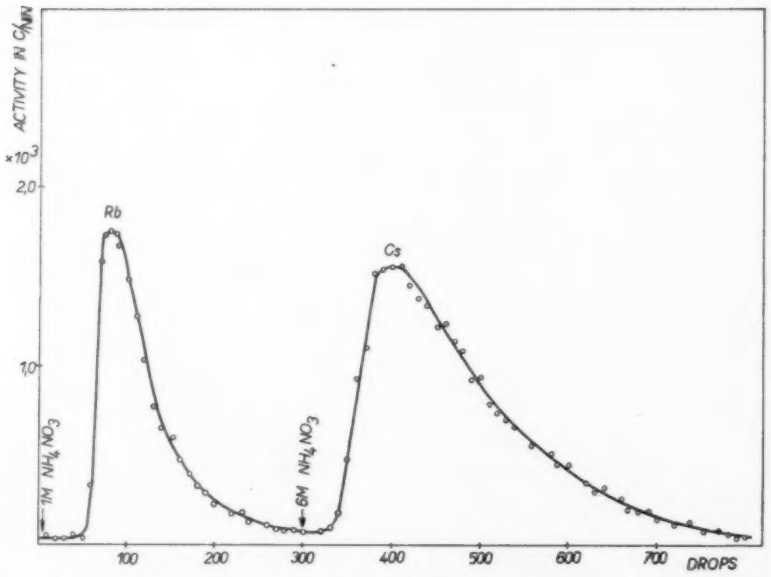

FIG. 3b.—Separation of macroamounts of Rb and Cs. 5 cm bed (0·4 g NH_4PW + 0·4 g asbestos); drop interval 35 sec 3·64 mg Rb, 4·72 mg Cs (molar ratio Cs/Rb = 0·840).

Then

$$K = \frac{[Cs]_S[NH_4]_L}{[Cs]_L[NH_4]_S}$$ (S indicating the precipitate and L the solution)

Static experiments were performed using 0·100 g NH_4PW and solutions containing a constant quantity of ^{137}Cs at the micro-level and variable amounts of NH_4NO_3; these were agitated in stoppered 2·5 ml tubes. The distribution of Cs between the

TABLE 1.—DISTRIBUTION COEFFICIENTS FOR Cs ON NH_4PW ON A FUNCTION OF NH_4^+ ION CONCENTRATION

Distribution coefficients for Cs, K_d	Equilibrium concentration of NH_4, (mole/l)	K'
100	0·065	6·50
59	0·111	6·55
32	0·230	7·36
20·7	0·314	6·46
13·2	0·500	6·60
6·6	1·010	6·66
4·2	1·480	6·21
3·17	2·030	6·43

VOL. 19 1961

phases was determined radiochemically and the ammonium ions concentration was taken to be equal to the initial value since changes in the ammonium ion concentration will be small and may be neglected. If the distribution coefficient is given by

$$K_d = \frac{[Cs]_S}{[Cs]_L}$$

and $[NH_4]_S$ is taken to be constant, equation (1) may be simplified to the form

$$K' = K_d[NH_4]_L.$$

Substituting the values for K_d and $[NH_4]_L$ we obtain constant values (Table 1).

$$K_d = \frac{\text{activity of Cs per 100 mg of } NH_4PW}{\text{activity of Cs per 2 ml of solution at equilibrium}}$$

The calculated value of K' (mean 6·6) corresponds to a value of $1{\cdot}9 \times 10^2$ for the stoicheometric equilibrium constant K in equation (1).

Acknowledgement—The author is indebted to Mr. V. KOUŘÍM for stimulating discussion.

J. Inorg. Nucl. Chem., 1961, Vol. 19, pp. 304 to 313. Pergamon Press Ltd. Printed in Northern Ireland

THE DECOMPOSITION KINETICS OF COPPER HYDRIDE IN THE PRESENCE OF ELECTROLYTES*

J. C. WARF†
Department of Chemistry, University of Indonesia, Djakarta, Indonesia

(*Received* 14 *September* 1960; *in revised form* 8 *November* 1960)

Abstract—The decomposition of copper hydride into the elements was known to be a first-order process, the rate being strongly influenced by electrolytes. Those electrolytes which do not interact with copper(I) influence the rate relatively little, but those which do interact with copper(I) have a pronounced effect. Low concentrations of chlorides, bromides and iodides inhibit the decomposition, but higher concentrations accelerate it. Hydroxides and fluorides strongly accelerate the reaction, the kinetics being quite complicated. In some runs, the data indicated two simultaneous first-order reactions, one of much shorter half-life than the other.

An interpretation in harmony with the observations is presented. This involves adsorption of ions on the surface of the copper hydride particles, leading to stabilization, and abstraction of copper atoms at higher halide concentrations, forming a complex ion and leaving a defect site which is a nucleus from which decomposition and disintegration of the particle commences.

IT was shown[1] earlier that the irreversible decomposition of copper hydride, suspended in water, is a first-order process involving a particle-by-particle mechanism, and that the rate is drastically affected by the presence of foreign substances. In particular, it was found that the decomposition is inhibited by sodium chloride, but accelerated by alkalies, presumably through preliminary adsorption of the anions. In the present work, the role of electrolytes in the decomposition of copper hydride is further explored.

EXPERIMENTAL

Preparation of copper hydride. The procedure described in the earlier work[1] was followed, employing copper(II) sulphate and hypophosphorous acid at 50°C using a stream of carbon dioxide for agitation and protection from the air. In some cases, when particularly acid-free copper hydride was desired, the well-washed preparation was treated with the basic form of an anion-exchange resin (Dowex 21K) held in an asbestos thimble for some hours, after which the aqueous phase was essentially neutral. Small vials were filled with the copper hydride slurry, and frozen until needed. All washing and transferring operations were carried out keeping the temperature as close as possible to 0°C and under carbon dioxide.

When sodium borohydride was employed as the reducing agent, 12·5 mmoles in 15 ml of ice-water was treated with 25 ml of previously chilled F $CuSO_4$, under a hydrogen atmosphere. After 10 min, the $Cu(OH)_2$ was separated from the CuH by treating with 25 ml of 2 F acetic acid, after which the normal washing procedure was followed.

Apparatus and procedure. An apparatus nearly identical with that previously described[1] was employed. A calibrated vacuum reservoir was attached to the line, so that in those runs in which the hydrogen volume exceeded the capacity of the burette, the final volume could be measured.

After each rate measurement, the quantity of copper hydride taken was determined by quantitative decomposition in boiling water, and observing the total hydrogen volume. But in many of the runs in which halides were present, the stabilization of the CuH was so pronounced that many hours of

* Presented at the XVIIth International Congress of Pure and Applied Chemistry, Munich, September, 1959.

† Present Address: Department of Chemistry, University of Southern California, Los Angeles 7, California.

[1] J. C. WARF and W. FEITKNECHT, *Helv. Chim. Acta* **33**, 613–639 (1950).

boiling were necessary to effect complete decomposition. In these cases, the system was opened, and some concentrated sodium hydroxide solution introduced into the reaction vessel through a funnel; the alkali accelerated the decomposition of the copper hydride, more than compensating for the inhibitory effect of the halides.

For each run, a vial of the frozen CuH slurry was thawed, and an approximately known amount pipetted into the reaction vessel against a stream of hydrogen. Some exposure to air was unavoidable. A measured quantity of a standard electrolyte solution was then added, and the decomposition begun. At the end, the aqueous phase was analysed.

Analysis. Copper determinations were carried out by the common iodide-thiosulphate titration method. Chlorides, bromides and iodides were titrated with silver nitrate, employing adsorption indicators as described by Fajans. Fluorides were titrated with thorium nitrate according to the procedure of ROWLEY and CHURCHILL[2].

RESULTS

Pure copper hydride

The decomposition rate of copper hydride suspended in pure water was determined at several temperatures ranging from 50 to 80°C. For the well-washed material prepared using hypophosphorous acid, rate constants k were determined by plotting the logarithm of the amount of hydride, obtained from the difference D between each volume of hydrogen and the volume on complete decomposition, against time (log D–t curves). The log k — $1/T$ data were least squared to equations of the Arrhenius form, and an activation energy of 18·9 ± 0·5 kcal/mole calculated, compared with 21·0 kcal/mole in the original work.[1] The pre-exponential factor was $2{\cdot}1 \times 10^{10}$ min^{-1}, compared to the earlier 6×10^{11} min^{-1}. Similar data from the copper hydride made using sodium borohydride gave the same activation energy but were somewhat less reproducible (18·9 ± 1·0 kcal/mole).

Non-interacting electrolytes

These were electrolytes which form no complexes or precipitates with copper(I). Decompositions of copper hydride were carried out suspended in solutions of H_2SO_4, Na_2SO_4, and several concentrations of $NaClO_4$. In general, it was found that the effect of these electrolytes was slight, although the decomposition rate was reduced somewhat by higher concentrations of $NaClO_4$ as is shown by typical data in Table 1. Surprisingly, some of the log D–t curves were not linear from the beginning of the

TABLE 1.—DECOMPOSITION OF CuH UNDER NON-INTERACTING ELECTROLYTES

Electrolyte	Formality	Temp (°C)	Reaction I half-life (min)	Reaction II half-life (min)
None	—	77·4	—	19·2
H_2SO_4	0·12	77·4	None	10·0
$NaClO_4$	0·064	77·4	None	22·0
$NaClO_4$	0·125	77·4	6·47	81·2
$NaClO_4$	1·79	77·4	5·12	148
None	—	50·0	—	190
Na_2SO_4	0·202	50·0	None	265

[2] R. J. ROWLEY and H. V. CHURCHILL, *Industr. Engng. Chm., Analyt. Ed.* **9**, 551 (1937).

J. Inorg. Nucl. Chem., 1961, Vol. 19, pp. 304 to 313. Pergamon Press Ltd. Printed in Northern Ireland

THE DECOMPOSITION KINETICS OF COPPER HYDRIDE IN THE PRESENCE OF ELECTROLYTES*

J. C. WARF†
Department of Chemistry, University of Indonesia, Djakarta, Indonesia

(*Received* 14 *September* 1960; *in revised form* 8 *November* 1960)

Abstract—The decomposition of copper hydride into the elements was known to be a first-order process, the rate being strongly influenced by electrolytes. Those electrolytes which do not interact with copper(I) influence the rate relatively little, but those which do interact with copper(I) have a pronounced effect. Low concentrations of chlorides, bromides and iodides inhibit the decomposition, but higher concentrations accelerate it. Hydroxides and fluorides strongly accelerate the reaction, the kinetics being quite complicated. In some runs, the data indicated two simultaneous first-order reactions, one of much shorter half-life than the other.

An interpretation in harmony with the observations is presented. This involves adsorption of ions on the surface of the copper hydride particles, leading to stabilization, and abstraction of copper atoms at higher halide concentrations, forming a complex ion and leaving a defect site which is a nucleus from which decomposition and disintegration of the particle commences.

IT was shown[1] earlier that the irreversible decomposition of copper hydride, suspended in water, is a first-order process involving a particle-by-particle mechanism, and that the rate is drastically affected by the presence of foreign substances. In particular, it was found that the decomposition is inhibited by sodium chloride, but accelerated by alkalies, presumably through preliminary adsorption of the anions. In the present work, the role of electrolytes in the decomposition of copper hydride is further explored.

EXPERIMENTAL

Preparation of copper hydride. The procedure described in the earlier work[1] was followed, employing copper(II) sulphate and hypophosphorous acid at 50°C using a stream of carbon dioxide for agitation and protection from the air. In some cases, when particularly acid-free copper hydride was desired, the well-washed preparation was treated with the basic form of an anion-exchange resin (Dowex 21K) held in an asbestos thimble for some hours, after which the aqueous phase was essentially neutral. Small vials were filled with the copper hydride slurry, and frozen until needed. All washing and transferring operations were carried out keeping the temperature as close as possible to 0°C and under carbon dioxide.

When sodium borohydride was employed as the reducing agent, 12·5 mmoles in 15 ml of ice-water was treated with 25 ml of previously chilled F $CuSO_4$, under a hydrogen atmosphere. After 10 min, the $Cu(OH)_2$ was separated from the CuH by treating with 25 ml of 2 F acetic acid, after which the normal washing procedure was followed.

Apparatus and procedure. An apparatus nearly identical with that previously described[1] was employed. A calibrated vacuum reservoir was attached to the line, so that in those runs in which the hydrogen volume exceeded the capacity of the burette, the final volume could be measured.

After each rate measurement, the quantity of copper hydride taken was determined by quantitative decomposition in boiling water, and observing the total hydrogen volume. But in many of the runs in which halides were present, the stabilization of the CuH was so pronounced that many hours of

* Presented at the XVIIth International Congress of Pure and Applied Chemistry, Munich, September, 1959.

† Present Address: Department of Chemistry, University of Southern California, Los Angeles 7, California.

[1] J. C. WARF and W. FEITKNECHT, *Helv. Chim. Acta* **33**, 613–639 (1950).

boiling were necessary to effect complete decomposition. In these cases, the system was opened, and some concentrated sodium hydroxide solution introduced into the reaction vessel through a funnel; the alkali accelerated the decomposition of the copper hydride, more than compensating for the inhibitory effect of the halides.

For each run, a vial of the frozen CuH slurry was thawed, and an approximately known amount pipetted into the reaction vessel against a stream of hydrogen. Some exposure to air was unavoidable. A measured quantity of a standard electrolyte solution was then added, and the decomposition begun. At the end, the aqueous phase was analysed.

Analysis. Copper determinations were carried out by the common iodide-thiosulphate titration method. Chlorides, bromides and iodides were titrated with silver nitrate, employing adsorption indicators as described by Fajans. Fluorides were titrated with thorium nitrate according to the procedure of ROWLEY and CHURCHILL[2].

RESULTS

Pure copper hydride

The decomposition rate of copper hydride suspended in pure water was determined at several temperatures ranging from 50 to 80°C. For the well-washed material prepared using hypophosphorous acid, rate constants k were determined by plotting the logarithm of the amount of hydride, obtained from the difference D between each volume of hydrogen and the volume on complete decomposition, against time (log D–t curves). The log k — $1/T$ data were least squared to equations of the Arrhenius form, and an activation energy of $18{\cdot}9 \pm 0{\cdot}5$ kcal/mole calculated, compared with 21·0 kcal/mole in the original work.[1] The pre-exponential factor was $2{\cdot}1 \times 10^{10}$ min^{-1}, compared to the earlier 6×10^{11} min^{-1}. Similar data from the copper hydride made using sodium borohydride gave the same activation energy but were somewhat less reproducible ($18{\cdot}9 \pm 1{\cdot}0$ kcal/mole).

Non-interacting electrolytes

These were electrolytes which form no complexes or precipitates with copper(I). Decompositions of copper hydride were carried out suspended in solutions of H_2SO_4, Na_2SO_4, and several concentrations of $NaClO_4$. In general, it was found that the effect of these electrolytes was slight, although the decomposition rate was reduced somewhat by higher concentrations of $NaClO_4$ as is shown by typical data in Table 1. Surprisingly, some of the log D–t curves were not linear from the beginning of the

TABLE 1.—DECOMPOSITION OF CuH UNDER NON-INTERACTING ELECTROLYTES

Electrolyte	Formality	Temp (°C)	Reaction I half-life (min)	Reaction II half-life (min)
None	—	77·4	—	19·2
H_2SO_4	0·12	77·4	None	10·0
$NaClO_4$	0·064	77·4	None	22·0
$NaClO_4$	0·125	77·4	6·47	81·2
$NaClO_4$	1·79	77·4	5·12	148
None	—	50·0	—	190
Na_2SO_4	0·202	50·0	None	265

[2] R. J. ROWLEY and H. V. CHURCHILL, *Industr. Engng. Chm., Analyt. Ed.* **9**, 551 (1937).

decomposition, but concave upward, and became linear only after 15–25 min. Typical curves are shown in Fig. 1.

Those log D–t curves which were not linear from the start were analysed by extrapolating the linear portion back to zero time, and plotting the logarithm of the difference between the two curves against time. In each case a second straight line was produced (Fig. 1). This demonstrated that there were two simultaneous first order

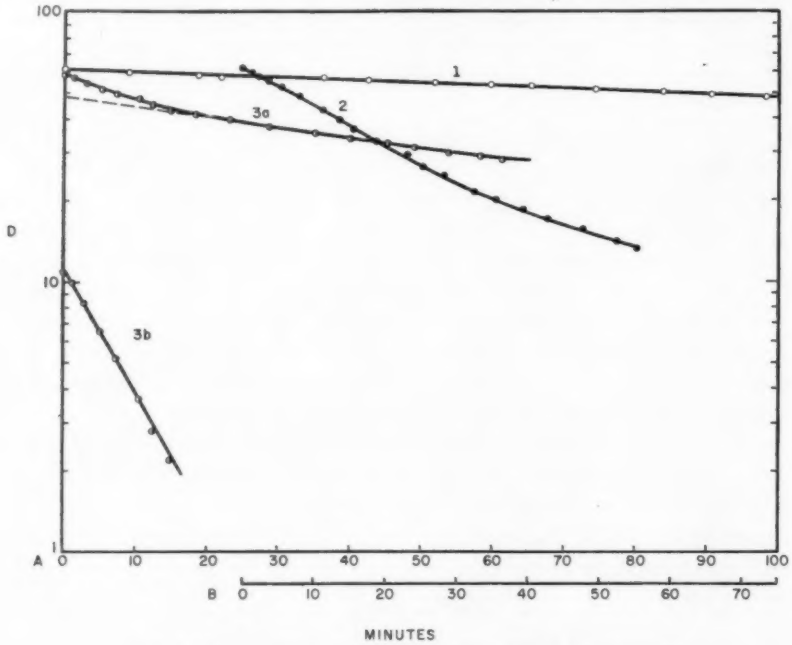

FIG. 1.—Decomposition of CuH under non-interacting electrolytes.
Curve 1—0·20 F Na_2SO_4 at 50·0°C (abscissa A)
Curve 2—0·064 F $NaClO_4$ at 77·4°C (abscissa B)
Curve 3a—0·125 F $NaClO_4$ at 77·4°C (abscissa A)
Curve 3b—Reaction I of curve 3a (abscissa A)

reactions, one of which was fast (called reaction I) and one of which was slow (called reaction II); some half-lives of both reactions are presented in Table 1.

No firm conclusion was reached as to the origin of reaction I (the slower reaction II was the "normal" decomposition of the copper hydride), but it is probable that it arises from the inadvertent presence of dissolved oxygen in some of the preparations (*vide infra*).

Interacting electrolytes

These were electrolytes which form precipitates or complexes with copper(I); they strongly affected the decomposition rate of copper hydride. Most of the log D–t plots (Fig. 2) were concave upward for the first portion of the decomposition, as in the case of the non-interacting electrolytes. They corresponded similarly to two first-order reactions, I, the faster, presumably oxygen-induced reaction, and II, the slower, main decomposition. The log D–t plots were found to be linear over two to three half-lives

for the faster decompositions (half-life under 50 min), and one to one and a half half-lives for the slower reactions.

Sodium chloride. Table 2 shows typical half-lives for reactions I and II for a variety of concentrations and temperatures, and Fig. 3 shows the dependence of the rate constant on concentration at constant temperature. The rates were sensitive to concentration, and reproducibility was poor (10–20 per cent). The inhibiting effect of

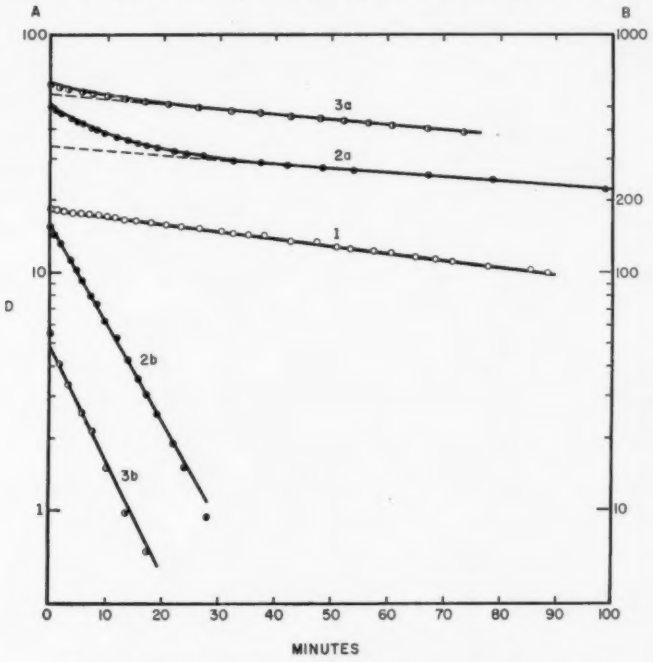

FIG. 2.—Decomposition of CuH under interacting electrolytes.
Curve 1—0·218 F $NaCuCl_2$ at 77·4°C (ordinate B)
Curve 2a—0·353 F NaI at 50·0°C (ordinate A)
Curve 2b—Reaction I of curve 2a (ordinate A)
Curve 3a—0·104 F NaCl at 77·4°C (ordinate A)
Curve 3b—Reaction I of curve 3a (ordinate A)

the chloride is seen clearly; but the rate constant went through a minimum at about 0·2 F NaCl, and the decomposition became accelerated in the more concentrated solutions.

The inhibiting effect of the chloride ion up to about 0·5 F was so great that it became impractical to achieve complete decomposition of the copper hydride by boiling at the end of each run. In these cases, therefore, the reaction bulb was cooled, and concentrated sodium hydroxide solution added through a funnel; the catalytic action of the alkali permitted complete decomposition on boiling. On each addition of the alkali, reddish copper(I) oxide was noted to precipitate. Analysis of the aqueous phases, removed prior to adding alkali, showed copper(I) concentrations ranging from 0·01 to 0·08 F, which represented 2–8 per cent of the total copper. Part of this dissolved copper is believed to result from small and variable quantities of dissolved oxygen.

One decomposition of copper hydride was carried out in which the concentration of copper(I) complex was very high. This was done by preparing $NaCuCl_2$ from Cu,

TABLE 2.—DECOMPOSITION OF COPPER HYDRIDE UNDER SODIUM CHLORIDE SOLUTIONS

Electrolyte	Formality	Temp (°C)	Reaction I half-life (min)	Reaction II half-life (min)
None	—	77·4	—	19·2
NaCl	0·015	77·4	5·57	94·3
NaCl	0·055	77·4	5·84	172
NaCl	0·104	77·4	6·11	162
NaCl	0·186	77·4	13·7	197
NaCl	0·366	77·4	12·0	108
NaCl	0·511	77·4	None	53
NaCl	1·88 ·	77·4	—	0·35*
NaCl	0·502	65·0	None	435
none	—	50·0	—	190
NaCl	0·091	50·0	None	857
NaCl	0·224	50·0	3·2	1190
NaCl	0·467	50·0	None	733
NaCl	0·935	50·0	None	703
NaCl	3·34	50·0	None	4·2

* The decomposition was too rapid to follow, but an approximate rate constant could nevertheless be estimated.

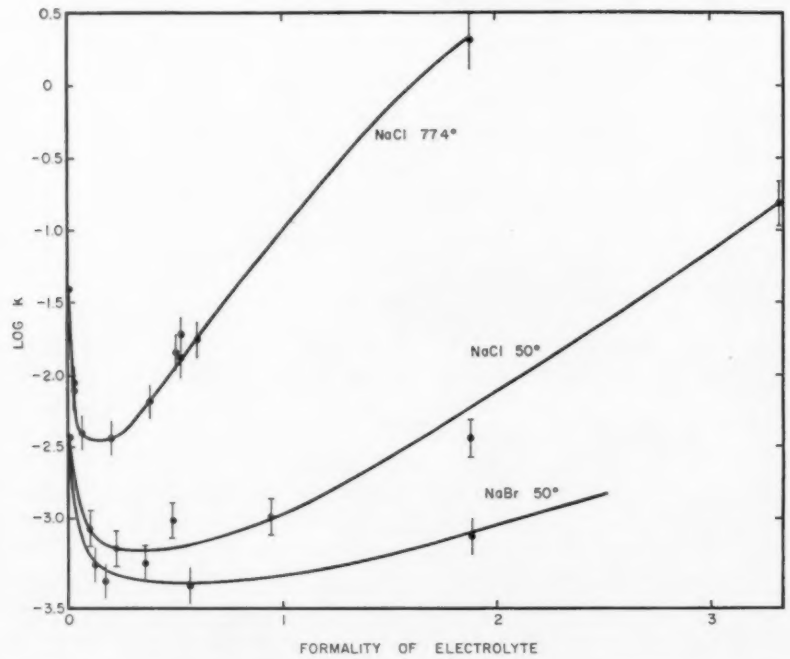

FIG. 3—Influence of electrolyte concentration on decomposition rate of CuH.

$CuCl_2$, and NaCl, and adding it to the copper hydride slurry. After the decomposition at 77·4°C, analysis showed the copper(I) concentration to be 0·218 F, and the total chloride concentration to be 1·92 F. The log D–t plot, shown in Fig. 2, was linear from the start, showing that reaction I was completely suppressed, probably owing to the consumption of any oxygen by the copper(I). The decomposition had been strongly inhibited (half-life = 100 min) despite the high chloride concentration.

Bromides. As the data in Table 3 show, sodium bromide inhibited the decomposition of copper hydride even more strongly than sodium chloride. In more

TABLE 3.—DECOMPOSITION OF COPPER HYDRIDE UNDER BROMIDE SOLUTIONS

Electrolyte	Formality	Temp (°C)	Reaction I half-life (min)	Reaction II half-life (min)
NaBr	0·515	77·4	1·6	48·5
NaBr	0·970	77·4	None	64·0
NaBr	0·493	65·0	Slight	68·3
NaBr	0·117	50·0	Slight	1480
NaBr	0·163	50·0	15·6	1940
NaBr	0·563	50·0	None	2130
NaBr	1·90	50·0	None	932
NH_4Br	0·194	65·0	None	344
	0·467	65·0	None	705
	1·58	65·0	None	1250

concentrated solutions, the rate increased, but not so much as in the preceding case. Ammonium bromide exerted an inhibitory effect still more pronounced than that of sodium bromide. At the end of each decomposition, the aqueous phase contained small amounts of copper(I) (0·002–0·05 F).

Iodides. The influence of iodides on the course of the decomposition of copper hydride was closely similar to that of the chlorides and bromides. Two simultaneous reactions (Table 4, Fig. 2) existed, and the decompositions became faster in the more concentrated iodide solutions (Fig. 3). In each case after complete decomposition, the

TABLE 4.—DECOMPOSITION OF COPPER HYDRIDE UNDER IODIDE SOLUTIONS

Electrolyte	Formality	Temp (°C))	Reaction I half-life (min)	Reaction II half-life (min)
NaI	0·240	77·4	1·4	57
NaI	0·0375	50·0	6·7	475
NaI	0·353	50·0	7·2	170
KI	0·0386	77·4	4·3	121
KI	0·0530	77·4	3·9	135
KI	0·209	77·4	4·6	195
KI	0·95	77·4	None	113
KI	1·03	77·4	None	93
KI	2·06	77·4	3·4	74

VOL. 19 1961

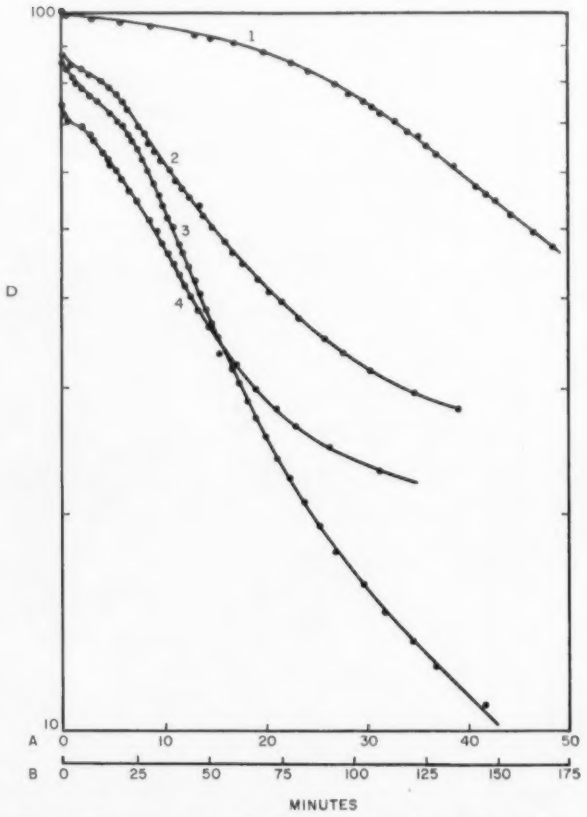

FIG. 4.—Decomposition of CuH under saturated $Ca(OH)_2$ solutions
Curve 1—10°C (abscissa A) Curve 2—3·5°C (abscissa A)
Curve 3—15°C (abscissa A) Curve 4—7·6°C (abscissa B)

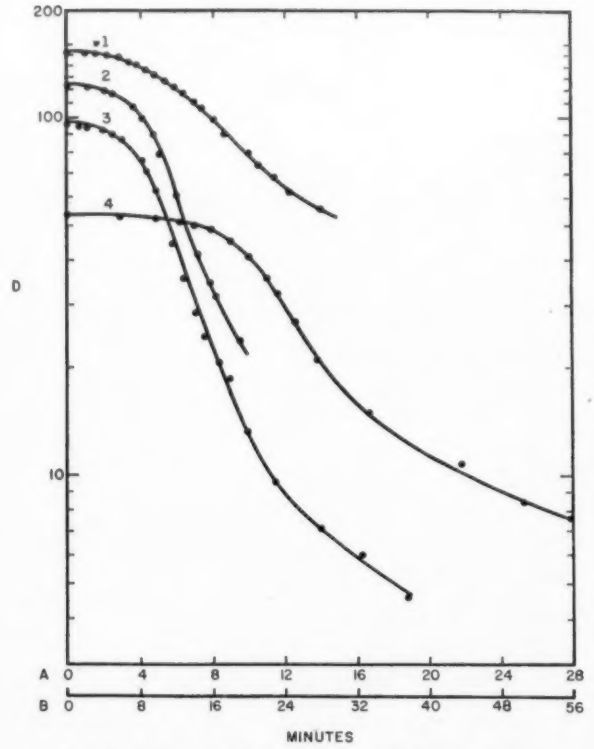

FIG. 5.—Decomposition of CuH under NaF solutions.
Curve 1—0·98 F NaF at 50·0°C (abscissa B) Curve 2—0·473 F NaF at 77·4°C (abscissa A) Curve 3—0·214 F NaF at 77·4°C (abscissa A)
Curve 4—Saturated NaF at 65·0°C (abscissa B)

residual copper contained 10–20 per cent copper(I) iodide, as found by weighing before and after treatment with sodium thiosulphate solution.

Sodium hydroxide and carbonate. As it had already been shown[1] that alkalies strongly catalyse the decomposition of copper hydride, dilute sodium hydroxide solutions at relatively low temperatures were employed. Even so, the decompositions were immeasurably fast (half-life less than 0·1 min) with 0·045 F NaOH at 40°C, 0·52 F NaOH at 13·2°C and 0·015 F Na_2CO_3 at 50°C (all concentrations being determined by titration of the aqueous phase at the end of the decomposition). But when an ice bath was used, the rates could be measured in sodium hydroxide solutions up to 0·15 F. The log *D–t* plots were linear. Since the decomposition of copper hydride is exothermic to the extent of approximately 5·1 kcal/mole,[3] the actual temperature inside the reaction vessel was somewhat higher than ice temperature. The half-life for the decomposition of well-washed and resin-treated copper hydride was found to be 2·20 min at 0·2°C in 0·069 F sodium hydroxide, and 2·38 min at 0·2°C in 0·15 F solution. The exact decomposition conditions were difficult to reproduce, as varying traces of phosphorus-containing ions were left with the copper hydride, evidently strongly adsorbed. This residual phosphorus-bearing acid precluded use of extremely dilute sodium hydroxide solutions.

VOL. 19 1961

Calcium hydroxide. Since the neutralization of very dilute sodium hydroxide by traces of phosphorus-bearing acids adsorbed by the copper hydride produced a variable basicity, a solution of controlled alkalinity was produced through the use of an excess of calcium hydroxide. Saturated calcium hydroxide is a buffer of pH 12·45 at 25°C.[4] Approximately 1 g of $Ca(OH)_2$ was added to the reaction vessel holding 18 ml of aqueous phase, pre-adjusted to the bath temperature (0–20°C).

The log *D–t* curves were of complicated sigmoid shape (Fig. 4). The most linear portions correspond to half-lives of 2–8 min, but these values probably have doubtful significance. The decompositions seemed to begin slowly, then grew faster until the bulk of the copper hydride was decomposed. A reaction bulb was designed to accommodate a glass electrode, and this equilibrated at 0°C with the agitator. Addition of calcium hydroxide to pure water, under the same conditions as in the decompositions, caused the pH to rise to 12·5 in less than 10 sec. This shows that the rate of dissolution of the $Ca(OH)_2$ is not the rate-controlling step.

Sodium fluoride. Since the fluoride ion resembles the hydroxide ion in size and charge, studies were made to determine the effect of this ion on the decomposition rate of copper hydride. The log *D–t* curves (Fig. 5) were sigmoid, resembling the cases with calcium hydroxide. The slopes of the most nearly linear portions corresponded to decomposition rates somewhat higher than in the absence of sodium fluoride. For example, in 0·214 F NaF at 77·4°C, the half-life was about 8·8 min, and in 0·57 F NaF at 50°C, 175 min, but the meaning of these data is doubtful.

Other substances. During the course of these investigations, several decompositions of copper hydride were made in the presence of compounds which interact with copper(I) to form precipitates or complexes. The log *D–t* curve representing the decomposition in 0·15 F ammonium hydroxide at 40°C was linear, and corresponded to a half-life of 284 min. This is about twice as fast as under pure water. The log *D–t* curves for decomposition under sodium azide solutions were also linear, corresponding

[3] A. Sieverts and A. Gotta, *Ann. Chem.* **453**, 289 (1927).
[4] R. G. Bates, V. E. Bower and E. R. Smith, *J. Res. Nat. Bur. Stand.* **56**, 305 (1956).

to half-lives of 306 min at 77·4°C in 0·50 F NaN_3, and 2280 min at 52°C in 0·75 F NaN_3. But the log D–t curves representing the decomposition in potassium thiocyanate solutions were sigmoid, resembling the case with calcium hydroxide. The curves corresponding to decomposition of copper hydride suspended in solutions of disodium ethylenediaminetetraacetate were linear at the beginning, but became concave downward, showing some sort of auto-catalytic action.

DISCUSSION

The work of a decade ago[1] disclosed that no detectable exchange occurs when CuH suspended in D_2O is catalytically decomposed by NaOD, and this observation is one of the principal points which support the view that the copper hydride decomposes particle-by-particle. It is thought that the surface of the hydride strongly adsorbs water, which cannot be removed without decomposition of the hydride. Sorption and desorption of hydroxide ions, perhaps removing copper atoms as Cu_2O, creates nuclei from which a chain-reacting zone of decomposition grows into the interior. As the decomposition is exothermic, the local temperature rise would be considerable, causing the entire particle to disintegrate into the elements, in which case the H_2 would escape exchange with D_2O or OD^-. This mechanistic picture is in agreement with the observed first-order decomposition.

In the case of "pure" copper hydride, made using hypophosphorus acid, there remains about 0·1 per cent phosphorus which cannot be washed out,[5] presumably adsorbed as a phosphorus-bearing acid. Desorption of these ions could, according to the view presented, give rise to decomposition nuclei.

The influence of chloride, bromide and iodide ions is to stabilize the copper hydride particles at low concentrations and accelerate their decomposition at higher concentrations (Fig. 3). This appears to be the result of two opposing factors. The first factor, stabilization of the surface by strong adsorption of chloride on active sites, i.e. ion exchange with the phosphorus-bearing ion, would predominate at low concentration, while the second factor, actual abstraction of copper atoms from the surface, forming $CuCl_2^-$, would be the over-weighing occurrence at high concentration. Higher concentrations of iodide ion are less effective than bromides or chlorides (Fig. 3), owing to the insolubility of copper(I) iodide, which perhaps forms a protective layer.

According to the interpretation developed, the catalytic role of the hydroxide ion would result from its preliminary adsorption and removal of copper atoms as highly insoluble copper(I) oxide. Only traces of this oxide would be formed, as it is necessary to create only a few nuclei on a copper hydride particle to cause the entire particle to disintegrate. Presumably, fluoride ion behaves similarly, causing disproportionation of copper(I) into copper metal and copper(II) ion. Abstraction of Cu^+ from the hydride lattice would leave a negative hole or defect, which is regarded as a nucleus from which decomposition grows. A parallel view for the formation of nuclei on the surface of lead azide crystals, via expulsion of azide ions, has been given by GRIFFITHS and GROOCOCK[6]. No rationale is offered for the complexity of the log D–t curves representing the decomposition of copper hydride under the influence of calcium hydroxide and sodium fluoride solutions.

[5] A. SIEVERTS and F. LOESSNER, *Z. Anorg. Chem.* **76**, 1 (1912).
[6] P. J. F. GRIFFITHS and J. M. GROOCOCK, *J. Chem. Soc.* 3380 (1957).

The existence of two simultaneous first-order decomposition reactions has been noted in a number of electrolytic media. It was mentioned earlier that reaction I could conceivably be attributable to nuclei formation on the copper hydride surface by dissolved oxygen, which is consumed or removed during the early stages of the decomposition, forming a copper(I)–halide complex. The presence of electrolytes is evidently necessary to observe reaction I.

An additional source of soluble copper(I) complexes is suggested by

$$CuH + 2Cl^- + H_2O \rightarrow CuCl_2^- + OH^- + H_2$$

which would be expected to occur in two steps. This could occur after consumption of oxygen, and probably took place mainly during the final decomposition by boiling. The hydroxide ion produced would be neutralized by adsorbed phosphorus-bearing acid, or consumed by

$$CuH + CuCl_2^- + OH^- \rightarrow 2Cu + H_2O + 2Cl^-$$

If the above reaction is slow, it could allow considerable $CuCl_2^-$ to accumulate. FEITKNECHT and SCHUTZ[7] have shown that the $CuCl_2^-$ ion does not form copper(I) oxide in 2 F chloride ion below pH 6–7, so most of the complex would not hydrolyse under the decomposition conditions. A similar case can be made for iodides, involving precipitation of copper(I) iodide. Probably there are partially compensating effects, the $CuCl_2^-$ ion inhibiting the decomposition, and the hydroxide ion accelerating it, each ion being of gradually varying concentration.

Acknowledgements—This study was in part subsidized by the General Research Fund of the University of Indonesia, for which I am duly grateful. In addition, I am indebted to Messrs. CHATTAM, RASIMIN and SUWANDI for their resourceful assistance in the laboratory.

[7] W. FEITKNECHT and W. SCHÜTZ, *Rev. Mét.* **52**, 327 (1955).

VOL. 19 1961

J. Inorg. Nucl. Chem., 1961, Vol. 19, pp. 314 to 327. Pergamon Press Ltd. Printed in Northern Ireland

SYNERGISM IN THE SOLVENT EXTRACTION OF DI-, TRI- AND TETRA-VALENT METAL IONS*—I

SYNERGIC EFFECTS OF DIFFERENT PHOSPHATE ESTERS

T. V. HEALY†
Argonne National Laboratory, Argonne, Illinois

(*Received* 5 *October* 1960; *in revised form* 7 *November* 1960)

Abstract—Synergic effects noted previously only in the solvent extraction of uranyl ions are now shown to exist for other ions. Examples of this greatly enhanced extraction from aqueous solution are given for rare earths, actinides and alkaline earths, the extracted species being $Ca(TTA)_2S_2$ $UO_2(TTA)_2S_1$ $UO_2(TTA)_2S_2$ $Pm(TTA)_3S_2$ $Tm(TTA)_3S_1$ $Tm(TTA)_3S_2$ $Am(TTA)_3S_2$ $Cm(TTA)_3S_2$ and $Th(TTA)_4S_1$ where S is a neutral organophosphorus ester varying from tri octyl phosphine oxide with its highly polar phosphorus oxygen bond to the very weakly basic tri phenyl phosphate, and TTA refers to thenoyl trifluoroacetone.

THE word "synergism" was first coined by American workers BAES *et al.*[1] to describe their discovery of a definite enhancement of the extraction of uranium (called synergic effect) from aqueous solution by a mixture of an acidic dialkyl phosphate and certain neutral organophosphorus esters, the resulting mixture giving a better extraction of uranium than either the acid or neutral phosphate alone. These workers considered that this synergistic enhancement seemed to be limited in their experiments to dialkyl phosphoric acid–neutral reagent combinations and that, out of several elements studied, uranium (UO_2^{2+}) was the only one which extracted synergistically. It is also possible that hexavalent plutonium (PuO_2^{2+}) also extracts synergistically from the dialkyl phosphoric acid–neutral phosphate ester mixture.[2] A few years prior to the above work CUNNINGHAM *et al.*[3] at Harwell showed that mixtures of HTTA (thenoyl trifluoroacetone) and TBP (tri-n-butyl phosphate) in benzene would extract praesodymium and neodymium to a greater extent than either reagent alone and they attributed this increase to the probable formation of the complexes $M(TTA)_3$, $M(TTA)_2$ TBP.NO_3, MTTA $(TBP)_2$ $(NO_3)_2$ and $M(TBP)_3$ $(NO_3)_3$. The present author decided to re-examine this work in the light of a possible synergic effect similar to that reported by BAES *et al.* and obtained a much greater enhancement or synergic effect in the system M/TTA/TBP where M is promethium or americium than that reported by BAES for uranium. The species extracted from dilute hydrochloric acid into benzene solution were identified as $Pm(TTA)_3(TBP)_2$ and $Am(TTA)_3(TBP)_2$ with equilibrium constants of $0{\cdot}91 \times 10^{-1}$ and $1{\cdot}1 \times 10^{-1}$ respectively. While this work was in progress, IRVING and EDGINGTON published a note[4] on the synergic effects in the enhanced extraction of uranium from aqueous nitric acid into HTTA and TBP in

* Based on work performed under the auspices of the U.S. Atomic Energy Commission.
† Harwell Exchange Fellow at the Argonne National Laboratory.

[1] C. A. BLAKE, C. F. BAES, K. B. BROWN, C. F. COLEMAN and J. C. WHITE, *Proceedings of the Second International Conference on Peaceful Uses of Atomic Energy, Geneva*, 1958, 15/P/1550 (1958).
[2] J. KENNEDY, F. A. BARFORD and P. C. SAMMOS, AERE/R-3077 (1959).
[3] J. G. CUNNINGHAM, P. SCARGILL and H. H. WILLIS, AERE/C/M 215 (1954).
[4] H. IRVING and D. N. EDGINGTON, *Proc. Chem. Soc.* London, 360 (1959).

cyclohexane. They showed the extracted species to be $UO_2(TTA)_2TBP$ and $UO_2(TTA)_2(TBPO)_3$ (TBPO being tributyl phosphine oxide) with equilibrium constants of $10^{3.9}$ and $10^{16.1}$ respectively. The present author has confirmed this work with uranium using TBP in benzene and obtained similar but slightly lower results than IRVING. This uranium work has also been extended to cover a number of phosphate esters varying from the highly extracting trioctyl phosphine oxide (TOPO) to the almost non-extracting triphenyl phosphate (TPP). The trivalent elements Pm, Am, Tm and Cm were all examined and found to give synergic effects with HTTA and a number of neutral organophosphorus esters. The tetravalent thorium and the divalent calcium also gave greatly enhanced extraction in the same manner. The study presently reported is concerned with the synergic effects obtained with these di, tri, and tetra-valent elements, HTTA and a number of neutral phosphorus esters. Solvent dependencies, acid dependencies and HTTA dependencies have been obtained leading to the identification of various species and to their mixed equilibrium constants.

VOL. 19 1961

EXPERIMENTAL

Sources of materials

Tri-n-octyl phosphine oxide (TOPO) and triphenyl phosphate (TPP) were obtained from Eastman Organic Chemicals and were sufficiently pure to be used without further purification. This was also true for triphenyl phosphine oxide (TPPO) m.p. 150°C obtained from Aldrich Chemical Co. Inc. The tri-n-butyl phosphate (TBP) received from Commercial Solvents Corporation has been purified as described previously:[5] Dibutyl butyl phosphonate (DBBP) from the Virginia Carolina Chemical Co., was also purified by a similar procedure.[5] Thenoyltrifluoroacetone (HTTA) received from the Dow Chemical Co., was recrystallized from benzene and had a molecular weight of 222·2. The β-active 2·6 year ^{147}Pm and 160 day ^{45}Ca were obtained from Isotopes Division of the Oak Ridge National Laboratory.

The β-active rare earth nuclide 129 day ^{170}Tm was obtained from ANL stocks. So also were the α-active nuclides 8×10^4 year ^{230}Th, $1{\cdot}6 \times 10^5$ year ^{233}U, 470 year ^{241}Am and 18 year ^{244}Cm. All the foregoing tracers were subjected to further purification cycles using liquid/liquid extraction techniques.

Determination of distribution ratios

The distribution ratio (K) of a specific nuclide was obtained by dividing the nuclide concentration in the organic phase by its concentration in the aqueous phase, after shaking together an equal volume of aqueous and organic phases for a minimum of four hours at room temperatures (22 $\pm$ 2°C). In several instances, re-equilibrations with fresh aqueous organic phases were carried out and K redetermined, to establish that equilibrium had been attained and that no appreciable concentration changes of the reagents in solution had taken place. Aliquots of each phase were evaporated on 3-mil platinum disks 15/16 in. in diameter, by means of induction heating, for α- and β-counting.

In some instances two nuclides were used in the same solutions, two pairs used being ^{241}Am–^{147}Pm and ^{244}Cm–^{170}Tm. In these cases, for both ^{147}Pm and ^{170}Tm the β-activity was counted through 10 mg of aluminium absorber. Sometimes a correction was required due to the presence of α-activity e.g. a correction of 13 counts/min per 10^3 counts/min of ^{241}Am is necessary when counting ^{147}Pm in the ^{241}Am–^{147}Pm mixture.

Much of this solvent extraction work involved solutions containing low molarities of individual reagents. In order to maintain a reasonably exact treatment of the solvent and other dependencies a constant aqueous activity was maintained and only dilute solutions of the ligands were used. The tracer was also kept at such a concentration level that it was less than a thousandth of the ligand strength. This necessitated, in some instances, using a rather low count in some of the α- and β-assays where the specific activity of the tracer was not very high and where the ligand was less than 10^{-6} molar.

[5] D. F. PEPPARD, W. J. DRISCOLL, R. J. SIRONEN and S. MCCARTY, *J. Inorg. Nucl. Chem.* **4**, 334 (1957).

RESULTS AND DISCUSSION

Extraction of Am, Cm, Pm *and* Tm

Initially, to ascertain whether a synergic effect was obtainable partition coefficients were obtained from a benzene phase 0·2 molar in HTTA or 0·2 molar in TOPO and an aqueous phase 0·010 normal in mineral acid and from mixtures of these benzene solutions with the same constant aqueous phase all containing tracer ^{241}Am and ^{147}Pm.

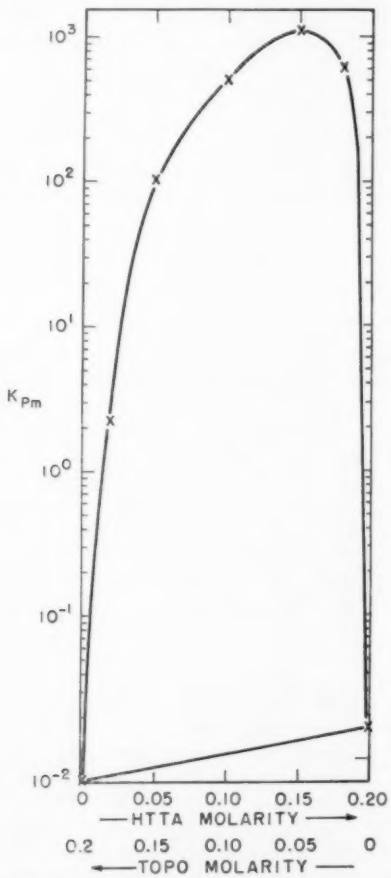

FIG. 1.—Synergic effects due to HTTA/TOPO mixtures (Aqueous phase is 0·01 N HCl).

It was found that the partition coefficients for both Am and Pm were increased by a factor of 10^5 using a benzene solution containing 0·15 molar HTTA and 0·05 molar TOPO when compared with the partition using either 0·2 molar HTTA or 0·2 molar TOPO alone. This large synergic effect is illustrated in Fig. 1.

To obtain information on the possible species being extracted into the benzene phase the three variables in the system $[H^+]$, HTTA and TOPO were examined, keeping two constant at a time. As expected from a trivalent metal–HTTA system it was found that on keeping hydrogen ion and TOPO concentrations constant, while varying the HTTA concentration a log/log plot of partition coefficients of tracer ^{241}Am

and ^{147}Pm against HTTA concentration produced a straight line of slope-3 (Fig. 2). A similar log/log plot varying only hydrogen ion gave a line of slope 3 (Fig. 3). On keeping both hydrogen ion and HTTA concentrations constant, variation of TOPO concentration gave a line of slope 2 (Fig. 4). It was found early in the experimental work that the ester dependency line varied from linearity at about 0·05 molar ester if nitric acid and tracer nitrates were used, but only above 0·1 molar ester if hydrochloric acid and tracer chlorides were used. As the partition coefficients were otherwise

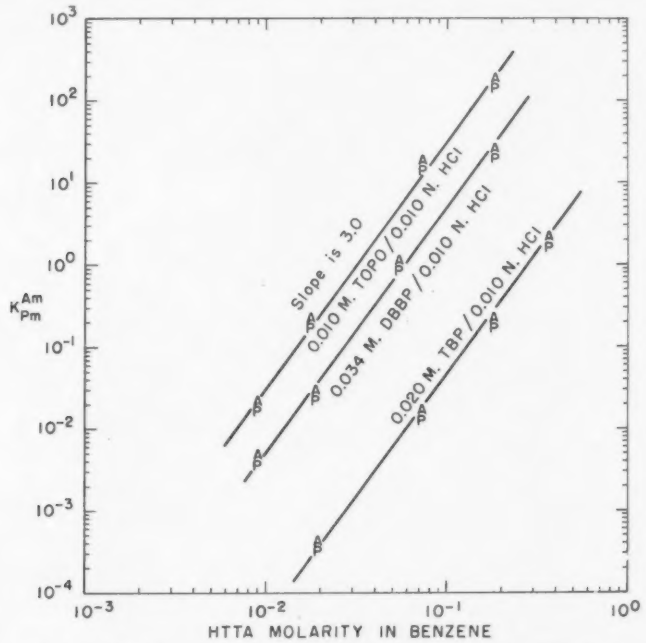

FIG. 2.—Third power dependency of HTTA in HTTA/ester synergistic system.

independent of the aqueous anion, hydrochloric acid and tracer chlorides were used throughout practically all this work.

Similar synergic effects were found with TBP, DBBP, TPPO and TPP and in all cases an ester dependency of two was found (Fig. 4). It is interesting to note that the synergic effect is greatest with the two phosphine oxides, somewhat lower with the phosphonate, appreciably lower with the tributyl phosphate and lowest of all with triphenyl phosphate where substitution of butyl by phenyl groups renders the phosphoryl oxygen atom less basic. Nevertheless the synergic effect produced with HTTA and triphenyl phosphate is still quite appreciable. This variation in synergic effect places the different neutral esters in the same order as their expected donor properties would suggest and in fact in the same order of efficiency of extraction of metal nitrates by these esters.[6] On using tracer ^{244}Cm in a similar series of experiments the same second power ester dependency is observed with both TOPO and TBP. For tracer

[6] T. V. HEALY and J. KENNEDY, *J. Inorg. Nucl. Chem.* **10**, 128 (1959); T. V. HEALY, J. KENNEDY and G. M. WAIND, *J. Inorg. Nucl. Chem.* **10**, 137 (1959).

thulium this second power dependency only appears to hold at high ester concentrations (Fig. 5). At lower ester concentrations and this is specially true for TOPO there appears to be a good first power ester dependency. For comparison the partition coefficients of Pm, Tm, Am and Cm are given together in Fig. 5 to illustrate the ester dependency at constant acidity and constant TTA concentration. It can be seen that the partition coefficients of Am are very slightly greater than those of Pm and slightly less than those of Cm. This is similar to their behaviour on extraction by

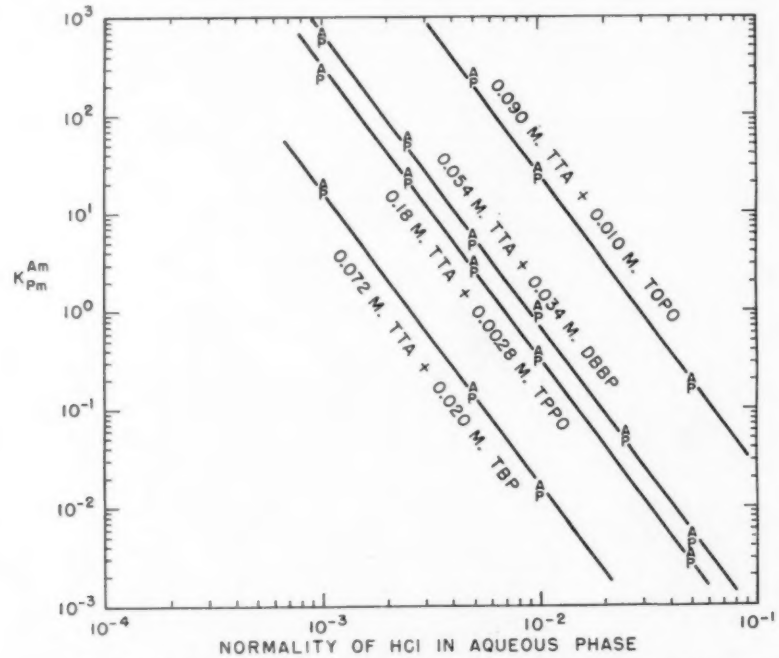

FIG. 3.—Inverse third power dependency of [H⁺] in HTTA/ester synergistic system.

neutral ester of HTTA alone. The partition coefficients of Tm are very different at low ester concentrations, whereas at high ester molarities they are similar to the other trivalent metals. Thus, while the synergic effect of HTTA plus ester only gives a low separation factor for Am, Cm and Pm (β for Cm/Am $\simeq 2$) this effect provides a larger factor for the separation of thulium from the other 3 (β for Tm/Pm $\simeq 100$).

From the above results we assume the reaction goes according to equation (1).

$$M^{3+} + 3HTTA + 2S = M(TTA)_3S_2 + 3H^+ \quad (1)$$

and the equilibrium constant $K = \dfrac{[M(TTA)_3S_2][H^+]^3}{[M^{3+}][HTTA]^3[S]^2}$ (2)

The following Table gives this K value (ignoring activities) for the different species.

Extraction of uranium

The synergic effect of TBP and TBPO on the HTTA extraction of hexavalent uranium has recently been briefly reported by IRVING and EDGINGTON[4] and work by

VOL. 19 1961

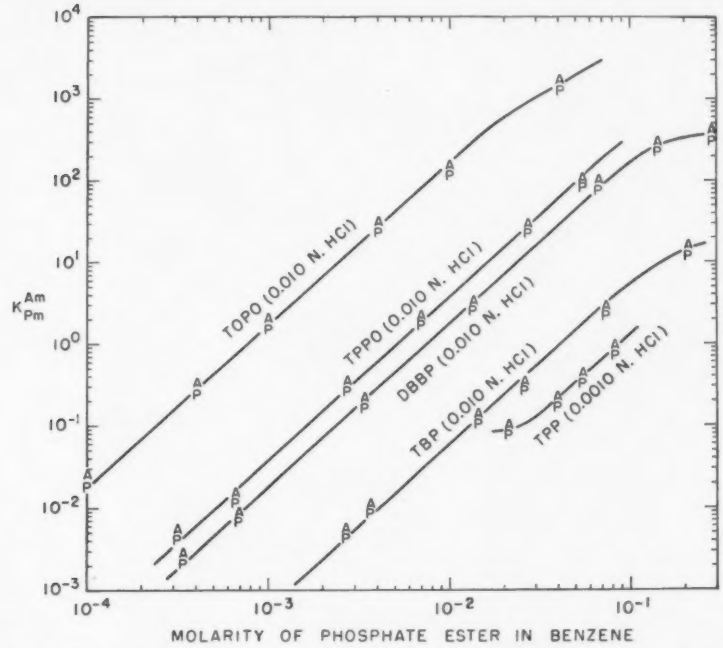

FIG. 4.—Second power dependency of ester in HTTA/ester synergistic system. (All solutions 0·18 M HTTA in benzene).

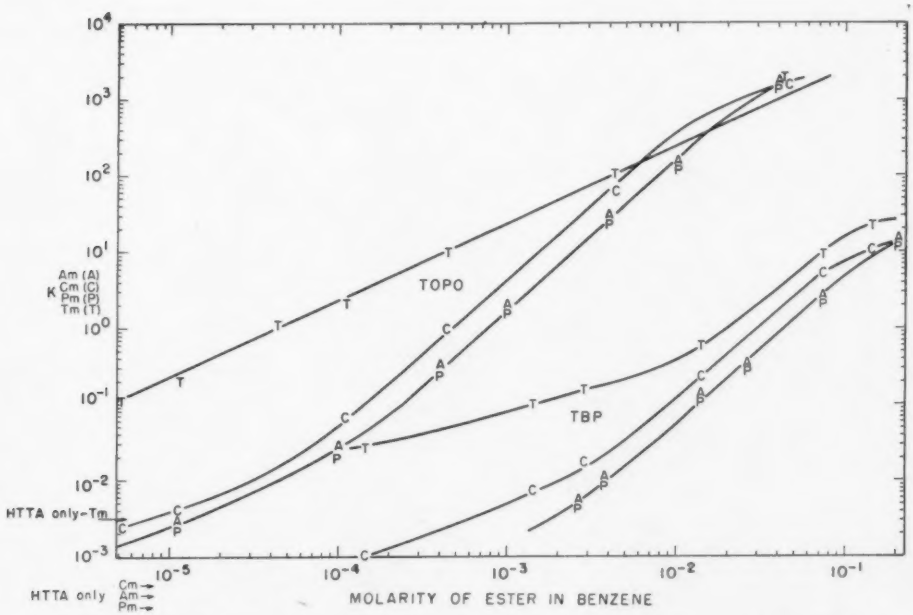

FIG. 5.—First and second power dependencies of ester in HTTA/ester synergistic system (All solutions 0·18 M HTTA in benzene).

TABLE 1.—MIXED EQUILIBRIUM CONSTANTS FOR SPECIES EXTRACTED INTO BENZENE

Solvent	TOPO	TPPO	DBBP	TBP	TPP	
Metal Am	$Am(TTA)_3(TOPO)_2$ $3{\cdot}2 \times 10^2$	$Am(TTA)_3(TPPO)_2$ 7·0	$Am(TTA)_3(DBBP)_2$ 3·2	$Am(TTA)_3(TBP)_2$ $1{\cdot}1 \times 10^{-1}$	$Am(TTA)_3(TPP)_2$ $2{\cdot}3 \times 10^{-5}$	Species *K* value
Cm	$Cm(TTA)_3(TOPO)_2$ $6{\cdot}7 \times 10^2$	—	—	$Cm(TTA)_3(TBP)_2$ $2{\cdot}0 \times 10^{-1}$	—	Species *K* value
Pm	$Pm(TTA)_3(TOPO)_2$ $2{\cdot}7 \times 10^2$	$Pm(TTA)_3(TPPO)_2$ 6·0	$Pm(TTA)_3(DBBP)_2$ 2·7	$Pm(TTA)_3(TBP)_2$ $9{\cdot}1 \times 10^{-2}$	$Pm(TTA)_3(TPP)_2$ $2{\cdot}0 \times 10^{-5}$	Species *K* value
Tm	$Tm(TTA)_3(TOPO)_1$	—	—	$Tm(TTA)_3(TBP)_2$ $4{\cdot}6 \times 10^{-1}$	—	Species *K* value

VOL 1 196

the present author confirms this effect. Fig. 6 shows the synergic effect of two other phosphine oxides TOPO and TPPO and the two phosphates TBP and TPP. Benzene was used as organic diluent and the aqueous phase was 0·010 molar HCl whereas IRVING used cyclohexane and 0·010 molar HNO_3 respectively. IRVING's work indicated formation of the complexes $UO_2(TTA)_2TBP$ and $UO_2(TTA)_2(TBPO)_3$. Fig. 5 shows slopes of unity for TPP, TBP and TPPO dependency but a slope of 2 for TOPO. Coupling these with hydrogen ion dependency of two (Fig. 7) the present work

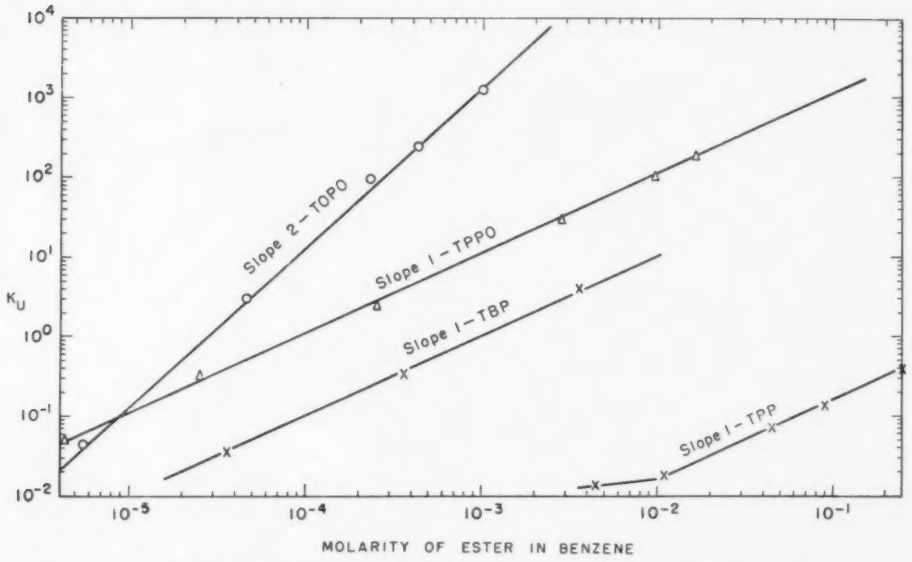

FIG. 6.—First and second power dependencies of esters in UO_2^{2+}/HTTA/ester synergistic system (All solutions 0·018 M HTTA in benzene, Aq. phase 0·01 N HCl).

indicates the following species $UO_2(TTA)_2TPP$, $UO_2(TTA)_2TBP$, $UO_2(TTA)_2TPPO$ and $UO_2(TTA)_2(TOPO)_2$. Assuming the reaction goes as in equation (3)

$$UO_2^{2+} + 2HTTA + xS = UO_2(TTA)_2S_x + 2H^+ \tag{3}$$

the equilibrium constant $K = \dfrac{[UO_2(TTA)_2S_x][H^+]^2}{[UO_2^{2+}][HTTA]^2[S]^x}$ (4)

and both the K value (neglecting activities) and the species are given in the following Table.

The mixed equilibrium constant for the species $UO_2(TTA)_2TBP$ recorded by IRVING[4] is somewhat greater than that in Table 2 but this is probably due to his use of cyclohexane instead of benzene as inert diluent—see Part II of this series.[7] Here also the synergic effects of the different phosphate esters is in the order to be expected from the electron donor properties of these solvents. Again it is interesting to note that triphenyl phosphate which normally extracts practically no uranium by itself can increase the HTTA extraction coefficient several hundred times.

[7] T. V. HEALY, Part II of this series. *J. Inorg. Nucl. Chem.* **19**, 328 (1960).

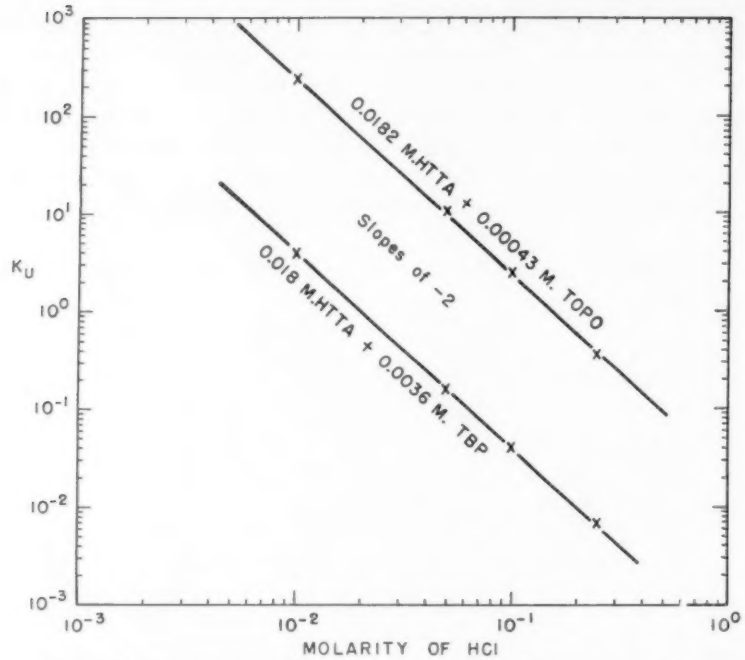

FIG. 7.—Inverse second power dependency of [H⁺] in HTTA/ester synergistic system.

TABLE 2.—MIXED EQUILIBRIUM CONSTANTS FOR URANYL SPECIES EXTRACTED INTO BENZENE

Solvent	TOPO	TPPO	TBP	TPP
Species	$UO_2(TTA)_2(TOPO)_2$	$UO_2(TTA)_2TPPO$	$UO_2(TTA)_2TBP$	$UO_2(TTA)_2TPP$
K Value	$4{\cdot}1 \times 10^8$	$3{\cdot}5 \times 10^3$	$3{\cdot}0 \times 10^2$	0·48

Extraction of calcium

Synergism has also been demonstrated with the alkaline earth calcium. An enhancement of 10^5 in the extraction rate is obtained if 0·06 molar TOPO is added to 0·18 molar HTTA in cyclohexane. A solvent dependency of two is shown in Fig. 8 for both TOPO and TBP in cyclohexane and a hydrogen ion dependency of two for the system TOPO–HTTA–$CaCl_2$–HCl (Fig. 9) indicating the species $Ca(TTA)_2(TBP)_2$ and $Ca(TTA)_2(TOPO)_2$ and the mixed equilibrium constants

$$K = \frac{[Ca(TTA)_2S_2][H^+]^2}{[Ca^{2+}][HTTA]^2[S]^2} \tag{5}$$

are $5{\cdot}4 \times 10^{-4}$ and $1{\cdot}1 \times 10^{-2}$ for S equal to TBP and TOPO respectively.

Extraction of thorium

Here again an exceptionally large synergic effect can be demonstrated as shown in Fig. 10. An enhancement of $>10^4$ in the extraction coefficient may be obtained when 1 per cent of the HTTA is replaced by TOPO. A solvent dependency of 1 is shown in

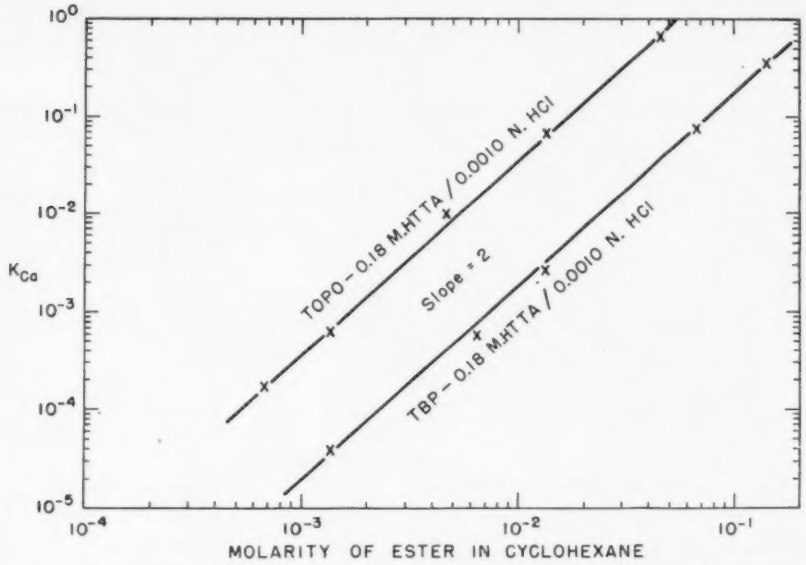

FIG. 8.—Second power dependencies of esters in Ca^{2+}/HTTA/ester synergistic system.

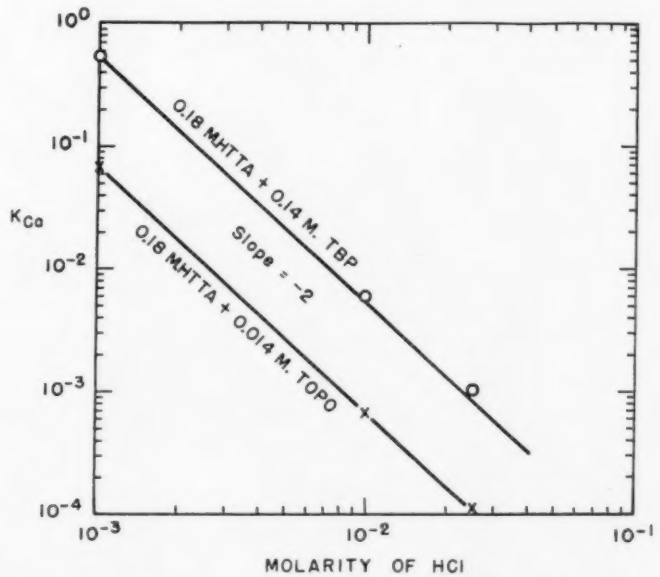

FIG. 9.—Inverse second power dependency of $[H^+]$ in HTTA/ester synergistic system.

Fig. 10 for all three esters TOPO, TBP and TPP. A hydrogen ion dependency and a HTTA dependency of $3\frac{1}{2}$–4 (Figs. 11–12) indicate that the species is probably $Th(TTA)_4S$. The mixed equilibrium constants, ignoring activities are $2{\cdot}8 \times 10^{10}$, $7{\cdot}0 \times 10^7$ and $3{\cdot}5 \times 10^5$ for the solvents TOPO, TBP and TPP respectively.

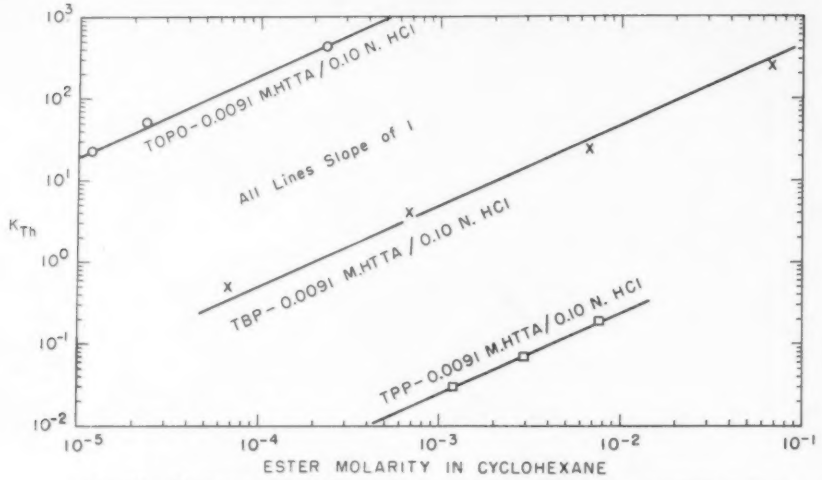
TOPO – 0.0091 M.HTTA / 0.10 N. HCl
All Lines Slope of 1
TBP – 0.0091 M.HTTA / 0.10 N. HCl
TPP – 0.0091 M.HTTA / 0.10 N. HCl
K_{Th}
ESTER MOLARITY IN CYCLOHEXANE

FIG. 10.—First power dependency of esters in Th^{4+}/HTTA/ester synergistic systems.

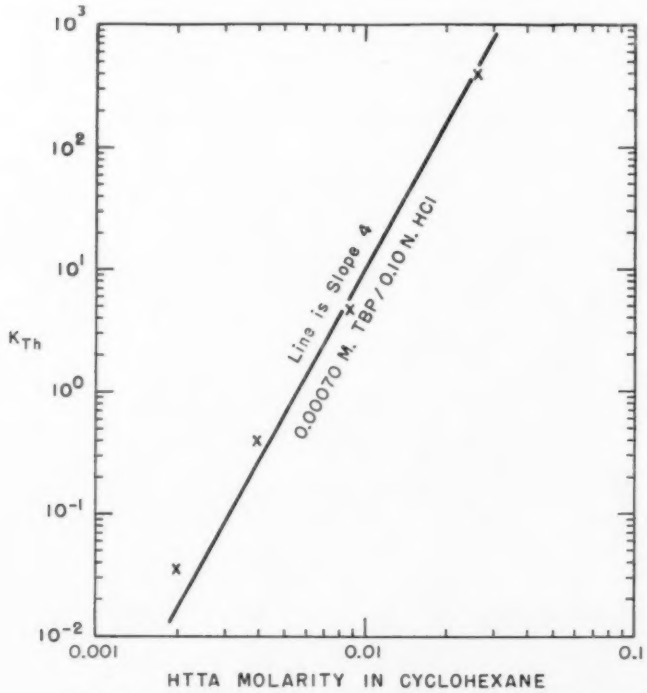

FIG. 11.—HTTA dependency in Th^{4+}/HTTA/TBP synergistic system.

Synergic effects with different metals

The above results show that synergism is by no means confined to uranyl ion but is demonstrated with divalent, trivalent and tetravalent ions. Only a few metals have been selected for this study and in all cases large synergic effects have been

demonstrated. It is most likely that the majority of metal ions, including monovalent ions, will also show similar synergic effects.

The degree of enhancement of the extraction of the metal into the HTTA–phosphate ester solution varies somewhat from metal to metal but is not always appreciably greater for the more extractable thorium and uranyl ions than the others although the actual partition coefficients may be very much higher.

Synergic effects with different neutral esters

Different types of organophosphorus esters were chosen in conjunction with HTTA to demonstrate the synergic effect. Trioctyl phosphine oxide contains an extremely powerful donor oxygen and is one of the most highly extracting of the neutral esters.

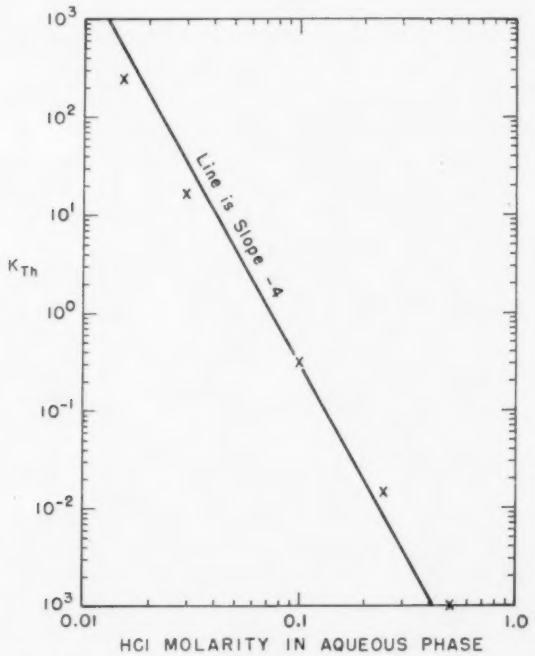

FIG. 12.—$[H^+]$ dependency in Th^4/HTTA/TBP synergistic system.

The synergic effect produced with HTTA and this ester was in all cases greater than the effects produced with HTTA and other less powerful phosphorus ester extractants. Another ester, triphenyl phosphine oxide was chosen because of possible steric hindrance effects, but no noticeable difference was found except the expected lower degree of extraction in conformity with its lower electron donor properties. Dibutyl butyl phosphonate and tributyl phosphate were chosen as typical examples of the neutral phosphonate and phosphate esters and again the relative extraction coefficient with HTTA was in conformity with their relative donor properties. Triphenyl phosphate was used as an example of an ester which gives practically no extraction of calcium, the rare earths and thorium and only a poor extraction of uranium. It was thought that this ester could have no synergic effect on HTTA extraction of these

metals but a very definite effect was recorded and in some cases the extraction with HTTA alone was increased by several hundredfold on addition of this very feeble ester extractant.

Although several neutral esters and several metals were examined in the synergistic system–metal/HTTA/neutral ester no variants for HTTA in the system are at present being reported although there is a strong possibility that some variants may prove to have a larger synergic effect than HTTA itself. It is hoped that the synergic effects of a number of variants will be the subject of a separate paper. The HTTA substitute should form a neutral complex, preferably a chelated complex with the metal, but it should not form such a weak complex that the direct co-ordinating effect of the ester overcomes the joint synergistic complex.

Rates of reaction

The rate of reaction in the synergistic system has been briefly studied with the rare earths. It was found that after addition of the organic solution of HTTA/TBP to the aqueous acid salt the partition coefficient gradually increased with time reaching a maximum within a few hours but in many instances this figure decreased again, sometimes by a factor of up to five, final equilibrium being reached within 4 hr. In the absence of the neutral ester, the time for equilibrium with HTTA alone was usually from 1 to 3 hr. In the case of the neutral ester alone (No HTTA) this time was usually a few minutes. However, after establishment of equilibrium in an aqueous acid salt/TTA-diluent mixture (1–3 hr), addition of the neutral ester caused a synergic effect on the partition coefficient of the metal by a factor of up to 10^5 in a few minutes, that is, upon establishment of the new equilibrium. This indicates that the rate determining step in the synergetic reaction of the metal/TTA/ester system is the usual slow keto-enol equilibrium,[8] and that the synergetic reaction must be caused by the action of the neutral ester on the metal–TTA complex.

Reaction mechanism

This enhancement of metal extraction or synergic effect, due to the combination of HTTA and a phosphorus ester, is extremely marked and is much greater than the previously reported synergic effects[1] due to a combination of a dialkyl hydrogen phosphate and certain neutral organophosphates such as TBP or TOPO. These latter effects on the extraction of uranium have so far been explained in two different ways[1,9] as in equations (6) and (7)

$$UO_2A_2(HA)_2 + B \rightleftarrows UO_2A_2(HA)_2B \quad (6)$$

$$UO_2A_2(HA)_2 + 2B \rightleftarrows UO_2A_2B_2 + (HA)_2 \quad (7)$$

The first mechanism (equation 6) postulated by the discoverers[1] of this effect assumes that this synergic effect is due to the addition of the nonionic molecule B (such as TBP) through a hydrogen bond to the extracted species, $UO_2A_2(HA)_2$ where $(HA)_2$ is a dimeric dialkyl acid phosphate. So far, there is inadequate experimental support for this hypothesis. Recently more adequate support[10,11] has become available for the second mechanism (equation 7) proposed by KENNEDY[9] which involves the

[8] E. L. ZEBROSKI, TID, 1098 (1955); J. C. REID, TID, 1112 (1956).
[9] J. KENNEDY, AERE/C/M, 369 (1958).
[10] D. DYRSSEN and L. KUCA, *Acta Chem. Scand.* 1945 **14**, (1960).
[11] A. M. DEANE, J. KENNEDY and P. G. SAMMOS, *Chem. and Industr.* 443, (1960).

substitution of two molecules of the neutral ester B for two molecules of the acid phosphate HA.

Neither of the above mechanisms for this synergic effect on uranium extraction appears to apply directly to the much larger general synergic effect found for a number of metals with HTTA and neutral phosphate esters. KENNEDY's suggested mechanism[9] also involves increasing the co-ordination number of the uranium above six and while this is possible in going from $UO_2(TTA)_2$ to $UO_2(TTA)_2S_x$, this mechanism cannot be used in the formation of the complex $Pm(TTA)_3S_2$.

One possibility for explaining the synergic effect is that an aquo metal TTA complex such as $Pm(TTA)_3(H_2O)_x$ is rendered less hydrophilic by the substitution of a neutral ester for the water group or groups such as $Pm(TTA)_3(TBP)_2$. In such a complex the neutral ester would probably be attached, through its P=O bond to the TTA. Supporting evidence for this mechanism comes from the macro isolation of the water insoluble crystalline white thorium and yellow uranium/TTA/TBP solid complexes with approximately the expected metal/TTA/TBP mole ratios which appear to contain practically no water. This does not preclude the possibility of formation of some metal/TTA/ester complexes which have retained some water of constitution in their complexes.

VOL. 19 1961

In view of the diverse types of complexes produced with metals of different basicities and neutral esters of different electron donor strengths, no satisfactory general explanation seems possible with direct co-ordination of the neutral ester to the metal. If one assumes that the HTTA and the ester both have monodentate bonds with the metal through the C—O and P=O bonds respectively, then one would expect some interaction between HTTA and the ester in the absence of the metal. Evidence from infra-red spectral work indicates no apparent interaction between HTTA and the esters TOPO and TBP but definite interaction in the mixed metal complexes. This infra-red work together with absorption spectra and water contents of organic phases and solid complexes carried out in collaboration with J. R. FERRARO will be discussed in Part III of this series.[12]

Acknowledgements—Thanks are due for valuable help in discussions to D. F. PEPPARD, G. W. MASON and J. R. FERRARO.

[12] J. R. FERRARO and T. V. HEALY, Part III of this series. To be published.

J. Inorg. Nucl. Chem., 1961, Vol. 19, pp. 328 to 339. Pergamon Press Ltd. Printed in Northern Ireland

SYNERGISM IN THE SOLVENT EXTRACTION OF DI-, TRI- AND TETRAVALENT METAL IONS*—II

SYNERGIC EFFECTS IN SO-CALLED INERT DILUENTS

T. V. HEALY†
Argonne National Laboratory, Argonne, Illinois

(*Received* 5 *October* 1960; *in revised form* 7 *November* 1960)

Abstract—Greatly enhanced extractions (synergism) for di, tri and tetravalent metals have been reported for the system M^{n+}/HTTA/S/diluent where HTTA is thenoyltrifluoracetone and S varies from the highly polar tri-octyl phosphine oxide to the weakly basic triphenyl phosphate. The extracted species $M(TTA)_nS_x$ is the same, whatever "inert" diluent is used, but the partition coefficients of the metal ion vary over several powers of ten, sometimes by a factor much greater than that obtained by the synergic effect itself. The effect, on the extraction, of so-called "inert" diluents such as cyclohexane, hexane, carbon tetrachloride, benzene and chloroform has been studied under various conditions. In all cases the distribution ratio decreases as the diluent is changed from cyclohexane in the above sequence, chloroform giving the lowest partition coefficient. This order is in the same sequence as the water solubility in the pure diluent and the diluent effect on metal extraction is probably connected through the diluent water content with the permanent or induced diluent dipole.

THE word "synergism" was first coined by American workers BAES *et al.*,[1] to describe their discovery of a definite enhancement of the extraction of uranium (also called synergic effect) from aqueous solution by a mixture of an acidic dialkyl phosphate and certain neutral organophosphorus esters, the resulting mixture giving a better extraction of uranium than either the acid or neutral phosphate alone. These synergic effects have recently been demonstrated by IRVING *et al.*,[2] who obtained a much larger enhancement for the extraction of uranium by substituting the acidic thenoyl trifluoracetone (HTTA) for the acidic dialkyl phosphate. The present author has shown similar very large enhancements for divalent, trivalent and tetravalent metals[3] by using HTTA with a large number of neutral organophosphorus esters. It has now been shown that certain so called "inert diluents" can have an effect on the enhancement of metal extraction by HTTA plus neutral ester which in some instances is much greater than the original synergic effect. A typical example is the comparison of the partition coefficient of Pm where, say, this figure is taken relatively as unity for either of the systems 0·01 N HCl/HTTA in benzene or cyclohexane or 0·010 N HCl/TBP in benzene or cyclohexane, and addition of 5 per cent of the TBP benzene system to the HTTA system in benzene gives a synergic enhancement from 1 to 500. However, addition of 5 per cent of the TBP cyclohexane system to the HTTA system in cyclohexane gives a synergic enhancement from 1 to 10^6. This means that substitution of one "inert" diluent cyclohexane for another "inert" diluent benzene gives a change in the partition coefficient by a factor of 2,000, that is, much greater than the synergic effect in benzene alone. This paper describes the effect of different so-called inert

* Based on work performed under the auspices of the U.S. Atomic Energy Commission.
† Harwell Exchange Fellow at the Argonne National Laboratory.

[1] C. A. BLAKE, C. F. BAES, K. B. BROWN, C. F. COLEMAN and J. C. WHITE, *Proceedings of the Second International Conference on Peaceful Uses of Atomic Energy, Geneva* 1958, 15/P/1550 (1958).
[2] H. IRVING and D. N. EDGINGTON, *Proc. Chem. Soc., London* 360 (1959).
[3] T. V. HEALY, Part I of this series. *J. Inorg. Nucl. Chem.* This issue, p. 314.

diluents on the synergic effect obtained by mixing HTTA and neutral esters with di-valent, trivalent and tetravalent metals.

EXPERIMENTAL

Sources of materials

Tri-n-butyl phosphate (TBP) was obtained from Commercial Solvents Corporation and has been purified as described previously.[4] Tri-n-octyl phosphine oxide (TOPO) and triphenyl phosphate (TPP) were obtained from Eastman Organic Chemicals and were sufficiently pure to be used without further purification.

The α-active nuclides 8×10^4 year ^{230}Th, $1{\cdot}6 \times 10^5$ year ^{233}U, 470 year ^{241}Am, and 18 year ^{244}Cm and the β-active nuclide 129 day ^{170}Tm were all obtained from ANL stocks. The other beta active nuclides 2·6 year ^{147}Pm and 160 day ^{45}Ca were obtained from Isotopes Division of the Oak Ridge National Laboratory. All the above tracers were subjected to further purification cycles using liquid/liquid extraction techniques.

Determination of distribution ratios

The distribution ratio (K) of a specific nuclide is defined as the concentration in the organic phase divided by that in the aqueous phase. A shaking time of 4 hr was found to be sufficient to reach equilibrium at room temperatures ($22 \pm 2°C$). In many instances, re-equilibrations with fresh aqueous or organic phases were carried out and K redetermined to ensure that equilibrium had been reached and that there was no appreciable changes in reagent concentration.

K values were determined by alpha or beta counting of aliquots of each phase after evaporations by induction heating on 3-mil platinum disks $\frac{1}{16}$ in. in diameter. In some instances two nuclides were used in the same solution and these were counted as described previously.[3] For solvent and other dependencies it was necessary to maintain a reasonably exact treatment so constant aqueous activities were maintained and only dilute solutions of the ligands were used and the conditions were generally similar to those described in Part I of this series.[3]

RESULTS AND DISCUSSION

"Inert" diluent effect on extraction of trivalent cations

It was first noticed that the large enhancement of extraction of promethium on using a mixture of HTTA and a neutral organophosphate ester was appreciably greater when using some inert diluents than others. A systematic study was therefore made using a series of diluents, these being the common non polar solvents which alone do not extract inorganic salts and are normally classed as "inert" diluents. Most surprising differences were found in the extraction rates of promethium and americium using these diluents, these differences sometimes being greater than the large synergic effects themselves. The following table gives the comparison of promethium partition coefficients (K_{Pm}) under identical conditions except for the variation of the diluent. The aqueous phase is 0·010 N HCl and the organic phase contains 0·18 M HTTA plus 0·18 M TBP in the various diluents. The figure in the last column is the K_{Pm} for HTTA alone with no TBP added i.e. the synergic effect is absent. K_{Pm} in the case of TBP or HTTA alone using different inert diluents varies overall by a factor of less than ten.

TABLE 1.—EFFECT OF "INERT" DILUENT ON Pm EXTRACTION UNDER OTHERWISE IDENTICAL CONDITIONS

Inert diluent	Cyclohexane	Hexane	CCl_4	Benzene	Hexone (MIK)	$CHCl_3$	HTTA/Benzene alone—no TBP
K_{Pm}	5×10^4	2×10^3	5×10^2	2×10	6×10^{-1}	10^{-1}	10^{-4}

[4] D. F. PEPPARD, W. J. DRISCOLL, R. J. SIRONEN and S. MCCARTY, *J. Inorg. Nucl. Chem.* **4**, 334 (1957).

This table shows that the synergic effect of the addition of TBP in $CHCl_3$ solution namely 10^3 is dwarfed by the much larger difference of 5×10^5 in changing from "inert" diluent $CHCl_3$ to another "inert" diluent cyclohexane. As reported previously[3] a log/log plot of the partition coefficients (K_{Pm}^{Am} of americium and promethium against the molarity of TBP at constant aqueous activity and constant HTTA molarity gives a slope of two indicating the complex $M(TTA)_3(TBP)_2$. This same slope at different levels is obtained with all the diluents tried from cyclohexane to chloroform despite the difference in K which varies by a factor of greater than 10^5. This slope of 2 for the different diluents is shown in Fig. 1. HTTA plus TBP in chloroform do not have a synergic effect on the metal extraction until 10^{-2} molar TBP is present in contrast to the other diluents. The order of the extraction is in the inverse order of increasing polarity of the diluents, so the effect of a solvent, hexone (methyl isobutyl ketone) which is more polar than chloroform, was examined. HTTA plus hexone do not have any appreciable synergic effect on the extraction of metals but hexone itself is a good extractant for those trivalent metals. Addition of TBP has practically no effect on the extraction from the HTTA/hexone mixture until about 10^{-2} molar TBP has been added and the synergic effect is only really apparent above 10^{-1} molar TBP. Thus it appears that in the more polar diluents particularly hexone the diluent arrests the formation of the double complex $M(TTA)_3(TBP)_2$. Fig. 2 gives a comparison of the direct effect of cyclohexane and benzene on the extraction of both the rare earths Pm and Tm and the trivalent actinides americium and curium. It is interesting to note that, in the case of thulium, the complex at low TBP concentrations changes from two solvent molecules $Tm(TTA)_3(TBP)_2$ to one $Tm(TTA)_3TBP$. This diluent effect was not particular to the HTTA/TBP/diluent system and Fig. 3 shows the same effect as Fig. 2 with the more strongly basic TOPO substituted for TBP. Once again the thulium appears at low TOPO concentrations to form the complex with one solvent molecule $Tm(TTA)_3TOPO$ as distinct from the other trivalent complexes $Pm(TTA)_3(TOPO)_2$ $Am(TTA)_3(TOPO)_2$ and $Cm(TTA)_3(TOPO)_2$. This is true for both diluents benzene and cyclohexane. Fig. 4 shows the same large difference in extraction rates for Pm and Am between benzene and cyclohexane in the solvent system HTTA/TPP/diluent using the much less basic triphenylphosphate which alone does not extract trivalent metals.

It has been shown in the previous paper[3] that the hydrogen ion dependency in the system M^{3+}/HTTA/phosphorus ester/benzene was inverse third power. Fig. 5 shows the same inverse third power dependency using either TBP or TPP with the diluent cyclohexane although the actual partition coefficients are much higher than are given in the benzene diluent system. Similarly Fig. 6 shows a third power dependency for HTTA in the system M^3/HTTA/TBP/cyclohexane as was found previously[3] with benzene as diluent.

"*Inert*" *diluent effect on extraction of uranyl ion*

A comparison of cyclohexane, carbon tetrachloride and benzene diluents was carried out with uranyl ion in the same manner as for the trivalent rare earths and actinides. By means of the same log/log plot of K_U against the phosphorus ester molarity, slopes of about unity were obtained in the system UO_2^{2+}/HTTA/TBP/diluent with both cyclohexane and benzene as diluents (see Fig. 7) indicating the species $UO_2(TTA)_2TBP$. Those two diluents however only show a difference in K_U by

VOL. 19 1961

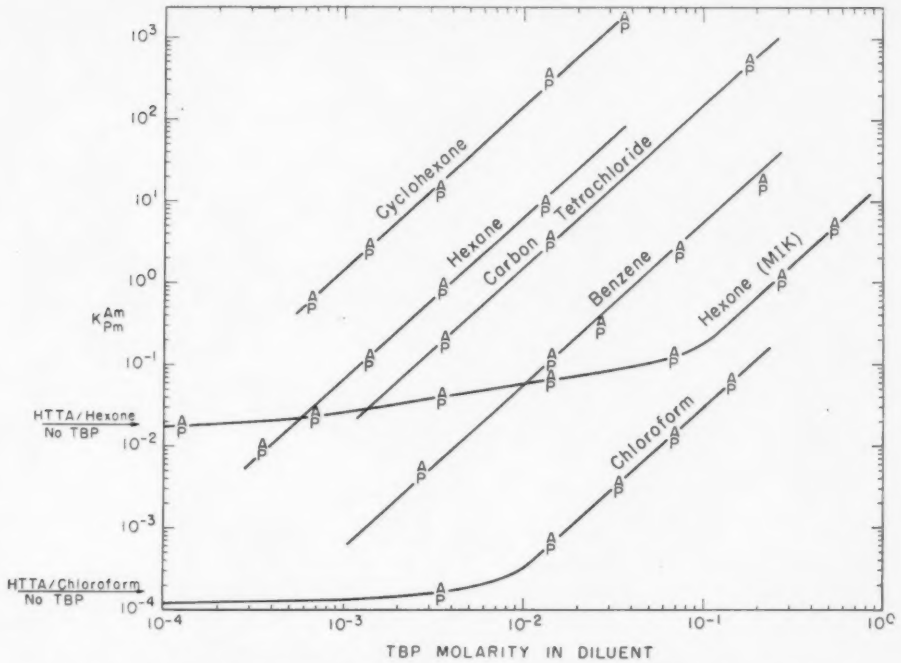

FIG. 1.—Effect of diluents on M^{3+} extraction by HTTA/TBP/diluent synergistic system. (All solutions contain 0·18 M HTTA/0·010 N HCl).

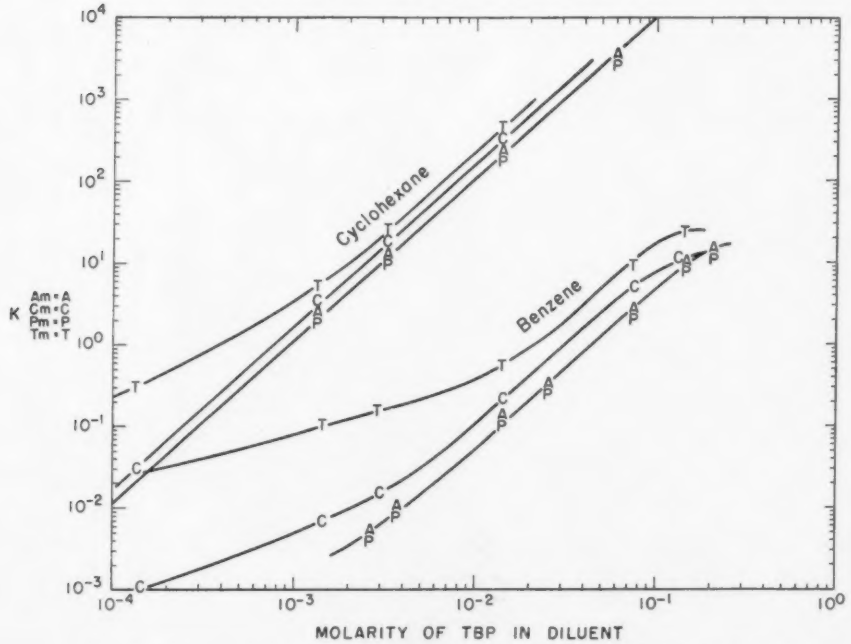

FIG. 2.—Comparative effect of two diluents in the M^{3+}/HTTA/TBP/diluent synergistic system. (All solutions 0·18 M HTTA/0·010 N HCl).

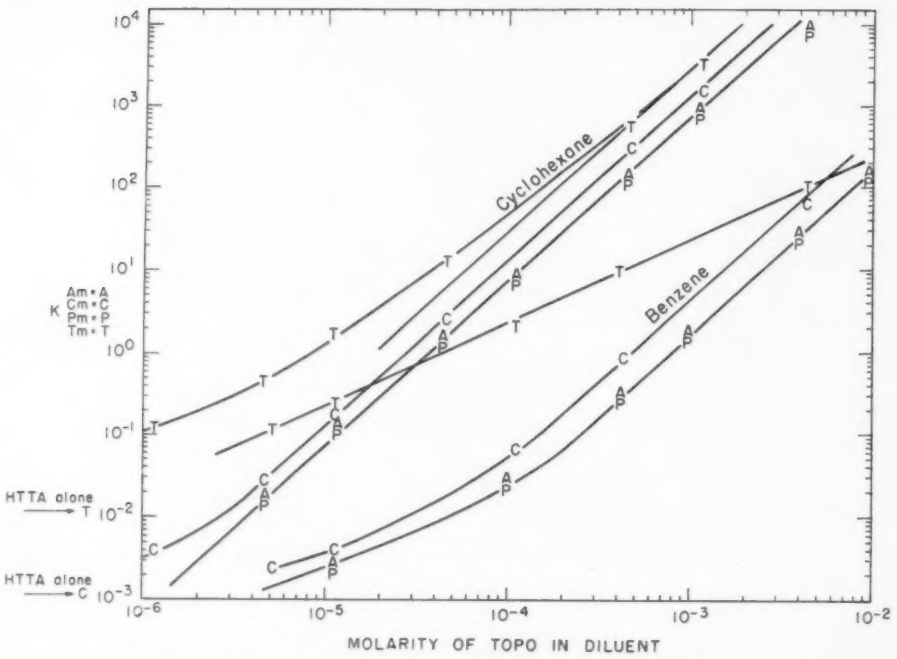

FIG. 3.—Comparative effect of two diluents in the M^{3+}/HTTA/TOPO/diluent synergistic system. (All solutions contain 0·18 M HTTA/0·010 N HCl).

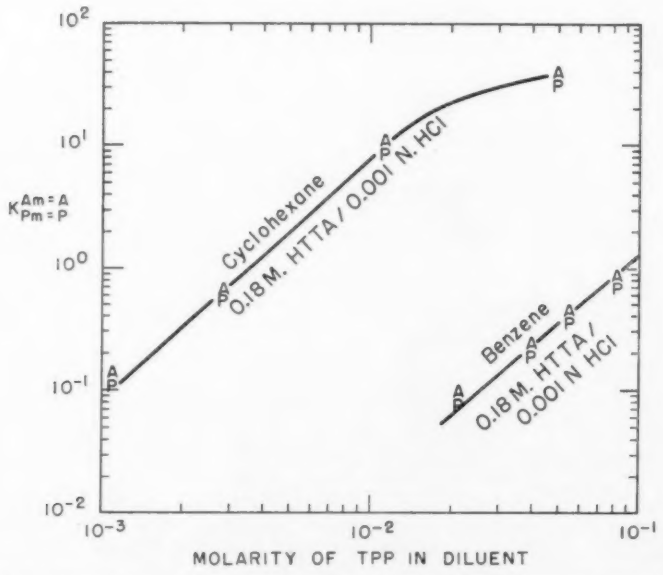

FIG. 4.—Second power dependency of TPP in M^{3+}/HTTA/TPP/diluent synergistic system.

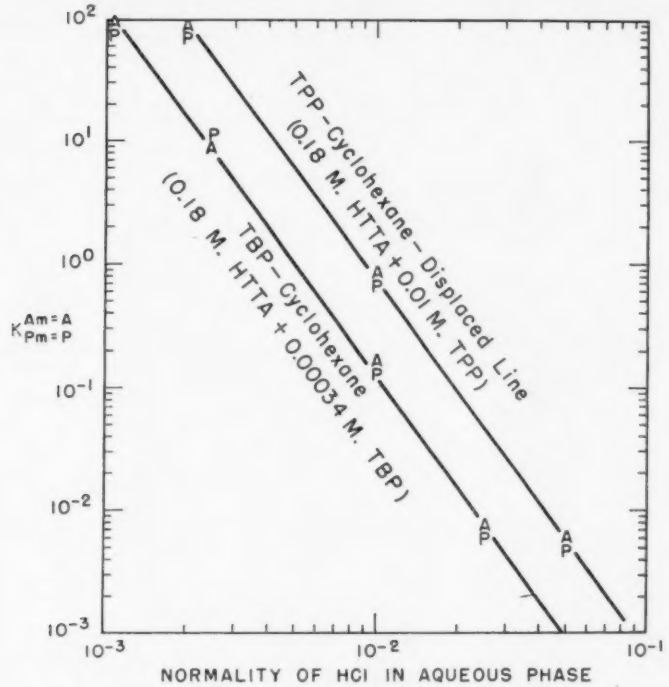
TPP-Cyclohexane-Displaced Line
(0.18 M. HTTA + 0.01 M. TPP)
(0.18 M. HTTA + 0.00034 M. TBP)
TBP-Cyclohexane
$K^{Am=A}_{Pm=P}$
NORMALITY OF HCl IN AQUEOUS PHASE

FIG. 5.—Inverse third power [H^+] dependency in M^{3+}/HTTA/ester/diluent synergistic system.

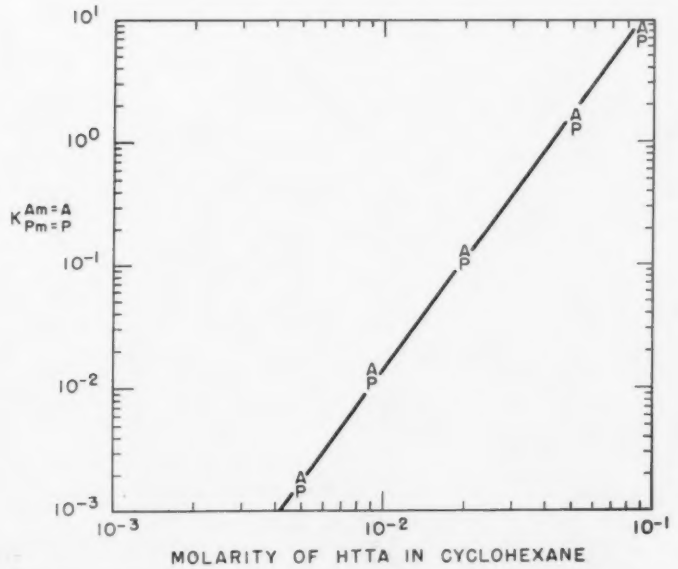

FIG. 6.—Third power dependency of HTTA in the M^{3+}/HTTA/TBP/cyclohexane synergistic system.

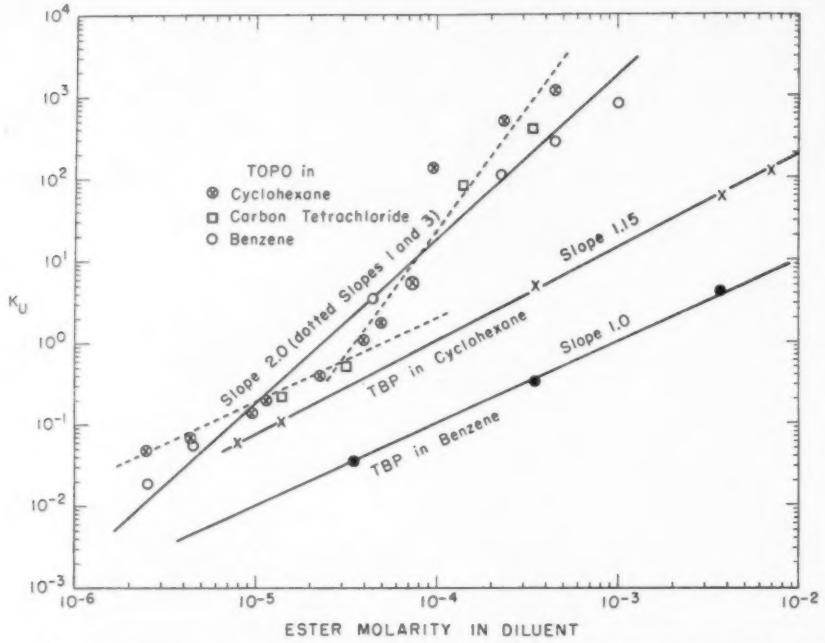

FIG. 7.—Comparative effect of diluents in the UO_2^{2+}/HTTA/ester/diluent synergistic system. (All solutions 0·018 M HTTA/0·01 N HCl).

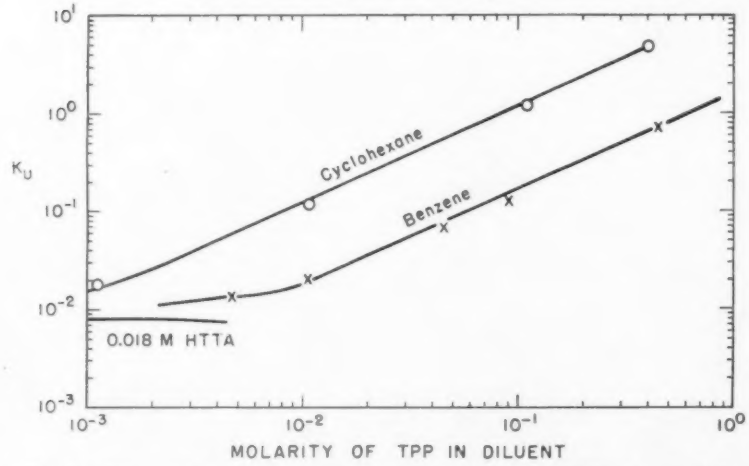

FIG. 8.—Comparative effect of diluents in the UO_2^{2+}/HTTA/TPP/diluent synergistic system. (All solutions 0·018 M HTTA/0·010 N HCl).

a factor of 10 in sharp contrast to the corresponding difference in the rare earth K_{Pm} of over 2000. As with the rare earths the $[H^+]$ dependency in this system is unchanged for the two diluents (see Fig. 9). Substitution of TBP by the more basic TOPO shows as even smaller variance in K_U among the three diluents cyclohexane, carbon tetrachloride and benzene but the slope of the line for TOPO dependency (Fig. 7) is approximately two. It appears more likely that at low TOPO concentrations it is

unity whereas at higher concentrations it is three indicating formation of the species $UO_2(TTA)_2TOPO$ and $UO_2(TTA)_2(TOPO)_3$.

Substitutions of TBP by the much less basic triphenyl phosphate also shows only a small variance in K_U between the diluents cyclohexane and benzene of somewhat less than ten, the extracted species being $UO_2(TTA)_2TPP$ (Fig. 8).

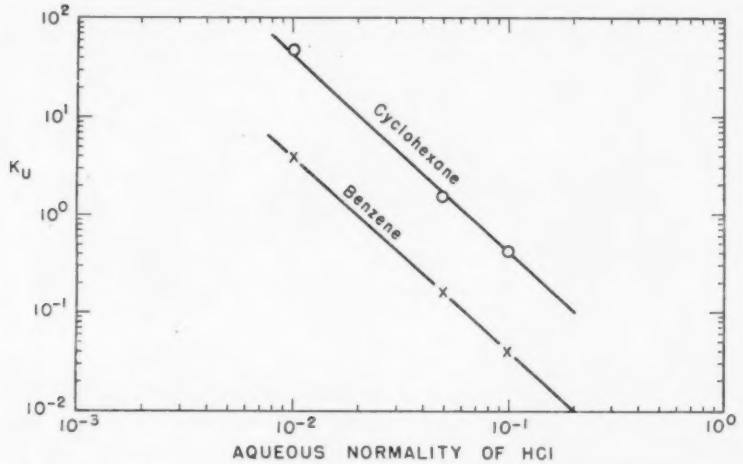

FIG. 9.—Inverse second power [H^+] dependency for the UO_2^{2+}/HTTA/TBP/diluent synergistic system. (All solutions 0·018 M HTTA plus 0·0036 M TBP).

"Inert" diluent effect on extraction of thorium

The synergistic system Th^{4+}/HTTA/ester/diluent has also been examined using the three diluents cyclohexane, benzene and chloroform. The TOPO dependency of unity indicating $Th(TTA)_4TOPO$ is the same in all three cases despite large differences in actual distribution ratios which vary by factors of 2500 : 5 : 1 for the three diluents respectively (Fig. 10). Here it is seen that this large diluent effect on partition coefficients of Th is similar to those of Am, Pm, Cm and Tm and looks very different from the small diluent effect on the uranyl ion. On varying the neutral organophosphorus ester from TOPO to TBP the same effect applies, the extraction ratios for the three diluents cyclohexane, benzene and chloroform being $>1000:10:1$ respectively. The TBP dependency is unity for benzene but the complex $Th(TTA)_4TBP$ appeared to be appreciably less soluble in benzene than in cyclohexane or chloroform. This low solubility is indicated by the poor mass balance for Th on reaching a certain low concentration of the complex in benzene. The TBP dependency in the other two diluents appeared to be close to unity (0·8 and 1·5 respectively) and no reason for this variation is apparent.

"Inert" diluent effect on Ca^{2+} extraction

A comparison of the effect of the two diluents cyclohexane and benzene in the synergistic system Ca^{2+}/HTTA/TOPO/diluent indicates in both cases extraction of the species $Ca(TTA)_2(TOPO)_2$ but the extraction factor is 25:1 in favor of the cyclohexane (Fig. 12). Thus the diluent effect in this calcium extraction is appreciably greater than

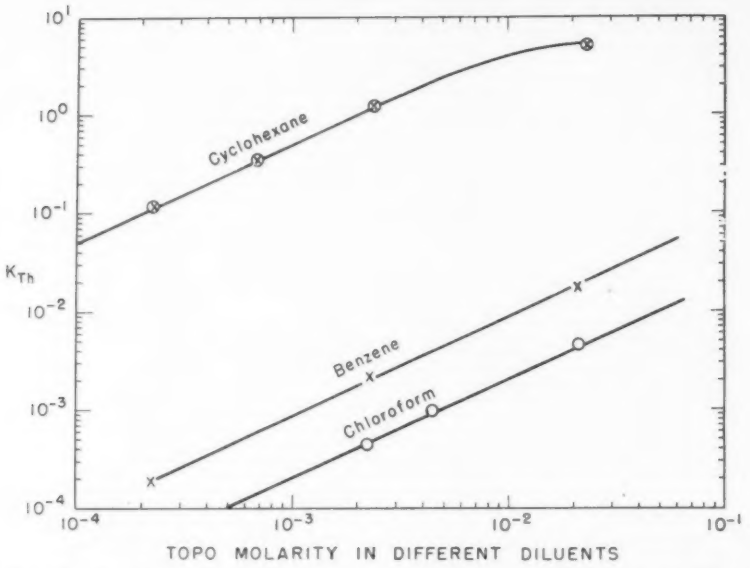

FIG. 10.—First power solvent dependency for Th^{4+}/HTTA/TOPO/diluent synergistic system. (All solutions 0·018 M HTTA/1·0 N HCl).

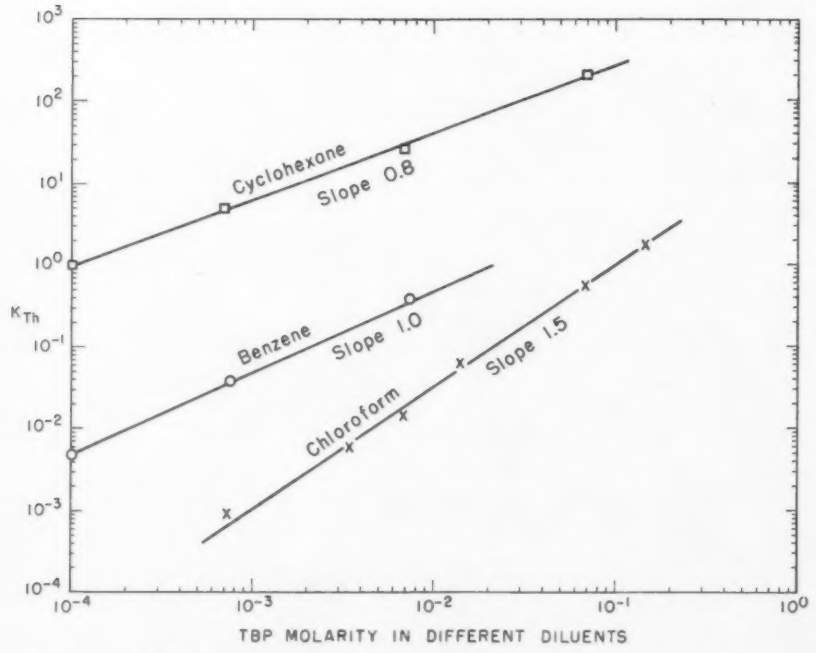

FIG. 11.—Solvent dependency for Th^{4+}/HTTA/TBP/diluent synergistic system. (All solutions 0·009 M HTTA/0·10 N HCl).

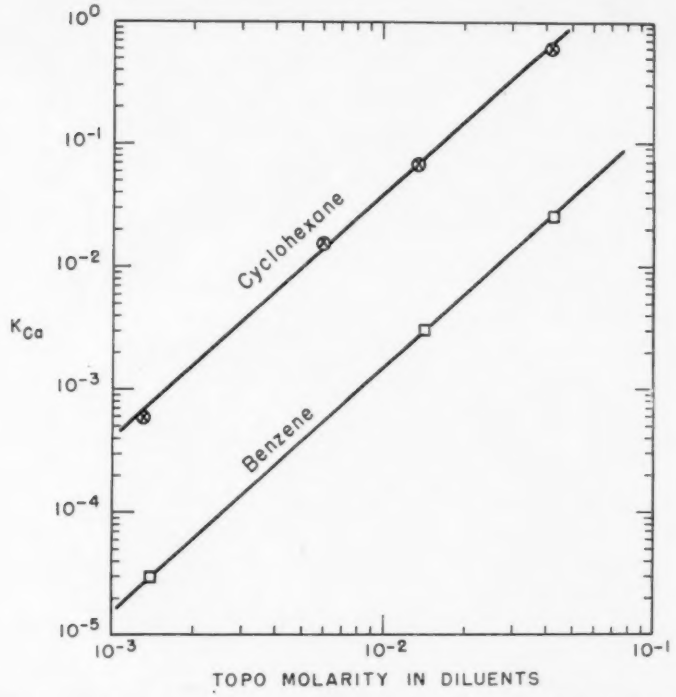

FIG. 12.—Second power solvent dependency for Ca^{2+}/HTTA/TOPO/diluent synergistic system. (All solutions 0·18 M HTTA/0·001 N HCl).

for the uranyl system but very much less than for the trivalent rare earths and actinides and thorium.

Comparison of the "inert" diluent effects on the extraction of different metals

A direct comparison may be made on the relative effects of the two "inert" diluents cyclohexane and benzene by comparing the extraction under similar conditions for the systems M/HTTA/ester/diluent and these are given in Table 2 where the figures are the cyclohexane/benzene extraction ratios.

On using cyclohexane as the diluent, all the metals studied are extracted to a greater degree than when benzene is used, and this effect is very great for the tetra and trivalent metals, fairly small for calcium and very small for uranium. There does not appear to be any trend in this effect if one varies the neutral ester from a strongly

TABLE 2.—EXTRACTION RATIOS FOR METALS USING CYCLOHEXANE AND BENZENE UNDER OTHERWISE IDENTICAL CONDITIONS

	TOPO	TBP	TPP	Species
Th^{4+}	600	150	—	$Th(TTA)_4S$
M^{3+}	500	2000	500	$M(TTA)_3S_2$
Ca^{2+}	25	—	—	$Ca(TTA)_2S_2$
UO_2^{2+}	2–4	12	7	$UO_2(TTA)_2S$

basic to a weakly basic ester. The effect of substituting one diluent, benzene, for the other diluent, cyclohexane, under otherwise identical conditions in the system Pm^{3+}/HTTA/TBP/diluent has been examined. Fig. 13 shows a log/log plot of the partition coefficient against the fraction substituted and a gradual curve is obtained indicating no correlation between the species extracted and either diluent.

The order of increasing extraction of the various metals by the organophosphorus esters is in the order TOPO > TBP > TPP both for the esters alone and for the synergistic combination of the esters with HTTA. This order is in the order expected

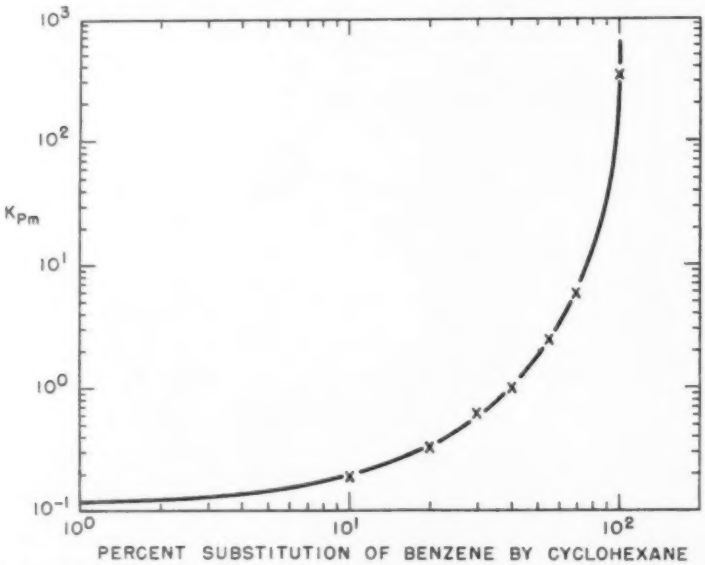

FIG. 13—Substitution of benzene for cyclohexane in the system Pm^{3+}/0·18 M HTTA/0·068 M TBP/diluent/0·010 N HCl.

from the donor properties of these esters.[5] The order of increasing extraction of the various metals (at constant aqueous activity and constant HTTA and phosphorus ester concentration) by the diluents examined in this work is also in a constant order which is also the same order as the solubility of water in the diluent. This is illustrated in the following table where the partition coefficient of Pm in the various diluents is in the same order as the water solubility of the diluent.

TABLE 3.—CORRELATION OF K_{Pm} WITH WATER SOLUBILITY OF DILUENT

Diluent	Cyclohexane	Hexane	CCl_4	Benzene	$CHCl_3$	Hexone
K_{Pm}	5×10^4	2×10^3	5×10^2	2×10	10^{-1}	6×10^{-1}
Water solubility of pure diluent (g/l.)	0·04	0·07	0·15	0·60	1·5	19

Hexone is slightly misplaced in this table as it extracts to a greater degree than chloroform but this is due to the fact that it forms a complex with the salt and by

[5] T. V. HEALY and J. KENNEDY, *J. Inorg. Nucl. Chem.* **10**, 128 (1959). T. V. HEALY, J. KENNEDY and G. M. WAIND, *J. Inorg. Nucl. Chem.* **10**, 137 (1959).

itself extracts the metal. Table 3 indicates that the diluent effect may be bound up with the water content of the pure diluent and the permanent or induced diluent dipole. Attention has been focussed recently by other workers[6] on the importance of the dielectric constant and dipole of the organic phase and its effects on the extraction of metal complexes. There may be a close correlation between the diluent and HTTA–TBP complex formation in the presence or absence of the metal, for example, a greater degree of complexing may take place between the more polar chloroform and the HTTA–TBP mixture than occurs with the non polar cyclohexane. The fact that the diluent effect on the uranyl system is very small may be coupled with the probability that uranyl complexes with TBP and HTTA are symmetrical and without a significant dipole moment and therefore dipole interaction with the diluent would play no appreciable role in the extraction mechanism.

In order to throw more light both on the mechanism of the large synergistic effects and on the large "inert" diluent effects more work is being done on water contents of the organic phases and of solid metal–TTA–TBP complexes, together with infrared study, isopiestic measurements and molecular weight determinations.

Acknowledgement—Thanks are due for valuable help in discussions to D. F. PEPPARD, G. W. MASON and J. R. FERRARO.

[6] A. G. GOBLE and A. G. MADDOCK, *J. Inorg. Nucl. Chem.* **7**, 94 (1958); G. H. MORRISON and H. FREISER, *Solvent Extraction* in *Analytical Chemistry*. J. Wiley, New York (1957); M. TAUBE, *J. Inorg. Nucl. Chem.* **12**, 174 (1959). H. IRVING and D. C. LEWIS, *Proc. Chem. Soc.*, London 222 (1960).

VOL. 19 1961

J. Inorg. Nucl. Chem., 1961, Vol. 19, pp. 340 to 347. Pergamon Press Ltd. Printed in Northern Ireland

STUDY OF PURE FORMIC ACID AS SOLVENT FOR ACID–BASE EQUILIBRIA*

A. I. POPOV† and J. C. MARSHALL
Department of Chemistry, State University of Iowa

(*Received* 11 *October* 1960; *in revised form* 8 *November* 1960)

Abstract—A study was made on the preparation of pure formic acid and its use as a solvent for the study of very weak bases. A glass closed system was constructed for carrying out the purification and all subsequent manipulations in an inert atmosphere. Potentiometric titrations were carried out on a number of substituted tetrazoles with satisfactory accuracy and reproducibility using quinhydrone electrodes and *p*-toluenesulphonic acid as the titrant. Attempts to use hydrogen electrodes in this solvent were unsuccessful.

ANHYDROUS formic acid should be a very interesting solvent for the study of acid–base equilibria. The strongly acidic character of this solvent makes it a very desirable medium for the study of very weak bases, moreover, it has a high dielectric constant of 56·1 at 25°[1], a convenient temperature range of the liquid state and it is a very good solvent for numerous organic as well as inorganic substances.[2] However, it does have certain drawbacks which perhaps can explain the paucity of studies made in this solvent. It is extremely hygroscopic and it is very difficult to obtain in rigorously pure state especially in view of the fact that it undergoes spontaneous decomposition by either or both of the following mechanisms.[3]

$$H—COOH \rightarrow H_2 + CO_2$$

$$H—COOH \rightarrow H_2O + CO$$

Formic acid has another serious limitation in that it is a highly dissociated solvent with the autoprotolysis constant being of the order of 5×10^{-7}[4]. This means that the "pH" scale in this solvent is narrower by nearly eight units than that of water, and consequently the useful potential range of a "hydrogen" electrode is only of the order of about 200 mV.

Literature search showed that the most significant studies on acid–base equilibria in formic acid were done by HAMMETT and DIETZ[4] and more recently by IZMAILOV and his co-workers in Russia.[5]

In the first case the authors have carried out potentiometric measurements in formic acid using the quinhydrone electrode and the hydrogen electrode. While the first electrode behaved reversibly if it was supported on gold instead of platinum, the behaviour of hydrogen electrode was highly erratic. IZMAILOV and his co-workers used

* Abstracted in part from the Ph.D. Thesis of J. C. MARSHALL, State University of Iowa, August, 1960. Presented at the 137th meeting of the American Chemical Society, Cleveland, Ohio, April 12, 1960.

† Present address: Department of Chemistry, Northern Illinois University, DeKalb, Illinois.

[1] J. F. JOHNSON and R. H. COLE, *J. Amer. Chem. Soc.* **73**, 4538 (1951).
[2] O. ASCHAN, *Chem. Z.* **37**, 1117 (1913).
[3] C. N. HINSHELWOOD, H. HARTLEY and B. TOPLEY, *Proc. Roy. Soc.* **100** A, 575 (1922).
[4] L. P. HAMMETT and N. DIETZ, *J. Amer. Chem. Soc.* **52**, 4795 (1930).
[5] A. M. SHKODIN, N. A. IZMAILOV and N. P. DZUBA, *Zh. Obshchei Khimii*, **20**, 1999 (1950); **23**, 27 (1953); Zhur. Anal. Khimii, **6**, 273 (1951).

glass electrode with satisfactory results for several acid–base titrations, but found that it loses its sensitivity with use. They determined pK_b values of several weak bases using ROLLER's method[6] which was originally proposed for the determination of titration errors in aqueous systems. The applicability of this method in formic acid systems is somewhat debatable especially since the authors arbitrarily assumed a titration error of 1 per cent from which they calculated the pK_b value.

Since sparse amount of previous work on formic acid solutions indicated its potential usefulness as a non-aqueous solvent, it was decided to investigate acid–base equilibria in this solvent in as rigorously pure state as conveniently possible and to carry out all the operations in a closed system under inert atmosphere. It should be pointed out that the literature shows considerable disagreement on the optimum purification procedure for formic acid and this problem had to be investigated in some detail. Likewise, in conjunction with some other studies in this laboratory on physicochemical properties of substituted tetrazoles, formic acid solutions presented a very advantageous medium for the determination of their relative basicities.

VOL. 19 1961

EXPERIMENTAL PART

Reagents. Formic acid of 98 + per cent purity was obtained from Eastman Kodak. The commercial acid was first dried for several weeks over anhydrous copper sulphate and then carefully purified with the aid of the apparatus shown in Fig. 1. This system consists essentially of three water jacketed flasks *A*, *B*, and *C*, three standard water jacketed condensers, *E*, *E'*, and *F*, with the latter being packed with glass helices. Purified nitrogen was admitted at *D* and at *D'*, and vacuum was applied at *G*. Use of two constant temperature baths allowed flasks *A* and *B* as well as *F* to be thermostated at either 25° or 4–6° depending on the adjustment of the water circulation system. The previously dried acid was first placed in flask *A* over freshly prepared boric anhydride and the temperature of this flask maintained at 4–6° for about one week. Following this, by manipulations of jacket and condenser temperatures the desired amount of formic acid was distilled at 15 mm pressure onto fresh boric anhydride in flask *B*. After the heat exchange between the water jacket and the formic acid in flask *A* had equilibrated the distillation proceeded smoothly, driven by the temperature gradient. During this distillation small amounts of formic acid carried over into flask *C*. The distillation was stopped by letting dry nitrogen into the system at *D*. The impure acid carried over into flask *C* was forced from the system with nitrogen pressure applied at *D'* and the flask dried under flowing nitrogen. The formic acid was then allowed to dry an additional week in flask *B* at 4–6° after which it was again distilled from flask *B* to flask *C*. The first fraction, comprising about one-fourth of the total of the sample was discarded. Acid purified in this way consistently melted between 8·3 and 8·5°. The average specific conductivity was $6{\cdot}6 \times 10^{-5}$ mho/cm. These results are in essential agreement with the best values found in the literature.[7,8]

There seems to be some ambiguity in the literature reports on the preparation and properties of anhydrous *p*-toluenesulphonic acid and in many cases the acid while assumed to be anhydrous was in reality in the form of monohydrate. This is due to the fact that the water molecule is held very tenaciously by the acid and attempts to dehydrate it by vacuum sublimation over drying agents or by precipitating it out of acetone solution with benzene led either to decomposition or, in the latter case, to recovery of the monohydrate. The anhydrous product was finally obtained by dehydration of the commercial monohydrate (Eastman Kodak-White Label) under vacuum in the absence of dehydrating agents. The anhydrous acid distilled over at 163–165° and was obtained as a colorless oil which was very difficult to crystallize. The observed m.p. was 32–35° while KRAFT and WILKE[9] report 38°. Incidentally, this seems to be the only mention in the literature of the pure, anhydrous acid. Analysis of the product gave C, 48·59, H, 4·62%; calcd. C, 48·82, H, 4·68%.

Boric anhydride was prepared by the dehydration of pure, granular boric acid at 120–140° over

[6] P. S. ROLLER, *J. Amer. Chem. Soc.* **54,** 3485 (1932).
[7] A. S. COOLIDGE, *J. Amer. Chem. Soc.* **50,** 2166 (1928).
[8] H. I. SCHLESSINGER and R. P. CALVERT, *J. Amer. Chem. Soc.* **34,** 1924 (1912).
[9] F. KRAFT and W. WILKE, *Ber. Dtsch. Chem. Ges.* **33,** 3208 (1900).

FIG. 1.—Purification system for formic acid

phosphorous pentoxide. The product obtained was in the form of fine powder which reacted violently with water with large evolution of heat. If this anhydride is prepared at higher temperatures as is usually suggested[10] the product is partially sintered and less active.

Sodium formate was of A.R. grade and it was further purified by three recrystallizations from conductivity water. It was dried for 24 hr at 110°–120° and then stored over phosphorus pentoxide.

Quinhydrone was obtained from Eastman Kodak (White Label). The commercial product was purified by recrystallization but in subsequent work no difference (in properties or in action) was observed between the original and the purified material.

TABLE 1.—STABILITY DATA FOR ELECTRODES IN FORMIC ACID

Electrode solution	Formic acid	Stability
0·20 M Sodium *p*-toluene-sulfonate 0·05 M Quinhydrone	Commercial 98+%	Poor
Saturated KCl 0·05 M Quinhydrone	Commercial 98+%	Poor
0·25 M Sodium Formate 0·05 M Quinhydrone	Commercial 98+%	±2·0–4·0 mV. 8 hours
0·25 M Sodium Formate 0·05 M Quinhydrone	Dried and distilled	±0·8–3·0 mV. 5–14 hr
0·25 M Sodium Formate 0·05 M Quinhydrone	Purified in closed system	±0·1 mV. 5 hr

Caffeine and theobromine were likewise obtained from Eastman Kodak and were purified by recrystallizations. Metrazole and other substituted tetrazoles were obtained from the Knoll Pharmaceutical Co. Metrazole was purified by previously described method[11] but other compounds were obtained in very small quantities and had to be used without purification.

Strychnine was purchased from Merck Chemical Co. as free base. It was dissolved in aqueous hydrochloric acid solution which was subsequently neutralized to give strychnine hydrochloride. After several additional recrystallizations the product was dried at 110°. Observed m.p. was 267–268°, lit. value 268°.

Electrodes. The stability of several electrodes was examined in this work and the data are summarized in Table 1. It is seen how important it is to exert utmost caution to purify formic acid and maintaining it in pure state for these measurements. Optimum results were obtained with quinhydrone–sodium formate electrode as described by PINFOLD and SEBBA[12]. Consistent with the report of the above authors this electrode was found to be stable and reproducible to ±0·1 mV for about 5 hr. Varying amounts of quinhydrone and the passage of small currents had no effect on the observed potential.

The reference electrode used was prepared according to the suggestion of PINFOLD and SEBBA[12]. The solution used in the work was 0·2493 M in sodium formate and 0·05 M in quinhydrone. The electrode itself was formed in a six inch test tube to which a side arm was fused. Liquid junction was made through an asbestos fiber sealed into the side arm. The amount of liquid flow through this junction was found to be negligible. Contrary to the reports of HAMMETT and DIETZ, either platinum or gold could be used for the electrode surface.

Hydrogen electrodes were of the Hildebrand type. They were prepared by standard platinizing methods and checked for accuracy and stability in aqueous buffers. Hydrogen gas was purified by passing it through a palladium catalyst tube and drying tubes containing magnesium perchlorate and ascarite. The electrodes were checked for stability in solutions of 98+% formic acid vs. aqueous

[10] W. C. FERNELIUS, (Editor) *Inorganic Synthesis*, Vol. 2, (1946).
[11] A. I. POPOV, C. CASTELLANI-BISI and M. CRAFT, *J. Amer. Chem. Soc.* **80**, 6513 (1958).
[12] T. A. PINFOLD and F. SEBBA, *J. Amer. Chem. Soc.* **78**, 2095, 5193 (1956).

calomel electrodes. The potential was found to rise steadily for about 45 min and then remain stable to ±5 mV for 1–3 hr. After this period the potential started to fall, eventually going to zero. The hydrogen electrode could be returned to its original potential by allowing it to stand in distilled water for several hours. When the above procedure was followed using carefully purified acid the equilibration was usually more rapid but stable readings were obtained for only about 30 min before the potential started to fall.

Electromotive force measurements were made with a Leeds and Northrup type K-2 potentiometer accurate to ±0·1 mV. Recently standardized low resistance Weston cell was used to check its accuracy.

Titration Procedure. Titrations in anhydrous formic acid were carried out potentiometrically in a completely closed system under a nitrogen atmosphere. The titration apparatus is shown in Fig. 2.

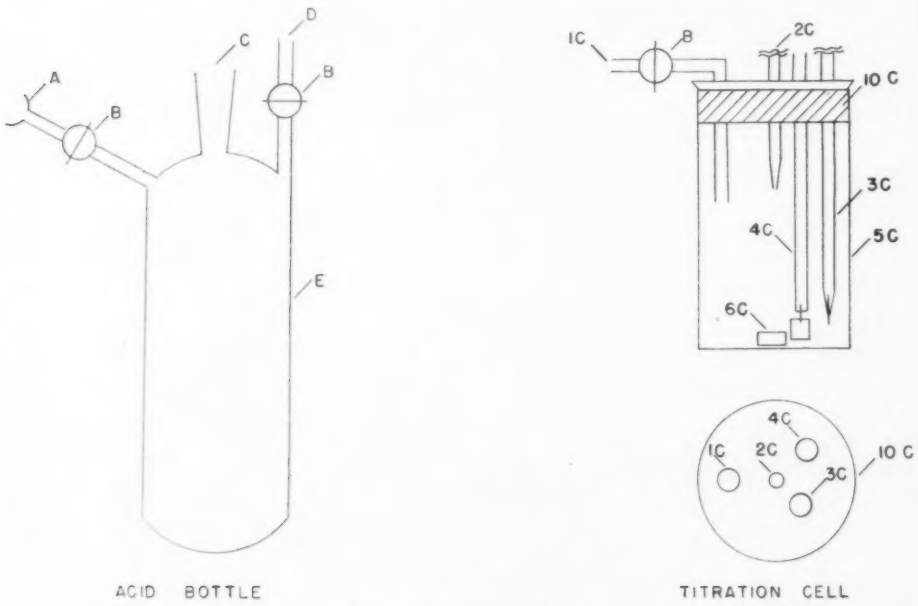

FIG. 2.—Titration apparatus.

The titrant acid solution was prepared by first placing approximately the desired amount of *p*-toluenesulphonic acid in the acid bottle in a dry-box. The acid bottle was then attached to a storage burette. Formic acid could be lead into the acid bottle by forcing it from the purification system under nitrogen pressure. A closed system, automatic zero burette of 10 ml capacity was placed in the acid bottle at *C*. This titrant solution was standardized by titrating a known amount of sodium formate, which served as a primary standard throughout the course of this investigation. All openings of the system to add components or materials were made under flowing nitrogen to exclude atmospheric moisture.

Titration cell (Fig. 2) consisted essentially of a 100 ml tall form beaker and #10 rubber stopper which was bored as shown, except in experiments involving the hydrogen electrode when a larger hole was drilled to accommodate the barrel of the electrode.

The procedure used to carry out a series of titrations may be described briefly as follows. The desired samples were weighed into the cells and the cell tops were assembled as shown, except that rubber plugs were placed in holes 2*c* and 3*c*. The cells were flushed with nitrogen, tared and stored in a desiccator until used. Likewise the desired amount of *p*-toluenesulfonic acid was placed in the acid bottle in a dry-box. On the day the titrations were to be performed the solvent was distilled, sample and reference electrode solutions, and the titrant acid solution were prepared. The concentration of the sample solutions was determined knowing the weight gain of the cell from the addition of

the solvent. The entire procedure required about 10 hrs, of which about two and one-half were required for the actual performance of the titrations.

Because of the limited stability of formic acid the purification and titration procedure must be performed in an unbroken sequence. The most serious experimental difficulty encountered in the use of formic acid for a solvent is its limited stability in acidic solutions. The usable stability period of a formic acid solution 0·2 M in hydrogen ion is about 3 hr at room temperature. After this time bubble formation from the decomposition of the solvent makes careful volumetric measurements impossible.

RESULTS AND DISCUSSION

Using the above procedure a number of potentiometric titrations were carried out in anhydrous formic acid, and the results are shown in Table 2. Quantitative evaluation of the procedure used was obtained by first standardizing the titrant acid

TABLE 2.—TITRATION DATA ON WEAK BASES IN ANHYDROUS FORMIC ACID

Sample titrated	M.E. taken	M.E. found	Error* (%)
Caffeine	1·00	0·98	
Caffeine	0·88	0·88	
Caffeine	0·88	0·89	−0·3
Theobromine	0·96	0·93	
Theobromine	0·99	0·99	
Theobromine	0·97	0·98	−0·7
Strychnine	0·98	0·99	
Strychnine	1·14	1·13	
Strychnine	1·05	1·06	
Strychnine	1·01	1·01	−0·3
Metrazole	1·01	1·01	
8-Tertiarybutylmetrazole	1·05	1·05	
7-Methyl-8-isopropylmetrazole	0·93	0·93	
7-Methylmetrazole	0·94	0·93	
8-Isopentylmetrazole	1·12	1·12	
1-Cyolohexyl-5-ethyltetrazole	1·04	1·06	
1-Methyl-5-cyclohexyltetrazole	1·01	1·00	
Sodium Sulphate	1·06	1·05	
Sodium Sulphate	1·22	1·20	−1·3

* Given for multiple titrations only.

against a known weight of sodium formate and then calculating the apparent number of milliequivalents of the sample from the titration curve.

Equivalence points in the titration curve were determined graphically and by using the derivative plots. The two methods gave essentially identical results. The e.m.f. at the end point of duplicate titrations was usually reproducible to $\pm 1{\cdot}0$ mV.

The observation, in itself, that very weak bases can be titrated in formic acid is, perhaps, of little practical importance. Rather elaborate procedure used above as well as fairly large experimental error of about $\pm 2{\cdot}0$ per cent, would not tend to popularize this method for routine analytical work. The nature of the potentiometric titration curves does, however, give some insight into acid–base behaviour in this solvent.

In comparison to water, the pH range available in formic acid is very small. Using an acid solution about 0·2 M in *p*-toluenesulphonic acid and base solutions about 0·03 M the potential jump found in the region of the end point was usually between 40 and 50 mV. The analogous aqueous titration would result in a potential jump in this

region of about 400 mV. It is seen then that this severely limits titrimetric procedures in formic acid since the potential jump is too small to allow a good degree of certainty in the location of equivalence point.

It is of interest to note that titrimetric curves for diprotic bases have never been observed in the formic acid media. This is particularly noteworthy in the case of

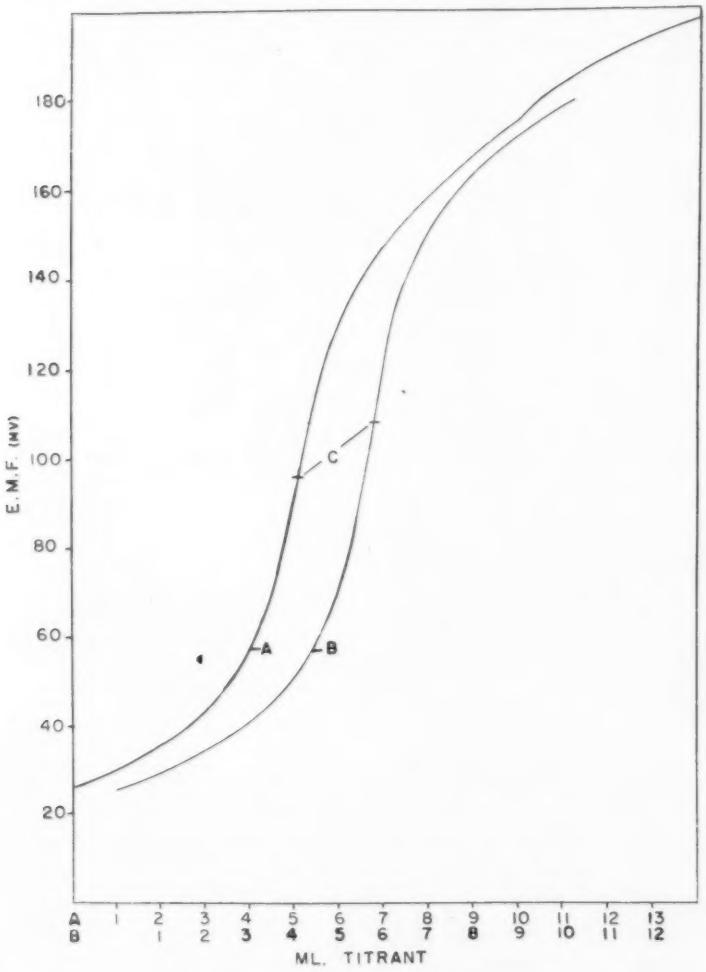

FIG. 3.—Titration curves in formic acid.
A—strychnine.
B—sodium formate.

strychnine which has respective pK_b values of 7·0 and 10·2 in water. Considering the fact that both caffeine and theobromine, which have pK_b values in aqueous solution of 13·49 and 13·89, respectively, are relatively easily titratable, it would seem on first glance that both nitrogens in the strychnine molecule should likewise be found in the potentiometric titration curve of this compound. However, only one break in the titration curve is actually observed. This is due to the fact that the pH range of the

solvent is too small and that by the time second nitrogen atom begins to be protonated, the concentration of the formate ion is high enough to compete with it for the available protons.

Consistent with the above arguments the titration curve of strychnine does show some unusual features. This curve, along with the titration curve for sodium formate for comparison, is shown in Fig. 3. The inflexion found in the region of the second equivalence point, although very small, was reproducible. This would then seem to indicate that strychnine is a diprotic base in anhydrous formic acid, but the second potential break is obscured by the limited pH range of the solvent.

An interesting evidence for the highly acidic nature of the formic acid media is illustrated in the case of metrazole. POPOV and HOLM[13] showed that metrazole is an extremely weak base in glacial acetic acid and its titration curve (when titrated with perchloric acid) shows rather small slope at the endpoint, even when concentrated solutions are used. On the other hand, in this work the titration curves for metrazole and for a series of substituted metrazoles and tetrazoles were well defined and characteristic of strong bases.

VOL. 19 1961

Attempts were made to use the hydrogen electrode as the indicator electrode for the titration of sodium formate with *p*-toluenesulphonic acid. This titration could not be carried out. The response of the hydrogen electrode became increasingly unstable as the titration progressed, the last reliable reading being in the region of the half-equivalence point.

The erratic behaviour of the hydrogen electrode in formic acid has also been observed by HAMMETT and DIETZ[4] and PLESKOV[14]. Contrary to this, TOMECEK and VIDNER[15] and MUKHERJEE[16] report good results with the hydrogen electrode in formic acid. It is of interest to note that these authors used formic acid which was neither pure nor anhydrous.

The fact that the hydrogen electrode is not useful in formic acid solutions is not surprising when it is considered that this electrode is poisoned by carbon monoxide. The observation that the hydrogen electrode was more stable in formic acid solutions containing water is probably due to the fact that the decomposition rate of formic acid is slower when water is present.[3] The increasingly erratic behaviour of the hydrogen electrode as a titration progressed is consistent with evidence that formic acid solutions containing excess formate are more stable than the pure acid.[4]

Acknowledgements—This work was supported by the Research Grant B-1095 from the National Institute of Neurological Diseases and Blindness, U.S. Public Health Service. We are also indebted to Dr. R. O. HAUCK of the Knoll Pharmaceutical Company for the substituted metrazole derivatives. One of us (J. C. M.) wishes to thank the Graduate College of the University of Iowa for Research Assistantships and the DuPont Company for a predoctoral fellowship.

[13] A. I. POPOV and R. D. HOLM, *J. Amer. Chem. Soc.* **81**, 3250 (1959).
[14] V. A. PLESKOV, *Zh. Fiz. Chimii* **20**, 153 (1940).
[15] O. TOMECEK and P. VIDNER, *Chem. Listy* **47**, 56 (1953).
[16] L. M. MUKHERJEE, *J. Amer. Chem. Soc.* **79**, 4040 (1957).

J. Inorg. Nucl. Chem., 1961, Vol. 19, pp. 348 to 358. Pergamon Press Ltd. Printed in Northern Ireland

THE LIMITATIONS OF SALT CRYOSCOPY FOR THE STUDY OF COMPLEX SPECIES IN AQUEOUS SOLUTION*

R. STUART TOBIAS
Department of Chemistry, University of Minnesota, Minneapolis

(*Received* 26 *September* 1960; *in revised form* 7 *November* 1960)

Abstract—The implications and the validity of the tacit assumptions made in the theory and in the application of the salt cryoscopic method as used for the study of charged poly- and mononuclear complexes have been examined. Data obtained from salt cryoscopy are compared with results obtained from different experimental methods. On the basis of this information, it appears that the method has limited value for the study of polynuclear complexes containing more than 3 or 4 metal atoms or for the study of systems containing a series of stepwise mononuclear complexes. Results in these cases should be considered indicative rather than conclusive. The conditions necessary for the interpretation of cryoscopic and e.m.f. data are compared, particularly for the case of polynuclear complexes, and it is seen that the conditions are much better satisfied in the case of the e.m.f. measurements.

MUCH attention has been given in recent years to the study of the products formed by the polymerization of the conjugate acids and bases which are produced by the hydrolysis of ions.[1] A variety of experimental methods have been used for studies, and because of the difficulty in interpreting data for concentrated electrolyte solutions it is highly desirable to have agreement between two or more independent methods.

One technique which has been widely used involves measurements of the depression of the freezing points or transition points of two component systems with three phases where one component is water and the other is an electrolyte. Systems such as the KNO_3-and $NaNO_3$-ice eutectics have been used as well as salt hydrates in the presence of excess anhydrous salt such as $Na_2SO_4 \cdot 10H_2O$–Na_2SO_4. These systems have been applied to the determination of the number of metal atoms in polymeric cations and anions[2–6] and also to the study of systems with mononuclear complexes.[7–9] Earlier work is reviewed by SOUCHAY[10]. Detailed mathematical methods for the computation of stability constants from freezing-point depressions have recently been given.[11]

In all of these studies, it is assumed that only ions not contained in the electrolytic component of the solvent system, i.e. the so-called foreign ions, will exhibit a cryoscopic effect. The thermodynamic foundations for this assumption were presented

* This work was supported by the United States National Science Foundation under grant NSF-14173.

[1] L. G. SILLÉN, *Quart. Revs.* **13**, 146 (1959).
[2] G. JANDER and H. PLUSKAL, *Z. Anorg. Chem.* **291**, 67 (1957).
[3] E. THILO and G. KRÜGER, *Z. Elektrochem.* **61**, 24 (1957).
[4] G. JANDER and D. ERTEL, *J. Inorg. Nucl. Chem.* **3**, 139 (1956).
[5] J. KENTTÄMAA, *Ann. Acad. Sci. Fennicae* **67**, (1955).
[6] K. F. JAHR and A. BRECHLIN, *Z. Anorg. Chem.* **270**, 257 (1952).
[7] G. KRÜGER and E. THILO, *Z. Phys. Chem.* (*Leipzig*) **209**, 190 (1958).
[8] J. KENTTÄMAA, *Acta Chem. Scand.* **12**, 1323 (1958).
[9] P. HAGENMÜLLER, *Ann. Chim.* **12:6**, 1 (1951).
[10] P. SOUCHAY, *Research* **4**, 11 (1951).
[11] F. J. C. ROSSOTTI and H. S. ROSSOTTI, *J. Phys. Chem.* **63**, 1041 (1959).

many years ago by LEWIS[12] and HOENEN[13]. The interpretation of the freezing-point data for these systems has been made in an analogous fashion to that used for the determination of molecular weights of nonionized complexes in organic solvents. Since the liquid phase of these multicomponent systems consists of a concentrated electrolyte solution, activity coefficients are assumed to be essentially invariant, and on this basis it is assumed that the freezing or transition temperature depression will vary with the concentration of the foreign solute in a similar way to that of a nonelectrolyte in a single component solvent. A linear extrapolation of the depression divided by the foreign salt concentration to infinite dilution of the foreign salt is assumed to give the product of the number of foreign ions per mole of solute and the molal depression for the solvent system. The approximate validity of the foregoing assumptions has been demonstrated many times.[3,6,9,14–17]

Although the assumption of the constancy of activity coefficients is common to most of the methods employed to study complexes in aqueous solution and the "constant ionic medium"[18] is used for this reason, the analysis of salt cryoscopic data is complicated by the presence of three or more phases.

VOL. 19 1961

Recently some discussion has arisen concerning the accuracy of the assumptions made in interpreting cryoscopic data because of the rather widespread extension of this method to the study of complexes containing from five to ten metal atoms, particularly the isopoly ions, where small uncertainties in the extrapolated values lead to substantial errors in the composition of the complex. In addition, more data are available for comparison, especially from careful e.m.f. measurements, and it has been noted that the agreement between these two methods is sometimes unsatisfactory.[19] SCHWARZENBACH and PARISSAKIS[20] measured the depression of the transition point of $Na_2SO_4 \cdot 10H_2O$ caused by a variety of known solutes. The data could all be fitted by equations of the type $\vartheta/m_2 = A + Bm_2$ where ϑ is the transition temperature depression, m_2 the foreign ion concentration in moles/kg $Na_2SO_4 \cdot 10H_2O$, and A and B are constants for a given solute. It was observed, however, that the values of A as well as B varied somewhat depending on the solute, and it was suggested that the van't Hoff law is not obeyed even in the limit of infinite dilution of the foreign solute. An effort was made to relate the values of A to the chemical properties of the solute, and using empirically adjusted values of A, degrees of aggregation of some polymeric anions were obtained which were in good agreement with other experimental methods.

JAHR and SCHOEPP[21] do not agree with these observations and have obtained degrees of aggregation in agreement with e.m.f. measurements without recourse to adjustment of the A values, i.e., the molal depressions, from solute to solute.

It is interesting to note that at one time DONNAN[22] questioned the validity of the van't Hoff osmotic pressure relation for the description of the osmotic pressure due to

[12] G. N. LEWIS, *Proc. Amer. Acad. Arts Sci.* **43**, 259 (1907).
[13] P. HOENEN, *Z. Phys. Chem.* **83**, 513 (1913).
[14] K. F. JAHR, A. BRECHLIN, M. BLANKE and R. KUBENS, *Z. Anorg. Chem.* **270**, 240 (1952).
[15] K. F. JAHR and R. KUBENS, *Z. Elektrochem.* **56**, 65 (1952).
[16] E. DARMOIS, *Bull. Soc. Chim. France* 1, (1950).
[17] J. KENTTÄMAA, *Acta Chem. Scand* **12**, 1323 (1958).
[18] L. G. SILLÉN, *J. Inorg. Nucl. Chem.* **8**, 176 (1958).
[19] G. LAGERSTRÖM, *Acta Chem. Scand.* **13**, 722 (1959).
[20] (a) G. SCHWARZENBACH and G. PARISSAKIS, *Helv. Chim. Acta*, **41**, 2425 (1958); (b) G. PARISSAKIS and G. SCHWARZENBACH, *Helv. Chim. Acta*, **41**, 2042 (1958).
[21] K. F. JAHR and L. SCHOEPP, *Z. Naturforsch.*, **14 B**, 468 (1959).
[22] F. G. DONNAN, *Trans. Faraday Soc.* **31**, 80 (1935).

a polyelectrolyte in the presence of a supporting electrolyte, even in the limit of infinite dilution of the polymeric solute. It has subsequently been shown that the van't Hoff expression does apply under these conditions.[23]

In view of these discrepancies, an examination of the freezing or transition temperature depressions and the component activities appeared to be in order to describe the tacit assumptions, the range of applicability, and the accuracy and hence general usefulness of the cryoscopic method.

1. *Freezing or transition temperature depression for multicomponent solvents*

In the following discussion, components which appear in both a pure solid and in the solution are designated by J or K, e.g. $NaNO_3$ and H_2O in the sodium nitrate–ice eutectic system. All concentrations are defined in terms of a fixed quantity of one of these components; normally the concentrations will be defined as moles per kilogram of water. The foreign ion under study which is present only in the solution phase is contained in a neutral component designated as 2. The nonpolymeric ions contained in the various components are designated by i, e.g., Na^+ in $Na_6[Mo_7O_{24}]$. As usual it is assumed that no solid solutions are formed. At constant pressure, T and the component molalities are chosen as variables, and the standard-state fugacities of the solid components are defined as equal to those of the components in the liquid phase. Square d's are used for the total change at equilibrium and round δ's for partial derivatives where all variables are held constant except the one specifically indicated as varying.

In general with a system consisting of n components and n + 1 phases, for any component K which appears in both a solid and the liquid phase,

$$\left(\frac{\delta \ln a_K}{\delta m_2}\right) + \Sigma_J \frac{dm_J}{dm_2}\left(\frac{\delta \ln a_K}{\delta m_J}\right) + \left(\frac{\delta \ln a_K}{\delta T}\right)\frac{dT}{dm_2} = \left(\frac{\delta \ln a_K'}{\delta T}\right)\frac{dT}{dm_2} \tag{1}$$

Primed quantities refer to the pure solid phases. Multiplying each equation (1) by m_K and summing over all components in the solvent system,

$$\Sigma_K m_K\left(\frac{\delta \ln a_K}{\delta m_2}\right) + \Sigma_J \frac{dm_J}{dm_2}\Sigma_K m_K\left(\frac{\delta \ln a_K}{\delta m_J}\right) + \frac{dT}{dm_2}\Sigma_K m_K\left(\frac{\delta \ln a_K}{dT}\right) = \frac{dT}{dm_2}\Sigma_K m_K\left(\frac{\delta \ln a_K'}{\delta T}\right) \tag{2}$$

Applying the Gibbs Duhem equation, since P = constant and T = constant freezing or transition point of system

$$\Sigma_K m_K\left(\frac{\delta \ln a_K}{\delta m_2}\right) + m_2\left(\frac{\delta \ln a_2}{\delta m_2}\right) = 0 \quad \text{and} \tag{3}$$

$$\Sigma_K m_K\left(\frac{\delta \ln a_K}{\delta m_J}\right) + m_2\left(\frac{\delta \ln a_2}{\delta m_J}\right) = 0 \tag{4}$$

Substituting (3), (4) into (2)

$$m_2\left(\frac{\delta \ln a_2}{\delta m_2}\right) + m_2\Sigma_J \frac{dm_J}{dm_2}\left(\frac{\delta \ln a_2}{\delta m_J}\right) = \frac{dT}{dm_2}\left(\Sigma_K m_K\left(\frac{\delta \ln a_K}{\delta T}\right) - \Sigma_K m_K\left(\frac{\delta \ln a_{K'}}{\delta T}\right)\right) \tag{5}$$

[23] G. SCATCHARD, *J. Amer. Chem. Soc.* **68**, 2315 (1946).

The activity of component 2 written in the usual form is

$$a_2 = m_2^{\nu_2}\pi_i m_i^{\nu_{2i}}\gamma_2 \tag{6}$$

Taking logs

$$\ln a_2 = \nu_2 \ln m_2 + \Sigma_i \nu_{2i} \ln m_i + \beta_2 \tag{7}$$

ν_2 = number of "foreign" ions in component 2
ν_{2i} = number of ith counter-ions in component 2
$\beta_2 = \ln \gamma_2$, where γ_2 is the component activity coefficient

For example, if the foreign ion were a polymeric anion with charge $-Z$, in a medium with Na^+, we could define component 2 as Na_ZP and write

$$\ln a_2 = \ln m_P + Z \ln m_{Na} + \ln \gamma_2 \tag{8}$$

To simplify the equations, we shall consider only two components, 1 and 3, besides the foreign solute and define the concentrations per kg. of component 1, H_2O.

Differentiating (7) with respect to m_3 and m_2, where m_3 is the concentration of the electrolyte component in the solution,

$$\left(\frac{\delta \ln a_2}{\delta m_3}\right) = \Sigma_i \frac{\nu_{2i}\nu_{3i}}{m_i} + \beta_{23}; \quad \beta_{23} = \left(\frac{\delta \ln \gamma_2}{\delta m_3}\right) \tag{9}$$

$$\left(\frac{\delta \ln a_2}{\delta m_2}\right) = \frac{\nu_2}{m_2} + \Sigma_i \frac{\nu_{2i}^2}{m_i} + \beta_{22}; \quad \beta_{22} = \left(\frac{\delta \ln \gamma_2}{\delta m_2}\right) \tag{10}$$

Substituting (9) and (10) into (5), we obtain

$$\nu_2 + \Sigma_i \frac{\nu_{2i}^2}{m_i} m_2 + \beta_{22} m_2 + m_2 \frac{dm_3}{dm_2}\left[\Sigma_i \frac{\nu_{2i}\nu_{3i}}{m_i} + \beta_{23}\right] = \frac{-dT}{dm_2}\left[m_1\left(\frac{\delta \ln a_1'}{\delta T}\right) + m_3\left(\frac{\delta \ln a_3'}{\delta T}\right) - m_1\left(\frac{\delta \ln a_1}{\delta T}\right) - m_3\left(\frac{\delta \ln a_3}{\delta T}\right)\right] \tag{11}$$

Substituting the temperature coefficients of the activities,

$$\nu_2 + \Sigma_i \frac{\nu_{2i}^2}{m_i} m_2 + \beta_{22} m_2 + m_2 \frac{dm_3}{dm_2}\left[\Sigma_i \frac{\nu_{2i}\nu_{3i}}{m_i} + \beta_{23}\right] = \frac{-dT}{dm_2}\left[m_1\left(\frac{\bar{H}_1 - \bar{H}_1'}{RT^2}\right) + m_3\left(\frac{\bar{H}_3 - \bar{H}_3'}{RT^2}\right)\right] \tag{12}$$

First it is of interest to consider the limiting value of (12) as $m_2 \to 0$. In the limit, the term $\Sigma_i \nu_{2i}^2 m_i^{-1} m_2$ will become 0 so long as none of the m_i are zero. With the restriction that all of the i counter-ions in the polymeric solute be found in one or more of the components of the solvent system, the values of m_i will be essentially determined by the concentration of the ions present in the pure solvent system. For example in the study of a polymeric cation in the $NaNO_3$–ice eutectic, $m_{Na^+} = m_{NO_3^-} = 6{\cdot}89$ molal. In general, the m_i are greater than unity with the solvent systems that have been used, e.g., KNO_3–ice, 1·21 molal KNO_3, $Na_2SO_4{\cdot}10H_2O$–Na_2SO_4, 3·5 molal Na_2SO_4.

The quantity $\beta_{22} m_2 = (\delta \ln \gamma_2/\delta m_2) m_2$ will also vanish at infinite dilution so long as β_{22} is finite. In general β_{22} will be small, since measurements have shown that the

VOL. 19 1961

activity coefficient of a component present at low concentration together with a second electrolyte at high total molality is approximately independent of the component concentration. With 1–1 electrolytes this is true to rather high concentrations, and β_{22} for HCl in the presence of NaCl at a total molality of 1 is zero to about 10^{-1} molal HCl.[24] With higher charge type electrolytes, deviations would be expected at somewhat lower concentrations.

The third quantity $m_2\left[\frac{dm_3}{dm_2}\Sigma_i\frac{\nu_{2i}\nu_{3i}}{m_i}+\beta_{23}\right]$ will vanish so long as the expression within the brackets is finite. The total derivative dm_3/dm_2 represents the change in the supporting electrolyte concentration caused by the addition of the foreign solute, e.g., with a salt–ice eutectic the addition of a foreign solute changes the eutectic composition slightly. Few data are available for ternary systems, but little change in m_3 has been observed in the cryoscopic measurements up to concentrations of the foreign solute as high as 1 molal. Again so long as none of the m_i are 0, $\Sigma\frac{\nu_{2i}\nu_{3i}}{m_i}$ will be finite. The value of $\beta_{23}=(\delta\ln\gamma_2/\delta m_3)$ while small is not zero at infinite dilution of the foreign solute and depends on the chemical properties of components 2 and 3 and the total molality.

The enthalpy terms in (11) become the enthalpy of fusion or transition of the quantity of pure eutectic or hydrate required to give 1 kg. of component 1, water, together with m_3 moles of component 3, the supporting electrolyte in the saturated solution; this is designated $\Delta H_m{}^0$.

If the melting or transition point of the system is θ, and $T=\theta-\vartheta$, we obtain the van't Hoff law in the limit as $m_2\to 0$.

$$\nu_2=\frac{-dT}{dm_2}\frac{\Delta H_m{}^0}{RT^2}=\frac{d\vartheta}{dm_2}\frac{\Delta H_m{}^0}{R\theta^2} \tag{13}$$

In view of the general behaviour of electrolyte solutions, there is therefore no reason to expect deviations from the van't Hoff expression in the limit of infinite dilution of the foreign solute. The more important question, however, is whether the limiting value $(\vartheta/m_2)_{m_2=0}$ and hence ν_2 can be obtained experimentally. Figs. 1 and 2 show data from several authors for the depression of the $Na_2SO_4\cdot 10H_2O$ transition point caused by some "known" solutes. It is clear that significant deviations from the limiting value of $(\vartheta/\nu_2 m_2)$ occur even at the lowest concentrations studied. This is to be expected, since the term $\Sigma_i\frac{\nu_{2i}{}^2}{m_i}m_2$ increases with the square of the charge on the ion and for the case of a foreign anion of charge 1 in the $Na_2SO_4\cdot 10H_2O$ melt will still amount to about 0·015 in 0·1 molal solution. While $\beta_{22}m_2$ will probably be quite small, $m_2\left[\frac{dm_3}{dm_2}\Sigma_i\frac{\nu_{2i}\nu_{3i}}{m_i}+\beta_{23}\right]$ will in general be different from 0 at finite concentrations.

2. *Temperature depressions at finite concentrations*

Since the usual experiments cannot be expected to yield values of $(\vartheta/m_2)_{m_2=0}$ directly, the method of extrapolation of the data to infinite dilution must be examined.

[24] H. S. HARNED and B. B. OWEN, *The Physical Chemistry of Electrolytic Solutions*, (3rd Ed.), p. 598 Reinhold, New York (1958).

If the linear extrapolation which has been used is valid, the equation describing (ϑ/m_2) as a function of m_2 can be obtained using Taylor's theorem. Thus if

$$\vartheta/m_2 = A + Bm_2 \tag{14}$$

$$A = \left(\frac{d\vartheta}{dm_2}\right)_{m_2=0} = -\left(\frac{dT}{dm_2}\right)_{m_2=0} = \frac{\nu_2 R\theta^2}{\Delta H_m{}^0} \text{ from (13)} \tag{15}$$

$$B = \frac{1}{2!}\left(\frac{d^2\vartheta}{dm_2{}^2}\right)_{m_2=0} = \frac{-1}{2!}\left(\frac{d^2T}{dm_2{}^2}\right)_{m_2=0} \tag{16}$$

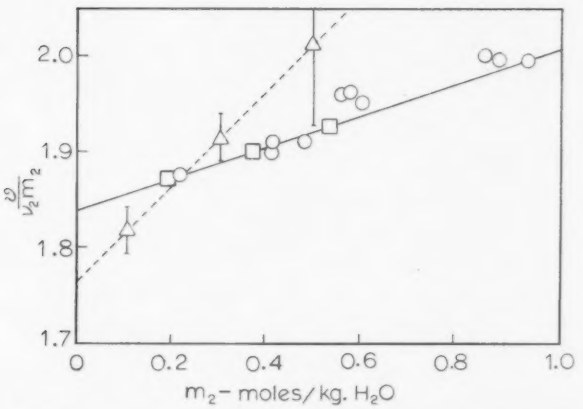

FIG. 1.—The reduced depression, $\vartheta/\nu_2 m_2$ as a function of concentration for the solute NaOH; □, data of JAHR and KUBENS[15]; ○, data of THILO and KRÜGER[3]; △, data of SCHWARZENBACH and PARISSAKIS[20]. The vertical lines represent the approximate range of the third set of data. The solid line is the extrapolation of JAHR and KUBENS, the broken line was constructed from the equation given by SCHWARZENBACH and PARISSAKIS.

In order to obtain $(d^2T/dm_2{}^2)_{m_2=0}$, we differentiate (5) with respect to m_2. Thus

$$\begin{aligned}
&m_2\left(\frac{\delta^2 \ln a_2}{\delta m_2{}^2}\right) + \left(\frac{\delta \ln a_2}{\delta m_2}\right) + 2m_2\Sigma_K \frac{dm_K}{dm_2}\left(\frac{\delta^2 \ln a_2}{\delta m_2 \delta m_K}\right) \\
&+ m_2\Sigma_J \frac{d^2 m_J}{dm_2{}^2}\left(\frac{\delta \ln a_2}{\delta m_J}\right) + \Sigma_J \frac{dm_J}{dm_2}\left(\frac{\delta \ln a_2}{\delta m_J}\right) + m_2\Sigma_{JK}\frac{dm_K}{dm_2}\frac{dm_J}{dm_2}\left(\frac{\delta^2 \ln a_2}{\delta m_J \delta m_K}\right) \\
&+ m_2\frac{dT}{dm_2}\left(\frac{\delta^2 \ln a_2}{\delta m_2 \delta T}\right) + m_2\frac{dT}{dm_2}\Sigma_J\frac{dm_J}{dm_2}\left(\frac{\delta^2 \ln a_2}{\delta m_J \delta T}\right) \\
&= \frac{-d^2T}{dm_2{}^2}\left[\Sigma_K m_K\left(\frac{\delta \ln a_K{}'}{\delta T}\right) - \Sigma_K m_K\left(\frac{\delta \ln a_K}{\delta T}\right)\right] + \frac{dT}{dm_2}\Sigma_K m_K\left(\frac{\delta^2 \ln a_K}{\delta T \delta m_2}\right) \\
&+ \frac{dT}{dm_2}\Sigma_J\frac{dm_J}{dm_2}\Sigma_K m_K\left(\frac{\delta^2 \ln a_K}{\delta T \delta m_J}\right) - \left(\frac{dT}{dm_2}\right)^2\left[\Sigma_K m_K\left(\frac{\delta^2 \ln a_K{}'}{\delta T^2}\right)\right. \\
&\left. - \Sigma_K m_K\left(\frac{\delta^2 \ln a_K}{\delta T^2}\right)\right] - \frac{dT}{dm_2}\left[\Sigma_K\frac{dm_K}{dm^2}\left(\frac{\delta \ln a_K{}'}{\delta T}\right) - \Sigma_K\frac{dm_K}{dm_2}\left(\frac{\delta \ln a_K}{\delta T}\right)\right]
\end{aligned} \tag{17}$$

An expression for dm_J/dm_2, the effect of the foreign solute on the concentration of the supporting electrolyte in the solution, can be obtained in the following way.

Again considering only a two-component solvent system and substituting the temperature coefficient of the activity in equation (1), we obtain for component 3

$$\left(\frac{\delta \ln a_3}{\delta m_2}\right) + \frac{dm_3}{dm_2}\left(\frac{\delta \ln a_3}{\delta m_3}\right) = \frac{dT}{dm_2}\left(\frac{\bar{H}_3 - \bar{H}_3'}{RT^2}\right) \tag{18}$$

Also

$$\ln a_3 = \nu_{3c} \ln m_c + \nu_{3a} \ln m_a + \beta_3 \tag{19}$$

ν_{3c} = number of cations in component 3
ν_{3a} = number of anions in component 3
$m_c = \nu_{2c} m_2 + \nu_{3c} m_3$ = molality cations
$m_a = \nu_{2a} m_2 + \nu_{3a} m_3$ = molality anions
$\beta_3 = \ln \gamma_3$, where γ_3 is the component activity coefficient

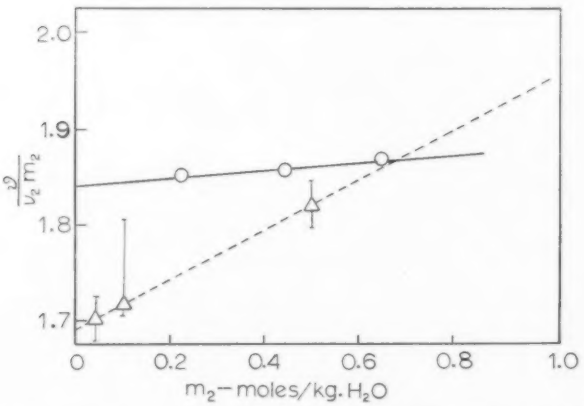

FIG. 2.—The reduced depression as a function of concentration for the solute NaCl; ○, data of JAHR and KUBENS[15]; △ data of SCHWARZENBACH and PARISSAKIS[20]. The vertical lines represent the approximate range of the second set of data. The solid line is the extrapolation of JAHR and KUBENS, the broken line was constructed according to the equation given by SCHWARZENBACH and PARISSAKIS.

$$\left(\frac{\delta \ln a_3}{\delta m_2}\right) = \left(\frac{\delta \ln a_2}{\delta m_3}\right) = \frac{\nu_{3c}\nu_{2c}}{m_c} + \frac{\nu_{3a}\nu_{2a}}{m_a} + \beta_{23}; \quad \beta_{23} = \left(\frac{\delta \ln \gamma_3}{\delta m_2}\right) \tag{20}$$

$$\left(\frac{\delta \ln a_3}{\delta m_3}\right) = \frac{\nu_{3c}^2}{m_c} + \frac{\nu_{3a}^2}{m_a} + \beta_{33}; \quad \beta_{33} = \left(\frac{\delta \ln \gamma_3}{\delta m_3}\right) \tag{21}$$

It is convenient to define component 2 so that dissolution of one mole gives ν_2 moles of ions in the solution. Thus for a polymeric anion P^{z-} in a medium containing the 1–1 electrolyte BX, component 2 would be $B_zP - (Z/2)BX$. This does not change the molality of component 2 from the more usual definition with the component simply B_zP. It does change the molality of component 3 slightly, but this effect becomes negligible in dilute solution.[25] In the general case, for a component which

[25] R. S. TOBIAS and S. Y. TYREE, *J. Amer. Chem. Soc.* **81**, 6385 (1959).

gives ν_2 moles of ions in solution, the numbers of the i ions necessary to make the component electrically neutral have been given by SCATCHARD[23].

$$\nu_{2c} = \frac{-\nu_2 Z_2 Z_c m_c^0}{Z_c^2 m_c^0 + Z_a^2 m_a^0} \tag{22}$$

$$\nu_{2a} = \frac{-\nu_2 Z_2 Z_a m_a^0}{Z_c^2 m_c^0 + Z_a^2 m_a^0} \tag{23}$$

ν_{2c} and ν_{2a} are the number of non-polymeric cations and anions respectively contained in component 2.

Z_2 = effective charge on "foreign" ion; although Z_2 is assumed to be constant, it may be less than the charge on the "foreign" ion because of the binding of counter-ions from the medium.

Z_a = charge on anion in component 3

Z_c = charge on cation in component 3

The superscript 0 indicates infinite dilution of component 2. For solutions dilute in component 2,

$$\left(\frac{\delta \ln a_3}{\delta m_2}\right) \simeq \frac{\nu_{2c}}{m_3^0} + \frac{\nu_{2a}}{m_3^0} + \beta_{23}^0 = \beta_{23}^0 \tag{24}$$

$$\left(\frac{\delta \ln a_3}{\delta m_3}\right) \simeq \frac{\nu_{3c}}{m_3^0} + \frac{\nu_{3a}}{m_3^0} + \beta_{33}^0 = \frac{\nu_3}{m_3^0} + \beta_{33}; \quad \nu_3 = \nu_{3c} + \nu_{3a} \tag{25}$$

Substituting these values together with the value of $(-dT/dm_2)_{m_2=0}$ from equation (13) into (18),

$$\beta_{23}^0 + \frac{dm_3}{dm_2}\left(\frac{\nu_3 + \beta_{33}^0 m_3^0}{m_3^0}\right) = -\nu_2 \frac{\Delta \bar{H}_3^0}{\Delta H_m^0} \tag{26}$$

Rearranging

$$\left(\frac{dm_3}{dm_2}\right)_{m_2=0} = -\left(\frac{\beta_{23}^0 + \nu_2 \Delta \bar{H}_3^0/\Delta H_m^0}{\nu_3 + \beta_{33}^0 m_3^0}\right) m_3^0 \tag{27}$$

This expression differs from the one describing the isothermal change in the solubility of a pure solute caused by adding a second electrolyte containing a common ion only by the addition of $\nu_2 \Delta H_3^0/\Delta H_m^0$, since the temperature decreases with the addition of solute. The quantity $\nu_2 \Delta H_3^0/\Delta H_m^0$ is small for these cryoscopic solvents because of the large enthalpy change involved in transferring 55·5 moles of water from solid to solution.

For a two-component solvent system, equation (17) in the limit as $m_2 \to 0$ can be reduced to the following expression by substituting the temperature coefficients of the activities and dT/dm_2 from equation (13)

$$\begin{aligned} m_2\left(\frac{\delta^2 \ln a_2}{\delta m_2^2}\right) + \left(\frac{\delta \ln a_2}{\delta m_2}\right) + \frac{dm_3}{dm_2}\left(\frac{\delta \ln a_2}{\delta m_3}\right) &= \frac{-d^2T}{dm_2^2}\frac{\Delta H_m^0}{R\theta^2} - \frac{\nu_2}{\Delta H_m^0}\left(\frac{\delta H_m}{\delta m_2}\right) \\ &- \frac{\nu_2}{\Delta H_m^0}\frac{dm_3}{dm_2}\left[m_1\left(\frac{\delta \bar{H}_1}{\delta m_3}\right) + m_3\left(\frac{\delta \bar{H}_3}{\delta m_3}\right)\right] - \nu_2^2 \frac{R\theta^2}{\Delta H_m^{02}} \Delta C_{pm}^0 \\ &- \frac{\nu_2}{\Delta H_m^0}\frac{dm_3}{dm_2} \Delta \bar{H}_3^0 \end{aligned} \tag{28}$$

VOL. 19 1961

ΔH_m^0 = enthalpy of fusion or transition of the quantity of solvent containing 1 kg H_2O at $T = \theta$

H_m = enthalpy of the quantity of fused medium containing 1 kg of water

$\bar{H}_1$, $\bar{H}_3$ = partial molal enthalpy of the solvent-system components in the fused solvent

ΔC_{pm}^0 = difference in heat capacity between the quantity of fused and solid medium containing 1 kg of water

$\Delta \bar{H}_3^0$ = enthalpy change in transferring one mole of the salt, component 3, from the pure solid to the pure fused solvent system

All derivatives are taken in the limit as $m_2 \to 0$.

Certain terms in equation (28) can be neglected to a first approximation. Considering the sodium sulphate decahydrate solvent system as an example, ΔH_m^0 is quite large and equal to 104·76 kcal;[26] hence division by this quantity tends to give small terms. The ΔC_p^0 term amounts to only about 0·5 kcal/°C,[26] and $\Delta \bar{H}_3^0$ can be estimated from heats of solution of Na_2SO_4 to be smaller than -1 kcal/mole.[27] Considering the high concentration of electrolyte in the solvent system and the fact that activity coefficients vary slowly with concentration in such solutions, the effect of the concentrations of components 2 and 3 on the partial molal enthalpies of the solvent will be small. With these restrictions, the last four terms in (28) may be neglected.

Further differentiation of (10) yields

$$\left(\frac{\delta^2 \ln a_2}{\delta m_2^2}\right) = \frac{-\nu_2}{m_2^2} - \Sigma_i \frac{\nu_{2i}^3}{m_i^2} + \beta_{222}; \quad \beta_{222} = \left(\frac{\delta^2 \ln \gamma_2}{\delta m_2^2}\right) \tag{29}$$

The quantity β_{222}^0 vanishes in the limit, since β_{22} is constant and probably zero in solutions where component 2 does not contribute appreciably to the total molality. Substituting from equations (10), (24), (27), and (29) into (28) in the limit as $m_2 \to 0$

$$\Sigma_i \frac{\nu_{2i}^2}{m_i^0} + \beta_{22}^0 = \beta_{23}^0 \left(\frac{\beta_{23}^0 + \nu_2 \Delta H_3^0/\Delta H_m^0}{\nu_3 + \beta_{33}^0 m_3^0}\right) m_3^0 = \frac{-d^2T}{dm_2^2} \frac{\Delta H_m^0}{R\theta^2} \tag{30}$$

Thus

$$B = \frac{1}{2!}\left(\frac{d^2\vartheta}{dm_2^2}\right)_{m_2=0} = \frac{-1}{2!}\left(\frac{d^2T}{dm_2^2}\right)_{m_2=0}$$
$$= \frac{1}{2!}\frac{R\theta^2}{\Delta H_m^0}\left(\Sigma_i \frac{\nu_{2i}^2}{m_i} + \beta_{22}^0 - \beta_{23}^0 \left(\frac{\beta_{23}^0 + \nu_2 \Delta H_3^0/\Delta H_m^0}{\nu_3 - \beta_{33}^0 m_3^0}\right) m_3^0\right) \tag{31}$$

Setting $R\theta^2/\Delta H_m^0 = \lambda$, the usual molal freezing-point depression, and substituting these values into equation (14), recognizing that β_{22}^0 is essentially 0,

$$\frac{\vartheta}{m_2\lambda} \sim \nu_2 + \left(\Sigma_i \frac{\nu_{2i}^2}{m_i^0} - \left(\frac{\beta_{23}^{02} + \nu_2 \beta_{23}^0 \Delta H_3^0/\Delta H_m^0}{\nu_3 + \beta_{33}^0 m_3^0}\right) m_3^0\right) \frac{m_2}{2} \tag{32}$$

Equation (32) has a form very similar to the equation describing the osmotic pressure due to a colloidal electrolyte in the presence of a supporting electrolyte.[23] The osmotic pressure of proteins several pH units from the isoelectric point has been observed to obey such a limiting law in the concentration range 0 to about 10^{-3} molal where the maximum value of $|Z_2 m_2|$ is less than 10^{-2}. In view of the fact that the

[26] G. BRODALE and W. F. GIAUQUE, *J. Amer. Chem. Soc.* **80**, 2042 (1958).

[27] (a) K. S. PITZER and L. V. COULTER, *J. Amer. Chem. Soc.* **60**, 1310 (1938); (b) Circular 500, of the National Bureau of Standards, Feb. 1, Washington, D.C. (1952).

cryoscopic measurements are usually carried out with values of m_2 in the range 0·1–1·0 molal where $|Z_2 m_2|$ generally has values greater than unity with solutes like the isopolyanions, it is highly unlikely that the limiting law would be obeyed. Since theory indicates that the limiting values of $(\vartheta/\nu_2 m_2)_{m_2=0}$ should be a constant for a given solvent system independent of the solute, the fact that the values obtained by the careful measurements of SCHWARZENBACH and PARISSAKIS[20] with known solutes vary from solute to solute indicates that a linear extrapolation of the data is not valid.

Qualitatively, equation (32) indicates that the values of (ϑ/m_2) at finite concentrations will be greater than the limiting value by an amount which depends on the charge on the foreign ion which governs the ν_{2i}. The observation that the values obtained by extrapolation of the data from the concentration range $m_2 > 10^{-2}$ molal increased with increasing charge density of the foreign ion[20] is qualitatively in accord with equation (32). The empirical corrections applied to the limiting values of (ϑ/m_2) by SCHWARZENBACH and PARISSAKIS[20] are, in effect, an approximate way of correcting the data to infinite dilution.

VOL. 19 1961

It is interesting to note that if all activity coefficients were constant as is generally assumed, the curve $\vartheta/m_2\lambda(m_2)$ would not have a limiting slope of zero but would have the value $\Sigma_i \nu_{2i}^2/m_i^0$, which depends, for a given solvent, on the square of the charge on the foreign ion. Since the β_{23}^0 will in general not be zero and appears as the square, it will reduce the magnitude of the slope, and this tends to account for the fact that the method of linear extrapolation does give approximately correct values of $(\vartheta/m_2)_{m_2=0}$. There is, however, no theoretical justification for the linear extrapolation of the data from concentrations as high as 10^{-1} molal to infinite dilution.

An examination of the careful measurements of SCHWARZENBACH and PARISSAKIS[20] reveals the following variations in the values of $(\vartheta/\nu_2 m_2)$ obtained by linear extrapolation of data with known solutes. For $Z_2 = 0$, 3·14 ± 0·06; $Z_2 = -1$, 3·22 ± 0·12; $Z_2 = -2$, 3·14 ± 0·06; $Z_2 = -3$, 3·08 ± 0·12; $Z_2 = -4$, 3·10 ± 0·07. For a series of mono and polyphosphates, the mean value of $(\vartheta/\nu_2 m_2)_{m_2=0}$ was 3·60 ± 0·32 with individual values ranging between 3·1 for NaH_2PO_4 to 4·05 for Na_3PO_4. These values are for concentrations defined in terms of a kilogram of $Na_2SO_4 \cdot 10H_2O$, i.e. per 559·3 g of water.

JAHR and KUBENS[15] obtained a mean value of $(\vartheta/\nu_2 m_2) = 3{\cdot}27 \pm 0{\cdot}03$ with urea and a series of solutes giving one univalent foreign anion in $Na_2SO_4 \cdot 10H_2O$. The theoretical value calculated using the enthalpy of transition of $Na_2SO_4 \cdot 10H_2O$[26] with concentrations defined per kilogram of $Na_2SO_4 \cdot 10H_2O$ is 3·16, while with concentrations defined per kilogram of water it is 1·77.

In the study of an unknown polynuclear complex, the concentrations are computed on the basis of the monomeric species, $m_2 = N^{-1}m'$, where m' is the monomer concentration and N is the number of monomer units, e.g. metal atoms in the complex. Thus, $(\vartheta/\lambda m')_{m'=0} = 1/N$. In view of the large uncertainties in the values of $(\vartheta/m')_{m'=0}$, the salt cryoscopic method cannot be relied upon to give unequivocal values of the degree of polymerization when the complex contains more than about three or four metal atoms.

3. *Systems with more than one species of foreign ions*

In the preceding discussion, it was assumed that the foreign solute was monodisperse. Actually in the study of the isopolyions, hydroxide ions are often present in

sufficient quantity to make a significant contribution to the temperature depression.[3] In the study of the stepwise formation of complexes,[8] several cryoscopically active ions are present in equilibrium. SCATCHARD[23] has shown that with the definitions, $m_2 = \sum_n m_n$, $Z_2 = \sum_n X_n Z_n$, and $\ln \gamma_2 = \sum_n X_n \ln \gamma_n$ where the X_n are the mole fractions of the cryoscopically active species and the summations are extended over all n active species, $\beta_{23}{}^0 = \sum_n X_n{}^0 \beta_{n3}{}^0$ and $\beta_{22}{}^0 = \sum_n \sum_m \beta_{mn}{}^0 X_m{}^0 X_n{}^0$. In a system with several mononuclear complexes, the equation $\vartheta\lambda^{-1} = A + B + \sum_n nAB_n$[11] involves rather severe assumptions when applied at high total concentrations of the ligand A, the central ion B, and the complexes AB_n. If we consider the case of an isopoly ion which is formed reversibly, the equilibria of which can be studied only in the presence of significant concentrations of hydroxide ion, substitution of the above values of m_2, Z_2, and $\beta_{23}{}^0$ into (22), (23) and (32) indicates that the depression at finite concentrations of a mixed foreign solute is not the same as the sum of the depressions caused by the pure components of the mixture. The term involving $v_i{}^2$ will contain cross products of the type $X_a X_b Z_a Z_b$ while $\beta_{23}{}^{02}$ will contain $X_a X_b \beta_{a3}{}^0 \beta_{b3}{}^0$. Here the subscripts a and b refer to the components of the foreign solute, e.g., the isopoly salt and a hydroxide. In the calculation of the depression attributable to polysilicate ions in the presence of NaOH in a $Na_2SO_4 \cdot 10H_2O$ medium,[3] subtraction of the depression caused by an equal concentration of pure NaOH will not accurately give the depression that would be caused by the pure silicate ions at finite concentrations. Considering the assumptions necessary for the interpretation of such cryoscopic data, it is not surprising that the results do not agree exactly with e.m.f. studies.[19]

4. *Comparison with other methods*

The most widely used method for the study of aggregation and complex formation equilibria in aqueous solution is the e.m.f. method. The e.m.f. method requires that the activity coefficients of all species which are measured directly as well as those involved in the equilibria must remain constant. Since all of the species under study can be maintained at quite low concentrations in a medium of high constant ionic strength or constant concentration of the ions of charge opposite to those under study, this assumption can be satisfied to a very good approximation.[28,29] On the other hand, even though the cryoscopic solvents consist of a highly concentrated electrolyte solution, an evaluation of the data from cryoscopy at finite concentrations even where the limiting law is obeyed would require a knowledge of the charge on the species as well as the $\beta_{23}{}^0$ term which differs from zero. In order to circumvent these difficulties an extrapolation to infinite dilution is required; however, unless data are taken for very dilute solutions, a linear extrapolation of the data cannot be expected to give an accurate value of $(\vartheta/m_2)_{m_2=0}$. The results of cryoscopic measurements, particularly in the case of systems with several complexes or poly-ions containing more than three or four metal atoms, are best regarded as indicative rather than conclusive.

[28] G. BIEDERMANN and L. G. SILLÉN, *Arkiv Kemi* **5**, 425 (1953).
[29] G. BIEDERMANN and T. WALLIN, *Acta Chem. Scand.* **14**, 594 (1960).

J. Inorg. Nucl. Chem., 1961, Vol. 19, pp. 359 to 376. Pergamon Press Ltd. Printed in Northern Ireland

VOL. 19 1961

NOTES

Hydrolytic and photolytic reactions in the system: water–hydrochloric acid–uranyl chloride–butyl phosphoric esters

(*Received* 9 *November* 1960)

THE publications on tri *n*-butyl phosphate (TBP) as an extractant for uranium are very numerous for systems containing uranyl nitrate and aqueous nitric acid solutions. Much of the published work on the extraction properties of TBP from aqueous solutions of acids other than nitric is rather limited in scope as the practical implications are the most important issue. In a series of papers, Kertes *et al.* recently reported the results of investigations into the solute–solvent interactions between TBP and hydrobromic acid,[1] perchloric acid[2] and hydrochloric acid,[3] and pointed out the difference in behaviour of these systems in comparison with that of TBP and nitric acid. In an extension of these investigations a hydration phenomenon in the hydrochloric acid—TBP system[4] has been studied, and we reported on the hydrochloric acid promoted hydrolysis of TBP.[5] In these studies special emphasis was placed on the important rôle that water plays in the distribution of electrolytes between aqueous solutions and the extractant.[6] A further difference between the nitric and hydrochloric acid systems was found in the extraction of hexavalent uranium, as uranyl chloride, by undiluted TBP, from aqueous hydrochloric acid solutions.[7] During this study, it was found that the homogeneous equilibrium organic layers, previously separated from the opposing equilibrium aqueous phases, and containing both hydrochloric acid and uranyl chloride in various concentrations, could not be kept unchanged after a period of 8–10 days under the normal laboratory conditions of light and temperature. After this period a solid began to separate out. Once the transformation has started it proceeds quite rapidly and is usually complete in a few days. The homogeneous organic layer, initially uranium (VI), turns from yellow to a greenish tinge, characteristic of uranium (IV), while forming the gel precipitate. The above phenomenon, completely unknown for the parallel nitric acid–uranyl nitrate system, is described in the present report.

Similar phenomena were mentioned in publications from other laboratories as observed in studies of uranium (VI) extraction by acidic phosphoric esters. BAES, ZINGARO and COLEMAN,[8] in a study of the extraction of uranyl perchlorate into di-(2-ethyl hexyl) phosphoric acid, observed that the organic solution resulting from uranium (VI) extraction, homogeneous and yellow in colour, developed a greenish tinge after several days storage on open shelves. When stored in the dark no transformation took place. By spectrophotometric examination the authors obtained absorption curves with a pronounced maximum at 650 mμ, characteristic of uranium (IV). These phenomena, although attributed to light, could not be explained by the authors. HEALY and KENNEDY[9] found that exposure of uranyl dibutyl phosphate to light resulted in photochemical decomposition, producing a greenish tinge of uranium (IV) and a rancid odour, due probably to butyric acid. These authors also offered no explanation for the phenomena. More recently, GRDENIĆ and KORPAR[10] in a study of the complexing of uranium (IV) with dialkyl pyrophosphoric acids, obtained compounds with chemical properties similar to those described in this study.

[1] A. S. KERTES and V. KERTES, *Canad. J. Chem.*, **38**, 612 (1960).
[2] A. S. KERTES and V. KERTES, *J. Appl. Chem.*, **10**, 287 (1960).
[3] A. S. KERTES, *J. Inorg. Nucl. Chem.*, **14**, 104 (1960).
[4] A. S. KERTES, *J. Inorg. Nucl. Chem.*, **12**, 377 (1960).
[5] A. S. KERTES and M. HALPERN, *J. Inorg. Nucl. Chem.*, in press.
[6a] W. H. BALDWIN, C. E. HIGGINS and B. A. SOLDANO, *J. Phys. Chem.*, **63**, 118 (1959).
[6b] H. IRVING and D. N. EDGINGTON, *J. Inorg. Nucl. Chem.*, **10**, 306 (1959).
[7] A. S. KERTES and M. HALPERN, *J. Inorg. Nucl. Chem.*, **46**, 308 (1961).
[8] C. F. BAES, JR., R. A. ZINGARO and C. F. COLEMAN, *J. Phys. Chem.*, **62**, 129 (1958).
[9] T. V. HEALY and J. KENNEDY, *J. Inorg. Nucl. Chem.*, **10**, 128 (1959).
[10] D. GRDENIĆ and B. KORPAR, *J. Inorg. Nucl. Chem.*, **12**, 149 (1959).

The similarity of our observations in systems containing uranium(VI) and the neutral ester tributyl phosphate with those of mono-acidic phosphoric esters, leads us to explain the phenomenon on the basis of hydrolytic decomposition of the esters involved, both the neutral trialkyl- and the acidic dialkyl ester, and on the basis of a primary photochemical transfer of electrons from hydrolytic products of the esters to the uranyl ion.[11]

The experimental results can be summarized as follows: One series of experiments carried out with a constant initial concentration of uranyl chloride (~0·1 M) and varying amounts of hydrochloric acid, up to 10 M, in the initial aqueous solution, have shown that the gel formation, in the separated equilibrium organic phase, takes place even at fairly low acidities of approximately 2 M in the initial aqueous solution. The quantity of the precipitate observed, under identical experimental procedures, is strictly dependent on the initial acidity, since the amount of uranyl chloride in the organic phase depends on the acidity of the initial aqueous solution.[7] The point at which the transformation begins seems also to be dependent upon the acidity: at higher acidities, the gel formation starts earlier. An additional set of experiments was carried out with constant concentration, 8·8 M, of hydrochloric acid and varying high concentrations of uranyl chloride of up to 3·2 M in the initial aqueous solution. In these experiments, under identical laboratory and working conditions, gel formation took place only when the uranium concentration before equilibration was not too high, about 1·2 M in the initial aqueous solution. In experiments with higher initial uranium concentrations, the freshly-separated homogeneous and yellow TBP phase turned to a deep green, very viscous solution after a few days, but without a solid phase being formed. In all experiments the presence of butanol, and/or butyraldehyde and/or butyric acid in the closed containers of the samples was detected by smell.

The green gel is completely soluble in chloroform and partially soluble in toluene, but insoluble in any of the following organic solvents: methanol, ethanol, *n*-butanol, acetone, benzene, carbon tetrachloride, *iso*-propylether, *iso*-amylalcohol, methyl *iso*-butyl ketone, methyl ethyl ketone, *n*-hexane, *n*-heptane, cyclohexane, ligroin, kerosene, cellosolve, ethylacetate, *n*-butylacetate and amyl acetate. It is also soluble in hot, concentrated nitric acid. The inconsistency of the phosphorous to uranium ratio in the different samples was taken as evidence that the gel precipitate contained various amounts of occluded TBP. In order to remove the occluded TBP from the gelatinous precipitate, it was washed with ethanol, and the washed precipitate was finally vacuum dried at about 70°C. This procedure leaves the product in the form of a pale green powder insoluble even in chloroform. The analysis of the different washed samples after their dissolution by sodium nitrate fusion revealed the same uranium:phosphorus ratio, thus indicating a definite chemical compound, formed under the various experimental conditions described above. No chloride could be found in any of the samples.

A part of the above experiments was repeated with dibutyl-(HDBP) and monobutyl-phosphoric acids (H_2MBP). These acidic esters were isolated from a commercial product—Butyl Acid Phosphate, purchased from ALBRIGHT and WILSON Ltd., Birmingham—and thoroughly purified by a solvent extraction method, similar to that of KENNEDY and GRIMLEY,[12] and described in detail elsewhere.[13] In order to study their behaviour under identical conditions, neither of these esters were diluted with carrier solvents. Using HDBP, the homogeneous, yellow organic phase had changed in colour within a few hours, and a precipitate was formed when the samples were kept on open shelves, but no change appeared even after six months when the samples were kept in the dark at room temperature, as in the case of TBP. With the aqueous solutions completely miscible, the H_2MBP transformation appeared only when the aqueous solution contained high concentrations of uranyl chloride. The product of HDBP, after washing with alcohol and drying, was very similar in appearance to that of TBP, but the H_2MBP product, after washing and drying, was an almost white powder.

The reduction of uranium(VI) became evident when comparing the spectra of the photolysed and unphotolysed samples of the same original organic solutions. The absorption spectra of the photolysed samples of the three esters (chloroform solution of the unwashed and undried gel) revealed the absorption peak characteristic of uranous ions,[14,15] but shifted somewhat to longer wavelengths

[11] B. JEZOWSKA-TRZEBIATOWSKA, A. BARTECKI, M. CHMIELOWSKA, H. PRZYWARSKA, T. MIKULSKI, K. BUKIETYNSKA and W. KAKOLOWICZ, *Proceedings of the Second Conference on the Peaceful Uses of Atomic Energy, United Nations, Geneva*, **28**, 253 (1958).
[12] J. KENNEDY and S. S. GRIMLEY, AERE CE/R–968 (1953).
[13] Y. HABOUSHA, M.Sc. Thesis, *The Hebrew University, Jerusalem*, (1960).
[14] L. J. HEIDT, *J. Amer. Chem. Soc.*, **76**, 5962 (1954).
[15] K. A. KRAUS and F. NELSON, *J. Amer. Chem. Soc.*, **72**, 3901 (1950).

probably as an effect of the medium.[11] A similar peak was not measured in the unphotolysed samples, nor were such spectra developed by the photolysed aqueous solutions containing uranyl chloride and hydrochloric acid. These differences in the spectra leave little doubt that uranium (IV) is produced s.by photolysi

Infra-red spectra of the solids, using the KBr disc method, were taken by means of the Baird-Atomic I.R. Spectrophotometer with NaCl prism. The absorption peaks observed for TBP and HDBP compounds were essentially identical, except that a negligible absorption of free–OH band appears in the region of 3350 cm^{-1} in the HDBP sample. The spectrum of the H_2MBP compound, in contrast to that of TBP and HDBP compounds, does not reveal weak bands at 920 cm^{-1}, attributed to the anti-symmetrical normal vibration of the uranyl ions probably present in traces in the isolated solids. The strength of the 3350 cm^{-1}–OH band is more intense in the case of H_2MBP–compound. High absorption was recorded for the whole region from 1020 to 1100 cm^{-1} in the case of all three compounds. The band strengths do not differ significantly in the three compounds.

Additional information concerning the nature of the three compounds was acquired from X-ray diffraction diagrams, as obtained by a Guinier monochromatizing-focussing camera. X-ray examination of the washed and dried samples showed them to be crystalline. The lines in the TBP and HDBP compounds were found to be exactly analogous. The X-ray pattern of the H_2MBP compound was quite different from that of TBP and HDBP samples, and showed that the crystal size was much smaller. The lines were diffuse and therefore no attempt was made to index them.

The uranium, phosphorus and the elementary analyses carried out on the three samples gave the following results:

	U	P	C	H
TBP-compound	24·1	10·4	35·7	6·74
HDBP-compound	23·8	10·9	34·9	6·31
H_2MBP-compound	41·3	10·9	17·2	3·57

All attempts to carry out molecular weight determinations of the samples which had been washed and purified by alcohol, but not dried, using the freezing-point depression method, with chloroform as the cryoscopic medium, proved futile.

For the sake of prudence, several experiments were carried out with the three esters and aqueous nitric acid solutions of uranyl nitrate. Under conditions identical with those described above, no change was observed in any of the samples after a couple of months.

DISCUSSION

The best-known photochemical reactions of hexavalent uranium are those with organic compounds. Rabinowitch[16] has thoroughly and critically reviewed the photosensitized reduction of uranium by fatty acids, but unfortunately this report does not include photochemical processes for uranium reduction by organic compounds other than normal and substituted aliphatic acids. It has been found that photo-activated uranyl ions react in water with sucrose and closely related substances,[17] in aliphatic alcohols[14,18] and in a mixture of formic acid and absolute ethanol.[19]

From the fact that in nitric acid systems with either the neutral or acidic butyl esters of phosphoric acid, no photo-sensitized reduction of uranium (VI) takes place, it is tempting to conclude that esters are unable to undergo photochemical excitation under the conditions of solvent extraction processes. In completely analogous hydrochloric acid systems, where the hydrolysis of the esters in the organic phase is about 250 times faster than in the nitric acid systems,[5,20] the hydrolysis products formed

[16] E. Rabinowitch, ANL–5202 (1954).
[17] L. J. Heidt and K. A. Moon, *J. Amer. Chem. Soc.*, **75**, 5803 (1953).
[18] S. K. Bhattacharayya and Sh. Gulvady, *J. Indian Chem. Soc.*, **29**, 649 (1952).
[19] B. Sahoo and D. Patnaik, *J. Indian Chem. Soc.*, **36**, 483 (1959).
[20] L. L. Burger, *Progress in Nuclear Energy*, Series III; *Process Chemistry*, Pergamon Press, London, **2**, 307 (1958).

VOL. 19 1961

and accumulated are able to undergo photochemical oxidation by excited uranyl ions. Unfortunately, no data are available on the rate of hydrolysis of the butyl esters in perchloric acid systems, but on the basis of analogy with the systems HCl–TBP and $HClO_4$–TBP, as far as the hydration of the acid in the organic phase is concerned,[2,21,22,23] the rate of hydrolysis in the perchloric acid system could be expected to be very similar to that in the hydrochloric acid system. The existence of photoreduction of uranium as observed by BAES, ZINGARO and COLEMAN[8] in perchloric acid systems with the dialkyl phosphoric acid is consistent with the above assumption on the rate of hydrolysis.

For the H_2MBP-compound, the precipitated entity may be formulated as $U(O_2BuOPO)_2$. This formulation is consistent with the analytical composition of the precipitate–theoretical FW 542·3; U 43·7%; P 11·4%; C 17·7%; H 3·34%. On the basis of the analytical data obtained for solids isolated from TBP and HDBP, a common formula $U[O(BuO)_2PO]_4$ can be postulated with the theoretical composition: FW 1074·9; U 22·2%; P 11·5%; C 35·8%; H 6·75%. This formulation is essentially analogous to that of the solid uranous-dialkyl pyrophosphate isolated by GRDENIĆ and KORPAR.[10] If the above patterns for the three compounds are correct, the uranium must be linked ionically to the phosphate through the acidic OH group of the esters and, therefore, the solvent: uranium molecular ratio depends upon the neutralizable hydrogen ions in the molecule of the extractant-ligand. The presence of the free OH band at 3350 cm^{-1} in both HDBP and H_2MBP compounds as well as that of the weak band at 920 cm^{-1}, characteristic of the uranyl ions, in the TBP and HDBP compounds, tends to weaken the above formulation, unless both bands are due to impurities occluded in the precipitate.* We believe this is the case since the intensity of the bands varied in different samples of the same compound.

Nevertheless, the formulae advanced are open to objection, since a number of complex factors must be taken into account. Firstly, we do not know the real uranous ionic species in solution before any precipitation occurs, and therefore the co-existence of several uranous species in the organic solution cannot be excluded. A second complication arises from the fact that organic molecules are dimerized and polymerized in the case of DBP and MBP, respectively.[24,25] In addition, in view of the complex nature of the organic solutions, polynuclear cation species are possible and are not ruled out by our data. Finally, it is possible that, during the formation of solid, several species are involved with varying formula weights or even in varying states of polymerization.

The formation of the gel was found to begin with almost the same velocity in HDBP and H_2MBP samples, provided that sufficient uranium was present in the case of H_2MBP. This indicates that the light absorption is approximately the same in both cases, and therefore it is unlikely that the light absorption is different in TBP samples, under identical experimental conditions. However, the formation of the precipitate starts and approaches completion much more slowly in the TBP samples. It should be noted that the HDBP and H_2MBP phenomena relate to systems in which the organic molecules entering the solid are present in large excess. On the other hand, in the TBP system, the formation of the organic molecules, HDBP, entering the solid, must be sufficient to reach the solubility product of the solid, which is probably greater in tributylphosphate than in dibutylphosphate, and to stabilize the uranium (IV) by the formation of the insoluble uranium (IV)-compounds from the reversible reaction uranium (IV) ⇌ uranium (VI).

Acknowledgements—It is a pleasure to thank Drs. E. MEIER, R. HELLER and Miss G. LACHOVER, Dept. of Microanalysis, The Weizmann Institute of Science, Rehovot, and Mrs. M. GOLDSTEIN, Chemical Engineering, Laboratory of Microanalysis, The Hebrew University, for the phosphorus and elementary analyses. The authors also wish to express their appreciation to Drs. B. S. FRAENKEL and Z. KALMAN, Department of Physics, The Hebrew University, for the X-ray analyses.

Department of Inorganic and Analytical Chemistry,
The Hebrew University,
Jerusalem, Israel.

A. S. KERTES
M. HALPERN

* The authors are indebted to the referee for the suggestion that the weak OH and uranyl ion bonds may be due to slight hydrolysis of the $U(DBP)_4$ compound.

[21] V. V. FOMIN and E. P. MAIOROVA, *Zhur. Neorg. Khim.*, **5**, 1100 (1960).
[22] S. SIEKIERSKI and R. GWOZDZ, *Nukleonika*, **5**, 205 (1960).
[23] E. HESFORD and H. A. C. MCKAY, *J. Inorg. Nucl. Chem.*, **13**, 156 (1960).
[24] D. F. PEPPARD, G. W. MASON and J. R. FERRARO, *J. Inorg. Nucl. Chem.*, **4**, 371 (1957).
[25] D. DYRSSEN, *Acta Chem. Scand.*, **11**, 1277 (1957).

Pressure measurements in the arsenic trichloride–chlorine system and the arsenic and antimony tribromide–bromine systems

(*Received* 25 *November* 1960; *in revised form* 20 *January* 1961)

Pentahalides such as PCl_5, PBr_5 and $SbCl_5$ are well known while the literature[1,2] indicates that $AsCl_5$, $AsBr_5$ and $SbBr_5$ have no stable existence. For example, the freezing point diagrams of the tribromide-bromine systems[3] of arsenic and antimony show simple eutectic formation. In order to examine the tendency for equilibrium pentahalide formation in solutions of the trihalide–halogen mixtures, pressure measurements were carried out.[4]

Experimental

Materials. Arsenic tribromide (City Chemical Corp., New York) was fractionated by vacuum distillation. It was necessary to keep the distillation assembly above 31·5°, the melting point of arsenic tribromide. The latter was accomplished by use of two infra-red lamps. The fractions were sealed in weighed ampoules and sublimed into the sickle gauge apparatus just prior to use.

Arsenic trichloride (Baker and Adamson, reagent grade) was purified by vacuum distillation followed by fractionation in the line. Samples were condensed and weighed directly in the 'reaction' ampoule.

Antimony tribromide (Fisher Scientific Co.) was weighed out directly from a freshly opened bottle using dry box techniques.

Chlorine gas (Matheson Co.) was passed through a spiral type bubbler containing concentrated sulphuric acid. It was dried over phosphorus pentoxide coated glass beads and fractionated in vacuum. The vapour pressure at −78·5°C was 68·2 mm (literature value,[5] 64·5 mm).

Liquid bromine (Baker's, analyzed reagent) was used from a freshly opened bottle and fractionated in the line. Vapour pressure at 0°C was 68·4 mm as compared to a literature value[6] of 65·9 mm.

Apparatus. The apparatus used for the pressure measurements is pictured in Fig. 1. It combines two glass sickle gauges; one for measuring the pressure in the section containing the halogen to determine the amount added in incremental fashion to the reaction section, the other for measuring the equilibrium pressures in the reaction section. The pressures are read by a null point method. The pressure inside the sickle gauge is adjusted by varying the external air pressure (an independent system is provided for each gauge), such that the pointer is brought back to a reference point. To accomplish this and obtain the necessary sensitivity the pointer movement is magnified by attaching a mirror to the end of the pointer and focussing the cross hairs of a cathetometer on a metre stick as seen reflected in the mirror, the metre stick being mounted permanently on the cathetometer. After pressure equalization, the external pressure is read on a mercury manometer by means of the cathetometer. For convenience the apparatus was constructed so that the pointer movements on the two sickle gauges, and the mercury levels in the associated manometers, could be read by swivelling the cathetometer from one permanent position. Pressures read to ±0·1 mm are readily obtained.

Dow Corning high vacuum silicone grease was used for all valves. Chlorine was not noticeably effected. Bromine initially discoloured the grease with an accompanying small loss in pressure but no further action was noted.

VOL. 19 1961

(1) N. V. Sidgwick, "*The Chemical Elements and their Compounds*", Oxford University Press, London, p. 791, Vol. 1 (1950).
(2) V. Gutmann, *Monatsh.*, **82**, 473 (1951).
(3) N. A. Pusin and J. Makuc, *Z. anorg. allgem. Chem.*, **237**, 177 (1938).
(4) The simple freezing point diagram observed for the arsenic tribromide–bromine system by Pusin and Makuc[3] had a eutectic at −31·5° at 79·5 atom % bromine. This corresponds to a freezing point lowering of 24·2° (mp. of bromine = −7·3°). Assuming ideal behavior one would expect a lowering of 26·8°. The value they obtained experimentally then, indicates very slight positive deviations from ideality. Considering the routine nature of the freezing point measurements, the latter may or may not be real. To decide would require detailed cryoscopic measurements of high precision. For example, a 0·1 molal solution would show a depression of 0·83° if association did not occur and 0·85° even if association to a 1:1 was 100% complete.
(5) W. F. Giauque and T. M. Powell, *J. Amer. Chem. Soc.*, **61**, 1970 (1939).
(6) R. E. Dodd and P. L. Robinson, "*Experimental Inorganic Chemistry*", Elsevier Publishing Co., Amsterdam, p. 174 (1954).

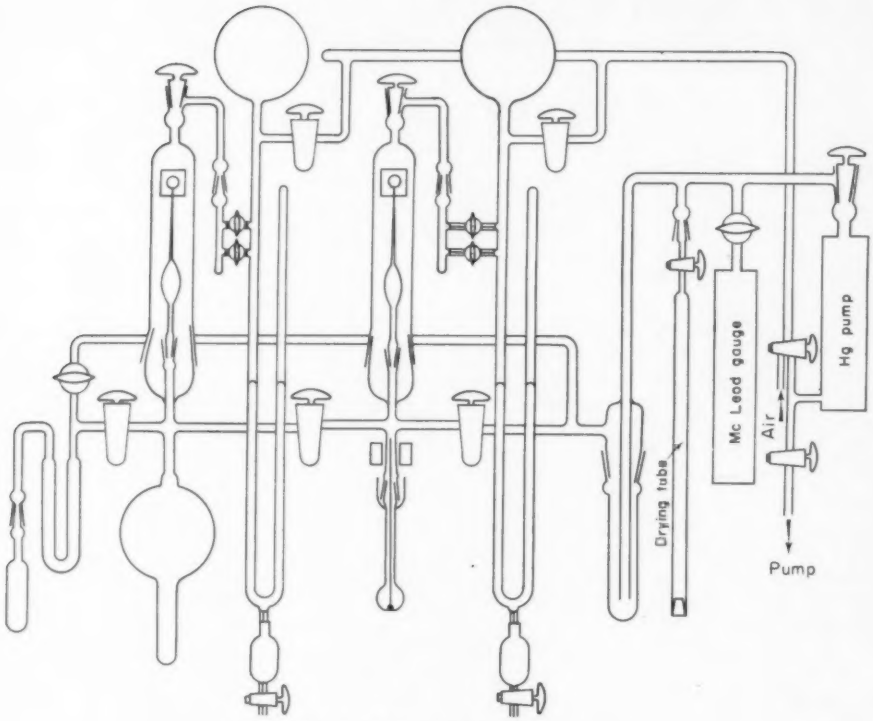

FIG. 1.—Sickle gauge apparatus.

Equilibrium was readily established after each addition in the systems studied as noted by no time-pressure dependence after a short period of stirring.

Results

Arsenic trichloride–chlorine system at 0°C;—the data for the measurements made on the arsenic trichloride–chlorine system at 0°C are listed in Table 1. The data reported here and in the following

TABLE 1.

The arsenic trichloride–chlorine system at 0°

Mole fraction chlorine	Total pressure mm
0·032	177
0·055	250
0·089	343
0·108	410
0·161	532

tables refer to condensed state compositions. In the case of arsenic and antimony tribromide, their contribution to the total pressure is negligible.

When plotted the data showed slight positive deviations from ideal liquid behaviour. In comparing with ideal behaviour, a value of 3·66 atm for the vapour pressure of chlorine at 0° was used.[5]

TABLE 2.

The antimony tribromide–bromine system at 0°C

Mole fraction bromine	Bromine pressure mm
0·13	53·3
0·325	54·8
0·505	55·0
0·776	54·9
0·816	56·5
0·846	58·4
0·869	59·7
0·895	62·2

VOL. 19 1961

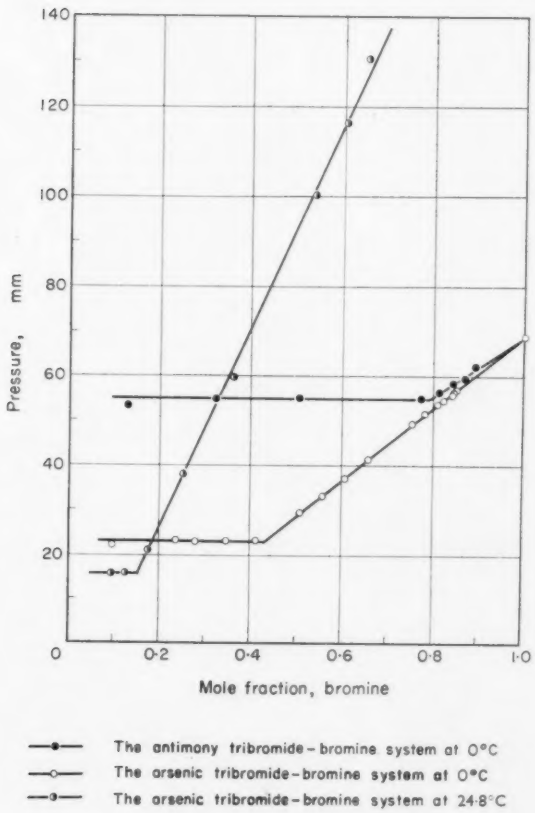

FIG. 2.—The antimony tribromide–bromine system.

Antimony tribromide–bromine system at 0°C;—the data for the measurements made on the antimony tribromide–bromine system at 0° are listed in Table 2 and shown graphically in Fig. 2. The plot shows a plateau corresponding to the pressures of a saturated solution of solid antimony

tribromide in liquid bromine. The solubility was calculated to be 56·5 gm $SbBr_3$ per 100 g Br_2. In the solution region a line showing almost ideal behaviour was obtained.

Arsenic tribromide–bromine system;—the data on the arsenic tribromide–bromine system at 0°C and 24·8°C are listed in Table 3 and shown in Fig. 2.

TABLE 3.

The arsenic tribromide–bromine system

0°C		24·8°C	
Mole fraction bromine	Bromine pressure mm	Mole fraction bromine	Bromine pressure mm
0·101	21·9	0·098	15·4
0·238	23·1	0·128	15·7
0·280	22·8	0·178	20·9
0·352	23·1	0·253	37·8
0·413	23·1	0·360	59·6
0·510	29·4	0·536	100·1
0·558	33·0	0·602	116·1
0·609	37·2	0·651	130·6
0·659	41·3		
0·755	49·0		
0·781	51·4		
0·811	53·5		
0·824	54·4		
0·840	55·8		
0·846	56·5		
0·852	56·9		

The plot shows plateaus corresponding to the pressures of saturated solutions of solid arsenic tribromide in liquid bromine. The solubility was calculated to be 261 g $AsBr_3$ per 100 g Br_2 at 0°C and 1036 g $AsBr_3$ per 100 gm Br_2 at 24·8°C. The solution region at both temperatures shows negative deviations from Raoult's law. The resultant value of the Henry's law constant, k, obtained from the relation, $P_{Br_2} = k\,N_{Br_2}$ is 79·8 mm at 0° and 228 mm at 24·8°.

Solutions of arsenic tribromide in liquid bromine at room temperature were tested for conductivity and showed no conductance within the limits of the bridge (the lower limit being $4{\cdot}0 \times 10^{-8}\,\Omega^{-1}$). Concentrations tested range from 0·0112 molal to 0·0657 molal.

Discussion

The results show no tendency for formation of $AsCl_5$ or $SbBr_5$. The negative deviations observed in the arsenic tribromide–bromine system tempt one to postulate an equilibrium involving the presence of some $AsBr_5$ in solution. However, the lack of existence of $AsCl_5$ does not make the existence of $AsBr_5$ seem reasonable, even in an association process. In view of the lack of any appreciable conductance of the solutions, formation of simple ions would be ruled out as an alternate possibility. However, ion pair formation would be in accord with the data, for example, formation of $Br_3AsBr^+ \ldots Br^-$.

Acknowledgement—The author wishes to express his appreciation to the National Science Foundation for a grant for support of this work.

ROBERT R. HOLMES

Department of Chemistry
Carnegie Institute of Technology
Pittsburgh 13, *Pennsylvania*

Polymorphism and melting in silver cyanide to 75,000 bars.

(*Received* 13 *January; in revised form* 21 *March* 1961)

THE high pressure modification of AgCN was discovered by BRIDGMAN,[1] who followed the transition curve to 147°C and 30,700 kg cm^{-2}. Bridgman's transition line was drawn on the basis of only three points at 22, 90 and 147°C, and deviated appreciably from a straight line, being strongly curved towards the P-axis in the P–T plane. It was consequently decided to reinvestigate the region of the P–T diagram studied by BRIDGMAN and simultaneously to extend the transition curve to higher pressures and temperatures.

Method

The experiments were carried out in a simple squeezer high-pressure high-temperature apparatus[2] The method described in detail elsewhere.[4] To observe the melting point, the resistance of the sample is measured and plotted as a function of temperature at constant pressure. A typical plot of resistance against temperature is shown in Fig. 1. The process of melting is accompanied by a fairly sharp

VOL. 19 1961

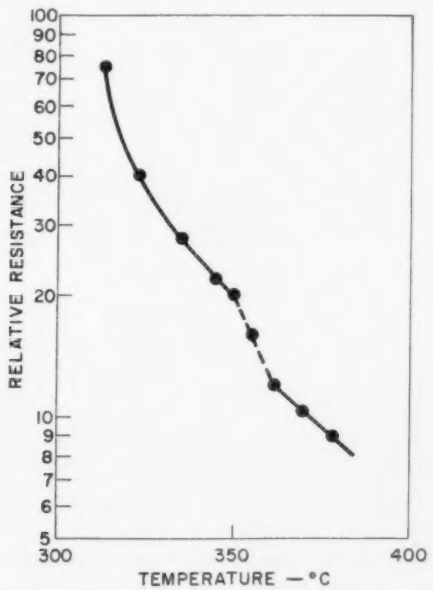

FIG. 1.—Typical plot of resistance of AgCN against temperature at 5·2 kB.

discontinuous decrease in the resistance. This procedure is repeated at various pressures, and a curve of melting temperature against pressure is obtained.

The polymorphic transition discovered by BRIDGMAN[1] is detected in a slightly different way. The temperature is kept constant and the pressure is increased by 1000 bar steps, the resistance being measured one minute after each increment. The transition appears as a very obvious discontinuity in the curve of resistance against pressure. Such a curve is shown in Fig. 2.

High-pressure Transition

AgCN was obtained from Johnsons of Hendon. Runs were made at 71°C, 200°C and 231°C.

[1] P. W. BRIDGMAN, *Proc. Amer. Acad. Arts Sci.* **72,** 46 (1937) *Proc. Nat. Acad.* **23,** 202 (1937).
[2] D. T. GRIGGS and G. C. KENNEDY, *Amer. J. Sci.* **254,** 722 (1956).
[3] C. W. F. T. PISTORIUS, *Z. Phys. Chem. Neue Folge*, in press.

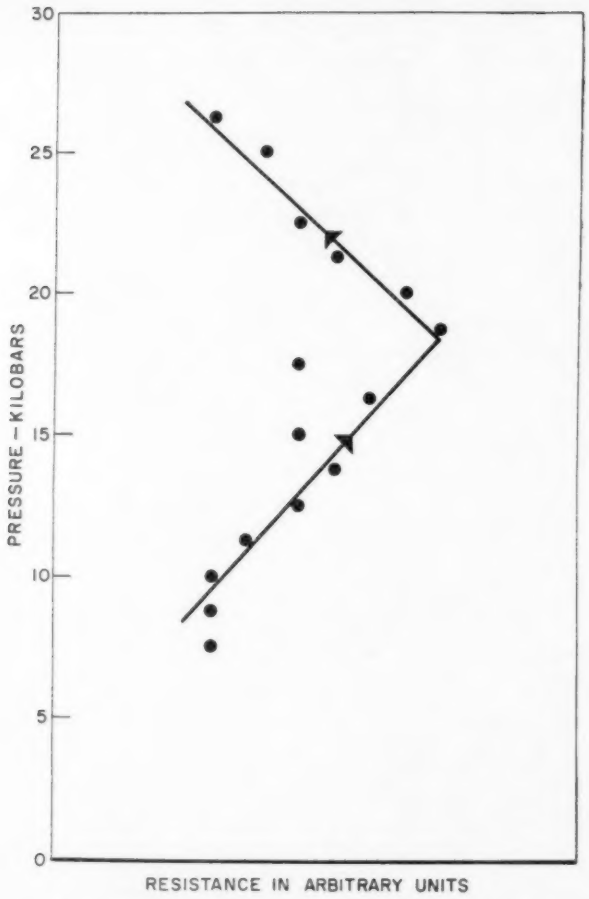

FIG. 2.—Typical plot of resistance of AgCN against pressure at 71°C.

The run at 71°C was in the region of the transition line investigated by BRIDGMAN, and served mainly as a check on the agreement between Bridgman's results and the present ones. The agreement was excellent within the stated limits of error.

The runs at 200°C and 231°C showed fairly conclusively that the transition line is, in fact, curved as found by BRIDGMAN. The final transition boundary is shown in Fig. 3. Unfortunately the boundary could not be extended beyond 57 kilobars because changes of resistance due to discontinuously changing sample geometry interfered.

The strong curvature of the transition line must be ascribed to the fact, discovered by BRIDGMAN, that the high pressure phase is distinctly less compressible than the low pressure phase. The original change of volume at the transition is approximately 0·0002 cm³/gm, and would obviously decrease with increasing pressure due to the compressibility relations. This would, according to the Clausius–Clapeyron relation, give rise to a curvature of the experimentally encountered type, if one assumes that the change of entropy remains approximately constant.

Thermal Expansion

The low-pressure phase of AgCN is rhombohedral, space group $R3c$, with $a_{rh} = 3{\cdot}88$ Å, $\alpha_{rh}: = 101°11'$, or $a_{hex} = 5{\cdot}99$ Å, $C_{hex} = 5{\cdot}26$ Å.[4] Measurements were made of the X-ray powder diffraction

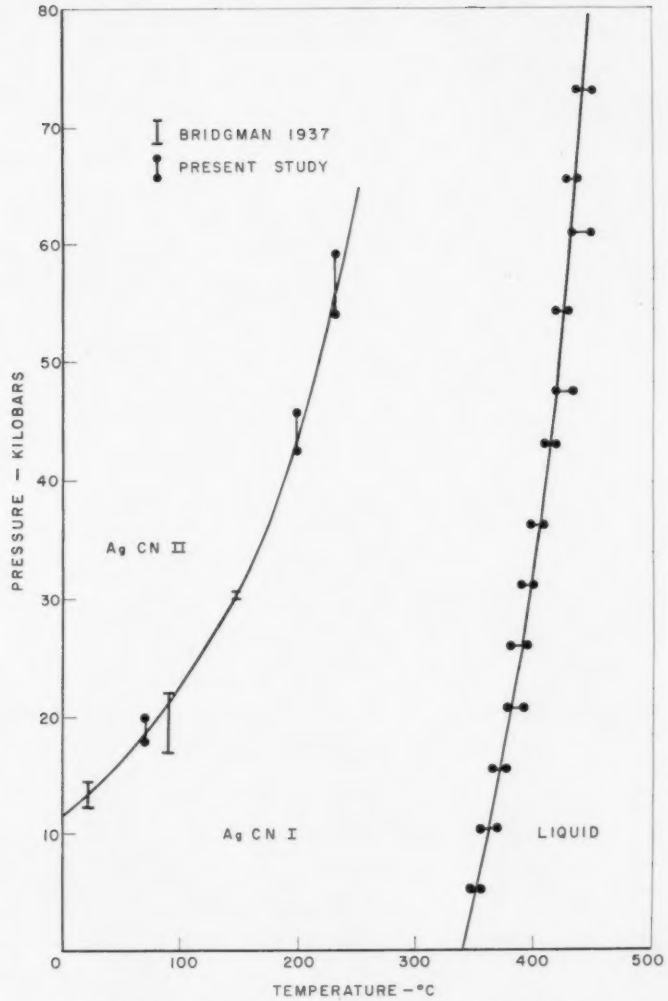

FIG. 3.—Phase diagram of AgCN in the range 0–80 kB and 0–500°C.

pattern of AgCN to 325°C in a high-temperature attachment to the Philips X-ray diffractometer.[5] The observed average thermal expansion coefficients in the range 25–325°C were as follows:

Coefficient along hexagonal *a*-axis = 0·000077/°C.
Coefficient along hexagonal *c*-axis = 0·000043/°C.
Coefficient of cubic expansion = 0·00020/°C.

The accuracy in all cases is approximately ±5 per cent.

The calculated density at 25°C is 4·05 g/cm³. Using these coefficients of volume expansion, the density of the solid at the melting point is 3·806 gm/cm³.

Melting Curve

The melting temperature is not strongly dependent on pressure. The melting curve was followed to

[4] J. WEST, *Z. Kristallogr.* **88,** 173 (1934).
[5] J. VAN NIEKERK, *J. Sci. Instrum.* **37,** 172 (1960).

73 kilobars, where the temperature of fusion is 443 ± 6°C. Up to 73 kilobars no transition lines intersect the melting curve, and it is consequently smooth. The curvature is obvious, and in the expected direction, i.e. towards the pressure axis in the P–T plane.

The melting curve is shown in Fig. 3. The curve extrapolates to a value of 346 ± 5°C at one bar pressure. This value must be considered a better value than the previous figure[6] of 320–350°C for fusion accompanied by decomposition, since in the present case decomposition is totally suppressed by the counter-effect of the high pressure. Any significant decomposition would have been revealed by a time-dependent change in the resistance, and no such effect was encountered. The original sample was unchanged, as shown by X-ray diffraction, after fusion even at 73 kB and 443°C.

The constants in the Simon fusion equation[7] are

$$c = 1{\cdot}5 \pm 0{\cdot}4$$
$$a = 300 \pm 100 \text{ kB},$$

where

$$P/a = \left(\frac{T}{619}\right)^c - 1.$$

Acknowledgements—The author would like to thank MR. E. TAPPERE and his staff for maintenance of the apparatus.

CARL W. F. T. PISTORIUS

National Physical Research Laboratory
Council for Scientific and Industrial Research
P.O. *Box* 395. *Pretoria*
Union of South Africa

[6] W. TRUTHE, *Z. Anorg. Chem.* **76**, 144 (1912).
[7] F. SIMON and G. GLATZEL, *Z. Anorg. Chem.* **178**, 309 (1929).

The preparation and some properties of the intermediate product leading to the formation of red zinc oxide

(*Received* 13 *March*, 1961)

KUTZELNIGG,[1] and EHRET and GREENSTONE,[2] have shown that mixtures of zinc oxide and ammonium nitrate produced a red coloured zinc oxide when fused and thermally decomposed above 300°C. The 2:1 (NH_4NO_3:ZnO) molar melt underwent the most vigorous decomposition and produced the most intensely coloured oxide. According to KUTZELNIGG,[1] the formation of red zinc oxide proceeded via zinc nitrate which was formed by the reaction of zinc oxide with fused ammonium nitrate.

$$ZnO + 2NH_4NO_3 \rightarrow Zn(NO_3)_2 + 2NH_3 + H_2O \quad (1)$$
$$Zn(NO_3)_2 \rightarrow ZnO + 2NO_2 + \tfrac{1}{2}O_2 \quad (2)$$

AUDRIETH and SCHMIDT[3] proposed equation (1) to represent the reaction of fused ammonium nitrate with zinc oxide. EHRET and GREENSTONE[2] did not consider the nature of the intermediate product leading to the formation of red zinc oxide.

This note describes the preparation and some properties of the product formed by reacting 1 mol of zinc oxide with 2 mols molten ammonium nitrate.

Preparation

Because of the potentially hazardous nature of molten ammonium nitrate,[4,5,6] only small quantities (20–30 g) were used, overheating was avoided, oxidisable matter was scrupulously excluded and all work was carried out behind an explosion screen.

[1] A. KUTZELNIGG, *Z. Anorg. Allg. Chem.* **208**, 23 (1932).
[2] W. EHRET and A. W. GREENSTONE, *J. Amer. Chem. Soc.* **65**, 872 (1943).
[3] L. F. AUDRIETH and M. T. SCHMIDT, *Proc. Nat. Acad. Sci.* **20**, 223 (1934).
[4] H. L. SAUNDERS, *J. Chem. Soc.* **71**, 710 (1922).
[5] J. R. PARTINGTON, *Textbook of Inorganic Chemistry*, Macmillan, London (1950).
[6] N. I. SAX, *Handbook of Dangerous Materials*, Reinhold, New York (1951).

Twenty-five grams (0·31 mol) C.p. ammonium nitrate, in a 150 ml beaker, was heated over a small bunsen flame until the temperature of the melt was 170°C. 12·7 g (0·15 mol) C.p. zinc oxide was slowly added to the molten ammonium nitrate, which was kept well stirred with a thermometer. With the continued addition of zinc oxide it was necessary to raise the temperature of the melt. At no time was the temperature allowed to exceed 215°C.

At first, the zinc oxide dissolved with only slight reaction taking place; water vapour and a little ammonia were evolved. On raising the temperature, the reaction became more vigorous, the water vapour and the ammonia were evolved with effervescence. Ammonia was never copiously evolved. All the zinc oxide did not react with the ammonium nitrate, as shown by the slight turbidity of the melt at the end of the addition of all the zinc oxide. Since the 2:1 (NH_4NO_3:ZnO) molar melt decomposed on heating (see under thermal decomposition), it was useless to lengthen the heating period in order that further reaction could occur.

On cooling the 2:1 (NH_4NO_3:ZnO) melt a white, fairly hard crystalline solid was formed. The solid was completely soluble in dilute or concentrated mineral acids and in molten ammonium nitrate. It was appreciably soluble in liquid ammonia and was slightly soluble in cold water without the evolution of heat. Had the solid been $Zn(NO_3)_2$ it would have dissolved readily in water with the evolution of heat.[7]

Cooling curve determinations showed that the solid was impure.[8] The freezing points of different samples ranged from 208–214°C. Attempts to purify the solid by removal of unreacted starting materials proved unsuccessful.

Analysis

Two independent preparations were analysed after being dried for two hours at 120°C. Only water was evolved during drying; the loss in weight was ~1 per cent. There was fairly close agreement between the analytical data obtained and that calculated for $Zn(NH_3)_2(NO_3)_2$:—

Zn found 28·7 ± 0·3 per cent calc. 29·3 per cent; NH_3 found 14·9 per cent calc. 15·2 per cent; NO_3 found 55·85 ± 0·05 per cent calc. 55·9 per cent.

A compound having the formula $Zn(NH_3)_2(NO_3)_2$ could be formed if 2 mols ammonium nitrate and 1 mol zinc oxide reacted as follows

$$ZnO + 2NH_4NO_3 = Zn(NH_3)_2(NO_3)_2 + H_2O.$$

By dissolving weighed amounts of solid in excess 0·1N HCl and back-titrating with 0·1N NaOH (bromophenol blue indicator), values of 119–120 were found for the equivalent weight; the calculated value for $Zn(NH_3)_2(NO_3)_2$ is 112.

Electrolysis

The 2:1 (NH_4NO_3:ZnO) molar melt conducted electricity very well showing the presence of ionic linkages. Using platinum electrodes and a potential of 4 V d.c., a red-grey deposit of zinc oxide was formed on the cathode. The gases evolved at the anode and cathode during electrolysis were not identified.

Since reduction occurs at the cathode, the formation of an oxide at this electrode is unusual. Zinc oxide formation at the cathode could possibly be due to the nitrate ions present in the melt oxidising cathodically deposited zinc. Dry nitrate ion is a much stronger oxidising agent than aqueous nitrate ion[9].

Thermal Decomposition

Both rapid (5–10 min) and slow (30–40 hr) thermal decomposition of the 2:1 (NH_4NO_3:ZnO) molar melt was investigated. The explosive nature of the solid necessitated using only small quantities (0·5–1·0 g).

Ammonia, water vapour and ammonium nitrate were evolved from the commencement of both rapid and slow thermal decomposition. The water vapour was probably produced by the oxidation of the ammonia and the —NH_3 groups in $Zn(NH_3)_2(NO_3)_2$ by atmospheric oxygen and the nitrate ions present in the melt. The ammonium nitrate was probably formed from the vapour phase by the reaction[5]

$$4NO_2 + O_2 + 2H_2O + 4NH_3 = 4NH_4NO_3,$$

the NO_2 being formed by the oxidation of the ammonia and the —NH_3 groups.

[7] E. PIETSCH (Editor), *Gmelins Handbuch der Anorganischen Chemie*, No. 32, Verlag Chemie, Berlin (1924).
[8] C. R. WITSCHONKE, *Analyt. Chem.* **24**, 350 (1952).
[9] G. KORTUM and J. O'M. BOCKRIS, *Textbook of Electrochemistry*, Vol. 2, Elsevier, Amsterdam (1951).

VOL. 19 1961

When the melt was rapidly decomposed, explosive decomposition with copious evolution of brown NO_2 fumes, water vapour, oxygen, and a puff of white smoke occurred in the region of 350–360°C. Chemical tests showed that the white smoke was ammonium nitrate and not zinc oxide. With the commencement of explosive decomposition the fumes evolved changed from alkaline to acidic. A rise in temperature of about 20°C within 10–15 seconds occurred during the explosive decomposition stage. Sometimes a vigorous deflagration commenced in the melt at a temperature below 350°C, the gases burning with an orange-yellow flame, not unlike that of ammonia burning in oxygen.[5]

When the melt was slowly decomposed (30–40 hours) at 240–250°C, the fumes evolved changed from basic to acidic some time before the final decomposition occurred. Only brown NO_2 fumes were observed to be evolved during the final decomposition stage which was not explosive.

Remaining behind at the end of the thermal decomposition of the 2:1 (NH_4NO_3:ZnO) molar melt was a crust of red zinc oxide. Slow thermal decomposition of the melt at temperatures below 360°C produced an oxide considerably paler than the brick red oxide produced by the rapid (5–10 min) thermal decomposition.

The percentage yield of red zinc oxide (35·6–36·3 per cent) obtained by both slow and rapid thermal decomposition of the 2:1 (NH_4NO_3:ZnO) molar melt corresponds to the reaction

$$Zn(NH_3)_2(NO_3)_2 \rightarrow ZnO + 2NO_2 + 2NH_3 + \tfrac{1}{2}O_2$$

for which 36·4 per cent ZnO would be expected.

R. A. EDGE

Department of Chemistry
University of Cape Town
Rondebosch, South Africa

Acknowledgements—The author is greatly indebted to Professor F. SEBBA for his interest, encouragement and advice during this work.

Bivalent nickel complexes of 1,10-phenanthroline and 2,2'-bipyridyl

(*Received* 22 *February* 1961)

Several nickel complexes of the type $Ni(chel)_2X_2$, xH_2O (where chel = 1,10-phenanthroline, 2,2′-bipyridyl; X = a univalent anion) have been reported in the literature;[1,2] but no systematic attempt appears to have been made to determine their structure or chemical behaviour. It has been noted that such compounds are, in general, unstable in aqueous solution, disproportionating to the tris-chelated species and, probably, the hexaquonickel(II) ion,[3] although the existence of both the bis and mono-chelated species has been demonstrated spectrophotometrically.[4] The aqueous nickel–phenanthroline system has recently been more extensively studied by WILKINS and WILLIAMS.[5]

By using non-aqueous solvents, such as acetone, methanol and ethanol, we have been able to extend considerably the range of known compounds, and are studying their behaviour in non-aqueous media. Some of the compounds so far isolated are listed in Table 1, together with their magnetic moments. These moments lie in the range 3·0–3·3 B.M., thus indicating an essentially octahedral arrangement of the ligand atoms about the nickel atom.

This is supported by the conductivity measurements in non-aqueous solvents (Table 2). The anhydrous dihalogeno-complexes have small conductivities in nitrobenzene, which may be due to the dissociation

$$[Ni(chel)_2X_2] + \text{solvent} \rightleftharpoons [Ni(chel)_2(\text{solvent})X]^+ + X^-$$

In the more polar nitromethane, this dissociation is more extensive, and the conductivity of the

[1] P. PFEIFFER, V. DOMINIK, A. FRITZEN and B. WERDELMANN, *Z. anorg. Chem.* **260**, 84 (1949).
[2] P. PFEIFFER and FR. TAPPERMANN, *Z. anorg. Chem.* **215**, 273 (1933).
[3] W. W. BRANDT, F. P. DWYER and E. GYARFAS, *Chem. Rev.* **54**, 959 (1954).
[4] W. C. VOSBURGH and G. R. COOPER, *J. Amer. Chem. Soc.* **63**, 437 (1941).
[5] R. G. WILKINS and M. J. G. WILLIAMS, *J. Chem. Soc.* 5414 (1957).

TABLE 1.

Compound	Colour	Magnetic moment (Bohr magnetons)
Ni $bipy_2(ClO_4)_2$, $2H_2O$	lilac	3·19
Ni $phen_2(ClO_4)_2$, $3H_2O$[1]*	lilac	3·13
Ni $phen_2(ClO_4)_2$	lilac	3·18
Ni $bipy_2$ Cl_2[2]*	green	3·17
[Ni $bipy_2(H_2O)Cl]Cl$, $2H_2O$	blue	3·20
[Ni $bipy_2(H_2O)Cl]ClO_4$, $0{\cdot}5H_2O$	lilac-blue	3·19
Ni $phen_2$ Cl_2[2]*	green	3·17
[Ni $phen_2(H_2O)Cl]Cl$, $3H_2O$[2]*	blue	3·19
Ni $bipy_2$ Br_2	green	3·18
[Ni $bipy_2(H_2O)Br]Br$	blue-green	—
[Ni $bipy_2(H_2O)Br]ClO_4$	blue	3·18
[Ni $bipy_2(H_2O)_2]Br_2$	lilac	3·16
[Ni $phen_2$ Br_2]†	green	3·22
Ni $phen_2$ Br_2, $2{\cdot}5H_2O$	green	3·11
[Ni $bipy_2$ I_2]	brown	3·10
[Ni $bipy_3$][Ni bipy I_4]	red	3·03
[Ni $bipy_2(H_2O)I]I$	olive-green	—
[Ni $bipy_2(H_2O)_2]I_2$	lilac	3·24
[Ni $phen_2$ I_2]	brown	3·25
[Ni $phen_2(H_2O)I]I$	olive-green	3·28
[Ni $bipy_2(NCS)_2$]	lilac	3·12
Ni $bipy_2(NCS)_2$	yellow-brown	3·10
[Ni $phen_2(NCS)_2$]	lilac	3·18

* Denotes compound already reported in the literature.
† Denotes compound previously prepared in this department (N. BARKER: Thesis, New South Wales University of Technology, (1956).

TABLE 2.—MOLECULAR CONDUCTIVITIES OF NICKEL COMPLEXES IN NITROBENZENE AND NITROMETHANE AT 25°C

Compounds	Nitrobenzene		Nitromethane	
	Molar Concentration	Conductance (in mho)	Molar Concentration	Conductance (in mho)
Ni $bipy_2(ClO_4)_2$, $2H_2O$	1×10^{-3}	34	1×10^{-3}	173
Ni $phen_2(ClO_4)_2$, $3H_2O$	1×10^{-3}	36	1×10^{-3}	170
Ni $bipy_2$ Cl_2	2×10^{-4}	5	1×10^{-3}	37
[Ni $bipy_2(H_2O)Cl]Cl$	Insoluble	—	1×10^{-3}	58
[Ni $bipy_2(H_2O)Cl]ClO_4$	1×10^{-3}	28	1×10^{-3}	86
Ni $bipy_2$ Br_2	2×10^{-4}	15	6×10^{-4}	74
[Ni $bipy_2(H_2O)Br]ClO_4$	5×10^{-4}	29	1×10^{-3}	86
[Ni $bipy_2(H_2O)_2]Br_2$	Insoluble	—	1×10^{-3}	69
[Ni $bipy_2I_2$] (brown isomer)	5×10^{-4}	14	1×10^{-3}	83
[Ni $bipy_3$][Ni bipyI_4] (red)	1×10^{-3}	66	1×10^{-3}	250
[Ni $bipy_2(H_2O)_2]I_2$	5×10^{-4}	25	1×10^{-3}	92
[Ni $bipy_2(NCS)_2$]	1×10^{-3}	1–2	1×10^{-3}	13

VOL. 19 1961

iodo-complex is of the order expected for a uni-univalent electrolyte. Conductometric titrations of [Ni bipy$_2$(H_2O)$_2$] (ClO_4)$_2$ with halide ions in nitrobenzene showed well-defined end-points at the addition of one mole-equivalent of halide, and weaker, but still well-defined, end-points at two mole-equivalents. On the other hand, the phenanthroline complex gave only single 1:1 end-points, but these were always high.

Mono-halogeno complexes have been isolated with the empirical formula [Ni bipy$_2$X]ClO_4, $(CH_3)_2CO$ (where X = Cl^-, Br^-). The infra-red spectrum of the bromide showed the carbonyl "stretching" frequency to be at a position almost identical with that in liquid acetone (1712 cm^{-1}). As co-ordination of the acetone is expected to lower this frequency markedly (e.g. $TiCl_4$, $(CH_3)_2CO$: 1625 cm^{-1})[6] these compounds are considered to be halogen-bridged polymers. In moist air, the acetone is lost with the corresponding gain of one molecule of water; and the colour change involved suggests a breaking of the halogen bridge, with the formation of the aquo-complex [Ni bipy$_2$(H_2O)X] ClO_4.

The behaviour of the hydrated perchlorate Ni phen$_2$(ClO_4)$_2$.3H_2O, first reported by PFEIFFER *et al.*,[1] is of some interest. This lilac compound has been dehydrated by heating to 144°C *in vacuo* over P_2O_5, with practically no change in colour (Found; 7·5 per cent loss in wt.; Calc.; 8·2 per cent) or in the magnetic moment (μ = 3·18 B.M.). This is in marked contrast to the behaviour of the ethylene-diamine analogue which, under similar conditions, gives the diamagnetic [Ni en$_2$](ClO_4)$_2$.[7] Further, in nitrobenzene solutions, the conductivity of the phenanthroline complex was of the order expected for a uni-univalent electrolyte. Thus it appears that the bond energy between the perchlorate ion and the nickel atom is sufficient to allow the former to displace a water molecule under these conditions. Such a bond would be expected to have a high degree of ionic character and would thus be favoured in solvents of low polarity. Indeed, in nitromethane, the conductivity was that of an essentially di-univalent electrolyte. Simple ion-pairing cannot be ruled out *a priori*, but we have recently obtained evidence for a similar phenomenon in nitrobenzene solutions of [Cu bipy$_2$(ClO_4)]PF_6. and [Cu bipy$_2$](ClO_4)$_2$, where the existence of the [Cu bipy$_2$ ClO_4]$^+$ ion has been demonstrated by both spectral and detailed conductance measurements.[8] The compound Ni bipy$_2$(ClO_4)$_2$.2H_2O behaves similarly in solution.

Two pairs of isomeric compounds, with empirical formulae Ni bipy$_2$$I_2$ and Ni bipy$_2$($NCS)_2$, have been obtained. Red and light-brown forms of the iodo-complex have been obtained from reactions in acetone solution: the former by the addition of a solution of bipyridyl or trisbipyridylnickel(II) perchlorate to nickel perchlorate and lithium iodide in acetone; and the latter by the addition of lithium iodide to an acetone solution of nickel perchlorate and bipyridyl (1:2), and evaporation of the solution on the waterbath. Conductivity data, colours and the mode of preparation of the compounds indicate that the red isomer is the dimeric salt [Ni bipy$_3$] [Ni bipyI_4], and that the brown isomer is the simple octahedral compound [Ni bipy$_2$$I_2$]. The red dimeric salt has not been obtained in the phenanthroline series, where similar conditions gave the salt [Ni phen$_3$][NiI_4]. Addition of an acetone solution of the tris-chelated species to solutions of $[NiBr_4]^=$ and $[NiCl_4]^=$ in acetone also gave salts of the type [Ni(chelate)$_3$][NiX_4]. The high magnetic moments obtained for these compounds (see Table 3) are evidence for the existence of tetrahedral $[NiX_4]^=$ units.[9]

Addition of bipyridyl to a cold acetone solution of nickel perchlorate and lithium thiocyanate gave a lilac-coloured compound Ni bipy$_2$($NCS)_2$, $(CH_3)_2CO$, which, in air, lost acetone and was converted to a yellow-brown form. Heating of the above lilac compound to 110°C, however, gave a lilac acetone-free complex, which also, slowly converted to the yellow-brown form. Recrystallisation of the latter from nitromethane gave the lilac compound Ni bipy$_2$($NCS)_2$, 2$MeNO_2$. This also lost the solvent in air, with conversion to the yellow-brown form. Infra-red measurements on the lilac, acetone-containing complex showed only one band (2080 cm^{-1}) in the C≡N "stretching" region. This is typical of nickel tetrammine complexes of known *trans*-octahedral structure, such as [Ni en$_2$($NCS)_2$],[10] [Ni py$_4$($NCS)_2$] and [Ni(NH_3)$_4$($NCS)_2$].[11] Also, the position of the carbonyl frequency of the acetone was at 1712 cm^{-1}, which, as previously mentioned, indicates that the acetone is present

[6] D. CASSIMATIC and B. P. SUSZ, *Helv. chim. acta* **43**, 852 (1960).
[7] H. GLASER and P. PFEIFFER, *J. prakt. Chem.* **153**, 300 (1939).
[8] N. BARKER, C. M. HARRIS and E. D. MCKENZIE. Submitted to proceedings of Chemical Society London. To be published shortly. N. BARKER: Thesis, University of New South Wales, (1960).
[9] N. S. GILL and R. S. NYHOLM, *J. Chem. Soc.* 3997 (1959).
[10] E. C. LINGAFELTER, *Nature, Lond.* **182**, 1730 (1958).
[11] C. PECILE, G. GIACOMETI and A. TURCO, *R. C. Acad. Ital.* **28**, 189 (1960).

TABLE 3.—MAGNETIC MOMENTS OF $[NiX_4]^{=}$ COMPLEXES

	μ/Ni	μ_{anion}*
[Ni $bipy_3$][Ni Cl_4]	3·46	3·7
[Ni $phen_3$][Ni Cl_4]$2H_2O$	3·45	3·7
[Ni $bipy_3$][Ni Br_4]	3·46	3·7
[Ni $phen_3$][Ni Br_4].$2H_2O$	3·45	3·7
[Ni $phen_3$][Ni I_4].$2H_2O$	3·31	3·5

* This value was calculated using $\mu = 3{\cdot}15$ for the cations [Ni $phen_3$]$^{++}$, [Ni $bipy_3$]$^{++}$

simply as solvent of crystallisation. These results are in favour of a simple octahedral diacidotetrammine structure of the lilac isomer. On the other hand, the infra-red spectrum for the yellow-brown isomer had two bands of equal intensity at 2084 and 2050 cm^{-1}. The higher wave number band appears to be typical of the thiocyanate covalently bound as Ni—NCS, while the lower wave number band is more typical of an ionic thiocyanate. It is interesting to note that a similar spectrum has been obtained for Cu $bipy_2(NCS)_2$.[12] By analogy with the corresponding iodide,[13] this latter compound is expected to have a 5-covalent trigonal bipyramidal structure.[14] There is as yet, however, insufficient evidence to support such a structure for the nickel complex. The possibility of *cis-trans* isomerism has been considered, but the only known nickel compound with a *cis*-octahedral structure of this type is [Ni(tren)$(NCS)_2$].[15] This molecule is unsymmetrical, the quadridentate ligand having one tertiary and three primary nitrogens, and the published bond lengths (Ni—NCS) are indeed unequal. Thus, the existence of two bands in the infra-red spectrum (Li F optics) at 2076 and 2089 cm^{-1}[12] is not unexpected and does not lend any support to the possibility of a *cis*-octahedral structure for the yellow-brown isomer. By contrast, only a stable lilac isomer has been obtained in the case of the phenanthroline analogue.

It is hoped that a more detailed conductometric study will give a better understanding of the behaviour of these complexes in solution. Spectrophotometric studies are also in progress.

Acknowledgement—The authors wish to acknowledge Dr. D. HALL (University of Auckland, N.Z.) for a sample of [Ni tren$(NCS)_2$].

C. M. HARRIS
E. D. MCKENZIE

Department of Inorganic Chemistry
University of New South Wales
Broadway, Sydney

[12] C. M. HARRIS, T. N. LOCKYER and E. D. MCKENZIE, Unpublished results.
[13] G. A. BARCLAY and C. L. KENNARD, to be published.
[14] C. M. HARRIS, T. N. LOCKYER and H. WATERMAN, to be published.
[15] S. E. RASMUSSEN, *Acta Chem. Scand.* **13**, 2009 (1959). D. HALL, M. D. WOULFE, *Proc. Chem. Soc.* 346 (1958).

Redetermination of the half-life of bismuth (ThC)*

In the course of investigating the chemical properties of carrier-free lead-212 deposited on platinum surfaces we had occasion to redetermine the half-life of bismuth-212 (ThC). Our data give a half-life of 60·60 minutes, with a standard deviation of 0·043 minutes. The previously measured half-life, reported[1] almost a half century ago, was 60·48 minutes, with a probable error of 0·035 minutes.

Procedure

A mixture of bismuth-212 and lead-212 was isolated from a solution of thorium nitrate by the method of KAHN and LANGHORST.[2] The separation of bismuth-212 from this mixture was based on the procedure of ERBACHER and PHILIPP,[3] wherein bismuth is removed from an acid solution by

* This communication is based on work done under the auspices of the Atomic Energy Commission (Contract No. AT (11–1)–733).

[1] F. V. LERCH, Sitzb. kais. Akad. Wiss., Wien., Abt. IIa, 123, 699–712 (1914).
[2] M. KAHN and A. L. LANGHORST, *J. Inorg. Nucl. Chem.* **15**, 384 (1960).
[3] O. ERBACHER and K. PHILIPP, *Z. Physik.* **51**, 309 (1928).

VOL. 19 1961

electrochemical deposition on nickel powder. Bismuth and lead carriers were added to the active 0·02*f* nitric acid solution, which was then passed through a nickel powder matte supported on a glass frit. The matte, which retained most of the bismuth and a few per cent of the lead, was dissolved in hot concentrated nitric acid and the solution diluted to 1*f* nitric acid. Then, additional lead carrier was added and the solution was passed through a second nickel matte supported on a small filter paper clamped between a porcelain filter cone and a glass chimney. The nickel matte was washed with water, dried with acetone, and mounted on an aluminum plate for counting. The decay of each of four such samples was followed for about six hours with a Los Alamos-type counting assembly consisting of a thin-window methane-flow proportional counter, a pulse amplifier, and a binary-type scaler. At least twenty-seven points were obtained for each decay; and at least 10,000 counts were taken for each point. The data were fitted by least squares to a single-component decay with an IBM 704 computer; dead-time losses and decay during counting were taken into account in the computer code. No statistically significant amounts of lead-212 were detected by attempts to fit the data to a two-component decay with the inclusion of lead-212 as the second component.

Chemistry Department
University of New Mexico
Albuquerque, New Mexico

K. R. Applegate
E. M. Morimoto
M. Kahn
J. D. Knight†

† Los Alamos Scientific Laboratory.

The ice region of the system $AgF \cdot HF \cdot H_2O$ at $-15°$

(*Received* 4 *May* 1961)

The results of an investigation in this laboratory of the system $AgF \cdot HF \cdot H_2O$ at 0° and −15° have been previously reported in this journal.[1] We have recently realized that ice should exist at at least one point at −15°C and that it would be surprising if it did not exist at low HF and AgF concentrations. Examination of the previously reported data showed that the region in which ice would most likely exist had not been investigated. We have therefore investigated this region.

The experimental procedure has been described in the previous paper.

The results are tabulated in Table 1. It seems quite clear that solid H_2O (ice) can exist on the HF concentration limits of from 0·00 per cent to 12·06 per cent provided the AgF concentration does not reach 37·72 per cent.

Acknowledgement—One of us (J. P. B.) would like to thank the Dow Chemical Company for a leave of absence which allowed him to participate in this work.

Table 1.—Analysis of the solution and wet residues

Solutions	Weight %	Wet Residues	Weight %	Composition of Solid Phase
HF	AgF	HF	AgF	
12·06	0	9·12	0	H_2O
10·74	4·96	7·97	3·81	H_2O
8·84	12·01	7·21	9·59	H_2O
7·40	17·85	5·70	13·79	H_2O
5·77	23·99	4·51	19·25	H_2O
3·50	30·64	2·89	25·67	H_2O
2·71	34·66	2·39	30·79	H_2O
0·10	37·72	0·09	50·34	H_2O and $AgF \cdot 4H_2O$

Chemistry Department
Agricultural and Mechanical College of Texas

John P. Buettner
Albert W. Jache

[1] H. J. Thomas and A. W. Jache, *J. Inorg. Nucl. Chem.* **13**, 54 (1960).

VOL
19
196

J. Inorg. Nucl. Chem., 1961, Vol. 19, pp. 377 to 381. Pergamon Press Ltd. Printed in Northern Ireland

LETTERS TO THE EDITOR

The preparation and properties of TcF_6

(*Received* 13 *January* 1961)

THE reaction of fluorine gas and technetium metal powder yields a volatile compound which we have identified as TcF_6. Two preparations have been made using 85 and 236 mg samples of Tc metal. The metal, prepared by reducing dry NH_4TcO_4 with H_2 at 600°C,[1] was reacted for two hours with excess F_2 gas in a closed nickel can at 400°C. The volatile product was purified by fractional sublimation techniques which have been described previously.[2] The yield of purified TcF_6 was greater than 90 per cent.

The experimental evidence which characterizes the volatile product as TcF_6 is:

(1) Measurement of fluorine consumption by Tc metal shows that 3 moles of fluorine are absorbed per mole of Tc.

(2) Two vapour density determinations gave molecular weights of 208 and 209. Within our experimental error, these results are in agreement with the formula weight of 213.

(3) Chemical analysis implies an empirical formula of $TcF_{5.8}$ (Given, 128 mg compound: Found: 58·5 mg Tc, 65·4 mg F; Calculated for TcF_6; 59·5 mg Tc, 68·5 mg F). The Tc was determined by counting.

(4) X-ray diffraction studies show that the solid compound undergoes a phase transition. The low and high temperature forms of the solid are isomorphous with the corresponding solid forms of the other known transition metal hexafluorides.[3] The solid-solid transition occurs at about −3.5°C.

(5) The infrared spectrum from 600–2000 cm^{-1} is similar to the infrared spectra of the other hexafluorides.[4] TcF_6 exhibits a strong fundamental absorption at 745 cm^{-1}.

At room temperature TcF_6 is a golden-yellow solid. The melting point determined in a thin-walled capillary was 33°C. Some preliminary vapour pressure measurements for solid TcF_6 are:

T (°C)	p (mm)
0	59
4·9	78
9·3	100
12·0	115
15·7	140

TcF_6 can be stored unchanged in nickel or dry Pyrex vessels for extended periods of time.

Upon hydrolysis with NaOH, TcF_6 yields a black precipitate which dissolves with the addition of H_2O_2. This behaviour is analogous to that of ReF_6 which disproportionates upon hydrolysis to yield insoluble ReO_2 and soluble ReO_4^-.[5]

Acknowledgements—Based on work performed under the auspices of the U.S. Atomic Energy Commission.

HENRY SELIG
CEDRIC L. CHERNICK
JOHN G. MALM

Argonne National Laboratory
Argonne, Illinois

[1] J. W. COBBLE, C. M. NELSON, G. W. PARKER, W. T. SMITH, JR. and G. E. BOYD, *J. Am. Chem. Soc.*, **74**, 1852 (1952).
[2] B. WEINSTOCK and J. G. MALM, *J. Inorg. Nucl. Chem.*, **2**, 380 (1956).
[3] D. NORTHRUP and S. SIEGEL, unpublished data.
[4] J. GAUNT, *Trans. Faraday Soc.* **49**, 1122 (1953).
[5] O. RUFF, W. KWASNIK and E. ASCHER, *Z. Anorg. Allgem. Chem.*, **209**, 113 (1932).

4A—(4 pp.)

VOL. 19 1961

The preparation of trivinylgallium

(*Received* 6 *March; in revised form* 10 *April* 1961)

Trivinylgallium has been prepared by the reaction of divinylmercury with excess gallium metal at room temperature. A 40 per cent yield based on the divinylmercury was obtained when the reaction was allowed to proceed for 24 hr at this temperature. Either longer reaction times or higher temperatures induced polymerization of the product and reduced the yield.

Other workers have reported[1] that divinylmercury and gallium metal react to give a vinylgallium compound, but its exact nature has not been described. This method has also been used in the preparation of other organogallium compounds, but under quite different conditions.[2]

The reaction products were separated by a low temperature crystallization. The purified trivinylgallium melts between -7° and -9°C. Its vapour pressure is given by the equation $\log_{10} P_{mm} = \frac{-2020}{T} + 6{\cdot}690$ between 30° and 70°C. Above 70°C the material undergoes a rapid polymerization to a brown oil with evolution of small amounts of ethylene. This polymerization also takes place slowly at room temperature as previously reported.[1]

Trivinylgallium is hydrolyzed by water or by dilute mineral acids producing ethylene. This hydrolysis is not complete, however, unless the reaction mixture is heated to 100°C for 6 to 8 hr with acid or for 48 hr with water; then, it proceeds quantitatively according to the equation:

$$Ga(C_2H_3)_3 + 3H^+ \rightarrow Ga^{+3} + 3C_2H_4.$$

The results of this reaction were used for analysis of the trivinylgallium and gallium analysis was

TABLE 1.

Sample	C_2H_4 moles $\times 10^3$		Ga moles $\times 10^3$	
	Calc.	*Found*	*Calc.*	*Found*
23·4 mg (acid hydrolysis)	0·465	0·461	0·155	0·146
42·5 mg (water hydrolysis)	0·842	0·835	0·281	0·257

carried out by titration with potassium ferrocyanide[3] while the ethylene was identified by its infra-red spectrum.[4]

The infra-red spectrum of a carbon tetrachloride solution of the pure compound had absorptions at 3013, 2935, 2909, 1394, 1264, 1042, 1017, 981, and 952 cm^{-1}. This spectrum indicated that the vinyl group[5] was present and that there were no other organic substituents.[6]

Trivinylgallium was further characterized by reacting 0·0993 m moles with excess anhydrous ammonia. The excess ammonia was then removed by distillation from the reaction vessel at room temperature. 0·0995 m moles of ammonia was retained indicating the formation of an 1:1 addition compound. This compound slowly decomposed at room temperature producing ethylene and an unidentified liquid product.

Trivinylgallium reacts with air to produce ethylene and a white crystalline product which is stable. This product has infra-red absorptions (KBr disk) at 700, 958, 1013, 1400, 1467, 1545, 1641, 2922, and

[1] F. E. BRINCKMAN and F. G. A. STONE, *J. Inorg. Nucl. Chem.* **11,** 24 (1959).
[2] L. M. DENNIS and W. PATNODE, *J. Amer. Chem. Soc.* **54,** 182 (1932); H. GILMAN and R. G. JONES, *ibid.* **62,** 980 (1940); E. WIBERG, T. JOHANNSEN and O. STECHER, *Z. Anorg. Allg. Chem.* **251,** 114 (1943).
[3] R. BELCHER, A. J. NUTTEN and W. L. STEPHEN, *J. Chem. Soc.* 2438 (1950).
[4] R. H. PIERSON, A. N. FLETCHER and E. GANTZ, *Analyt. Chem.* **28,** 1218 (1956).
[5] H. D. KAESZ and F. G. A. STONE, *Spectrochim. Acta,* **15,** 360 (1959); H. D. KAESZ and F. G. A. STONE, "Organometallic Chemistry," ACS Monograph No. 147, Edited by H. Zeiss, Reinhold Publishing Corporation, New York, (1960) pp. 88–149.
[6] L. J. BELLAMY, "*The Infra-red Spectra of Complex Molecules,*" John Wiley and Sons, New York, (1954).

3404 cm^{-1}. The absorption at 3400 cm^{-1} is characteristic of the OH group,[6] while the others are characteristic of the vinyl group.[5] This product is under further study.

All reactions were carried out under a nitrogen atmosphere or in standard vacuum equipment.

Acknowledgements—The authors wish to thank the Research Corporation for a Frederick Gardner Cottrell grant which made this work possible.

JOHN P. OLIVER
L. G. STEVENS

Department of Chemistry
Wayne State University
Detroit 2, Michigan

The thermodynamic properties of dilute solutions of UCl_3 in LiCl-KCl eutectic

(*Received* 24 *March* 1961)

VOL. 19 1961

THREE independent studies of the thermodynamic properties of dilute solutions of UCl_3 in LiCl–KCl eutectic have recently been made.[1,2,3] Each study has involved measurement of the e.m.f. of galvanic cells of the form

$$U/UCl_3 \text{ in LiCl–KCl eut.//AgCl in LiCl–KCl eut./Ag}$$

and the compositions examined have been in the range 0 to $5{\cdot}6 \times 10^{-3}$ mol fraction UCl_3 at temperatures between 440° and 550°C. The e.m.f. E, of the cell is given by the equation

$$E = E^{\circ}_{UCl_3} - E^{\circ}_{AgCl} - \frac{T}{15129}\log_{10} a_{UCl_3} + \frac{T}{5043}\log_{10} a_{AgCl} + Ej \text{ volts}$$

where $E^{\circ}_{UCl_3}$, E°_{AgCl} are the e.m.f. values corresponding to the free energies of formation of pure UCl_3 and AgCl from the elements at T°K and 1 atm pressure, a_{UCl_3}, a_{AgCl} are the activities of UCl_3 and AgCl in LiCl–KCl eutectic, mol fraction basis, T is the temperature in °K, and Ej denotes the junction potential that may be present, arising from the difference in composition of the salt in the two halves of the cell. $E^{\circ}_{UCl_3}$, E°_{AgCl} and a_{AgCl} are known, so that the measured cell e.m.f. may be used to deduce a_{UCl_3} provided the junction potential Ej is either known or else is assumed to be negligibly small.

The experimental evidence suggests that for the concentrations of interest here the junction potentials, with either the silica frit junction used by GRUEN and OSTERYOUNG or the continuous Pyrex glass membranes used by INMAN *et al.* and YANG *et al.*, were in fact negligibly small.[4]

From their experimental results INMAN *et al.* calculated a_{UCl_3} and found that at a UCl_3 mol fraction, $N_{UCl_3} = 5{\cdot}6 \times 10^{-3}$ the activity coefficient, γ_{UCl_3}, was 0·07 at 463°C. YANG *et al.* used their results to derive a value of $\gamma_{UCl_3} = 0{\cdot}84$ at $N_{UCl_3} = 5{\cdot}0 \times 10^{-3}$ and 497°C. This apparent wide disagreement is due in some part to the values used by the different workers for $E^{\circ}_{UCl_3}$, E°_{AgCl} and a_{AgCl}, and to enable a proper assessment of the data to be made the results for a_{UCl_3} and γ_{UCl_3} have been re-derived[4] on the basis of the most reliable data at present available for $E^{\circ}_{UCl_3}$, E°_{AgCl} and a_{AgCl}. The experimental results of GRUEN and OSTERYOUNG, who did not derive activity data from their measurements, have also been used to calculate a_{UCl_3}.

Thus, taking $E^{\circ}_{UCl_3}$ from the free energy data of BREWER *et al.*,[5] E°_{AgCl} from the results of SALSTROM[6] and a_{AgCl} from the recent work of YANG and HUDSON[7], and re-deriving the activity data it is found that good agreement exists between the results of GRUEN and OSTERYOUNG and those of

[1] D. INMAN, G. J. HILLS, L. YOUNG and J. O'M. BOCKRIS *Trans. Faraday Soc.* 55, 11, 1904 (1959).
[2] D. M. GRUEN and R. A. OSTERYOUNG *Annals N.Y. Acad. Sci.* 79, Art 11, 897 (1960).
[3] L. YANG, R. G. HUDSON and C. CHIEN *AECU* 4544 (1960).
[4] B. PARTRIDGE AERE–R. 3682 (1961).
[5] L. BREWER *et al.* TID 5290, Paper 33 (1958).
[6] E. J. SALSTROM *J. Amer. Chem. Soc.* 55, 2426 (1933).
[7] L. YANG and R. G. HUDSON *Trans. Met. Soc.* of *A.I.M.E.* 215, 4, 589 (1959).

YANG *et al.* However, the earlier, more limited experimental results of INMAN *et al.* are in marked disagreement with the other work and the reason for this is not apparent. Nevertheless, the degree of agreement between the data of GRUEN and OSTERYOUNG and of YANG *et al.* leads to confidence in the combined results, which give, at 500°C,

N_{UCl_3}	2×10^{-3}	4×10^{-3}	6×10^{-3}
a_{UCl_3}	$1{\cdot}13 \times 10^{-2}$	$2{\cdot}11 \times 10^{-2}$	$3{\cdot}05 \times 10^{-2}$
γ_{UCl_3}	5·65	5·28	5·01

Therefore the conclusion is reached that UCl_3 exhibits marked positive deviations from Raoult's Law in LiCl–KCl eutectic at temperatures around 500°C and that the activity coefficient at infinite dilution is approximately 6·3 at 500°C. It must be remembered that this conclusion is based upon the quoted data for $E^{\circ}_{UCl^3}$, E°_{AgCl} and a_{AgCl} and may be modified when more precise data on these quantities (in particular on $E^{\circ}_{UCl_3}$) become available.

B. A. PARTRIDGE

Chemical Engineering Division
Atomic Energy Research Establishment
Harwell

The half-life of Br^{83}

(*Received* 1 *May* 1961)

DURING recent investigations of the proton-induced fission of the actinide elements, it was necessary to redetermine the half-life of Br^{83}, which has been variously reported as having the values 140 ± 10 min[1], 138 ± 3 min[2], 140 min[3,4], 144 min[5] and 147 ± 6 min[6].

Since these different values could have been due to contamination by a nuclide or nuclides of similar half-life, several different methods of preparation were employed. Accordingly samples of Br^{83} were prepared by the (n, γ) reaction of pile neutrons both with natural metallic selenium and with selenium which had been enriched to 82 per cent in Se^{82}; by the fission of natural uranium with pile neutrons, and by the fission of thorium, uranium and plutonium with protons of 30 and 50 MeV.

Method of preparation	Activity at start of the usable decay curve (counts/min)	Half-life (min)	Standard Deviation (min)
Nat Se(n, γ)	17550	144·08	0·10
Nat Se(n, γ)	4850	143·03	0·27
82 per cent $Se^{82}(n, \gamma)$	45510	145·71	0·10
82 per cent $Se^{82}(n, \gamma)$	86180	144·13	0·09
82 per cent $Se^{82}(n, \gamma)$	17350	142·74	0·09
U(n, f)	13000	145·59	0·43
U(n, f)	7600	145·83	0·41
Th(p, f) 30MeV	114000	145·51	0·14
Th(p, f) 50MeV	472000	144·58	0·08
U(p, f) 30MeV	278000	143·95	0·08
U(p, f) 50MeV	147500	144·96	0·09
Pu(p, f) 30MeV	28800	144·94	0·16

[1] F. STRASSMAN and O. HAHN *Naturwiss* **28**, 817 (1940).
[2] P. SWINBANK and J. WALKER *Proc. Phys. Soc.* A **66**, 1093 (1953).
[3] A. LANSDORF and E. SEGRE *Phys. Rev.* **57**, 105 (1940).
[4] R. N. H. HASLAM and H. M. SKARSGARD *Phys. Rev.* **81**, 479 (1951).
[5] S. KATCOFF, B. FINKLE and N. SUGARMAN NNES–9, Paper 59.
[6] A. M. SNELL *Phys. Rev.* **52**, 1007 (1937).

In all cases the material containing the active bromine was taken into solution with bromine carrier and the bromine activity was separated from all other activities by several successions of solvent extraction into carbon tetrachloride as Br_2 (by oxidising bromide with potassium permanganate solution in the presence of acid), and into water as bromide (using H_2SO_3). Several specific separations from iodine were performed, the iodide carrier being introduced at various stages and removed as I_2 (which does not oxidise the bromide to Br_2). The bromine was finally collected in the form of silver bromide, in which state it was counted.

The decay curves were followed on either a 2π methane-flow β-proportional counter of a type similar to the AERE 1222A as developed at Harwell, or on one of three 2π β-proportional counters of the type developed by SUGARMAN. These latter counters had anti-coincidence shielding associated with them, which reduced the background to less than 2 counts/min.

When the active bromine was made by the fission process, the activities taken at times earlier than 400 min from the end of the irradiation were ignored. The contamination due to Br^{84}, which has a half-life of 31·8 minutes, was thus reduced to less than 0·02 per cent of its original value. Since the irradiations were of a few minutes only, this corresponds to less than 0·1 per cent at 400 min assuming equal formation cross sections. Corrections were also made in these cases for the activity due to Br^{82}.

A summary of a least squares fit, weighted according to the variance on each point of the decay curves is given in the Table. The standard deviation quoted in each case is on the best fit to the experimental decay curve.

Considering these results, a value of 144·6 $\pm$ 1·0 minutes is proposed for the half-life of Br^{83}.

Atomic Energy Research Establishment B. J. BOWLES
Harwell
Didcot, Berkshire

VOL. 19 1961

J. Inorg. Nucl. Chem., 1961, Vol. 19, pp. 382 to 383. Pergamon Press Ltd. Printed in Northern Ireland

BOOK REVIEWS

Annual Review of Nuclear Science, Edited by EMILIO SEGRE, Vol. 10, 1960. Annual Reviews, Inc., Palo Alto, California. 617 pp. $7.

THE present volume, which marks the tenth anniversary of the Annual Review of Nuclear Science, is very much along the lines of previous volumes, with authoritative survey articles on selected topics; cumulative indexes of chapter titles and contributing authors for Volumes one to ten are included.

This review is up to the high standard set previously. Most of the articles are of course concerned with physics, but there is one article—on the labelling of organic compounds by recoil methods, by A. P. WOLF—which will be of interest to chemists; in addition to a brief discussion of the mechanisms involved, the article deals with recoil labelling of a great variety of organic compounds with carbon-14, with tritium and briefly with other elements. There are also articles on cellular radiobiology, on vertebrate radiobiology (metabolism of internal emitters and late effects), and on nuclear methods for subsurface prospecting which may be of interest to chemists.

Of the physics sections, one of the articles—that on bubble chambers by H. BRADNER—is very interesting not only because of the physics involved but because it mentions the cost of some of this equipment; chemists whose researches involve only rather small amounts of cash can only admire the facility of physicists in extracting megabuck quantities from the public purse for their fundamental research.

In addition to the topics mentioned there are articles on neutrino interactions, nuclear reactions of heavy ions, cosmic ray showers, optics of high-energy beams, nuclear structure effects in internal conversion, recoil techniques, theoretical interpretation of energy levels in light nuclei, and nucleon–nucleon scattering experiments.

G. WILKINSON

D. P. GRADDON: **An Introduction to Co-ordination Chemistry,** International Series of Monographs on Inorganic Chemistry, Vol. 3, Pergamon Press, Oxford, 1961. vii + 111 pp., 25s.

AN introduction to this rapidly advancing subject will be welcomed by students who might possibly find some of the larger works, for example the excellent volume edited by LEWIS and WILKINS, rather beyond their scope. In fact the author states in his preface that the book is intended primarily for students.

The first of the seven chapters provides a brief (13 page) and interesting historical introduction. This is followed by a longer chapter (26 pages) which aims at a presentation of current valency theory applied to co-ordination chemistry. The theory includes a brief treatment of non-bonding pairs and of magnetism, but the second half of the chapter is concerned with ligand-field theory and here one cannot help feeling it is unfortunate that DR. ORGEL's excellent monograph on transition metal chemistry was published almost simultaneously. It would probably have been better had DR. ORGEL's book appeared well before DR. GRADDON's, and could have been included in the bibliography of the latter.

The remaining five chapters deal with particular aspects of co-ordination chemistry. Chapter 3 (11 pages) on polymerization and co-ordinate saturation contains a good deal of descriptive matter, and refers to such compounds as trimethylaluminium, basic beryllium acetate, silver cyanide, the associated *A* sub-group alkoxides, and Prussian blue. The next chapter (14 pages) provides a useful summary of methods for measuring stability constants, and a brief discussion of some of the factors which influence them. There follows a surprisingly brief chapter (7 pages) on oxidation potentials and valency state stabilization.

The longest chapter (VI, 16 pages) is on the subject of carbonyls and π-complexes, but the discussion of valency in this chapter is rather less clear than elsewhere in the book. Clarity would have been improved if, for example, the author had shown which acetylenic, cyanide or carbon monoxide orbitals are involved in σ and π bonding, how these orbitals interact with metal orbitals, and why this kind of complex is particularly characteristic of metals in low oxidation states. Some use of the symmetry properties of atomic and molecular orbitals would have improved the treatment of olefin π-complexes, cyclopentadienyls and arenes. Many students, after reading this chapter as an introduction to the subject, would draw erroneous conclusions about the symmetries of cyclopentadienyl π-electron orbitals. The structure (illustrated) of gaseous copper(II) nitrate is not that described by BAUER and ADDISON, who determined it.

The final chapter (12 pages) contains a useful discussion of various practical applications of complex formation, including the selective precipitation of oxine complexes, solvent extraction, and sequestration.

G. E. COATES

VOL.
19
1961